

Seismic Vulnerability of Cultural Heritage Buildings in Switzerland

THÈSE N° 4167 (2008)

PRÉSENTÉE LE 3 OCTOBRE 2008

À LA FACULTE ENVIRONNEMENT NATUREL, ARCHITECTURAL ET CONSTRUIT
LABORATOIRE D'INFORMATIQUE ET DE MÉCANIQUE APPLIQUÉES À LA CONSTRUCTION
PROGRAMME DOCTORAL EN STRUCTURES

ÉCOLE POLYTECHNIQUE FÉDÉRALE DE LAUSANNE

POUR L'OBTENTION DU GRADE DE DOCTEUR ÈS SCIENCES

PAR

Mylène DEVAUX

ingénieure civile diplômée EPF
de nationalité suisse et originaire de Lamboing (BE)

acceptée sur proposition du jury:

Prof. J.-F. Molinari, président du jury
Dr P. Lestuzzi, directeur de thèse
Prof. P. B. Lourenço, rapporteur
Dr K. Pfyl-Lang, rapporteur
Prof. B. Zimmerli, rapporteur



ÉCOLE POLYTECHNIQUE
FÉDÉRALE DE LAUSANNE

Suisse
2008

Acknowledgements

The research presented in this thesis comes within the framework of a national project that began in 2001. The project is aimed at the preservation of the Swiss Cultural Heritage Buildings against earthquakes. Without the support of the Swiss Federal Office of Civil Protection and especially Rino Büchel, Hans Laupper and Ivo Zemp, this thesis would not have been initiated. I take this opportunity to express my sincere gratitude to them. I am also grateful for their helpful comments and advice.

I sincerely thank my thesis supervisor, Pierino Lestuzzi, for guiding me towards successful completion of my thesis in such a challenging field of research. I thank him for his valuable comments, advice and support during the four years of doctoral study. I would like to thank everyone who helped me in gathering data on damage observed after past earthquakes. In particular, I thank Stefan Fritsche (Swiss seismological Service), Pierre Dubuis (Lausanne University), the teams of the cantonal archives of Valais and the bishopric of Sion. The authorities of the canton of Valais and in particular, Christophe Valentini and Bernard Attinger, are also acknowledged for their collaboration. I am also very grateful to Stéphane Rossier (SCIA MAPS SA) for his help and support regarding the numerical modelling as well as Pascale Favez for her important input in carrying out the experimental investigation. The members of the technical commission of Lausanne Cathedral are also acknowledged for their interest in this research work and for having put at our disposal sandstone blocks from the removed parts of the buttresses of the Lausanne Cathedral. I thank Léopold Pflug for his interest and his help in collecting study material that proved to be very useful. Finally, I would like to express my gratitude to Kerstin Pfyl-Lang (EMPA), Paulo B. Lourenço (Minho University, Portugal) and Bruno Zimmerli (Technical University, Luzern) for taking the time to be in my committee and for their valuable comments and corrections.

I would like to thank Ian F. C. Smith for giving me the opportunity to carry out my research work at the Applied Computing and Mechanics Laboratory (IMAC) as well as his interesting comments for my oral defence.

The English language of the present PhD thesis has been corrected by Prakash Kripakaran (IMAC); his cooperation is gratefully acknowledged. The German part has been reviewed by Jürg Hegner and I also thank him.

I have really enjoyed my four-year stay at IMAC; I have been fortunate to work within such a nice environment. Many thanks go to all the members of IMAC for the interesting discussions we had at coffee breaks and the nice time we spent during the IMAC hiking and ski days.

My final thanks are addressed to my family, Vincent and my friends for their support and constant encouragement all along my PhD research work.

Abstract

Seismic risk for cultural heritage buildings has been underestimated for years in Switzerland. A strong earthquake can occur at any time in this region, as it has been shown during the last centuries. As reminder the 1356 seismic event that destroyed the city of Basel can be quoted; this event, whose intensity is assessed as having been I=IX on the European Macroseismic Scale (EMS-98), is recorded as the most violent earthquake that struck central and northern Europe.

Since 2003 or even 1989, the seismic safety of common buildings is well defined through modern building codes (Swisscodes (SIA)). However, this is not the case of cultural heritage buildings whose seismic vulnerability has been only partly addressed. This PhD thesis was initiated in order to fill in this void of knowledge by creating a methodology for assessing the seismic vulnerability of historical edifices.

Surveys carried out on cultural heritage buildings after seismic event showed that such kind of structures are particularly vulnerable under seismic actions. This vulnerability is essentially due to their particular structure that is characterized by slender components (pillars), wide open spaces, quite big masses located at high levels (vaults and their filling, lantern towers, etc.) on one hand; on the other hand, they generally have few components that can resist the lateral actions perpendicular to the nave and their masonry fabric is non-ductile. Moreover the non-existence of a stiff horizontal component (or a deformable one in case of wooden ceilings) and heavy masses concentrated in walls rather at floors make it impossible to apply models that have been developed for common buildings.

The methodology that is presented in this report is composed of four steps. It gives the possibility to first sort out the sacred edifices that are seismically vulnerable from the ones that are not vulnerable. The second step allows engineers to determine the seismic vulnerability of a given edifice by the use of simplified models that give valuable results. In case more accurate results are required, more sophisticated models can be applied, as the Finite Element Method. In the last step, the seismic vulnerability of the edifice is put in parallel with the expected peak ground acceleration of the region. This last phase permits to set if the given edifice can be damaged by earthquakes, which damage is expected and which retrofitting is required.

Key words: Seismic vulnerability, methodology for the assessment of the seismic vulnerability, cultural heritage buildings, old masonry, structural behaviour, Romanesque churches, theory of plasticity, preservation of the building heritage.

Résumé

Le risque sismique pour les bâtiments historiques a pendant longtemps été sous-estimé en Suisse. En effet, un fort tremblement de terre peut arriver à tout instant dans cette région, comme l'ont démontré les importants séismes qui se sont produits durant les siècles passés. A titre d'illustration, on peut citer le tremblement de terre qui a secoué la région de Bâle en 1356, dont l'intensité maximale est évaluée à I=IX sur l'échelle macrosismique européenne (EMS-98). Il s'agit de la plus violente secousse sismique répertoriée au nord de l'Europe.

En 1989, un chapitre traitant de la sécurité parasismique du bâti courant a été introduit dans la norme de construction suisse (SIA); ce dernier a été remanié en 2003 afin d'intégrer les derniers résultats de la recherche en génie parasismique. Les bâtiments historiques n'ont pas été traités de la même manière et la norme suisse de construction ne donne pas d'indications quant au moyen de déterminer leur sécurité face aux séismes. Afin de palier à ce manque, ce travail de doctorat, dont le but est de fournir une méthodologie permettant d'évaluer la vulnérabilité sismique des bâtiments historiques, a été initié.

Les reconnaissances réalisées sur les édifices historiques après séisme montrent que ce type de structures s'avère particulièrement sensible aux actions sismiques. Cette vulnérabilité est essentiellement due à leurs particularités structurales telles que l'élancement des piliers, l'existence de grands espaces ouverts et d'importantes masses situées à des hauteurs élevées. En outre, ils contiennent peu d'éléments résistants aux forces latérales perpendiculairement à la nef et leurs murs sont généralement composés d'un matériau pierreux non ductile. Par ailleurs, l'absence de diaphragme (ou l'existence d'une structure en bois déformable en tant qu'élément horizontal) et la concentration de la masse dans les murs plutôt qu'à des étages rend caduque l'utilisation des modèles développés pour le bâti courant.

La méthodologie présentée dans ce rapport pour l'évaluation de la vulnérabilité sismique des édifices historiques est composée de quatre niveaux. La première étape consiste à sélectionner les édifices sacrés vulnérables au séisme. Lors de la deuxième étape, la vulnérabilité sismique d'un édifice est déterminée à l'aide de modèles simplifiés donnant des résultats fiables. Dans le cas où des résultats plus détaillés sont souhaités, un troisième niveau de calculs permet de les obtenir par simulation numérique (FEM). En dernier lieu, il s'agit de comparer la demande sismique avec la résistance de l'édifice étudié. Cette dernière phase permet de définir si l'édifice présente un risque d'endommagement et si oui, dans quelles parties et pour quelles raisons.

Mots-clés: Vulnérabilité sismique, méthodologie d'évaluation sismique, bâtiments historiques, maçonnerie ancienne, comportement structural, églises romanes, théorie de la plasticité, protection du patrimoine bâti.

Zusammenfassung

In der Schweiz wurde das Erdbebenrisiko bei historischen Gebäuden lange Zeit unterschätzt. In der Tat sind auch in der Schweiz starke Erdbeben möglich und jederzeit zu erwarten, wie anhand bedeutender historischer Erdbeben verdeutlicht werden kann. Zur Veranschaulichung kann das Basler Beben von 1356 zitiert werden, welches mit einer geschätzten Intensität $I=IX$ bezüglich der Europäischen Makroseismischen Skala (EMS-98) die Stadt Basel weitgehend zerstörte. Es handelt sich dabei um das bisher schwerste der bekannten Erdbeben nördlich der Alpen.

Im Jahre 1989 wurden Bestimmungen zur Erdbebensicherung von gewöhnlichen Bauwerken in die Schweizerischen Baunormen (SIA-Normen) eingeführt. Diese Bestimmungen wurden 2003 angepasst, um wissenschaftliche Fortschritte im Erdbebeningenieurwesen zu integrieren. Dabei wurden jedoch die historischen Gebäude nicht in gleicher Masse mitberücksichtigt, und in den SIA-Normen ist kein Verfahren enthalten, um die Erdbebensicherheit dieser Art von Bauten abzuschätzen. Ziel der vorliegenden Doktorarbeit ist es, diesen Mangel zu beheben; das heisst, eine Methode zu entwickeln, damit Bauingenieure und Architekten die seismische Verletzbarkeit von historischen Gebäuden evaluieren können.

Schadensbilder vergangener Erdbeben zeigen auf, dass historische Gebäude unter seismischer Beanspruchung besonders verletzlich sind. Gründe dafür sind im wesentlichen tragstrukturelle Besonderheiten wie schlanke Pfeiler, beträchtliche, hochgelegene Massen sowie Decken und Gewölbe mit hohen Spannweiten. Ausserdem sind im allgemeinen nur wenige Tragelemente senkrecht zum Kirchenschiff angeordnet, über welche Erdbebenkräfte abgetragen werden können. Zudem fehlen steife horizontale Tragelemente, die eine Diaphragmawirkung sicherstellen könnten. Auch ist die Masse, im Gegensatz zu gewöhnlichen Bauwerken, meist in den Mauern statt in den Geschossdecken konzentriert. Des weitern verfügen die benutzten Steinmaterialien über praktisch keine Duktilität. Aus diesen Gründen ist die Verwendung von Modellen, die für herkömmliche Gebäude entwickelt wurden, nicht möglich.

Die im vorliegenden Bericht vorgestellte Methodik zur Abschätzung der seismischen Verletzbarkeit von historischen Gebäuden ist in vier Schritte unterteilt. Das Ziel des ersten Schrittes ist ein Auswahlverfahren der Gebäude anhand ihrer seismischen Verletzbarkeit. Der zweite Schritt ist die Abschätzung der seismischen Verletzbarkeit mittels einfacher, verlässlicher Modelle. Sind genauere Ergebnisse erwünscht, so kann in einem dritten Schritt die Finite-Element-Methode angewendet werden. Der letzte Schritt besteht darin, den Erdbebenwiderstand des untersuchten Gebäudes den aufzunehmenden Erdbebenkräften gegenüberzustellen. Anhand dieses letzten Schrittes ist es möglich, abzuschätzen, ob für das betrachtete Gebäude ein Schadensrisiko besteht und wo beziehungsweise aus welchem Grund allenfalls solche Schäden auftreten.

Schlagwortliste: seismische Verletzbarkeit, Methodik zur Beurteilung der Erdbebensicherheit, historische Gebäude, altes Mauerwerk, Tragverhalten, Romanische Kirchen, Plastizitätstheorie, Denkmalschutz.

Table of contents

CHAPTER 1	<i>Introduction</i>	<i>1</i>
1.1	Motivation	2
1.1.1	Seismic vulnerability of the Swiss Cultural Heritage Buildings	3
1.1.2	Assessment of the seismic vulnerability of the Cultural Heritage Buildings: present methodologies in Switzerland	4
1.2	Objectives	5
1.2.1	Methodology	5
1.2.2	Experimental investigations	6
CHAPTER 2	<i>State of the Art</i>	<i>7</i>
2.1	Introduction	7
2.2	Existing methodologies for sacred buildings	8
2.2.1	Vulnerability index methodologies	9
2.2.2	Structural methodologies	10
2.2.3	Probabilistic methodologies	12
2.2.4	Hybrid methodologies	12
2.3	Discussions and Conclusions	13
CHAPTER 3	<i>Pre-Romanesque and Romanesque sacred edifices in Switzerland</i>	<i>15</i>
3.1	Introduction	15
3.2	Architectural account	15
3.3	Structural account	18
3.3.1	Pre-Romanesque period	18
3.3.2	Romanesque period	19

3.4 Pre-Romanesque and Romanesque edifices in Switzerland: global shape	21
3.4.1 Discussions	23
3.5 Characterization method	24
3.5.1 Standard units	25
3.5.2 Applications	34
3.6 Discussions and conclusions	42
CHAPTER 4 <i>Observed damage on churches due to seismic events</i>	43
4.1 Introduction	43
4.2 Damage observed in Switzerland	43
4.2.1 Seismic event of 1356, Basel	44
4.2.2 Seismic event of 1755, Brig/ Naters (Valais)	46
4.2.3 Seismic event of 1855, Törbel (Valais)	47
4.2.4 Seismic event of 1946, Sierre (Valais)	52
4.2.5 Seismic event of 1964, Sarnen (Obwald)	55
4.2.6 Seismic event of 1991, Vaz area (Graubünden)	56
4.2.7 Seismic event of 2005, Balmes Pass (France)	57
4.3 Damage observed in Italy	59
4.3.1 1976 Tolmezzo earthquake	59
4.3.2 Damage recorded on sacred edifices	60
4.4 Discussions	64
4.4.1 Seismic vulnerability of churches and their structural components, based on recorded damage	64
4.4.2 Impact of the structural characteristics and constructive details	68
4.4.3 Impact of the connection between the roof structure and walls	71
4.4.4 Impact of the structural transformations	72
4.4.5 Impact of the masonry state of maintenance	74
4.4.6 Impact of the foundations and soil quality	76
4.5 Conclusions	76

CHAPTER 5	<i>Application of existing methodologies</i>	77
5.1	Introduction	77
5.2	Existing methodologies for unique edifices	78
5.2.1	Lourenço's method	78
5.2.2	Risk-UE method	80
5.2.3	Lagomarsino's method	83
5.2.4	Augusti's method	91
5.2.5	Summary	96
5.3	Application of existing methodologies for unique edifices	96
5.3.1	Sample set of churches	96
5.3.2	Lourenço's method	99
5.3.3	Risk-UE method	103
5.3.4	Lagomarsino's method	105
5.3.5	Augusti's method	108
5.3.6	Discussions	110
5.4	Conclusions	111
CHAPTER 6	<i>Masonry</i>	113
6.1	Introduction	113
6.2	Masonry types from history	114
6.2.1	Pre-Romanesque masonry types (Carolingian era)	114
6.2.2	Romanesque times	114
6.2.3	Gothic era	116
6.3	Masonry types in Switzerland	116
6.3.1	Types of stones	117
6.3.2	Types of mortars	117
6.3.3	Recorded bondings and cross-sections	118
6.3.4	Foundations	122
6.3.5	Transformations	122
6.4	Mechanical properties of stone masonry	123
6.4.1	Stone	124
6.4.2	Mortar	126

6.4.3 Properties of the mortar-stone interface	128
6.5 One-leaf stone masonry failure: criterion	129
6.5.1 Compressive strength	130
6.5.2 Shear strength	139
6.6 Multiple-leaf stone masonry failure: criterion	143
6.6.1 Distribution of load within a multiple-leaf masonry wall	143
6.6.2 Determination of the compressive strength	145
6.6.3 Determination of the shear strength	151
6.7 Degradation	151
6.8 Discussions and conclusions	151
CHAPTER 7 <i>Old masonry: experimental investigations</i>	153
7.1 Purpose	154
7.2 Description of the test specimen	154
7.2.1 Test set-up	155
7.2.2 Measurement equipment	157
7.3 Testing program	158
7.3.1 Testing unfolding	160
7.4 Test results	164
7.4.1 Hysteresis loops	165
7.4.2 Energy dissipation	169
7.4.3 Sample load-bearing and deformation capacity	171
7.4.4 Sample shear strength	173
7.5 Interpretation	174
7.5.1 Shear-loading capacity: analytical models	174
7.6 Discussions and conclusions	179
CHAPTER 8 <i>Churches: seismic behaviour</i>	181
8.1 Introduction	181
8.2 Seismic behaviour of churches.	181
8.3 Walls	182
8.3.1 Out-of-plane behaviour	183

8.3.2	Out-of-plane behaviour of walls with openings	202
8.3.3	In-plane behaviour	202
8.4	Vaults: seismic behaviour	208
8.4.1	Structural behaviour under self-weight	209
8.4.2	Structural behaviour under seismic actions	216
8.5	Bell-towers: seismic behaviour	217
8.6	Churches: global behaviour	219
8.7	Churches: local behaviour	220
8.7.1	Front walls	220
8.7.2	Apses	229
8.7.3	Choirs	229
8.7.4	Transept	229
8.7.5	Chancel arch	230
8.7.6	Lateral walls	232
8.8	Discussions and conclusions	246
CHAPTER 9	<i>Assessment of the seismic vulnerability: methodology</i>	249
9.1	Introduction	249
9.2	Methodology: concept	249
9.3	General survey	251
9.4	Study: Level 1	252
9.5	Study: Level 2	254
9.5.1	Description of the structure	254
9.5.2	Seismic demand	254
9.5.3	Local behaviour	255
9.5.4	Global behaviour	266
9.6	Study: Level 3	266
9.7	Diagnosis	267
9.8	Discussions and conclusions	267

CHAPTER 10	<i>Application of the methodology</i>	267
10.1	Introduction	269
10.2	General survey	269
10.3	Study: level 1	271
10.3.1	Index 1	271
10.3.2	Index 2	271
10.3.3	Index 3	271
10.3.4	Discussions	272
10.4	Study: level 2	272
10.4.1	Description of the structure	272
10.4.2	Local behaviour	273
10.4.3	Global behaviour	289
10.5	Study: level 3	293
10.6	Diagnosis	293
10.7	Discussions and conclusions	293
CHAPTER 11	<i>Discussions and future work</i>	295
CHAPTER 12	<i>Conclusions</i>	299
CHAPTER 13	<i>References</i>	301
CHAPTER 14	<i>Symbols</i>	313
CHAPTER 15	<i>Glossary</i>	317
CHAPTER 16	<i>Appendices</i>	321
A.1	Swiss Pre-Romanesque and Romanesque edifices	321
A.1.1	A brief description	321
A.1.2	Architectural account	324

A.2 Observed damage	336
A.2.1 EMS-scale	336
A.2.2 Quotation from the re book of Basel city	339
A.2.3 Damage recorded after the 1946 earthquake (Epicentre: Sierre, Switzerland)	340
A.2.4 Damage recorded after the 1976 earthquake. in Friuli (Italy)	342
A.3 Existing methodologies	361
A.3.1 Risk-UE:correctiong factors	361
A.3.2 Lourenço’s method: application	362
A.3.3 Risk-UE method: application	372
A.3.4 Lagomarsino’s method: application	377
A.3.5 Augusti’s method: application	406
A.4 Masonry	414
A.4.1 Geology of Switzerland: a brief description	414
A.4.2 Types of stones	415
A.4.3 Mechanical properties of the main stones used for the construction in Switzerland	417
A.4.4 Definition of the thickness	421
A.4.5 Diagram of failure of masonry under different stress loading; after Page	423
A.5 Sample	423
A.5.1 Young’s modulus of the masonry with molasse blocks	423
A.5.2 Results from the defometer targets	425
A.6 Flow of forces within a barrel vault	426
A.7 Seismic response of standard units	427
A.7.1 Front walls	427
A.8 Seismic hazard in Switzerland	430

Switzerland is rich in cultural heritage buildings of national, European and international importance. Being in the centre of Europe, the present Swiss ground was for a long time under the influence of many great European kingdoms which left political, artistic and architectural marks in Switzerland. The traditions of each kingdom, especially its architecture, merged with each other. The architecture of the cathedral of Basel, for instance, was greatly influenced by Lombard and Burgundian architecture whereas Burgundian as well as Norman features are visible on the cathedral of Lausanne.

Swiss cultural heritage goods have withstood the ages without much deterioration due to weather, wars, etc. Nevertheless, many of them, especially monumental buildings and statues, sustained serious damage resulting from seismic events whose epicentres were either in Switzerland or in the bordering countries.

Switzerland has a moderate risk for earthquakes. According to research carried out at the Swiss seismological service, from the 10th to the 21th century, forty earthquakes of an intensity higher than or equal to VII, twelve with an intensity higher than or equal to VIII and finally, one very strong earthquake whose intensity was equal to IX were recorded [We 02], [Fä 03].

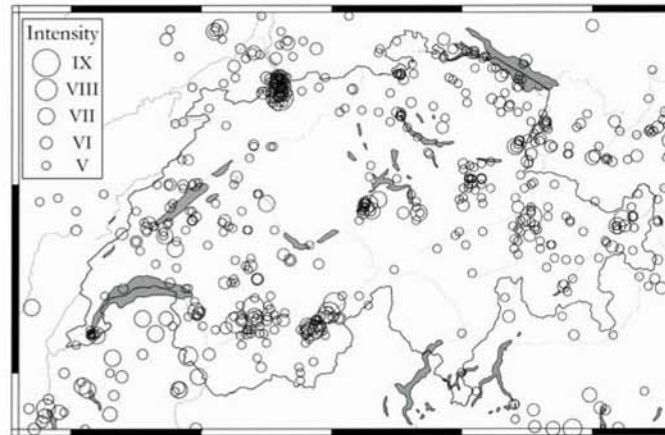


Figure 1.1 : Historic earthquakes with an intensity higher than or equal to V between 1000 and 2001 (source: Swiss seismological service [Fä 03]).

These seismic events are due to a peculiar geological situation; Switzerland is actually situated at the intersection of the European and African tectonic plates, which resulted in the creation of the alpine arch. Enclosing a large part of the Alps, the Valais is the region with the highest seismic hazard in Switzerland; the Graubünden canton, the Basel region, the Rhine valley and the central part of Switzerland also present an important seismic hazard.

Based on damage surveys carried out after seismic events, cultural heritage buildings are observed to be more seriously damaged than traditional housing. Their structure, which is characterized by large open spaces, slender walls, ceiling with vaults and a lack of horizontal thrusting elements, is more vulnerable to seismic loads [Ol 03]; churches are especially vulnerable even in case of low-intensity earthquakes [La3 04]. One of the main goals of this dissertation is to assess the seismic vulnerability of the Swiss cultural heritage buildings, especially of churches since they constitute the largest part of cultural heritage buildings in this country.

1.1. MOTIVATION

Cultural heritage buildings are highly vulnerable to earthquakes. Everyone remembers the earthquakes that happened in Italy (Friuli region (1976, $M^1=6.5^2$), Basilicata Region (1980, $M=7.2^2$), Umbria-Marche region (1997, $M=6.4^2$)), in the Azores and more recently in Iran (Bam area (2003, $M=6.6^2$) and their catastrophic consequences. In every case, the cultural heritage buildings suffered severe damage and many of them were partially or even totally destroyed (Cathedral of Noto (Sicily), St-Francis of Assisi, Citadel of Bam, etc.). Many edifices which partially collapsed lost a part of their cultural value (damaged or destroyed frescos, statues, paintings, valuables and so on), which is often irrecoverable.

1. Magnitude on the Richter's scale.
2. Values from the US geological survey.

Unlike catastrophes quoted above occurred elsewhere in Europe, Switzerland has also had many disastrous earthquakes. Amongst seismic events that hit Switzerland, we can list the earthquake occurred in Basel (1356) which destroyed almost every building of the city. Valais has experienced three earthquakes equally spaced in time (1755, 1855 and 1946); the first two events essentially hurt the upper part of the canton of Valais while for the last one the epicentre was situated to the north of Sion. The three events were of a magnitude higher than or equal to 6. More recently, the seismic event which occurred in the Central part of Switzerland in 1964 seriously damaged the Church of Sarnen [Lau 04].

1.1.1. SEISMIC VULNERABILITY OF THE SWISS CULTURAL HERITAGE BUILDINGS

Churches in Switzerland have a high seismic vulnerability. Many of them, especially the edifices situated in the Canton of Valais, in the Basel region, in the Central part of Switzerland and also in the Canton of Graubünden, suffered from earthquakes. They were slightly, moderately or even highly damaged.



Figure 1.2 : Engraving of the city of Basel after the earthquake which occurred in 1356 in this region (Source: Swiss Reinsurance Company: Historic earthquakes in Europe).



In regard to almost every church, seismic events resulted in masonry dislocation, especially in the upper parts of structural elements. According to archives (engravings, drawings, pictures and surveys records carried out after earthquakes), the most vulnerable components of churches are: the bell tower, the vaults-pillars system and the front wall in its out-of-plane direction.

Figure 1.3 : Our-Lady-of-the-Moor damaged by the earthquake of 1946, Sierre. (Source: Le Nouvelliste, 30.01.1946).

In a few cases, the vaults, which are highly vulnerable to seismic events, also broke down, as in the church of Chippis in 1946.



Figure 1.4 : Church of Chippis after the earthquake occurred in 1946 (Source: Keystone/Photopress).



Certainly one of the most seriously damaged edifices after an earthquake in Switzerland is the last chapel of the Visperterminen Procession lane (Valais) in 1855.

This church of standard size (~15 m x 10 m and 15 m high) collapsed under the seismic loads.

It constitutes a very interesting case study in order to assess the seismic vulnerability of churches.

Figure 1.5 : Visperterminen: chapel which collapsed during the earthquake of 1855 (picture taken in May 2005).

The valuable goods contained in sacred edifices, like statues and frescoes, are likely amongst the most vulnerable elements when an earthquake occurs. Under cyclic actions, the statues can be moved out of their support; they can fall down onto the floor and break. The frescoes are also highly vulnerable since they are tightly bound to the walls which are deformed during an earthquake.



Figure 1.6 : Damage on the Chapel of Lourdes (Sachseln, Obwald) resulting from the earthquake which occurred in the Central part of Switzerland in 1964 [Lau 04]; Photo Reinhard, Sachseln.

1.1.2. ASSESSMENT OF THE SEISMIC VULNERABILITY OF THE CULTURAL HERITAGE BUILDINGS: PRESENT METHODOLOGIES IN SWITZERLAND

Lately, new building codes which deal with the seismic vulnerability of new buildings with modern structural system replaced the previous Swiss code in 2003 [SIA 261 03]; the existent common buildings are dealt with in the SIA 2018 [SIA 2018 04]. Nevertheless, there is still no available methodology for the seismic vulnerability of historical and monumental buildings.

Procedures for the assessment of the seismic vulnerability of common buildings and of cultural heritage buildings are a lot different. The main goal of the former is to save people in case of earthquake whereas for the latter it is essential to also safeguard the cultural value of the edifice. Moreover, as their life span is longer than that of the common buildings, the return period of the seismic hazard that has to be considered is therefore also longer.

The seismic hazard in Switzerland, although moderate, can still seriously endanger the Swiss cultural heritage. On the context of adequate cultural heritage preservation, it is therefore essential that earthquakes are taken into account.

The present research work comes within the framework of a national project began in 2001 about the seismic risk of Swiss monumental buildings [Lau 04]. One of the main purposes of this national project is to define the seismic vulnerability of the Swiss cultural heritage and to provide a methodology to assess it.

1.2. OBJECTIVES

This research, which has been carried out for three years is aimed at filling a knowledge void in the field of safety of cultural heritage buildings in Switzerland. Moreover, a methodology is created in order to give the authorities efficient tools to assess the seismic vulnerability of cultural heritage buildings, especially of sacred edifices. However, there is a wide variety of types of structures among sacred edifices in Switzerland. For instance, Romanesque, Gothic and Baroque edifices have indeed different structural features. Due to this diversity of structures and also of the time available to set up a methodology, it is decided to focus the methodology on the Pre-Romanesque and Romanesque edifices. This choice is based on chronological reasons.

Besides the creation of a methodology, experimental investigations have been carried out in order to obtain the shear strength and ductility of old typical masonry walls.

1.2.1. METHODOLOGY

The topic of the seismic vulnerability of cultural heritage buildings is quite new in Switzerland; in fact, knowledge in this topic is almost at its beginning. Consequently, parts of this PhD thesis are based on the knowledge gained in foreign countries like Italy, Greece, Portugal, Spain and to a lesser extent from the USA.

As Swiss cultural heritage buildings are different from the aforementioned countries, the methodology that is presented in this report gives a procedure to take their structural particularities into account. Besides, this methodology allows us to assess the whole seismic response of sacred build-

ings instead of only the collapse stage. In this way, this method is well adapted for Switzerland for it is characterized by a moderate seismic hazard.

1.2.2. EXPERIMENTAL INVESTIGATIONS

Because of its historical value, old masonry has not been rigorously tested to get its mechanical properties. Nevertheless, these properties are salient for the understanding and description of the seismic response of cultural heritage buildings made of masonry. Therefore we set up a testing program; the test specimen is composed of sandstone (molasse) blocks that came from the abutments of the Lausanne cathedral¹ and lime mortar. This experimental investigation on a wall made up with such a particular masonry appears among the first to be carried out in the world. The obtained results indicate a high shear strength as well as good ductility.

1. Because of the bad state of certain parts, it was a necessity to change and replace them with new blocks. We had the opportunity to get some of them to build a testing wall.

2.1. INTRODUCTION

The assessment of the seismic vulnerability of cultural heritage buildings is complex because of numerous challenges and uncertainties. From material properties to structural behaviour, every aspect is related to the process of vulnerability assessment.

Besides, the most difficult part of the process is likely to define the structural behaviour, either static or dynamic. The available structural models, which are essentially confined to the field of elasticity, do not generally fit calculations of monumental edifices since they are characterised by non-linear structural behaviour. Besides these non-linear characteristics, the successive structural transformations they have experienced as well as the degradation of materials (masonry) with time have a great sway on the structural behaviour.

A few decades ago, all these difficulties and uncertainties made this topic too complex to be treated well due to the lack of efficient numerical tools; these became available in the 80's. From another point of view that is not scientific, seismic response of cultural heritage buildings began to be addressed in the 80's essentially because of two reasons:

- the awareness of the need of protecting and conserving the heritage buildings for the next generation (Charte d'Athènes, 1931),
- the definitive loss of cultural heritage buildings due to earthquakes, like the situation of the Friuli region after the 1976 earthquake.

In this chapter a list of methodologies that have been developed for the assessment of the seismic vulnerability of sacred edifices is presented. Nevertheless, as the methodology which is going to be developed in the dissertation framework will be mainly related to

churches, the state of the art knowledge in the different fields mentioned above is essentially linked to them.

2.2. EXISTING METHODOLOGIES FOR SACRED BUILDINGS

The necessity of developing ad hoc procedures for the assessment of the vulnerability of churches has been identified by Doglioni et al. [Do 94] after the Friuli earthquake of 1976. The earthquakes occurred in Sicily as well as in the Marche and Umbria regions (1997) have emphasized the need for developing and/or refining methodologies.

All available methodologies nowadays could be gathered in four groups according to their nature, the type of results they allow us to obtain and their structure:

- vulnerability index methodologies
- structural methodologies, based on engineering models
- probabilistic methodologies
- hybrid methodologies, merging two or more of the above mentioned methodologies

The choice of the methodology which will be applied in order to assess the seismic vulnerability of sacred buildings depends mainly on the need, the expected accuracy and also on the available time.

The seismic vulnerability evaluation of a cultural heritage building requires, in principle, the determination of its non-linear dynamic response. Nevertheless, as this kind of calculation, even if possible, is complex and highly time-consuming, many methodologies to assess more quickly and accurately the seismic vulnerability of edifices have had to be developed. This fact explains the development of the above presented methodologies.

In 1994, Doglioni et al. [Do 94] showed that, based on damage observed on churches after the Tolmezzo earthquake (1976), churches could be considered as an assembly of structural elements which behave more or less independently during seismic events (structural predominant features). All these sort of puzzle pieces were identified in almost every studied church damaged by earthquakes in Italy. Since then, as this assumption presents many advantages, it has been at the basis of almost every developed procedure in Italy and Italian universities have been amongst the first to develop methodologies to assess the seismic vulnerability of monumental buildings. Their approaches based on macro-elements have been adopted by other European universities.

Prior to presenting the existing methodologies, it is worth understanding the macro-elements approach.

MACRO-ELEMENTS APPROACH

Based on their survey of the damage observed on churches after the Friuli earthquake (1976), Doglioni et al. have developed what they called the macro-elements approach. It considered a church as an assemblage of a few macro-elements which detached from the rest of the structure under high seismic actions. This means that each macro-element, from that moment, had a structural behaviour which is independent from the other structural parts of a same church. Amongst the main macro-elements, there are the front wall, lateral walls, nave with vaults, chancel and the apse [Do 94]. This list of macro-elements was based on churches surveyed in the Friuli region;

later, the list was upgraded by Lagomarsino et al. [La 98] who carried out further surveys after earthquakes occurred from the 80's up to the beginning of the 2nd millennium in Italy. The macro-elements list can be found in the chapter 5.

2.2.1. VULNERABILITY INDEX METHODOLOGIES

The determination of vulnerability indexes is usually based on data (observed damage) coming from surveys carried out after seismic events. The use of these data for the definition of the vulnerability index can be made in a statistical, structural and/or probabilistic way. In general, researchers who developed vulnerability index methods exploited one or more of the three ways.

Nevertheless, the determination of a vulnerability index (and then, the development of a vulnerability index method) always requires a data base with a listing of the recorded damage on sacred edifices due to earthquakes. The bigger the data base is, the better (i.e. more accurate) is the method. This fact is especially important for the statistical approach, which is a suitable way to assess seismic vulnerability at a territorial scale [La1 04]. As the macro-elements approach allows comparison amongst similar churches, it is therefore perfectly adapted to this methodology. For contrast, Switzerland has no database with an extensive damage recording; therefore, it is difficult to apply a statistical method.

The numerous surveys carried out in the damaged regions in Italy have provided them with a wide database of damage recorded on churches after seismic events. However, the Italian database can be used for the methodology developed for Switzerland, even if edifices (materials, building techniques, etc.) differ between both countries.

The first country to begin developing a vulnerability index method, to our knowledge, is Italy. In the 90's, the GNDT (National Group for the Defence against Earthquakes, Italy) studies of damage sustained by churches in Italy due to earthquakes (Friuli, 1976; Umbria-Marche, 1997) led researchers, especially Lagomarsino, to propose a classification of damage to churches into several categories through the definition of a damage index. In the framework of the method proposed by Lagomarsino, this index measured the average level of damage that a sacred edifice would sustain; the index value was within 0 and 1. The damage classification was based on 18 relevant damage mechanisms¹; and their propensity to be activated is defined through the vulnerability index i_v [Ol 03]. To each value of the vulnerability index it was possible to associate a curve that correlated the expected damage and the macroseismic intensity or the peak ground acceleration [La3 04].

DAMAGE PROBABILITY MATRIX METHOD

The principle of the DPM method is very close to the vulnerability index method. It mainly differs in three aspects: first, the application of this method allows the definition of a vulnerability curve for groups of churches; secondly, it is based on the concept of the mean damage grade D , which is defined by six levels ($k=0$ (No damage), 1, 2, 3, 4, 5 (collapse)) according to the EMS-98 scale. Finally, the damage to an edifice is given by a probabilistic value.

1. Doglioni et al. carried out a survey of the damaged churches and bell towers in Friuli after the earthquake of 1976. This analysis let them catalogue the encountered typologies, structural details and the associated damage. The type of cracks and their direction help in interpreting collapse mechanisms. Similar survey was carried out by Lagomarsino et al. on the churches in Umbria and the Marche (damaged by the 1997 earthquake), on churches in Catania and also in Lunigiana [Ol 03].

In the DPM method, buildings are divided into groups of different typologies which are then dispatched into classes of similar seismic vulnerability (from a structural and architectural point of view). The buildings (according to their seismic vulnerability) are then connected to damage values (see above) according to the EMS-98 scale. For each class and for a certain seismic intensity, the damage foreseen is represented by a histogram of occurrence or by a probability distribution based on the mean damage grade D [La2 04].

INDICES BASED ON DIMENSIONAL RATIOS

This method has been developed by the working group at the University of Minho, Portugal [LR 06]. Contrary to the previous methods, this one is not directly based on a data base of observed damage.

In fact, this methodology was based on the fulfilling of a sort of check-list for each church. The form contained on one hand a statement of general characteristics (inventory) as the national classification, the period of construction, a brief description of the structure and also a few words about possible damage due to earthquakes occurred in the past. It also contains a more technical part with indexes (ratios between important values of the structure) and other key structural features. Following indexes have been defined:

- Index 1: in-plane area ratio
- Index 2: area to weight ratio
- Index 3: base shear ratio

The other key structural features were:

- the presence or not of a vault, its type (barrel vault, rib-vault, etc.) and its geometrical dimensions
- data for columns (height, diameter, etc.)
- data for perimeter walls

Finally, the last element was the seismic loading.

2.2.2. STRUCTURAL METHODOLOGIES

The term Structural methodologies includes every calculation method to analyse the structural behaviour of structures under seismic actions. The evaluation of the seismic vulnerability of a monumental building requires, in principle, the calculation of its non-linear seismic response and the estimation of the resulting damage when the building is subjected to earthquakes of different magnitudes [ACG 00].

Besides, these methodologies have to deal with two distinct but highly related aspects, i.e how to take the seismic input into account and how to analyse the seismic response of a given edifice.

2.2.2.1. Seismic input

The choice of the seismic action level depends on the calculations method. For analytical methods, which are generally based on simplified models, the seismic action is usually defined according to the building codes of the concerned country. For instance, in Switzerland, the seismic input is defined according to the Swiss codes (SIA). The seismic input is usually modelled by a quasi-

static loading, i.e. through horizontal loads proportional to the permanent loads, that is the self-weight.

In case of more sophisticated models, like a numerical one for which the FEM (Finite Element Method) would be used, a recording of a real earthquake (or even a synthetic one) could be implemented. Then, the seismic response could be more precise and real or at least looks like *a priori*; nevertheless, it must be kept in mind that besides the difficulty to interpret the numerical results, the recorded earthquake corresponds to something unique. Such an earthquake necessarily differs from another one. Consequently, a building that collapses under the action of one earthquake might be stable for another earthquake even if they are of the same magnitude. The duration of the seismic event as well as its frequency content can result in very different damage on the same building.

2.2.2.2. Seismic response of structures

Present methods for analysis of seismic behaviour of monumental buildings, or at least the seismic strength, range from the simplest to the hardest. One of the most simplified methods, which is also one of the most frequently applied and almost the only analytic method, is the limit equilibrium analysis from theory of plasticity. This method is actually the basis of many methodologies for the assessment of the seismic vulnerability of churches.

At present, the structural behaviour of cultural heritage buildings is often addressed through numerical calculation (FEM; Finite Element Method). Nevertheless, it could be highly time-consuming (depending on the meshing) and requires experienced specialists to interpret the obtained results. In this case, seismic input can be implemented through time step algorithms which require the ground acceleration of a recorded earthquake (or of a synthetic earthquake).

THEORY OF PLASTICITY (LIMIT EQUILIBRIUM ANALYSIS)

Simple-to-use models based on collapse mechanisms (application of the upper bound theorem of plasticity theory) have been used often to assess the seismic vulnerability of edifices. However this kind of method requires the definition of prior patterns for collapse mechanisms (generally on macro-elements) and establishing minimum energy concepts [Ol 03]. The application of this method is based on the following assumptions: (1) masonry behaves as a rigid body and (2) masonry does not resist any tensile stresses.

In most of the limit equilibrium analyses, seismic loads are identified with horizontal loads proportional to the quasi-permanent vertical loads; in other words, a quasi-static loading is taken into account and both the dynamic properties of the building and the spectral properties of the earthquake are neglected [ACG 00], [Gi 93], [La 05].

In order to improve the results obtained by common limit equilibrium analyses (as described here above), Augusti G. et al. [AC 00] proposed another approach that complements it by a probabilistic procedure. Though the proposed method is also based on the macro-elements approach and the theory of plasticity, Augusti applies a probabilistic description of relevant collapse mechanisms. The whole structural system is modelled through a logical diagram [Au 01] (chapter 5) which describes the relation between the collapse of each macro-element. Based on such a scheme, the probability of damage and collapse of each macro-element and therefore of the whole building is assessed.

FINITE ELEMENT ANALYSIS (FEM)

Many kinds of numerical methods are available today: from 1D to 3D analyses, linear or non-linear. The use of sophisticated models such as 3D finite element discretizations has been developed in recent years. Examples of such refined models are discrete blocky elements model (with friction between blocks) or models being able to deal simultaneously with small and large displacements [Ol 03]. There are a few cases of churches (Lourenço et al. [Lo 94]) which were dealt with. In Italy, Gambarotta and Lagomarsino [GL 96], [GL 97] have developed a macro-element model which can simulate two-plane masonry failure modes, bending-rocking and shear-sliding (with friction) mechanisms. This model can also take into account, by means of internal variables, the shear-sliding damage development that controls strength (softening) and stiffness reduction [Lo 01].

It is worth noting that numerical analysis seems to be the only one possibility to describe the seismic behaviour accurately.

2.2.3. PROBABILISTIC METHODOLOGIES

Such methodologies give probabilistic results; with respect to the seismic vulnerability of religious edifices, they allow the obtention of fragility curves. Such curves are indeed valuable tools for assessing the seismic vulnerability of sacred buildings. However, the application of probabilistic methods requires the definition of probability functions for the collapse (or damage) of the structure (or parts of it) and also of the collapse of the whole structure. The definition of the failure of the whole edifice appears indeed to be quite complex.

Furthermore, for determining the collapse probability functions (for parts of the structure or for the whole edifice) probabilistic methods are based on results coming from either statistical or structural data. By structural data, it is meant data that are obtained by the application of structural models. Consequently, probabilistic methodologies are in fact hybrid methodologies.

Only one method using probabilities, which has been developed for sacred buildings, has been recorded; this is the Augusti's method.

2.2.4. HYBRID METHODOLOGIES

Almost every methodology applied to assess the seismic vulnerability of churches is actually a hybrid methodology. Generally, they often contain several steps that steadily increase accuracy regarding either the input or the output.

The first step is generally about basic information, that is, the name, the location, etc. of the given building; according to its architectural typology, the building is provided with a vulnerability value related to statistical data. The second step usually deals with an assessment of the seismic vulnerability; at this stage of the study, only simplified calculation methods are applied. The last step, which is not necessarily addressed in every case, deals with the given building in a more accurate way, i.e. by sophisticated mechanical models, like the FEM.

One of the first hybrid methodologies which have been developed within the last two decades is the one developed by Lagomarsino and his team at the University of Genoa; they have also participated in the Risk-UE project by redacting the part 4 about the seismic vulnerability of cultural heritage buildings.

Augusti and his team have also developed their own hybrid methodology that is based on the three characteristics given under the chapter 2.2 (statistical, structural and probabilistic)

2.2.4.1. Risk-UE

The methodology developed for the Risk-UE (2004) for the assessment of the seismic vulnerability of cultural heritage buildings, is based on two levels of increasing refinement [La4 04]:

Level 1: based on typological and statistical studies on the observed vulnerability

Level 2: analysis through simplified mechanical models of single parts of a given building

2.2.4.2. Lagomarsino's method

The methodology developed by Lagomarsino et al. for the assessment of the seismic vulnerability of cultural heritage buildings, is based on three levels of increasing refinement [La3 04], [La1 04], [La2 04]:

Level 1: based on typological and statistical studies on the observed vulnerability

Level 2: analysis through simplified mechanical models of single parts of a given building

Level 3: more accurate analysis (FEM for instance) of the whole edifice or single parts

Note: this method is similar to the Risk-UE one.

2.2.4.3. Augusti's method

Augusti G. et al. [ACG 00], [Au 01] proposed a probabilistic procedure to assess the seismic vulnerability of churches. This latter is based on the macro-elements approach (structural model), and on the probabilistic description of the relevant quantities: the whole structural system is thus broken into few macro-elements whose behaviour can be typified and is significant for the response of the entire building.

Cultural heritage buildings are modelled through a logical diagram [Au 02], which described the relationship between macro-elements collapse and the one of the whole edifice. Based on such a diagram and on the collapse probability of each macro-element, the probability of collapse of the whole edifice is calculated.

2.3. DISCUSSIONS AND CONCLUSIONS

The methods, which were presented in the previous chapter, each have advantages as well as disadvantages with respect to the required data for applying them, the time involved for a correct application or the obtained results (type and level of accuracy). Some methods need more data than others; for instance, the implementation of a numerical model requires the mechanical properties of masonry and the perfect knowledge of the modelled structure, whereas only the dimensions, the unit volume weight of masonry and the internal angle of friction are needed for the method developed by Lourenço.

The time devoted to the application of a methodology is also of prime importance, especially in the practical (private engineer offices) context. No doubt that FEM consumes more time than other presented methodologies. Nevertheless, results are also of higher accuracy.

Another matter that must also be highlighted is the data base or the statistics on which a methodology is based. This remark especially concerns the first step of the Risk-UE methodology since the data this level refers to, were recorded in Italy and not in Switzerland. The question is: is it correct to use a methodology (or a part of it) that is based on statistics from a different kind of structures knowing that the Swiss heritage buildings are not similar to the ones in Italy.

In order to answer this question and also to assess the advantages and disadvantages of the presented methodologies for cultural heritage buildings in Switzerland, the methods will be applied to Swiss sacred edifices in chapter 5.

3.1. INTRODUCTION

This chapter gives a brief account of the architecture between the early Christian Period and the Romanesque times.

Due to the diversity of cultures, the building techniques development, the historical contexts and the geographical relief, each Pre-Romanesque and Romanesque edifice in Switzerland differs in its shape. The creation of a methodology to evaluate the seismic vulnerability of a large non-homogeneous group of edifices is consequently difficult.

Nevertheless, a more in-depth study showed that, though differently disposed, all sacred edifices are composed of similar structural parts. Therefore, the development of a methodology, which is focused on the seismic vulnerability of these «common» structural parts (that are later called «standard units»), becomes then possible.

Furthermore, as will be seen later, this way of proceeding, i.e. to look at structural parts, is justified since it coincides with the seismic response of churches.

3.2. ARCHITECTURAL ACCOUNT

The purpose of this chapter is to give an overview of the architecture development throughout time. The present thesis deals with Pre-Romanesque and Romanesque sacred edifices, knowing that this period of time extends from the beginning of Christianity up to the second half of the 12th century. In order to set it in historical context, it is also complemented by a historical (mainly related to Christian history) account.

BEGINNING OF CHRISTIANITY

In the 2nd century, even if prohibited by Roman authorities, the Christian faith propagated from Rome through the main roads of the Roman

Empire. Christianity settled in the Swiss region in the end of the Western Roman Empire; bishoprics already existed in the 4th century.

In the end of the 4th century, Germans attacked the Roman Empire: Burgundians invaded the western part of the Swiss region, while Alamannen conquered the eastern part. In the Italian territory, Theodoric the Great, King of the Ostrogoths, conquered Ravenna in 493. Finally, the Franks, with Clovis at their head, invaded the Burgundians territory as well as the Alamannen in the 6th century.

In the end of the Antiquity, the one-nave small edifice with one apse was the most widespread sacred building. In the city of the bishopric seat, larger edifices were built; the Roman basilica was chosen as an example for the shape of the new Christian important edifices. However, while this pattern was applied in Western Europe, the octagonal (or square) plan was used throughout the Byzantine area. Almost every sacred edifice were erected to shelter saints relics; this led to the beginning of pilgrimages of pious people all over Europe.¹

MEROVINGIAN PERIOD

The Merovingian Dynasty, which started with Clovis, lasted until the middle of the 8th century. It reigned over almost the whole current French, Belgian and Swiss territories.

Merovingian period was characterized by the coming of missionary monks (many came from Ireland). Two Irish monks played an important role in the Christianization of Switzerland: Saint Columban and Saint Gall (Columban's disciple). They built a monastery in an old Roman castle close to the current city of Zurich. Moreover, while his master went on to Italy, Saint Gall stopped in the Steinachtal where he founded the future foyer of the Christian culture in Alemannia, i.e. Saint Gall's abbey.

Except the baptistery of Riva San Vitale, no sacred buildings from this age survived because of abandon, destruction by humans, deterioration over time, etc.²

CAROLINGIAN PERIOD

In the beginning of the 8th c., Charles Martel (688-741) was the leading member of one of the most important aristocratic families within the Frankish kingdom. By the 8th c., he had amassed such a large support base that he was the recognised acting leader of the Franks though he did not have the title of a king. Moreover, Charles Martel also supported the spread of the hierarchical, Roman form of Christianity in the Frankish kingdom. Eventually, Martel's son, Pippin III, used this blossoming relationship with the papacy to formally obtain the title of king (in addition to the practical power of king that he inherited from his father) and finally supplanted the last of the Merovingian Dynasty in 751. In 768, Charlemagne (747-814), the 3rd of the Carolingian line, inherited the Frankish kingdom; he influenced the whole of Europe through his strong (and long) leadership of the Carolingian Empire. In 774, Charlemagne's armies conquered Lombardy; from then on, the Swiss region was geographically in the heart of the great Empire. Among others, this increased the importance of the Alpine passes and the Swiss territory became a sort of gravity centre of the

1. The reader can refer to the Appendix A. 1. 2. 1 for further information.

2. The reader can refer to the Appendix A. 1. 2. 2 for further information.

Carolingian culture, which is proven by the primordial rights received by Swiss monasteries (Saint Gall for instance).

Under the Carolingian Reign, Europe came through a relatively peaceful period which was good for an architectural renewal. Although Roman techniques were still applied, the original Roman model of a basilica for the church was abandoned for new architectural shapes. In fact, the Empire's emblem became the cathedral which was designed to show the union between temporary and spiritual powers. Cathedrals shape was based on the famous plan of Saint Gall (presented at synods in 817 or 818), given by the bishop of Basel (Haitto) to Gozbert, who wanted to erect a cathedral at Saint Gall's hermitage place: it was characterized by a Westwerk (with the Emperor tribune), a Carolingian feature that symbolized the Imperial power. The basilica had then a nave whose extremities were composed of apses, a choir area and a transept with a lantern-tower. The nave became then the link between the Episcopal seat and the Emperor's.

Carolingian churches in Switzerland were usually composed of a nave with three apses. Famous example still standing are the convents of Mistail and of Mustair in Rhetia (8th c.). It is worth noting that foundations of many great Swiss sacred buildings date from the Carolingian period like the Fraumünster of Zürich, the cathedral of Saint Gall or the abbey of Saint Maurice.¹

HIGH MIDDLE AGES

Upon Charlemagne's death in 814, his only surviving son, Louis, became the king of Franks and the Emperor. When the Emperor Louis himself died, a civil war erupted amongst his sons Lothar, Charles the bald and Louis II for the throne. This conflict was finally solved in 843 by the treaty of Verdun that split the Holy Empire into three parts: western (France), central (Lorraine-Burgundy-Italy) and eastern (Germany). So Switzerland was then split between Burgundy and Germany for a while. But soon the central Empire decayed and around 900 the German king had seized control over Burgundy and Italy. From an economical and social point of view, this was a difficult and dangerous period in Switzerland. However, since 962, when Otto I was crowned Emperor of the Holy Roman Empire in Rome, the political and economical situation became stable enough to lead towards an Artistic renewal after the long interruption due to political troubles after Charlemagne's reign. People were once again able to make long journeys and pilgrimages throughout Europe without problems; this situation was also favourable to cultural and economic exchanges as well as new artistic currents.

In parallel, monastic societies became powerful, as the Cluny's congregation (Benedictine); they built many monastic communities throughout Europe and also many existing communities asked for joining them; at its apogee, Cluny's monastery had 1500 convents under its control. Eastern Switzerland was influenced by the abbey of Hirsau, which was the most prestigious monastery united with Cluny. The abbey of Schaffhausen (The all Saints' church, 1150) is probably the most famous example of the architecture from Hirsau. The power and wealth of Cluny softened the initial principles of the Benedictine monastic rule. In 1115, to counteract what he thought to be a decline of the Benedictine rule, Bernard de Clairvaux and other monks founded a new monastic order: the Cistercians. At Bernard's death, 343 abbeys were under the Cistercian protection. In 1153, the abbey of Bonmont was founded in Switzerland, then came Lucelle in Eastern Switzer-

1. The reader can refer to the Appendix A. 1. 2. 3 for further information.

land and finally Canobbio in Ticino. About 30 abbeys and Cistercian convents were founded in Switzerland between the 12th and the 13th centuries.

Romanesque period actually corresponds to an era of revival of Art and growth in Europe. Nevertheless, building techniques as well as the configuration of sacred buildings did not differ a lot from the ones applied during the Carolingian era, which were inspired from Roman techniques [CVLR 82].

The plans, though different all over Europe, had similar features due to liturgy. Most churches adopted the basilica configuration. The Carolingian basilica was enlarged and the new architectural style added an area between the chancel¹ and the area for the laics: the transept. The basilica was broadly composed of one or three naves, transept, lantern-tower, towers, crypt, and chancel with choir and sometimes an ambulatory; there was sometimes also a narthex. The chancel ground was often slightly raised above the nave floor, which was also sometimes the crypt ceiling. Whereas the chevet had a semicircular cross-section at the beginning of the Romanesque era, it became flat towards the end (premises of Gothic style [CVLR 82]). It is worth noting that only a few parts of the church were vaulted at first; later, the whole edifice was vaulted and then the cupola placed on the transept crossing appeared too. The west entrance was sometimes conceived, as in the areas of the Holy Roman Empire, as a space independent (the Westwerk) from the rest of the church and was flanked by towers (Carolingian legacy). Windows were quite small, except in buildings whose covering was a timber framework; the outer side of walls was ornamented by lesenes and arcatures.²

Note: the reader can find a map with Pre-Romanesque and Romanesque edifices in Switzerland under the Appendix A. 1. 1. 1.

3.3. STRUCTURAL ACCOUNT

To begin this chapter, it is worth noting that the building techniques applied during both the Pre-Romanesque and the Romanesque period essentially followed from the Roman ways of building.

3.3.1. PRE-ROMANESQUE PERIOD

3.3.1.1. Structure

As Roman civilisation became more or more stifled by German invasions, their building techniques were applied less and less. Roman art of building was based on experience and had been taught on building sites, however due to anarchy, less and less people knew how to build as the Romans did. Compared to Antiquity, the quality of workers (stonemasons, stonecutters, master builders, etc.) became poor. According to Yves-Marie Froidevaux [Fr 93], patterns got simpler, Roman building techniques got lost and the edifices lacked strength. For him, Pre-Romanesque buildings were simply a bad plagiarism of Roman construction. Walls usually were composed of

1. The reader can find the definition of this word in the chapter 14 (Glossary).

2. The reader can refer to the Appendix A. 1. 2. 4 for further information.

two sides made up of small stones, which were more or less well cut, filled with a pebbles and mortar. Walls erected with large dressed-stones were rare and only the Emperor (Carolingian era) buildings were erected with such luxuriousness.

From a general standpoint, the Carolingian churches (untransformed since their completion) in Switzerland have a simple structure. They are basically composed of two lateral walls, a front wall, a chancel arch, one or three apses and a wooden ceiling with a timber framework (Mistail church, for instance).

3.3.1.2. Masonry

As aforementioned, Pre-Romanesque masonry was composed of pebbles, small stones or of medium-size dressed-stones, which were later preferred to pebbles for important edifices. The courses were small, horizontal, reticulated or also fishbone-shaped and sometimes interrupted with two or three tiles layers; these courses played a role of bond headers and of a horizontal layer [Fr 93]. The type of stone, which was used, depended on the material available around the building site (quarry, etc.). Carolingians also arranged the bonds to be somehow decorative by positioning the stones and using colour. Mortar, which was made up of quick lime and sand, was often of poor quality; sometimes it was even mixed with pieces of tiles.

Walls were quite thick because of structural reasons; nevertheless they got thinner as it rises to the roof. The churches usually were devoid of abutments; however, it is possible to see pilasters along the outer sides of the chapel in Aachen. A sort of alternation of niches and vertical flat pilasters (lesenes) in Milan (Saint Vincent of the meadows) as well as the very flat abutments of the church of Saint Philibert of Grandlieu were the premises of the Romanesque style [En 02].

Regarding the tools used to cut stones, they were quite basic at that time; only the pick, the mass and the stone chisel were used [Fr 93], [BBJPSS 99].

3.3.2. ROMANESQUE PERIOD

3.3.2.1. Structure

During construction, stone vaults were the main preoccupation of Romanesque architects. Main naves were covered by pointed arch vaults or barrel vaults while the low-aisles, narthexes and crypts were covered by groined-vaults. Transept crossing was often crowned by a cupola on pendentives (or pendentive bracketing) [Je 76]. Though the use of vaults was more frequent, edifices with a wooden ceiling were still erected (in the Holy Roman Empire, North and Northeast of France). In Switzerland, Romanesque churches with a wooden ceiling are mostly found in Eastern Switzerland.

The structural equilibrium of the main nave was usually ensured by massive lateral walls and the low-aisles vaults that resisted the thrust coming from the main nave vault. Sometimes, there were also buttresses along low-aisles walls to transfer the horizontal thrust from the vaults of the central nave. The walls, which were the main supports, were sometimes quite slender. To reinforce them, overlapping quoins were laid at the corners and lesenes along the outer faces of walls. Romanesque supports, except in a few cases in Germany and Italy, were no longer round but cross-shaped pillars (often reinforced by semi-columns or pilasters [CVALR 96]). The Romanesque architecture

reinforced the wall that was weak around each opening, through a pillar which was usually linked to its opposite counterpart by a transverse arch.

It is worth noting that according to the materials at their disposal, the northern countries had rather used wood (timber framework) for long whereas in the south areas, buildings were erected in stones (stone vaults) [CVLR 96]. Stones came from quarries in the close surroundings because of the high travel costs (transport and tolls between feudal kingdoms). In the 11th century, good quarries were worked and stone reefs were carefully chosen. The monks became knowledgeable about all aspects of handling stones, right from the quarry to stone cutting.

The development of building techniques and the experience gave builders a very good mastery of stone-dressing. It also resulted in the education of qualified masons and stonecutters who gathered in societies of journeymen; however, this phenomenon developed slowly. Workers were rare in the Middle-Ages; skilled and intelligent labour could only be found in small quantities. Construction sites were consequently composed of a few workers and it was difficult to use large dressed-stones as in Roman times when the labour was easily available. Romanesque masonry was made up of pebbles or small dressed-stones, which did not require many workers to extract, to cut and finally to lay. Stone-cutting technique was not new-developed up to the 11th century end: the cutting tools were thick and their use resulted in an irregular dressed face and they also let visible tracks of cutting. In the end of the 11th century, a beautiful cutting technique, which was carried out through the use of a «straight cutting tool», appeared in Burgundy. According to [Fr 93], stone cutting achieved perfection thanks to contributions from Syrian artists.

In general, light came into the edifice through the chancel and low-aisles windows. Only edifices with a wooden ceiling and one-nave churches had direct lightning.

Already conceived in Armenia, Syria and in a few early examples in Lombardy, the rib was used to reinforce vaults of porches and also of crypts [CVLR 96]. This prefigures their timid use at the beginning in the first half of the 12th century in the area of Paris, which is usually considered as being the starting point of the Gothic style.

3.3.2.2. Masonry

The usual Romanesque bond is composed of medium-sized stones that are 20 cm to 40 cm thick and 30 cm to 60 cm long. Romanesque masons no longer used small-sized stones that were used in the Carolingian period and which required a lot of mortar. The height of courses was defined by the width of quarry layers, in order to use it rationally, as well as the stone properties; it often happened that masonry was made up of courses with irregular heights. Walls were composed of two outer walls and of an inner one made up of pebbles and mortar.

Note: it was however not rare that the masonry of small edifices was made up of pebbles.

This kind of walls is sensitive to humidity coming in the middle part through the outer walls joints; water leads to the weathering of the mortar-stone combined material and results then in the desegregation of the outer sides under thrusts [Fr 93].

Every architectural element (columns, pillars, etc.) is integrated in a course height; for instance, a column put side-by-side with a wall is included within it through masonry courses. Corners are carried out with overlapping courses.

3.4. PRE-ROMANESQUE AND ROMANESQUE EDIFICES IN SWITZERLAND: GLOBAL SHAPE

WESTERN SWITZERLAND

Many of the Romanesque churches in Western Switzerland are basilicas; they are composed of a nave, a transept whose crossing is surmounted by a lantern-tower, a choir and apses.

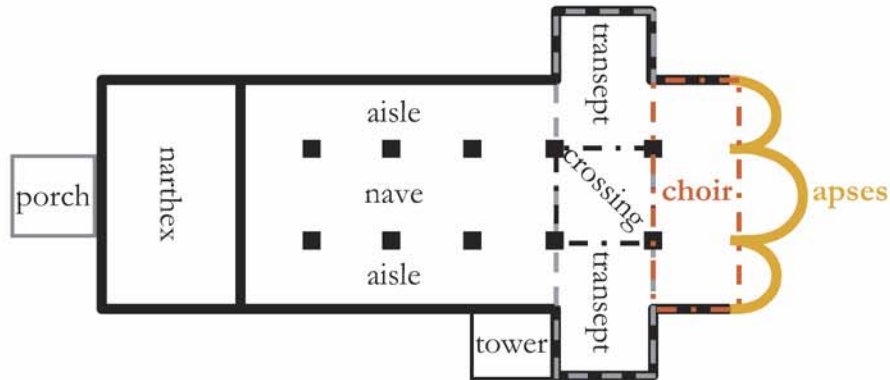


Figure 3.1 : General plan of Romanesque churches in Western Switzerland.

Contrary to most churches, only the abbey churches of Romainmôtier and Payerne have a narthex in front of their nave. Moreover, Romainmôtier has a porch on its west side. Though it is not shown in the Figure 3.1, the transept crossing of Romanesque churches is generally surmounted by a lantern-tower. Except edifices within the south area, Romanesque churches in Western Switzerland have no bell-tower erected along nave (aisles) side. In the canton of Valais, massive towers (Lombard style) were actually built either in front of the edifice or beside it.

Note: the above figure shows all the architectural features that can be found in Western Switzerland; however, many of the Pre-Romanesque and Romanesque edifices can have three naves but no transept, for instance. The comment is also valid for the religious Pre-Romanesque and Romanesque buildings in Eastern (Figure 3.2), Southern and South-eastern (Figure 3.4) Switzerland.

EASTERN SWITZERLAND

Romanesque churches in Eastern Switzerland are also mainly basilicas; they are composed of a nave, a transept, a choir, one or three apses and one tower

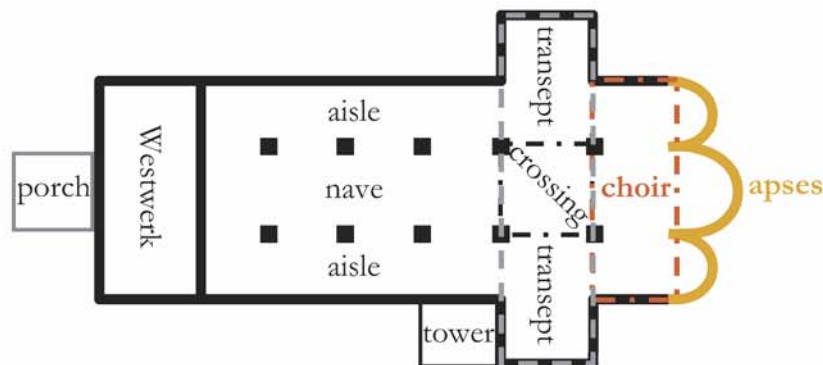


Figure 3.2 : General plan of Romanesque churches in Eastern Switzerland.

Note: though there might be a crypt under the choir (as for the following cases), it has not been taken into account in this thesis.

The main difference between churches of both areas (Western and Eastern Switzerland) are the presence of a Westwerk (the narthex structure in Western Switzerland is different) and the ceiling. The Westwerk is composed of two towers along each side of the front wall middle part; it is typical of important German edifices (Carolingian legacy). Only two edifices present this characteristic in Switzerland: the cathedral of Basel and the Grossmünster in Zürich. In respect to ceilings, a few churches in Eastern Switzerland^a have their nave covered by a wooden ceiling, while it does not exist in the western part.



a. This is also the case of a few churches in Southern Switzerland.

Figure 3.3 : View of the Basel cathedral Westwerk.

For a few sacred buildings, the opposite side of the Westwerk may be somehow irregular (chancel without any symmetric axis; Grossmünster in Zürich) or sometimes the choir is surrounded by a chevet (i.e. an ambulatory with small apses (Cathedral of Basle)).

Almost every sacred edifice in Eastern Switzerland is completed with a bell tower. However, this one can be differently placed around the edifice: sometimes it was erected outside the building (though connected to it) and sometimes above another church part. It is worth noting that the tower was often built earlier or later than the rest of the church. Moreover and in many cases, the tower is the only Romanesque part of the original sacred complex which is still standing nowadays.

SOUTHERN SWITZERLAND¹

Romanesque churches in this region are essentially small one-nave churches, except mainly the cathedral of Chur, Saint Victor's church in Muralto and the church in Biasca, which are basilicas. Though it is not representative of the majority, the plan below (Figure 3.4) must also apply for the singular cases of the Cathedral of Chur, the church in Muralto and the one in Biasca. In accordance to the Lombard way of building churches (which highly influenced the architectural style of churches in the Italian speaking region), almost every edifice has a crypt beneath its choir, semi-dominical apses and quite a slender tower along one of their sides. Moreover, it is worth noting that for most of them, churches have sustained many structural transformations since their erec-

1. The denomination of Southern Switzerland includes the cantons Ticino and Graubünden.

tion. In fact, many were vaulted in the Gothic period for instance and often deeply transformed during Baroque times.

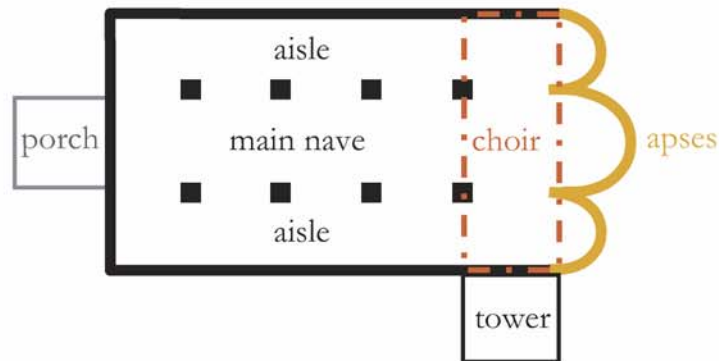


Figure 3.4 : General plan of Romanesque churches in Southern and South-eastern Switzerland.

Usually, churches in the southern and south-eastern Switzerland have no porch; Biasca and Muralto consist in two exceptions though their porch was added in the Baroque period. As aforementioned, most sacred edifices in these areas are composed of one nave, a crypt, a choir, one or more apses and one tower.

Due to its singular octagonal plan, the baptistery of Riva San Vitale cannot be represented by this plan.

Regarding masonry, it must be said that it is generally made up of well-dressed stones and is sometimes dry for a few edifices in the Ticino region; on the contrary, it is difficult to identify the type of masonry in the Graubünden because of the lime covering the walls. It is worth noting that though shapes are quite similar, the way of building churches in Ticino differed from the one in Graubünden.

3.4.1. DISCUSSIONS

It is worth noting that there are more Romanesque bell towers that still exist as they initially were after their completion than Romanesque edifices. Naves and chancels of churches have often been later transformed according to new architectural currents (particularly in the Gothic and Baroque periods) whereas the tower of the previous edifice was kept intact.

Pre-Romanesque and Romanesque edifices are either quite simple one-nave churches or basilicas¹. All the existing edifices can be roughly gathered into 16 types, depending on the ground plan, the

1. Cathedrals are generally more sophisticated basilicas and cannot be dealt with in the framework of a general methodology. However, if the structure of a given cathedral is not too much complex, the method can be treated with the proposed methodology.

kind of chancel, the type of ceiling (wooden planks or vaults), the presence of a bell-tower and of a transept (see the figure below).

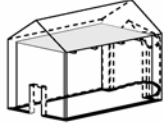
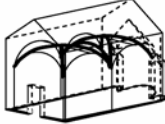


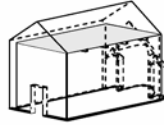
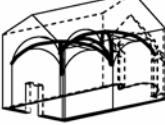

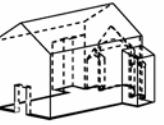
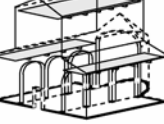

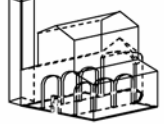

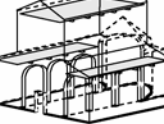

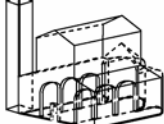
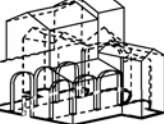
	Wooden ceiling	Vaulted ceiling	Bell-tower	Transept/ Lateral chapels
Simple church with one apse				
Simple church with two/three apses				
Basilica with one apse				
Basilica with three apses				

Figure 3.5 : Types of Pre-Romanesque and Romanesque churches.

Note: churches with a bell-tower or with a transept can be either vaulted or simply covered by a wooden ceiling.

Though built in different times, Pre-Romanesque and Romanesque churches have similar structural components. For instance, they all have a front wall, a chancel arch, lateral walls, etc., even if the shape differs. In fact, a more in-depth study shown that each component can have different shapes, though not too many. In consequence, every Pre-Romanesque and Romanesque church can be characterized as an assembly of structural components that were beforehand listed.

This observation combined with the fact that structural parts of churches behave independently from each other under high lateral ground acceleration¹, justifies considering churches as an assembly of structural components (from now on, these structural components are called «standard units») and to deal with each of them separately. This approach speeds up the analysis process, since it is possible to assess the seismic strength of every Pre- and Romanesque church by simply picking up the corresponding components from a list and adapting them to the given case.

1. That is, enough to make masonry enter the non-linear field.

3.5. CHARACTERIZATION METHOD

All the Swiss Pre-Romanesque and Romanesque edifices have too much different structural features. It is consequently difficult to find representative shapes for correctly identifying them. Figure 3.1, Figure 3.2 and Figure 3.4 show edifices that have all the structural features that can be found in the three areas of Switzerland; however, a chosen building can have only one nave, no bell-tower and one apse. Therefore, a characterization method must be developed.

In order to be able to characterize quickly every Pre-Romanesque and Romanesque edifice in Switzerland with common denominators of structural features, a characterization method is set up. This method, which allows the characterization of any Pre-Romanesque and Romanesque buildings through the use of a few similar structural components, so-called standard units, is presented in this chapter. The list of structural components was drawn up on the basis of a survey carried out in the context of this PhD thesis on Swiss Pre-Romanesque and Romanesque sacred edifices.

After a listing of the identified standard units, the method is applied to a few sacred edifices in Switzerland that are located in the three areas aforementioned.

3.5.1. STANDARD UNITS

The common denominators of structural components of Pre-Romanesque and Romanesque edifices, i.e. the so-called standard units are:

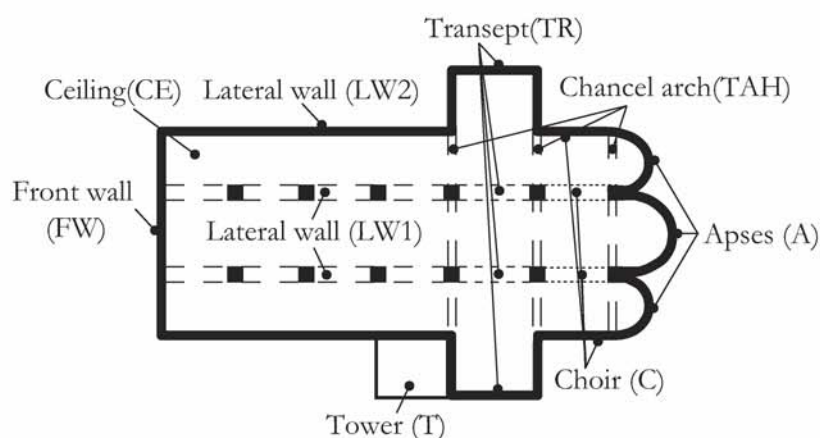


Figure 3.6 : Standard units designation.

3.5.1.1. Chancel part

In the framework of this report, the chancel part corresponds to the eastern area (according to the building rules of that time that required to erect a church along the west-to-east nave axis). It is composed of apses and the choir area; the church sanctuary (chancel) actually is located within both these zones.

In Switzerland, the eastern side of Romanesque churches is generally composed of apses (one or more), which may have various shapes (see below under the section apse units).

However, for most cases, the east side is composed of three apses: two small ones around a larger one. Moreover, the apses are built side by side with the choir area. With an ambulatory, the chevet of the Basel cathedral is a particular case of Romanesque churches; though smaller, Lausanne cathedral, also presents a similar Romanesque chevet.

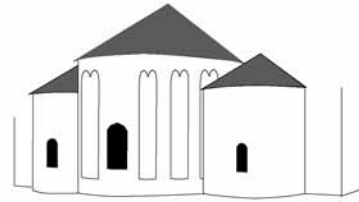


Figure 3.7 : Representative eastern side of Romanesque churches in Switzerland.

Although the three-apse configuration (Figure 3.7) is the most frequent one in the given area, other patterns can also be found. In Figure 3.7, the chancel is enclosed within the main apse area. However, in some cases the sanctuary occupied a wider surface than the semicircular floor area of an apse: the choir (Figure 3.8). This pattern is usually found in churches with transept (middle-size edifices).

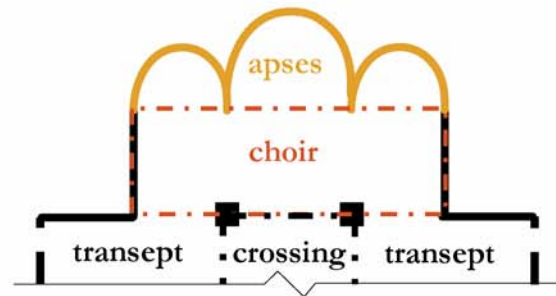
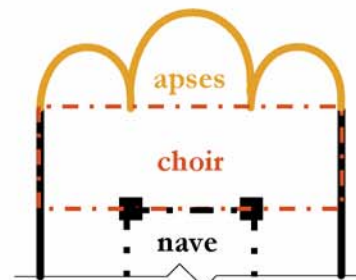


Figure 3.8 : Plan of the chancel of Pre- and Romanesque churches with transept in Switzerland.

The configuration in Figure 3.9 has actually been found in two churches in the Ticino canton. Other churches have only one or two apses; for instance, the cathedral in Chur has a choir but only one apse. Contrary to many churches in Western and Eastern Switzerland, the edifices in the south have no transept.

Figure 3.9 : Plan of the chancel of Pre- and Romanesque churches without transept in Switzerland.



To deal with those different existing configurations of the chevet and the sanctuary, one has to divide it into standard structural units which can be identified in every Romanesque church.

Note: the crypts are not considered in this study.

The identified units within the surveyed Romanesque churches are presented in the following chapters.

APSES UNITS

Seven units have been identified amongst Pre- and Romanesque churches in Switzerland.

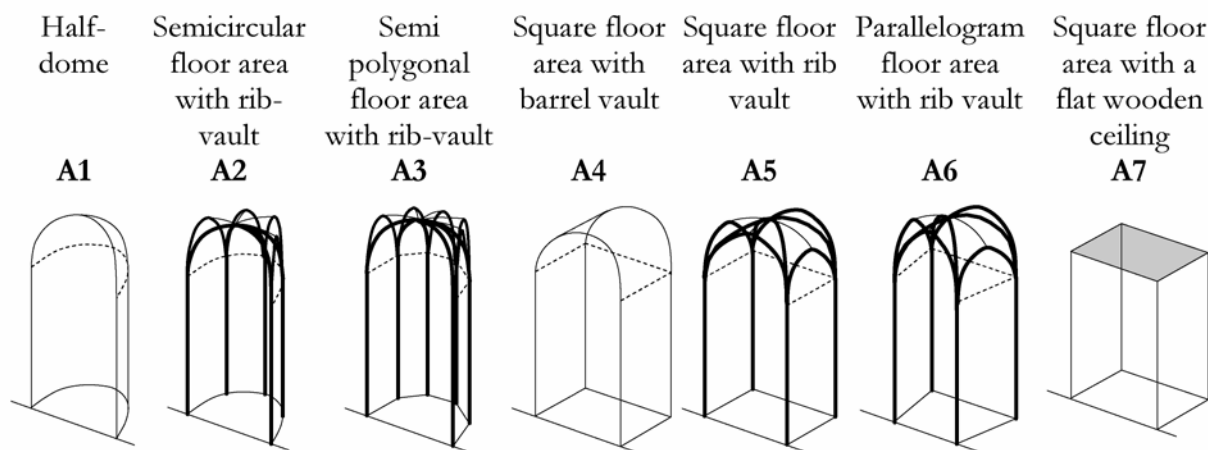


Figure 3.10 : Standard structural units for apses.

Each type of apse can have different dimensions and also different opening configurations; their number and size depend on the construction period, the region and the religious congregation who built the edifice. Regarding the identification of the apse units, the opening configuration does not matter in the framework of the characterization methodology.

The apses of Pre-Romanesque and Romanesque churches actually were half-domed or barrel-vaulted; nevertheless, most of them were later transformed, especially during the Gothic and the Baroque periods. This is why the apse units are so numerous¹.

Note: if the church was transformed during the Baroque period (frequent case in Eastern Switzerland), the whole edifice sustained transformations unlike during the Gothic era.

1. Considering only the untransformed Romanesque apses, would have been incorrect.

CHOIR UNITS

Choirs are usually composed of plain walls or pillars-wall system, as in the main nave; from the survey carried out on Pre- and Romanesque churches in Switzerland, the following patterns were recorded:

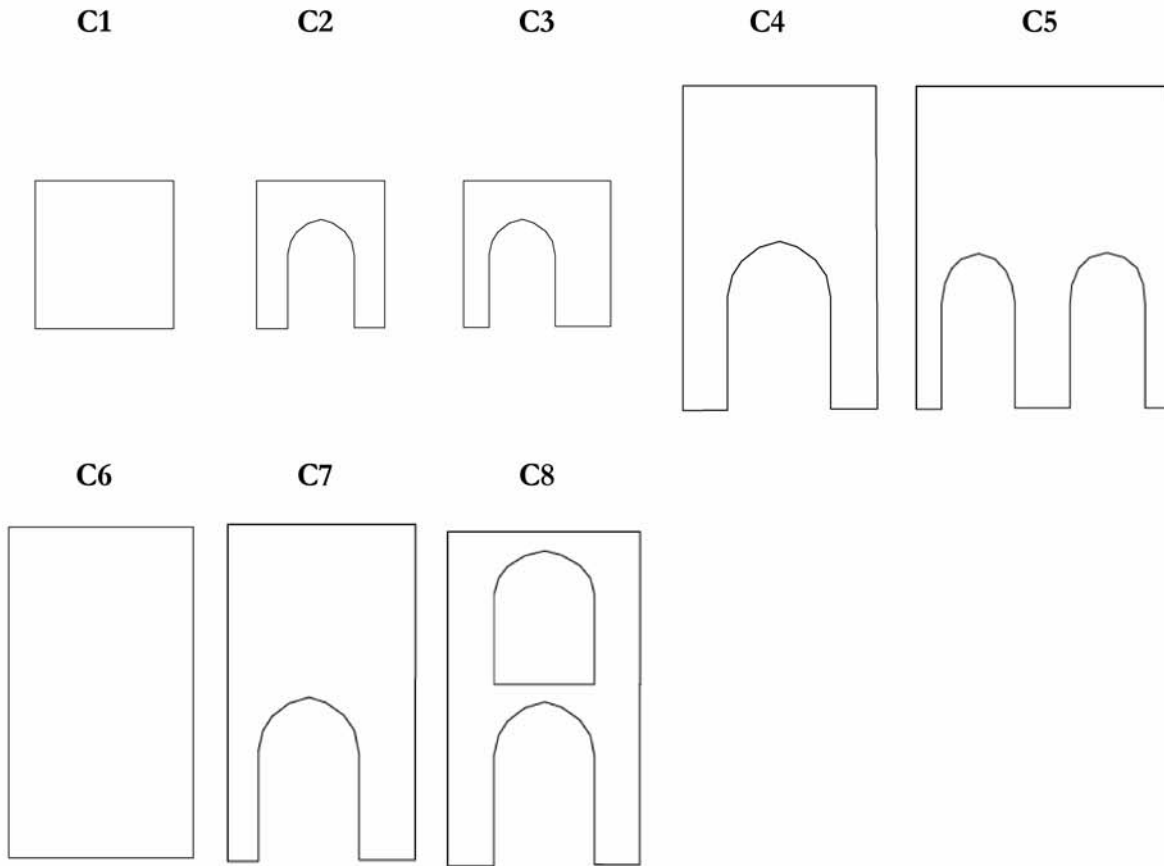


Figure 3.11 : Standard units of choirs.

The units C1, C2 and C3 corresponds to the parts that are in continuum with the low-aisles or with the transept aisles. Moreover, C1 is typically a outer wall¹.

Units C4, C5, C6 and C7 are part of the choir middle area, following the main nave direction. C8 is a particular unit that corresponds to a two-floor choir that can be found in the Basel Cathedral.

Note: arches can be either pointed or semicircular; the above standard units might have a gable.

3.5.1.2. Chancel arch

This structural part, which is usually either situated between the transept and the nave, between the choir and the transept or between the eastern side (apses) and the adjoining structural element,

1. There can be an opening.

is found in cathedrals, churches and chapels. Most chancel arches in basilicas have the TAH3 or TAH 4 shape. Chancel arch of smaller churches have a TAH1 or TAH2 shape.

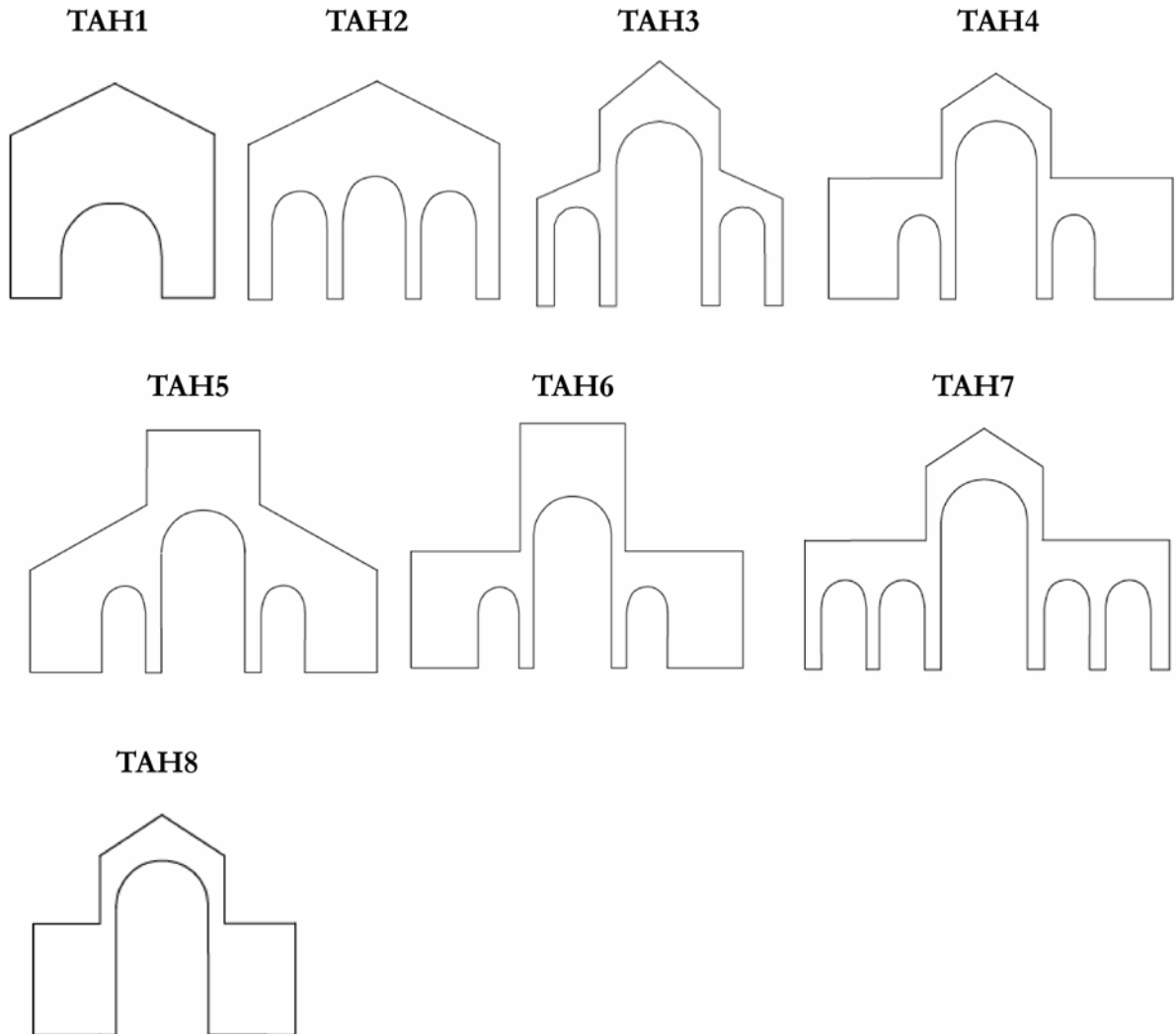


Figure 3.12 : Standard units for chancel arches.

TAH7 type of chancel arch is quite unique and is found only in the Abbey of Payerne.

The chancel arch might be coupled to a bell tower, as it is in the church in Amsoldingen.

3.5.1.3. Transept

The structural units belonging to the transept actually are part of either the chancel arch standard units or of the nave walls standard units (TR1 and TR2 in Figure 3.13); the other units are lateral parts, that is, in the nave continuum (TR3 and TR4 in Figure 3.13).

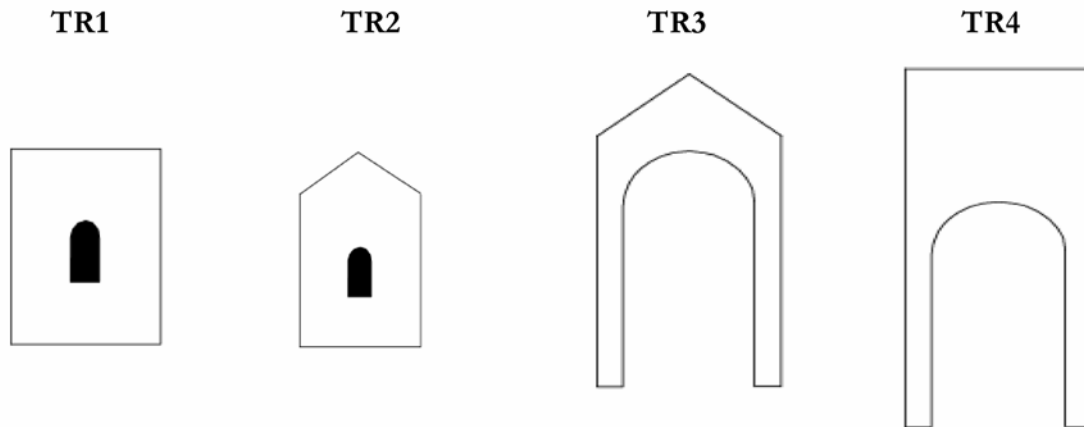


Figure 3.13 : Standard units for transepts.

3.5.1.4. Nave and Lateral Walls

For basilicas, lateral walls correspond to the vertical panels that divide the main space into a main nave and two low-aisles. In case of simple churches, lateral walls are indeed the outer walls of the nave. Only three types of lateral walls were recorded for sacred edifices in Switzerland:

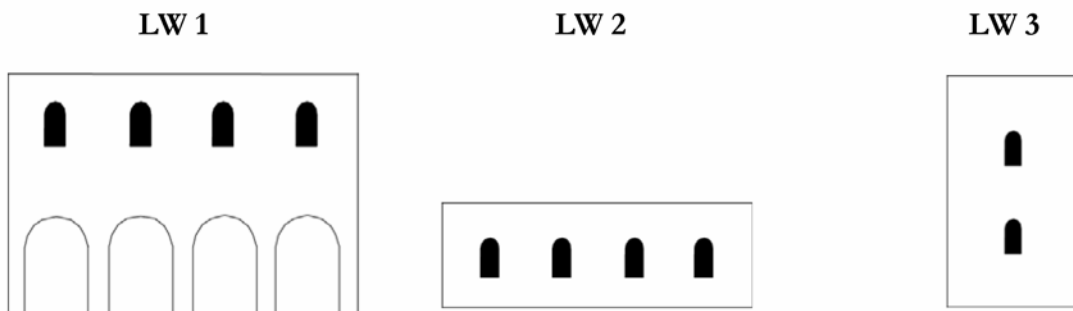


Figure 3.14 : Standard units of lateral walls.

Note: the number of openings (arches or windows) vary.

3.5.1.5. Ceiling

Ceilings in sacred churches are usually of two kinds: vaulted ceilings and the ones composed of wooden planks.

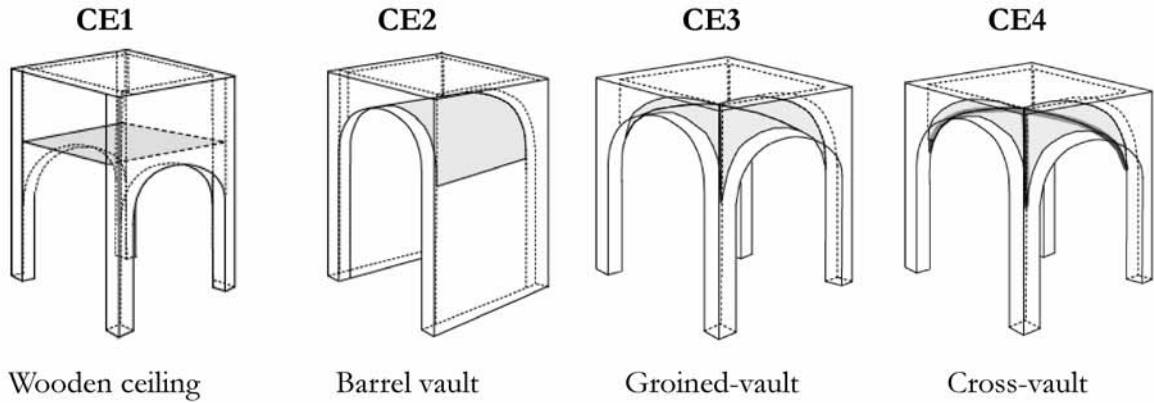


Figure 3.15 : Nave standard units.

These units are also used for describing the ceiling of the transept, choir, narthex and the Westwerk. Furthermore, the cupola on pendentives is also put into the nave standard units category (Figure 3.16).

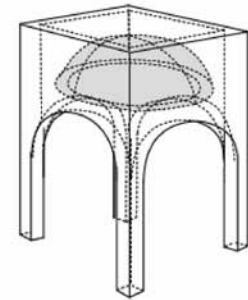


Figure 3.16 : CE5 nave standard units.

3.5.1.6. Front wall

The side opposite to the choir is the front wall; in a few cases, this side might not be clearly visible since a tower, a narthex, a Westwerk or a porch could have been erected in front of it. Nevertheless, even if the front wall is not clearly visible, it must be taken into account because of its contribution to the transversal rigidity of the church.

The front walls essentially differ in their dimensions and also in the opening configuration.

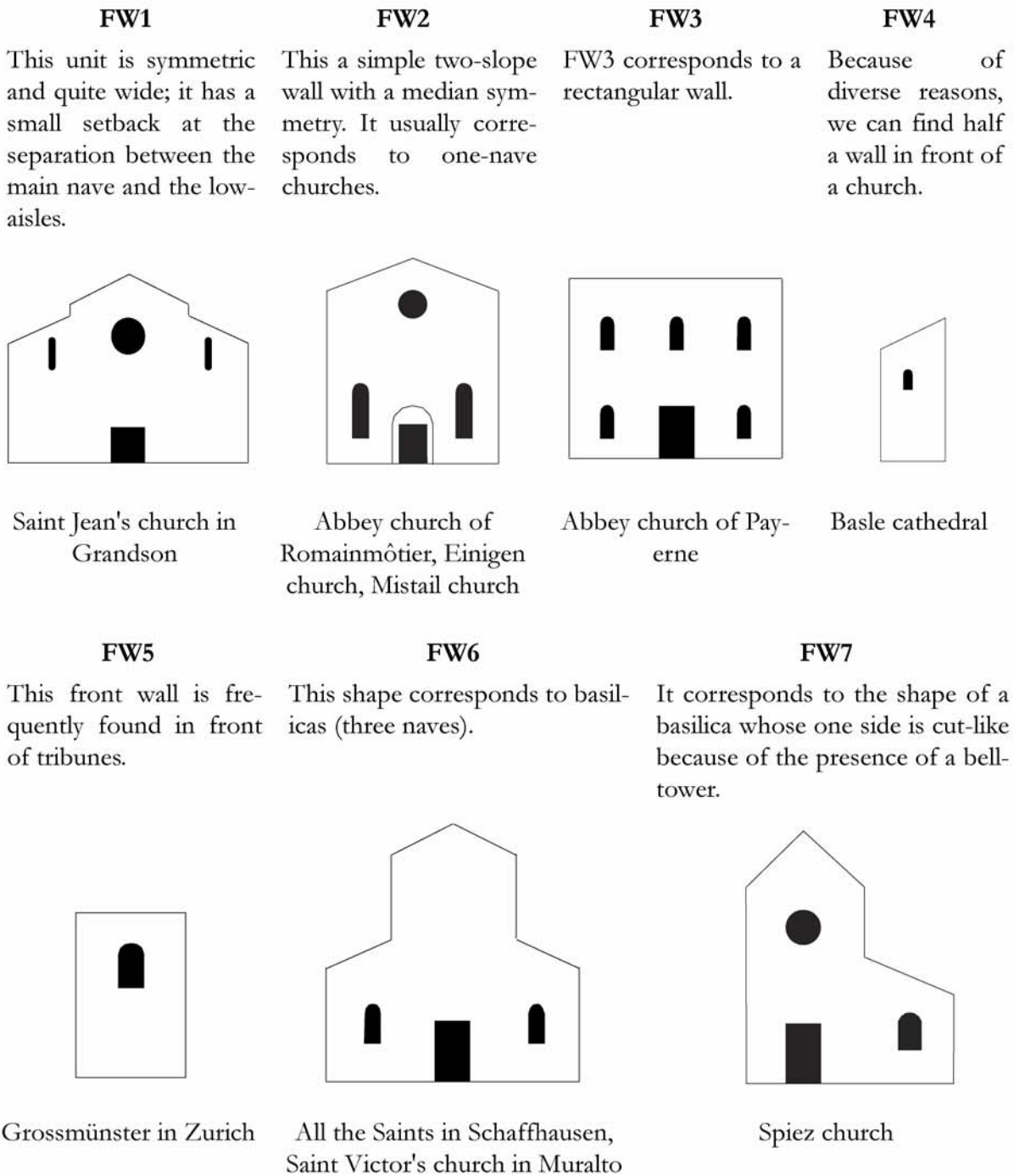


Figure 3.17 : Front wall standard units.

The configuration of openings is schematic; there might be more or less openings, smaller or bigger and also differently situated.

3.5.1.7. Bell-tower

Contrary to other parts in Switzerland, Romanesque churches do not usually have any bell tower in the west part. Nevertheless, a few edifices are flanked by a tower which is generally situated in front of the church (linked to the front wall). This is the case of the churches in the canton of Valais and in the northern part of western Switzerland (Saint-Imier and also in Saint-Ursanne). In the south, the presence of towers is due to the Lombard architecture influences and in the north of western Switzerland, towers were generally built later and probably on an original narthex. In eastern Switzerland, almost every church has a tower and sometimes even two (Westwerk).

It is worth noting that the Ticino area essentially has Lombard towers (massive with small gemel windows and a pyramidal spire) whereas the Graubünden region towers with a small two-slope roof are more frequent. In eastern Switzerland, many different types can be found. All the recorded types are listed below:

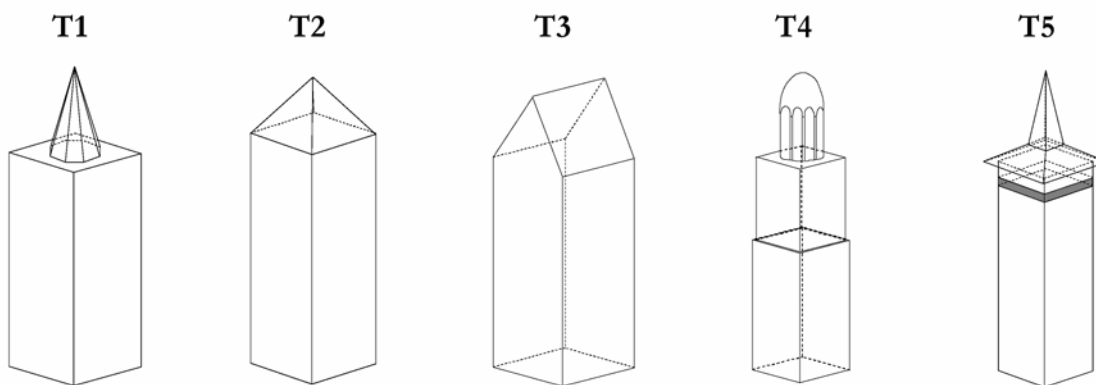


Figure 3.18 : Standard units of bell-towers.

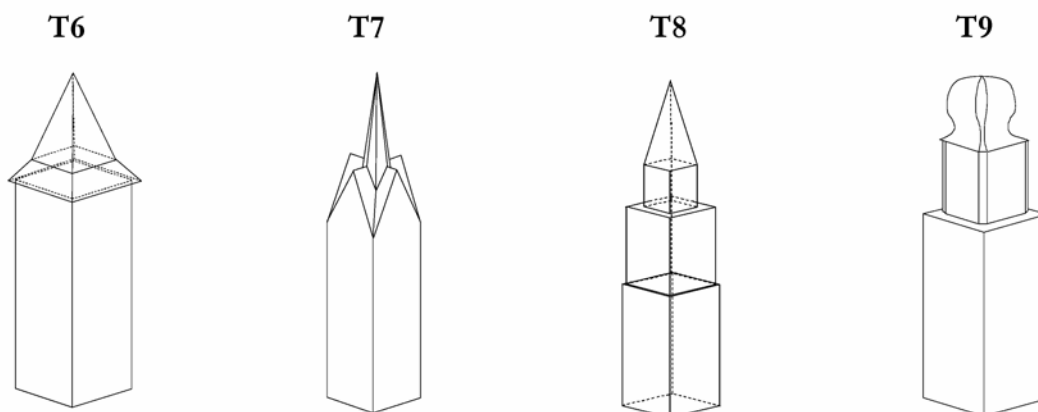


Figure 3.19 : Standard units of bell-towers.

Note: the spire of bell-towers do not necessarily date from the Romanesque era or earlier, as is the case of T9.

3.5.1.8. Buttresses

Buttresses are taken into account as being a part of the lateral walls or the walls that are connected to the given buttresses.

As the seismic response of flying buttresses has not been addressed in this research work, they are not included in this characterization method.

3.5.1.9. Narthex, Westwerks

Narthexes and Westwerks are taken into account by the method through front wall, lateral wall and tower units. Nave units are used for their interior.

3.5.1.10. Porches

Porches are not considered in this method because their structural response under seismic loading is not addressed.

3.5.2. APPLICATIONS

The method, which has been presented in the previous sections, is applied to four Romanesque edifices in Switzerland; they are: the abbey of Payerne (Western Switzerland), the church in Saint-Imier (Northern Switzerland), the castle church in Spiez (Central Switzerland) and the church in Mistail (Eastern Switzerland).

3.5.2.1. Payerne

A canon community came to Payerne between 940 and 950; this community was actually affiliated to the Cluny congregation in 961-965 and Payerne became one of the main Benedictine monasteries in western Switzerland [St 72]. This probably explains the new style of the east side that is one of the best examples of the 11th century Cluny architecture in Switzerland.



Figure 3.20 : Outer views of the abbey church (north-west side, Eastern side) [Me 96]; inner view of the main nave (eastward).

STRUCTURE

As aforementioned, the east side configuration differs from other Benedictine churches in Switzerland of that time: there are five apses (one median and four small lateral apses) of a different height. Moreover, each apse is covered by a different kind of vault.

The six-bay nave, which narrows towards the narthex, is composed of one main nave flanked by two low-aisles. Those are covered by groined-vaults, whereas the main nave ceiling is made up of a barrel vault with transverse arches.

The two-storey narthex contains a chapel dedicated to Saint Michel at the first floor.

Masonry is characterized by small courses and small units of Jurassic stone which probably came from the Roman ruins of Aventicum [Sc 71].

It seems worth noting that the edifice was restored and slightly transformed in 1920 [St 72].

FOUNDATIONS

The canon community erected a church in the beginning of the 10th century on the foundations of a villa built in the 3rd century. It was later transformed and a narthex was added as well as an atrium. The present church, which seems to have been designed by Odilon, was erected in the end of the 10th century without using the foundations of previous edifices. A few decades later, there was a plan to rebuild the edifice completely; however, building work was interrupted and only a new east side was erected.

APPLICATION OF THE METHOD

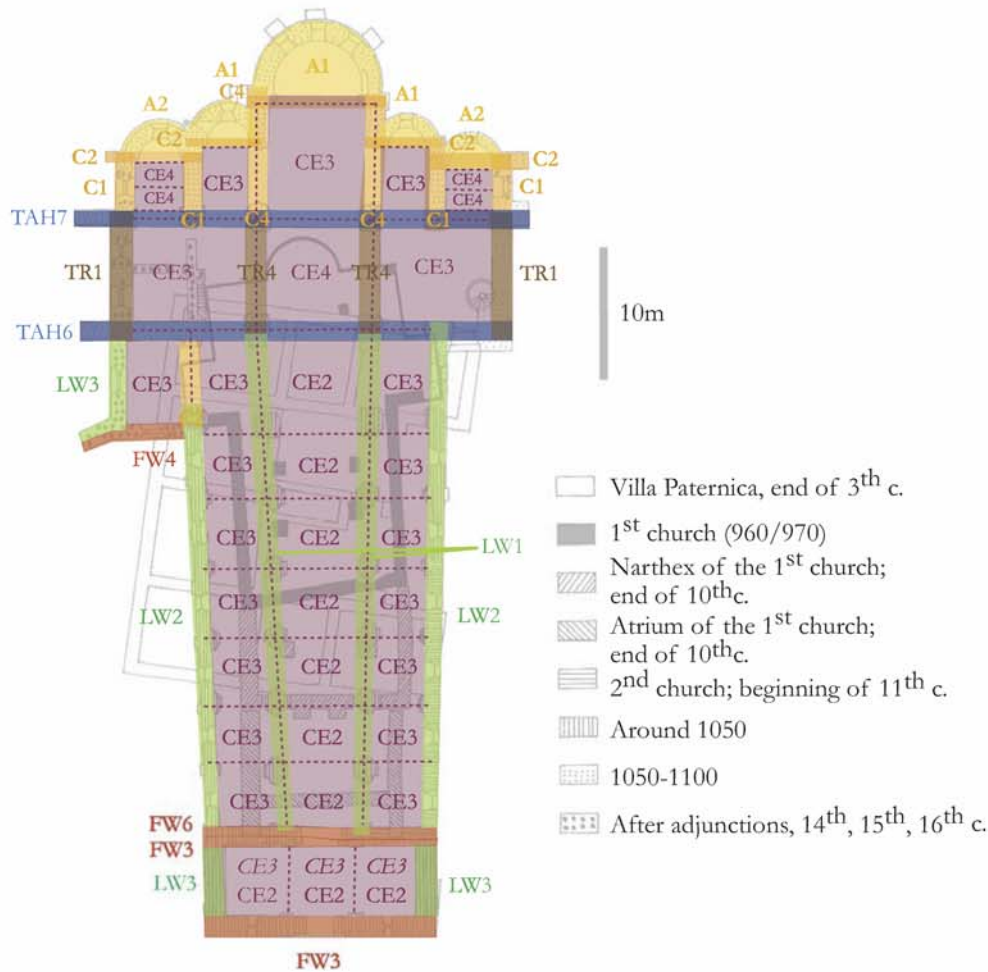


Figure 3.21 :Application of the method on the Abbey of Payerne.

Church part	Units	Comments
East side	A1 (3x), A2 (2x)	The east side is composed of a half-dome-shaped main apse with four semicircular rib-vaulted apses.
Choir	C1 (4x), C2 (4x), C4 (3x), CE3 (3x), CE4 (4x)	A few C2 (connected with the apses) and one C4 have a gable. The ceiling of the four secondary choir elements is groin-vaulted, whereas the main one is covered by a rib-vault.
Chancel arch	TAH6, TAH7	TAH7 type of chancel arch is quite unique and is found only in the Abbey of Payerne.
Transept	TR1 (2x), TR4 (2x), CE3 (2x), CE4 (1x)	The crossing is covered by a rib-vault. The lantern tower, which is above it, is taken into account by the chancel arches and the TR4 type of transept. Both transept arms have a groin-vault as a ceiling.

Nave	LW2 (2x), LW1 (2x), CE3 (14x), CE2 (7x)	The main nave ceiling is a barrel-vault (that is rather more elliptic than semicircular) which is structured through transverse arches along its axis. The low-aisles bays are groin-vaulted.
Chapel	FW4 (1x), LW3 (1x), CE3 (1x), C2 (1x)	This new chapel (built after the building completion) is taken into account based on the assumption that its walls are well connected to that of the church.
Front wall	FW6 (1x), FW3 (1x)	The wall separating the nave from the narthex is rectangular, whereas the front wall of the nave is of a basilica type.
Narthex	LW3 (2x), CE2 (3x), <i>CE3 (3x)</i>	The structure of the narthex's second floor is composed of groin-vaults, while the first floor seems to be constituted by a barrel-vault. The words in italic indicate the structure of the second floor ceiling.
Front wall	FW3	The front wall of this church also corresponds to the narthex wall.

Note: the stairs leading to Saint Michael's chapel is situated in the nave and along the front wall.

3.5.2.2. Saint-Imier

The church was erected in the beginning of the 11th century and a narthex was added in the 12th century.

A fire partially damaged the edifice in 1512; the transept as well as the nave was repaired. The frescoes painted on the crossing walls date from this period.

On the contrary, the paintings in the apse, which were discovered in 1930, are Romanesque.



Figure 3.22 : Inner and outer view of Saint-Imier's collegiate church [BKQ 97].

The apsidal chapels were destroyed in the 19th century and directly reconstructed.

STRUCTURE

The three-nave basilica has a flat ceiling and the six-bay nave is as wide as the churches of Amsoldingen and Schönenwerd. On the contrary, the chancel type differs since in this case, a transept crosses the nave and separates it from the three-apse chevet of the church.

The east side of the church is composed of a median apse flanked by two lateral smaller apses whose ceiling has a cul-de-four shape. The main apse is taller than the other ones and as tall as the transept upper edge. There is no visible buttress.

Masonry seems (according to a picture) to be made up of small dressed stones.

APPLICATION OF THE METHOD

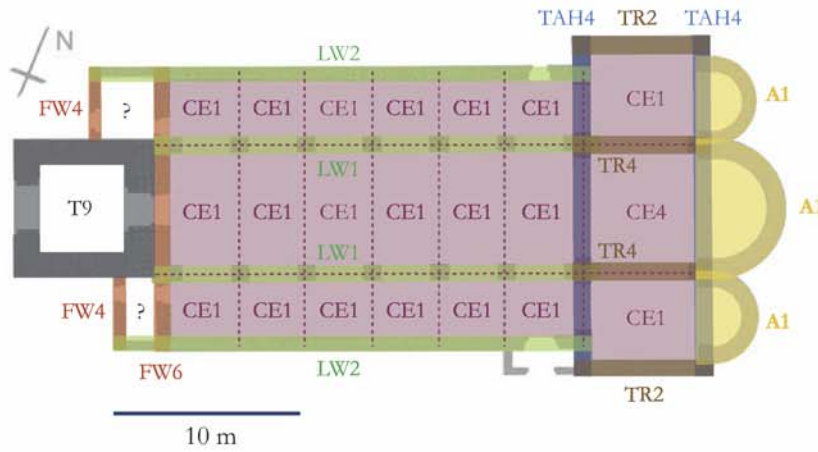


Figure 3.23 : Application of the method on the church in Saint-Imier.

Church part	Units	Comments
East side	A1 (3x)	The east side is composed of half-dome-shaped apses.
Chancel arch	TAH4 (2x)	The chancel arches of this church are the most frequently found in Pre- and Romanesque churches in Switzerland.
Transept	TR2 (2x), TR4 (2x), CE1 (2x), CE4 (1x)	The crossing is covered by a rib-vault. Both transept arms are covered by a wooden ceiling.
Nave	LW2 (2x), LW1 (2x), CE1 (18x)	The nave is covered by wooden ceilings.
Front wall	FW6 (1x), FW4 (2x)	The wall separating the nave from the tower is of FW6 type; new rooms were made in front of the FW6 element and two FW4 were required to close them. Nevertheless, the configuration of these rooms is unknown.
Tower	T9	The tower was transformed after its completion.

3.5.2.3. Spiez: castle church

As stated above, the castle church of Spiez is a part of a group of Romanesque churches around the lake of Thune. They were all founded by the old Burgundian dynasty and were probably built by Lombard craftsmen [Ha 74].

Noticeable Romanesque frescoes from the beginning of the 11th century were discovered when they restored the church in 1950 [SS 79].

Figure 3.24 :View of the castle church in Spiez [Mo 72].



STRUCTURE

The present edifice was built on a previous church whose tower and wall were kept (a clear change of masonry confirms it [Ha 74]).

This three-nave church is about 25 m long and 10 to 15 m wide; moreover, the four-bay nave ends by a three-apse chevet, without transept. The naves are separated by arcades built on massive pillars (with a squared cross-section), which were erected on the previous edifice foundations. Like other important edifices of this area, the chancel was raised in order to cover a crypt.

Whereas the ceiling of the main nave is made of wooden planks, the median apse is barrel-vaulted and both lateral apses are covered by a groined vault [Mo 72].

Figure 3.25 : Inner view of the Castle church in Spiez [Mo 72].



In elevation, it is worth noting that the roof ridge of the presbytery is lower than the one of the choir which is itself lower than the nave roof ridge [Ha 74].

FOUNDATIONS

Archaeological excavations (the knight grave gave much information regarding the date of building) showed that there was already a previous edifice at the place of the present church. Like in Wimmis, it was a hall-church with lateral appendices.

APPLICATION OF THE METHOD

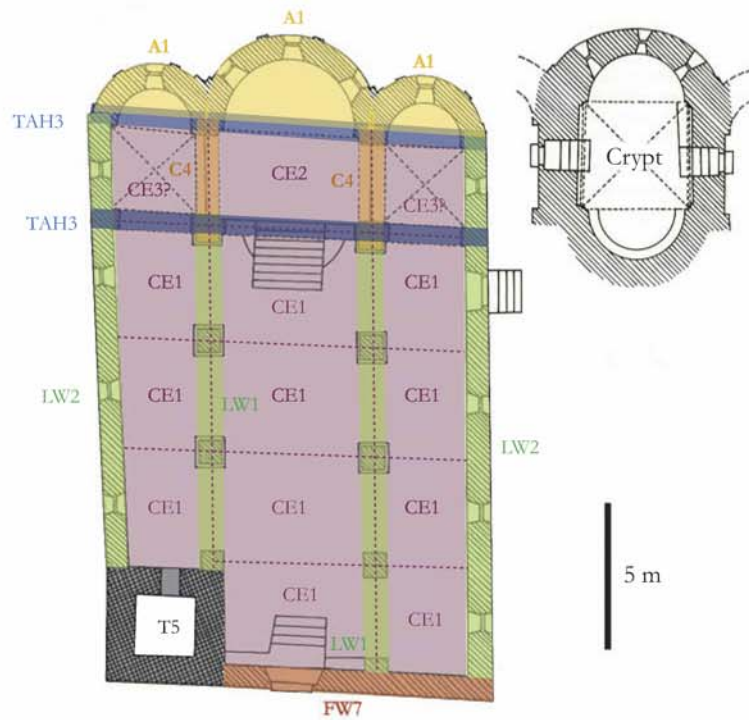


Figure 3.26 : Application of the method on the castle church in Spiez.

Church part	Units	Comments
East side	A1 (3x)	The east side is composed of three half-dome-shaped apses.
Chancel arch	TAH3 (2x)	There are two similar units that share the east side of the church; at each times, the roof ridge is upraised.
Choir	C4 (2x), CE3? (2x), CE2 (1x)	Both lateral parts are supposed to be covered by groined-vaults, whereas the central part is barrel-vaulted.
Nave	LW2 (2x), LW1 (2x), CE1 (11x)	The whole nave is covered by wooden ceilings.
Front wall	FW7 (1x)	The surface on the left of the eastern side belongs to the bell-tower.
Tower	T5	The tower, which has a square cross-section, is crowned by a timber roof (characteristic of the Bernese region).

Note: there is a crypt; nevertheless, it is not allowed for in this method because the seismic response has not been addressed.

3.5.2.4. Mistail: Saint Peter's church

This edifice was built at the junction of a few military and economically strategic valleys; it was situated close to an important road during the Middle Ages period, which was called the bishop road and connected Chur or Domschleg to the Septimer and the Julier pass.

Saint-Peter's church dates from the second half of the 8th century; it was enlarged (sacristy and bell tower) in the 14th century (consecrated once again in 1397). Large structural transformations were held at the Baroque period, i.e. in 1640-1690.



Figure 3.27 : Outer view of the church [Br 79].



This church is probably the oldest Pre-Romanesque edifice (not being a baptistery) which is still standing in Switzerland. Moreover, with Müstair, this is one of the best examples of the characteristic Carolingian architecture of this area.

The church is composed of a rectangular nave which is crowned eastwards by three semi-domical apses. The tower, which stands to the west of the edifice, as well as the sacristy, were made higher in the Baroque period [Br 79].

Figure 3.28 : Inner view of the church (apses).

APPLICATION OF THE METHOD

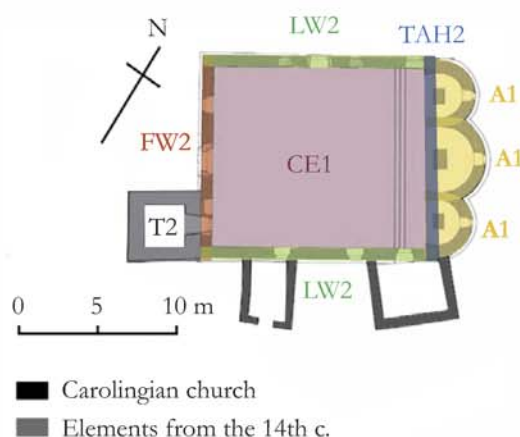


Figure 3.29 : Application of the method on Saint Peter's church in Mistail.

Church part	Units	Comments
East side	A1 (3x)	The east side is composed of three half-dome-shaped apses well interconnected (no clearly separated) to each other. There is only one small window per each apse; the covering is a slate roof (there is no timber framework)
Chancel arch	TAH2 (1x)	The chancel arch, whose shape is the same as the front wall's, has three large openings.
Nave	LW2 (2x), CE1 (1x)	The main nave is covered by a wooden ceiling. This type of nave is also typical of chapels.
Front wall	FW2 (1x)	Two-slope front wall with a tower erected in front of the south part of the front wall.
Tower	T2	Tower with a pyramidal spire; it was erected in the 14 th century.

Note: the two small annexes are not taken into account since their walls are probably not well connected to the rest of the church; however, this point should be checked in case of a real application of the method.

3.6. DISCUSSIONS AND CONCLUSIONS

As shown within this chapter, Switzerland is rich in Pre-Romanesque and Romanesque edifices. Moreover, they can be very different because of numerous reasons such as the place, the monastic congregation that built them, the culture, material at disposal, etc. In order to be able to deal with all of them, they must be simplified or characterized differently than as a whole. In this study, the characterization approach is adopted and a method to make it is developed.

This method, which was presented under the chapter 3.5, actually constitutes the first step of the global methodology¹ proposed in this report; it allows the engineer or the architect to characterize a given edifice as a juxtaposition of structural components. This step prepares the application of the level 2 of the methodology (chapter 9), which is based on the macro-elements approach, proposed for assessing the seismic vulnerability of sacred buildings. Macro-elements indeed correspond to the standard units; the former term refers to them as structural components (civil engineering standpoint), while the second term describes them as architectural components.

1. That is, the methodology for the assessment of the seismic vulnerability of Cultural Heritage Buildings in Switzerland.

Observed damage on churches due to seismic events

4.1. INTRODUCTION

A survey of damage suffered by cultural heritage buildings due to earthquakes is of prime importance since it gives interesting hints on their seismic response. Furthermore, the weakest links of such kinds of structures (or of masonry) can be identified according to the frequency of occurrence of different types of damage.

Such a survey has been carried out for Switzerland on the basis of the information in archives. Cantonal and communal archives as well as archives from the bishopric of Sion and parishes were used. Information from papers written by members of the Swiss Seismological Service was also gathered and has been of prime interest. In respect to the aforementioned archives, it must be said that reports about damage on buildings after earthquakes were sometimes missing.

In addition to events in Switzerland, relevant observations recorded after the Tolmezzo earthquake that struck Italy are also presented in this chapter.

4.2. DAMAGE OBSERVED IN SWITZERLAND

The observed damage on churches in Switzerland are described in this section. This is classified according to the seismic event that created it. This approach allows us to compare damage that resulted from a seismic event, although the peak ground acceleration that subjected churches within the struck area was not the same.

Only the events that resulted in significant damage to sacred buildings are recorded. Consequently, the damaged churches are not necessarily Pre-Romanesque and Romanesque.

The time required to list the damage on churches recorded after an earthquake, long after the seismic event can be significant; indeed, the search of archive documents proved to be difficult. Since it was not a focus of this PhD thesis the search of documents has been carried out according to the time at disposal and the research needs. The list of damage given below is not exhaustive though it likely includes most recorded damage.

4.2.1. SEISMIC EVENT OF 1356, BASEL

In October 1356, the ground shook in the area of Basel; this earthquake, whose intensity reached the level of IX on the EMS-98 scale at the epicentre, is known at the strongest earthquake that occurred in northern Europe since the first millennium.

A multi-disciplinary study enabled researchers to set up an isoseist map (Figure 4.1).

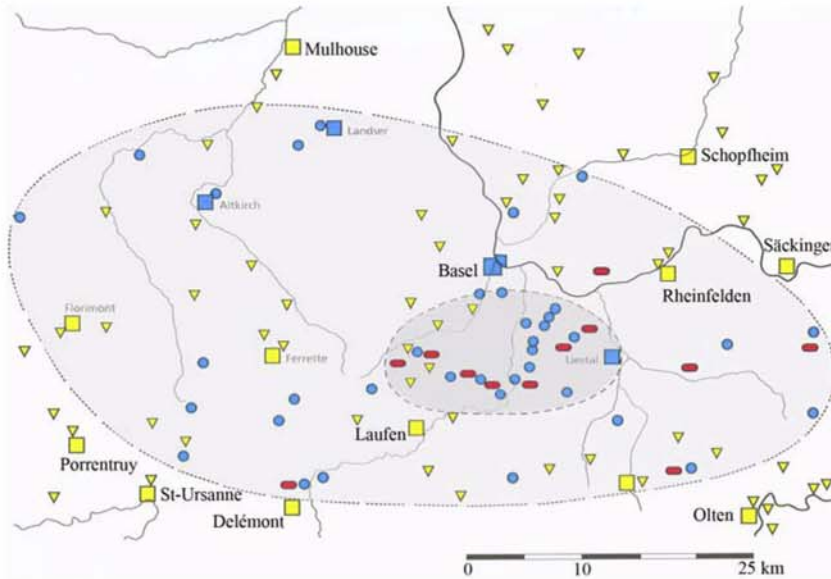


Figure 4.1 : Isoseist map of the 1356 Basel earthquake [We 03], [MC 79]; damage recorded in the area of Basel [Me 05].

Legend:

<ul style="list-style-type: none"> City, highly damaged City, without damage or slightly damaged 	<ul style="list-style-type: none"> Town, highly damaged but rebuilt (repaired) later Town, damaged in 1356, neglected and finally disappeared Town, undamaged or slightly damaged
--	--

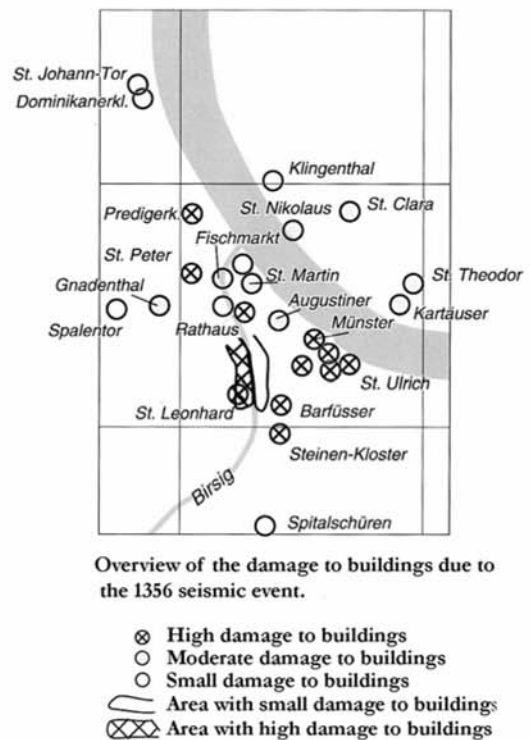
In a radius of about 30 Km almost every church, castle and fortification was destroyed as written in the «Red book» of Basel city¹.

1. The reader can found the actual text in German in Appendix A. 2.2.

«One should know that this city was destroyed by an earthquake; no church, no tower and no masonry house survived it, either in the city or in the surroundings, every building was highly damaged. The city ramparts also partly collapsed. [...] as fire set in the night and lasted during the next eight days people was no longer able to face with the earthquake. The part of the city enclosed within the city walls burnt almost completely...».

As aforementioned, the city of Basel was struck hard; an indication of the damage sustained by edifices is shown in Figure 4.2. Masonry buildings, as sacred edifices, were highly damaged; for instance, the cathedral of Basel and the church of the preacher sustained severe damage.

Figure 4.2 : Overview of the damage to buildings due the 1356 earthquake in Basel; source: Swiss Seismological Service.



Overview of the damage to buildings due to the 1356 seismic event.

BASLER CATHEDRAL

It is likely that the Basler Cathedral was one of the most damaged masonry buildings of the city due to the seismic event. According to specialists, the choir vaults fell down [Me 06], the transept vaults also must have sustained damage, the main nave vaults (it is written in [Me 06] that the west tower was broken and its upper part fell down on the vaults of two bays) got damaged, one lateral tower collapsed without being reconstructed and the facade of the Gallus' gate cracked (the «wheel of the fortune» (rosace) collapsed while the facade was moderately damaged). Whereas vaults were rebuilt, the damaged (or collapsed) tower was not replaced. The Gallus' gate facade, was repaired and the rosace rebuilt; however a crack however still exists and can be easily seen by passers-by.

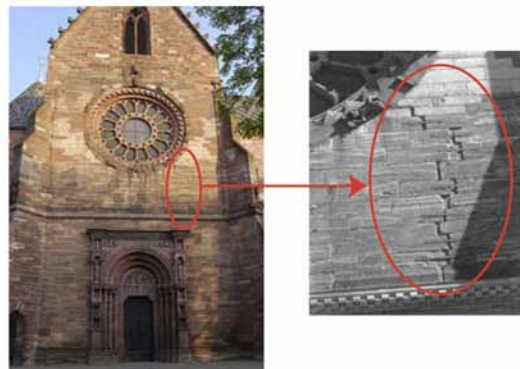


Figure 4.3 : Crack beneath the so-called «the wheel of the fortune» rosace, Galluspforte (Gallus gate).

CHURCH OF THE PREACHER

Specialists observed a change of masonry within the fabric of the church of the preacher (in English: the preacher church); the interface was found all along the wall of one aisle from the level of choir down to the front wall (Figure 4.4). The choir as well as the front wall were still standing after the earthquake; this might be explained by the compactness (from a structural point of view) of the choir and the abutments on the front wall that reinforced it.

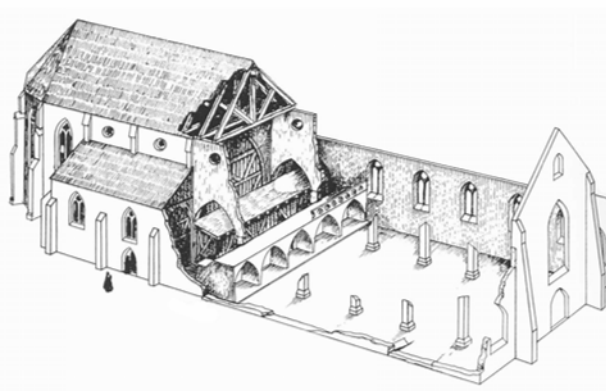


Figure 4.4 : State of the church of the preacher after the 1356 seismic event [Me 05].

It must however be kept in mind that the Figure 4.4 is only a reproduction.

4.2.2. SEISMIC EVENT OF 1755, BRIG/ NATERS (VALAIS)

On December 9, 1755, the region of Brig (Valais) shook under a very strong earthquake. The epicentral Intensity (I_0) was estimated to be VIII (Epicentre: Brig/Naters) and the Moment-Magnitude (M_w) was 6.1 (Richter's scale) [ECOS 02]. This region was struck many more times in the following days and months by smaller seismic events that were characterised by magnitudes between 2 and 4 on the Richter's scale; about 22 events were recorded in the same area.

4.2.2.1. Damage

Below are the important damage that were reported at that time (i.e. in 1755).

BRIG

In a chronicle, a Jesuit priest who witnessed the event gave some details of it; he wrote: «*On December 9, at 2:30 p.m., a terrible noise was heard that came from the underground, as to make people going out from their house. Then we thought Brig was about to collapse.[...]. The earth shook during about 40 seconds; every house shaking along north-south direction cracked. Almost all chimneys were thrown down; churches suffered great damage; towers were split from top to bottom.*» [Be 56]. Moreover, the church of the Jesuit college sustained serious damage: their mansion cracked almost in all parts and the temple vault fell down.

Other cultural heritage buildings also suffered from the earthquake such as the Stockalperpalast that sustained severe damage to its outer walls.

GLIS

A wall part of the bell tower of Maria Himmelfahrt Kirche fell down on the vault and destroyed it as well as the altar that was beneath it [Be 56]. It is added in another source [JWK 97], that the falling part destroyed the arch of the church; that probably corresponds to the chancel arch. It is worth noting that the tower (about 30 m high (without roof); 1230-1290) was built on the basis of the Sion Cathedral bell tower.

According to all sources, Glis suffered more than Brig from the 1755 earthquake.

NATERS

According to the archives of the city of Visp [Visp ArP], the church in Naters was highly damaged by the 1755 earthquake. In [Gi 04], it is written that *«the arch of the bishop's church collapsed, sweeping away two bells and destroying the organ and some part of the interior»*. Furthermore one can read in [Be 56] that the vault also collapsed.

At this point, damage recorded by both sources does not exactly correspond to each other; it may be accepted however that the vault (that was maybe called an «arch» in the first source) actually collapsed and destroyed the organ and a part of the interior.

4.2.2.2. Summary

According to the above survey, vaults and bell-towers were the most damaged parts of churches due to the 1755 earthquake. Unfortunately, it is difficult and also specious in most cases to draw conclusions or hints on the seismic response of the damaged buildings because their initial (before the seismic event) state and sometimes their shape is at present unknown. Nevertheless, since the shape of the Glis bell-tower was not modified after the earthquake and as it is still standing today, it is possible to make some conclusions about its seismic response. First, the presence of tie-rods only in the upper part of the tower indicates that the largest deformations were concentrated at this level; the initial reinforcement of the corners by quoins was probably not enough efficient. Moreover, the replacement of the roof, which may initially have been made up of masonry like the bell tower of the Sion Cathedral, into a lighter structure in wood shows that this part must have been damaged.

The long duration (40 seconds according to [Be 56]) of the 1755 earthquake can also be an important factor in the damage to buildings; nevertheless, this factor must be considered with precaution because of the difficulty in assessing time on the spur of the event and also because the movement of buildings usually lasts more than the seismic event.

4.2.3. SEISMIC EVENT OF 1855, TÖRBEL (VALAIS)

On July 25, 1855, the region of Visp (Valais) was struck by another strong earthquake. The epicentral Intensity (I_0) was estimated to be VIII (Epicentre: Törbel), whereas the Moment-Magnitude (M_w) was assessed to be 6.4 (Richter's scale) [ECOS 02]. This region was once again struck on the next day by two seismic events of magnitudes 5.6 and 5.2 [ECOS 02]. The earth continued to shake during the next month: a dozen of earthquakes of smaller magnitude were then recorded.



Figure 4.5 : Isoseist map of the 1855 earthquake in Switzerland [Sc 89] (updated by data from the Swiss Seismological Service).

4.2.3.1. Damage

CHALAIS

In 1855, the earthquake seriously damaged the previous church of Chalais, whose existence was already attested in the 13th century [MMS 97]. It was damaged so badly that a new one was built and consecrated in 1858 [Cha ArP]; this is actually the present one.

GRÄCHEN

D. Lenoir wrote in [Le 49] that the vault of the church was cracked; the present church was later modified and the stone vault was changed into a wooden one. This fact is confirmed in the list of reparations that were planned after the earthquake [Sion ArC]: 2 tie-rods in the choir, 4 tie-rods in the nave, the ceiling of the ossuary, to repair paintings, one arch, the ceiling and to repair the vault. For all the reparations, 900 CHF were calculated.

Besides the church, the chapels (the chapels «auf der Luin» and «an der Egge») also sustained important damage. The Chapel «auf der Luin» was less damaged while the bell gable and the nave of the chapel at the corner («an der Egge») had to be repaired [Sion ArC]



Figure 4.6 : Chapel «an der Egge» and the parish church at the time of the 1855 earthquake.

NATERS

According to E. Jossen [Jo 00], the church in Naters was highly damaged by the 1855 earthquake. The part of the nave vault that was along the front wall broke down and resulted in destroying the organ that laid on the tribune. The portal also collapsed. All the reported observations show that the tower moved so much that it catapulted the bells out of the windows.

SANKT-NIKLAUS

Most reports described Sankt-Niklaus as the town that suffered the most from the 1855 earthquake. According to the archives of the State of Valais [Sion ArC], the vault of the church collapsed (the whole vault had to be repaired as well as 7 arches), two dozen square meters of walls had to be repaired, many cracks had to be refilled, the organ and most pews were destroyed or heavily damaged. Moreover, 12 arches of the bell tower and the roof also had to be repaired; 8 tie-rods had to be inserted into masonry. The damage was so heavy that Nöggerath even wrote the church was irreparable [Nö 55].

The church was erected in the 1750s after the previous one was smashed away by an avalanche; the bell tower dated from the 17th century.



Figure 4.7 : Views of the parish church in Sankt-Niklaus of 1855.

STALDEN

According to both Nöggerath [Nö 55] (translation from German: S. Fritsche [FFGGb 06]), Stalden was at least as much disrupted as Visp. The church and its tower were cracked in many places and the wall separating the vault of the nave from the choir collapsed. Nevertheless, this information was not confirmed by Heusser [He 56].

The parish church, Saint-Michael, which was built in 1777, is the oldest of the Visp valley. The reported damage after the 1855 earthquake are in [Sion ArC]: rebuilding of the arches of 9 windows, the tower arch (probably the chancel arch) and keystone, 4 keystones in the bottom part of the tower, refilling cracks and making a survey of the foundations (to the south). Every description of damage survey is unfortunately depending on the vocabulary used by the reporter; with time it becomes indeed more difficult to know exactly what a word precisely meant. For instance, we do not know accurately what corresponds to the tower arch.

Nevertheless, the survey carried out in 2005 (May) of this church showed the following features: there are vertical cracks above upper windows as well as in the anchorage area. Moreover, vertical splits were observed along the inner side of the nave at the connection between the nave, the chancel arch and the tower. There is no proof that this damage results from an earthquake.

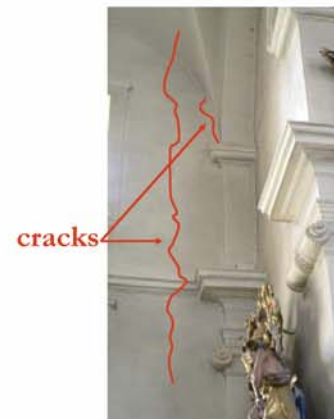


Figure 4.8 : Vertical cracks along the connection of the nave to the bell tower.

TÖRBEL

In the diary of the priest of Törbel, who was in office at that time, it is written that the vault of the church collapsed and damaged the organ in the tribune, the pulpit, the pews, statues and the altars [FFGG 06].

VISP

Vaults of both churches in Visp (St Martin's church and the Three kings' church) collapsed; the pinnacle of the St-Martin's bell tower broke down and fell, while the rest of the structure and especially the lateral walls were highly cracked. In [Nö 1855], it is written (translation from German [FFGG 06]): «... in the St-Martin's church, the con-rods tightening the lateral walls below the vaults [...], partly broke, partly had been pulled out of the walls». This fact is confirmed by [He 1856], who added that the walls of both churches were disrupted in many places.



Figure 4.9 : Engraving of the St-Martin's church (J.V. von Osterwal) around 1825 [Sc 01] and after the 1855 earthquake (J. C. Heusser, 1856).

Moreover, Heusser mentioned the fact that even the ground (rock) was cleft around the St Martin's church (erected at a hill top). He recorded one half-foot to one foot wide cracks. It is worth noting that all the above recorded damage reflect the situation after at least the main shock and both aftershocks that occurred the day after; it is written in [RCom 60] that keystones in both churches in Visp collapsed, the ceiling fell down and the square was covered by a 3 feet high layer of plaster, rubble and all kinds of rubbishes.

In [Ru 84], it is observed that the chancel vault of the Three-King church was damaged whereas the ceiling vaults fell down, destroying the organ (toward the front wall; on the tribune) and the pews.

Like the parish church in Stalden, a vertical crack in the west lateral wall of the nave is observed at the connection of the nave with the bell tower.

VISPERTERMINEN

The spire of the parish church was broken and its walls highly cracked; likewise, chapels along the procession lane were also heavily damaged. The most damaged building was the Gnadenkapelle (also called Waldkapelle) whose vault collapsed.

The so-called alte Waldkapelle (old chapel in the forest) in Visperterminen was built in 1730-40. According to G. Studer-Freuler [St 94], it was roomy and made with a good taste. The chapel shape was similar to the one of the Three Kings' church in Visp and it reminded more generally the pattern of Baroque churches from Southern Germany. The architect came from the Vorarlberg region (Austria).

It is important to note that this chapel was already damaged by the seismic event of 1755 [Sion ArB]; according to [St 94], it resulted in two cracks: one in the choir walls and one in the portal (or in front of it; it is not clear). At that time everyone thought it was due to the soil conditions but they changed their mind after removing the covering. According to [St 94], it seems indeed obvious that damage was caused by the timber framework. Nevertheless, the type of connection between the framework and the walls is not known.

After displacing the altar to the new parish church in the middle of the town, villagers no longer visited the chapel.

The damaged chapel collapsed during (or after) the earthquake of 1855 whose epicentre was situated in the town of Törbel (Visp valley).



Figure 4.10 : Damaged chapel in Visperterminen; picture taken in 2005.

4.2.3.2. Summary

Once again, in comparison with the damage recorded after the 1755 earthquake, vaults and bell-towers are the most damaged parts of churches. Nevertheless, the record of damage highlighted a few more hints on the seismic vulnerability of vaults and bell-towers. For instance, vaults close to a rigid facade, like the front wall, collapsed first (Stalden church). Moreover, the fact that lateral walls can move differently (out of their plane) was proved by the surveys carried out by Nöggerath [Nö 55] and Heusser [He 56].

With respect to bell-towers, their seismic vulnerability was confirmed by the damage observed after the 1855 earthquake. The spire was damaged and the upper part was cracked and corners showed signs of dismantling since they were always reinforced by tie-rods (St-Niklaus, Stalden and Naters).

Finally, the chancel arches showed serious damage (Naters and Stalden); this fact is interesting since it highlights the enhancement of the seismic vulnerability of chancel arches because of the closeness (that is, a wall of the bell-tower is supported by a part of masonry belonging to the chancel arch) of a bell-tower.

4.2.4. SEISMIC EVENT OF 1946, SIERRE (VALAIS)

In January 25, 1946, the Alpine region was struck by an earthquake of moderate magnitude (6.1 on the Richter's scale was measured at the epicentre (Sierra)). This main shock was followed by two after-shocks: on January 26 (5.2 on the Richter's scale) and February 4 (5.1 on the Richter's scale) [ECOS 02].



Figure 4.11 : Isoseist map of the 1946 earthquake [Sc 00].

4.2.4.1. Damage

Figure 4.12 shows the recorded damage on churches after the 1946 earthquake¹.

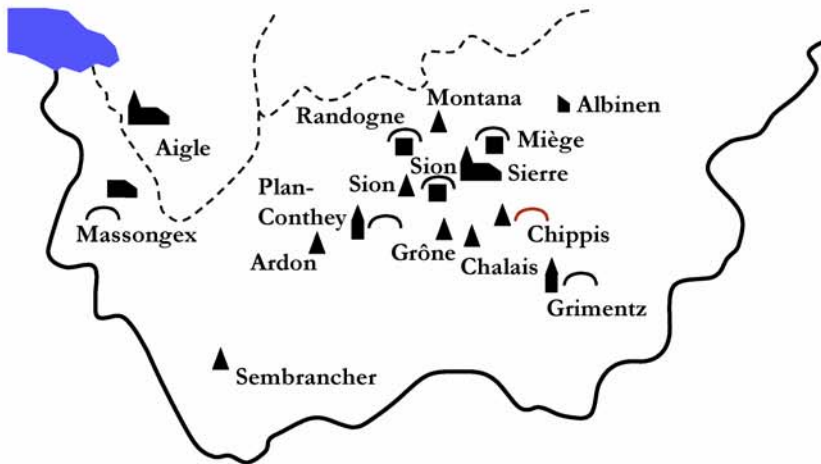


Figure 4.12 : Recorded damage after the 1946 earthquake.

Legend:

	Whole church is damaged		Bell-tower spire is damaged
	Bell-tower is damaged		Vault is damaged
	Nave walls are damaged		Masonry vault is damaged
	Apse is damaged		

1. The list of the damage showed above can be found in appendices; it is worth reminding that this list is not exhaustive.

According to this list of damage, the most damaged part was the spire of the bell tower (Sembrancher, Ardon, Sion, Grône, Chalais, Chippis, Sierre and Montana). For every case the damage consisted of the sliding of the spire's upper part; the volume of this part was different for each tower. In both following pictures, the spire of the church in Chalais (left) was hollowed whereas only the top of the bell tower of the church in Chippis dislocated and slightly slid aside.

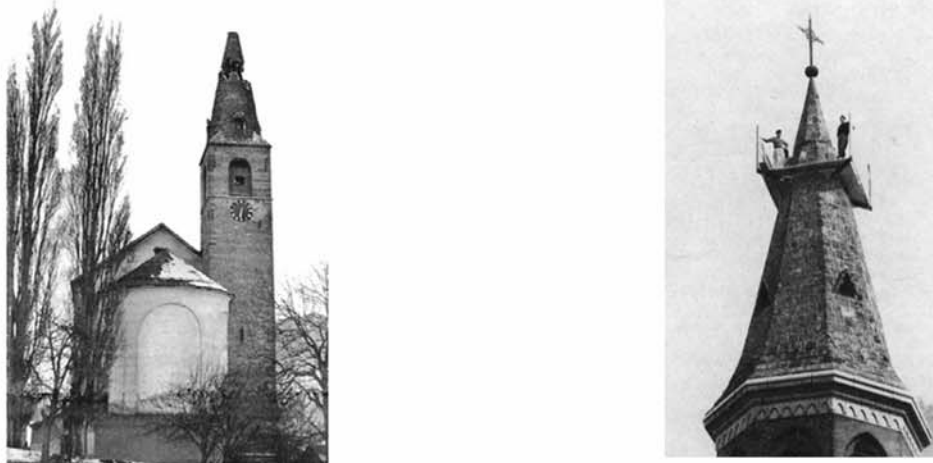


Figure 4.13 : Damage to the bell-tower of the churches in Chalais and in Chippis [AR 05] and [Chippis BP].

The case of Our-Lady-of-the-Moor in Sierre was probably one of the worst ones; the whole spire was split (Figure 4.14). Moreover the rest of the church was also highly cracked.

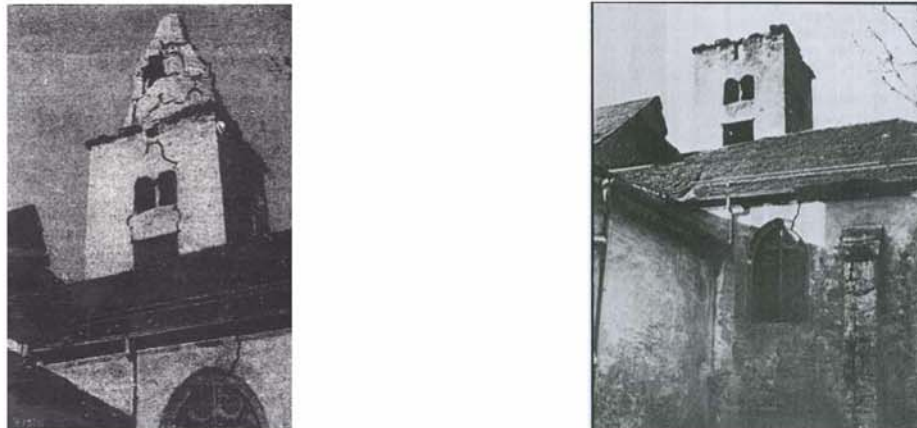


Figure 4.14 : State of Our-Lady-of-the-Moor in Sierre after the main shock of the 1946 earthquake. Source: Le Nouvelliste, 30.01.1946.

The vaults of the collegiate of Valère, the parish church of Massongex and the one of Miège were moderately cracked. The plaster vault (built in 1922) of Saint Urban church in Chippis, on the contrary, fell down after the seismic shock happened in May 30, 1946. The vault was particularly cracked next to the organ tribune; the vault collapse started at this point and lasted a few seconds (the ceiling just fell down slowly (according to the priest who was in the church when the vaults collapsed)).

According to people memories, the masonry barrel vault in the church in Grimentz was cracked in such a way [MMS 97] that they decided that the vault had to be destroyed and rebuilt. Nevertheless, its destruction turned out to be more difficult than they had expected. Unfortunately, the damage pattern is unknown. In Grimentz, it must be added that the bell-tower was also slightly damaged.

The damage to vaults in the church in Conthey was more serious than in Grimentz. It was probably the most damaged sacred edifice after the 1946 earthquake. The parish church in Plan-Conthey collapsed after the second seismic aftershock, on February 4, 1946, (Mw=5.1, Ayent). According to human memories (see description in Appendices), the tower and the vault had so many cracks that people were afraid to enter the church or ring the bells.



Figure 4.15 : Parish church in Plan-Conthey^a

a. Found Raymond Schmid, Sion Bourgeoisie, Médiathèque, Valais.



The chapel in Randogne was also highly damaged, as is shown in the left picture.

Figure 4.16 : View of the damaged chapel in Randogne [Cr 03].

4.2.4.2. Summary

Vaults apparently were the structural parts that showed the highest seismic vulnerability; this was especially true in many sacred edifices as the chapels or churches in Chippis (St-Urban), Plan-Conthey, Grimentz and Randogne. It is worth noting that both collapses (Chippis and Plan-Conthey) were due to aftershocks, whereas the other cases were characterized only by serious cracking.

Bell-towers were also damaged, especially at their top, i.e. the spire (Chalais, St Urban in Chippis, Sion cathedral, Montana, Ardon and Grône). The bell-tower of the church Our-Lady-of-the-Moor was the most damaged tower and probably more than the bell-tower of the Plan-Conthey church. Moreover, lateral walls of Our-Lady-of-the-Moor also showed serious cracking (see Figure 4.14); in this case, it is important to indicate that this edifice was erected, as its name explains it, on soft (kind of clay-silt soil) ground and this fact certainly had a great impact on the peak ground acceleration felt by the church.

The nave vaults were certainly replaced whereas the ones in the choir were kept intact.

It is also worth noting that the damp atmosphere (as some pictures taken during Winter 2005-2006 highlight it (apparition of micro-organisms on the washed surfaces (dark zones on Figure 4.17))) might have had some impact on the masonry quality.

Figure 4.17 : State of the bell-tower of the church Our-Lady-of-the-Moor in Sierre.



Other kinds of damage can be found in the structure of the Collegiate of Valère; most serious ones were: the front wall was separated from the nave and the rosace that was above the main arch of the chancel arch fell apart. This edifice sustained other damage that are listed in Appendix A. 2.3.

4.2.5. SEISMIC EVENT OF 1964, SARNEN (OBWALD)

On February 17, 1964, the earth shook in the area of Sarnen, Central Switzerland. The epicentral Intensity (I_0) was estimated to be VII (Epicentre: Flüeli/ Naters) and the Moment-Magnitude (M_w) was 5 (Richter's scale) [ECOS 02]. The damage listed below were recorded after this seismic event; a second earthquake happened a month later. On March 14, 1964, the earth shook again in this area. The epicentral Intensity (I_0) was VII (Epicentre: Kerns/ Naters) and the Moment-Magnitude (M_w) was 5.7 (Richter's scale) [ECOS 02].

Except for the survey carried out by F. Pfister [Pf 81], no information about the state of the church after the second earthquake is available.

4.2.5.1. Damage

The 1964 earthquake of January is introduced here only because of the damage caused to the Saint Peter und Paul church in Sarnen.

According to the report written by F. Pfister [Pf 81], the three vaults of the nave showed many long lateral and transversal cracks as well as smaller ones. The cracks in the areas along the vault apex are the largest ones (up to 4 mm wide and a few meters long; Figure 4.18). Moreover the engineer is quite sure that there are longitudinal cracks along one side of the church that crossed the vault (it is, however, not noticed on the sketch on Figure 4.18). Nevertheless most cracks only crossed the

roughcast of the vault. Contrary to the main nave ceiling, the vault of the side-aisles and the chor's were only slightly damaged.

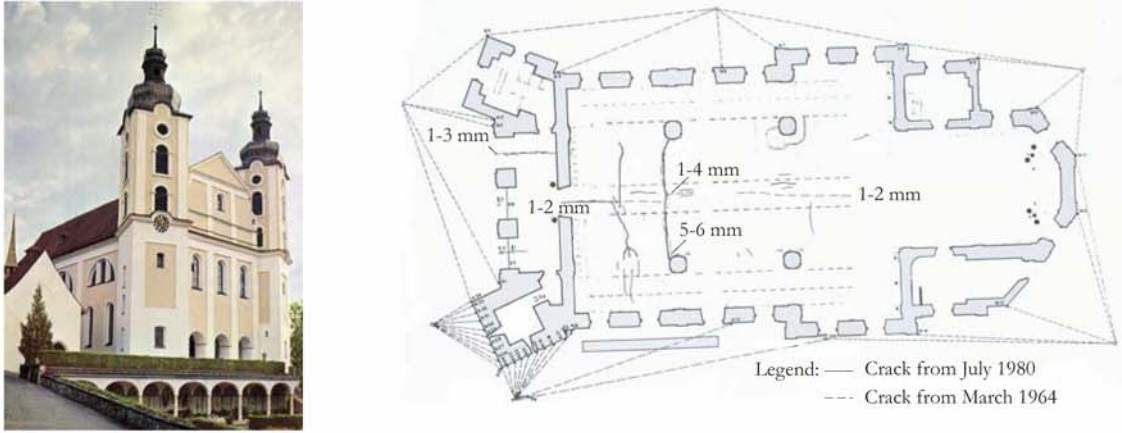


Figure 4.18 : View of the main facade of the church [De 70] and of the recorded cracks after the earthquake in 1964 and a few decades later (1980) [Pf 81].

The towers were not too much damaged *a priori* compared with the church pillars and the framework.

Amongst walls, the front wall was certainly the most damaged. A vertical crack, that crossed the front wall, was observed close to its connection with the bell tower (on the mountain side). Walls and pillars did not show any important deformation.

It is interesting to see that further cracks happened long after the earthquake (recorded cracks in 1980 had indeed not been reported in 1964). This shows that a first damage (for instance, due to an earthquake) can result in other damage later.

It might be worth noting that the church was already reinforced by transversal tie-rods through the nave. It means that there were already cracks (due to the shape and material) before the earthquake. According to F. Pfister [Pf 81], the vault of the main nave was probably in a bad state; nevertheless he also wrote that the vaults were not at risk and just made a proposal to repair it.

4.2.6. SEISMIC EVENT OF 1991, VAZ AREA (GRAUBÜNDEN)

On November 20, 1991, the area of Vaz (Eastern Switzerland) was struck by an earthquake. The epicentral Intensity (I_0) was VI (Epicentre: Vaz) and the Moment-Magnitude (M_w) was 4.6 on Richter's scale [GWF 05], [ECOS 02]. This main shock was followed by about thirty aftershocks, until May 1992, whose Moment-Magnitudes were between 1.8 and 3.4 on Richter's scale.

The resulting damage to buildings was of moderate scale: most damage was thin cracks in walls as, for instance, on a wall of the church in Vaz.

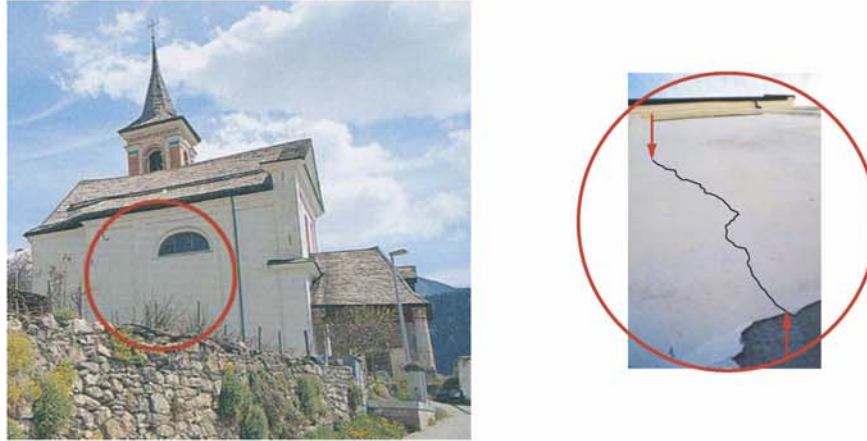


Figure 4.19 : Church in Vaz: views of a damaged part [GWF 05].

4.2.7. SEISMIC EVENT OF 2005, BALMES PASS (FRANCE/ VALAIS)

On September 8, 2005, the area close to the Balmes pass (at the border between France and Switzerland) was struck by an earthquake of moderate magnitude. The estimate of the epicentral Intensity (I_0) was V (Epicentre: Vallorcine (France)) and the Moment-Magnitude (M_w) was assigned to 4.7 (Richter's scale) [ECOS 02].

A survey of the churches in the following towns was carried out within a week after the event: Finhaut, Trient, Salvan and Le Trétien.

4.2.7.1. Damage

FINHAUT

The church in Finhaut was hit by the earthquake right after a restoration. It essentially consisted of restoring the roughcast on the outer side of the walls and also probably their inner faces. This means that every crack was made visible by the movement induced by the 2005 earthquake.

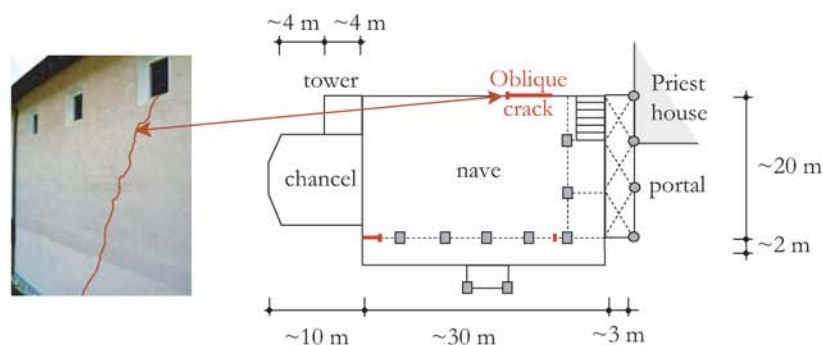


Figure 4.20 : Diagram of the church plan and its observed damage.

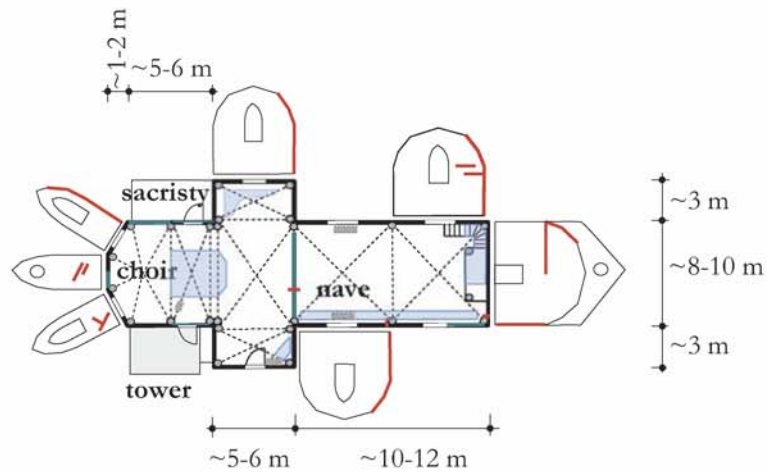
SALVAN

No particular damage was observed in the church in Salvan, which was transformed in Baroque times.

TRIENT

The Neo-Gothic church in Trient showed a few cracks that was probably present since the end of the construction in 1869. Most of them were essentially vertical, at the connection between the pillars of the ribs and the walls, and some of them followed the interface between the vault bays and the side-by-side lateral wall of the church (meaning detachment). Another kind of damage observed on this church was the scattering of small roughcast parts, which belonged to the ceiling and that fell down on the ground due to the earthquake. These parts that scattered on a few areas have been transferred to the next figure. Small holes were also visible in the roughcast layer of the vault bays.

It might be worth noting that the exterior was restored in 1959 and the interior in 1989



Legend:

- crack
- detachment
- ▨ holes in the roughcast layer
- roughcast scattered on the floor

Figure 4.21 : Outer view of the church and schema showing the observed damage after the earthquake.

4.2.7.2. Summary

What strikes most observers are the numerous cracks at connections between two structural elements. For instance, the cracks between the front wall and the nave or the nave and the chancel arch (Trient church). Moreover, a crossing crack appeared at the middle of half the arch of chancel arch (Figure 4.21); this highlights the position change of the trust line due to the seismic movements.

An oblique crack was observed in a lateral wall indicating that the wall was subjected to shear during the earthquake.

4.3. DAMAGE OBSERVED IN ITALY

Recording all the damage due to earthquakes in Italy could be the object of a book. Such an exhaustive survey is not the goal of this PhD thesis; this is why only a few cases are discussed below. Because of the comprehensive nature of the survey carried out by Doglioni et al. [Do 94] after the 1976 Friuli earthquake (also called Tolmezzo earthquake), the next chapters essentially list the damage observed after this seismic event.

4.3.1. 1976 TOLMEZZO EARTHQUAKE

This earthquake, which occurred in 1976, was so-called since its epicentre was situated in the city of Tolmezzo in the Friuli (north of Italy). The main seismic shock was on May 6 and was followed by many smaller shaking movements. On September 15 of the same year, a second seismic event of equal intensity to the first one occurred.

The intensity of the earthquakes reached a value of X on the MCS (Mercalli, Cancani, Sieberg) scale at the city of Tolmezzo. The event of May was the worst earthquake that the region had experienced for many centuries. The seismic magnitude reached indeed about $M_s=6.5$ [AS 05] and the ground acceleration at Tolmezzo was about ^a 3.5 m/s^2 .

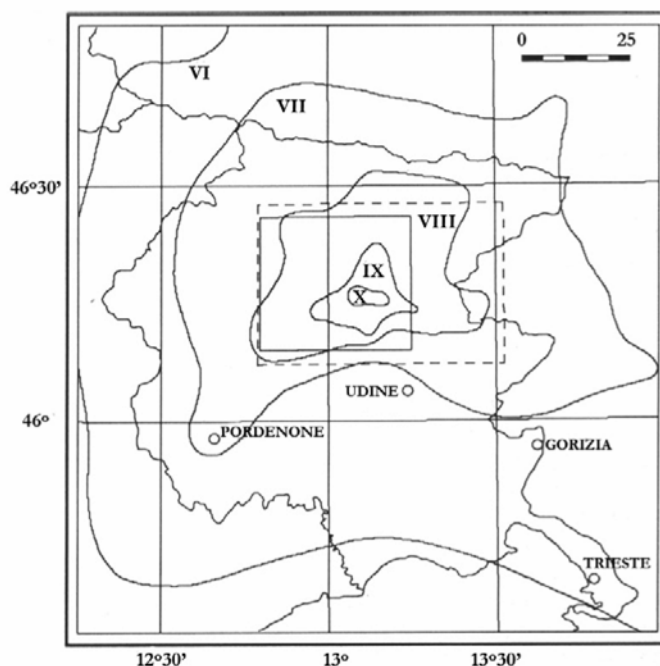


Figure 4.22 : Seismic intensity lines in the Friuli region [Do 94].

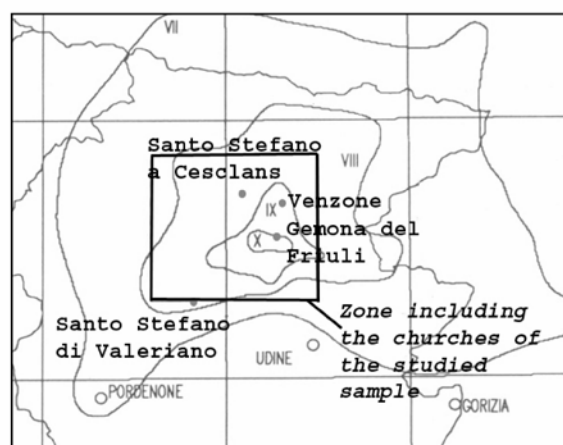
a. This value has been reevaluated to 1.9 m/s^2 (without site effects) by [BPVR 07].

4.3.2. DAMAGE RECORDED ON SACRED EDIFICES

The information was taken from the book written by F. Doglioni et.al. [Do 94] who studied a large sample of churches damaged by the earthquake in 1976. The level of the observed damage ranged from VIII to X on the MCS scale. The sample contained about 243 churches.

Five edifices are specifically addressed because of the quality of the damage record, the representativeness of the other churches from the sample and also because they present most of the important structural features whose impact on the seismic response must be assessed. These edifices are: the church of Santa Maria del Fossale (Gemona), the church of Sto (Santo) Stefano a Cesclans, the church of Sto Stefano di Valeriano, the Duomo di Gemona and the Duomo di Venzone.

Figure 4.23 : Location of the five edifices that have been chosen from the sample studied by [Do 94].



Note: only the church of Santa Maria del Fossale is presented; the reader can find a description of the four other edifices, as well as the related damage, under Appendix A. 2.4.

4.3.2.1. Santa Maria del Fossale a Gemona

Geologically, the ground under the town of Gemona is composed of a Jurassic limestone bedrock and alluvium (so-called alluvioni torrentizie) of about 50 m. thickness, made up of homogeneous gravel mixed with silt sand. In 1976, this situation could likely have amplified the amplitude of the seismic waves and therefore created more damage.

STRUCTURAL CHARACTERISTICS

The church, which was about 10 m wide, 20 m long and 13 m high, was built in 1659 and transformed in 1735. It was composed of a simple nave extended by an apse and had a sacristy as appendix (mainly connected to the apse); a chancel arch divided the nave and the apse. There was no bell tower.

All parts of the walls are made of masonry.

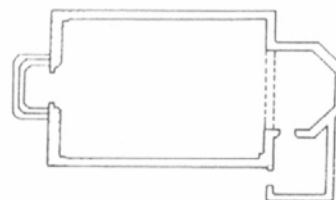


Figure 4.24 : Plan of the church Santa Maria del Fossale [Do 94].

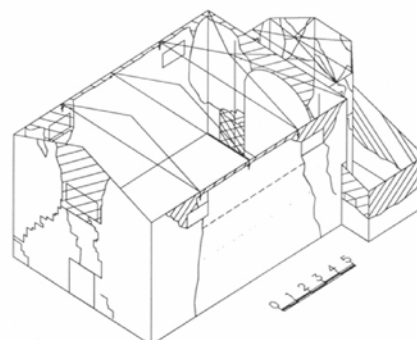
The roof structure was made up of timber trusses that were supported by the lateral walls and were spaced 2.8 m apart. The church did not encompass stone vaults.

The reader can find further information about the structural characteristics of the Santa Maria del Fossale church in appendix.

OBSERVED DAMAGE

According to the damage observed on the church, the transversal displacements (in the plan of the main facade) appeared to be higher than the lateral displacements. From a structural engineer's point of view, the main mechanism of damage on the main facade was of an in-plane type, while the damage on the lateral walls seemed to be the result of an out-of-plane mechanism.

Figure 4.25 : Observed damage to the fabric of the church Santa Maria del Fossale [Do 94].



All structural elements of the church are taken into account; they are: the front wall, the lateral walls, the chancel arch, the apse and the annexes. The classification was made according to the approach of F. Doglioni et. al. in [Do 94].

1. The front wall

After the main seismic shock (May 1976):



The main damage observed included the following: a major part of the tympanum tumbled down along with the stones that were between the tympanum and the window. The brickwork between the window and the door dislocated and slightly detached from the fabric. The left part of the front wall was diagonally cracked and the front wall was detached from the left lateral wall (left-hand figure).

Figure 4.26 : Front wall damaged by the main seismic shock occurred in May 1976 [Do 94].

After the second seismic shock (September 1976):



There was no remains from the previously dislocated masonry between the window and the door: there was instead a big hole from the tympanum to the door. The left part of the wall cracked further and the whole facade was detached from the lateral walls (left-hand figure).

Figure 4.27 : Front wall after the second seismic event [Do 94].

2. Lateral walls

The masonry of both lateral walls was dislocated all along the upper edge and especially above the openings. There was a vertical fracture, which started from the bottom edge of the left opening (see the opposite figure) along the corner with the front wall; at the opposite corner, the crack surrounded the corner itself.

Outline of the damage observed on the right lateral wall of the church:

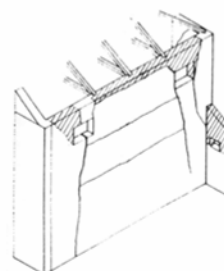


Figure 4.28 : One lateral wall damaged by the main seismic shock in 1976 [Do 94].

3. Chancel arch

The failure of both piers was observed (intersection of the lateral walls with the chancel arch). They also experienced a translation towards the apse (see also Figure 4.30). Following the failure of its corners (that promoted an opposite movement of both arch pillars), the arch broke down at the crown and a big part of masonry fell down on the ground.

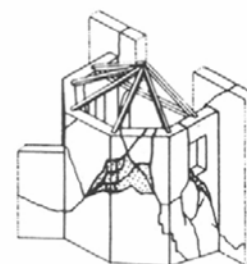
Figure 4.29 : Chancel arch after the main seismic shock in May 1976 [Do 94].



4. Apse

The apse part that was connected to the left branch of the chancel arch collapsed and completely detached from the rest of the fabric. Otherwise, the angles were surrounded by cracks and a diffuse cracking pattern was observed on every area as well as the expulsion of stones from the rest of the fabric.

Figure 4.30 : Outline of the damage suffered by the apse [Do 94].



DAMAGE MECHANISMS

1. Front wall

During the main seismic event (May 1976), the major damage mechanism was due to in-plane shear forces (diagonal and in-cross cracks). The presence of openings (bull's eye window in the tympanum and square window in the front wall) led to the formation of cracks and extended towards the appearance of a hole. During the second seismic event, every cracking pattern that was created by the main seismic shock became more visible (cracks enlargement, brickwork more divided and so on) and led to the situation of the Figure 4.26.

The cracking pattern was mainly due to configuration of the openings and could occur because of the good cohesion in the fabric. The type of failure at the corners shows that the connection with

the lateral walls was better on the right side than on the left one. Also, the inefficient connection between the tympanum and the facade was mainly at the root of the collapse of the central part that encompassed the bull's-eye window.

2. Lateral walls

The dislocation of the masonry along the upper edge of the lateral walls was merely due to the movement of the roof structure trusses (hammering phenomenon). Concerning the fractures close to the corners, the crack near the front wall was due to the detachment of the latter and the one close to the chancel arch looked like caused by the thrust due to a roof rafter at the corner of the lateral walls with the chancel arch.

The diverse horizontal cracking pattern of the walls was likely due to a membrane-like structural behaviour of the lateral walls. The metallic connection between the roof structure and the walls fixed the wall horizontally along its upper edges and then created a kind of membrane partially restrained along its edges. According to the observations, the mechanism of damage appeared to be essentially of an out-of-plane type.

3. Chancel arch

Because of the thrust from two roof rafters, the corners (between each lateral wall and the chancel arch) cracked and finally detached from the rest of the fabric. The translation of both corners towards the outside, increasing the distance between the chancel arch piers, promoted the cracks that cut the upper part of the arch and led to its collapse. On the left side, this phenomenon was accentuated by the discontinuity from an ancient opening. On the right side, the connection with a wall of the sacristy also affected the cracking process.

The failure of the corners between the lateral walls and the chancel arch highlights the sway of constructive discontinuity that result from transformations carried out during the construction life.

4. Apse

Following the disconnection and translation of the left part of the chancel arch, the apse fabric that was connected to, also failed. The detachment of the corners was probably due to the thrust from the roof rafters as well as to the discontinuity resulting from a transformation that occurred in 1735.

The loss of cohesion in the fabric, as well as the expulsion of the roughcast, had its root in the masonry cohesion and in the way of building.

CONCLUSIONS

Every kind of discontinuity, either due to a change of masonry or due to structural transformations, may highly influence the cracking pattern and the damage mechanisms of structural elements (under dynamic action). In the case of the church Santa Maria del Fossale, the masonry discontinuity at the joint between the front wall and the lateral walls helped (the damage was also due to the front wall motion) to promote the vertical crack right at the intersection. Also, the structural transformation of 1735 led to the collapse of the parts belonging to the apse wall and those that were joined to the chancel arch.

The roof structure and especially its connection with the walls that support it, appear to be very important. In the case of the Santa Maria del Fossale, the roof structure that was connected to the

lateral walls by metallic anchorage, contributed then to a good connection between opposite walls, only the very upper edges were damaged. However, this link resulted in a membrane-like structural behaviour of the lateral walls.

Regarding the slip of the stones out of the wall, it seems that masonry made up of relative big stones may be more sensitive to out-of-plane actions than a masonry composed of smaller stones that are well cemented together.

After several successive seismic events, the damage history (say the cracking history), appears to influence highly the mechanisms of damage of the structural elements. The parts that are just separated from the rest of the structure will indeed behave independently from each other and then may totally differ from the initial structural behaviour.

The reader can find other cases of damage recorded after the Friuli earthquake in Appendix A. 2.4.

4.4. DISCUSSIONS

Damage to sacred buildings is related to the types of structures, that is, the shape of the given global structure and those of each components, the connections between them (quality), masonry (bonding type, rock and general quality), transformations and the constructive details.

Based on the damage observed in Switzerland and in Italy, the impact of each aforementioned feature on the seismic response of buildings is discussed here after.

4.4.1. SEISMIC VULNERABILITY OF CHURCHES AND THEIR STRUCTURAL COMPONENTS, BASED ON RECORDED DAMAGE

4.4.1.1. Churches shape

The observations of churches did not provide a clear idea about the influence of the global shape of churches on their dynamic response and on the damage due to earthquakes. Nevertheless, it appears that masonry behaves more or less linearly under very small ground acceleration and non-linearly when ground waves are stronger (the level of ground acceleration that leads to non-linear behaviour depends on the structure, the dimensions of the components and the type (quality) of masonry). In fact, the part of linear behaviour is very small compared with the non-linear one since masonry rapidly enters the non-linear domain. That means cracks appear quite quickly (generally at connections because of stresses concentrations or weak points) and the global structure turns out to be composed of separated components. These are called macro-elements.

In fact, the seismic response of churches consists of analysing the seismic behaviour of each part separately and their interaction rather than an analysis of the structure as a whole. For instance, the interaction between the tower and the front wall can lead to the damage to the latter because of two different seismic responses (see the cases of Santo Stefano a Cesclans and the one of Santo Stefano di Valeriano).

The tower closely interacts with another structural part of the church (with the front wall as seen above, with chancel arch, etc.) due to its different seismic response. It must also be said that even due to their self-weight, bell towers generate vertical cracks in the masonry of the connected parts

(a very frequent case in Swiss churches). These cracks make the parts disconnected even before earthquakes.

4.4.1.2. Front wall

With respect to the front wall, the impact of the shape especially concerns the structural parts, such as gables, that are disconnected from perpendicular structural elements. Since they are restrained only along their base, such structures behave as cantilevers under seismic loading. However, as masonry does not resist (or at small level) tensile stresses, this type of structure can overturn; this is typically what happened to the gable of the church Santo Stefano di Valeriano, the one of the Duomo di Gemona and the one of the Duomo di Venzone too. Nevertheless, no such case has been recorded in Switzerland. The out-of-plane collapse mechanism (overturning) can also happen for the whole front wall; this situation was recorded on the church Santa Maria del Fossale. The presence of abutments can highly reduce the activation of this mechanism (as for the church of the preacher in Basel).

Besides the out-of-plane collapse mechanism, the in-plane failure is also observed on edifices; sometimes, both mechanisms can happen on the same front wall, as, for instance, on the church Santa Maria del Fossale. The failure pattern of this front wall also shows that two close openings (along the vertical) can result in cracking the volume in-between.

Problems are also generated by the connection of two structural components that are structurally different. It is observed that the configuration of a bell-tower put side-by-side with a front wall (connected to or not) can result in cracking the front wall (shear crack) and damaging the bell-tower. This case is recorded on the church Santo Stefano a Cesclans.

4.4.1.3. Lateral walls

On the basis of the observation of damage, lateral walls (either main nave lateral walls and the low-aisles ones) are not particularly seismically vulnerable. However, damage to low-aisles walls is more often recorded than to main nave walls (as the case of the church of the preacher in Basel or the Duomo di Gemona).

In respect to smaller churches (one-nave edifices), out-of-plane damage to lateral walls seems to be due to timber framework (rafters) hammering combined with the presence of openings (Santa Maria del Fossale). On the other hand, the recorded in-plane damage (church in Vaz, in Finhaut and the Our-Lady-of-the-Moor in Sierre) is likely due to the presence of openings.

Furthermore, it is worth noting that lateral walls are often separated from the bell-tower, if there is any beside, before any seismic event.

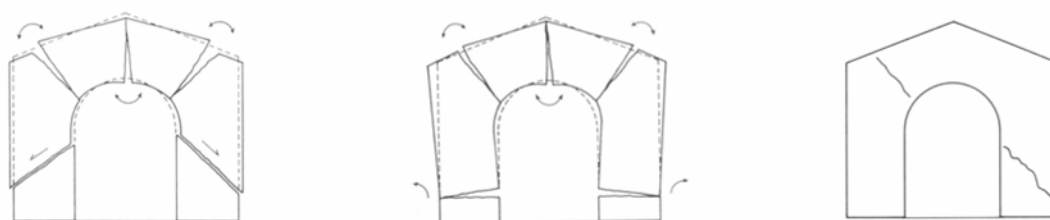
4.4.1.4. Vaults

Cracked or even collapsed vaults is one of the most recorded damage after a seismic event (Church in Conthey, in Chippis, in Sarnen and in Grimetz, for instance). However, it is difficult to draw any conclusions regarding the causes (shape, masonry, state of maintenance, etc.) that led to the cracking or the fall of vaults. Also the fall of vaults does not necessarily happen right after the main shock but often due to aftershocks (church in Plan Conthey or the one in Chippis); this highlights the importance of the initial state, that is the configuration of cracks (number and place), of the vaults.

4.4.1.5. Chancel arch

According to the damage pattern that was observed in the studied sample the structural response under dynamic action of a chancel arch mainly depends on the arch shape (thrust line position) and particularly on the boundary conditions, i.e. if there is an appendix building beside the chancel arch. Note that the structural response was mainly of an in-plane type.

Based on their observations after the Friuli earthquake, Doglioni et al. have set down three damage mechanisms for chancel arches, which are:



Shear mechanism beginning inside the piers and resulting in the enlargement of the distance between opposite piers, finally causing the failure along the upper part of the arch.

Rotation of both piers and formation of five hinges that lead to failure.

Formation of oblique cracks resulting from particular boundary conditions especially along the upper edge of the arch (caused by a cord for instance).

Figure 4.31 : Damage mechanisms set down by Doglioni et al. [Do 94].

The first one was mainly recorded on the «Regular» type of chancel arches (with quite a small opening). The second mechanism has been generally recorded into the «big opening» category.

These collapse mechanisms show the impact of the pier movements on the chancel arch damage; it is important to note that, in Switzerland, such damage mechanisms would rarely occur. In fact, chancel arches are made of an arch (series of voussoirs) that supports the above masonry. Consequently, the apex hinge as shown on Figure 4.31 (on a whole cross-section) would not be created. Instead, the hinge would appear in the arch, which supports masonry, and after reaching the material strength, the voussoir would fall, making the above masonry break down too.

Based on the survey made in the church in Trient, the main arch of the chancel arch could cracked quickly.

4.4.1.6. Apse

The apses of the churches belonging to the sample were cylindrical, polygonal or square. The study of the observed damage leads to conclude that the only mechanism of damage recorded on cylindrical apses was actually a kind of cut by an oblique plane (Figure 4.32). As for the other two shapes, it is difficult to determine exactly whether the shape is a very essential parameter on the dynamic response of the apse.

Nevertheless, the roof structure and the position of openings appeared to have a lot of influence (see the chapter on the impact of constructive details) on the damage following a quake.



Figure 4.32 : Main mechanism of damage of cylindrical apses [Do 94].

4.4.1.7. Bell-towers

In general, damage appeared in the upper parts of bell-towers; this fact was observed both in Switzerland and in Italy. It was noticed, especially in Italy, that windows located at the top of the tower were often at the origin of damage; this case was also observed on the church Lady-of-the-Moor in Sierre and on the church in Visp.

However, the most frequent damage recorded on Swiss bell-towers, in particular in the canton Valais, is the sliding of a masonry part of the spire. Sometimes, there is more than a sliding, as was the case for the church in Chalais where a part of the spire broke down.

Apparently, damage appears where:

- the vertical action (weight) is low, that is, in the upper parts of the tower
- there are windows (in the upper part)
- at the connection with very stiff structural parts such as wide front walls (boundary conditions).

Based on their observations of churches after the Tolmezzo earthquake, Doglioni et al. [Do 94] set down five frequent collapse mechanisms. Except for the 3rd mechanism, they essentially corre-

spond to failures that occurred on dependent towers, i.e. towers whose walls (one or more) belong both to the towers and to one another part of the church. These mechanisms are:

1. Rotation of the upper part of the bell tower around a horizontal axis (flexion).
2. Cyclical movement of the upper part of the tower along one direction or two directions (usually horizontal) (flexion).

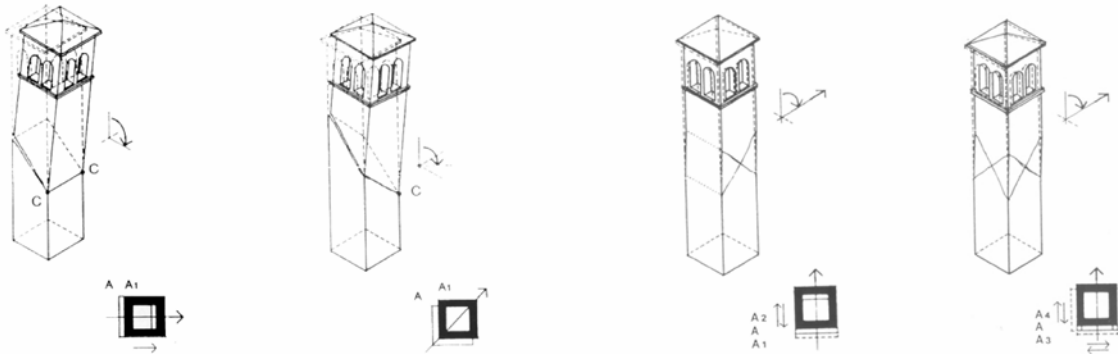


Figure 4.33 : Most frequent damage mechanisms observed on bell-towers by [Do 94] after the Tolmezzo earthquake.

3. Rotation of the structure parts enclosing the cell pillars and the corresponding parts of the tower.
4. Torsion around a vertical axis.
5. Translation of the upper part of the tower.

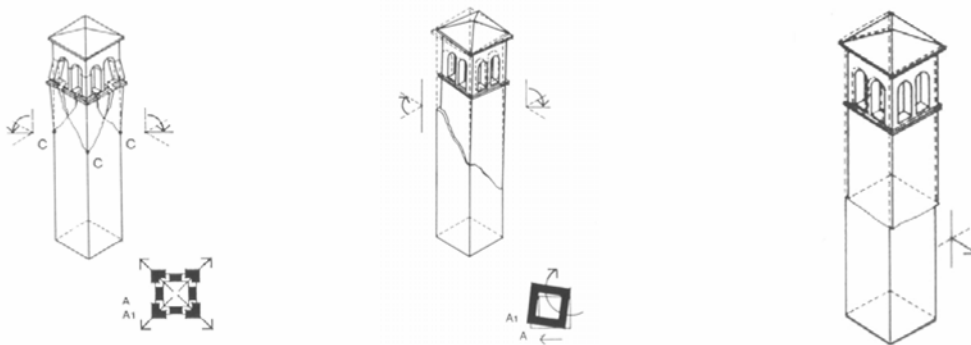


Figure 4.34 : Most frequent damage mechanisms observed on bell-towers [Do 94].

The configuration of openings and the previous damage level (decay, structural transformations, past earthquakes, and so on) of the structure have a high influence on the mechanism types. Moreover, campanile strengthened by metallic ties improve resistance to dynamic actions.

4.4.2. IMPACT OF THE STRUCTURAL CHARACTERISTICS AND CONSTRUCTIVE DETAILS

In the previous chapter, a summary of the observed damage was carried out on each structural component. It appeared that the shape of certain structural elements may have some influence on

the damage, but it was noted that damage may also have its root, and often in a preponderant way, in some unsuitable constructive details, such as masonry type and quality.

4.4.2.1. Influence of the masonry type and wall structure (one-leaf or multiple-leaf)

According to observations, the type of masonry seems to have a certain importance, especially regarding the way and degree of cracking (thin or thick cracks, cracks following the masonry units or not, etc.). Moreover, the wall structure seems to be also highly relevant regarding the structural behaviour of masonry walls.

MASONRY KIND

It is quite difficult to assess the influence of the masonry type on the damage caused by earthquakes on the basis of archive quotations or pictures; moreover, most of the time walls are covered by a roughcast layer that make it even more difficult to have any judgement of the impact of masonry type on the damage. However, it is possible to observe that the cracking was mainly scattered in masonry composed of pebbles while cracks generally followed blocks for ashlar masonry with dressed stones.

However, it seems that the most important factor in the masonry response under earthquake is the inner structure of walls.

WALLS INNER STRUCTURE

Amongst the churches in the studied sample set, there were one-leaf walls and multiple-leaf ones. The first type of fabric is compact enough to behave monolithically. The second type appeared to mainly depend on the kind of masonry of the outer leaves and especially on the connection between every part of the wall. If the connection between the inner core and the outer leaf cannot resist the out-of-plane action (due to the earthquake), a part of the outer leaf might detach from the rest of the wall, as shown in the next picture:

Before the earthquake of May:



After the earthquake of May:



Figure 4.35 : Detachment of a part of masonry belonging to the outer leaf wall caused by the earthquake (Duomo di Venzone).

According to [Do 94], walls with a core made with lime have their inner and outer parts better connected to each other than those with a core of non-cohesive material. There are indeed fewer cases of detachment of the fabric belonging to the outer part of such walls.

In the church of Santo Stefano a Cesclans and the church Santo Stefano di Valeriano, the leaves of the apse walls separated during the earthquake. The outer part of these walls was actually made up of small stones surrounded by a small quantity of mortar. This resulted in a weak connection that appears to be at the origin of the damage mechanism.



Figure 4.36 : Separation of the parts belonging to the structure of the apse wall (S.Stefano di Valeriano) [Do 94].

Obviously, the slender the wall is, the higher is the probability of a detachment of a part of the outer leaf. Moreover, the detachment of a part of the wall leads to not only the expulsion of a few stones but also a loss of stiffness. This in turn might promote or even activate a mechanism of failure.

4.4.2.2. Influence of the walls configuration (openings, etc.)

The vulnerability of the walls seems to also depend on the link to the structural orthogonal elements, the presence of openings, discontinuities (masonry discontinuities (openings), corners), etc.

CORNERS

Quality of the connection between two orthogonal walls is of prime importance. In fact, the stronger the connection is, the better is the resistance of the connected out-of-plane loaded wall.

A good connection is provided either by a good interconnected masonry (of both orthogonal walls) or the presence of tie-rods.

When two perpendicular walls with different quality of masonry are connected, fractures were observed along the exact change of masonry as was the case of the church Santa Maria del Fossale (Figure on the right).



Figure 4.37 : Santa Maria del Fossale: crack between the front wall and the lateral wall mainly due to the difference in masonry and the out-of-plane motion of the front wall [Do 94].

Large and well dressed quoins (a case actually often observed in the campaniles) seemed to improve the tie between two orthogonal walls. On the other hand, they might sometimes behave like pillars after being separated from the rest of the fabric.

OPENINGS



It appeared that every kind of openings (oculus windows, half oculus, gothic windows, baroque windows (square shaped), door), promotes cracks formation around them when the walls, which encompasses them, are struck by an earthquake.

The fracture type (size, length, angle, etc.) depends on the structure configuration (distance and area between openings, etc.).

The distance between windows (as the case of the church Our Lady of the Moor), between a door and a window appeared to be also important (Santa Maria del Fossale).

Figure 4.38 : Bell-tower of the church Our-Lady-of-the-Moor in Sierre (Source: Le Nouvelliste, 30.01.1946).

In the next pictures it is quite easy to see the impact of openings as the fracture started from openings and sometimes even ran along them:

Sta Maria delle Grazie (Gemona) before May 1976



Sta Maria delle Grazie after May 1976



Figure 4.39 : Two pictures of the same church taken before and after the main seismic shock of May 1976 [Do 94].

4.4.3. IMPACT OF THE CONNECTION BETWEEN THE ROOF STRUCTURE AND WALLS

The timber structure belonging to the studied churches were generally composed of transversal timber trusses put on lateral walls. The roof covering was generally laid on a series of parallel purlins that were fixed to the rafters.

It is observed that the connection between the front wall and the roof structure do not often exist amongst the analysed churches. Also, trusses are not laterally braced; the purlins are often the only transversal elements.

Timber frameworks are often simply laid on lateral walls; however, main beams are sometimes embedded in the wall masonry. As shown in the picture to the right, this type of connection can damage the upper part of the walls (local damage).

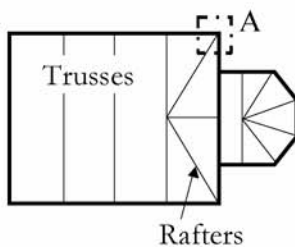


Figure 4.40 : Walls hammered by roof rafters [Do 94].

However, if the trusses are not well connected to the vertical structure, they might hammer the latter. To reduce damage, the components of timber frameworks should be well connected to each other; on the basis of the observations, any tight connection between the timber framework and walls generates damage to the structure.

When the connection between the timber framework components is loose or even non-existent (as is sometimes found in apses), their movement can result in large damage (case of the chapel in Visperterminen).

Plan of the roof structure:



Damage at the corner [A]:



Oblique rafters without horizontal ties generally result in activating out-of-plane mechanisms of damage or a detachment of a part of masonry (by thrust) (see Figure 4.41).

Figure 4.41 : Damage caused to a corner of a church due to the thrust from a roof rafter.

4.4.4. IMPACT OF THE STRUCTURAL TRANSFORMATIONS

The main structural transformations carried out on cultural heritage edifices are:

1. Enlarging of the church: widening and/or lengthening of the nave and the apse with partial or complete enclosing of the pre-existing structures into the new construction,
2. Raising of the church and the bell tower,
3. Enlargement of the edifice by adding appendix buildings such as sacristies and chapels,
4. Complete architectural and functional reorganization; for instance: change of the entrance place,
5. Opening or filling of windows.

As it is difficult to ensure a good connection between the structural elements of an old construction and a new one, a transformation of the fabric generally constitutes a discontinuity within the

edifice. The impact of such discontinuities on the seismic vulnerability depends on their place within the structure and on the type of forces that transfer through it.

The structural element including a discontinuity will show a different cracking pattern than if there were no cracks. These usually occur where the material is no longer able to resist the forces due to the outer action. Discontinuities constitute supplementary weak parts within the structure and these alter the configuration of cracks compared to a situation without any discontinuities.



Figure 4.42 : Impact on the damage, following an earthquake, due to the adjunction of an appendix (Duomo di Venzone) [Do 94].

4.4.4.1. Transformations carried out to improve the seismic performances of edifices

According to [Do 94], the structural transformations may be divided into two groups:

1. Transformations using traditional techniques (like metallic ties)
2. Transformations based on modern techniques of construction

TRANSFORMATIONS USING TRADITIONAL TECHNIQUES

The main traditional technique that was applied is the metallic link. This denomination includes metallic bars, angular nails (cramps), pins, etc.

A vertical crack crossed a campanile alongside one of its corners (Figure 4.43); this was supposed to have appeared after the earthquake of 1928 [Do 94]. It was restored by means of metallic cramps that should tight the parts separated by the crack. The main seismic shock occurred in may 1976 caused the same kind of cracking pattern as the seismic event of 1928 but the split was situated just few decimetres from the previously repaired crack.



Figure 4.43 : Formation of a crack parallel to the pre-existing fracture caused by a previous earthquake in 1928 (San Marino ad Artegna church) [Do 94].

Two bell towers were transformed at the same time (raising of the tower and filling up the previous cell windows). Only one of the towers was strengthened by metallic ties. After the main seismic shock, the reinforced bell tower was still standing while the other (Figure on the left) collapsed at the cell level because of the discontinuity resulting from the openings of the previous cell^a.

Figure 4.44 : Unreinforced and reinforced bell towers after the main seismic shock of May 1976 [Do 94].

Without ties (Santo Stefano a Nimis):



With ties (Duomo di Tolmezzo):



a. This comparison shows the difference (relative and not absolute, since the peak ground acceleration was certainly not the same) in seismic vulnerability between a reinforced bell-tower and an unreinforced one.

The bell towers were not the only structural elements to be reinforced; many front walls were repaired and reinforced as they also experienced serious damage caused by earthquakes.

Tie-rods were often put at corners in order to reinforce the tower; on the basis of the observations carried out after earthquakes, this technique has proven to be effective.

Another method that has often been used through centuries is simply the reparation (or maintenance) of masonry with mortar. This keeps the components of masonry well connected to each other and as aforementioned, a compact masonry has a better resistance than a loose one.

This technique was improved in the end of the 20th c.: instead of putting mortar on walls sides, it was directly injected into masonry. According to observations, this approach enhanced the fabric cohesion and then, the seismic vulnerability of the so-reinforced walls.

TRANSFORMATIONS USING MODERN TECHNIQUES

Amongst modern techniques, there is mainly the seismic strengthening by a cord of reinforced concrete. This technique, which was particularly applied in Italy since the 50's proved to be inefficient and increases the damage to cultural heritage buildings. As it has not been applied in Switzerland, its impacts are not discussed in the present report.

4.4.5. IMPACT OF THE MASONRY STATE OF MAINTENANCE

With time, masonry suffers the meteorological actions such as bad weather (rain and wind), thermal cycles, freezing and thawing cycles, etc. All these actions account for the decay of masonry and especially of sedimentary rocks. Note that the stones may also have been biologically affected (by any kind of vegetation (lichens)).

On the other hand, structural problems, such as soil settlements, also damage the structure, especially by causing cracks.

4.4.5.1. Impact of decay

Although it is currently well known that the decay of stones or masonry may highly weaken their stiffness and resistance (masonry is less compact), it is difficult to clearly establish to what extent it has an influence on the damage observed on a church. Moreover it is actually impossible to assess it in the observed cases since the state of decay of the churches before the considered seismic event is unknown. Even with pictures taken before the earthquake, it is difficult to clearly see in which state of decay the masonry was before the event.

Like masonry, the wood decay of the roof structure is also difficult to analyse. The problems with wood are generally situated within the support area. As the beams are generally put inside the walls and as masonry lets water seep into the wall, the wood might then easily rot.

4.4.5.2. Impact of pre-existing cracks

The impact of pre-existing cracks on the damage resulting from a seismic event is only visible with the studied sample in Italy because pictures were taken after the main shock and also after the second main shock.

Observations showed that the impact of pre-existing damage or cracks is very important and may be the most relevant one compared to the other factors that might affect the seismic vulnerability of cultural heritage buildings under seismic actions. This fact is illustrated by the following pictures of the Duomo di Gemona: it showed large cracks in the webs of the apses vaults before the main seismic shock and the ceiling fell down during the earthquake (Figure 4.45).

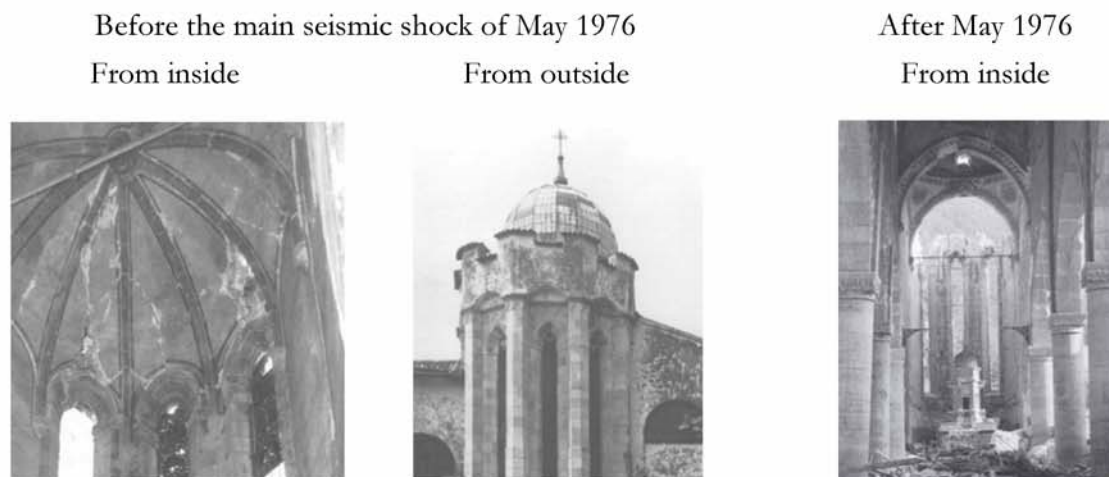


Figure 4.45 : Views from in- and outside of the apse of the Duomo di Gemona, before and after the main seismic shock of 1976 [Do 94].

Combined with the loss of resistance in walls, the decay of masonry that resulted in separating the fabric into masonry areas influenced a lot the mechanisms of failure and damage. The change of failure mechanism seems to have occurred when the masonry was particularly dislocated.

Moreover, it is important to keep in mind that once a crack exists in masonry, it won't disappear.

4.4.6. IMPACT OF THE FOUNDATIONS AND SOIL QUALITY

The impact of foundations on damage resulting from an earthquake is very difficult to assess on the basis of pictures of short surveys. Therefore, no conclusions can be made on this topic.

On the contrary, the effect of the soil quality could be qualitatively assessed with observations made on the church Our Lady of the Moor in Sierre. When compared with other buildings, the damage observed on this church after the 1946 earthquake is particularly severe. This may be due to the structure of the church but it is clear that the bad quality ground (alluvium) on which the church was erected is somehow also responsible for the high level of sustained damage.

4.5. CONCLUSIONS

Observations of damage recorded on cultural heritage buildings after earthquakes lead to the conclusion that, at first, a church under dynamic loading does not behave like a monolithic structure but rather like a set of walls (or macro-element [Do 94] that actually are structural elements) more or less strongly tied together. In fact, the roof structure and the ceiling do not play a role of diaphragm (as the concrete slab does in common buildings); it is generally not advisable to consider a monolithic structural behaviour of edifices.

Furthermore, a few other parameters are also important for the damage to a church loaded by seismic waves. The type of masonry, that is, one-leaf walls or multiple-leaf walls, ashlar masonry or loose masonry, for instance, also play a role. For instance, it has been noticed that multiple-leaf walls can be seismically vulnerable out of their plane. Regarding the type of masonry, a masonry with dressed-stones will probably better resist actions in its plane than a masonry with pebbles. Besides, the shape of structural elements, the type of openings and the distance in-between can be of importance especially with respect to the in-plane loading. Another prevalent factor is the pre-existing damage because it may influence a lot the damage mechanisms (chapel in Visperterminen).

Apart from the edifice structure, the soil properties can increase the seismic waves by increasing the peak ground acceleration that strikes the edifice (Our-Lady-of-the-Moor church).

Finally, it must be pointed out that the evolution of damage is highly influenced by the duration of the seismic event.

5.1. INTRODUCTION

In this chapter, readers are presented the application of existing methods, which have been developed since the middle of the '90s, that allow us to assess the seismic vulnerability of cultural heritage buildings and more specifically of churches. Four methodologies are popular today in Europe; other continents have not developed such kinds of methodologies or they have not been published.

All available methodologies nowadays could be gathered into four groups according to their basis:

- statistical methodologies, based on damage statistics
- structural methodologies, based on engineering models
- probabilistic methodologies, based on probabilities
- hybrid methodologies, that merge two or more of the above mentioned methodologies

Almost every methodology applied to assess the seismic vulnerability of churches is actually a hybrid methodology. In general, they contain several levels that are characterized by an increasing accuracy regarding either the input or the output.

The first step is generally about basic information, that is, the name, the location, etc. of the given building; according to its architectural typology, the building is given a vulnerability value (index) from statistical data. The second step usually deals with an assessment of the seismic vulnerability; at this stage of the study, only simplified calculation methods are applied. The last step, which is not necessarily undertaken in every case, deals with the given building in a more accurate way, i.e. by using sophisticated mechanical models.

5.2. EXISTING METHODOLOGIES FOR UNIQUE EDIFICES

Amongst existing methodologies, one is based on a collection of three indices (Lourenço et al.(2006)) while the other three other are hybrid methodologies (Risk-UE (2004), Lagomarsino et al. (2006) and Augusti et al. (2002)). In these three methods, seismic vulnerability is assessed through different levels of increasing refinement; the first level is generally typological, i.e. that the index depends on the architectural typology of the given buildings, and on damage recorded after earthquakes that happened in the past. Through the other levels, seismic vulnerability is assessed more accurately by usually using structural models or numerical models (e.g. Finite Element Method).

These four methodologies have been applied to two cultural heritage buildings: the chapel in Visperterminen (in ruins today) and the collegiate church of Valère. These buildings were chosen because they were moderately damaged or even destroyed by earthquakes (case of the chapel in Visperterminen); the observation of damage gives the opportunity to compare the results obtained by the application of the already existing methodologies with reality.

5.2.1. LOURENÇO'S METHOD

This method has been developed by the working group at the University of Minho, Portugal (P.B. Lourenço) [LR 06].

The developed methodology is based on the fulfilling of a check-list for each church. The form contains on one hand a statement of general characteristics (inventory) as the national classification, the period of construction, a brief description of the structure and also a few words about possible damage due to earthquakes that occurred in the past. On the other hand, it also contains a more technical part with indices (ratios between dimension values describing the structure) and other key structural features. Following indices have been defined:

- index 1: in-plane area ratio
- index 2: area to weight ratio
- index 3: base shear ratio

The other key structural features are:

- the presence or absence of a vault, its type (barrel vault, rib-vault, etc.) and its geometrical dimensions
- data for columns (height, diameter, etc.)
- data for perimeter walls

Finally, the last element is the seismic loading (for index 3).

5.2.1.1. Index 1: In-plane ratio

This first index $\gamma_{1,i}$, which is associated with the base shear strength, is the ratio between A_{wi} the area of the earthquake resistant walls in each main direction and S the ground surface of the buildings.

$$\gamma_{1,i} = \frac{A_{wi}}{S} \quad [-] \quad (\text{EQ 5.1})$$

In cases of high seismicity, a minimum value of 10% is recommended for historical buildings [LR 06].

Note: index 1 ignores the wall slenderness and also the mass of the construction. Moreover, after EC 8, walls are considered as earthquake resistant if the thickness is larger than 0.35 m and if the height-thickness ratio is smaller than 9.

5.2.1.2. Index 2: Area to weight ratio

The second index $\gamma_{2,i}$ is the ratio between A_{wi} the in-plane area of the earthquake resistant walls in the i direction and G the total weight of the construction.

$$\gamma_{2,i} = \frac{A_{wi}}{G} \quad [\text{m}^2/\text{MN}] \quad (\text{EQ 5.2})$$

This index corresponds to the horizontal cross-section of the building per unit of weight.

In cases of high seismicity, a minimum value of 1.2 m^2/MN is recommended for historical masonry buildings [Me 98] in [LR 06].

5.2.1.3. Index 3: Base shear ratio

The base shear ratio provides an indication of the shear strength of the building. The seismic demand is simulated by an equivalent static force: $F_E = \beta \times G$, where β is an equivalent seismic static coefficient related to the design ground acceleration.

The shear strength of the structure comes from the contribution of all earthquake resistant walls $F_{Rd,x \text{ or } y} = \Sigma A_{wi} \times \tau_S$, where τ_S is the material shear strength. According to EC 8 and based on Coulomb's law, $\tau_S = c + 0.4\sigma_n$, where c is the cohesion and $\tan\varphi$ is equal to 0.4 ($\varphi=22^\circ$; defined in the EC 8). The normal stress in the walls is assumed to be only due to self-weight.

The third index is the ratio between the shear strength of the structure and the seismic demand:

$$\gamma_{3,i} = \frac{F_{Rd,i}}{F_E} \quad [-] \quad (\text{EQ 5.3})$$

If the cohesion c is assumed to be zero, the index then becomes:

$$\gamma_{3,i} = \frac{A_{wi}}{A_w} \cdot \frac{\tan\varphi}{\beta} \quad [-] \quad (\text{EQ 5.4})$$

Where:	$\gamma_{3,i}$	third index in regard to the direction i
	A_{wi}	plan area of earthquake resistant walls in the direction i
	A_w	ground surface of the earthquake resistant walls of the given building
	φ	internal angle of friction
	β	equivalent seismic static coefficient related to the design ground acceleration

To ensure the safety, $\gamma_{3,i}$ must be greater than 1.

5.2.2. RISK-UE

The methodology developed for the assessment of the seismic vulnerability of cultural heritage buildings within the framework of Risk-UE (2004), is based on two stages of increasing refinement [La1 04], [La4 04]:

- Level 1: based on typological and statistical studies of the observed vulnerability; this index gives a qualitative value of the vulnerability of a given edifice.
- Level 2: analysis through more refined mechanical models of single parts of a given building; this index is defined through a capacity curve.

The Risk-UE methodology was developed for all kinds of cultural heritage buildings, such as palaces, monasteries, castles, churches, oratory/chapels, theatres, towers, urban walls, bridges, chancel arches, obelisks and statues.

5.2.2.1. Level 1

In this level, poor data is used. Consequently, results are of typological nature and the information about the seismic vulnerability is simply connected to the kind of edifice.

The model for the assessment of the seismic vulnerability at level 1 is based on the capacity curve of its typological group. Each capacity curve has been defined through statistics on one hand and an analogical basis on the other hand [La4 04]. Statistically, Lagomarsino et al. were able to define DPM (Damage Probability Matrices) thanks to the numerous damage surveys (1976 in Friuli, 1997 in Umbria and Marches and 2002 in Puglia and Molise earthquakes) they had at their disposal. These matrices provide the distribution of damage levels of given typologies and for diverse seismic intensities. In other words, vulnerability curves for each building category are characterized by a vulnerability index V_i^* and a coefficient of variability β (the typologies definition is based on the EMS-98). Cathedrals and medium-size churches are not included within the church typology.

The index value is based on the typology to which a given edifice belongs. Furthermore, the obtained value V_i^* is then corrected through modifier scores that are correlated to factors (see Appendix A.3.1), such as the state of maintenance, material quality, symmetry of the structure and constructive characteristics: $V_i = V_i^* + F_c$. The value ranges of V_i (between V_i^- and V_i^+) for each typology are given in Table 5.1 (taken from [La4 04]):

Table 5.1: Value ranges for each typology [La4 04]

Typology	V_i^-	V_i^*	V_i^+	κ
Palaces/ buildings	0.496	0.616	0.956	2.3
Monasteries	0.616	0.736	1.076	2.3
Castles	0.356	0.456	0.766	2.3
Churches	0.77	0.89	1.26	3
Chapels/ oratories	0.65	0.77	1.14	3
Mosques	0.67	0.73	0.94	2.65
Theatres	0.616	0.736	1.086	2.65
Towers	0.636	0.776	1.136	2.3
Bridges	0.216	0.296	0.566	2.3
Walls	0.396	0.496	0.746	2.3
Chancel arches	0.376	0.456	0.706	2.3
Obelisks	0.396	0.456	0.746	1.95
Statues/ fountains	0.236	0.296	0.606	1.95

Where: V_i^* average of the vulnerability index
 V_i^+ average value and maximal standard deviation
 V_i^- average value diminished by the maximal standard deviation
 κ parameter that controls the slope of the curve; given in [La4 04].

According to Risk-UE [La4 04], the average vulnerability index of churches is equal to: $V_i^*=0.89$; this index was determined on the basis of a large data base of damage recorded after seismic events occurred in the past, especially in Italy.

Once the vulnerability index is determined, the mean damage grade (according the EMS-98 scale) can be calculated with the following equation that was developed by Sandi (1994):

$$\mu_D = 2.5 \cdot \left[1 + \tanh\left(\frac{I + 6.25 \cdot V_I - 13.1}{\kappa}\right) \right] \quad [-] \quad (\text{EQ 5.5})$$

Where: μ_D mean damage grade
 V_I vulnerability index
 I EMS-98 intensity
 κ parameter related to the typology

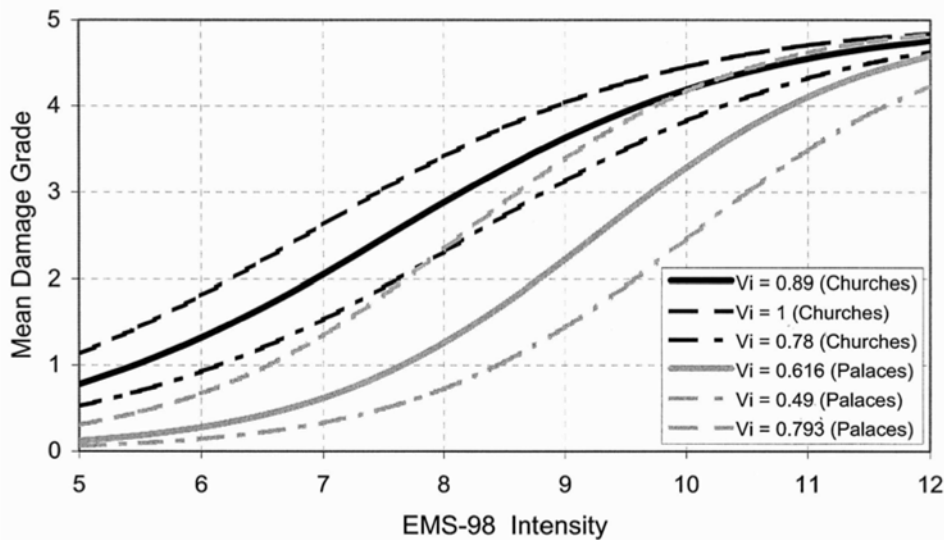


Figure 5.1 : Mean Damage Grade in function of EMS-98 Intensity; taken from [La4 04].

5.2.2.2. Level 2

Unlike level 1 for which the seismic vulnerability of a given edifice is based on the vulnerability curve of its typology, it is based on its capacity curve in the level 2.

finding a capacity curve that describes the global seismic response of a church is infeasible. According to [La3 04], churches are composed of diverse parts that behave independently under seismic actions. These structural parts are called macro-elements and for each of them a capacity curve has to be determined.

The capacity curve can be defined either by simple or by complex models. Amongst simplified methods, there is the equilibrium limit analysis. Non-linear analysis is listed under sophisticated methods.

EQUILIBRIUM LIMIT ANALYSIS

The equilibrium limit analysis is often applied to masonry by considering it as a rigid body with no tensile strength. The seismic load is usually simulated by a horizontal static force that is proportional to the structural mass. In consequence, the multiplier for the mass when the structure collapsed is also only the spectral acceleration.

This approach is based on the observation of the real behaviour of masonry structures [La3 04]. Though they generally have small elastic deformations, rotations and large displacements are also possible because of cracks.

The method has the following steps:

1. Overview of the structure (dimensions and structural study)
2. Identification and selection of the macro-elements that will be analysed
3. Listing of the potential collapse mechanisms and selection of the ones to be analysed

-
4. Analysis of the chosen macro-elements for the most likely collapse mechanisms
 5. Definition of the capacity curve for each analysed macro-element.

For further information, refer to the next method, that is Lagomarsino's method. In fact, while the original Risk-UE method was published in 2004 by Lagomarsino et al., it has since been refined.

5.2.3. LAGOMARSINO'S METHOD

According to Lagomarsino et al. [La1 04], an analysis of the seismic vulnerability of monumental buildings at a territorial scale has to be partially based on a typological classification (statistical approach). They make exceptions for certain famous buildings that require more refined models.

The proposed methodology is organised on three levels of progressively increasing accuracy.

- Level 1: based on data obtained from damage observed after earthquakes on diverse typologies of buildings; the seismic input is the macroseismic intensity,
- Level 2: is the analysis of a single part of the structure (macro-element), considering simplified mechanical models that are suitable at a territorial scale; the seismic response (capacity curve) is then compared with the capacity spectrum corresponding to the shaking event taken as a reference for a given region.
- Level 3: based on the use of more refined models than at level 2; the seismic demand is expressed by the capacity spectrum method.

5.2.3.1. Level 1

The first level is based on the attribution of a vulnerability index V_i^* for a given building. It is defined on the basis of the building typology and refined through behaviour scores related to a few characterizing parameters such as the maintenance state, the material quality or the structural regularity.

For further information, refer to the previous chapter about the Risk-UE method.

5.2.3.2. Level 2

The second level of Lagomarsino's method is based on the application of the Equilibrium Limit analysis that provides indeed a reasonably adequate description of the damage mechanisms in masonry structures. However, it must be kept in mind that the use of these models is based on the following assumptions:

- masonry is considered as a rigid body,
- masonry has no tensile strength.

In this level, the equilibrium analysis is applied on the so-called macro-elements. From the systematic survey carried out by Doglioni et al. [Do 94] on the churches damaged by the 1976 Friuli earthquake, it is observed that the seismic response of churches could be described as a combination of the recurrent behaviour of different structural parts each of which shows an almost autonomous structural behaviour. These structural parts are called macro-elements. It is worth noting that this method is *a priori* unsuitable for the analysis of complex buildings whose elements are highly interconnected.

As aforementioned, since it is assumed that macro-elements behave independently from each other, it is incorrect to characterize the global behaviour of the church using one capacity curve. Instead, a capacity curve must be defined for each macro-element. The capacity curves are analytically defined through the application of the Limit Equilibrium analysis. The upper bound theorem is applied to masonry that is assumed to be an assembly of rigid blocks, which are held together by forces of compression and liable to crack when tensile stresses appear. This assumption is true according to what has been observed on site after earthquakes.

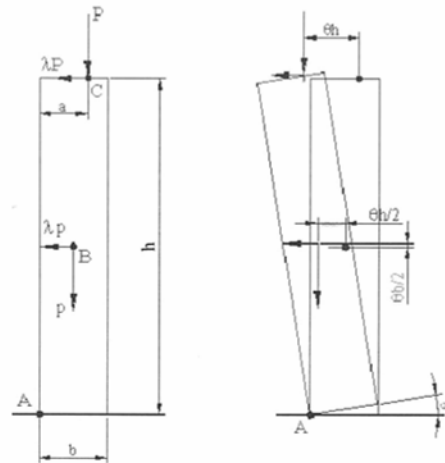
The earthquake is simulated as a horizontal static force proportional to the structure mass. The multiplier is the spectral acceleration; this is a single degree of freedom model. This multiplier is representative of the seismic coefficient because it can be assumed that inertial actions, which are dynamically amplified by the response spectrum, are proportional to the masses [LPR 02]. Once a set of potential collapse mechanisms is identified (which also means that the structure can be considered as a chain of rigid body connected to each others), the next step is to find the effective collapse multiplier that is, in case of the upper bound theorem, the smallest value of the calculated multipliers. The effective collapse multiplier determines an admissible stress state in the whole structure. In case of masonry, there must be no tension along the section.

Applying the theorem of virtual work, the work of every load acting on the wall under seismic actions is:

$$\lambda p \cdot \theta \frac{h}{2} + \lambda P \theta \cdot h - p \cdot \theta \frac{b}{2} - P \theta \cdot a = 0 \quad (\text{EQ 5.6})$$

$$\Rightarrow \lambda = \frac{(pb/2 + Pa)}{(ph/2 + Ph)}$$

Figure 5.2 : Calculation of the collapse multiplier of a wall restrained at one extremity.



Lagomarsino et al. has defined the capacity curve of each macro-element through the determination of five parameters that characterize five limit states defined in the 98-EM scale. These five parameters are:

- Limit state 1 (no damage) is defined by: $S_a = 0.7\lambda$
- Limit state 2 (slight damage) is defined by: $S_a = \lambda$
- Limit state 3 (moderate damage) is defined by: $S_d = 1/8 S_u$
- Limit state 4 (extensive damage) is defined by: $S_d = 1/4 S_u$
- Limit state 5 (complete damage) is defined by: $S_d = 1/2 S_u$

Where: λ | collapse multiplier
 S_d | spectral displacement

S_a	spectral acceleration, that in the case of rigid blocks is equal to the peak ground acceleration
S_u	described as the ultimate horizontal displacement of the gravity centre

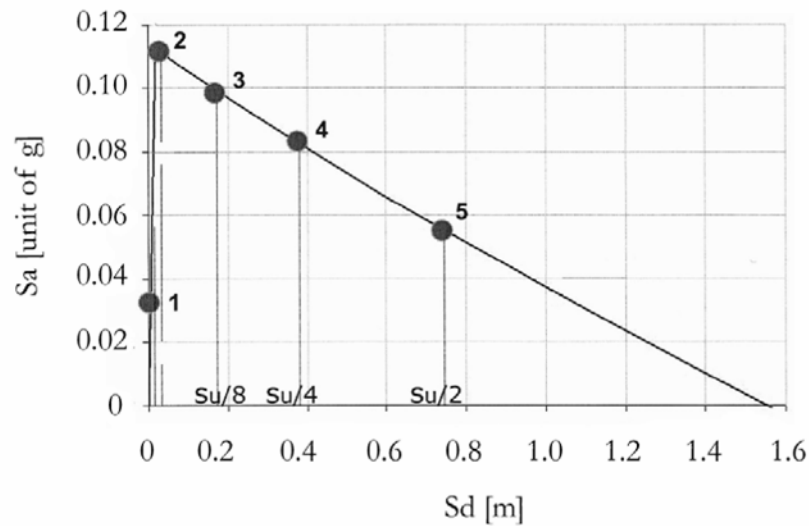


Figure 5.3 : Capacity curve with the damage limit states [La4 04]

The seismic vulnerability is then evaluated through the Capacity Spectrum Method: the damage scenario is defined by the intersection (performance point) between the capacity curve and the response spectrum. It is worth noting here that before comparison between the seismic demand and the macro-element seismic response, the suitable capacity spectrum has to be defined (regarding the damping value to be chosen).

LIST OF THE MACRO-ELEMENTS

The macro-element approach was developed by Doglioni et al. [Do 94], after they surveyed the damage on churches after the 1976 Friuli earthquake. The next figure shows the identified macro-elements.

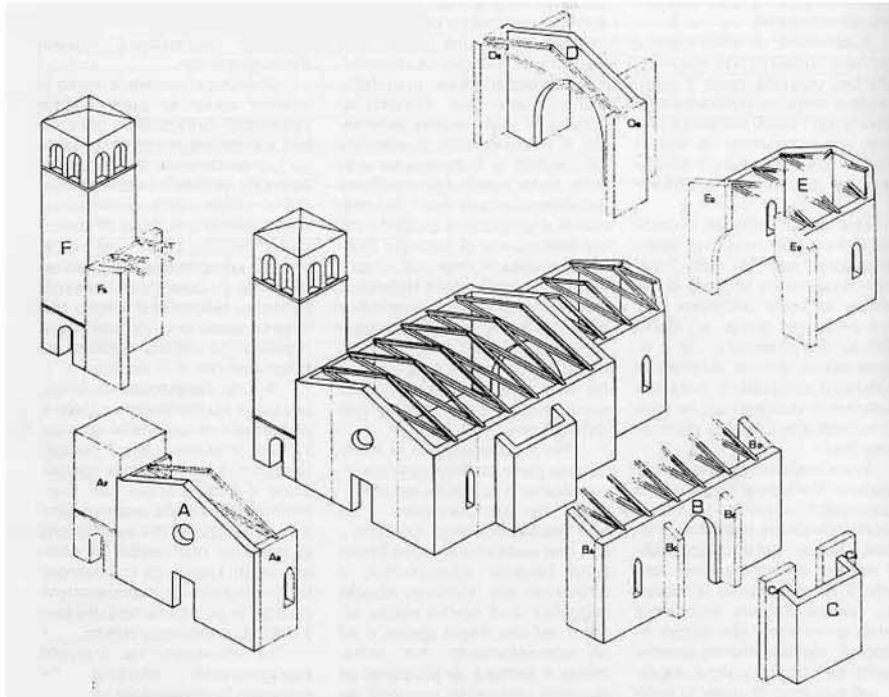


Figure 5.4 : Macro-elements that were identified by Doglioni et al. [Do 94].

Legend: A	Macro-element: main facade (front wall)
B	Macro-element: lateral walls; nave
C	Macro-element: lateral chapel
D	Macro-element: chancel arch
E	Macro-element: apse
F	Macro-element: tower/ bell tower

1. Front wall

This macro-element does not only correspond to the main facade of a church but also to the facade of the transept.

Figure 5.5 : Sketch of a facade (front wall).



2. Nave, lateral walls

According to Lagomarsino et al. [LPR 02], in case of a long nave (4 bays and more), it can be assumed that the central bay is no longer subject to the edge effects due to the front wall or the

chancel arch/ transept. Consequently, it is possible to analyse it as an independent part that is to say as a macro-element. The following diagrams are taken from [La 06]:

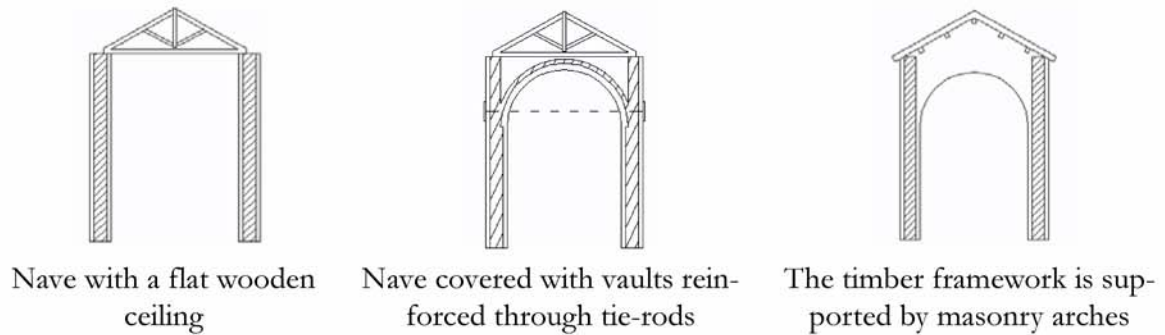


Figure 5.6 : Sketches of the nave macro-elements.

3. Chancel arch

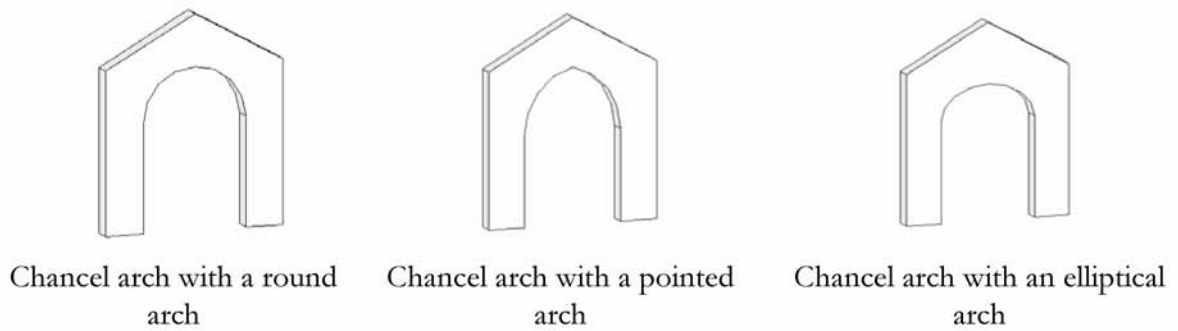


Figure 5.7 : Sketches of the chancel arch macro-elements.

4. Apse

The listed typologies in [La 06] are:

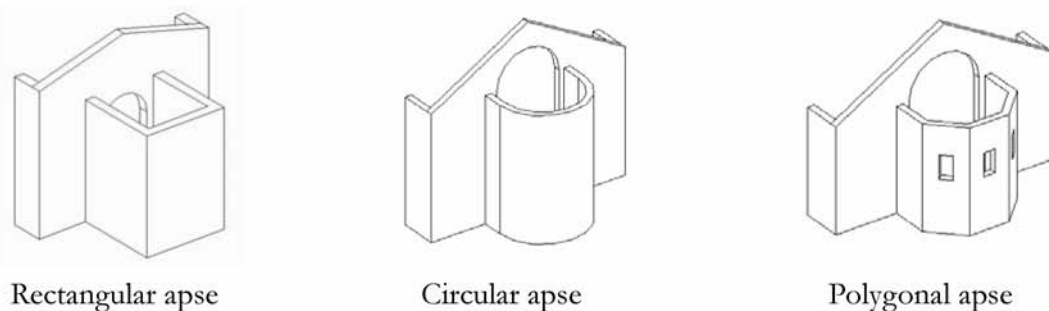


Figure 5.8 : Sketches of the apse macro-elements [La 06].

5. Tower, bell-tower

Towers with a rectangular ground surface are allowed; the top of the model is composed of a kind of cell (*cella* in Italian) and a small four-slope roof.

LIST OF THE OBSERVED COLLAPSE MECHANISMS

The following 18 possible collapse mechanisms have been identified from the damage observation after earthquakes. This approach allows the development of a classification based on the architectural styles, the age and the regional particularities (due to technical or cultural know-how). Moreover, Lagomarsino et al. have written in [La2 04] that a clear similarity was found in the seismic behaviour of churches all over Italy.

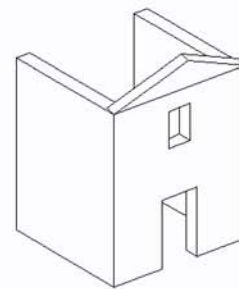
1. Front wall

Due to seismic loads, the front wall is subjected to out-of-plane actions as well as shear forces (in-plane actions). The following collapse mechanisms were observed by Lagomarsino et al. after seismic events in Italy.

A. Out-of-plane collapse mechanisms

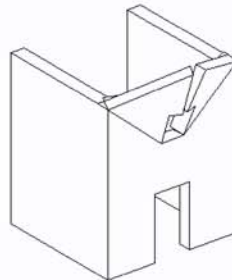
1. Gable overturning around horizontal yield-line

The gable overturns. To find the collapse multiplier λ , it is assumed that the gable behaves as a rigid body.



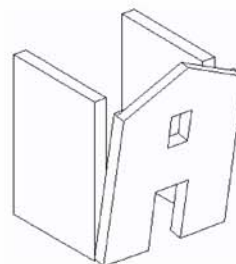
2. Tympanum overturning through oblique yield-lines.

The front wall upper part overturns through the creation of oblique yield-lines.



3. Overturning of the whole front wall

The front wall completely overturns through the creation of a horizontal yield-line at the basis.

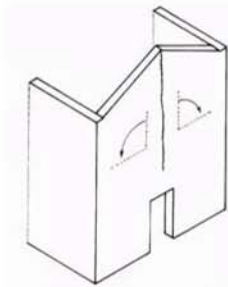


Note: the pictures on the right are taken from [Do 94]; church in the Friuli region after 1976. The small sketches are taken from [La4 04].

Figure 5.9 : Sketches of the out-of-plane collapse mechanisms of the macro-element «front wall».

B. In-plane collapse mechanisms

1. Shear collapse mechanism through the creation of a vertical crack.



2. Shear collapse mechanism through the creation of an oblique crack.

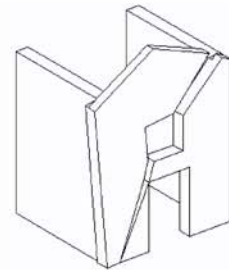


Figure 5.10 : Sketches of the in-plane collapse mechanisms of the macro-element «front wall».

2. Nave/ lateral walls

Only the transversal seismic response of the nave is treated with the Limit Equilibrium analysis.

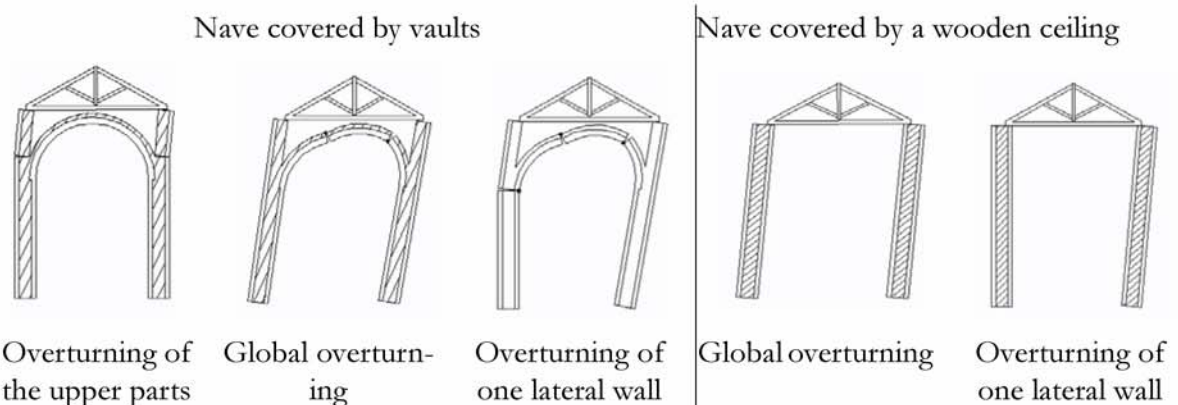


Figure 5.11 : Sketches of the collapse mechanisms of the nave (lateral mechanisms).

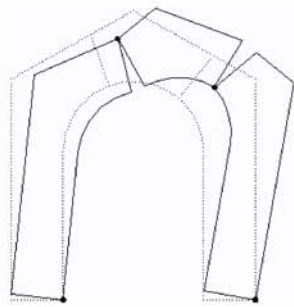
3. Chancel arch

Chancel arches collapse mainly in their plane. However, this collapse mechanism is possible only if the church is not completely surrounded by other buildings.

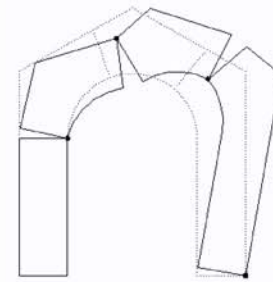


Figure 5.12 : Damaged chancel arch [Do 94].

Collapse mechanisms:



Two-pier overturning

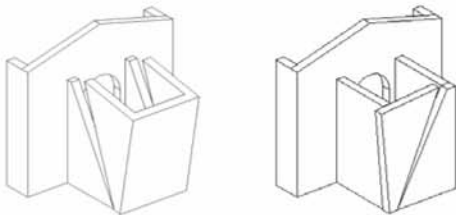


One-pier overturning

Figure 5.13 : Sketches of the in-plane collapse mechanisms of the chancel arch.

4. Apses

Collapse mechanisms for rectangular apses



Collapse mechanism for a cylindrical apse



Collapse mechanism for a polygonal apse

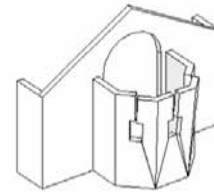
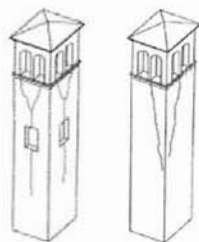


Figure 5.14 : Sketches of the out-of-plane collapse mechanisms of the macro-element «apse».

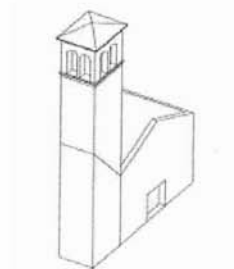
5. Towers, bell-towers

Creation of cracks at the interface between the cell and the main body of the tower



Two-pier overturning

Creation of cracks at the interface between the main body of the tower and the nave



One-pier overturning

Figure 5.15 : Sketches of the collapse mechanisms of the macro-element «bell-tower».

5.2.3.3. Level 3

At this level, the capacity curve is calculated through the use of more refined methods such as the FEM (Finite Element Method) or non-linear structural models. Non-linear methods give the pos-

sibility of more precisely taking into account the real masonry behaviour as, for instance, the stiffness degradation and the tensile behaviour of the material.

5.2.4. AUGUSTI'S METHOD

Augusti's method is, like Lagomarsino's and the Risk-UE method, based on the approach by macro-elements. As in many analyses of the seismic behaviour of masonry structures, he proposed the use of quasi-static loads. Augusti shows how, assuming appropriate probabilistic properties of the relevant quantities and a logical diagram, which describes the relation between the collapse of the macro-elements and the whole building, the probability of collapse and damage of each macro-element and then of the whole building can be calculated under given horizontal loads [Au 01]. Furthermore, calculations are also based on the upper bound theorem of the Limit Equilibrium analysis (structural components behave as rigid bodies).

The procedure proposed by Augusti et al. to assess the seismic vulnerability of churches is constituted by the following steps:

- evaluation of the collapse probability for each macro-element and then for the whole church
- evaluation of the probability distribution of damage for each macro-element and then for the church.

5.2.4.1. Evaluation of the probability of collapse

Under seismic actions, the structure is assumed to be loaded by vertical (W) and quasi-static horizontal loads αW . The coefficient α , which is the ratio between horizontal and vertical loads, is conventionally taken as the ratio a_g/g , i.e. the peak ground acceleration by the gravity acceleration¹. In this context, a_g is considered as a first good approximation measure of the seismic load.

FOR EACH MACRO-ELEMENT

First, macro-elements that define the structural organism of the building and also characterize its seismic response are identified. Then:

1. The most significant collapse mechanisms (i) for each macro-element (j) are identified,
2. The nominal values of the seismic coefficient C_{ij} (corresponding to the activation of the i mechanism in the j macro-element) are evaluated through the application of the upper bound theorem of the Limit Equilibrium analysis,
3. The probability functions (PDF) $f_{C_{ij}}$ of the seismic coefficients C_{ij} ; C_{ij} , which is assumed to be normally distributed, are calculated with a mean value $E[C_{ij}]$ equal to the value defined in step 2; the estimation of the coefficient of variation (c.o.v) is based on the number, the significance and the uncertainties of the parameters allowed under step 2,

1. It corresponds to the λ used in Lagomarsino's method.

4. For each given peak ground acceleration a_g , the probability P_{ij} of activation of the i^{th} mechanism for the j^{th} macro-element is calculated as follows:

$$P_{ij} = \text{Prob}\left[C_{ij} \leq \frac{a_g}{g}\right] = F_{C_{ij}}\left(\frac{a_g}{g}\right) = \int_0^{a_g/g} f_{C_{ij}}(C_{ij})dC_{ij} \quad [-] \quad (\text{EQ 5.7})$$

Where $f_{C_{ij}}$ is the probability density function defined under 3 and $F_{C_{ij}}$ the corresponding cumulative distribution function (CDF),

5. The collapse probability P_j of the j^{th} macro-element (defined as the activation of any i mechanism) is calculated for given values of a_g . It is assumed that the collapse mechanisms of a macro-element can be either independent (ind) or mutually exclusive (me) [DSC 96] the corresponding probabilities of collapse $P_{j,\text{ind}}$ and $P_{j,\text{me}}$ are given by:

$$P_{j,\text{ind}} = \sum_i P_{ij} - \sum_{i_1 \neq i_2} P_{i_1 j} P_{i_2 j} - \sum_{i_1 \neq i_2 \neq i_3} P_{i_1 j} P_{i_2 j} P_{i_3 j} - \dots \quad [-] \quad (\text{EQ 5.8})$$

$$P_{j,\text{me}} = \sum_i w_{ij} \cdot P_{ij} \quad [-] \quad (\text{EQ 5.9})$$

Where w_{ij} is a weighing factor (defined in [Au 01]), whose value is related to the probability of activation of the i^{th} collapse mechanism in the j^{th} macro-element.

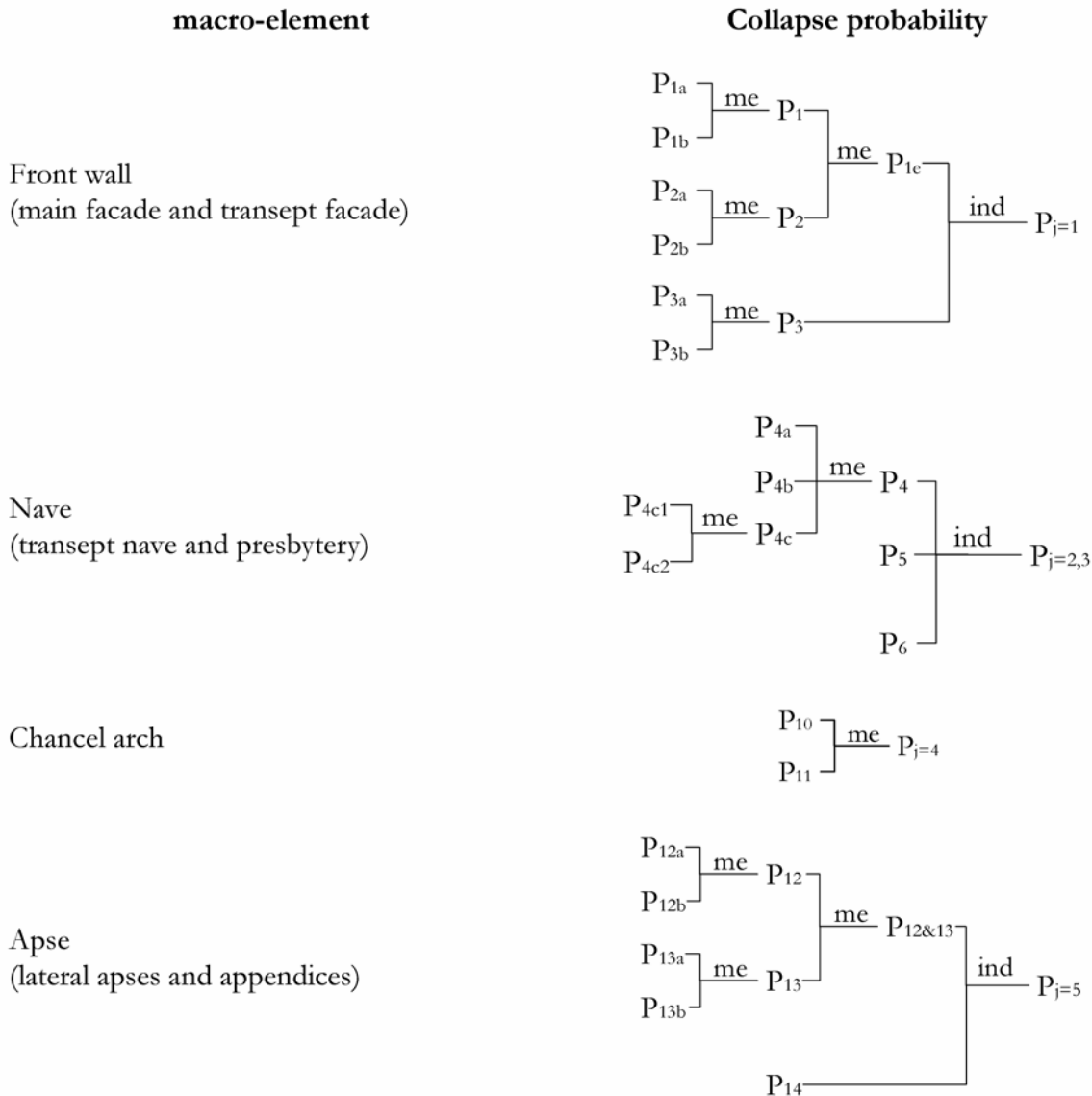
Table 5.2 lists the macro-elements and the relevant related collapse mechanisms that were taken into account in this method [Au 01].

Table 5.2: List of the macro-elements with the related collapse mechanisms.

Macro-element	Collapse mechanisms	
Front wall	1a	Out-of-plane rotation due to the development of a horizontal cylindrical hinge at the base of the facade; detachment of the facade from the orthogonal walls
	1b	Out-of-plane rotation due to the development of a horizontal cylindrical hinge at the top of the openings (entrance, windows) and to the detachment from perpendicular walls
	2a	Out-of-plane rotation of the top of the facade
	2b	Out-of-plane rotation due to the development of oblique cylindrical hinges
	3a	In-plane failure due to x-shaped cracks
	3b	Detachment of the middle of the facade and translation in the plane of the facade.
Nave, lateral walls	4a	Out-of-plane rotation of a wall restrained on three sides but free on the top side

	4b	Out-of-plane rotation of a wall restrained on four sides
	4c	Out-of-plane rotation of a wall restrained on the bottom side and free on the other three sides (4c1: cylindrical hinge at the base of the wall; 4c2: cylindrical in correspondence of openings, such as windows)
	5	Collapse due to localized thrusts from the roof
	6	Planar sliding due to oblique (X shaped) cracks
Nave as a whole	7	Collapse due to transversal seismic action: cracks in the transversal arches; crushing or cracking at the base of the nave pillars
	8	Collapse due to transversal seismic action: cracks in the longitudinal arches; crushing or cracking at the base of the nave pillars
	9	Cracks and/or disconnection of the rib vaults
Chancel arch	10	Shear failure of haunches
	11 a	Rotation of one haunch
	11 b	Rotation of both haunches
Apse	12a	Rotation and translation of the top with detachment along an inclined plane (often in circular and polygonal apses)
	12b	Out-of-plane rotation due to the development of a horizontal cylindrical hinge at the base of the apse end wall (usually in rectangular apses)
	13a	Out-of-plane rotation due to the development of hinges at the edges
	13b	Out-of-plane rotation of vertical bends
	14	Planar sliding due to x-shaped cracks
Presbytery	4a, 4b, 4c, 5, 6, 7, 8 and 9	
Transept facade,	1a, 1b, 2a, 2b, 3a and 3b	
Transept nave	4a, 4b, 4c, 5, 6, 7, 8 and 9	
Lateral chapels	2a, 12b, 13a and 14	

The following diagram shows a few examples of combinations that give an evaluation of the collapse probability P_j of each considered macro-element.



Note: me and ind mean: mutually exclusive and independent mechanisms respectively.

FOR THE WHOLE CHURCH

Collapse of a church does not result from the collapse of only one single macro-element because each has a different impact on the building under seismic loads. According to Augusti et al. [ACZ 02], the probability of collapse of a given church would be underestimated if it were measured by the probability of collapse of only one macro-element. He stated that the collapse probability of a whole church is a function of the collapse probabilities of macro-elements according to a functional logic of the whole. The collapse condition thus depends on the structural integrity of the church. This is defined by the interaction between macro-elements that is described by a logical diagram.

1. Macro-elements are divided into two groups: critical and non-critical ones. Contrary to the non-critical macro-elements, the collapse of the critical ones involves the destruction of the whole building. The church can be seen then as a series system, composed by critical macro-elements and in parallel subsystems that are composed of non-critical macro-elements
2. For given values of peak ground acceleration (a_g), the collapse probability of each subsystem (made up of macro-elements put in parallel) is evaluated by:

$$P_{f, \text{par}} = \prod P_k \quad [-] \quad (\text{EQ 5.10})$$

Where P_k is the collapse probability of each branch k of the parallel subsystem (numbers 4 and 5 in Figure 5.17).

3. The collapse probability of the whole church is then evaluated using the relation usually used for series systems:

$$P_f = 1 - \prod (1 - p_m)_m \quad [-] \quad (\text{EQ 5.11})$$

Where P_m can correspond either to the collapse probability of each critical macro-element (P_i) or the collapse probability $P_{f, \text{par}}$ of each subsystem.

LOGICAL DIAGRAMS

On the figure on the right is an example presented in [ACZ 02]. The chosen church, Santa Maria Maddalena in Flagogna, is situated in the Friuli region, Italy.

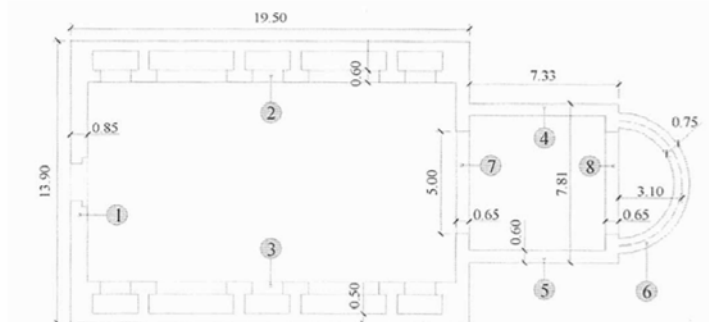


Figure 5.16 : Plan of Santa Maria Maddalena church in Flagogna; taken from [Au 02].

Legend:	1	Facade	2	Nave left wall	3	Nave right wall
	4	Presbytery left wall	5	Presbytery right wall	6	Apsse
	7	Chancel arch (nave-presbytery)		Chancel arch (presbytery-apse)		

Augusti et al. proposed the following logical diagram to describe Santa Maria Maddalena church.

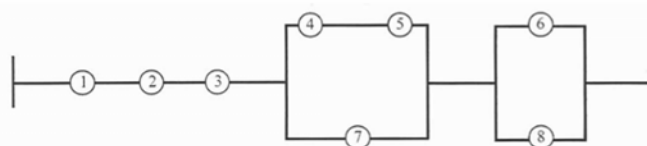


Figure 5.17 : Logical diagram of Santa Maria Maddalena church in Flagogna (Friuli region, Italy); taken from [ACZ 02].

Note: numbers in Figure 5.16 correspond to the macro-elements indicate in Figure 5.17.

Macro-elements 1, 2 and 3 are considered as critical whereas elements 4, 5, 6, 7 and 8 are non critical. In other words, the collapse of the critical macro-elements (i.e. 1, 2 and 3) involves the collapse of the whole structure while the collapse of the non critical macro-elements does not necessarily imply the overall failure of the church. On the other hand, the collapse of the whole church might also happen either if macro-elements 4, 5 and 7 collapse or if parts 6 and 8 collapse.

5.2.5. SUMMARY

Table 5.3: Summary of the existing methods presented in this report.

Method	Type	Input Data	Output data
Lourenço's method	Index method	Edifice dimensions, weight per unit of volume, internal angle of friction, peak ground acceleration	$\gamma_{1,i} = A_{wi}/S$; $\gamma_{2,i} = A_{wi}/G$; $\gamma_{3,i} = A_{wi}/A_w * \tan\phi/\beta$
Risk-UE method	Hybrid method	Edifice dimensions, weight per unit of volume, plans	Vulnerability curves (level 1); capacity curves (level 2)
Lagomarsino's method	Hybrid method	Edifice dimensions, weight per unit of volume, plans, mechanical properties of the material (FEM)	Vulnerability curves (level 1); capacity curves (level 2); seismic structural behaviour (FEM)
Augusti's method	Hybrid method	Edifice dimensions, weight per unit of volume, plans	Fragility curves

5.3. APPLICATION OF THE METHODOLOGIES TO SWISS SACRED BUILDINGS

Every method presented in the previous chapter is applied here below; however, only the results are given in this chapter. Details of calculations can be found in Appendix A.3.

5.3.1. SAMPLE SET OF CHURCHES

In order to assess the reliability and the applicability of the developed methods to the sacred buildings in Switzerland, a sample set of churches is chosen according to a few criteria. It contains different types of structures as well as fabrics and building techniques (time of construction, regions, etc.) have to be represented (if possible). On the other hand, it is judicious to select buildings which were slightly, moderately, strongly damaged by earthquakes in the past in order to make a comparison between the results from methodologies and the reality. Finally, the following sacred buildings are selected:

Sacred buildings	Type	Reasons
Old chapel, Visperterminen	Chapel	It was damaged by the seismic event of 1755 and collapsed after the earthquake of 1855.
Collegiate church of Valère	Fortified church	It was slightly damaged after the seismic event of 1946 (damage was recorded).

5.3.1.1. Chapel in Visperterminen

The so-called old chapel in the forest (alte Waldkapelle) in Visperterminen was built in 1730-40. According to German Studer-Freuler [St 94], it was roomy. The chapel shape was similar to the one of the so-called Three-king church (Dreikönige Kirche) in Visp and it resembled the pattern of Baroque churches from Southern Germany (the architect came from the Vorarlberg region (Austria)).

It was damaged by the seismic event of 1755; according to [St 94], it resulted in two cracks (their configuration is not known): one in the choir walls and one in the portal¹. At that time everyone thought it was due to the bad quality of the soil but they changed their opinion after removing the covering. In fact, they found out that the rafters timber framework was just laid on walls without horizontal links to the rest of the framework and it probably hammered masonry.

Because of the damage, villagers displaced the altar to the new parish church in the middle of the town and no longer visited the chapel.

The damaged chapel collapsed during (or after) the earthquake of 1855 whose epicentre was situated in the town of Törbel (Visp valley).

Figure 5.18 : View of a part of the ruined chapel choir (2005).



- Notes:
- *there probably were other windows along the same wall*
 - *there were small circle-windows above every «normal» window*
 - *lintel of both choir doors were arched; they still remain*
 - *main windows are rectangular framed (with a timbre plank to support the lintel)*

Based on photographs of the ruins taken in 2005, the chapel seems to have been about 6 m high.

The plan and elevation of the chapel were reconstituted based on the in-situ surveys and archive sources [St 94].

1. It is not clear if the crack appeared in the front wall or in a portal; the text was unfortunately not clear enough.

5.3.1.2. Collegiate church of Valère

The Valère collegiate church was built from the beginning of the 12th c. to the 13th c.; consequently, at least two diverse architectural styles are merged together (i.e. Romanesque and Gothic). Another particular feature, the crenellation (along the top edge of the apse) shows this is a fortified edifice [Sc 71].

In the end of the 18th century, the canons community came down town and Our-Lady of Valère became less occupied. The collegiate church was not maintained well and it was in a bad state of conservation one century later. In 1892, J.-Rahn warned the authorities that it was in ruins. The edifice was restored from 1896 to 1903.

Regarding cultural goods, the church shelters Romanesque capitals (ornaments from the 12th c.) and the apse is completely decorated with frescoes dating from the 15th c. Furthermore, it encloses the oldest organ over the world that is still used.

STRUCTURE

The inferior part of the eastern side and the transept, as well as the south-east chapel, the basis of the nave walls and the north portal, date from the first half of the 12th c. The erection of the tower, the construction of the chancel vaults and the nave pillars took place in the end of the 12th c. The upper part of the polygonal apse and the chancel vault were built according to Gothic architectural style. The last structural parts being built were the low aisles, the front wall and finally the jube (end of 13th c.; Burgundian Gothic).



Figure 5.19 : Inner view of the collegiate church.

The edifice is entirely vaulted: transversal barrel vault for the transept and rib-vaults above the nave ground. The nave is split into four bays; the fourth one, which is dedicated to the canons, is raised in comparison to the floor of the other bays and cut from them by a jube (13th c.) (it is actually the only jube in Switzerland which is still in its original place). Besides, the nave ended in a semicircular apse (polygonal in its upper part) and is flanked by two chapels (parallel to the church axis).

The vault thrust is transferred to the ground through massive buttresses; furthermore, in order to limit the horizontal force, tie-rods were put between the opposite springings of each bay vault.



Figure 5.20 : Outer view of the north side of the edifice.

The collegiate church, like the abbey churches of Romainmôtier and Payerne, has a narthex in front of its front wall; this is the only part of the edifice to be covered by a one-slope roof.

Masonry seems to be of good quality. The church was badly maintained for about six centuries; however, it was restored in the end of the 19th and during the 20th centuries. The edifice is situated on a rock hill.

5.3.2. LOURENÇO'S METHOD

5.3.2.1. Chapel in Visperterminen

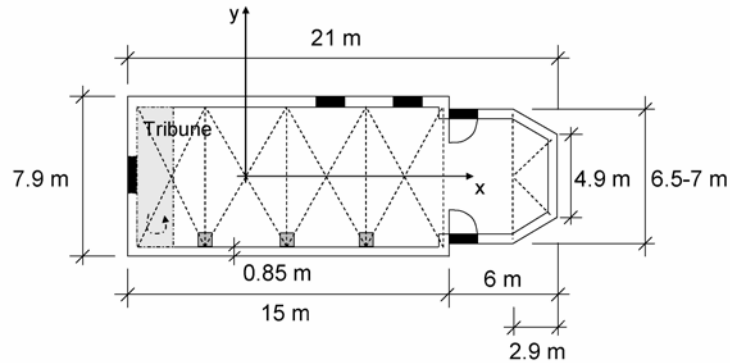


Figure 5.21 : Reconstituted plan of the chapel in Visperterminen.

Index 1: $\gamma_{1,x}=0.23$ and $\gamma_{1,y}=0.09$

Index 2: $\gamma_{2,x}=3.88$ and $\gamma_{2,y}=1.54$

Table 5.4: Values for the index 3.

Index 3:	Z1 ($a_{gd}=0.06$ g)	Z3b ^a ($a_{gd}=0.16$ g)	$a_{gd}=0.2$ g
$\gamma_{3,x}$	4.77	1.79	1.43
$\gamma_{3,y}$	1.9	0.71	0.57

a. There are four areas of seismic hazard in Switzerland (Z1, Z2, Z3a and Z3b [SIA 261 03]); each zone is characterized by a peak ground acceleration for an earthquake with a return period of $T=475$ years. Further information can be found in Appendix A.8.

Both indices 1 and 3 show that the chapel is seismically vulnerable along its y-axis. Index 2 shows that the chapel is not seismically vulnerable; however, this index is exact only for the reconstituted elevation that does not exactly represent the original structure of the chapel. While the reconstructed plan is right, the elevation is based on an assumption; consequently, the self weight is also an assumption. This explains the greater uncertainty for the values of the index 2 than of both other indices.

5.3.2.2. Collegiate church of Valère

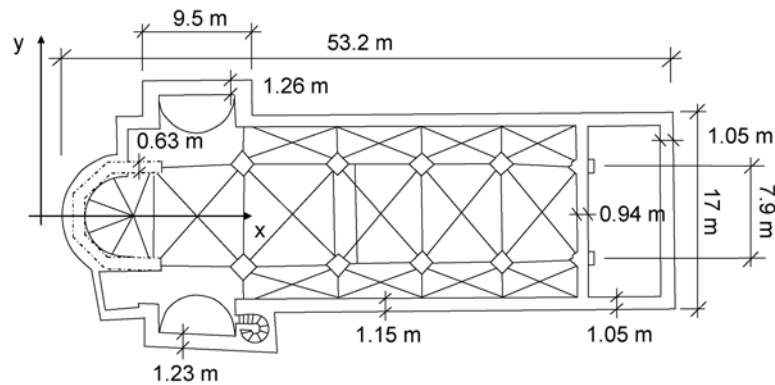


Figure 5.22 : Plan of the Collegiate church of Valère.

 Index 1: $\gamma_{1,x}=0.14$ and $\gamma_{1,y}=0.08$

 Index 2: $\gamma_{2,x}=1.4$ and $\gamma_{2,y}=0.97$

Table 5.5: Values for the index 3.

Index 3:	Z1 ($a_{gd}=0.06$ g)	Z3b ($a_{gd}=0.16$ g)	$a_{gd}=0.2$ g
$\gamma_{3,x}$	3.94	1.48	1.18
$\gamma_{3,y}$	2.73	1.02	0.82

The three indices show that the collegiate church is seismically vulnerable along its y-axis and might suffer quite high damage under the seismic actions defined for the hazard zone 3b. As the values of indices 1 and 3 are close or equal to the safety value, it cannot be said that the collegiate church is clearly vulnerable; nevertheless, in these limit cases, it is reasonable to undertake more refined methods in order to see whether it is vulnerable.

Note: the reader can find calculations under the Appendix A.3.

5.3.2.3. Pre-Romanesque and Romanesque churches in Switzerland

Conditions of non-vulnerability: $I_1 = \frac{A_{wi}}{S} \geq 0.1$ $I_2 = \frac{A_{wi}}{G} \geq 1.2$ $I_3 = \frac{A_{wi}}{A_w} * \frac{tg(\varphi)}{\beta} \geq 1.0$

Table 5.6: Application of Lourenço's method to Pre-Romanesque churches; results.

Edifice	Seismic hazard area	$\gamma_{1,x}$	$\gamma_{1,y}$	$\gamma_{2,x}$	$\gamma_{2,y}$	$\gamma_{3,x}$	$\gamma_{3,y}$
Romainmôtier	1	0.16	0.09	/	/	4.25	2.42
Payerne, abbey church	1	0.19	0.09	/	/	4.46	2.2
St Sulpice, priory church	1	0.14	0.23	/	/	2.5	4.18
Grandson, priory church	1	0.22	0.15	/	/	3.94	2.73

Chésereux, abbey of Bonmont	1	0.21	0.12	/	/	4.25	2.41
Donatyre, St Etienne's chapel	1	0.21	0.21	/	/	3.3	3.3
Basel, Cathedral	3a	0.13	0.098	/	/	1.74	1.34
Spiez, Castle church	2	0.16	0.12	1.67	1.17	2.3	1.7
Schaffhausen, All-the-saints' abbey	1	0.13	0.07	/	/	4.39	2.28
Stein am Rhein, St George's church	1	0.18	0.09	/	/	4.4	2.27
Zürich, Grossmünster	1	0.14	0.07	/	/	6.66	4.16
Mistail, St Peter's church	2	0.13	0.12	/	/	2.03	1.97
Müstair, St John's church	2	0.21	0.17	/	/	2.22	1.78
Muralto, St Victor's church	1	0.2	0.13	2.09	1.36	3.96	2.7
Biasca, St Peter and Paul's church	1	0.19	0.1	/	/	4.31	2.35
Chur, Cathedral	2	0.22	0.13	/	/	2.52	1.48
Mendrisio, St Martin's chapel	1	0.15	0.072	/	/	4.52	2.14
<i>Chapel in Visperterminen^a</i>	<i>3b</i>	<i>0.23</i>	<i>0.09</i>	<i>3.88</i>	<i>1.54</i>	<i>1.79</i>	<i>0.71</i>
<i>Collegiate church of Valère</i>	<i>3b</i>	<i>0.14</i>	<i>0.08</i>	<i>1.4</i>	<i>0.97</i>	<i>1.48</i>	<i>1.02</i>
Santa Maria del Fossale (I)	$a_{gd}=3.5 \text{ m/s}^2$ ^b	0.09	0.06	2.23	1.58	0.76	0.38
Santo Stefano a Cesclans	$a_{gd}=3.0 \text{ m/s}^2$	0.11	0.06	2.35	1.34	0.85	0.42
Santo Stefano di Valeriano	$a_{gd}=2.5 \text{ m/s}^2$	0.3	0.15	3.5	1.7	1.08	0.52
Santo Stefano di Valeriano ^c	$a_{gd}=2.5 \text{ m/s}^2$	0.2	0.09	3.4	1.7	1.08	0.52
Duomo di Gemona	$a_{gd}=3.0 \text{ m/s}^2$	0.12	0.08	/	/	0.78	0.66

a. Since results for the chapel in Visperterminen exist, they are inserted within the above table even if it is not Romanesque.

b. The values of the peak ground accelerations are not reevaluate according to [BPVR 07]

c. With smaller wall thickness (0.7 m instead of 1.08 m).

- Notes:
- x : nave axis (from entrance to apse); y is the perpendicular axis.
 - indices that do not satisfy safety is indicated in bold.
 - index 2 is calculated only for buildings whose elevation and plan are available; in case nothing is available the cell has a slash character inside.
 - the index 3 is calculated with respect to the seismic hazard characterizing the zone where the building is situated. Moreover, $\tan\varphi=0.4$, as proposed in [LR 06]. Moreover, the quality of the soil was defined as good (category A in the SLA 261 [SLA 261 03]).
 - indices for the chapel in Moutier, Saint Leonard's chapel, Saint Columban's chapel (Andermatt) and Saint Martin's chapel (Cazis) are not given because of lack of information.
 - the value of the peak ground acceleration for the Friuli earthquake is taken from [Do 94]; an $a_{gd}=3.5 \text{ m/s}^2$ was measured in Tolmezzo during the first seismic event (May 1976). This value was then adapted for the surrounding regions (assumed loss of 0.5 m/s^2 for one Intensity degree in regard to Figure 4.22).
 - details on the plans and elevations of Italian churches can be found in Appendix A.3.2.2.1; their damage is recorded either in chapter 4.3.2 or in the Appendix A.2.4.

Index 1 appears to be the most conservative one; in most cases, this is the first one whose safety conditions are not satisfied. The values of the index 3 collected in the Table 5.6 show that this index depends a lot on the peak ground acceleration. Many of Swiss churches would be qualified as vulnerable through the index 3 for an $a_{gd}=2 \text{ m/s}^2$. This fact is proved by the cases of the Italian churches for which the value of index 3 is lower than the safety condition. Index 2 essentially depends on the height of the edifice and the presence of vaults; in fact, it is quite high for squat churches while it decreases for slender edifices.

The reliability of this method is good and is showed by the four Italian examples. In fact, they are characterized at least by one index as seismically vulnerable and they were indeed moderately or highly damaged after the seismic events of 1976 in the Friuli region. It is worth noting that if more reasonable thickness is considered for the church Santo Stefano a Cesclans, there are at least two indices that show they are vulnerable. However, it must be kept in mind that these indices are based on the in-plane seismic response of walls; the out-of-plane behaviour, deterioration or damage due to the hammering of rafters is not taken into account.

In a more global point of view, the above table shows that churches are more seismically vulnerable in the direction perpendicular to the nave. This is particularly true for Swiss heritage buildings amongst which, nine Pre-Romanesque and Romanesque sacred edifices are at risk (in this direction).

Note: the obtained indices that are close to the limit values have to be regarded with care since they are calculated on the basis of imperfect (taken from books) plans and elevations¹ (for two edifices). With more exact calculations they might be higher or lower than the limit values simply because of uncertainties in given dimensions.

DISCUSSIONS

Based on observed damage, this method is proven to be reliable, especially when the given edifice is seismically more vulnerable in the plane of its components than out of their plane.

1. When elevations were available.

Calculations for indices 1 and 3 are quite simple and can be done rapidly whereas the index 2 requires more plans, information about walls, materials, etc. and it is also more time-consuming. Italian examples show that churches whose value for index 1 does not satisfy the safety condition were indeed seismically vulnerable. Values of index 3 are particularly low for these examples, compared to the cases of Swiss churches; however, when taking into account the peak ground accelerations proposed in the SIA 261 (Z3b; $a_{gd}=1.6 \text{ m/s}^2$)¹, the same values become higher than 1 for every church in x-direction and also for two edifices in the y-direction).

Finally, the choice of the value for the internal angle of friction could be discussed since this value is $\tan\phi=0.72$ in the SIA V178 and not $\tan\phi=0.4$.

5.3.3. RISK-UE METHOD

5.3.3.1. Application to the chapel in Visperterminen

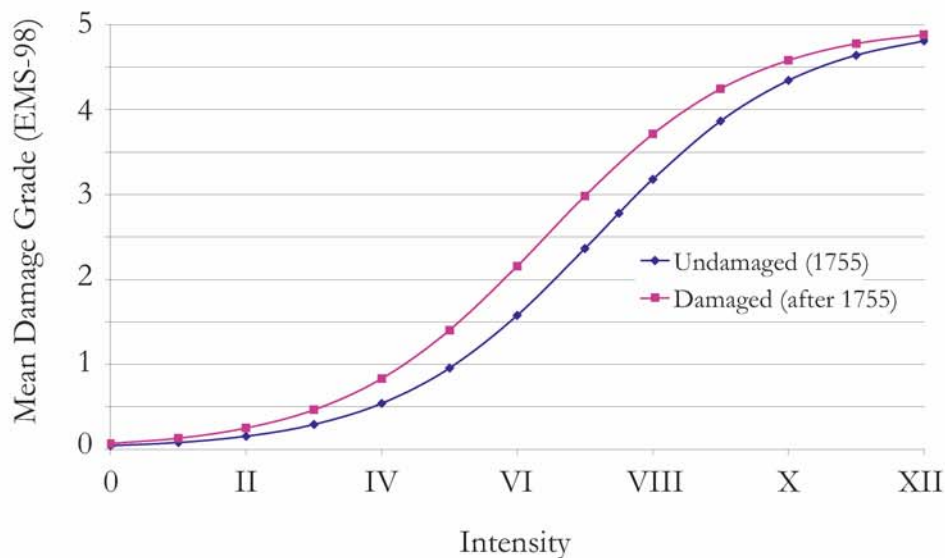


Figure 5.23 : Vulnerability curves for the old chapel in Visperterminen before and after 1755 earthquake.

1. This peak ground acceleration corresponds to an earthquake whose return period is $T=475$ years (Swiss Seismological Service). This value was defined for determining the design spectrum for common buildings.

Though the damage grade observed after the 1755 and the 1855 earthquakes were different (MDG=3 in 1755 (I=VIII)^a and MDG=4-4.5 in 1855^b (I=VIII)^c), both curves on the above graph are in fact not really far from each other; compared with the observed damage, this is incorrect. Since the intensity was I=VIII for both earthquakes, the MDG would be, according to Figure 5.23, ~3.2 and ~3.5 for 1755 and 1855 earthquakes, respectively. Though not completely wrong, these values do not fit reality.



- a. Place within the area of I=VIII; from [ECOS 02]
- b. These values correspond to evaluations based on archives.
- c. Place within the area of I=VIII; from [ECOS 02]; see chapter 4 too.

Figure 5.24 : View of the damaged chapel (from the east, westwards, 2005).

5.3.3.2. Application to the collegiate church of Valère

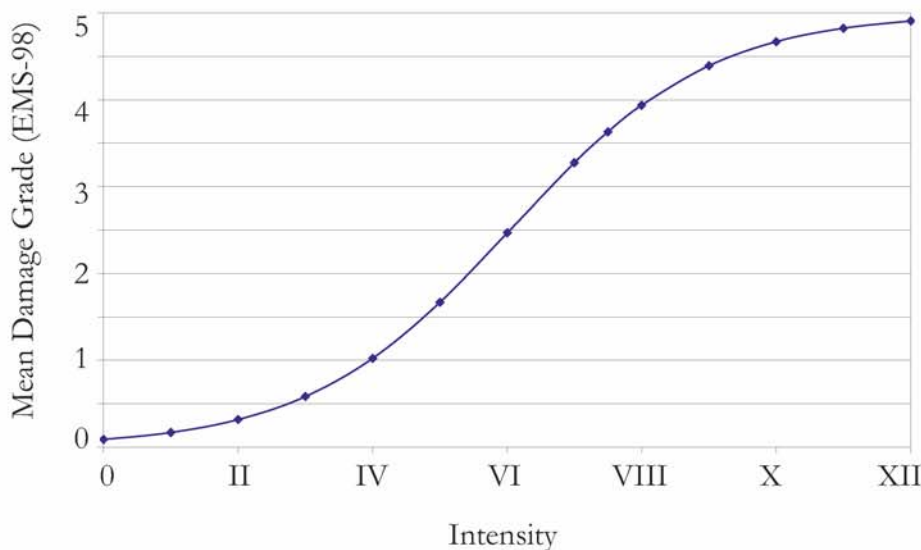


Figure 5.25 : Vulnerability curves of the collegiate church of Valère.

According to this method, the collegiate church is more vulnerable than the old chapel in Visperterminen for the same intensity. For instance I=VIII, the mean damage grade of the collegiate church would be MDG~3.9 whereas it is ~3.5 for the chapel in Visperterminen.

The mean damage degree that suits to the collegiate church after the earthquake of 1946 is assumed to be a value around MGD~2 in July 1946 (after the survey by L. Blondel) on the EMS-98. According to calculations, such a damage degree could have only been caused by a seismic intensity between V and VI. Because of the attenuation of the seismic waves, this result is in agree-

ment with reality; furthermore, as the collegiate church is situated on a hill, there must also have been a site effect.

Nevertheless, one must pay attention to the fact that there were two aftershocks (end of January 1946 and beginning of February 1947) that must have had an impact. Unfortunately, this impact is difficult to evaluate by applying the proposed method.

Note: the reader can find calculations under the Appendix A.3.3.

5.3.4. LAGOMARSINO'S METHOD

5.3.4.1. Application to the chapel in Visperterminen

RESULTS SUMMARY

Table 5.7: Main results of Lagomarsino's method on the chapel in Visperterminen.

Macro-element	Collapse mechanism	$S_a=0.7\lambda^a$	$S_a=\lambda^a$	$S_d=S_u[m]$
Front wall	Gable overturning (horizontal yield line)	0.45	0.64	0.43
	Gable overturning (oblique yield line)	0.2	0.29	0.43
	Whole facade overturning	0.1	0.14	0.43
	Overturning of the upper part of the front wall	0.27	0.39	0.43
	Shear collapse (two halves of the facade)	0.33	0.47	1.9
	Shear collapse (oblique crack and overturning of a part)	0.41	0.58	1.64
	Shear collapse in the bottom part of the front wall and overturning of every rigid block	0.36	0.51	1.6
Nave, lateral walls	Overturning of the upper parts	0.21	0.3	0.35
	Global overturning	0.08	0.11	0.35
	Overturning of one lateral wall	0.09	0.13	0.35
Chancel arch	Overturning of both pillars	0.23	0.33	0.73
	Overturning of one pillar	0.19	0.27	0.73
Apse	Overturning of a vertical band of masonry (on x-axis)	0.06	0.09	0.27
	Overturning of a vertical band of masonry (on y-axis)	0.11	0.15	0.44

a. In unit of g.

According to Table 5.7, the chapel front wall was seismically vulnerable out of its plane and might have easily collapsed under a spectral acceleration equal or lower than the peak ground acceleration defined in the Swiss code 261 for the given zone (3b) ($a_{gd}=1.6 \text{ m/s}^2$). Though the front wall does no longer exist, which confirms the obtained result, the real state of the facade after the seismic events of 1755 and 1855 is unknown.

The collapse multiplier value is 0.09 g for the chapel transversal seismic response. That would indicate that the most probable collapse mechanism would have been a global overturning. Nevertheless, according to the still ruins of the chapel, one lateral wall is still standing (though its upper part collapsed) and half the height of the other one is also still standing. In this case, the collapse mechanisms proposed by Lagomarsino do not match the real mechanism.



Figure 5.26 : View of one lateral wall of the chapel (2005).

With respect to the chancel arch collapse mechanisms, since both of its pillars are still standing (there are cracks, but no collapse), they must have moved apart from each other making the arch collapse.

Results show that the apse is the most vulnerable part of the chapel under seismic actions; however, the related collapse multiplier was actually calculated for a collapse mechanism defined according to the apse damaged pattern (that is not listed by Lagomarsino et al.). In fact, there is no reason *a priori* for the activation of such a mechanism, save the hammering of the timber framework rafters. Moreover, calculations show that the given part of masonry that has been dealt with had much probability to turn around the x axis than around the y-axis while the contrary happened.

Note: the reader can find calculations under the Appendix A.3.4.

5.3.4.2. Application to the collegiate church of Valère

First, as noted before, Lagomarsino's method has not been developed for three-nave churches and in consequence, it is not well adapted to the collegiate church of Valère that is a three-nave edifice. However, since this kind of sacred buildings constitutes a large part of the Pre- and Romanesque edifices in Switzerland, it is interesting to address them with this method.

Furthermore, for the method is not adapted for such kind of edifices, the collapse mechanisms of the nave and the chancel arch are not defined by Lagomarsino et al. and must be determined.

RESULTS SUMMARY

Table 5.8: Summary of the chosen collapse mechanisms and the related collapse multiplier.

Macro-element	Collapse mechanism	$S_a=0.7\lambda^a$	$S_a=\lambda^a$	$S_d=S_u[m]$
First wall ^b	Gable overturning (horizontal yield line)	0.12	0.17	0.54
	Whole wall overturning	0.08	0.11	0.54
	Shear collapse and overturning of the moving part (oblique crack)	0.62	0.88	5.7
Front wall	Gable upper part overturning (horizontal yield line)	0.32	0.5	0.42
	Gable overturning (horizontal yield line)	0.095	0.14	0.42
	Gable overturning (oblique yield line)	0.15	0.21	0.42
	Whole facade overturning	0.04	0.05	0.42
Transept facade	Whole facade overturning (with the impact of the timber framework)	0.05	0.07	0.63
	In-plane collapse mechanism	0.15	0.22	2.17
Lateral walls	Global overturning	0.17	0.25	0.22
Chancel arch	Overturning of both pillars	0.05	0.07	0.31
Apse	Overturning of the crenels	0.29	0.41	0.44
	Overturning of parts hammered by the timber framework	0.16	0.22	0.57
Tower	Overturning of the upper part	0.37	0.52	0.83

a. In unit of g.

b. It corresponds to the narthex wall (the last wall in y direction on Figure 5.22).

DISCUSSIONS

According to the obtained results, the three studied facades, i.e. the first wall, the main facade and the transept facade, lose their stability under an out-of-plane acceleration $a_{gd}=0.11g$, $0.05g$ and $0.07g$ respectively. Amongst them the most vulnerable is the main facade. According to oral sources, there are vertical cracks between the main facade and the lateral walls; moreover L. Blondel [Bl 46] recorded a large vertical crack in the south lateral wall¹ as well as in the vaults of the first bay. Though the obtained values for the collapse multipliers are low, it must be kept in mind that calculations have not taken into account the possible presence of tie-rods connecting the facades to their perpendicular walls². In this case, the multiplier scores would have been higher and the seismic vulnerability lower.

1. Perpendicular to the front wall.

2. Their position is not well known, as are their anchorage length and strength.

The nave, i.e. the lateral walls, is not particularly seismically vulnerable. According to L. Blondel [Bl 46], the low-aisles are particularly damaged. The vaults were transversally cracked (crossing the centre of the vaults) as well as laterally. Moreover, the vaults of the low-aisles were detached from the main nave walls and the arch voussoirs were also detached; at one place the keystone even fell down. From a structural point of view, 10 hinges are required to have a mechanism under horizontal actions (or 8 for a partial mechanism) according to Lagomarsino's model; all the above recorded cracks, if they crossed the wall or the vault, can be regarded as hinges. In case there are 10 cracks that can be considered hinges, the model that was used for calculations could be right; however, there is no certainty.

The chancel arch is characterized by a high seismic vulnerability. Since the choice of the collapse mechanism is arbitrary, this result must be carefully considered. As a reminder, the collapse multiplier obtained by applying the upper bound theorem of the Limit Equilibrium Analysis can be either higher or equal to real collapse mechanisms that can happen. If it is lower than the real one the assessment of the seismic vulnerability is unfavourable and wrong. That might be the case here. Moreover, the transversal movement is stopped in one direction by the presence of the tower; there is consequently no collapse (at least not the chosen collapse mechanism) in this direction. The apse and the tower are not seismically vulnerable, at least for the chosen collapse mechanisms. This result is in agreement with their dimensions and the observed damage [Bl 46].

At last, it must be said that the collegiate church was struck at least twice in one month since a second earthquake happened two weeks after the main shock. In consequence, it is difficult to assess not only the damage that resulted from each seismic events but also to assess the evolution of the edifice's seismic vulnerability.

Note: the reader can find calculations under the Appendix A.3.4.

5.3.5. AUGUSTI'S METHOD

5.3.5.1. Application to the chapel in Visperterminen

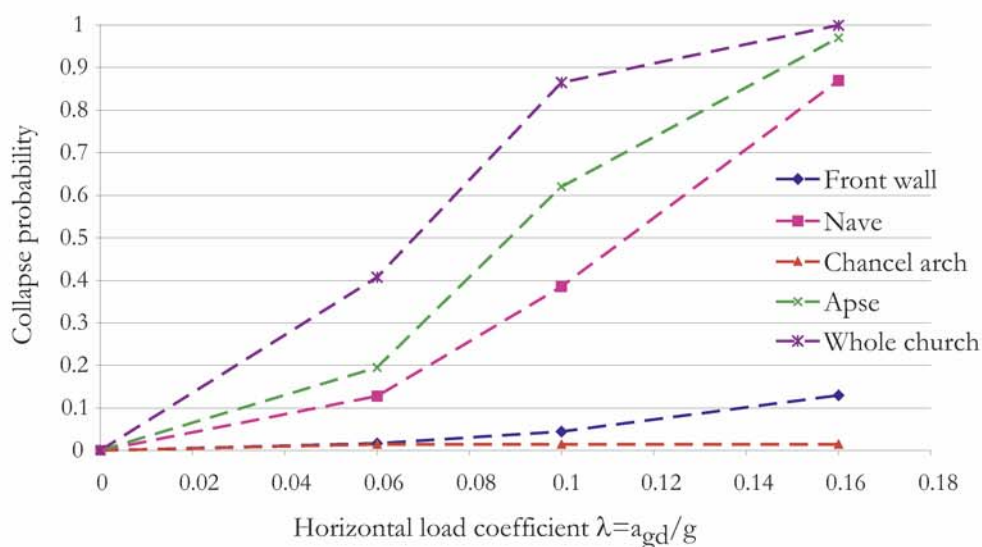


Figure 5.27 : Fragility curves (collapse probability vs. horizontal load coefficient) of the macro-elements and the whole chapel in Visperterminen.

DISCUSSIONS

According to Figure 5.27, the whole chapel would have a probability of 1 to collapse under a peak ground acceleration of 1.6 m/s^2 that characterized the zone 3b where Visperterminen is situated [SIA 261 03]. If the total collapse of the church means the total destruction, that is, no more than stones piles are left, this result is overstated (lateral and apse walls are still standing, though damaged)¹. Moreover, while the peak ground acceleration of the 1755 earthquake was probably close to 1.6 m/s^2 , it is close to 2 m/s^2 during the 1855 earthquake, and that did not result in the total collapse of the chapel.

Once again, as with Lagomarsino's method, the most seismically vulnerable part is the apse, then the nave (transversal movement), the front wall and finally the chancel arch. This is logical since the collapse mechanisms and the way to calculate the collapse multipliers are the same.

However, this method makes it possible to obtain not only probabilistic results (collapse probability versus the collapse multiplier), but it also gives information about the global seismic response of a whole edifice. This method is an interesting tool for having a global view of a church.

Nevertheless, the most important point to note is that the collapse probability of the whole chapel should be lower than the collapse probability of each component leading (according to the logical diagram) to the chapel ruin; this is not the case simply because of the equation applied (Eq 5.11).

Note: the reader can find calculations under the Appendix A.3.5.

5.3.5.2. Application to the Collegiate church of Valère.

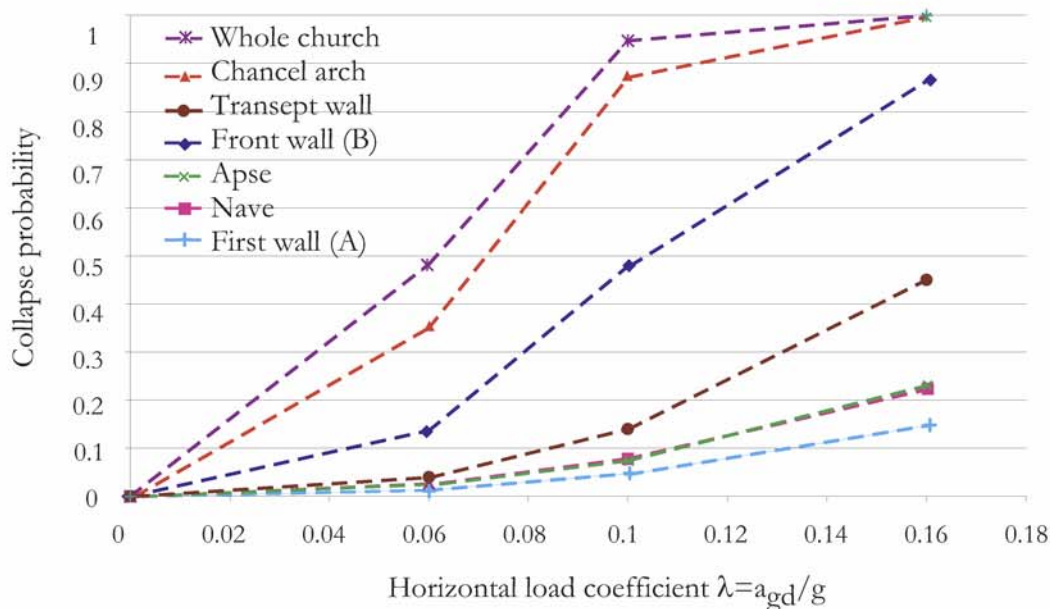


Figure 5.28 : Fragility curves (collapse probability vs. horizontal load coefficient) of the macro-elements and the whole collegiate church of Valère.

1. Furthermore, specialists think that the peak ground acceleration at that place was probably of 2 m/s^2

DISCUSSIONS

According to Figure 5.28, the whole collegiate church would collapse under a peak ground acceleration of $\sim 1.6 \text{ m/s}^2$. The most seismically vulnerable part of the collegiate church is the chancel arch; it is not surprising since the chosen collapse mechanism is the same as the one chosen for the application of Lagomarsino's method. Obviously, the same observations have to be made regarding this result; though the chancel arch is probably seismically vulnerable, this result is certainly overstated.

The collegiate church front wall is also highly vulnerable under out-of-plane seismic actions. The transept wall (out-of-plane mechanism), the apse, the nave (transversal collapse mechanism) and the first wall are less vulnerable. The apse and the nave (transversally) seem to be the least vulnerable in case of a seismic event. It is worth reminding that this conclusion is correct only in case of an undamaged structure, which is not necessary the case.

To sum up, it is worth noting that this method, like Lagomarsino's method, has been developed for small (one-nave) churches and not for medium-size edifices. Consequently, the validity of the results must be considered with caution.

Note: the reader can find calculations under the Appendix A.3.5.

5.3.6. DISCUSSIONS

LOURENÇO'S METHOD

The calculations for indices 1 and 3 are quite simple and can be done fast whereas the index 2 requires more plans, information about walls, materials, etc. and it is also more time-consuming. However, both examples (the chapel in Visperterminen and the collegiate church of Valère), which were studied in details, show that index 2 not only follows the same trend than index 1, but confirms the result.

Index 3, since it takes into account the seismic hazard of the area where the given edifice is situated, permits us to balance results of both first indices as a function of the place where the edifice is situated.

RISK-UE METHOD

This takes into account many important parameters that can have an impact on the seismic vulnerability of churches. Though it seems to suit more or less the case of the undamaged chapel in Visperterminen and the collegiate church of Valère, the curves of the undamaged chapel and the damaged one do not represent reality. This observation also shows that this method gives a good trend of the seismic vulnerability of sacred buildings (it shows that a mean damage grade of 3 can be expected from an intensity of VI/ VII for churches). However, it does not provide more accurate results since there are no substantial differences between the studied examples (the chapel and the collegiate church) although they are structurally very different.

Moreover, this method is based on statistics that have been collected in Italy on Italian churches. It is obvious that both kinds of building heritages are not necessarily the same (different structures, materials, etc.). Consequently, this statistical basis might simply not be suitable to Swiss churches.

With respect to the second level of the method, which is the same as the level 2 of Lagomarsino's method, see the following chapter.

Note: the fact the vulnerability curves do not reach a mean damage grade of 5 is a problem of the method itself.

LAGOMARSINO'S METHOD

This method has given interesting results for both given edifices even if the results are sometimes overstated or do not completely match the observed damage resulting from earthquakes.

In comparison with the chapel in Visperterminen, it is worth noting that the application of this method becomes more difficult with sophisticated buildings like the three-nave churches (collegiate church of Valère) or cathedral. Consequently, results obtained with the collegiate church of Valère must be taken into account as indicative.

When only considering the chapel in Visperterminen, the range of the peak ground acceleration values that would activate the chosen collapse mechanism is overstated. Specialists of the Swiss Seismological Service think that the chapel might have been subjected to a peak ground acceleration of 2 m/s^2 during the 1855 earthquake that is higher than the obtained values.

AUGUSTI'S METHOD

This method is based on the same assumptions as Lagomarsino's, that is, the macro-elements approach, the same list of collapse mechanisms and finally, the upper bound theorem of the Limit Equilibrium analysis. Consequently, it shows the same advantages as well as disadvantages.

However, this method prioritizes a probabilistic approach, that is, fragility curves can be obtained instead of capacity curves (deterministic approach). This way of doing is an advantage since seismic vulnerability is not deterministic but probabilistic. Moreover, the method gives a view of the seismic response of the whole church; nevertheless, it must be pointed out that the probabilistic law that is used for the whole edifice has proved to be incorrect.

5.4. CONCLUSIONS

All the presented methods are based on reasonable assumptions as well as procedures and have given interesting results. The index method proved to be quite easy and quick (especially for the indices 1 and 3) to apply. However, since indices correspond to ratios that simplified reality, the obtained answers are also related to the simplicity of the ratios. Nevertheless, it has been proved that the results do correspond to reality.

The three other methodologies are composed of steps with increasing refinement in the applied calculation methods; this process has proved to be efficient. For instance, a first step whose results are quickly obtained and reliable is appropriate to sort out edifices depending on their seismically vulnerability. For instance, the first level of the Risk-UE method and Lagomarsino's is based on parameters, which can have a great impact on the seismic vulnerability of churches, and also on statistical data collected during surveys (on damage to religious buildings) that were carried out after seismic events. Beside, the application of this first level is quick and easy.

The second level of both methods, i.e. the Risk-UE method and Lagomarsino's, is pretty interesting. Nevertheless, collapse mechanisms have to be chosen and in case the real collapse mechanisms are unlisted (or unknown), the obtained results differ from reality. Otherwise, the approach by macro-elements seems to be quite suitable to assess the seismic vulnerability of churches. This problem related to the collapse mechanisms is somehow weighted in Augusti's method by the use

of probability. However it leads to other problems: how to assess the weighting factors and how to define a suitable logical diagram? Moreover the obtained results with this method seem to be slightly overstated because of the probabilistic treatment.

To sum up, all the above presented methods present advantages and disadvantages with respect to the type and reliability of the obtained results. The development of a new methodology should take advantage of the above conclusions.

6.1. INTRODUCTION

Constructions in stone masonry constitute a large part of the building heritage in Switzerland. Beside old farms and individual houses (even contemporary), there are numerous cathedrals, churches, castles, town halls and Roman ruins.

As the topic of this report is the seismic vulnerability of such kind of buildings, the mechanical and structural properties of stone masonry must be well understood. Consequently, the study of this composite material is essential and it is why a chapter is devoted to it.

Stone masonry is made up of natural stones and mortar. Masonry is usually described by many parameters regarding both the stones and the mortar, i.e.:

- size and shape (and the regularity of size and shape) of the stones
- regularity of the courses
- mechanical properties of stones (strength)
- physical properties of stones (porosity)
- mechanical properties of the mortar
- size of the joints
- quality of the interface between stones and mortar

All these parameters are treated in the following sections. At first, it gives an overview of the masonry kinds that can be found in Switzerland. The mechanical properties of stone, mortar and masonry are discussed then in chapter 6.4.

6.2. MASONRY TYPES FROM HISTORY

The choice of the masonry type depends on a lot of different factors, which have furthermore changed with time mainly because of political, economical (transports were very expensive, the closer the quarry was the better) and artistic reasons. Originally, the place of the building site set the rock type(s) to be quarried and used for the edifice; this lasted until the Renaissance era at least. Mechanical properties, resistance against bad weather and height of rock layers also swayed the choice of the stone quality and the masonry type as well as the walls (one-leaf or multiple-leaf walls) and dimensions of the rock blocks. Finally, masonry type was also highly influenced by the building techniques used by the masons (local masons or itinerant companies) and the building master.

As aforementioned, since building as well as rock dressing techniques and the economical, social, religious and political context has changed in the course of history, so have masonry types.

6.2.1. PRE-ROMANESQUE MASONRY TYPES (CAROLINGIAN ERA)

Pre-Romanesque masonry was composed of pebbles, small stones or of medium-size dressed-stones, which were later preferred to pebbles to build important edifices. The courses were small, horizontal, reticulated or also fishbone-shaped (Figure 6.5) and sometimes interrupted with two or three tile layers that actually played the role of header bond [Fr 93]. The type of stone which was used depended on the material at disposal in the building site surroundings (quarry, etc.). Carolingians also arranged the bonds to be decorative through the stones position and colour. Mortar, which was made up of quick lime and sand, was often of bad quality; sometimes it was mixed with pieces of tiles.

Walls were quite thick because of stability; nevertheless they were thinner at the top. The churches were usually devoid of abutments; however, it is possible to see pilasters along the outer sides of a few edifices, as for instance, the chapel in Aachen. In fact, this sort of alternation of niches and vertical flat pilasters as well as very flat abutments was the premises of the Romanesque style [En 1902].

Regarding the tools used to cut stones, they were quite basic at that time; only the pick, the mass and the stone burin were used [Fr 93].

6.2.2. ROMANESQUE TIMES

The usual Romanesque bond is composed of medium-sized (and of medium-hardness) stones that are 20 cm to 40 cm thick and 30 cm to 60 cm long. Romanesque masons did not use small-size stones that was of common use during the Carolingian period and which required a lot of mortar. The height of the courses was defined by the thickness of quarry layers as well as the characteristics of the stone. Moreover, because of a rational use of the quarry blocs, it often occurs that stoneworks were made up of courses with irregular heights. Walls are composed of two outer masonry walls and of an inner one that is a conglomerate made up of pebbles and mortar. Romanesque masters already put bonder stones in order to tie outer and inner leaves to each other [Ha 05]. To strengthen masonry edifices, master builders also applied the in-and-out bond principle that can also be considered as abutments. For the same reason, they put bigger stones at corners (quoins bonding); nevertheless, according to [Ha 05], this system can also initiate cracks in masonry

(if the stones are big). It might be worth noting that unlike in Roman buildings, head joints in Romanesque masonry are not put every two courses (irregular stonework).

Though quite easy and rapid to be built, this kind of multiple-leaf walls have a few disadvantages: it is not only sensitive to humidity but also to differing deformation between the inner and the outer leaves (loss of homogeneity) (Figure 6.1).

Humidity, which comes from outside, enters the middle part through the outer wall joints. Water weathers the mortar-stone composite material and leads to the desegregation of the outer sides under the resulting lateral thrusts [Ha 05], [Co 70]. The outer leaves deformation under weight is smaller than the inner part settlement that may result in a rupture at the interface.

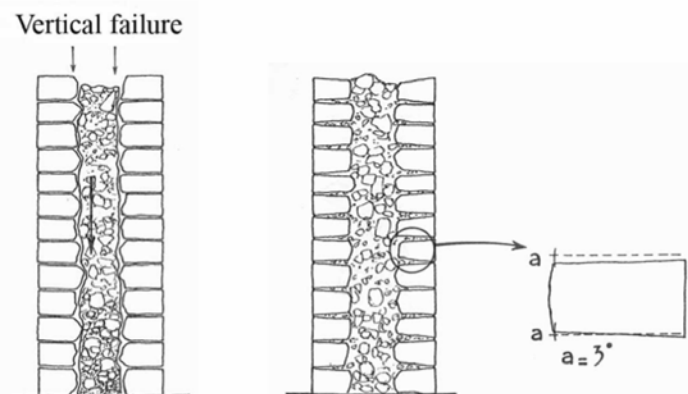


Figure 6.1 : Vertical failure between layers of a multiple-leaf walls; right: Cistercian method to avoid cracking [Ha 05].

Later, masons solved this problem by making thicker joints by placing stones of different lengths on each other (structure more homogeneous) or, as Cistercians did (Figure 6.1), also by dressing prism-shaped stones that have a smaller area in contact with the filling. In regard to walls, there is one more structural characteristic of Pre-Romanesque and Romanesque architecture (and which disappeared in Gothic period) that is worth noting: the archivolt. Abutments (rather flat pilasters) run along the outer facing of walls that bear archivolts, themselves supporting the upper part of walls; this system can bring more stiffness to the whole structure and it also make possible to build thinner walls (because unloaded by archivolts). However, the archivolts that can be seen in Switzerland are more aesthetic than structural, that is, they do not significantly stiffer the wall.

Like walls, columns and pillars are composed of two parts: an outer skin of stones that surrounds a kind of filling.

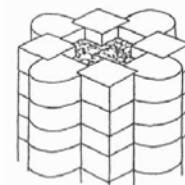


Figure 6.2 : Pillar cross-section [Ha 05].

Vaults, which are essentially barrel-shaped or groin-shaped (groin vault is used from the 11th century for covering the aisles), are made up of very light material so that walls are not heavily loaded. Moreover, building masters learned from experience that vaults without filling in the vault haunches cracked at one fifth of the arch (30° to 35°); so they stacked pebbles and mortar (that gave a kind of conglomerate) between the extrados and the nave walls.

Another characteristic of Romanesque building techniques is that every architectural element (columns, pillars, etc.) is integrated in a course height (it is no longer found in Gothic buildings); for

instance, a column put side-by-side with a wall is included within it through masonry courses. Corners are carried out with overlapping courses.

Regarding foundations, it has been noted [Ha 05] that they usually are of bad-quality. They are often, especially for small- or medium-sized churches, constituted of a masonry block that is itself composed of quarry waste or of river pebbles. Furthermore, foundations are not very deep (1.5 m) in order to minimize raw materials whose transport was expensive.

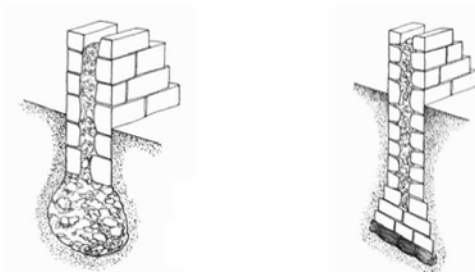


Figure 6.3 : Usual Romanesque and Cistercian foundations [Ha 05].

However, Benedictine and Cistercian edifices are sustained by foundations of better quality. They are 3 m deep and have the same structure as the multiple-leaf walls above; moreover, they widen as they go deeper and end with a footing which is one and one-half as wide as the walls are (stepped footing). Footings rest on fascines that are put into a cement matrix.

The walls of small edifices were often built in masonry with pebbles.

6.2.3. GOTHIC ERA

While Romanesque builders used medium-hard rocks and small stonework masonry, Gothic builders tended to use harder and of bigger size raw materials from the end of the 12th century.

As within the Romanesque era, each architectural piece, especially protruding ones such as capitals, cornices and lintels, was included in one course for each level. In consequence, each stone piece had to be dressed before being set in walls. Gothic masters rationalized these techniques and protruding components were linked to the rest of the structure through only a few courses (for instance, one per three courses).

In Romanesque period, the structure of walls was slightly changed: in place of an unorganized filling leaf, all parts of the walls were carried out course by course. Thus, courses of the wall outer leaf correspond to the courses of the interior leaf; this approach made masonry more homogeneous. Moreover, when walls were not too thick, bondstones were placed.

Compared to the massive Romanesque constructions, gothic masters tended to erect light, homogeneous and quite deformable (less sensitive to soil settlements or to structural deformation) edifices.

Besides prestigious edifices, common buildings were built with simple ashlar masonry or pebble masonry.

6.3. MASONRY TYPES IN SWITZERLAND

The kinds of stones that are used in a given masonry generally come from the same area as the constructed building. Similarly, it is erected by local workers and also according to local building techniques. These aspects are particularly true for Pre- and Romanesque edifices mainly because

of the economical system (feudal taxes), the political insecurity and the loss of the Roman building knowledge of that time (see chapter 3.2).

As a consequence, stone masonries are generally typical of the region where they were erected and lots of different kinds of masonries can be recorded. This fact is particularly true in Switzerland, not only because of the diverse cultures gathered in one country but also because of the high diversity of stones due to the proximity to the Alps. Moreover, beside raw materials and building techniques, the era when the construction was carried out is also of interest since the construction techniques evolved with time.

6.3.1. TYPES OF STONES

As aforementioned, stones used for a given building were extracted from the area around the building site. Consequently, their characteristics depend on the geological configuration of the place. Types of stones used for construction in Switzerland range from limestone, sandstone and granite to gneiss and even marble, which has been mainly used as stone facing.

In order to give an idea of the type of stones that might be found at different places as a function of the geological situation, an overview of the geology of Switzerland (as well as the mechanical properties of stones) is given in appendix (Appendix A.4.2).

6.3.2. TYPES OF MORTAR

Mortar is composed of solid materials (aggregates), binder and water.

AGGREGATE

Aggregate, sand, gravel and small pebbles are generally used; Romans also added Pozzolans¹ to their mortars, especially for underwater parts. While pebbles are brought from riverbeds, gravel and sand can be found either in rivers or in lakebeds. Moreover, aggregate might also result from crushed rocks and from blast furnace slag. Sand used in Swiss heritage buildings is generally either siliceous or calcareous.

Aggregates contribute to strengthen mortars and ensure them a better force distribution in masonry. They also help reduce shrinkage and a good (uniformly distributed) grading curve diminishes porosity [BSI 96]. The diameter of grains can exceed 4 mm in old mortars.

BINDER

Ancient mortars essentially used non-hydraulic lime, magnesia lime, blue lias lime and sometimes Portland cement for recent (before the 90's) transformations. In Switzerland, according to [EA 03], most cultural heritage buildings were erected with non-hydraulic lime until around 1750. In parallel to common lime, Blue lias lime was used from the 18th century end until 1900 when Portland cement began to be used and superseded both common and blue lias hydraulic limes. It is worth noting that though Roman Pozzolanic mortars -strictly speaking- were employed until the end of

1. Pozzolans, which constitute an artificial (roof tiles) or natural (from the region of Roma) adjunction of Alumina, Silica and Iron, react with the slaked lime and water to result in stable hydrates (suitable for underwater constructions).

the Roman Empire, masons put parts of tiles (or even of other kind of materials) into masonry until the 20th century these brought it close to the famous Pozzolan Roman mortar.

A few words about the binder types:

- Magnesia lime

Instead of pure limestone that is used in common lime, dolomitic limestone, in which magnesia carbonate is associated with calcium carbonate, is used for magnesia lime.

- Blue lias lime

This type of lime is made with impure limestones. Pure limestones are actually rather rare and they are usually interstratified with marls and claystones rich in iron, alumina and silica. At the burning stage, the calcium of limestone combines with iron, alumina and silica resulting in silicate, aluminates and iron-aluminates of calcium. By absorbing water, all these elements become insoluble hydrates that give the binder waterproof characteristics [BSI 96].

6.3.2.1. Mortar quality in the course of history

In Europe, as mortar was made with rocks extracted in the surroundings of the building site (that were essentially marled limestones or sandstones), the binder was very often blue lias lime [Re 91].

Without going back too far in Antiquity, it can be said that Greeks already knew how to make common lime. Romans borrowed Greek techniques and simply enhanced lime quality; while Greek people used lime for ornament or to whitewash facades, Romans applied it to small stonework masonry. It allowed them to erect resistant (because of better homogeneity and load distribution) and easy-built masonry.

After the Roman Empire collapse, Europe faced a long period of economical and politic instability; from a technical point of view this time of crisis led to a loss of knowledge and Roman building techniques were partially forgotten; constructions were badly erected. However, lime mortars were still applied but only for important edifices like castles, dwellings of nobility and bridges [BSI 96]; common buildings were actually erected with bad-quality raw materials and earthen mortar.

In the Romanesque period, the quality of mortars improved marginally and was of good quality in the Gothic period; nevertheless, until Renaissance, mortar quality varied a lot because of a partial knowledge and understanding of lime making process. Lime making actually requires not only excellent raw materials but also care in the limestone burning and a suitable proportioning of elements. All these points were satisfied with difficulty since many of the identified Romanesque mortars have defects as being lean (not enough lime) or being made with earthen sand, for instance. Moreover, these mortars had a very slow setting process that often resulted in deformations in walls. Lean mortars can be desegregated by water since the matrix was not compact.

In Renaissance, mortars quality was good.

6.3.3. RECORDED BONDINGS AND CROSS-SECTIONS

Walls are composed of either one or three leaves with a rubble filling in-between; there are several types of multiple-leaf masonry walls. The outer leaves are usually described through the way (bonding) and the quality of the cutting of stones as well as the type of mortar. The inner part might be made either of random rubble masonry or of a simple filling (sand and rubble mostly).

Regarding the masonry bonding, the usual combinations in Switzerland are¹:

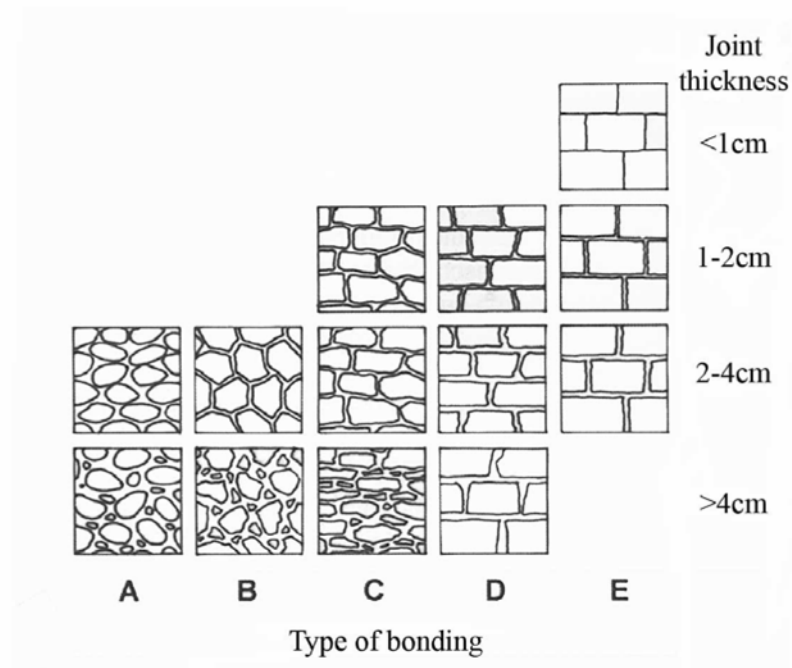


Figure 6.4 : Bonding types that can be found in Switzerland [SIA 266 07].

Where:

Bonding type	Description	Explanations
A	Rubble stone masonry	Masonry made up of round stones taken from riverbeds and/or from meadows.
B	Squared rubble masonry	Masonry of undressed stones that are initially angular; there is no horizontal course. For instance, the cyclops masonry belongs to this category.
C	Regular-coursed masonry with squared rubble.	Regular masonry mostly with squared flat-shaped rubble (limestone, gneiss, sometimes sandstone).
D	Regular-coursed masonry	Regular-coursed masonry made up of squared rubble that have been either roughly dressed or directly taken from quarry benches.
E	Ashlar masonry	Masonry made up of squared stones with well-made bed and head joints.

1. However, other combinations exist.

Other types might also be found in Switzerland:



Figure 6.5 : Other types of masonry bonding [SIA 266 07].

The fishbone masonry is seldom found in Switzerland; there is no wall that was completely made with this pattern (and which is still standing nowadays). It is more usual to see parts of a wall that are made up with such a configuration.

Walls made up of dry masonry can be essentially found in the canton of Tessin (south of Switzerland); this is the case, for instance, of the church Saint Nicola in Giornico. Nevertheless, there are so few sacred edifices (less than five) built using dry masonry in Switzerland, that this type of masonry is not taken into account in this report.

6.3.3.1. Cross-sections

Amongst the main cross-sections of masonry walls in cultural heritage buildings, there are essentially one-leaf and multiple-leaf walls.

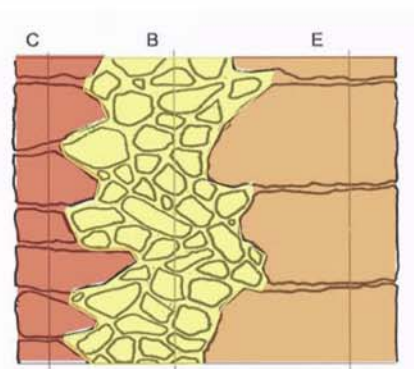
The one-leaf masonry wall can mostly be found in small churches, like the ones of small towns in the countryside or in towers (bell towers). The size and the type of the stone blocks can range from small stone rubble up to large squared stones. Depending on the quality (size and type) of the stones and mortar, each vertical edge of this kind of wall may be reinforced at the corners through big quoin stones of good quality.



Type 1

Figure 6.6 : One-leaf wall cross-section.

A multiple-leaf wall is defined as a heterogeneous construction (walls or pillars) which is composed of an inner leaf made (B on the right figure) of one or many materials. The inner leaf is compounded by two outer leaves (C and E on figure on the right) made of ashlar or simply regular-coursed masonry. Masonry of the outer leaves might be of different types; furthermore it is not infrequent that their thickness differs too.



Type 2

Figure 6.7 : Multiple-leaf wall cross-section.

The masonry type of the inner leaves depends essentially on the building process. This layer may be a kind of loose masonry (with blocks of bad quality compared with the masonry of outer leaves), a multi-layer masonry or simply a kind of filling with rubble.

The first solution -the loose masonry- which is composed of small stone blocks put in mortar and generally carried out at the same pace than the outer leaves, is probably the best from an engineering point of view. In this case, the outer leaves play the role of wall facing. The second solution -the multi-layer masonry (opus spicatum)- is carried out by putting quite good dressed stones onto a mortar layer; it results in a quite high concentration of holes. Because of its heterogeneity this kind of inner leaf does not have an efficient bearing capacity. The last possibility (opus caementitium), is filling in the empty room between the outer leaves that are already erected, with a mixture of rubble and mortar. If the filling is carefully carried out in steps of 50 cm, the inner leaf would be stronger than if it is entirely filled in at the end.

The connection between the inner leaf and the outer ones is provided by friction in the mortar joint (smooth interface), by crossing blocks or by cantilever blocks that are in the outer leaves and enter the inner part (crenellated interface). Nevertheless, several experiments and surveys on medieval multiple-leaf walls, show that only a few of them are connected through bond headers (crossing blocks) [Fr 93].

Note: the one-leaf masonry wall is the more efficient way to take loads. The multiple-leaf masonry wall is a solution that appeared because of the need for alternative materials as well as labours and time. According to [EA 03], this technique was already applied by Egyptians in the 3rd millennium BC.

6.3.3.2. DIMENSIONS

On the basis of many observations, Egermann [Eg 93] comments on multiple-leaf walls that:

- the average thickness is about 50 cm
- the relation between inner leaf and outer leaves thickness is between $t_i/t_o=1$ and $t_i/t_o=5^1$
- the relation between the aforementioned ratios and the thickness of the whole wall section is constant.

With respect to isolated walls (based on the survey of many edifices) Rondelet wrote in his treaty [Ro 1852] that a wall has a good stability if its thickness corresponds to the eighth of its height. If the thickness is the tenth of the height, it is still stable but this ratio cannot be lower than 1/12. For further information, the appendices can be consulted (Appendix A.4.4).

1. Where it corresponds to the thickness of the inner leaf and to the outer leaf.

6.3.3.3. Cross-section types as a function of the thickness

Besides the aforementioned rules, the type of cross-sections and its width can also be statistically linked:

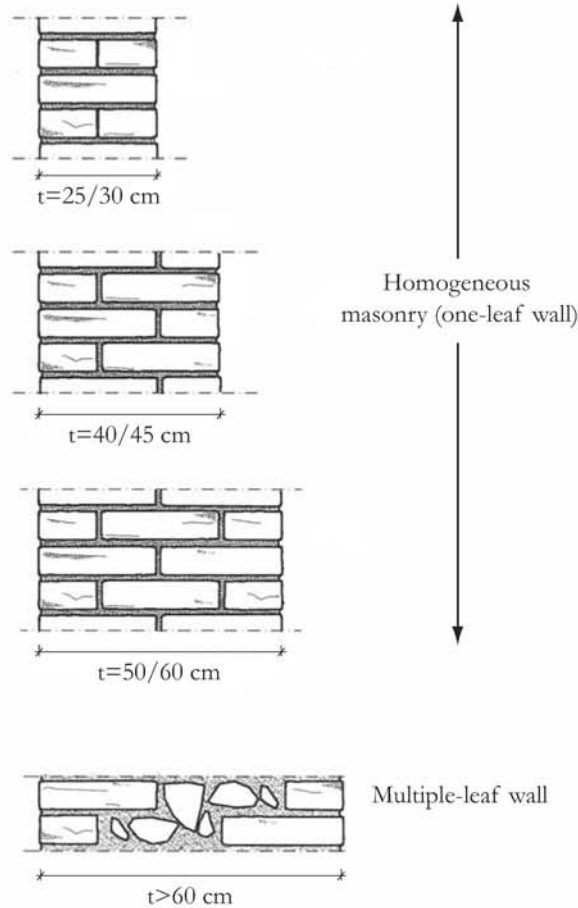


Figure 6.8 : Types of cross-sections as a function of the thickness [BP 06].

6.3.4. FOUNDATIONS

As already aforementioned, Romanesque foundations for churches were not of very good quality. They are not deep (1.5 m). Cistercian and Benedictine congregations made better foundations (chapter 6.2.2).

6.3.5. TRANSFORMATIONS

Cultural heritage buildings were frequently transformed with time. As the economical and political situation usually changed between two transformations, it is seldom to find different kinds of masonry in one wall, as illustrated on the below example:

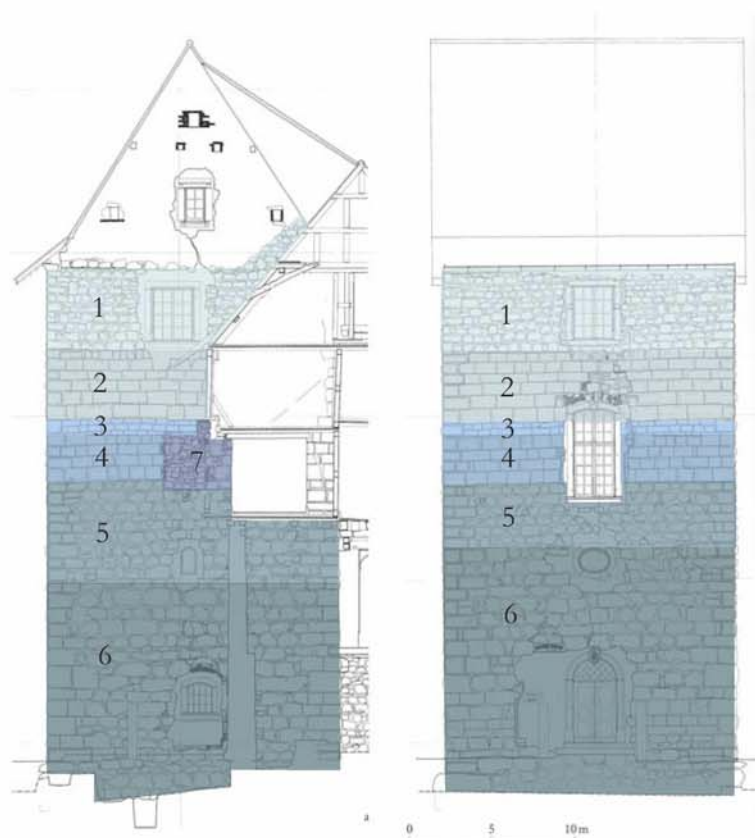


Figure 6.9 : Wall composed of masonries made at different period of time [Gr 03].

On the previous figure, at least six different kinds of masonry can be distinguished; they correspond either to a raising of the wall, the closing of an previous opening or a restoration after some damage.

Nevertheless, though churches sustained transformations of masonry after their completion, there was seldom a small part that was changed but rather a large part (a whole wall for instance). Such a case can be seen for masonry composed of stones sensitive to bad weather, such as molasse (sandstone).

6.4. MECHANICAL PROPERTIES OF STONE MASONRY

Masonry is a composite material whose structural behaviour (strength, stiffness and ductility) depends on many parameters, such as mechanical properties of stones and mortar, bonding type (geometry of stones, thickness of joints and the horizontality of courses), state of maintenance and thermal coefficients¹.

1. Though it may create supplementary stresses up to a certain degree, the impact of thermal coefficient will not be taken into consideration in this report.

Except in the case of dry masonry, masonry is a composite material composed of two different materials, i.e. stones and mortar¹. Forces can be transferred throughout masonry: under compression, mortar allows forces to be uniformly distributed from one course to another and it also gives a better resistance to horizontal forces through friction and adhesion. On the other hand both these materials are characterized by very different mechanical properties. This may lead to an incompatibility in deformation when the load achieves a certain level. For instance, stones usually have a higher Young modulus than mortar and especially old mortar which is much more ductile than stone. For instance, the sandstone's E modulus can reach a value of ² 15'000 MPa whereas the value of the same modulus for mortar is about 1000 MPa, i.e. a tenth of the former value. Furthermore, mortar failure can happen at a strain of 0.7% while the stone strain at failure is about 0.25 % [Hu 00].

Because of all the aforementioned features, which influence the stone masonry's mechanical behaviour as well as their variations, it is very difficult to calculate the exact value of the failure. Nevertheless, it is possible, under a few conditions, to determine strength values [Hu 00] through models; it is however important to be aware of the influence of the model assumptions in order to assess the quality (and the domain of application) of the obtained values. Models, which have been developed in order to assess stone masonry collapse values, are presented and discussed within the next few chapters.

Before describing the mechanical behaviour of masonry, each of its components, i.e. stone and mortar, is dealt with.

Note: though a few cultural heritage buildings are built with dry masonry, like the Saint Nicola's church in the canton of Tessin, it is not studied in this report because they constitute a small group of edifices. Moreover, these kinds of churches are situated in areas that are not characterized by a high seismic hazard.

6.4.1. STONE

Stones are characterized according to their mechanical properties as well as their conditions of failure.

6.4.1.1. Mechanical properties

Stones are brittle or quasi-brittle materials: under compression, stone is characterized by a more or less elastic behaviour up to a brittle failure. Under tension, stones have low resistance.

As shown on the previous figure, the mechanical behaviour of quasi-brittle materials (such as stone) under tensile load, as well as compressive (though less visible) shows a softening phase. This important feature is due to progressive internal crack growth that is commonly attributed to the heterogeneity of material [RGÖL 98]. Stone is heterogeneous because of micro-cracks in its structure. Under load, these micro-cracks grow until the beginning of the creation of macro-cracks. This corresponds to the peak load; from then onwards, load can only decrease as macro-cracks are unstable.

1. Sometimes, other materials, such as tiles, can be found in masonry.

2. It is worth keeping in mind that sandstone mechanical properties vary a lot from one type to another because of the quarry and the layer from which it was taken and the way it was laid within masonry.

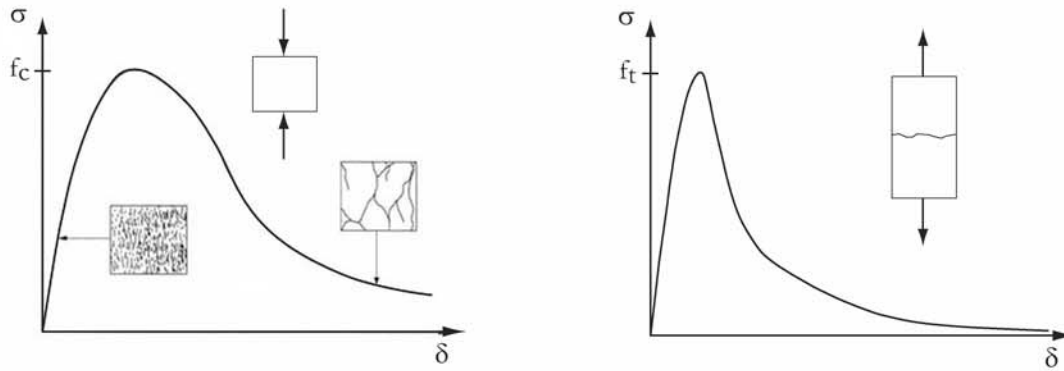


Figure 6.10 : Typical behaviour of quasi-brittle materials under uniaxial compressive and tensile force, respectively [RGÖL 98].

The relation between compressive strength and tensile strength is situated between 30:1 and 15:1 [SA 91]. It may be worth noting that this ratio for stone is higher than the one for concrete (ratio of 10:1). Poisson's ratio is between 0.01 and 0.09.

6.4.1.2. Stone failure: criterion

During one of his experiments on stone materials, Coulomb discovered in 1773 that the collapse plane of stone under compressive load was oblique. He concluded then that such materials collapsed by sliding on such a plan where shear (τ) and the normal stress (σ) had values linked together by a linear law. This criterion was then enlarged by Mohr (1900 to 1914) and then Caquot (1935) [Fr 94]. Mohr's theory can be applied to assess the strength of brittle materials; it says that failure happens on a plan where the tangential stress τ achieves a certain value in relation to the perpendicular stress:

$$f(\sigma) = \tau \quad (\text{EQ 6.1})$$

This curve, which is called the intrinsic curve, is the envelope of Mohr circles at failure for one material. In general, three circles are drawn: each from compression, tensile and plain shear experiments.

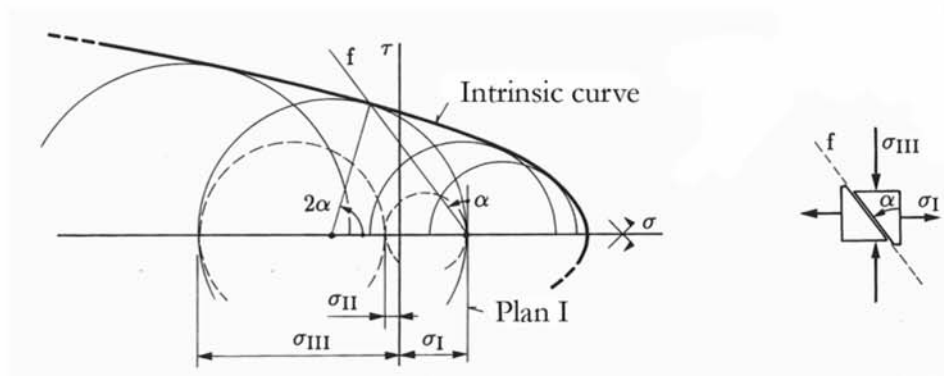


Figure 6.11 : Intrinsic curve [Fr 94].

A block of stone in masonry is indeed loaded by compression and tension; the mass above the blocks and its own weight create compression and its co-existence with mortar results in tension in the block (at the mortar-stone interface, see chapter 6.4.3) due to the deformation of mortar.

Another way failure criterion for stones was proposed (Figure 6.12): this gives the interaction between the material compressive strength and its tensile strength. A few experiments and analytic models have been carried out on the mechanical behaviour of bricks under compression and tension in order to obtain the material failure curve in function of the compressive and tensile strength.

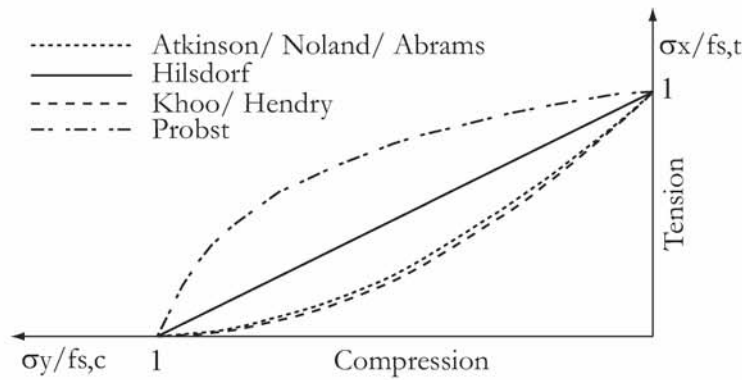


Figure 6.12 : Bricks failure curves [Eb 96].

Based on a similar failure curve, another method for calculating the strength of masonries composed of sandstone blocks was proposed by Berndt and Schöne [BS 91, BS 94]. The given equation was drawn from experimental investigations. According to Berndt and Schöne, the failure of masonry always happens because of the tensile failure of stone.

$$\frac{\sigma_{x,s}}{f_{s,t}} = 1 + 0.7 \cdot \frac{\sigma_y}{f_{s,c}} \quad (\text{EQ 6.2})$$

Where: $\sigma_{x,s}$: stress along x-axis

$f_{s,t}$: stone tensile strength

σ_y : stress along y-axis

$f_{s,c}$: stone compressive strength

Ebner [Eb 96] also recommends the application of the Berndt and Schöne equation with a curve slope between 0.5 to 0.7. for sandstone masonry.

6.4.2. MORTAR

Mortar is composed of solid materials, binder and water. While the diameter of grains cannot exceed 4 mm in present mortars, it used to be the case in old ones. Ancient mortars essentially enclose lime, hydraulic and quicklime. The type and quantity of binder has a great influence on the time for hardening as well as on the mortar strength.

6.4.2.1. Mechanical properties of lime mortars

Mechanical properties of mortars depend on the following parameters:

- water-binder relation
- absorption capacity of stones
- age of mortar
- ambient temperature
- contact with air (quantity)
- boundary conditions for shrinkage of mortar
- concentration of binder
- joint height

Like stones, mortars have low resistance to tensile forces and are better in compression; furthermore, the force-displacement curve looks like that of stone (though more deformable).

Because of the aforementioned parameters, the mechanical properties (mortar strength, etc.) obtained by tests cannot be directly used as absolute values. Moreover, the mechanical properties of mortar are different for a masonry joint because the boundary conditions can differ even along a joint. Nevertheless, a few researchers carried out many tests on mortars which allowed them to set mortar failure criteria.

6.4.2.2. Mortar failure criterion

Two teams carried out experiments on mortar in order to determine its failure curve [Eb 96]. Based on the assumption of a confining pressure, Koo and Hendry [KH 73] described the mortar failure curve as a function of its compressive strength:

$$\frac{\sigma_1}{\sigma_0} = 1 + 2.91 \cdot \left(\frac{\sigma_2}{f_{m0,c}} \right)^{0.805} \quad (\text{EQ 6.3})$$

Where: σ_1 : major principal stress

σ_2 : minor principal stress

$f_{m0,c}$: compressive strength

Note: this equation has been developed for 1:0.25:3 and 1:1:6 (concentration in weight of: cement, lime, sand) mortars.

6.4.3. PROPERTIES OF THE MORTAR-STONE INTERFACE

Mortar and stones are characterized by different mechanical properties, especially in their stiffness (Young’s modulus).

Because of different mechanical properties, problems of compatibility appear at the mortar-stone interface; three cases can arise with respect to the tightness of connection between mortar and stone. The first, is the case where connection is almost inexistent. The second, which constitutes the other limit, is encountered when the connection between mortar and stone is fully restrained.

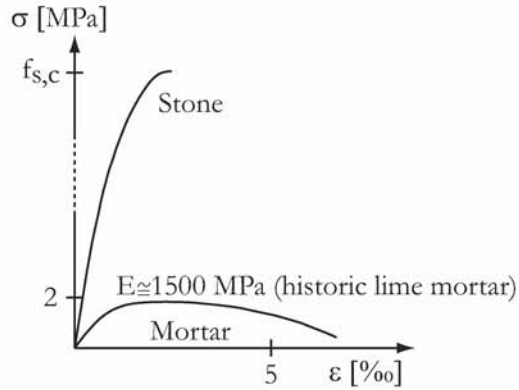


Figure 6.13 : Stress-deformation curve of stone and mortar.

In between, there is a third case which characterizes a connection whose efficiency is situated between both above-mentioned limits. Generally, bed joints suffer from this problem more than head joints.

Case 1: Stresses in mortar are independent of the ones within stones.

Case 2: At the interface, stresses must be similar both in the stone and in mortar (assumption).

As mortar is less stiff than stone, its deformation is actually restrained and this situation results in compressive stresses in mortar and tensile stresses (counterpart) in the stone. If the joint is thin, the stress distribution on the joint height can be assumed as constant. On the contrary, the distribution of stresses in a direction perpendicular to the action is rather parabolic in thick joints.

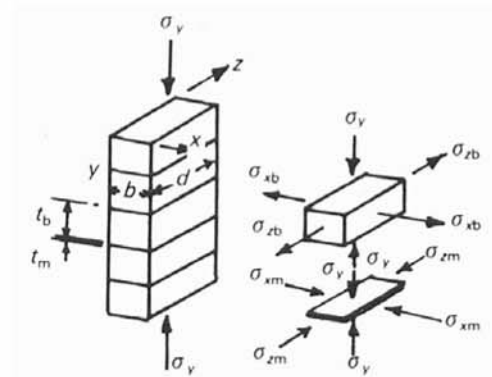


Figure 6.14 : Stresses in stone-block-mortar composite; taken from [He 90].

The following equation evaluates stresses perpendicular to the action direction (assuming that deformation in both directions of the plan is the same):

$$\sigma_y = f_{m_{o,c,p}} + m \cdot \sigma_{rm} \tag{EQ 6.4}$$

Where: σ_y : vertical stress (σ_N)

$f_{m_{o,c,p}}$: mortar compressive strength on prism

σ_{rm} : radial stress

m: slope of the envelope curve

Tensile stresses in stones result in cracks in both directions (in the plane perpendicular to the action direction). The above equation can be applied only if the following conditions are satisfied:

- Joint height must be thin enough so that the distribution of stresses is constant on the thickness
- Mortar shear strength is high enough to stand the shear force at the interface

While these above conditions are generally satisfied in brick masonry, this is no longer the case in stone masonry. Old lime mortar is indeed more deformable than the cement mortar of brick masonry. Consequently, it tends to increase the shear stress at the interface between stone and mortar. However, instead of resulting in cracks in stones, it is more likely to cause the separation between the two materials.

Case 3: representing the reality, i.e. a situation when the connection between mortar and stone is not perfectly ideal (with the stone whole surface tied to a mortar which is strong enough to stand the shear force resulting from perpendicular actions).

Note: even when mortar is vertically cracked, in the case of vertical compression actions, vertical stresses can be still transferred from a stone to the one under it. This is due to the mortar confinement (3D compressive stress state) and its friction capacity.

Besides the transfer of forces in the mortar and at the interface, forces must also get through stones. The force flow within stones depends on the rock structure (micro-cracks and cracks) and on the boundary conditions. If stones do not completely (on the whole surface) lie on mortar, flow of forces is no longer vertical and it consequently results in tensile stresses within the stones.

A regular masonry with rectangular stones and constant-thickness mortar joints will collapse because of cracks in stones (because of the incompatibility of deformation at the interface). On the contrary, collapse of irregular masonry will occur due to cracks in mortar. The force flow always follows the highest stiffness, which is actually provided by stones.

Note: when mortar yields, it no longer resists an increasing of loads; this often happens in the edge zones. The surface that transfers loads is then smaller and this area is consequently more loaded than before.

6.5. ONE-LEAF STONE MASONRY FAILURE: CRITERION

Compared with ordinary masonry (masonry composed of bricks with perpendicular head, bed joints and regular courses), the surface of ashlar masonry is usually irregular. The difference of mortar thickness due to irregular stone surfaces leads to a concentration of stresses in bed joints, especially where it is particularly thin. These aspects of heterogeneity result in a more complex situation compared to ordinary masonry.

Roughly, two approaches have been adopted to deal with the mechanical behaviour of masonry: the first one is based on principal stresses, while the second one uses the shear and normal stresses ($\tau=f(\sigma)$).

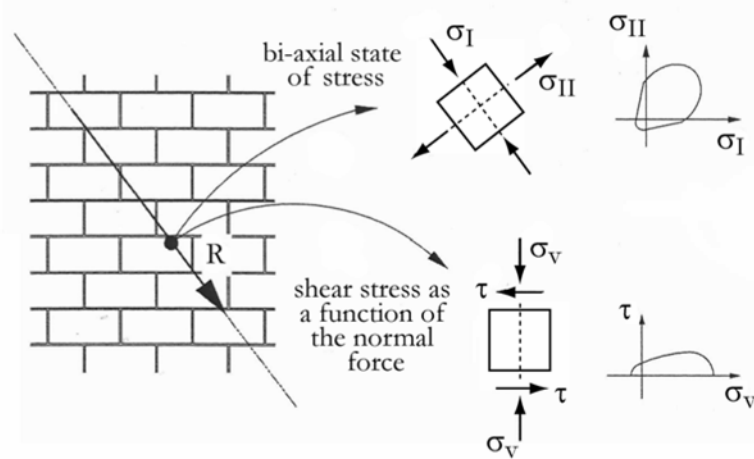


Figure 6.15 : Main approaches to describe masonry failure; taken from [Cr 98].

The natural stone masonry failure can be either due to the failure of mortar or that of stone (tensile failure). All the following models are based on one of these assumptions. Every model which is based on the failure of stone takes into account the non-linear behaviour of mortar; the yield surface that is generally used is Drucker-Prager's. The minimal vertical stress that causes the stones to fail is determined by the stresses in stones when they achieve the failure surface of the rocky material. These stresses are due to the incompatibility of deformation at the mortar-stone interface. This minimal value of vertical stress is usually considered as the failure stress of the wall¹.

When masonry failure is defined by the failure of mortar, the Mohr-Coulomb's yield surface is usually applied.

Note: no model considers the influence of vertical joints on the masonry compressive strength.

The definition of the above model's yield surface requires the value for the material strength, that is, the compressive, tensile and shear strength.

6.5.1. COMPRESSIVE STRENGTH

Many experiments have been carried out in order to study the compressive strength of masonry; it has led to the determination of empirical formulae as well as analytical ones. Before listing them (see the next chapters), it is worth noting general masonry features that have been drawn from standard tests.

GENERALITIES

Recent research work has shown that the compressive strength is influenced by the characteristics of units, mortar and masonry [He 90]. Characteristics are shown on the following table:

1. The diminution of the loaded surface due to the mortar yielding along is not allowed for.

Table 1 : Factors that influence the compressive strength of masonry.

Unit characteristics	Mortar characteristics	Masonry characteristics
Strength	Strength	Type of bond
- Type of stone and geometry of units	- Water/ cement ratio	Direction of loading
- Solid	Relative deformation	Local stress raisers (e.g. discontinuities)
Relative height	Relative thickness	
Absorption of stone		

The compressive strength of masonry varies approximately as the square root of the unit strength and as the third or fourth of the strength of the mortar. In what concerns the material properties of the bed joints, it was observed that the «smoother» the mortar is, the lower is the compressive strength. Experiments have shown that the presence of aluminium sheets, mortar (1:0.25:3) or soft rubber bonds may decrease the masonry compressive strength to 96%, 35% and 17% of the unit strength, respectively. Moreover the joint thickness may have a great influence on the masonry compressive strength: this value tends to the unit strength when the mortar joints are thin. Thick joints decrease the masonry compressive strength (the units split quite rapidly (depending on the loading level)).

Many empirical equations were developed to determine the compressive strength of masonry; a few of them are listed here below.

6.5.1.1. Compressive strength according to the Swiss code 178 [SIA V178 80]

The compressive strength of different new natural stone masonries is calculated according to the following diagram ($f_{m,c}(f_{s,c})$).

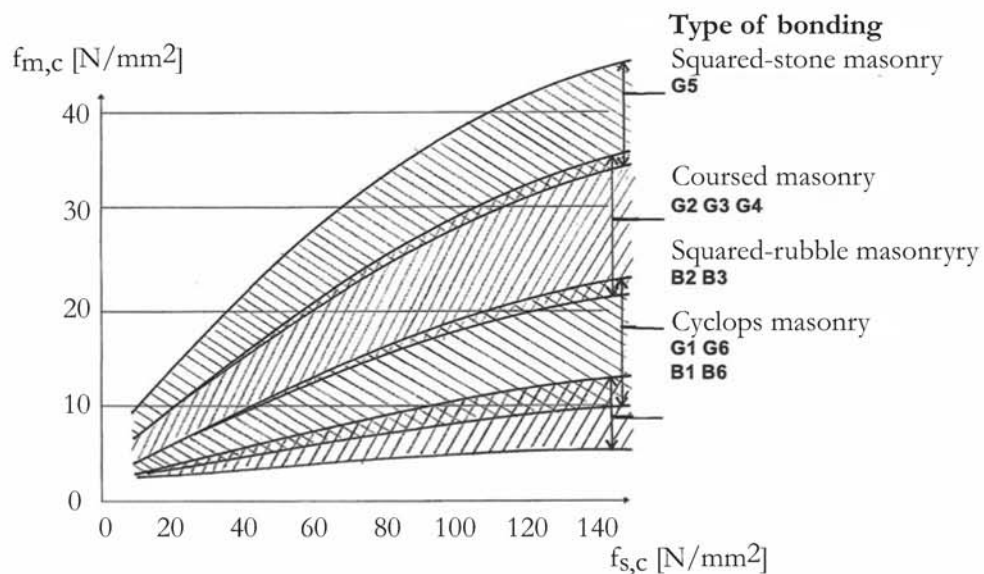


Figure 6.16 : Determination of the compressive strength of different types of masonry [SIA V178 80]

- for every masonry except the cyclopean one: $f_{m,y} = 0.5 f_{m,x}$
- for cyclopean masonry: $f_{m,y} = f_{m,x}$

Note: though the results that are obtained with the above diagram seem to be quite good, specialists agree that this diagram gives too great values of compressive strength of masonry compared with reality.

This diagram reflects the fact that masonry compressive strength depends highly on the quantity of mortar, that is to say (according to the above diagram):

- compressive strength of random rubble masonry is quasi-proportional to the mortar strength,
- because of alternate courses with more or less thick joints, the compressive strength of squared rubble masonry is between the units and the mortar compressive strength,
- ashlar masonry compressive strength is very close to the stone strength because of the small proportion of mortar.

The Young's modulus of masonry is:

$$E_{m,x}^a = E_s \cdot \text{volume of the stone part [\%]} + E_{mo} \cdot \text{volume of the mortar part [\%]} \quad [\text{MPa}] \quad (\text{EQ 6.5})$$

a. x corresponds to the x-axis (vertical).

6.5.1.2. Compressive strength according to the EC 6

The method developed by the Eurocode 6 [EC6 96] to calculate the compressive strength of masonry is based on the stone strength and the mortar strength as well as on a coefficient K that increases or decreases the given masonry strength according to its bonding type and the stone type.

$$f_{m,c,k} = K \cdot f_{s,c}^{0.65} \cdot f_{mo,c}^{0.25} \quad (\text{EQ 6.6})$$

Where: $f_{m,c,k}$: specific compressive strength of masonry (5% fractile)

$f_{s,c}$: average compressive stone strength along the load direction (on a 100x100mm sample that was dried in ambient air)

K: correction factor, depending on the stone category, bonding in cross-section and mortar type

$f_{mo,c}$: average value of the mortar compressive strength

For the value of K, the reader can consult the EC6.

Moreover, the strength of the rocky material is decreased by a partial coefficient that ranges between 1.7 and 3.0 corresponding to combinations IA and IIC (MGr) respectively.

6.5.1.3. Compressive strength of ashlar masonry in sandstone, after Pöschel [PS 96]

Pöschel's model was based on a combination of both compressive tests and FEM analyses. Under compression cracks appear early in stones, under a low level of load, along their perimeter. Failure occurs through vertical (parallel to the action direction) cracks in the middle of stones.

The yield criteria is based on stone failure; it occurs when the combination of stresses in the middle of stone exceeds the stones strength. The value of such stresses is calculated by a formula using the damage state of mortar (defined through the height of the damaged mortar) and on the stone width.

$$f_{m,c} = \frac{2 \cdot \frac{t}{b} \cdot f_{mo,c} \cdot \left(2.32 \cdot \frac{f_{s,t}}{f_{s,c}} + 1.6 \right) + f_{s,t}}{\frac{t}{b} \cdot \left(2.32 \cdot \frac{f_{s,t}}{f_{s,c}} + 1.6 \right) + \frac{f_{s,t}}{f_{s,c}}} \quad (\text{EQ 6.7})$$

Where: $f_{m,c}$: compressive strength of masonry

$f_{mo,c}$: compressive strength of mortar

$f_{s,c}$: compressive strength of stone

$f_{s,t}$: tensile strength of stone

t: joint height

b: stone width

Note: the relationship between stone height and joint height is not considered, though it has a great influence on the masonry strength.

6.5.1.4. Failure model for ashlar masonry after Berndt and Schöne [BS 91], [BS 94]

For this model, the failure criterion is based on the multi-axial strength of stone units and mortar. Cracks in stones are assumed to be due to:

- The incompatibility in deformation in the plane perpendicular to actions at the stone-mortar interface results in cracks within stones
- Cracks in the middle of stones because of damaged mortar (non-uniform distribution of stresses in stones)

These two sources of cracks are taken into account and the proposed equation is a function of them. Here below is the equation describing the stone failure:

$$\frac{\sigma_{s,x}}{f_{s,t}} = 1 + 0.7 \cdot \frac{\sigma_y}{f_{s,c}} \quad (\text{EQ 6.8})$$

Moreover, the yielding behaviour of mortar is modelled through a deformation **factor** **and** the interal friction coefficient ϕ . Masonry strength can be calculated with the help of the following equation:

$$f_{m,c} = \frac{f_{s,c}}{\left(\frac{t}{h'} \cdot \frac{v_m}{1-v_m} + K_1 \cdot \frac{d'd}{dh''} \right) \cdot \frac{f_{s,c}}{f_{s,t}} + 0.5 \dots 0.7} \quad (\text{EQ 6.9})$$

Where: $f_{m,c}$: masonry compressive strength

$f_{s,t}$: tensile strength of stone

ν_m : Poisson's coefficient of mortar ($\nu_m=0.3$ (MGr I), 0.4 (MGr II), 0.5 (MGr III))

h'' : stone height or 20 cm (the smaller value is prevalent)

d : wall thickness

t : joint height

$d' = t + t / (\tan(45 + \varphi/2))$

where: $\varphi=20$ for MGr I¹

$\varphi=30$ for MGr II

$\varphi=40$ for MGr III

h' : stone height or 10 cm (the smaller value is prevalent)

$f_{s,c}$: compressive strength of stone

K_1 : decreasing factor for the maximal cracking strength at the middle of the stone

Eq 6.9 can be represented by the following diagram showing the failure curve of stone:

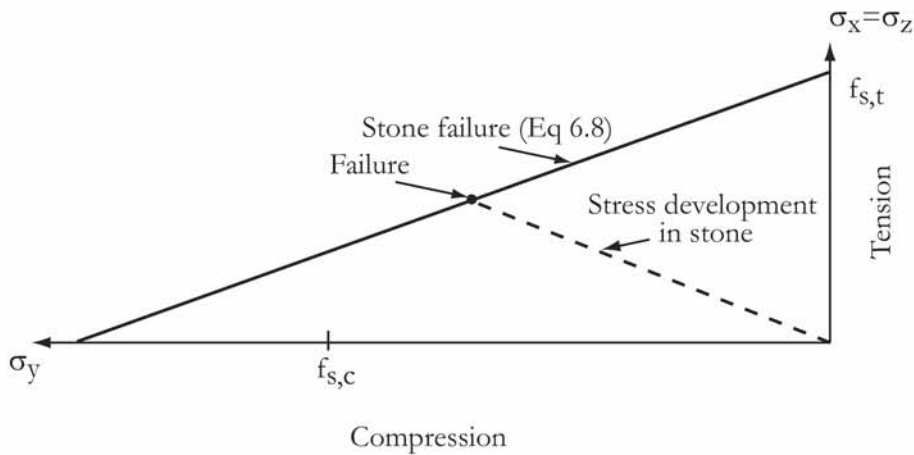


Figure 6.17 : Criterion of natural stone masonry after Berndt and Schöne [BS 91].

The depth of damaged mortar is calculated as a function of the joint height and the friction angle of mortar. Berndt gave different values of the friction angle in regards to the mortar quality (from 20° (bad quality) up to 40° (good quality)).

Note: the proposed equation is reliable for one-leaf asblar masonry if the E-modulus of stone is much higher than the mortar E-modulus. However, the equation is not applicable in the case of thick mortar joints.

6.5.1.5. Failure model for one-leaf stone masonry (irregular courses) after Ebner [Eb 96]

Ebner has carried out a series of three experiments related to three types of masonry: two-leaf walls without filling, three-leaf walls with sand (without mortar) as filling and three-leaf walls with

1. Mortar groups depending on their quality

an inner layer composed of small ashlar and lime mortar. She also numerically modelled the structure in order to better understand the results obtained through the experiments. According to Ebner, there are three possible failure modes of a one-leaf masonry wall under compressive loading:

- the stones fail due to the influence of head joints
- the stones fail due to the incompatibility of deformation at the stone-mortar interface
- the mortar fails

According to her observations, head joints influence the load distribution along the horizontal surface. This also leads to higher horizontal tensile stresses in stone blocks. These stresses may be determined by using a factor that multiplies the horizontal tensile stresses resulting from the restrained deformation. This factor essentially depends on the head joint and bed joint thickness as well as the mortar strength. She then calculated the minimal vertical stress due to the head joints with the following equation:

$$\sigma_y = -\frac{f_{s,t}}{k_{SF} \cdot K_q + m_s \cdot \frac{f_{s,t}}{f_{s,c}}} \leq f_{s,c} \quad (\text{EQ 6.10})$$

Where: $f_{s,t}$: stone tensile strength (on prism)

σ_y : minimal vertical stress in stone (compressive) (σ_N)

$f_{s,c}$: stone compressive strength (on prism)

m_s : slope of the stone failure envelope curve ($m_s = 1.0$ to 0.5)

K_q : factor

$$K_q = \frac{1 - \sin \varphi}{1 + \sin \varphi} \cdot \frac{h_m}{h_s}$$

h_s : stone height

$\tan \varphi$: mortar internal angle of friction

h_m : bed joint height

K_{SF} : factor

$$K_{SF} = 3.4 \cdot \frac{b_s^{0.2}}{\sqrt{h_m \cdot \frac{1 - \sin \varphi}{1 + \sin \varphi}}}; b_s \leq 70 \text{ mm}$$

b_s : head joint width

The second criterion is linked to the horizontal tensile stress resulting from the restrained deformation at the stone-mortar interface. Ebner [Eb 96] took it into account in the following equation:

$$\sigma_y = -\frac{f_{s,t}}{K_q + K_{TF} + m_s \cdot \frac{f_{s,t}}{f_{s,c}}} \leq f_{s,c} \quad (\text{EQ 6.11})$$

Where: $f_{s,t}$: stone tensile strength (on prism)

σ_y : minimal vertical stress in stone (compressive)

$f_{s,c}$: stone compressive strength (on prism)

m_s : slope of the stone failure envelope curve ($m_s = 1.0$ to 0.5)

K_q : factor

$$K_q = \frac{1 - \sin \varphi}{1 + \sin \varphi} \cdot \frac{h_m}{h_s}$$

h_s : stone height

$\tan \varphi$: mortar internal angle of friction

h_m : bed joint height

K_{TF} : factor

$$K_{TF} = K_1 \cdot \left(0.07 - 0.25 \cdot \frac{1 - \sin \varphi}{1 + \sin \varphi} \cdot \frac{h_m}{h_s} \right) \geq 0$$

For calculating K_1 :

$$b_{gr1} = h_m \cdot \left(\frac{\sqrt{2}}{\tan \varphi} - 2 \right) + h_s \tan 30^\circ$$

$$b_{gr2} = h_m \cdot \left(\frac{\sqrt{2}}{\tan \varphi} + 2 \right) + h_s \tan 30^\circ$$

$$K_1 = 1 \text{ for } d < b_{gr1}$$

$$K_1 = 2 \text{ for } b_{gr1} < \text{or } = d < \text{or } = b_{gr2}$$

$$K_1 = 1 \text{ for } d > b_{gr2}$$

The last criterion is about the mortar strength: the minimal vertical stress that can be supported by the mortar is given by the following equation:

$$\sigma_y = c \cdot \left(\frac{d_{\min}}{2.4 \cdot h_m \cdot (1 - 2 \tan \varphi)} \right)^{2.5} \quad (\text{EQ 6.12})$$

Where: d_{\min} : smallest stone width

σ_y : minimal vertical stress in stone (compressive) (σ_N)

$\tan\varphi$: mortar internal angle of friction

c: cohesion

The smallest vertical stress that is obtained with the above equations corresponds to the masonry failure stress. This value for one-leaf wall is then calculated for the whole cross-section with the defined failure stress¹.

$$f_{m,c} = \left(1 - 1.2 \cdot \frac{h_m}{d} (1 - 2 \tan \varphi) \cdot \left(\frac{\sigma_y}{c}\right)^{0.4}\right) \cdot \left(1 - \frac{n \cdot b_s}{l}\right) \cdot \sigma_y \quad (\text{EQ 6.13})$$

Where: $f_{m,c}$: failure stress of one-leaf masonry wall

σ_y : minimal vertical stress in stone (compressive) (σ_N)

h_m : stone compressive strength (on prism)

d: wall thickness

n: number of head joints above or beneath one bed joint

b_s : head joint width

l: wall length

c: cohesion

Note: if stone blocks are of different height, each bond must be allowed for.

Ebner [Eb 96] proposed a way to adapt these results for squared-stone masonry to another kind of masonry, such as the ashlar masonry made up of dressed blocks instead of perfect rectangular ones. Since the compressive strength of a well-dressed-stone masonry is higher than the one of a simple ashlar masonry, Ebner proposed to reduce the value obtained for the former in order to get the strength of the latter.

$$f_{m,c,am} = \frac{f_{m,c,ssm}}{\alpha} \quad (\text{EQ 6.14})$$

Where: $f_{m,c,am}$: failure stress of an ashlar masonry

α : factor ($\alpha=3.3$)

$f_{m,c,ssm}$: failure stress of a square-stone masonry

Note: the stone characteristics must be the same in both cases, as well as the wall dimensions.

It is important to keep in mind that this model for calculating the compressive strength of regular ashlar masonry, is based on both numerical and experimental tests. It essentially depends on the mortar internal angle of friction as well as its cohesion (Mohr-Coulomb yield surface). As the definition of the mortar mechanical properties (φ and c) is a difficult and uncertain task, the application of this model is actually complex.

1. This value differs a little bit for small-sized wall; for further information, the reader can refer to [Eb 96].

6.5.1.6. Discussion about the models

In [Hu 00], the above-mentioned methods are compared through their application to three case studies (two of a similar masonry type but with different mortars and the third case was an irregular-course masonry) each corresponding to a sample that was experimentally tested by Warnecke [Wa 95]. It emerged that though every method gives different values of compressive strength from the test results, they are all close to each of them.

The determination of the masonry strength by the Eurocodes (EC 6) gives values that are 20% to 33% higher than test results. Once again, the equation allowing us to obtain the compressive strength of stone masonry was initially developed for and from brick masonry. The equation terms are then essentially compressive strengths (both of stone and mortar) and consequently many factors that might influence the mechanical behaviour of stone masonry are simply not allowed for. However, Huster [Hu 00] wrote that this method could be applied for regular ashlar masonry with thin joints.

Pöschel's method also gives a higher compressive strength (20-80% high). This relation is actually independent of the joint height and assumes that cracks appear in the middle of the stones; this assumption requires a cubic stone (in regards to the stone friction angle). The collapse mechanism consequently corresponds to a state of pure shear; this assumption is actually too restrictive.

Compared to all other above-mentioned rupture models, the one developed by Berndt, according to Huster [Hu 00], has the best fit with the test results (6-55 % of difference). Not only did this theory give better results for the stone masonry with a mortar of bad quality, the values obtained for other types of masonry are also quite good. Moreover, it may be worth noting that the model was initially set up for ashlar masonry. Contrary to the other models, Berndt's takes into account important parameters that may greatly sway the strength of masonry, like the joint height (regarding the failure load level), the connection between the stone width and height and the place where the first cracks appear.

Regarding the results obtained with the SIA 178, the difference between experimental measurement and the method result is more than 100% for the first case¹ (regular ashlar masonry), while it reduces to 0 and 6% for both other cases (regular masonry with good quality mortar and irregular ashlar masonry, respectively).

Ebner's method has not been applied because the masonry cohesion was unknown.

To sum up, the SIA model is applied in the next chapters since it gives good results for calculating the compressive strength of masonry.

6.5.1.7. Discussion about masonry strength under compressive loading

- the smaller is the angle of internal friction and the slope of the mortar failure envelope curve, the smaller is the safe bearing capacity.
- mortar thickness has a great influence on the non-linear loss of bearing capacity (mortar failure is already predominant with thin mortar joints).
- stone height is also a prevalent factor: the larger the depth of course is, the larger is the failure load; this impact is amplified for thick joints.

1. Comparison is made with average values.

6.5.2. SHEAR STRENGTH

Masonry walls can be subjected to shear actions simultaneously with vertical compressive load; this is especially true during earthquakes. Consequently, the shear behaviour of masonry has been investigated in several countries for years now. The purpose here is not to make an exhaustive list with every experimental investigation that was carried out in order to model the structural behaviour of walls under shear actions. Only a few ones that are relevant to the study of the old masonry behaviour under seismic actions are presented here below.

First, scientists focused their research on determining the masonry shear strength based on the Mohr-Coulomb failure surfaces; however, the beginning of the computer use in the 70' led them to develop other material failure criteria for numerical implementations. These models were no longer based on the Mohr-Coulomb's law but rather on the principal stress block (Figure 6.15).

Scientists originally focused on the application of the Mohr-Coulomb equation on different kinds of masonries. Many tests were carried out in order to find values for the cohesion ($c=\tau_0$) and the internal friction term (μ or $\tan\phi$) for diverse types of masonries for they depend on the properties of the materials used, the form of the test specimens and the loading arrangements. Hendry and Sinha [HSD 04] proposed the following equation to calculate the shear strength of masonry according to a Mohr-Coulomb formulation ($\tau = \tau_0 + \tan\phi \cdot \sigma$):

$$\tau = 0.3 + 0.5 \cdot \sigma_N \quad (\text{EQ 6.15})$$

Where: τ : shear strength of masonry

σ_N : vertical stress

Note: this relationship was found to be valid for values of $\sigma_N=2\text{MPa}$ [He 90].

This equation was defined on the basis of a series of tests carried out on full-scale structures built of wire-cut bricks in 1:1/4:3 lime mortar.

Sinha [Si 67] showed that the initial mode of joint failure represented by the Mohr-Coulomb equation is indeed replaced under a certain pre-compression value by another failure mode: the cracking through units (bricks/stones). The curve of this mode (tensile failure, see on Figure 6.18) was characterized by Mann and Müller [MM 82]; the shear strength for this mode is:

$$\tau = 0.45 \cdot f_{s,t} \cdot \sqrt{1 + \frac{\sigma_N}{f_{s,t}}} \quad (\text{EQ 6.16})$$

Where: τ : shear strength of masonry

σ_N : normal stress

$f_{s,t}$: unit tensile stress

In [MM 82], a value of $0.033 f_b$ (f_b is the unit compressive strength) is given for the tensile strength of solids and $0.025 f_b$ for highly perforated units.

The failure mode changes once again under higher normal stress and corresponds then to the crushing failure of masonry. The envelope curve given by Mann and Müller is shown on Figure 6.18.

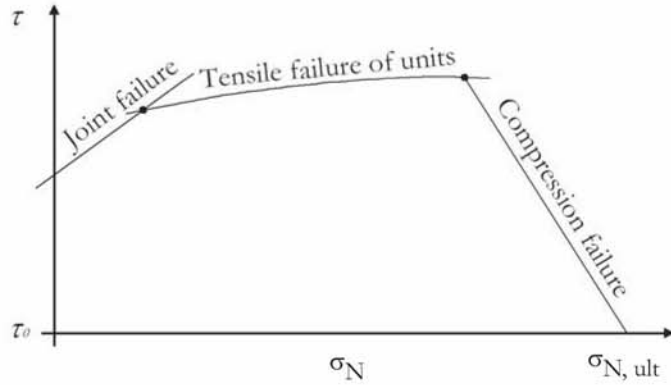


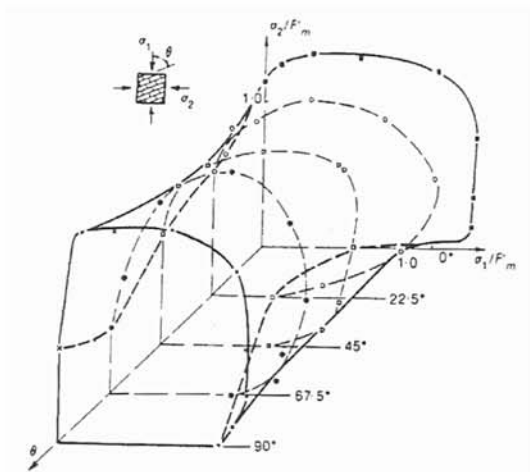
Figure 6.18 : Shear failure modes of masonry under vertical compression [He 90].

The other approach is to study masonry shear strength by considering the loading of masonry through the principal stress block.

In 1980 and 1981, Samaringhe, Page and Hendry [SPH 81] defined failure surfaces for brickwork under an orthogonal tensile-compressive stress. They applied normal stresses to brickwork specimens with different inclinations in regard to the bed joint direction.

Page carried out experimental investigations in 1982 [Pa 82] on masonry walls with different bed joint angles. The loading was either uniaxial or biaxial. From the test results, Page was able to set up three failure mechanisms and deduced from them a failure criterion (see the next figure).

Figure 6.19 : Failure criterion proposed by Page [Pa 82].



Failure diagrams proposed by Page can be found in Appendix A.4.5.

In the same direction, Ganz and Thürlimann also carried out similar experimental investigations on squared masonry walls with sloped bed and head joints (0° , 22.5° and 45° with respect to the horizontal) [GT 84]. Based on the obtained results, Ganz proposed a failure model for masonry that is confined by five failure areas (it is assumed that the stone does not resist tensile stress and the mortar cohesion is neglected).

The failure criterion developed by Ganz can also be described by a two-axis graph:

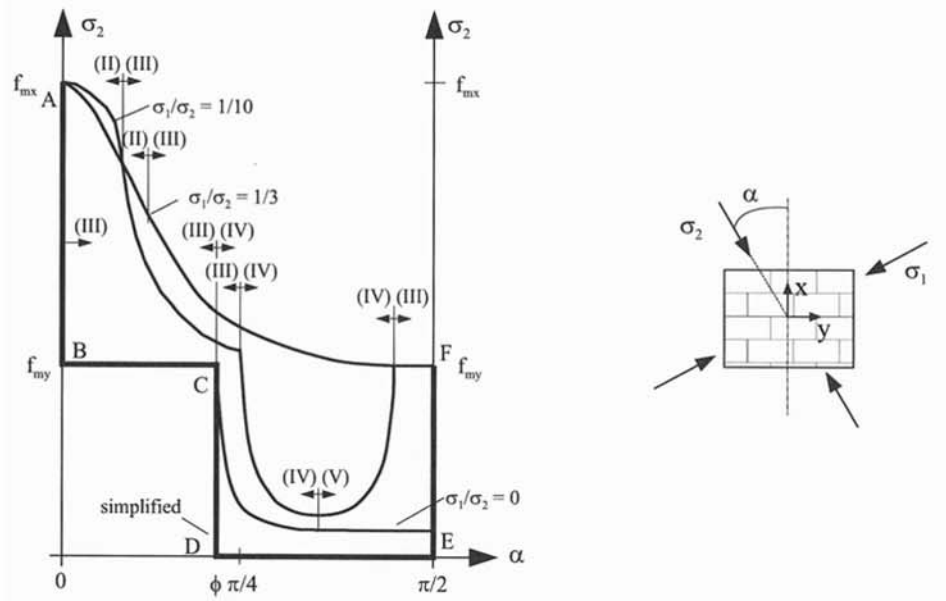


Figure 6.20 : Compressive strength as a function of the angle α ; proposed by Ganz [Ga 85].

According to Ganz, the failure conditions for unreinforced masonry can be described by five mechanisms:

I) Tensile failure of stones

$$\tau_{xy}^2 - \sigma_x \sigma_y \leq 0 \quad (\text{EQ 6.17})$$

II) Compressive failure of stones

$$\tau_{xy}^2 - (\sigma_x + f_{mx}) \cdot (\sigma_y + f_{my}) \leq 0 \quad (\text{EQ 6.18})$$

III) Shear failure of stones

$$\tau_{xy}^2 - \sigma_y \cdot (\sigma_y + f_{my}) \leq 0 \quad (\text{EQ 6.19})$$

IV) Sliding failure of stones

$$\tau_{xy}^2 - (c - \sigma_x \cdot \tan \phi)^2 \leq 0 \quad (\text{EQ 6.20})$$

V) Tensile failure in the mortar beds

$$\tau_{xy}^2 - \sigma_x \cdot \left(\sigma_x + 2c \tan \left(\frac{\pi}{4} + \frac{\phi}{2} \right) \right) \leq 0 \quad (\text{EQ 6.21})$$

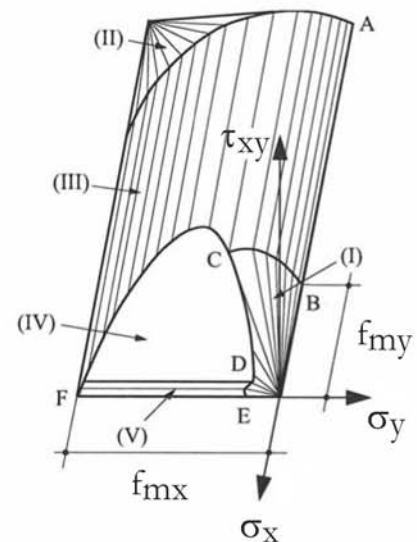


Figure 6.21 : Ganz's failure model.

Furthermore, Ganz proposed a way to determine the maximal lateral force (or maximal shear force) that can be withstood by a squat wall with or without openings. This method is based on the use of stress fields. He indeed proposed in [Ga 95] three different equations for calculating the shear strength force as a function of three levels of vertical load.

It is also interesting to note that according to Ganz [Ga 85], the angle of internal friction ϕ is almost the same for all types of masonry; the value of the internal angle of friction is situated between $0.7 < \tan \phi < 0.8$. Moreover, the ratio f_{my}/f_{mx} , which depends on the type of masonry (stone, type of bonds, mortar, etc.), ranges from 0.3 to 0.5 for brick and lime masonry. This is confirmed by [RGÖL 98] in which it is stated that the initial internal friction angle ϕ_i , associated with a Coulomb friction model ranges from $\tan \phi_i = 0.7$ to 1.2 for different unit-mortar combinations; the residual internal friction angle ϕ_r is approximately constant and equal to $\tan \phi_r = 0.75$.

Como and Grimaldi [CG 83] used another way to address the problem: they applied the upper bound theorem instead of the lower bound theorem that has been used for the previously shown models. The concept of Como's and Grimaldi's model is to first define the possible collapse mechanisms of a wall and then to calculate the minimal multiplier of the collapsing part of the wall that can lead to a loss of equilibrium. For instance, if we consider the collapse mechanism of a entire wall, this multiplier factor will be:

$$\lambda = \frac{G}{T} \cdot \frac{b}{2H} \cdot \left(1 - \frac{\sigma_N}{\sigma_k} \right) \quad (\text{EQ 6.22})$$

Where: σ_N : vertical stress (due to the wall self-weight)

σ_k : masonry strength (in the case of the self weight, σ_k corresponds to the masonry compressive strength).

H: wall height

T: resultant of the lateral actions

b: wall length

G: wall self weight

In 1993, Vermeltfoort and Raijmakers [VR 93] investigated the shear response of 0.99 m x 0.1 m x 1.0 m (width x thickness x height) walls; some had an opening in their middle (though not exactly right in the middle) and others were plain. The walls, which were made up of 18 brick courses, were subjected to a lateral load as well as a vertical one at their top. They obtained interesting failure patterns (cracks); nevertheless, they did not create failure criteria based on their results.

In 1996, for the first time, the shear strength of natural stone masonry was investigated. Berndt [Be 96] carried out shear tests on sandstone square-stone and ashlar masonries (bed joints were either 15 mm or 25 mm thick). It was observed that failure happened by sliding along the bed joints under a vertical load of 5.5 MPa, while the stone blocks cracked under a higher vertical load. Because of this observation, Berndt deduced that failure actually occurs due to the incompatibility of deformation at the mortar-stone interface. Consequently, Berndt's failure model is also based on this assumption.

Grauben and Simon [GS 01] proposed in 2001 a method for calculating the shear strength of masonry walls made up of big-size stone blocks with thin joints. Their method is based on the failure model that was developed by Mann and Müller [MM 82] and is characterized by four failure criteria (instead of three in the Mann and Mueller's model).

6.6. MULTIPLE-LEAF STONE MASONRY FAILURE: CRITERION

The construction of multiple-leaf walls was introduced by Romans; Pre- and Romanesque builders reused this technique. Any medieval wall, which is thicker than 50 cm, is generally composed of three leaves (see chapter 6.3.3).

Contrary to one-leaf walls, the structural behaviour of multiple-leaf walls has been analysed by only a few researchers. Most of them have essentially focused their research on the flow of forces amongst the layers as well as between them since it is usually the most important factor in the multiple-leaf wall strength. The flow has usually been determined by numerical application (FEM) or sometimes simply by analytical models. In fact, only a few experimental investigations have been carried out on the shear strength of multiple-leaf walls. Drawing conclusions from the experimental tests, which might be applied for many other kinds of multiple-leaf walls, proved to be quite difficult.

6.6.1. DISTRIBUTION OF LOAD WITHIN A MULTIPLE-LEAF MASONRY WALL

As aforementioned, the distribution of loads within multiple-leaf walls sways influences a lot the wall bearing capacity [Eb 96]. Almost every researcher agrees on the fact that this distribution depends on the mechanical properties of each leaf, their dimensions (stiffness) [Da 85] and the way they are connected to each other [PLBA 05], [BFA 91] and [WRB 95].

Dahmann described in [Da 85] the impact of the stiffness of leaves on the loads distribution¹:

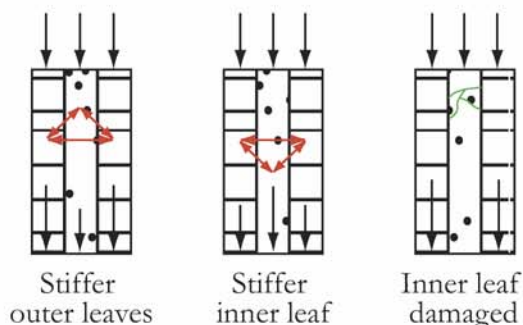


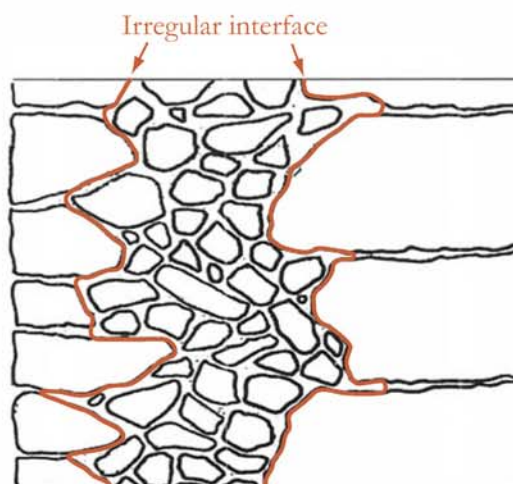
Figure 6.22 : Distribution of loads as a function of the stiffness of leaves.

1. It is assumed that the load transfers from one leaf to another; this transfer is ensured either by friction between leaves or by the stones themselves (resulting in an irregular interface; see the Figure 6.23).

Unfortunately, the mechanical properties of the layers, such as their stiffness (especially of the inner leaf) are usually not known. Binda et al. [BFA 91] proposed then to take into account two limits:

- limit 1: the stone blocks are wider than the average thickness of the outer leaves (or they even cross through the inner leaf); consequently, forces are transferred from one leaf to another.
- limit 2: every stone block is of similar thickness; in this case, forces can only be transferred from one leaf to another by friction. It is important to note that this coefficient of friction is generally unknown.

Figure 6.23 : Irregular surface that allows a better transfer of loads within the wall.



In order to better understand the transfer of forces within multiple-leaf walls, Binda et al. [BFA 91] carried out two numerical studies (FEM) on multiple-leaf walls: in the first model both outer leaves were connected through rigid links that permitted the transfer of loads. In the second model, the transfer of load was ensured by the mortar joint between leaves. In the first case, results showed that there was a transfer of load from the inner leaf to the outer leaves¹. This was not the case for the second model as the joint between leaves was unable to transfer high shear loads from one leaf to another.

Apart from numerical modelling, experimental investigations have been carried out; they have shown that the shear strength (at the interfaces) of straight collar joints (regular interface) is mainly influenced by the stones physical properties, such as porosity that provides a better adherence of the mortar. Moreover, it was observed that failures were brittle and left the wall with a small residual strength. The failure of such kind of walls (with regular interfaces) results from the development of vertical shear cracks along the connections at the interfaces. In this case, failure appears by the separation of every leaf at the interfaces. Shear strength values at the interfaces obtained for straight collar joints are between 0.09-0.17 MPa for a smooth and a hard stone, respectively.

The structural behaviour of keyed collar joints walls (irregular interfaces) is different. The failure is no longer brittle; the stress-strain curve has an elastic part followed by a yielding area. According to experimental results, the shear strength (at interface) of keyed collar joints walls is influenced by the stone strength, as the cracking pattern depends on the type of stone. For a low E-modulus stone, damage was observed in outer and inner leaves, while the sample with a high E-modulus showed cracks only in the inner leaf. Moreover, due to a higher strength and a small adherence with mortar, cracks went only around the blocks in the inner leaf, without crossing them. In this case, only the inner leaf collapses. Shear strength values obtained for keyed collar joints vary between 0.58-0.81 MPa for a smooth and a hard stone, respectively.

1. Outer actions loaded the inner leaf.

Finally, the experiments carried out showed that horizontal deformation increases when the outer leaves are disconnected from the inner leaf.

To summarize, if connections at the interfaces are ensured by only vertical joints (straight collar joints), there is no important transfer of loads from one leaf to another. On the contrary, a better connection (with keyed collar joints) ensures a transfer of loads within the multiple-leaf walls, as a function of each leaf stiffness.

6.6.2. DETERMINATION OF THE COMPRESSIVE STRENGTH

Very few researchers have published papers on this topic; these studies have resulted in a few methods which are presented here.

6.6.2.1. Failure model for multiple-leaf stone masonry after Egermann [Eg 93]

Egermann's failure model, which is limited to regular course masonry, is based on results from theoretical and experimental investigations; they are based on the following assumptions and limitations:

- the outer leaves of the samples are made up of brick masonry
- geometry and mechanical properties are similar for both outer leaves
- inner leaf with cohesion
- the interface between outer leaves and inner leaf is smooth
- there is no deformation in length direction (infinite wall)
- lateral deformation is restrained at the wall crown as well as its foot.
- both surfaces, at the crown and at the foot, stay flat
- vertical loading is uniformly distributed at the crown surface

Egermann's recommendations for assessing the bearing capacity can also be used for any kind of natural stone masonry if the structure of outer leaves approaches the one of brick masonry. For instance, it could be applied to square stones masonry or to regular ashlar masonry.

According to Egermann [Eg 93], the compressive strength of the inner leaf is increased by the biaxial loading (proved by numerical as well as analytical calculations).

Note: this method is based on an efficient interface between leaves.

MODEL FAILURE

Egermann's model takes into account the strength of each leaf, its stiffness and its dimensions; the strength (in regard to vertical loads) of a multiple-leaf wall is then calculated with the following equation:

$$f_{ml} = \theta_{o,1} \cdot f_{o,1} \cdot \frac{A_{o,1}}{A} + \theta_{o,2} \cdot f_{o,2} \cdot \frac{A_{o,2}}{A} + \theta_i \cdot f_i' \cdot \frac{A_i}{A} \quad (\text{EQ 6.23})$$

Where: f_{ml} : failure strength of a multiple-leaf wall (with two outer leaves)

$\theta_{o,1 \text{ or } 2}$: correction factor for the failure strength of the outer leaf n ($\theta_{o,1 \text{ or } 2} = 0.75$ [Eg 94])

$A_{o,1\text{or}2}$: ground surface of the outer leaf n

$f_{o,1\text{or}2}$: failure strength of the outer leaf n

θ_i : correction factor for the failure strength of the inner leaf ($\theta_i=1.3$ [Eg 94])

A_i : ground surface of the inner leaf

f'_i : failure strength of the inner leaf

Failure strength of the outer leaves

Through the correction factors, different structural behaviours of both the inner leaf and the outer leaves are taken into account. The bearing capacity of the outer leaves is diminished due to the connection with the inner leaf, while the inner leaf capacity is increased because of the bi-axial compressive loading (resulting from the presence of two outer leaves).

Failure strength of the outer leaves is calculated with the following equation:

$$f_a = f_{m,c} \cdot \alpha_\lambda \cdot \alpha_\varphi \quad (\text{EQ 6.24})$$

Where: α_λ : factor for the slenderness

α_φ : factor for the influence of the loading direction

f_a : failure strength of the outer leaf

$f_{m,c}$: compressive strength of masonry

According to the author's own words, this equation can be applied only for masonry that is homogeneous and well-maintained. However it is possible to use the above equations for an irregular masonry. The obtained value must be diminished through factors that reflect the exact situation of the given masonry.

The correction factor for slenderness is defined in regards to the buckling load (if $P_{cr} < 0.5 P_0$):

$$\alpha_\lambda = \frac{P_{cr}}{0.5P_0} \quad (\text{EQ 6.25})$$

Where: α_λ : factor for the slenderness influence

P_{cr} : critical buckling load

P_0 : load for compressive failure

Egermann proposed to calculate the critical load with the following equation:

$$P_{cr} = \frac{\pi^2 \cdot 0.7 \cdot E_{stat} \cdot I}{L^2} \quad (\text{EQ 6.26})$$

Where: L: buckling length

E_{stat} : Young's modulus ($E_{stat} = 1000 \cdot f_{m,c}$)

0.7: decremental factor for taking into account the cracked state of the cross-section

P_{cr} : critical buckling load

I : moment of inertia of the uncracked cross-section

The correction factor for the positive impact due to confinement provided by the outer leaves is then considered:

Spanning direction parallel to vertical load direction $\alpha_\varphi=1$

Spanning direction perpendicular to vertical load direction $\alpha_\varphi=2$

The compressive strength of masonry is calculated by Berger's method [Be 89] (joint core sample):

$$f_{m,c} = f_{w,FK} \cdot \frac{1 + 3.24 \sqrt{\frac{t_m}{d_{FK} - t_m}}}{1 + 3.24 \sqrt{\frac{t_m}{t_s}}} \quad (\text{EQ 6.27})$$

Where: $f_{m,c}$: compressive strength of masonry

$f_{w,FK}$: strength of a stone-mortar-stone sandwich according to Berger's method

t_m : average thickness of joints in masonry

t_s : average height of stones in masonry

d_{FK} : core sample diameter

Failure strength of the inner leaf

The inner leaf failure strength is defined through experiments: Egermann [Eg 93] proposed that at least five core samples of the studied masonry be made. These core samples must satisfy dimensional criteria; the obtained values are then corrected for the slenderness of the samples. No analytical method to calculate the inner leaf failure strength is proposed.

6.6.2.2. Failure model for multiple-leaf stone masonry (irregular courses) after Ebner [Eb 96]

The Ebner's failure model is based on the following assumptions:

- the multiple-leaf wall is subjected to compressive loads
- vertical load is distributed into leaves as a function of their deformation capacity
- the failure of outer leaves highly diminishes the bearing capacity of multiple-leaf walls
- the inner leaf stays in the elastic field; there is no yielding
- the influence of slenderness has not been taken into account
- the definition of the bearing capacity of multiple-leaf walls results from the comparison of the analytically calculated values for natural stone masonry and the values obtained with experimental tests (carried out on symmetrical multiple-leaf samples).

As the author underlined it, it must be kept in mind that the recommendations are for one type of stones, i.e. the sandstone. However, this method can be applied for other stone varieties, but the results have to be considered with caution.

LOAD DISTRIBUTION IN THE WALL

The distribution of stresses in one multiple-leaf wall can be determined with a spring-model, whose stiffness corresponds to that of the wall leaves. Consequently, the stiffness values, i.e. the Young's modulus, of each leaf must be known.

Moreover, based on the assumption that the stone's Young's modulus is much higher than that of the mortar, Ebner proposed to calculate the stress distribution with this equation:

$$E_{o,i} = \frac{E_{m_o} v_{m,o,i}}{(v_{m,o,i} + v_{H,o,i})} \quad (\text{EQ 6.28})$$

Where: $E_{o,i}$: Young's modulus of the outer leaf, inner leaf respectively

E_{m_o} : mortar's Young's modulus

$v_{m,o,i}$: part in unit of volume of the mortar in the outer leaves, inner leaf respectively

$v_{H,o,i}$: part in unit of volume of holes in the outer leaves, inner leaf respectively

FAILURE MODEL

Ebner [Eb 96] proposed to evaluate the bearing capacity of multiple-leaf walls by the calculation of the bearing capacity of both outer leaves, with almost the same procedure as the one used for determining the bearing capacity of one-leaf walls.

To remind, the failure of the outer leaves can result from three kinds of failure, according to Ebner:

1. Stone failure resulting from horizontal tensile stresses due to restrained horizontal deformation: Eq 6.10.
2. Mortar failure: Eq 6.11.
3. Stone failure due to the influence of vertical joints: Eq 6.9.

If the studied masonry is irregular, the failure stresses are determined by using average values of stone and joint dimensions¹ in a square surface of 1*1 m.

Like for one-leaf walls, if the masonry is made up of ashlar masonry instead of square-stone masonry (that were used by Ebner for the experiments), a factor (α) should be applied for taking into account the irregular surface of stones and variation in the thickness of mortar. Then, the adapted failure stresses are:

$$f_{m,c,am} = \frac{f_{m,c,ssm}}{\alpha} \quad (\text{EQ 6.29})$$

1. With average values for joints thickness, stone height, vertical joints thickness and average value of how many vertical joints there are along horizontal joints.

Where: f_{am} : failure stress of an ashlar masonry

α : factor ($\alpha=3.3$)

f_{ssm} : failure stress of a square-block masonry

6.6.2.3. Failure model for multiple-leaf stone masonry after Pina-Enriques et al. [PLBA 05]

Pina-Henriques et al. [PLBA 05] carried out compression experiments on multiple-leaf walls made up of the so-called Noto stone, which is characterized by an $E_s=9000$ MPa and by a compressive strength $f_{s,c}=19.1$ MPa. Amongst the obtained results, it was shown that when both outer leaves were simultaneously loaded:

- there was a shear failure along connections (interfaces); it was followed by the transfer of the load to the external elements,
- the strength of the outer-leaves was approximately 45% of the stone strength, while the inner leaf is characterised by a compressive strength of 20% of the stone strength. The result is more or less similar for a harder stone, especially concerning the outer-leaves.
- the outer leaves were brittle,
- the peak load of tested walls is not much higher than the one of each outer leaf,
- the walls with straight collar joints failed because of cracks in the outer-leaves; the inner leaf was almost undamaged,
- the collapse load of the walls with keyed collar joints was slightly higher than the one of the straight collar joints walls.

Based on the experiments, they were able to plot the following stress-strain graph:

It can be seen from the previous stress-strain diagrams (for both types of connections) that the vertical deformation of the inner leaf is not similar to that of the outer leaves. Furthermore, the inner leaf had already yielded as the walls failed and the global shape of the curves seem to be more influenced by the behaviour of the outer leaves. In consequence, the inner leaf contribution to the walls strength can be considered to be negligible.

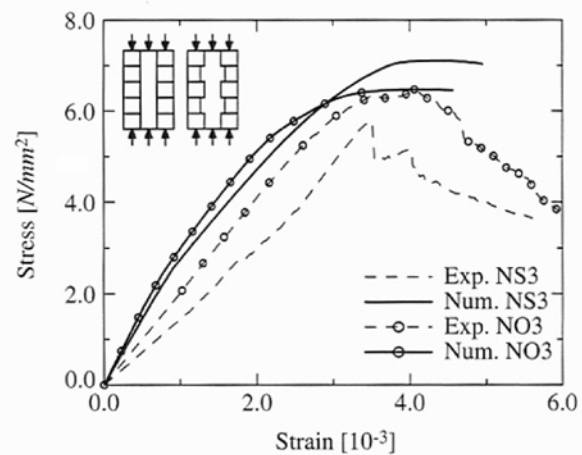


Figure 6.24 : Experimental and numerical stress-strain curves of two kinds of multiple-leaf walls [PLBA 05].

Pina-Henriques et al. [PLBA 05] compared the compressive strength obtained by experiments with values calculated through three equations that consider three possibilities of load distribution within the walls. They are:

1. The external load is completely supported by the stiffer elements (outer leaves):

$$f_{c,w} = \frac{2t_e}{2t_e + t_i} \cdot f_{c,e} \quad (\text{EQ 6.30})$$

Where: $f_{c,w}$: compressive strength of the wall

$f_{c,e}$: compressive strength of the external leaves

t_i : thickness of external leaves

t_e : thickness of the inner leaf

2. The external load is supported by each leaf according to its cross-section:

$$f_{c,w} = \frac{2t_e}{2t_e + t_i} \cdot f_{c,e} + \frac{t_i}{2t_e + t_i} \cdot f_{c,i} \quad (\text{EQ 6.31})$$

Where: $f_{c,w}$: compressive strength of the wall

$f_{c,e}$: compressive strength of the external leaves

$f_{c,i}$: compressive strength of the inner leaf

t_i : thickness of the inner leaf

t_e : thickness of external leaves

3. The external load is supported by each leaf according to its cross-section and adjusted through correction factors (according to Egermann [Eg 94]):

$$f_{c,w} = \frac{2t_e}{2t_e + t_i} \cdot \theta_e \cdot f_{c,e} + \frac{t_i}{2t_e + t_i} \cdot \theta_i \cdot f_{c,i} \quad (\text{EQ 6.32})$$

Where: $f_{c,w}$: compressive strength of the wall

$f_{c,e}$: compressive strength of the external leaves

$f_{c,i}$: compressive strength of the inner leaf

t_i : thickness of the inner leaf

t_e : thickness of external leaves

θ_i : correction factor for the inner leaf

θ_e : correction factor for the outer leaves

The results showed that the compressive strength obtained by the first equation is similar to the experimental results. This comparison highlights that in the case of a straight collar joint walls, the compressive strength is essentially provided by the outer leaves. It is worth noting that the Egermann's equation also gave a good result.

The compressive strength of keyed collar joints walls is slightly higher than the ones with straight collar joints; in this case, the second equation gave the same value than that obtained by experiments. Therefore, it can be drawn up that the inner leaf augments the compressive strength of the whole wall when it is connected to the outer leaves. The value given by the Egermann's equation is only a bit smaller than that obtained experimentally. In fact, Egermann's equation gives either the same values or values smaller than the ones obtained by experiments. Thus, it can be seen as a rather conservative way of obtaining the compressive strength of multiple-leaf walls.

6.6.3. DETERMINATION OF THE SHEAR STRENGTH

There is actually no model that permits the calculate of the shear strength of multiple-leaf walls. However, one can assume first assume that the multiple-leaf wall is compact enough to be considered as an one-leaf wall. The shear strength can be calculated according to the models shown within the previous sections (Ganz's model, for instance).

In case a given multiple-leaf wall turns out to have three clearly separated leaves, for instance because of degradation, each leaf must be checked separately: the seismic loads are to be applied to each leaf for which the shear strength can be defined as for one-leaf walls.

6.7. DEGRADATION

Masonry is considered as degraded when there are cracks or the rock units and/or mortar are in a bad state. Degradation can be due to either outer actions, such as earthquakes, settlements and bad weather, or inner actions, such as vault thrust or masonry creep. Degradation can also result from a combination of both types of actions. For more information about damage to old (historical) masonry, the reader can refer to [Ma 02] or [MG 92].

Cracks or/and a masonry in a bad state of maintenance can have an impact on the seismic response of a church. In consequence, the state of masonry must be taken into account when addressing the church seismic vulnerability.

6.8. DISCUSSIONS AND CONCLUSIONS

Within the first sections, it was shown that Swiss sacred buildings are composed of numerous types of masonry essentially due to the variety of rocks, the evolution of the building techniques and periods of art. Consequently, the determination of the compressive strength of the existing masonries (in Switzerland or else where) requires a method or a model that gives the possibility to obtain this value for many kinds of masonries. In fact, many models (or failure criteria) have been developed for addressing the compressive strength of masonry (brick masonry and stone masonry). In particular, it was seen that the SIA 178 model of Berndt's model are well adapted to one-leaf stone masonry.

During the last two decades, the mechanical properties of multiple-leaf walls, which are the most frequent type of wall in Swiss sacred buildings, have also been analysed. A few reliable models have indeed been drawn from experimental as well as numerical investigations.

The structural behaviour of masonry under static and vertical loads has been addressed. However, the matter of interest when evaluating the seismic vulnerability of sacred buildings is the shear strength and ductility of stone masonry as well as the in-plane behaviour of one-leaf and multiple-leaf walls under seismic loads. Ganz's model can be applied to calculate the shear strength of stone masonry; however, models based on Coulomb's failure criterion for determining the shear strength of stone masonry are very few. In fact, shear strength values of stone masonries are missing. Moreover, models for determining the shear strength of multiple-leaf walls simply do not exist or have not been published.

To fill this knowledge void, an experimental investigation is carried out at EPFL on a stone ashlar masonry wall (composed of sandstone blocks) in order to obtain a value for the shear strength of such masonry and also study its ductility. Moreover, this testing allows us to validate some models such as Ganz's.

7.1. PURPOSE

Masonry is a material whose structural behaviour and in particular the mechanical characteristics are still not well known. Moreover, the behaviour of old masonry, which is composed of stone blocks or bricks generally bonded with lime mortar, is even less understood because of its historical nature (it is indeed difficult to remove a part of masonry from a cultural heritage building to perform experimental investigations). Though old masonry behaviour under compressive stress has been studied for a few decades, the shear behaviour of such a kind of masonry has been scarcely addressed.

Calculation of the seismic response of sacred buildings requires the knowledge of the shear capacity¹ of old masonry. In fact, very few experimental investigations were carried out in order to address it and most of them focused on masonry of common old buildings (vernacular architecture).

To fill in this knowledge void, experiments to understand the shear behaviour are undertaken. The flying buttresses of the Lausanne Gothic cathedral were removed from 2002 to 2008. Also thanks to the generosity of the technical committee of the Cathedral, about ten big stone blocks were taken from the cathedral building site for testing at EPFL. The main element was a part of wall; besides, a few specimens were made in order to determine the mechanical characteristics of the stone blocks and of the mortar.

The wall was tested under a static-cyclic lateral loading (static-cyclic experiment). The expected results were the shear strength of this

1. The flexural failure mechanism is related to wall dimensions and the axial force; it can be therefore easily calculated.

wall, the associated hysteresis loop and its maximal displacement (ductility). As only the shear collapse mechanism is of interest, rocking and sliding are restrained by a judicious choice of dimensions and compressive load.

7.2. DESCRIPTION OF THE TEST SPECIMEN

The goal is to simulate the real forces in a part of one-leaf masonry wall, which is made up of well-dressed sandstone blocks, that is situated at the basis of a wall and subjected to seismic actions.

The test specimen (Figure 7.1) is composed of three parts:

- the masonry specimen consisting of four courses of sandstone (Molasse) masonry
- a supporting course made up of limestone
- a reinforced concrete head slab

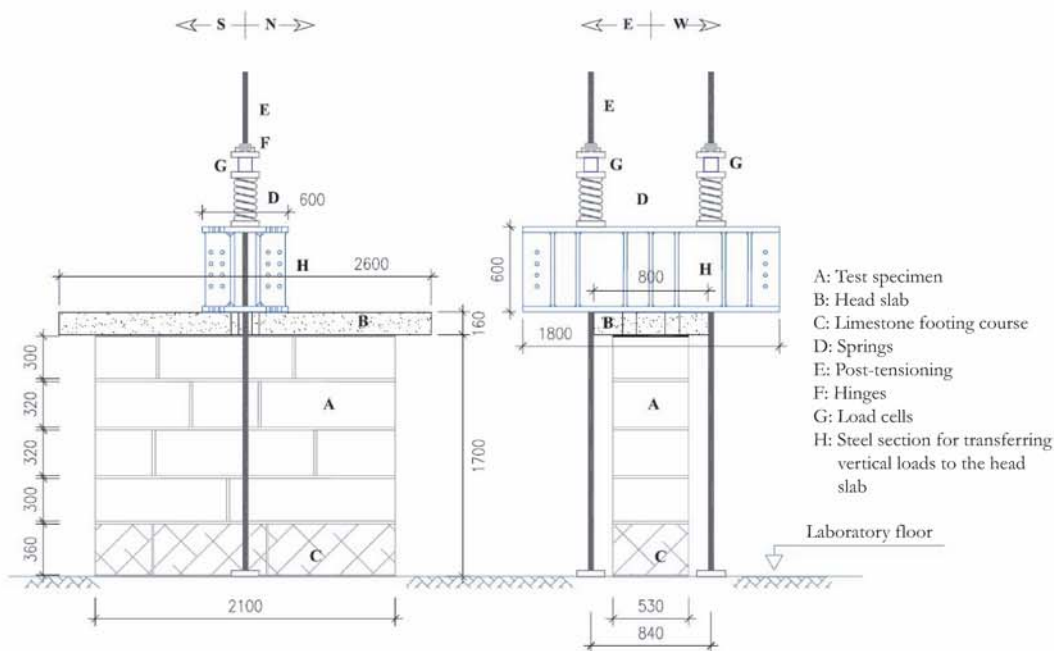


Figure 7.1 : Test specimen [Fa 07].

The bottom course is 2.1 m long and 0.36 m high, while the masonry specimen is 1.24 m for the same length; the whole specimen is 0.53 m thick.

The mechanical characteristics of sandstone were obtained by compressive tests on three samples, whose dimensions were: 0.13 m x 0.3 m x 0.17 m (height x length x width). They are given in Table 7. 1.

Table 7. 1 : Mechanical characteristics of sandstone (Molasse).

Samples	Loading speed [N/s]	Maximum Load [kN]	Compressive strength [MPa]	Young's modulus [MPa]
Sample 1	418.2	1650.4	32.4	1386.1

Sample 2	1148.8	1598.0	31.3	1578.8
Sample 3	1089.5	1565.6	30.7	1680.3
Average			31.5	1548.4
Standard-deviation			0.8	149.4

Bed and head joints are about 2-3 cm thick; since the visible surfaces of stone blocks are not entirely flat and the corners are not at 90 degrees, the visible joints looked thicker than they really are in the middle of the sample. The mortar, which is used, is the same as the one used for reconstructing the new abutments of the Lausanne cathedral. The mortar is composed of dry sand, hydrated and hydraulic lime as well as a part of silica cement; the whole composition is:

Table 7. 2 : Composition and mechanical characteristics of the mortar (mean values on 3 samples 40 x 40 x 160 mm (according to the EC NBN EN 1015-11)) [Fa 07].

Composition	Compressive strength [MPa]	Tensile bending strength [MPa]	Young's Modulus [MPa]
20.0 vol dry sand 0-5 mm grain size distribution			
1.50 vol powdered hydrated lime	9.6	2.4	1993.2
2.00 vol powdered hydraulic lime			
1.50 vol silica cement			

In order to avoid the crushing of the bottom molasse course, a first course in limestone is placed at the bottom of the wall; this material is chosen because it is harder than the used sandstone. Moreover, this situation corresponds to reality: walls made up of sandstones are often erected on a first course of limestone because of humidity reasons.

The reader who is interested in the construction of the specimen can consult the master thesis of P. Favez [Fa 07].

7.2.1. TEST SET-UP

The test-set up is composed of:

- test sample
- reaction frame
- post-tensioning bars
- actuators
- measure equipment (displacement sensors, load cell, etc.)

The reaction frame is ensured by double steel frames on each side of the sample that are each composed of six HEB 360 columns restrained by the lab floor. Twelve angle sections (eight C 560/2700 and four C320/1650) are used to stiffen the columns (Figure 7.2). Every screw is pre-stressed.

Each actuator is supported by two angle sections (C320/2060 and C320/1660), themselves fixed to the angle sections placed above and under it.

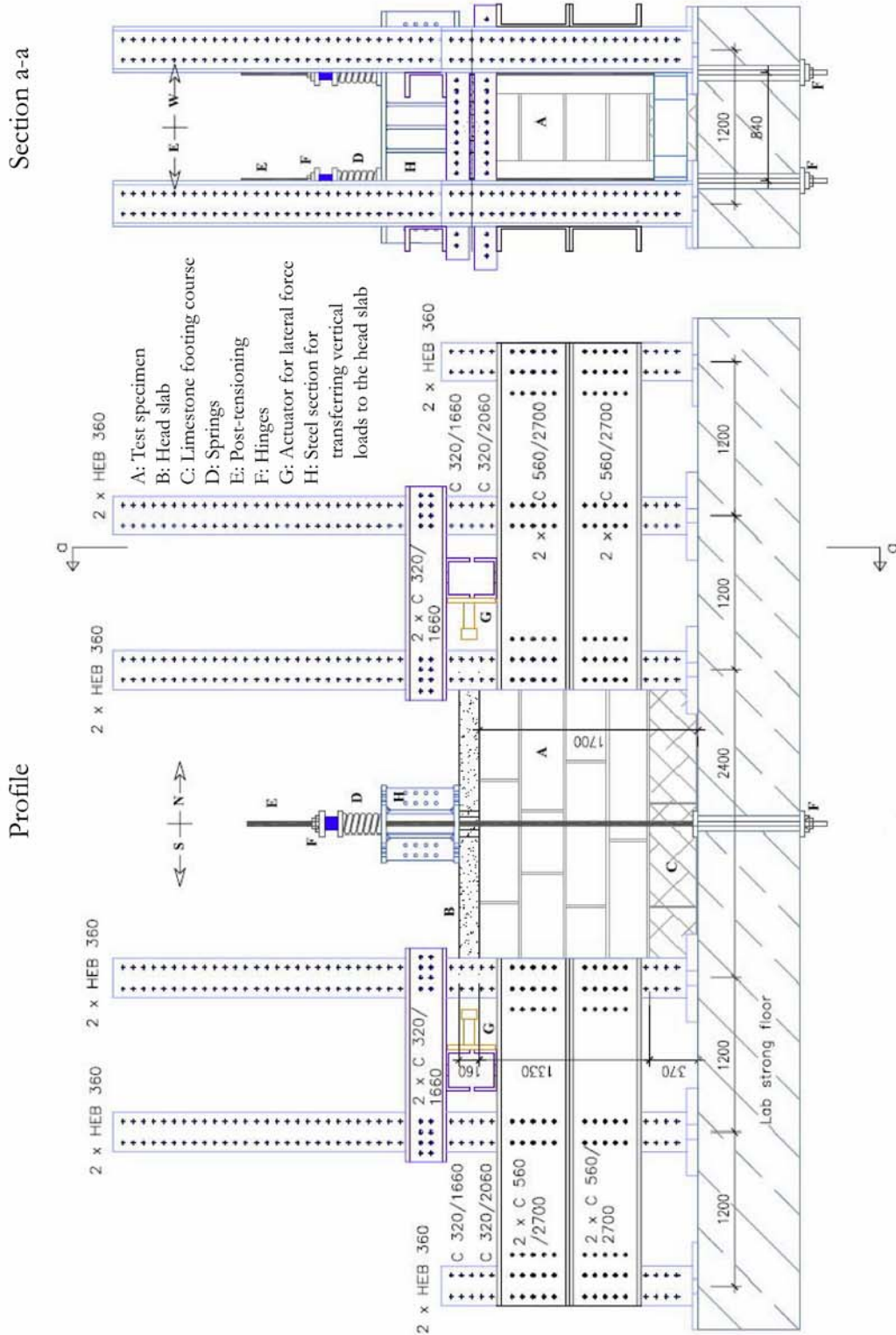


Figure 7.2 :Test set-up [Fa 07] (dimensions in [mm]).

The upper part of the sample, i.e. the reinforced concrete slab (0.8 m wide, 2.6 m long and 0.16 m thick), is rigid enough to distribute the post-tensioning action to the sample and the lateral load applied alternatively at one of its extremities. The connection between the reinforced concrete slab and the upper molasse course is probably one of the most important parameter for this test because it must ensure the correct transfer of the applied lateral force to the masonry sample. In order to guarantee this connection, the bottom surface of the slab is made rough (with a pneumatic-drill) and the joint between the slab and masonry is made with an epoxy resin (Sikadur 311) developed by the firm SIKA SA.

Two post-tensioning bars of 36 mm diameter are used to subject the wall to an axial loading; this action not only simulates a possible weight of masonry above the sample but it essentially helps create the shear collapse that we are looking for. A steel section is used to transfer the vertical post-tensioning load to the head slab and then to the masonry sample. The bars are placed at mid-length of the specimen on both sides of the wall. Circular ducts of 112 mm diameter that are placed at both extremities of the post-tensioning bars prevent any contributions of the bars to the lateral stiffness of the specimen. Anchoring is provided to the post-tensioning bars by anchor-hinge plate and nut systems that are placed above the steel section and below the laboratory strong floor (800 mm reinforced concrete). Before the static cyclic test, the bars are alternately post-tensioned in 10 KN increments up to the target force of 125 KN per bar with the help of an hydraulic jack and a hand pump. Springs are used between the steel section and the anchors of the post-tensioning bars in order to avoid increments in the post-tensioning force due to elongation of the bars. Each post-tensioning bar is subject to a force of approximately 130 KN. This is in addition to 64 KN of self-weight from steel section, concrete slab and masonry wall. This nominal normal force (324 KN) corresponds to a uniformly distributed compressive stress of 0.29 MPa.

The lateral cyclic load is applied by pushing the head slab with two actuators applying a maximum force of 200 KN that are operated alternately. The quasi-static load is applied manually using a hydraulic jack and hand pump up to a target force or a target displacement, according to the testing program. Then the hydraulic flow jack was shut off in order to record the displacement between deformer targets while the wall is loaded. During this time the force usually decreased by 15-20%; the specimen is then gradually unloaded.

7.2.2. MEASUREMENT EQUIPMENT

The test specimen was equipped with several devices as shown in Figure 7.3. Eighteen inductive linear displacement transducers (numbers 0-17 on the Figure 7.3) measured vertical, horizontal and diagonal displacements. Vertical and horizontal deformations in bed joints were measured by catching displacement between deformer targets (1-24 on the right part of the Figure 7.3). The

forces in the post-tensioning bars as well as the lateral force at the top of the wall are measured using three load cells.

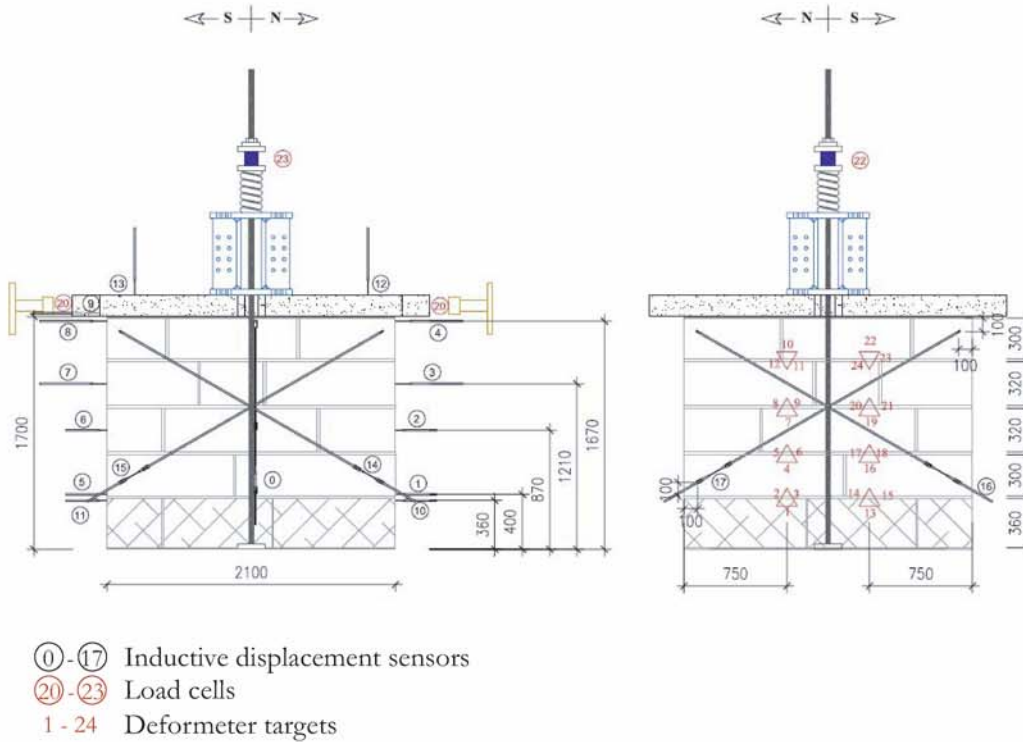


Figure 7.3 : Measurement equipment [Fa 07].

7.3. TESTING PROGRAM

The typical cyclic loading sequence adopted for the test is shown in Figure 7.4. It consists of a series of force and displacement-controlled cycles. During the first part (force-controlled) of the experiment, the force is gradually increased in a fixed loading increment. At each loading stage, the test specimen is subjected to a complete cycle, i.e. the force is applied alternately in both directions. From these force-controlled cycles allowed the maximum elastic displacement of the top of the wall is determined. In the second (displacement-controlled) part of the experiment, each load-

ing stage consists of two or three complete cycles. The displacements given in a cycle depend on the differences in the test specimen behaviour between the first and the second cycle.

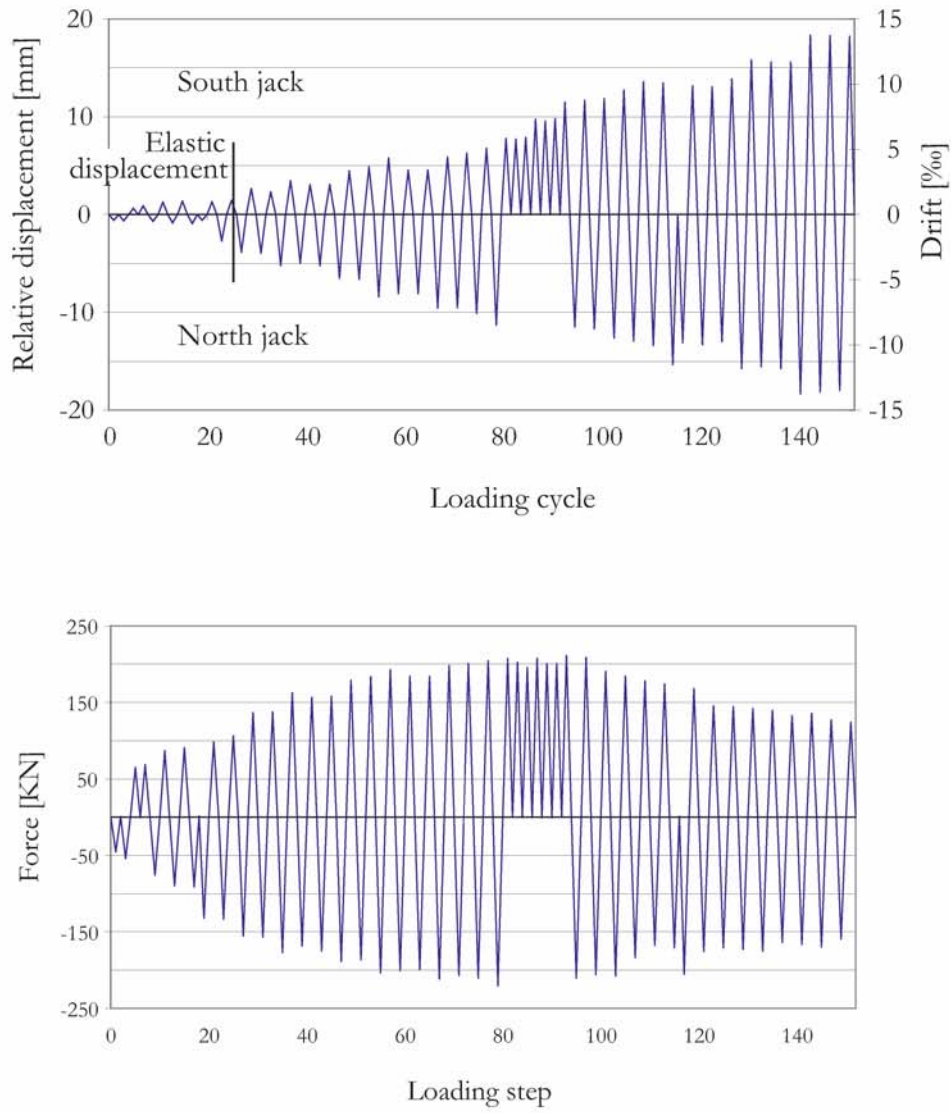


Figure 7.4 : Loading history (horizontal load) [Fa 07].

7.3.1. TESTING UNFOLDING

During the first three cycles (force-controlled), the force is gradually increased in increments of approximately 10 kN. At each loading stage, the specimen is subjected to a complete cycle (i.e. loading in both directions (north-south and south-north)).

After these three cycles, the force-displacement curve shows that the elastic limit has been exceeded; the subsequent loading cycles are displacement-controlled. The displacement increment is fixed at 1‰ of the wall height (1700 mm), that is 1.7 mm.

The next four stages are displacement-controlled, with a drift of respectively 2, 3, 4 and 5 ‰ of the wall height.

First cracks occur at 2‰ (3.4 mm displacement); they appear in horizontal and vertical mortar joints as shown in Figure 7.5; the lateral load is about 132 kN in the north-south direction.

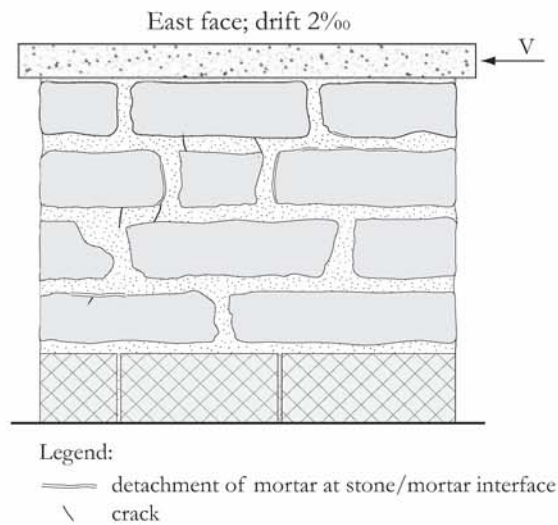
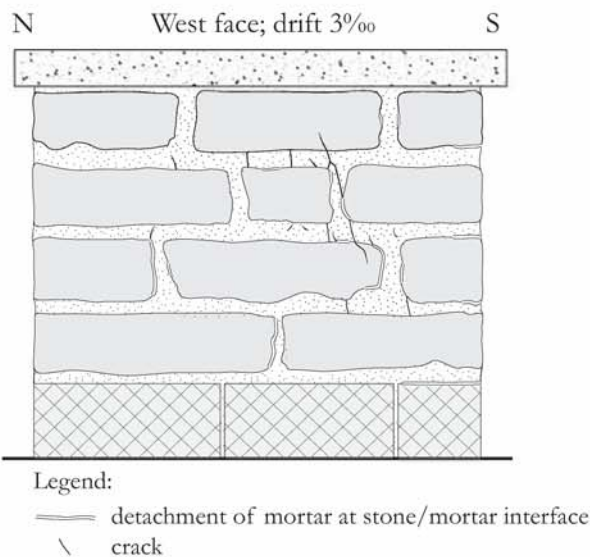


Figure 7.5 : Crack patterns on the sample under a drift of 2‰.



At the 3‰ displacement level (5.1 mm), diagonal cracks appear in the stone along the north-south diagonal as shown in Figure 7.6 and in the bed joint between molasse and limestone courses; the lateral load is about 156 kN in the north-south direction.

Figure 7.6 : Crack patterns on the west side of the sample for a drift of 3‰.

DRIFT 5‰

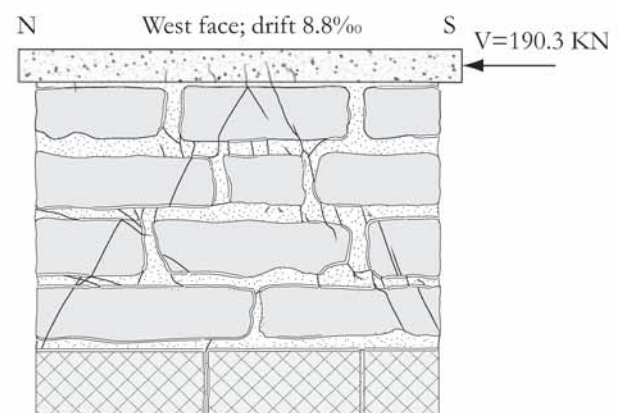
At a drift of 5‰ (over the total wall height) the limestone footing transducers indicate that this course is sliding slightly on the reaction slab (sensor 10 and 11 on Figure 7.3). Although footing sliding is restrained by iron angles, the measured displacement is important relating to the wall drift. In consequence, thin aluminium plates are added behind the angles in order to restrain the specimen base. To compensate for the small increase in the lateral action due to sliding, the test sample is subjected to two more cycles at this stage after being restrained. A next stage with a wall drift of 6‰ (8.04 mm) is then completed for three complete cycles. However, the thin aluminium plates are unable to fully restrain the footing layer; the drift is then linked to the molasse part (1.34 m) and no longer to the total height of the sample (1.7 m), for a reason of accuracy. At this point, it is observed that the specimen is not as loaded as it is in the opposite direction. In consequence, the wall is subjected to south-north loading through two series of three semi-cycles with 6‰ (8 mm) and 7‰ (9.4 mm) drift, respectively (Figure 7.4).

DRIFT 8‰ – 9‰

The experiment is continued with a further stage of three complete cycles at 8‰ relative displacement composed. At the end of the third complete cycle in the south-north direction, a sudden loss of strength is observed under a lateral force of 208.2 kN and a drift of 11.66 mm (8.8‰). The drop in lateral force is accompanied by an audible cracking sound. After the next semi-cycle of the south-north loading direction, cracks appear along the left diagonal (see Figure 7.7).



Figure 7.7 : Crack patterns on the west side of the sample for a drift of 8.8‰.



Legend:

- detachment of mortar at stone/mortar interface
- \ crack

The test continues with a stage of 9‰ (12.06 mm); during the first semi-cycle, cracks widen, especially those in the bottom course of molasse. Under a load of 207.4 kN (and a drift of 12.62 mm), a significant cracking sound occurs and further cracks along the north-south diagonal are created. During the second cycle of this stage a loss of strength is observed in the north-south direction. After the formation of the diagonal crack, the lateral load (to the left on Figure 7.8) goes down to 183 kN.

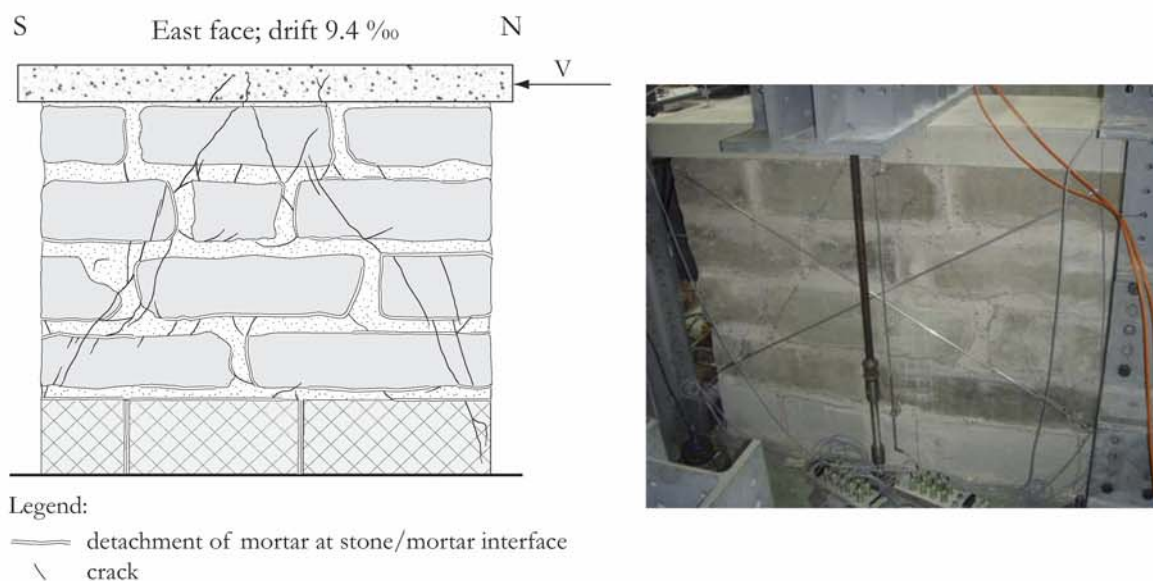


Figure 7.8 : Crack patterns after the loss of strength along the north-south direction (first semi-cycle of the stage 9‰).

A toe crack in the northern side of the limestone course compromises the transducer (number 10 on the Figure 7.3) that is used to measure the relative displacement of the molasse part of the wall. As the toe crack expands in the southern side, a new transducer is fixed on the eastern side of the footing to measure the displacement of the whole limestone course which is supposed to behave as one piece.

A second stage of three complete cycles at 9‰ relative displacement is performed to prevent mistakes due to the opening of the footing crack at the previous stage. One cycle later, still with a drift of 9‰, cracks along the failure surface widen and new cracks also appear.

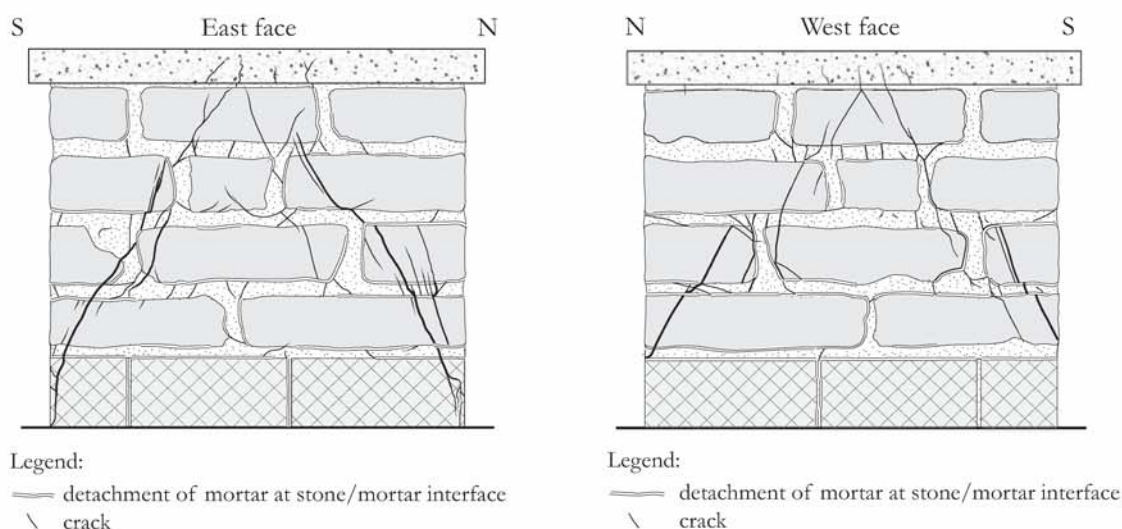


Figure 7.9 : Crack pattern on both faces at a drift of 10‰.

After a few cycles of reaching the maximal shear strength in both directions (two diagonal cracks), the increase of the relative displacement increment is fixed at 2‰ because the masonry force-displacement curve enters the softening phase. Cracks that split the blocks at the bottom courses of the sample are seen to get larger and the separated parts of the split rocks move away during each semi-cycle.

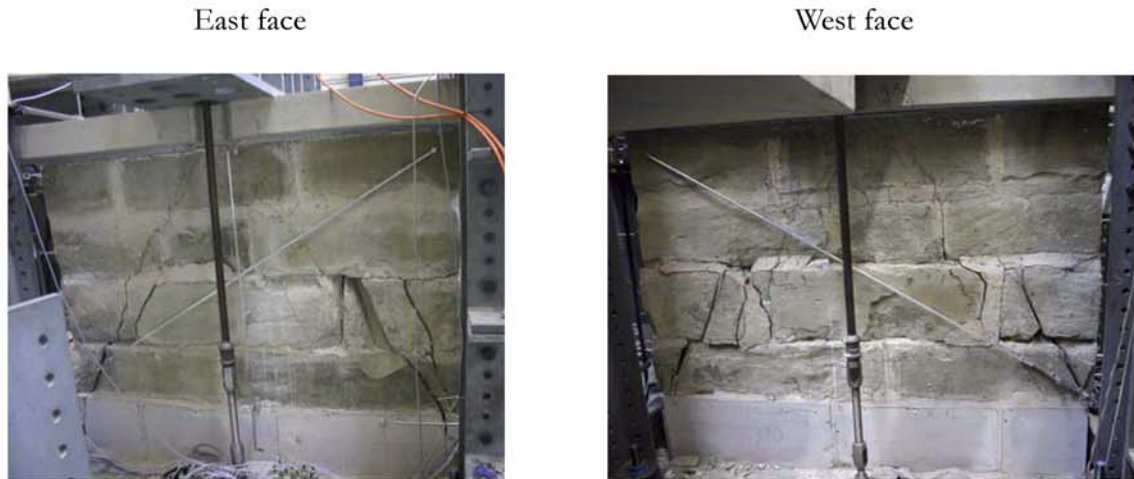


Figure 7.10 : Crack patterns on the east and west faces at the end of the 9‰ cycles.



Figure 7.11 : Crack patterns on the east and west faces at the end of the 11‰ cycles.

Two further stages of 3 complete cycles each at 11 and 13‰ relative displacement are completed. As a stone fall compromises the test safety and also as there is a beginning of a rocking behaviour around a plastic hinge at the wall core (the upper part of test specimen has a rotational motion around that hinge, Figure 7.12), the test run is stopped at the 13‰ relative displacement stage.

Figure 7.12 : End of the experiment: the hinge in the middle of the wall is easily recognizable.



7.4. TEST RESULTS

The main objective of this experimental investigation is to study the shear behaviour of a typical masonry of sacred buildings. In this case, a square-stone sandstone masonry is chosen; this is representative of medium-size and big churches. Sandstone is, with limestone, probably the most frequently used type of stone in construction, in Switzerland.

The global behaviour is studied with a hysteresis loop; it individualises the different stages of the wall reaction to the lateral wall and the released energy. The shear-loading capacity of such a masonry and its ductility can also be drawn from the hysteresis loop. Moreover, it defines an idealised bi-linear curve for the given masonry.

7.4.1. HYSTERESIS LOOPS

Here below are the complete hysteresis loops of the test according to both sensors (4 and 8 on Figure 7.13) that are located on both sides of the wall (at the top of the molasse part).

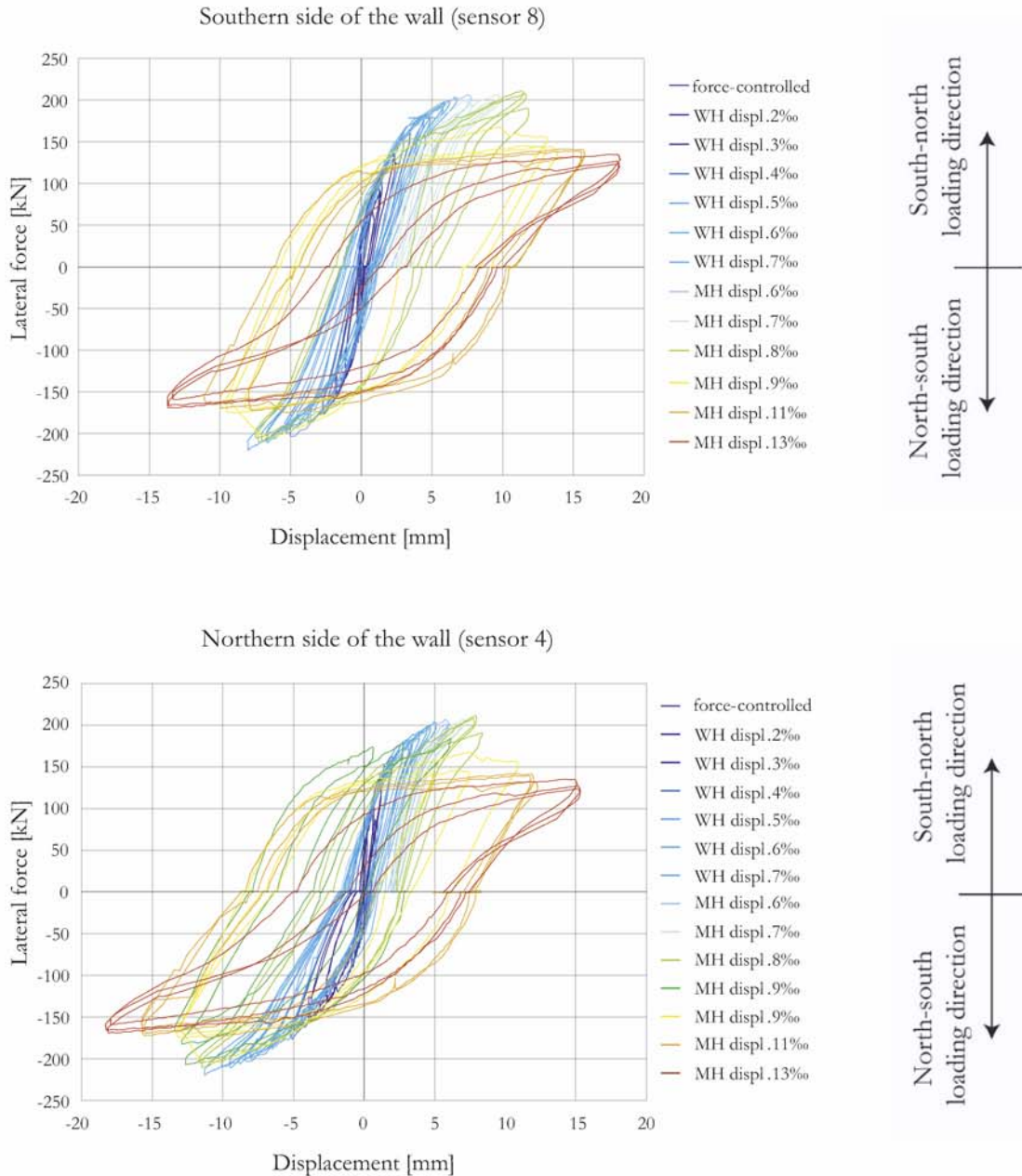


Figure 7.13 : Hysteretic loops of the test specimen drift.

Notes: WH displacement corresponds to a percentage of the whole sample height whereas the MH displacement is related to the height of the molasse part.
The above part on the graph corresponds to the shear behaviour under south-north directed loading, while the bottom part corresponds to the shear behaviour under north-south loading.

Obviously, both groups (each group being related to each sensor) of hysteresis loops look similar; the values of displacements vary a little bit since the lateral displacements measured at one side does not match exactly with the displacements measured at the other side. In the same manner, and as a consequence of this phenomenon, the loops are shifted differently along the x-axis.

Nevertheless, both graphs display phases in the shear behaviour of the sample¹. The first phase, which spans the start of the test to the point just before failure, is almost linear, at least at the beginning. The residual deformation is small and little energy is released. Nevertheless, after reaching a lateral force of 165 kN, the curve is no longer straight when lateral force decreases, contrary to what happened during the previous cycles. In fact, this phenomenon is due to the closing of cracks.

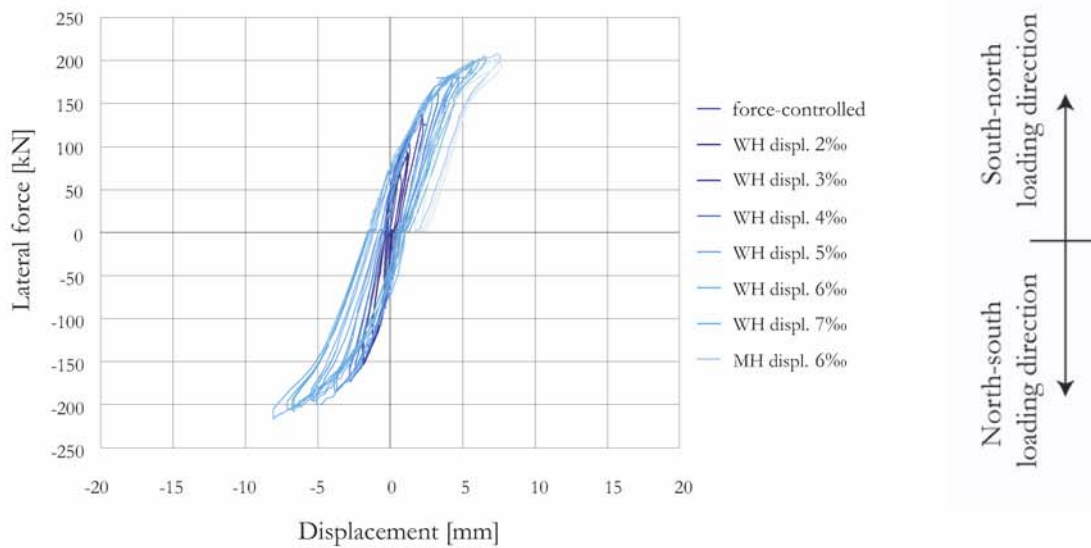


Figure 7.14 : Hysteresis loops from the beginning to 6‰ relative drift.

A sudden loss of strength happens for a 8‰ MH (Molasse Height) drift; from then on, shear strength of masonry decreases while its deformation increases (Figure 7.15). Consequently, there

1. Since graphs from both sensors (4 and 8) do not differ much in the phases, only the hysteretic loops given by the sensor 8 (south side) are dealt with.

is more energy released in this phase than during the first phase. The phenomenon of cracks-closing is still recognizable for high lateral loads.

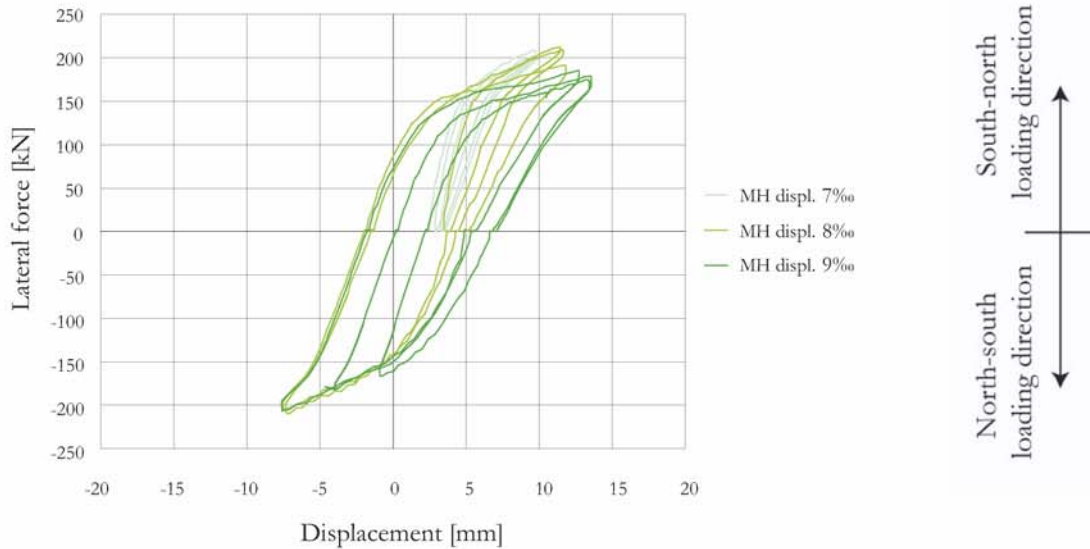


Figure 7.15 : Hysteresis loops from 7‰ to 9‰ relative drift.

In the next phase, the upper part of the wall (both upper courses) moves or slides along the bed joints of the bottom part. Failure planes of the extremity blocks of the second course (from the wall base) enlarges and separated parts move apart (Figure 7.11). Deformations increase due to the sliding along the middle bed joint. Also, more energy is consequently released (Figure 7.16).

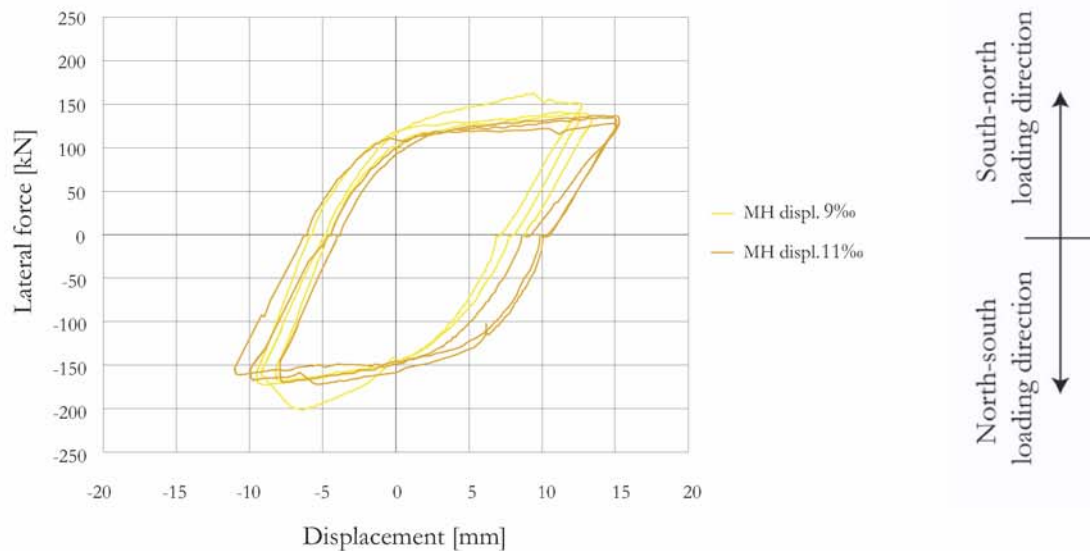


Figure 7.16 : Hysteresis loops from 9‰ to 11‰ relative drift.

The last phase slowly tends to a rocking movement (Figure 7.17); the upper part of masonry begins to rotate around a masonry core (Figure 7.12). This movement is easily recognizable by its small

residual deformation when the lateral load decreases down to zero and by the typical s-shape of the graph when rocking occurs.

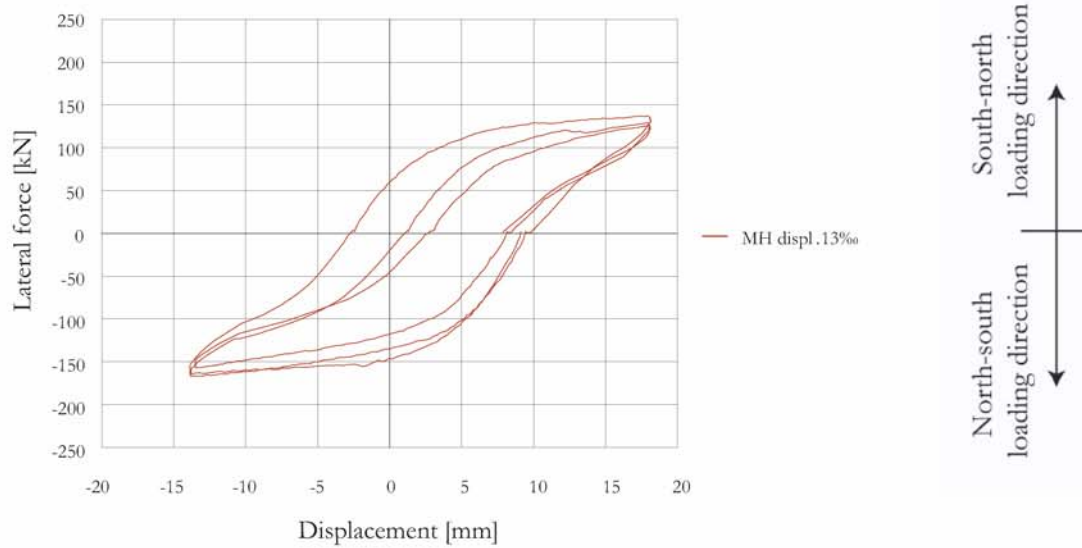


Figure 7.17 : Hysteresis loops at 13‰ relative drift.

When rocking is the dominant behaviour under lateral load, the maximal deformation for a constant force depends on the aspect ratio of the moving parts. The test is therefore stopped since there is no interest to proceed to find values depending on geometry.

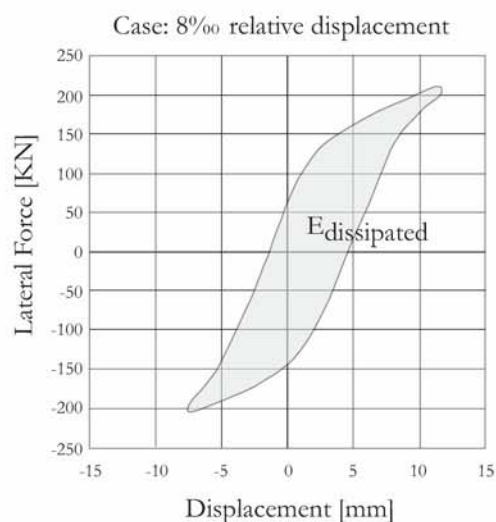
The above data on drifts can be completed from results obtained with the deformer targets (Appendix A.5.2).

7.4.2. ENERGY DISSIPATION AND STIFFNESS DEGRADATION

The amount of energy dissipation is a valuable result from the analysis of the masonry response under lateral loads. It gives information on how and up to what extent a given masonry can dissipate the energy transmitted by an earthquake.

The dissipated energy corresponds to the area within a load cycle (Figure 7.18); consequently, the larger the area is, the more is the energy dissipated.

A dissipative structure means the energy coming from the earthquake is dissipated, for the most part, through masonry deformation. In consequence, the ductility demand is lower for such a construction than for a non-dissipative structure. In present design codes, this reduction of the seismic response is taken into account through the behaviour coefficient^a that reduces the elastic seismic demand of a structure.



a. In fact, the behaviour coefficient also takes into account the over-strength.

Figure 7.18 : Dissipated energy in one loading cycle.

It is observed that energy is dissipated essentially after a sudden loss of strength in both directions (part 3 under chapter 7.4.1; from 7‰ to 9‰ MH drift in Figure 7.13); experimental investigations on shear walls with ancient masonry (whose units were in granite) showed similar results [Fa 05]. This sudden dissipation of energy is due to the creation and opening of the whole diagonal cracks; it increases up to $E_{\text{diss}}=4408$ J for a 11‰ MH drift. The shear response is characterized by an increase in the energy dissipation; sliding, which is particular case of the shear behaviour and

essentially takes place between a drift of 7‰ and 9‰ (MH), shows the higher dissipation of energy of the test (Figure 7.19).

The change of response, that is, from a shear response to a rocking one, results in a sudden decrease of energy dissipation. Nevertheless, though it dissipates less energy than shear, a rocking behaviour reaches higher drifts than shear response.

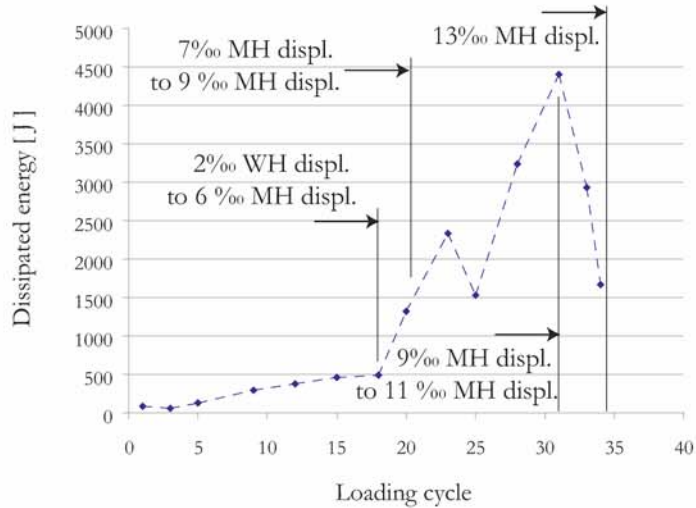


Figure 7.19 : Evolution of the dissipated energy.

The ratio between the input energy, that is, the energy provided through the lateral load in the experiment (the energy generated by a given seismic event in reality), and the dissipated energy is also a valuable tool to indicate the masonry response. More globally, it represents the seismic response of a masonry structure. The input energy is simply given by the integration of the lateral load-drift curve, as shown in Figure 7.20.

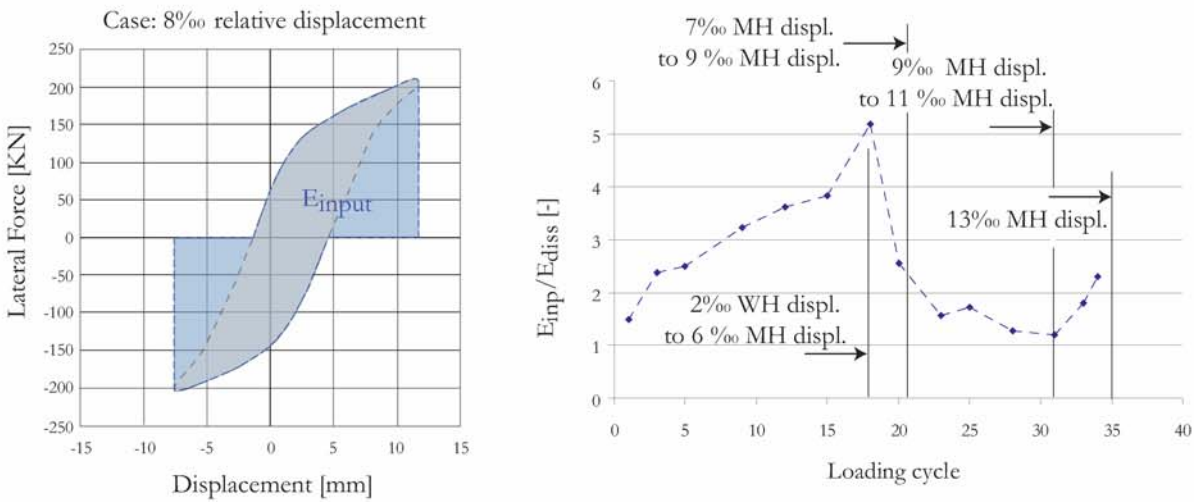


Figure 7.20 : Input and dissipated energy for one loading cycle.

The ratio between the input and the dissipated energy increases from the beginning of loading until the maximal lateral load in one direction (N-S) is reached. After achieving the lateral strength in the other direction, the dissipated energy abruptly decreases. After failure, the dissipated energy is close to the input energy; this means the structure in such a state does not store up energy and then does not collapse. Nevertheless, it must be kept in mind that such a structure is already highly damaged.

7.4.3. SAMPLE LOAD-BEARING AND DEFORMATION CAPACITY

The load-bearing and deformation capacity of the studied sample can be defined by the lateral-displacement versus lateral resistance hysteresis loop envelope.

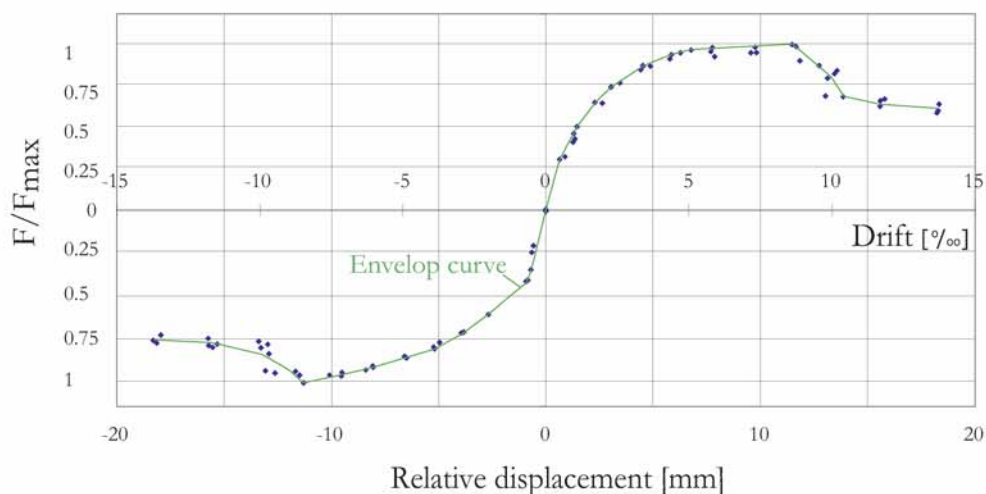


Figure 7.21 : Envelop curve of the lateral-displacement vs lateral resistance hysteresis loops.

In order to easily define both types of capacity, the hysteretic behaviour of the sample that was subjected to a constant vertical load and lateral load reversals, is simplified. The most frequent method of simplification is to idealise the experimental envelope curve as a bi- or thrilinear relationship [To 99]; a bilinear curve is chosen. First, the following points (limit states) must be defined:

1. the crack limit: appearance of the first significant cracks that change the envelope curve slope (point defined by H_{cr} , d_{cr})
2. the maximum resistance: corresponds to the actual maximum resistance achieved during the test (H_{max} , d_{Hmax})
3. the ultimate state: that is, the maximal displacement during test (H_{dmax} , d_{max})

Similar to the ideal force-displacement curve of materials, the bilinear envelope is composed of one linear elastic segment and one yield part (horizontal). The elastic curve, is defined by a modulus of elasticity smaller than the initial slope of the actual envelope curve. It actually corresponds to the secant stiffness (K_e) at the formation of cracks; it can be calculated by the following ratio: $K_e = H_{cr}/d_{cr}$.

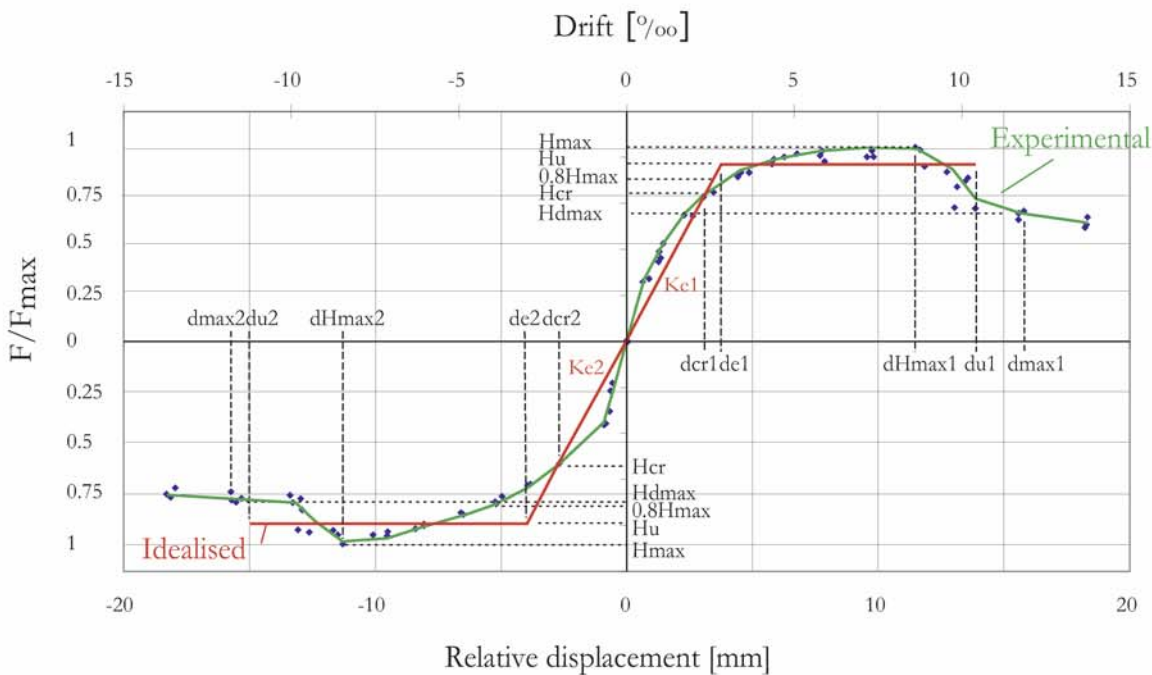


Figure 7.22 : Experimental and idealised envelop curves of the lateral-displacement vs lateral resistance hysteresis loops.

This idealised curve provides a simplified lateral-displacement vs lateral resistance curve of the tested masonry. This simplified curve is characterized by:

- a stiffness (secant stiffness, K_e)
- the shear strength (H_u)
- the displacement capacity (d_u, μ_u)

In this case, they are:

- the secant stiffness: $K_{e1} = H_{cr1}/d_{cr1} = 51.74 \text{ KN/mm}$; $K_{e2} = H_{cr2}/d_{cr2} = 49.4 \text{ KN/mm}$ (knowing that $H_{cr1} = 157.55 \text{ KN}$; $d_{cr1} = 3.045 \text{ mm}$; $H_{cr2} = 132.86 \text{ KN}$ and $d_{cr2} = -2.69 \text{ mm}$)
- the shear resistance: $H_{u1} = 194.76 \text{ KN}$; $H_{u2} = 189.85 \text{ KN}$

The ultimate displacement ductility factor (μ_u) is defined as the ratio of $d_u/d_e = \mu_u$. d_e is the elastic idealised limit. d_u is the ultimate idealised displacement that is the displacement value where the idealised line intersects the descending part of the experimental curve [To 99].

- the displacement capacity: $d_{u1} = 13.9 \text{ mm}$, $\mu_u = 3.9$; $d_{u2} = 13.4 \text{ mm}$; $\mu_u = 3.4$

The ratio between the initial stiffness K_o and the secant stiffness is: $K_o/K_e = 106.2/51.7 = 2.1$.

The maximal shear-loading capacity H_u of the idealised curve is determined by allowing for an equal dissipation of energy for the actual situation (described by the experimental curve) and the idealised one (described by the idealised curve). H_u is then [To 99]:

$$H_u = K_e \left(d_{\max} - \sqrt{d_{\max}^2 - \frac{2A_{\text{env}}}{K_e}} \right) \quad (\text{EQ 7.1})$$

Where: H_u : maximal shear-loading capacity of the idealised curve

K_e : secant stiffness

d_{\max} : maximal lateral displacement (experimental curve)

A_{env} : area below the experimental curve.

7.4.4. SAMPLE SHEAR STRENGTH

If we consider that the whole cross-section of the wall resists the shear force and also that the shear stresses are uniformly distributed on the section, the shear strength (for an axial force of about 280 kN) of the sample is:

$$\tau_{1,S} = V_1/A = 210.95 \text{ kN}/1.113 \text{ m}^2 = 0.2 \text{ MPa} = \tau_{2,S} = V_2/A$$

In fact, shear stresses are not uniformly distributed on the sample area; consequently, the actual shear strength of the tested masonry under such conditions of forces must be higher than 0.2 MPa¹. However, the weakest cross-section (regarding the shear strength) is the area at the interface between the slab and the wall because the axial force is the smallest within the wall. In consequence, the above approximate values are certainly not far from the actual shear strength of this masonry.

Nevertheless, the matter of interest is the way to calculate the shear strength as a function of the axial force, since it depends on it. As mentioned in chapter 6, masonry shear strength depends on the axial force, the cohesion and the internal angle of friction φ ; according to Coulomb's model: $\tau_{ss} = c + \sigma \tan \varphi$. If the cohesion is zero, a common assumption when calculating the masonry shear strength, φ is the angle of the resultant with the vertical direction: $\tau_{ss}/\sigma = \tan \varphi$. In case of the given masonry, that is, a well-dressed masonry with large blocks, this assumption is relevant since the cohesion does not have a great influence on the composite material failure (molasse has no cohesion [Du 69];). In the present case, this angle (internal angle of friction) is, in both directions:

$$\varphi_1 = \arctan(V_1/N) = \arctan(210.95 \text{ kN}/280 \text{ kN}) = 36.9^\circ ; (\tan \varphi = 0.75)$$

$$\varphi_2 = \arctan(V_2/N) = \arctan(220.11 \text{ kN}/280 \text{ kN}) = 38.2^\circ ; (\tan \varphi = 0.79)$$

The above values are interesting but such high values for φ are not exactly confirmed by experimental investigations (see Figure 7.23). However, it is difficult to compare a calculated angle of

1. In order to determine the shear strength more accurately, the actual distribution of stresses must be defined by numerical non-linear calculation.
2. The axial force consists of the post-tensioning force, the concrete slab and steel-section dead load.

friction with an angle measured on a sample because the definition of a straight line corresponding to the group of diagonal failure cracks¹ cannot be accurate (see Figure 7.23). However, the calculated values and measured ones figure within the same range ($\tan\phi = 0.7 - 0.79$).

What is relevant here is the dispersion of this value: it can vary from $\tan\phi = 0.7$ to $\tan\phi = 0.79$. This shows one of the main problems of the stone masonry: the dispersion of the mechanical properties of the stone blocks.

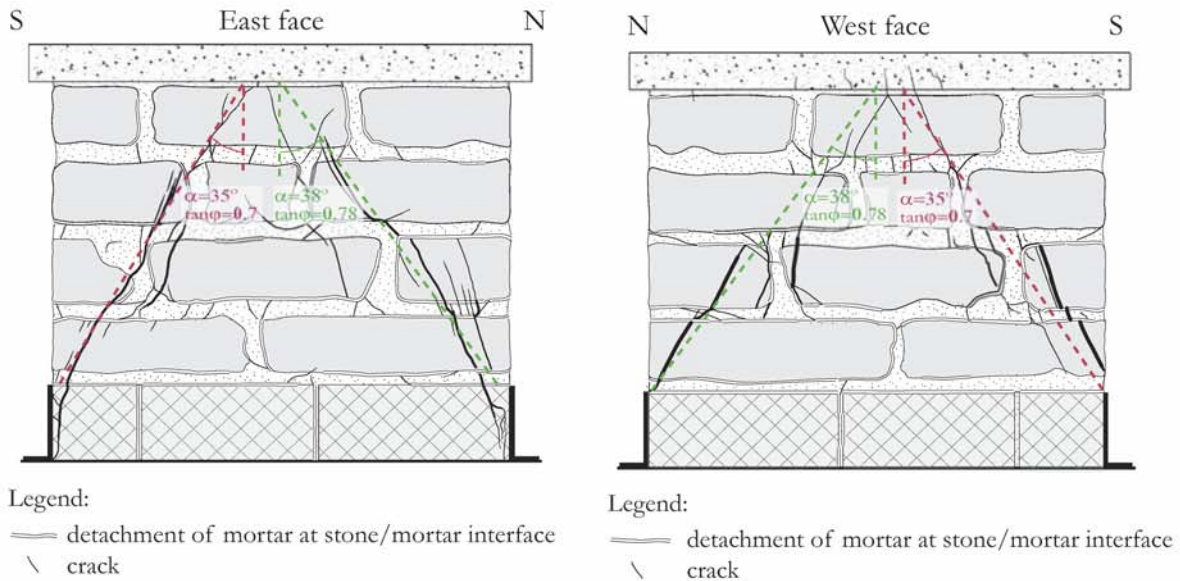


Figure 7.23 : Measured angles of internal friction.

7.5. INTERPRETATION

7.5.1. SHEAR-LOADING CAPACITY: ANALYTICAL MODELS

Three models are considered: the FEMA, the EC 6 and then the Swisscode V178².

7.5.2.1. FEMA model

1. Shear failure

The maximal lateral load is calculated with this equation:

$$V_{R,S} = 0.67 \cdot v_d \cdot t_w \cdot l_w \quad (\text{EQ 7.2})$$

Where: $V_{R,S}$: maximal lateral load (in case of a shear failure)

1. This is due to the fact that stone is a naturally generated material (heterogeneous material with weak points) and also because the masonry weight changes the stress state according to the height.
2. The maximal loads that are calculated are not design values.

v_d : design shear strength of masonry

l_w : wall (or sample) length

t_w : wall (or sample) height

As a reminder, the values characterizing the sample are:

v_{mk}	0.3 MPa ^a	t_w	0.53 m	l_w	2.1 m
N	280 KN ^b	v_d	0.19 MPa	h_w	1.7 m ^c

a. Recommended value for masonry made up of plain silico-calcareous bricks [SIA D 0211 05]

b. Post-tensioning, self-weight of the iron section and of the reinforced concrete slab are included

c. It corresponds to the height of the whole sample (including the limestone course)

In consequence, the maximal lateral load that leads to the shear failure is: $V_{R,S}=177.7$ KN

2. Flexural failure (Rocking)

The maximal lateral load is calculated with this equation:

$$\text{Flexural failure} \quad V_{R,R} = 0.9 \cdot N \cdot \frac{l_w}{2 \cdot h_w} \quad (\text{EQ 7.3})$$

Where: $V_{R,R}$: maximal lateral load (in case of a rocking failure)

N : vertical load (axial load)

l_w : wall (or sample) length

h_w : wall (or sample) height

As a reminder, the values characterizing the sample are:

N	325KN ^a	h_w	1.7 m ^b	l_w	2.1 m
-----	--------------------	-------	--------------------	-------	-------

a. Post-tensioning, self-weight of the iron section, the reinforced concrete slab and the sample masonry are included.

b. It corresponds to the height of the whole sample (including the limestone course)

In consequence, the maximal lateral load that leads to a flexural failure is:

$V_{R,R}=180.7$ KN; nevertheless, if only the height of the molasse part is taken into account (N is then equal to 314 KN and $h_w=1.34$ m), this value becomes: $V_{R,R,Molasse}=221.4$ KN.

7.5.3.2. EC 8 model

1. Shear failure

The maximal shear force (shear failure) is calculated with the following equation.:

$$V_{R,S} = f_{sd} \cdot l'_w \cdot t_w \quad (\text{EQ 7.4})$$

Where: $V_{R,S}$: maximal lateral load (in case of a shear failure)

f_{sd} : design shear strength

l_w : wall (or sample) length that is under compression

h_w : wall (or sample) height

The application of the Eq 7. 4 requires the knowledge of the dimensions of the compressed part (l_w and t_w). Considered values are:

N	325 KN ^a	h_w	1.7 m ^b	l_w	2.1 m
t_w	0.53 m	$f_{s,c}$ ^c	15 MPa		

- Post-tensioning, self-weight of the iron section, the reinforced concrete slab and the sample masonry are included.
- It corresponds to the height of the whole sample (including the limestone course)
- The stone compressive strength is determined on the basis of compression tests; masonry compressive strength is defined according to the SIA V 178.

In consequence, the maximal lateral load that leads to the shear failure is:

$$V_{R,S} = 328.2 \text{ KN}$$

2. Flexural failure

The maximal shear force (flexural failure) is calculated with the following equation:

$$\text{Flexural failure} \quad V_{R,R} = \frac{l_w \cdot N}{2 \cdot h_w} \cdot \left(1 - 1.15 \cdot \frac{N}{l_w \cdot t_w \cdot f_{m,c}} \right) \quad (\text{EQ 7.5})$$

Where: $V_{R,R}$: maximal lateral load (in case of a rocking failure)

N: vertical load (axial load)

l_w : wall (or sample) length

t_w : wall (or sample) height

$f_{m,c}$: masonry compressive strength (design value)

h_w : wall (or sample) height

As a reminder, the values characterizing the sample are:

N	325 KN ^a	h_w	1.7 m ^b	l_w	2.1 m
t_w	0.53 m	$f_{s,c}$ ^c	15 MPa		

- Post-tensioning, self-weight of the iron section, the reinforced concrete slab and the sample masonry are included.
- It corresponds to the height of the whole sample (including the limestone course)
- The stone compressive strength is determined on the basis of compression tests; masonry compressive strength is defined according to the SIA V 178.

Consequently, the maximal lateral load that leads to a rocking collapse is:

$V_{R,R}=196.2$ KN; nevertheless, if only the height of the molasse part is taken into account (N_x is then equal to 314 KN and $hw=1.34$ m), this value becomes: $V_{R,R, Molasse}=240.7$ KN.

7.5.4.3. Ganz's model

Ganz's model is based on the concept of the stress fields¹.

The maximal shear load that the whole wall (molasse courses and the limestone footing) can resist according to the Ganz's model and the Swisscode SIA V178 ($\tan\phi_{max}=0.72$, $c=0$) is $V=169.6$ KN, the axial force being $N=280$ KN (Figure 7.24). This maximal shear load is lower than the $V_2=220.11$ KN or even $V_1=210.95$ KN that is experimentally obtained.

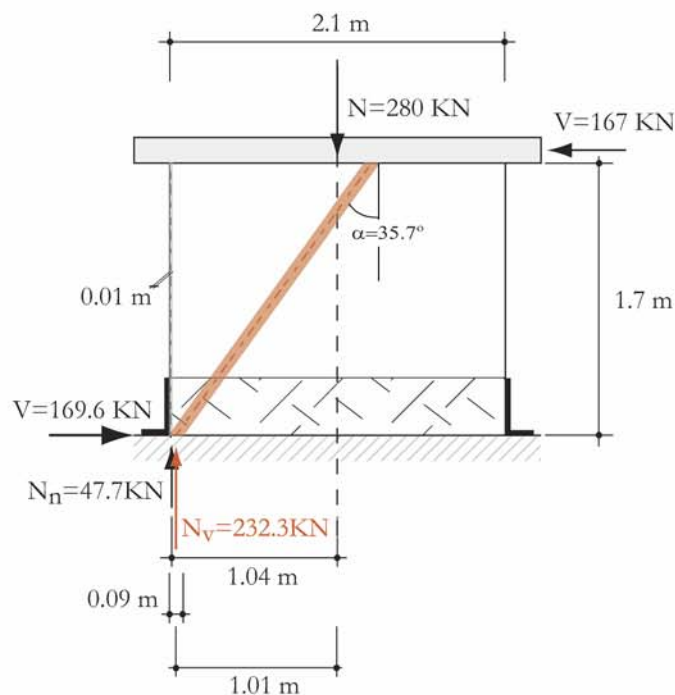


Figure 7.24 : Maximal shear load according to the Ganz's model for the whole wall.

Since the lateral force is higher than 169.6 KN, it directly transfers to the ground through the iron angles at the wall extremities. The lateral force no longer passes through the interface between the ground and the limestone footing; consequently, only the molasse part is loaded by shear. Since the shear strength of the molasse part was searched for, the aim of this test is reached.

With only the height (for the reason explained here above) and the internal angle of friction modified, the maximal shear load is 213 KN (Figure 7.25). The chosen value for the angle corresponds

1. For more information, the reader can read the chapter 8.3.3.

to the internal angle of friction of the rock material ($\varphi=38^\circ$, medium-grained sandstone firmly cemented, blocks put on their bed face [Du 69]).

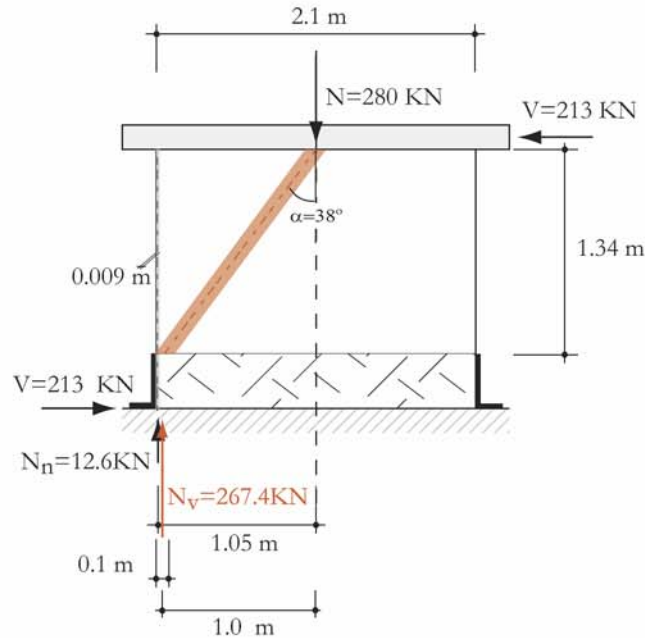


Figure 7.25 : Maximal shear load according to the Ganz's model, for different boundary conditions.

The highest value for the shear force ($V=226$ kN ($f_{mx}=15$ MPa)) is obtained with an axial force of $N= 297$ kN ($\varphi=38^\circ$, $c=0$)¹.

7.5.5.4. Discussion

SUMMARY OF MODEL RESULTS

Table 7. 3 : Summary of the model results.

Units: [m, kN]	FEMA		EC 8		GANZ' MODEL		
h_w	1.7	1.34	1.7	1.34	1.7	1.34	1.34
Shear failure	177.7	177.7	328.2	328.2	169.6	213	226 ^a
Flexural failure	180.7	221.4	196.2	240.7	b/	/	/

a. Half the weight of the molasse part is included within the axial force.

b. The dash indicates that the given model is not used to calculate the given failure (see the reasons in the above section).

1. It includes the post-tensioning, self-weight of the iron section, the reinforced concrete slab and half the dead load of the molasse courses.

With respect to shear failure, the FEMA model is about 15% lower than the experimental values (210.95 kN or 220.11 kN). The shear strength obtained with the EC8 is really too high. On the contrary, Ganz's model gives good estimates that closely match the experimental results.

Regarding rocking failure, good results are obtained with the FEMA and the EC 8 models. The lateral forces that are calculated for the rocking failure of the whole wall (180.7 kN and 196.2 kN) corresponds to the beginning of the phenomenon of closing cracks (at the tips of the hysteretic loops on the Figure 7.14). However, when approaching the maximal shear force (220.11 kN), there is no sign of rocking failure. This statement indicates that the rocking failure would appear at a higher level of shear force. Nevertheless, it does not mean that the value obtained by the EC8 is more accurate. In fact, since the sample failed by shear, an accurate evaluation of the performance of the models for rocking failure cannot be made.

7.6. DISCUSSIONS AND CONCLUSIONS

According to the obtained results, it can be stated that the kind of masonry that is tested (square-stone masonry (regular ashlar masonry)), shows a good displacement ductility compared to common brick masonry. Based on an idealised curve, this value is situated between $\mu_u=3.4$ and $\mu_u=3.9$; the maximal displacements reached before the beginning of rocking are high: $d_u=13.4$ or 13.9 mm. Such drifts of 10‰ are good compared with what can be reached with common brick masonry. On the other hand, this type of masonry resists high shear forces and dissipates a lot of energy at failure because of the sliding along bed joints.

Regarding the approach to calculate the shear strength of such a masonry, the experimental investigation allow us to make the following conclusions. First, the influence of cohesion can be neglected and the angle of internal friction can be assumed between $\tan\phi=0.75$ and $\tan\phi=0.79$; these values tend to the internal angle of friction of the stone¹. Consequently, the shear strength could be calculated with the following equation: $\tau_s=0.75\sigma_y$. However, it must be kept in mind that this equation results from only one test and therefore cannot be generalized. More experimental investigations must indeed be done in order to calibrate it. This notice also goes for the capacity displacement.

To sum up the previous statements, the FEMA model gives good results regarding the rocking failure and Ganz's model gives the best results for the shear failure.

This experimental investigation on old masonry, which figures among the first investigations of this kind to have been carried out in the world, gives interesting and useful results concerning the structural behaviour of such a masonry under cyclic loading. However, another masonry would have another response under a similar loading that is unknown today but is also of interest regarding the seismic safety of sacred buildings (whose masonry is not necessarily made up of molasse squared-stones). This statement shows that it is important to carry on further experimental investigations on other old masonries in order to be able to characterize the structural behaviour of each masonry under seismic loading.

1. This would no longer be the case for masonry with no squared-stones and a lot of mortar.

8.1. INTRODUCTION

Churches present different structural features compared with common buildings. Unlike them, their bearing structure is, save for small churches or chapels, irregular in elevation though generally regular and very often symmetric in plan. Moreover, on the contrary to common buildings, the masses are not concentrated at floors level but in the walls themselves; vaults are relatively light in comparison to walls since they are often made up of light materials like tuff. Timber frameworks are also very light compared to masonry. As vaults and timber framework constitute the only horizontal structure, there is no real diaphragm effect; walls structural elements behave then more or less independently from each other save from walls they are linked to. The only connection between structural elements is their corners; consequently the seismic response of each structural element depends on their own stiffness, strength, weight and on the type and quality of their connections to the other elements. This particularity highlights that the description of the seismic behaviour of churches has to be done through the description of the structural behaviour of each wall or part (bell tower, vaults) and the connections between them.

On the other hand and contrary to common buildings, sacred edifices have a few walls, that make them even more seismically vulnerable.

8.2. SEISMIC BEHAVIOUR OF CHURCHES

Since mass is essentially distributed in the masonry of walls, there are no concentrated masses like in common multi-floor buildings. Consequently, ground acceleration loads the mass of walls in both directions.

For instance, if considering an one-nave church with only one apse, the front wall, as a mass, sustained inertia forces in and out of its plane, as well as the lateral walls and the chancel arch.

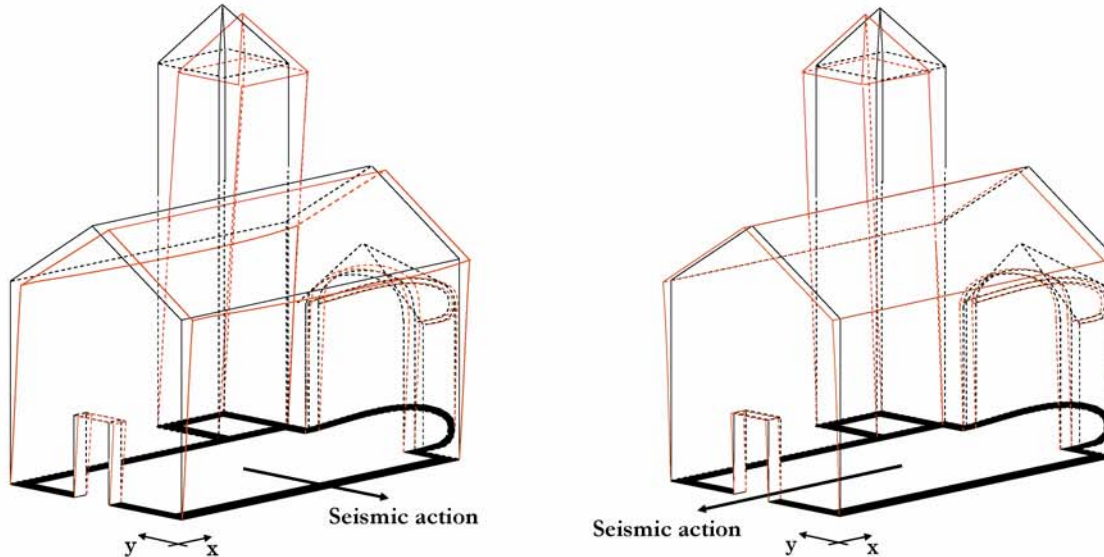


Figure 8.1 : Seismic response in both directions of a simple church with a bell-tower.

As aforementioned, churches have no stiff diaphragm that distributes forces among structural elements and makes the building behave in a compact way. Instead, masses (walls especially) move more or less independently from each other (depending on the boundary conditions (tightness of corners)). Because of this reason, each wall or part of masonry must be dealt with separately. The analysis of the seismic response of every structural part constitutes the first step of the study of the churches seismic behaviour; this step is called the local behaviour in this report.

Nevertheless, the closeness of structural parts that are characterized by different stiffness (or natural frequency regarding the bell-tower) or the double use of a wall area for two structural parts can result in damaging one or both given parts. This is essentially the case of the coexistence of a bell-tower and a nave wall that can be either the front wall, a lateral wall or the chancel; it can also be a transept wall in case of more complex churches. In order to prevent damage that can result from this situation, the second step of the analysis is the study of what is called the global behaviour.

The local behaviour, that is, the study of the seismic behaviour of each structural parts (walls, bell-towers) is the first to be treated in this chapter. Moreover, since they composed the most part of churches, the first structural parts to be dealt with are the walls.

8.3. WALLS

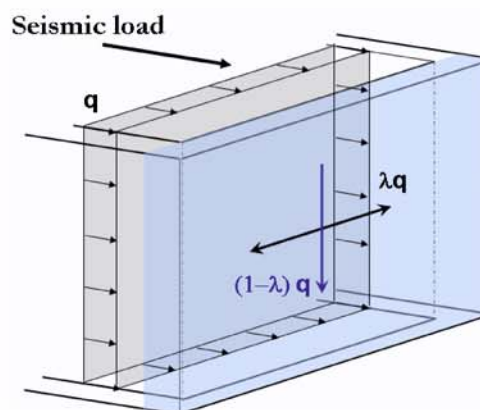
The out-of-plane seismic response of walls is considered first; then comes the in-plane behaviour.

8.3.1. OUT-OF-PLANE BEHAVIOUR

The impact of the seismic actions on the out-of-plane strength of walls is largely dependant on their direction. Actions that are inward directed will indeed load walls differently than the outward-directed ones. Because of this difference it makes sense to deal with each situation separately.

8.3.1.1. Outward-directed seismic actions: one-leaf walls

When seismic waves subject a given wall out of its plane, it induces inertia forces perpendicularly to its plane. To counteract it, forces can transfer to the lateral walls (arch effect; λq)^a and/or directly to the ground $(1-\lambda)q$ ^b. Forces transfer to the ground and to the lateral walls according to the wall dimension proportions, the quality of connection with perpendicular walls, and the presence or not of tie rods or abutments.



a. It is assumed that the arch effect is uniform along the height.

b. If there is tie-rods along the wall upper edge, the transfer of forces will be different.

Figure 8.2 : Distribution of outward-directed seismic actions within a wall.

Regarding the inertia forces, an important statement is made: it is assumed that walls behave like rigid bodies; their spectral acceleration corresponds then the peak ground acceleration. Moreover, each part of walls sustains the same lateral acceleration.

The transfer of the aforementioned decoupling of forces satisfies the conditions required by the application of the lower bound theorem of the limit analysis (i.e. actions and inner forces are in equilibrium and the bending moments are smaller than the yielding moment). It is worth noting that according to the application of the lower bound theorem, the lateral actions (i.e. the seismic actions) leading to collapse is actually equal or lower than the real one. Furthermore, the superimposition of two transfers of forces is based on the assumption that the wall material stays in the elastic field in every part of the wall, which is quite right since masonry resists very few tensile stresses.

The purpose is to determine the peak ground acceleration (a_{gd}) that can be counteracted by the wall.

First, the situation of three orthogonal walls is simulated; a given wall (in grey on Figure 8.3) is modelled by a beam (with similar characteristics, dimensions, etc.) with three damper bearings.

It is assumed that both corners have similar mechanical characteristics.

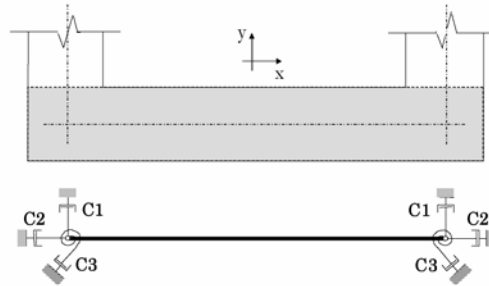


Figure 8.3 : Structural system of one wall that is connected to two orthogonal walls at its corners.¹

Damper bearings that model masonry corners have no constant characteristics; since they depend on masonry mechanical characteristics, such as cohesion, they change with the loading force accordingly. For instance, they can resist up to a certain level of the force; reaching this level, masonry cracked and the bearing strength decreases down to a lower level of strength (Figure 8.4)². Having reached this level means a definitive loss of strength; the next cycle (in the framework of seismic actions), the corners won't be able to resist a force as high as the one before.

The damper bearings C1, C2 and C3 can also be more or less characterized by a diagram; nevertheless, the value C3 can vary because of the loss of friction strength and the increasing cracking of the cross-section.

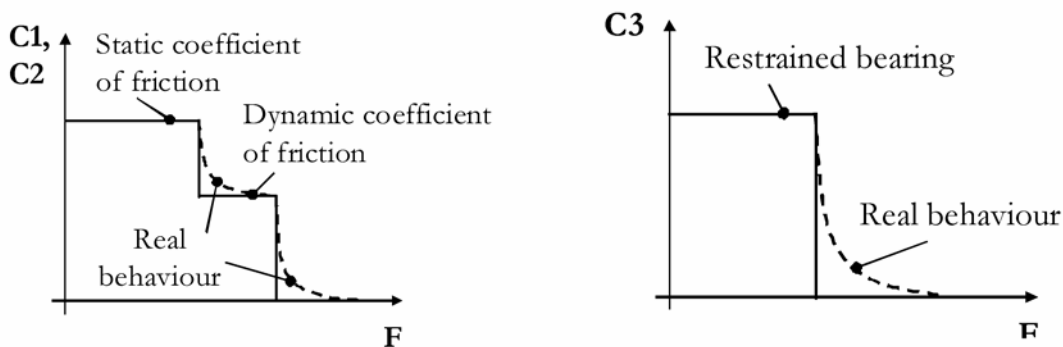


Figure 8.4 : Stiffness of the damper bearings of the beam that models a given loaded wall.

Though the previous figures show the real behaviour of the bearings, the diagrams will be simplified: the dynamic coefficient of friction will not be taken into account.

1. The situation on Figure 8.3 corresponds to a front wall made up of a compact and stiff masonry with lateral walls composed of less good quality.
 2. The strength actually does not brutally decrease as shown on the Figure, but more smoothly. This curve of decreasing strength depends on the masonry type and quality; it is difficult to give a curve matching to every kind of masonry. Nevertheless, it does not matter to give a perfectly matching curve since only the result (the lower value) is of interest.

In [Cr 98], Croci shows that a kind of arch effect can be found in masonry walls that are restrained at least along two opposite edges (e.g.: (part of) wall between two floors or two lateral walls). Moreover, he wrote that in case the wall is restrained along four edges a vault effect might be formed.

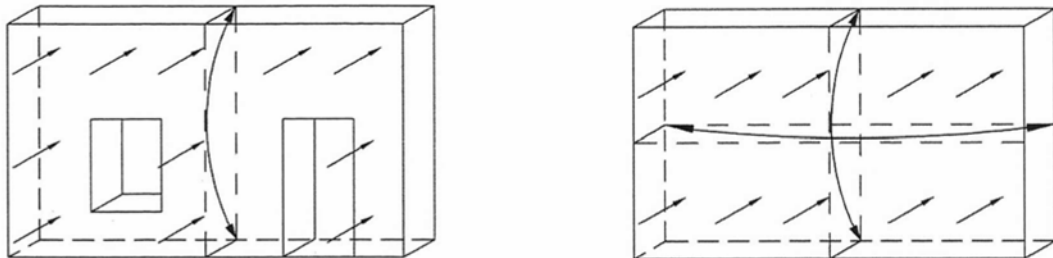


Figure 8.5 : Arch effect in one or two directions (vault effect) [Cr 98].

It is assumed that bearings (along edges) do not move.

Based on the aforementioned observations, the bearing capacities of such walls can be determined using the lower bound theorem of the limit analysis.

ARCH EFFECT WITHOUT TIE-RODS

If connections with lateral walls are strong enough (or if there are tie-rods that link the given wall to the orthogonal elements) to resist tensile stresses, an arch can be formed. The connection must resist the arch components:

$$H_x = \frac{q \cdot L^2}{8 \cdot a} \quad (\text{EQ 8.1})$$

$$H_y = \frac{q \cdot L}{2} \quad (\text{EQ 8.2})$$

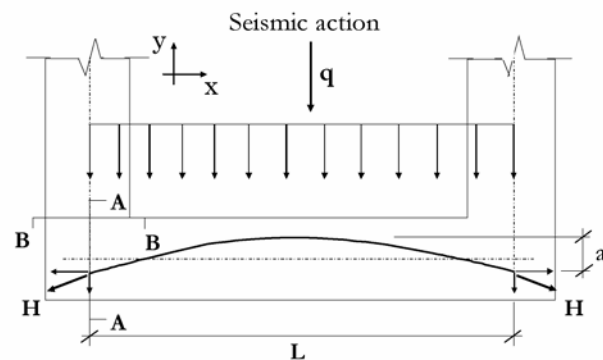


Figure 8.6 : Arch effect within a wall.

In fact, the formation of an arch under outward-directed actions in the wall requires a strength that usually cannot be ensured by masonry.

Note: there is no safety coefficients in the equations here below.

To create an arch, the bearings must be strong enough, then:

1. Bearing strength along y:

The actions resulting from the formation of an arch must be supported by the connection to the lateral wall along the section A-A and B-B (if considering only one corner; the process is the same for the other corner, by symmetry) and also by the transfer to the ground within the corner volume

with the help of this volume weight. In consequence, the strength by friction (connection) must be defined as well as the possibility of transferring the load to the ground:

$$H_y = H'_y + H''_y \geq q \cdot \frac{L}{2} \quad (\text{EQ 8.3})$$

Where: H_y : component of H along the y-axis

H'_y : bearing reaction by friction¹

H''_y : bearing reaction by transfer to the ground

- Friction strength²:

$$H'_y = \frac{W}{2} \cdot \tan\varphi + c \cdot A_F \quad (\text{EQ 8.4})$$

Where: c: cohesion

H_y : component of H along the y-axis

W: weight of the studied part of the corner

q: seismic action

$\tan\varphi$: angle of internal friction

A_F : friction area

It is assumed that the corner is made up of the same materials and has a homogenous weight per unit of volume.

- Possible transfer to the ground (without traction):

$$H''_y = W \cdot \frac{(t/2) - n}{h} \quad (\text{EQ 8.5})$$

Where: c: cohesion

H''_y : bearing reaction by transfer to the ground

W: weight of the studied part of the corner

t: y-cross-section thickness

n: H_x eccentricity

h: height of the given corner part

2. Bearing strength along x:

Like the previous case, the actions resulting from the formation of an arch must be supported by the connection to the lateral wall (if considering only one corner) and also by the transfer to the ground within the corner volume with the help of its volume weight. In consequence, the strength

1. Further information about the calculation of the bearing reaction by friction is given in chapter 8.3.1.6.
 2. This value corresponds to C1 on the Figure 8.4.

by friction (connection) must be defined as well as the possibility of transferring the load to the ground.:

$$H_x = H'_x + H''_x \geq \frac{q \cdot L^2}{8 \cdot a} \quad (\text{EQ 8.6})$$

Where: H_y : component of H along the y-axis

H'_x : bearing reaction by friction

q: seismic action

L: beam length

a: arch deflection

H''_x : bearing reaction by transfer to the ground

- Friction strength:

$$H'_x = \frac{W}{2} \cdot \tan\phi + c \cdot A_F \quad (\text{EQ 8.7})$$

Where: c: cohesion

H_x : component of H along the x-axis

W: weight of the studied part of the corner

$\tan\phi$: angle of internal friction

A_F : friction area

It is assumed that the corner is made up of the same materials and has a homogenous weight per unit of volume.

- Possible transfer to the ground (without traction):

$$H''_x = W \cdot \frac{2(t/2)}{h} \quad (\text{EQ 8.8})$$

Where: H''_x : bearing reaction by transfer to the ground

W: weight of the studied part of the corner and axial force from the part above it

t: x-cross-section thickness

h: height of the given corner part

There is no eccentricity of the arch force along x axis; moreover, the corner inertia force due to seismic actions is along the y-axis.

ARCH EFFECT WITH TIE-RODS

This time, connections with lateral walls are ensured by masonry strength as well as tie-rods (T1, T2 and T3 on Figure 8.7). If they are strong enough to resist tensile stresses, an arch can be formed. The connection must resist the arch thrust components (EQ 8.1 and EQ 8.2).

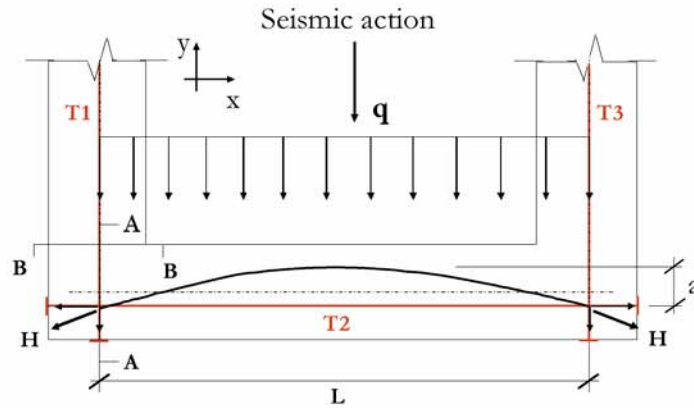


Figure 8.7 : Arch effect within a wall subjected to actions out of its plane.

In fact, since the formation of an arch under outward-directed actions in the wall requires a strength that usually cannot be ensured by masonry; the presence of tie-rods is of prime importance. The volume of masonry on which tie-rods have an impact, that is, within which an arch can be formed because of the tie-rods, depends on the area of the tie-rods head.

To create an arch, the bearings must be strong enough, then:

1. Bearing strength along y:

The actions resulting from the formation of an arch must be supported by the connection to the lateral wall (if considering only one corner; the process is the same for the other corner, by symmetry) and also by the transfer to the ground within the corner volume with the help of this volume weight. In consequence, the strength by friction (connection) must be defined as well as the possibility of transferring the load to the ground:

$$H_y = H'_y + H''_y + H'''_y \geq q \cdot \frac{L}{2} \tag{EQ 8.9}$$

Where: H_y : component of H along the y-axis

H'_y : bearing reaction by friction

H''_y : bearing reaction by transfer to the ground

H'''_y : bearing reaction provided by tie-rods¹

q: seismic action

L: wall length

- Friction strength:

With EQ 8.4.

1. Further information about the way of calculating the bearing reaction given by tie-rods can be calculated is proposed under chapter 8.3.1.6.

- Possible transfer to the ground:

With EQ 8.5.

- Tie-rod strength:

$$H_y''' \leq H_{y, \max}''' = f_{\text{yield}} \cdot A_{\text{TR}} \quad (\text{EQ 8.10})$$

Where: H_y''' : bearing reaction provided by tie-rods

$H_{y, \max}'''$: maximal bearing reaction provided by tie-rods

f_{yield} : yield strength of steel

A_{TR} : area of the given tie-rod cross-section

2. Bearing strength along x:

Like the previous case, the actions resulting from the formation of an arch must be supported by the connection to the lateral wall (if considering only one corner) and also by the transfer to the ground within the corner volume with the help of its volume weight. In consequence, the strength by friction (connection) must be defined as well as the possibility of transferring the load to the ground.:

$$H_x = H_x' + H_x'' + H_x''' \geq \frac{q \cdot L^2}{8 \cdot a} \quad (\text{EQ 8.11})$$

Where: H_y : component of H along the y-axis

H_x' : bearing reaction by friction

H_x'' : bearing reaction by transfer to the ground

H_x''' : bearing reaction provided by the tie-rods

q: seismic action

L: beam length

a: arch deflection

- Friction strength:

With EQ 8.7.

- Possible transfer to the ground:

With EQ 8.8.

- Tie-rod strength:

$$H_x''' \leq H_{x, \max}''' = f_{\text{yield}} \cdot A_{\text{TR}} \quad (\text{EQ 8.12})$$

Where: H_x''' : bearing reaction provided by tie-rods

$H_{x, \max}'''$: maximal bearing reaction provided by tie-rods

f_{yield} : yield strength of steel

A_{TR} : area of the given tie-rod cross-section

Note: the anchorage strength of tie-rods must be first checked (see EQ 8.26).

TRANSFER OF FORCES TO THE GROUND

Forces can transfer down to the ground as long as their resultant stays within the cross-section in order to avoid the loss of stability for the wall. Moreover the wall must resist sliding and the material must resist the high compressive stresses along the loaded edge.

The sliding condition is simply linked to the masonry cohesion and angle of internal friction:

$$Q \leq N \cdot \tan \varphi + c \cdot A \quad (\text{EQ 8.13})$$

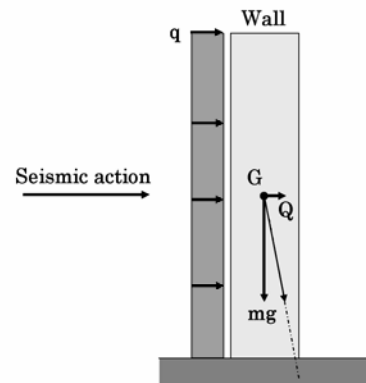


Figure 8.8 : Transfer to the ground of actions horizontally loading a wall.

Where: Q : resultant of the seismic action

N : resultant of the masonry weight

$\tan \varphi$: angle of internal friction

c : masonry cohesion

A : ground surface

The loss of stability condition is (the cohesion is neglected):

$$\tan \varphi = \frac{Q}{mg} = \frac{q \cdot L \cdot h}{mg} \leq \frac{t}{h} \quad (\text{EQ 8.14})$$

Where: Q : resultant of the seismic action

m : wall mass

$\tan \varphi$: angle of internal friction

h : wall height

t : wall thickness

Note: the above equation suggests that masonry has an infinite compressive strength; since this not the case, the wall thickness should be normally shortened in order to come closer to reality.

The material compressive strength cannot be exceeded¹:

$$\sigma = \frac{2N}{3bc} \leq f_x \quad (\text{EQ 8.15})$$

Where: N: axial force; it more or less corresponds to the weight of the corner masonry

b: thickness of the given section

σ : stress

c: distance from the cross-section edge to the force application ($c=h/2-e$)

f_x : masonry strength in the given direction

The assumption that under the above conditions, especially regarding the transfer of forces down to the ground, the wall loses its stability is correct in a static or motionless context. Nevertheless, earthquakes are cyclic events and the dynamic notion must be allowed. This is done when treating the out-of-plane collapse mechanisms, i.e. the so-called overturning mechanism (see chapter 8.3.1.5).

8.3.1.2. Outward-directed seismic actions: multiple-leaf walls

If the three parts of the wall are well (tightly) connected to each other, i.e. compact, and that bearings are enough strong, an arch can be created as for a simple-leaf wall. Nevertheless, the bearings are also composed of three parts characterized by different stiffnesses as well as strength. In consequence, the way of calculations their resistance differs from the one for one-leaf masonry walls.

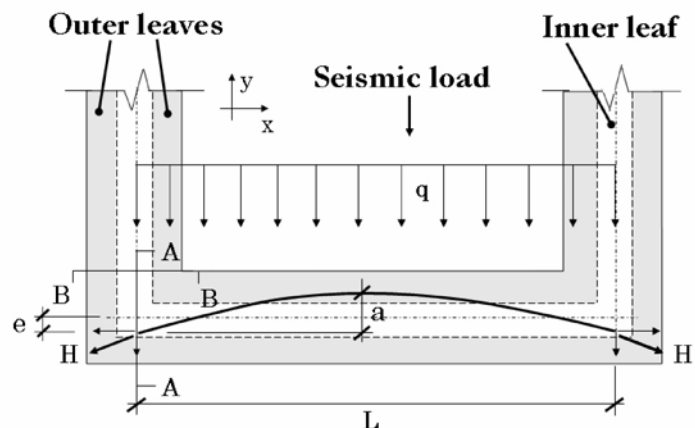


Figure 8.9 : Scheme of the creation of an arch within a multiple-leaf wall.

Globally, four cases may appear:

- the multiple-leaf wall is compact (layers are tightly connected to each other)
- the interface between the leaves 1 and 2 is loose
- the interface between the leaves 2 and 3 is loose
- both interfaces are loose.

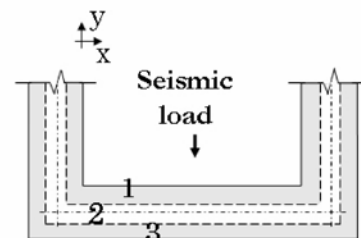


Figure 8.10 : The three leaves of a multiple-leaf wall.

1. A triangular distribution of stresses (perpendicular to the cross-section) is assumed.

The best situation is when the three leaves are well connected while the worst is probably when each layer is disconnected from its neighbour. Nevertheless, the in-between situations are quite bad too. The four situations are illustrated here below:

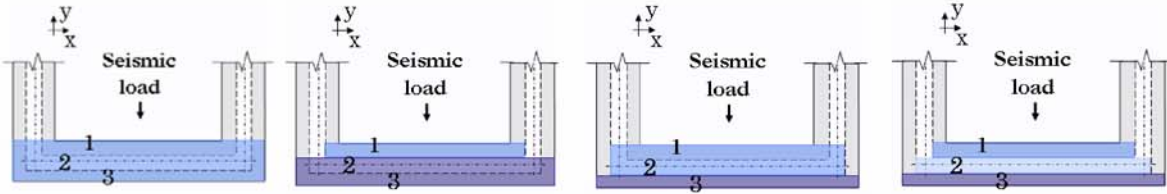


Figure 8.11 : Four situations of connections between the leaves of a wall.

Assumption: the quality of the interface is the same in the three orthogonal walls.

Globally, the peak ground acceleration that will lead to the collapse of the above presented multiple-leaf wall is situated between two limits:

- the wall is compact
- each leaf is independent from each other

ARCH EFFECT WITHOUT TIE-RODS

It is usually difficult not only to know or to obtain values of the shear strength of the interfaces between leaves, but also to be certain that the strength value is uniform in the whole surface of the interface.

Because of this uncertainties, it is proposed to calculate both limits of the given wall strength according to the process presented for one-leaf walls. This way of doing was also proposed by [Gi 91].

8.3.1.3. Inward-directed seismic actions: one-leaf walls

As for the previous case, the wall subjected to inward-directed seismic waves out of its plane can resist them by transferring the forces to its lateral edges and/or to the its foot.

As reminder, the static model is the same as for the previous situation of a wall subjected to outward-directed seismic actions. The model is composed of one beam bore by two fixed and partially restrained bearings.

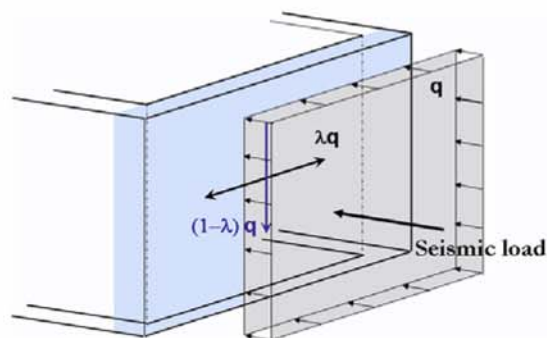


Figure 8.12 : Distribution of forces within a wall subjected to inward-directed actions.

ARCH EFFECT WITHOUT TIE-RODS

In this case, there is more probability that an arch is formed than when the seismic actions were outward directed, since the lateral walls can resist the y component of the thrust. However, the counteracting of the x component must be checked.

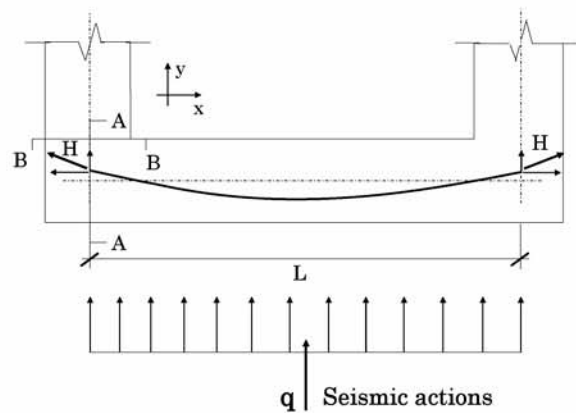


Figure 8.13 : Arch effect within a wall subjected to inward-directed actions.

One proposes to calculate the bearing strength according to the way presented in the previous section.

ARCH EFFECT WITH TIE-RODS

In this case, this is especially the tie-rods in the x direction that can bring more resistance to the wall.

As the previous case, the equations presented in the previous section can also be applied.

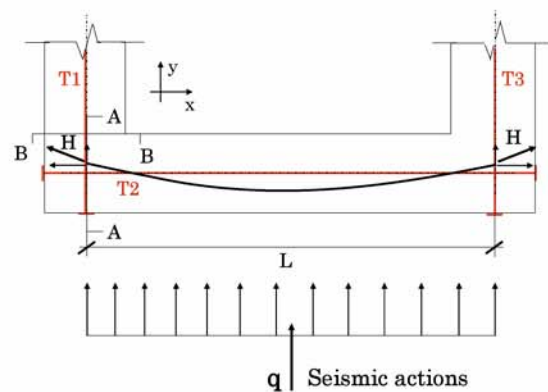


Figure 8.14 : Arch effect within a wall subjected to actions out of its plane.

8.3.1.4. Inward-directed seismic actions: multiple-leaf walls

Assumptions expressed in the chapter 8.3.1.2 are still valid in this case and can be then once again applied.

8.3.1.5. Overturning

If there are no tie-rods nor abutments at a given wall corners, these edges will constitute the weak link of the system. That means the cracks will appear there first and then detachment. The whole impact of the seismic actions (lateral forces) will be then directly led down to the ground thanks to the masonry weight and the wall becomes and behaves like a rigid block. The forces increasing, the cross-section on the ground will crack more up to reach the point of stability (gravity centre on the vertical plan including the turning edge); nevertheless, as the seismic loading is cyclic, to be on the point to loose stability does not mean it effectively. After one cycle that led the wall on the edge,

the next cycle will bring it back and then forth, etc. At that point, the loss of stability has to be allowed for from the energy point of view.

Note: the spectral acceleration also corresponds to the peak ground acceleration since it is a rigid block.

This matter has been dealt with by Betbeder [Be 03]; their assumptions as well as results are presented here below.

Based on the above diagram, the equation of movement of the above rigid block overturning around the point O is:

$$I_0 \cdot \ddot{\theta} = m\gamma \cdot r \cos(\alpha - \theta) - mg \cdot r \sin(\alpha - \theta) \quad (\text{EQ 8.16})$$

Where: I_0 : moment of inertia of the block (rocking around the edge O)
 m: block mass
 γ : horizontal acceleration (peak ground acceleration)

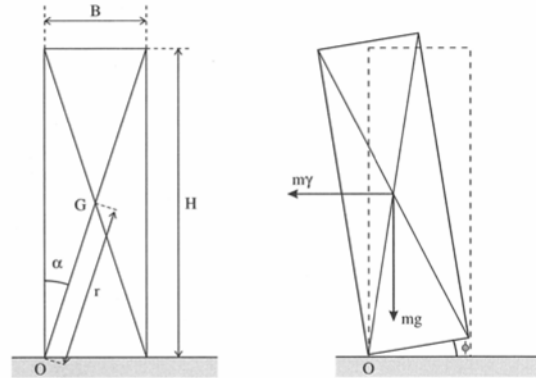


Figure 8.15 : Rocking movement of a slender rigid block [Be 03].

The block moment of inertia is: $I_0 = 4/3mr^2$; if we assume that the rocking movement is small and that the block is slender (small value of α), the previous equation becomes ($\cos \varphi = \cos \alpha = 1$ and $\sin \alpha = \alpha$, $\sin \varphi = \varphi$):

$$\ddot{\theta} - \frac{3}{4r}(g + \alpha\gamma)\theta = \frac{3}{4r}(\gamma - \alpha g) \quad (\text{EQ 8.17})$$

When the block does not move, i.e. $\varphi = 0$ and the rocking acceleration = 0, the impulsion must be higher than $\alpha g < \gamma$, $\alpha g = \gamma$ being the static criterion for stability.

Starting from this equation, Betbeder studied the movement of rocking block during a period of time t, assuming that the block sustained a constant horizontal acceleration during a time T (after this time, the support is motionless). The block was motionless at time $t_0 = 0$. The EQ 8.17 has then two solutions, corresponding to both phases of the movement: one for the period of time between t_0 and T and a solution for $t > T$.

The obtained solutions are:

a) For the time from to up to T:
$$\theta = \frac{\gamma - \alpha g}{g + \alpha \gamma} (\text{ch} \Omega t - 1) \quad (\text{EQ 8.18})$$

b) For the time from to up to infinity
$$\theta(T) = \frac{\alpha}{\phi + \sqrt{\phi^2 + \alpha^2}} \quad (\text{EQ 8.19})$$

Where: $\Omega^2 = (3/4r)(g + \alpha\gamma)$ and $\phi = \gamma / \alpha g$

Note: the assumption that has been applied to find the second solution is: the second phase of movement is finished when the block reaches its limit of stability, i.e. when the centre of gravity is on a vertical line with the rotating

edge ($\alpha=\theta$) without speed.

At that point, what may interest us is to compare the support speed (V_s) and the one that is required to move the block from its motionless state to its stability limit. This speed, which is specific to each block, is called the reference speed (v_r) by Betbeder. This ratio, called here σ is:

$$\sigma = \frac{\gamma T}{\alpha \sqrt{gr}} = \frac{V_s}{v_r} \quad (\text{EQ 8.20})$$

This ratio is always higher than 1 because the transfer from the support translation (horizontal acceleration) to the block rotation is not perfect - there is a loss of energy (otherwise σ would be equal to 1). The energy from one movement to another one is not conserved indeed; only the kinetic moment is conserved. Based on this conclusion it is demonstrated that the support speed when the block starts rocking is:

$$V_s = \frac{2}{\sqrt{3}} \cdot \frac{v_r}{\cos \alpha} \quad (\text{EQ 8.21})$$

Ishiyama [Is 82] showed that the maximal speed that a given block can reach at its loss of stability must be lower than the support speed of a factor k : $V < kV_s$. Based on a statistical survey (calculations and also experiments), Ishiyama gave to k a value of 0.4. If the support speed is converted in a rotating speed in order to be compared with the block rocking speed, this equation becomes:

$$V < \frac{2}{\sqrt{3}} \cdot k \cdot \frac{\sqrt{2gr(1-\cos\alpha)}}{\cos\alpha} \quad (\text{EQ 8.22})$$

For slender walls, i.e. α small, the equation becomes:

$$V < \frac{1}{2} \cdot \alpha \cdot \sqrt{gr} \quad (\text{EQ 8.23})$$

Even if the aforementioned procedure is related to quite a simple model, especially in what concerns the description of the ground acceleration (seismic actions cannot be so easily modelled by only horizontal acceleration), it has been proved good by many experimental, statistical, numerical and theoretical studies.

Here below are two graphs that are taken from one of these studies (experiments using a vibrating table [ST 99]). Both figures prove that the previous equation tallies well with experimental results: almost every block that is situated above the criterion given by the equation did not overturn while

the ones being under the line mostly collapsed. It is worth noting that the vertical acceleration does not have so much impact on the overturning.

The graphs show the stability of blocks with different height (H) and thickness (B) that sustained the El Centro accelerogram, in regards to the overturning collapse mechanism.

The cross points show blocks that did not rock; blocks that rocked are described by rectangular point. The blocks that collapsed are given by points.

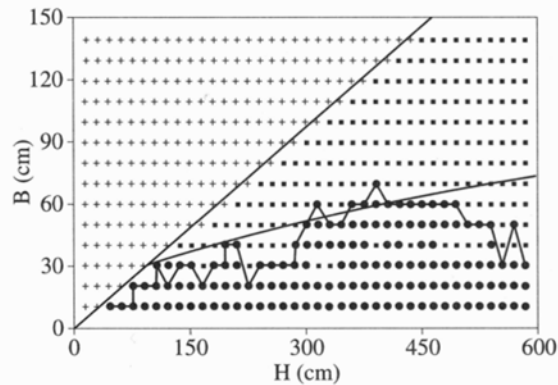


Figure 8.16 : Stability to overturning moments of rigid bodies subjected to the horizontal component of the El Centro earthquake [ST 99], [Be2 03].

The line starting from the point 0;0 corresponds to the static criterion while the equation of the other one is

$$V = \frac{1}{2}\alpha\sqrt{gr}$$

At this point it is worth noting that when most blocks collapse, some others with similar characteristics did not. This fact highlights the rather random feature of the ruin resulting from earthquake.

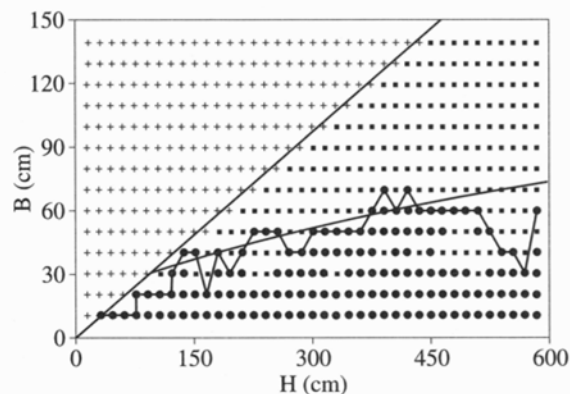


Figure 8.17 : Stability to overturning moments of rigid bodies subjected to the horizontal and vertical components of the El Centro earthquake [ST 99], [Be2 03].

According to Betbeder, this random feature of the collapse due to seismic events is also found for more complex structures than rigid blocks. Furthermore, he wrote in [Be 03] that it is quite frequent to observe buildings, which initially looked very similar, that were differently damaged by the same earthquake. Nevertheless, there must have been differences between them, either regarding the seismic actions (even for small distance) or regarding the real structure of the buildings. Furthermore, the successive seismic waves result in more and more damage to the structures (e.g. mechanical properties of materials and/or assemblies) and a more damaged structure becomes more sensitive to smaller change in the seismic demand. Another phenomenon that can lead to small difference in the structural behaviour of buildings close to collapse is the fact that parameters that did not much influence the seismic response at first, can become predominant when the structure is highly damaged. For instance, the vertical ground acceleration has not a great impact on the rocking waves of a rigid body if their displacement amplitude is small; this is however no longer the case if they are of great amplitude.

DISCUSSIONS

In order to define the degree of stability of walls, which are unconnected to perpendicular walls, a few calculations have been made on different walls. On the below graph, it is showed the peak ground acceleration required to make walls overturn; three different common thicknesses of walls that can be found in cultural heritage buildings in Switzerland are considered: 0.8 m, 0.9 m and 1 m.

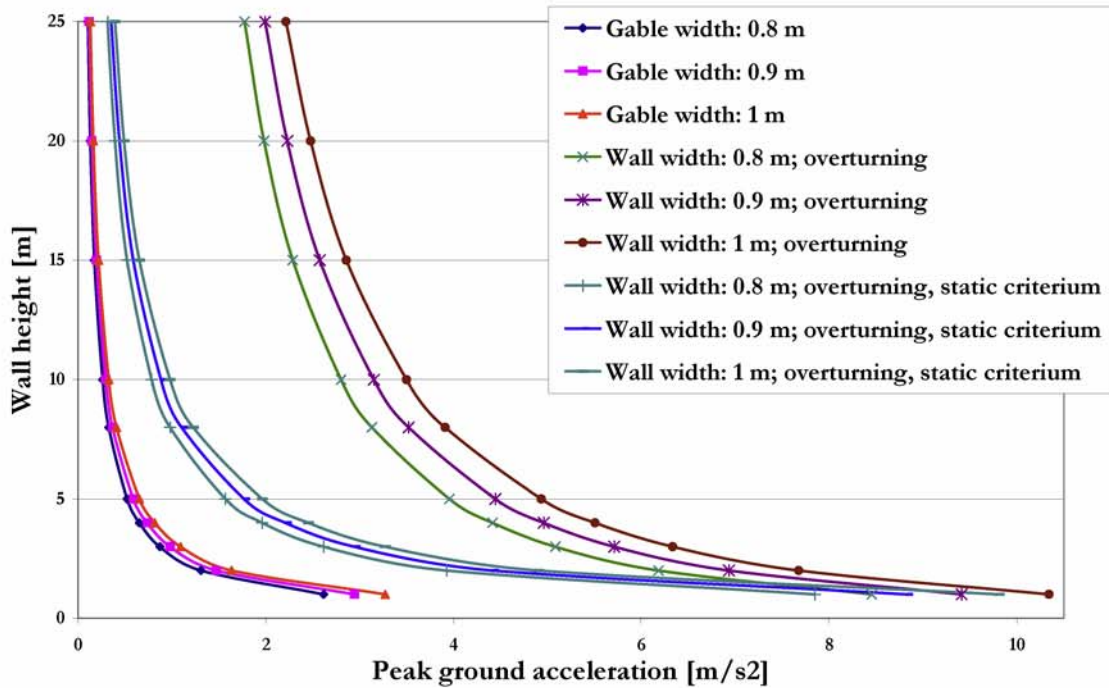


Figure 8.18 : Peak ground acceleration that leads to collapse (overturning) of simple walls or gables.

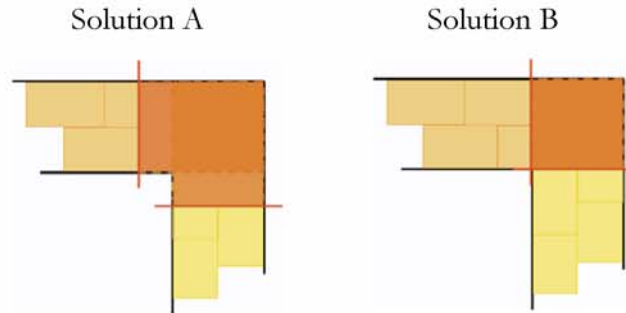
8.3.1.6. Corner strength

The quality of connection at the corners between two perpendicular walls mainly depends on the following parameters:

- Type of masonry (bonding, stones and mortar)
- Normal force (dead load)
- The presence or not of tie-rods
- State of maintenance of masonry

If we look at the first parameter, which is related to masonry, the interlocking of quoins is of most importance: the more they are interlocked, the stronger is the connection.

For instance, the solution A is better than the solution B because the surface of friction that linked both orthogonal walls is larger^a. Obviously, this surface of friction depends on the bonding type of masonry.



a. The solution B is rather seldom and must be allowed for a very schematic.

Figure 8.19 : Schema of the friction surface between two perpendicular walls at one corner.

A few examples of masonry quoins that can be found in Switzerland:

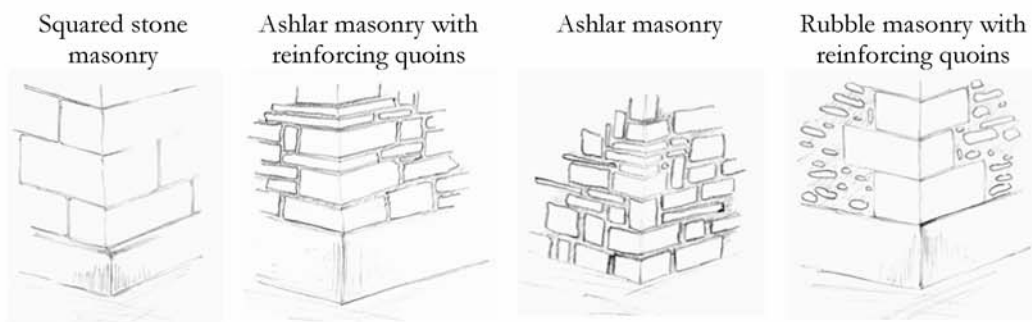


Figure 8.20 : Diverse types of quoins as a function of masonry.

Assuming that masonry is in a good state of maintenance and regarding the corners strength, the squared stone masonry is better than the three other ones. On the contrary, rubble masonry with reinforcing quoins offers quite a bad quality connection.

In respect to the dead-load, it is clear that the higher the force is, better the walls will be connected. Similarly, the presence of vertical tie-rods (or more frequent: post-tensioning cables) contribute to enhance the friction between the masonry components. Horizontal tie-rods also make the wall more resistant, especially when the connection of the wall, which is loaded out of its plane, with the corner is weaker than the one with the perpendicular wall. By the way, it is worth noting that any opening that is close to the corners constitutes a kind of weakness. In such a case, the failure might occur at the section with the opening instead of the corner section.

ASSESSMENT OF THE CORNER STRENGTH

Either for one-leaf walls or multiple-leaf walls, there are two possibilities that can result from the out-of-plane movement of one wall that is connected to two perpendicular walls:

- the friction force that connects the loaded wall with the corners is not high enough to counteract the resulting lateral action and the loaded wall gets separated from the corners

- the friction force that connects the loaded wall with the corners is high enough to counteract the resulting lateral action and the loaded wall gets separated from the lateral walls (the quoins being part of the loaded wall). In such a case and if the quoins are thin, the tensile strength of stones must also be checked.

A way to calculate the connection strength at the corners of a wall/two perpendicular walls is presented here below.

1. Simple-leaf walls

On the figure on the right, the wall along the z axis is subjected to a seismic action. Its connection to the perpendicular wall (along x axis and the z axis) must resist the force resulting from the out-of-plane loaded wall. This connection is made through the friction surface between elements belonging to both walls, i.e. the quoins at the corner (in green in the Figure 8.21).

Since friction increases with the normal force, it is obvious that the connection is better at the bottom than at the top. Similarly, the wider the surfaces are, the higher the cohesion and the stronger the connection are.

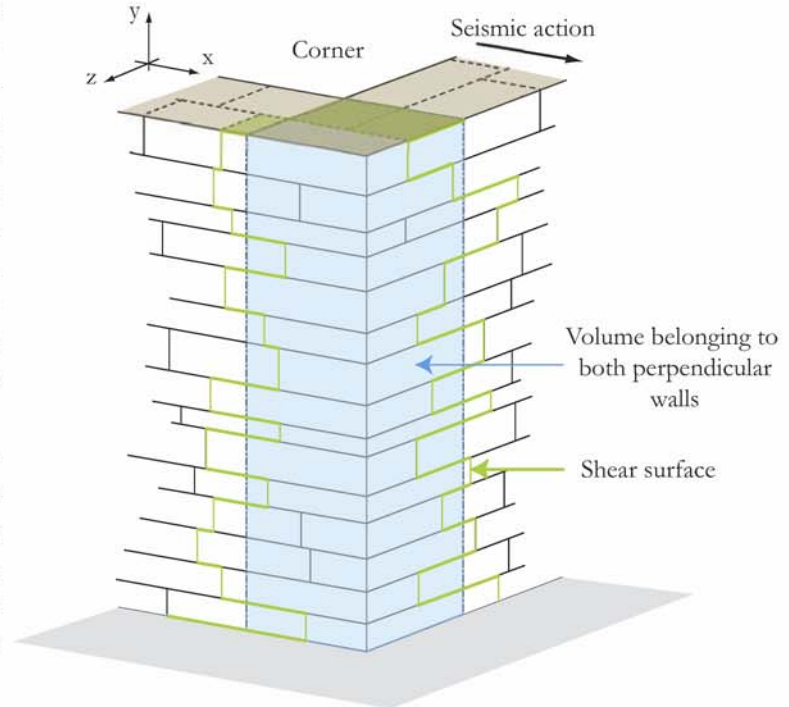
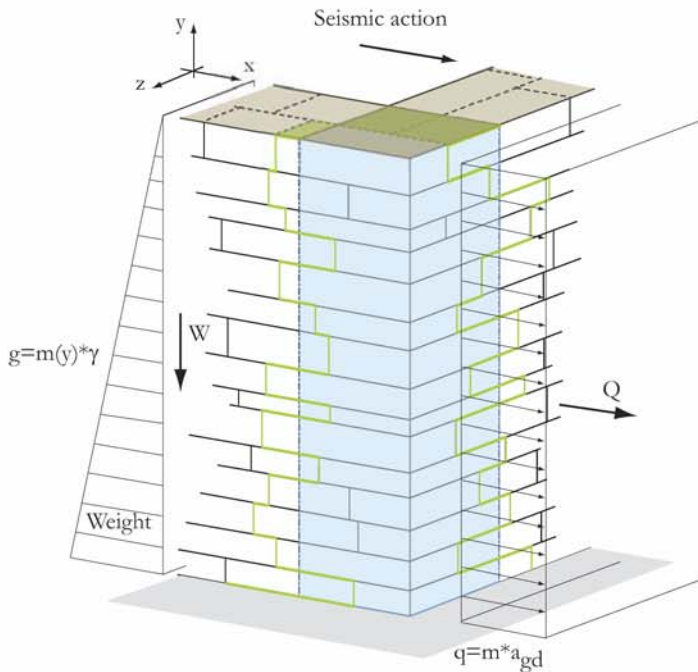


Figure 8.21 : Friction surfaces (ashlar masonry) at the corner between two perpendicular walls.



The case shown on Figure 8.21 under increasing out-of-plane acceleration can have two issues: either the wall gets separated on its side or on the perpendicular wall one. Of course, it depends on the masonry type as well as quality (especially in case of heterogeneous masonry) and on the size of the friction surfaces. For instance, corners of squared stone masonry resists better than an angle with pebbles masonry and a damaged (erosion of mortar for example) masonry also counteract the out-of-plane action to a less extent than a masonry in a good state of maintenance.

Figure 8.22 : Forces generated by an out-of-plane acceleration loading a wall, at a masonry corner of the same wall.

To answer the first question, that is, are the friction surfaces strong enough to resist the forces resulting from the seismic action, their strength must be calculated.

For the aforementioned case the reaction force R_x is^{1, 2} (Coulomb's assumption):

$$R_x = \Sigma A_{z,x} \cdot c + W \cdot \tan \varphi \quad (\text{EQ 8.24})$$

Where: R_x : bearing reaction along x

$A_{z,x}$: sum of the cross-section area of every bound that connect both perpendicular walls

c: cohesion

W: weight of the above masonry ($W = H \cdot t \cdot l \cdot \gamma$)

$\tan \varphi$: masonry strength

Assumptions: the vertical surfaces do not contribute to connection due to friction

1. This reaction force is for both sides of the corners.
2. The strength provides by the vertical surfaces is not taken into account since the tensile strength of mortar is zero. Nevertheless, if there are tie-rods, this contribution can be allowed for, considering then the axial force provided by the tie-rods

Calculations show that cohesion is the most significant parameter; the bearing reaction can vary with a factor of 100 whether there is a cohesion or not (or whether cohesion is taken into account or not). Unfortunately, this parameter is also very difficult to define since it depends on the quality of mortar as well as the mortar-stone interface that themselves depend on time.

It is possible to increase the friction contribution by grouting inclusion into masonry (increasing cohesion)¹ and/or introducing vertical tie-rods (increasing the vertical force); it is also possible to put horizontal anchorages in order to enhance the friction on the vertical contact surfaces:

$$R_x = R_{a,x} + \Sigma A_{z,x} \cdot c + W \cdot \tan \varphi \quad (\text{EQ 8.25})$$

Where: R_x : bearing reaction along y

$R_{a,x}$: lateral resistance provided by horizontal anchorages

$A_{z,x}$: sum of the cross-section area of every bound that connect both perpendicular walls

c : cohesion

W : weight of the above masonry

$\tan \varphi$: masonry strength

The part of the reaction force that can be taken by the tie-rods depends on their anchorage and on their strength; the critical part usually is the anchorage. Their strength is generally calculated with the following equation:

$$R_{a,x} = \pi \cdot D_s \cdot L_s \cdot \tau_s = \pi \cdot D_s \cdot L_s \cdot (c + \sigma \cdot \tan \varphi) \quad (\text{EQ 8.26})$$

Where: $R_{a,x}$: anchorage strength along y-axis

D_s : diameter of the anchorage

L_s : length of the anchorage

c : cohesion

σ : perpendicular stress

$\tan \varphi$: masonry strength

It is very important here to keep in mind that no pre-tensioned anchorages can give any resistance only after a certain deformation of the wall subjected to seismic action. If this part of masonry had moved after putting the anchorages, which might be due to masonry creep for instance, restraining them, their resistance can be simply directly added to the resistance by friction of the connection. Otherwise, their maximal strength must be allowed for only in case of the ultimate state, when the out-of-plane loaded wall begins to overturn.

The impact of tie-rods must be considered through the definition of an equivalent length (surface) in order to allow for the distribution of the force within masonry.

1. It is worth noting that this solution has been applied on cultural heritage buildings for years in Switzerland.

2. Multiple-leaf walls

The assessment of the connection strength at the corner between two perpendicular multiple-leaf walls is similar to the simple-leaf walls one. In fact, instead of taking into account the friction surfaces of one wall, the areas of both outer leaves must be allowed for. The main difference between simple-leaf walls connection and the multiple-leaf walls one is the middle part, that is, the filling, and also the connection between the inner leaf to the outer ones. However, though this layer can also be characterized by a cohesion as well as an angle of internal friction, these values are very difficult (often impossible) to be assessed. It is why, as a simplification mean (but putting the obtain result in the safe side), the contribution of the middle layer of multiple-leaf walls is not considered if its mechanical properties are not known.

8.3.2. OUT-OF-PLANE BEHAVIOUR OF WALLS WITH OPENINGS

Compared with plain walls, openings generate weaknesses around them when walls are loaded either in their plane or out of their plane. However, as stated within the first chapters, masonry encircling windows (or doors, but to a less extent) can resist the out-of-plane loading¹ thanks to the arch effect. In order to take this resistance into account and to determine the global strength of a wall out-of-plane loaded, the strips method is applied [Hi 75].

In consequence, the main point in the application of such a method is the definition of the strips configuration in regards to a given loading case, or in other words, to figure out a transfer of forces corresponding to the actions loading the wall.

Furthermore, this way of proceeding makes possible to assess the evolving of the transfer of forces and consequently, the damage development.

8.3.3. IN-PLANE BEHAVIOUR

Under lateral loading (seismic actions), the collapse mechanisms of masonry are generally grouped in two main modes: flexural failure and the shear failure (divided into shear and sliding).

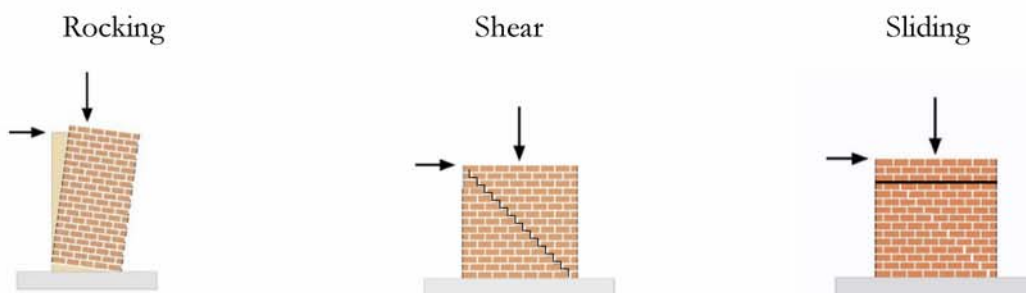


Figure 8.23 : Failure modes of masonry walls in their plane and under lateral actions.

Because of the importance of building seismically safe, shear behaviour of masonry walls under lateral loading has been quite thoroughly addressed for years. For the same reason building codes of almost every country proposed a way to calculate the strength of masonry walls in their plane.

1. The in-plane behaviour is dealt with in the next section.

As this does not serve on purpose to dress an exhaustive list of every existing method, only a selection is presented here below. They are based on models presented under chapter 6. It is important to keep in mind that the above methods have been developed for common buildings and brick masonry. Nevertheless, even if their field of application does not correspond to the cultural heritage buildings, they could be adapted to them. This is why they are presented in this report.

8.3.3.1. Analytical failure models

FEMA [FEMA 310 98]

The FEMA (Federal Agency Management Agency) proposed four simplified models for calculating the lateral withstanding of walls in respect to rocking and also to shear; only two models are taken into account in this section. For the flexural failure, it is assumed that the compression area is more or less equal to a tenth of the wall length and also that the structure behaves like a rigid body.

In what concerns the shear failure, the wall strength depends on the sliding strength along the bed joints.

The associated equations are:

Flexural failure
$$V_{Rd,R} = 0.9 \cdot N_{xd} \cdot \frac{l_w}{2 \cdot h_w} \quad (\text{EQ 8.27})$$

Where: $V_{Rd,R}$: design maximal lateral load (in case of a rocking failure)

N_{xd} : vertical load (axial load)

l_w : wall (or sample) length

h_w : wall (or sample) height

Shear failure
$$V_{Rd,S} = 0.67 \cdot v_d \cdot t_w \cdot l_w \quad (\text{EQ 8.28})$$

Where: $V_{Rd,S}$: design maximal lateral load (in case of a shear failure)

v_d : design shear strength of masonry

l_w : wall (or sample) length

t_w : wall (or sample) height

Note: the value of 0.67 seemed to be more suitable for masonry [LM 06].

The shear strength of masonry can be calculated with the following equation:

$$v_d = 0.5 \cdot \left(0.75 \cdot v_{md} + \frac{N_{xd}}{l_w \cdot t_w} \right) \quad (\text{EQ 8.29})$$

Where: v_d : design shear strength of masonry

N_{xd} : design vertical load (axial load)

l_w : wall (or sample) length

t_w : wall (or sample) width

v_{md} : design shear strength of the bed joints mortar; it corresponds to $v_{md} = v_{mk} / \gamma_m < 0.35$ MPa

v_{mk} : shear strength of the bed joints mortar

$\gamma_m = 2$ for masonry

EC 8

The Eurocode 8 [EC 8 04] deals with the rocking failure more precisely than the FEMA does; instead of assuming the dimensions of the area in compression, the compressive strength of masonry is involved in the calculations in order to calculate them more accurately. It is once again assumed that the given wall behaves as a rigid body.

The associated equations are:

Flexural failure
$$V_{Rd,R} = \frac{l_w \cdot N_{xd}}{2 \cdot h_w} \cdot \left(1 - 1.15 \cdot \frac{N_{xd}}{l_w \cdot t_w \cdot f_{xd}} \right) \quad (\text{EQ 8.30})$$

Where: $V_{Rd,R}$: Design maximal lateral load (in case of a rocking failure)

N_{xd} : Design vertical load (axial load)

l_w : Wall (or sample) length

t_w : Wall (or sample) height

f_{xd} : Design masonry compressive strength (design value)

h_w : Wall (or sample) height

Shear failure
$$V_{Rd,S} = f_{sd} \cdot l'_w \cdot t_w \quad (\text{EQ 8.31})$$

Where: $V_{Rd,S}$: design maximal lateral load (in case of a shear failure)

f_{sd} : design shear strength (design value)

l'_w : wall (or sample) length that is under compression

h_w : wall (or sample) height

The shear strength of masonry can be calculated with the following equation:

$$f_{sd} = f_{vm0} + 0.4 \cdot \frac{N_x}{l'_w \cdot t_w} \leq 0.065 f_m \quad (\text{EQ 8.32})$$

Where: f_{vm0} : Shear strength of masonry without vertical load (corresponds to cohesion)

f_m : Mean compressive strength of masonry

GANZ

Ganz's model is based on the lower bound theorem of the plasticity theory: the lateral action must be sustained by a statically admissible stress field in the wall that satisfies both the equilibrium conditions and the materials strength.

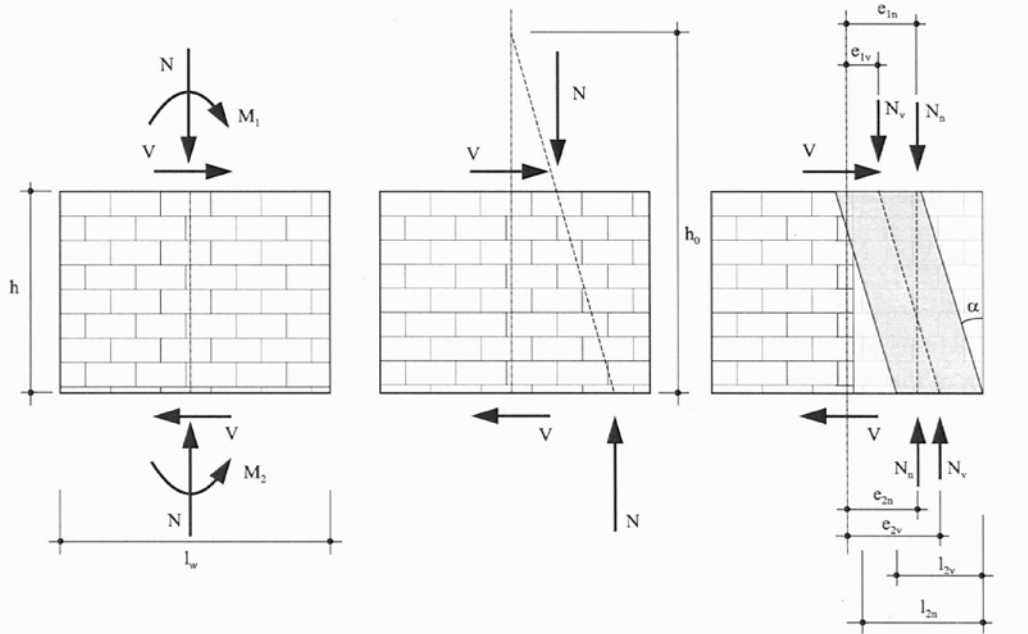


Figure 8.24 : Internal forces and the related stress fields of a wall, according to Ganz; figure taken from [La 02].

There are four equilibrium equations:

$$N = N_v + N_n \quad (\text{EQ 8.33})$$

Where: N: Vertical load

N_v : Component of N that corresponds to the oblique stress field

N_n : Component of N that corresponds to the vertical stress field

$$M_1 = N_v \cdot e_{1v} + N_n \cdot e_{1n} \quad (\text{EQ 8.34})$$

Where: M_1 : Moment on the cross-section at a height of h (see Figure 8.24)

e_{1v} : N_v eccentricity at the cross-section 1

e_{1n} : N_n eccentricity at the cross-section 1

$$M_2 = N_v \cdot e_{2v} + N_n \cdot e_{2n} \quad (\text{EQ 8.35})$$

Where: M_2 : Moment on the cross-section at the wall basis

e_{2v} : N_v eccentricity at the wall basis

e_{2n} : N_n eccentricity at the wall basis

And for satisfying the equilibrium, the shear force transferred in the oblique stress field is:

$$V = N_v \cdot \tan \alpha \quad (\text{EQ 8.36})$$

Then, there are three materials conditions:

$$N_v \leq f_y \cdot l_{2v} \cdot t_w \cdot \cos^2 \alpha \quad (\text{EQ 8.37})$$

Where: N_v : Component of N that corresponds to the oblique stress field

f_y : Masonry strength along the y axis (horizontal)

l_{2v} : Length of the oblique stress field

t_w : Wall width

$$N_n \leq (f_x - f_y) \cdot l_{2n} \cdot t_w \quad (\text{EQ 8.38})$$

Where: N_v : Component of N that corresponds to the oblique stress field

f_x : Masonry strength along the x axis (vertical)

f_y : Masonry strength along the y axis (horizontal)

l_{2n} : Length of the vertical stress field

t_w : Wall width

$$\tan \alpha \leq \mu_d = \tan \varphi \quad (\text{EQ 8.39})$$

Where: α : Angle of the oblique stress field

φ : angle of internal friction

With:

$$l_{2v} = l_w - 2e_{2v} \quad (\text{EQ 8.40})$$

$$l_{2n} = l_w - 2e_{2n} \quad (\text{EQ 8.41})$$

The maximal lateral load that can be sustained by the wall is then iteratively calculated by increasing or decreasing the applied shear action (V_{Rd}) until one of the above conditions is violated.

SWISSCODE SIA 266, SIA V178

Swisscodes SIA 266 and SIA V178 are based on the model developed by Ganz [Ga 85] for calculating the maximal lateral force a wall can sustain.

The model applies the lower bound theorem of the plasticity theory: the lateral action must be sustained by a statically admissible stress field in the wall that satisfies both the equilibrium conditions and the materials strength. Nevertheless, equations in the Swisscode SIA 266 are based on

the use of charts that were developed for bricks masonry. This fact makes its use not well adapted to walls in old stone masonry.

DISCUSSIONS

These methods have been developed to calculate the strength of common building walls under seismic actions. In this case, masses are concentrated on floors and not in the walls themselves. As this is not the case for cultural heritage buildings, the seismic response of walls must be assessed. The best way to evaluate the structural behaviour of walls (with openings and a uniformly distributed mass) under seismic loading is the numerical simulation. The results obtained by numerical calculations are then combined with the methods presented in the previous sections in order to determine the in-plane strength of walls.

The numerical simulation allows the determination of the flow of forces (stress fields) within a given structure under different peak ground accelerations. The strength of this structure, which is calculated with the simplified models that are aforementioned, is then compared with the internal forces generated by chosen peak ground acceleration.

Failure happens when either the compressive strength of masonry is achieved or the shear force is higher than the shear strength determined by Coulomb's assumption.

Nevertheless, failure happens in places and then does not mean the collapse of the whole structural element. A large crack that might lead to the collapse of the element is due to a certain number of small failures. Finally, the collapse strictly speaking of a given element only happens when one or many parts that separated from each other by cracks fall down.

8.3.3.2. Numerical modelling

In order to find out the real flow of forces under seismic actions in the walls plane, we have resorted to numerical modelling. In consequence, every part of churches whose in-plane structural behaviour under seismic actions may have an impact on the seismic vulnerability of given edifices has been numerically modelled.

Almost every structural element that has been listed in chapter 3.5.1 has been modelled in order to analyse its structural behaviour under seismic actions. The models have been implemented on one numerical support: ESA PT developed by Nemetschek, Scia SA.

Results of the numerical modelling have been used for defining the flow of forces, as shown on Figure 8.48, Figure 8.49, Figure 8.50, Figure 8.51, etc.

DESCRIPTION OF MODELS

Elements: shells

Meshings were automatically generated by the software.

Although the 2D numerical modelling only considers one-leaf walls, it can also be applied to multiple-leaf walls. What differs between them is the treatment of the numerical results, especially in what concerns the masonry shear and compressive strength.

Thanks to the numerical modelling it has become possible not only to define the flow of forces under lateral acceleration but also and essentially to obtain the zones where the masonry fail under a given acceleration. Each model is loaded by an increasing lateral acceleration (by step of 0.5 m/

s²) and the stresses (σ_x , σ_y and τ_{yx}) of each node of the mesh are checked with the failure criteria developed by the SIA V178 for the compressive strength (f_x) and Coulomb's assumption for the shear strength in order to control if there is failure or not.

For obtaining a homogeneous set of results, every initial model (structural part) was composed of the same type of masonry as well as the material. In order to exploit the results that were obtained by the experimental investigations, the stone material correspond to sandstone (molasse) and the mortar has the same mechanical properties than the one used for the test (chapter 7). As reminder, they are:

SANDSTONE

$$E_x = E_y = E_z = 4497 \text{ MPa}^1$$

$$f_x = 32.1 \text{ MPa}^2; f_y = 0.5 f_x \text{ [SIA V178 80]}.$$

$$\text{Self weight: } \gamma = 23 \text{ KN/m}^3$$

MORTAR

$$E_x = E_y = E_z = 1933 \text{ MPa}^3$$

$$f_x = 9.58 \text{ MPa}^4$$

MASONRY

$$E_x = E_y = E_z = 4497 * 0.97 + 1933 * 0.03 = 4412.40 \text{ MPa}^5$$

$$f_x = 15.5 \text{ MPa}^6; f_y = 0.5 f_x \text{ [SIA V178 80]}.$$

$$\text{Self weight: } \gamma = 23 \text{ KN/m}^3$$

Poisson's ratio: 0.15

Note: for every structural part the initial thickness is 1.0 m; thickness only have an impact on the weight. Moreover, the value of the Young's modulus has no impact on the collapse mechanisms.

8.4. VAULTS: SEISMIC BEHAVIOUR

In respect to vaulted ceilings, barrel-vaults, groined-vaults and cross-vaults are the most frequent patterns that were used during medieval times to cover wide spans in many sacred edifices.

-
1. This value is taken from [MP 04].
 2. The compressive strength of sandstone is taken from the compression test carried out at the EPFL (chapter 7).
 3. The Young's modulus is taken from the compression test carried out at the EPFL (chapter 7)
 4. The compressive strength of mortar is taken from the compression test carried out at the EPFL (chapter 7).
 5. The considered masonry is made of square well-dressed stones; stones constitute 97% of the volume and mortar 3%. The equation is proposed in the Swisscodes [SIA V178 80]. Calculations are in Appendix A. 5.1.
 6. The compressive strength of masonry is calculated with the help of the Figure 6.16, chapter 6.5.1 [SIA V178 80].
-

8.4.1. STRUCTURAL BEHAVIOUR UNDER SELF-WEIGHT

8.4.1.1. Barrel vault

From an engineering point of view, barrel vaults actually correspond to a succession of arches. In this way, self-weight is uniformly distributed along the vault continuous bearings that are the lateral walls of a nave if considering a church.

In consequence, instability of barrel vaults, in their plane and for uniformly distributed loads, can reasonably be addressed as for arches.

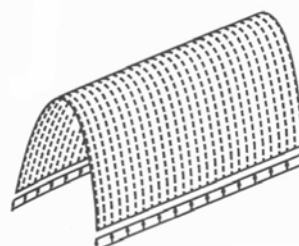


Figure 8.25 : Flow of forces within a barrel vault [Mu 04]¹.

Note: models deriving from the simple barrel vault, like the system found in the church in Payerne (barrel vault with arches), behave structurally the same way.

STRUCTURAL BEHAVIOUR

An arch can be compared to a cable; the only difference between both structures is the way for withstanding their self-weight: the cable will withstand it by traction whereas the arch will be essentially compressed to counteract its own self-weight. Under the dead load, a cable will take the so-called chain shape that corresponds to the optimal configuration to counteract the self-weight loading. Accordingly, the best shape for an arch is also a chain like shape².

Nevertheless, arches cross-section in sacred edifices (especially for Pre- and Romanesque edifices) is seldom a parabola but rather semicircular. In consequence, any stable arches must contain the chain-like trust line that result from their self-weight.

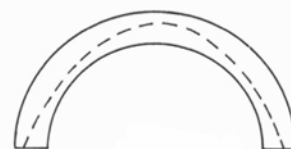


Figure 8.26 : Sketch of the trust-line of a semicircular arch [He 95].

Since the trust-line shape does not correspond to the semicircular arch, there are parts of masonry that are subjected by traction (in cross-sections where the trust-line eccentricity is higher than the third of the thickness). As masonry cannot resist traction (or very slightly), the situation of the Figure 8.26 results in the creation of cracks where masonry is subjected to tensile stresses. Nevertheless, such a situation does not correspond to the failure of the arch. The arch of the Figure 8.26 will collapse when its cross-section will be too much cracked at different places to counteract the trust line generated by the arch self-weight. Based on the assumptions of Heyman [He 95], which are related to the upper-bound theorem of the plasticity theory, the collapse of the given arch will be activated when four hinges are created. As reminder, it must be added here, that such an arch is

-
1. The cross-section of this barrel-vault actually is a parabola whose trust-line exactly corresponds to the cross-section shape.
 2. The chain shape is very close to a parabola which would correspond to the cable shape under uniformly distributed load. The main difference is the difference of slopes between the chain and the parabola at the bearings. Nevertheless, this difference can be neglected for small ratios between the rise and the span.

statically indeterminate; to make it statically determinate, three hinges are required and collapse occurs when four hinges are formed.

Note: Heyman's assumptions are [He 95, p. 14):

- masonry has no tensile strength
- stresses are so low that masonry has effectively an unlimited compressive strength
- sliding failure between voussoirs does not occur

I would add one more:

- subjected to compressive stress, masonry behaviour is linear-elastic

As said by Heyman, if a given arch or a barrel-vault stands 5 minutes after its completion, it will stand forever under similar conditions (no decay, no deformation of the bearings). In consequence, such structures collapse under their own weight almost only because of the movement of their bearings.

According to this movement, two limits can be given for the arch of the Figure 8.26: the situation (a) and the situation (b) on the right-hand figure. As can be seen, hinges location will obviously be different if the bearings give way (a on Figure 8.27) or come closer (b on Figure 8.27). In the cross-sections where the thrust-line is more or less parallel to the intrado or the extrado, i.e. also meaning close to them, kind of hinges are created. At these places, a small part of the cross-section is subjected to high compressive stresses, whereas the rest of the section is fully cracked.

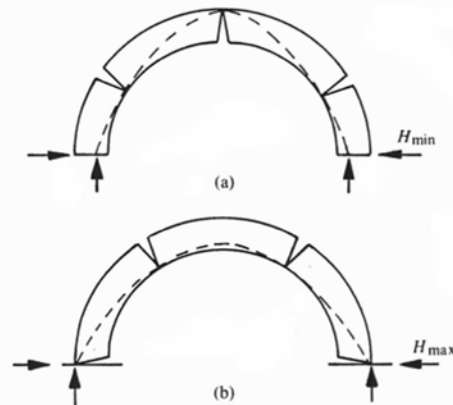


Figure 8.27 : Semicircular arch under its own weight, with minimal abutment (a) and maximal abutment (b) [He 95].

The situation (b) is no longer stable while the situation (a) on Figure 8.27 requires two more hinges; this would be done if the given arch would have been thinner like the arch (b) and (c) on Figure 8.28.

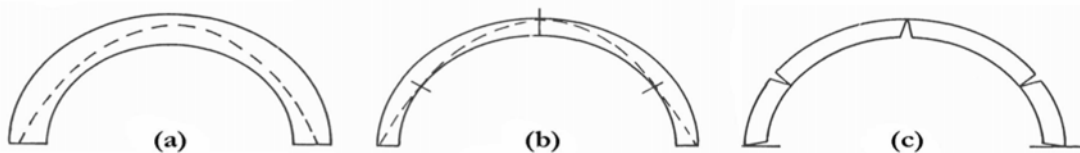


Figure 8.28 : Stable semicircular arch (a) and the one with minimum thickness ((b) and (c)) [He 95].

STABILITY

As aforementioned, arches and also barrel vaults whose cross-section corresponds to a semicircular arch, require a massive thickness for assuring their stability. The cross-section must be thicker than $R/10$, where R is the radius, at minimum, that is, to cover the thrust line under the structure

dead load. Nevertheless, bearings can spread under the trust and change consequently the trust line pattern. If the cross-section is exactly $R/10$ thick, this bearings deformation will result in the collapse of the barrel vault. In order to avoid the failure of arches due to the change of the boundary conditions (including loading cases), the arch must be thicker than $R/10$. At this point, it is worth introducing the concept of geometrical safety factor that was proposed by Heyman [He 96] for masonry arches. This geometrical factor is related to the arch thickness; it corresponds to the ratio between the actual thickness and the minimum one (R_a/R_{mt}). If this factor were 3 would indicate that the trust line of the given arch could be contained within the middle third of the actual thickness; it corresponds to the so-called middle-third rule that was an elastic concept concerned with the need to avoid any tension in the arch cross-section. Safe practical values for the geometrical factor of safety for arched constructions is indeed about 2 [He 95]; thus, arch cross-section must be at least thicker than $R/5$ (which corresponds to the condition $(R/6)$ given by Muttoni in [Mu 04]) in order to assure the arch stability against surimposing loading, asymmetries of bearings or their settlement.

If a barrel vault was erected according to the aforementioned constructional rules, it can lose under self-weight, its stability essentially due to the bearings movements (because of settlements or deformations; see the previous section), as aforementioned. The collapse of barrel-vaults under asymmetrical loading cases can be more or less easily defined; on the contrary, the failure resulting from the movement of bearings is more difficult to define since the cross-section shape gets also deformed accordingly. In order to take into account the constant change of shape of the vault cross-section, complex iterations must be carried out. Barthel [Ba 91] addressed it in his dissertation through a numerical calculation on two kinds of vaults: the first one is considered with the fill in the vaulting pocket, the second is opened on 55° . Both vaults are uncracked under their own weight. In addition to the self-weight, a displacement was imposed to the bearing (at the vault foot) in stages up to 4 mm.

A crack appeared very quickly along the intrado at the crown; then another crack occurred at 40° from the crown along the extrado¹. Nevertheless, further cracks appeared below as the bearing displacement increased. When the horizontal displacement was 4 mm, the main crack (approaching a hinge) was located at 49.3° from the crown. Barthel theoretically defined hinges as places where the trust-line is tangential to the extrado or the intrado (that is, eccentricity is $e = t/2$, where t is the

1. Masonry was assumed to have a certain level of tensile strength (0.6 MPa).

cross-section thickness), depending on the situations. Nevertheless, as they cannot be achieved with FEM models, he defined them as being located at places where the eccentricity is the highest.

On the Figure 8.29, the evolving of the horizontal force for the 55° vault is shown (results for a vault with a fill that is along 40° of the cross-section are similar since the fill restrains the structure). The above figure is about a 50 cm thick arch while the bottom figure concerns a thinner cross-section.

It is interesting to notice that the horizontal reaction of the vaults bearings changes quite quickly under small bearing displacements. In consequence, H achieves swiftly a value close to the limit states defined by Heyman with Hmax and Hmin.

Moreover, the 50 cm thick cross-section is more rapidly cracked than or at least as quick as 25 cm thick arch. This indicates that a thicker arch is not stronger than a thinner one.

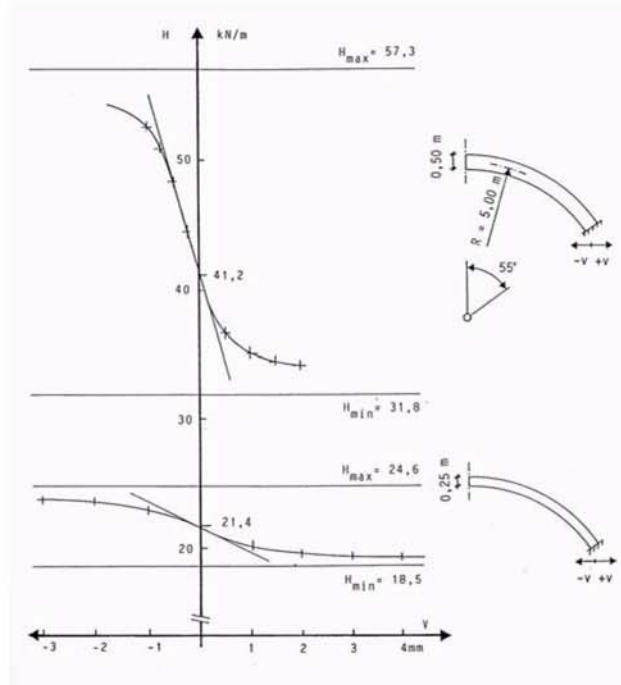


Figure 8.29 : Change of the horizontal force (H) as a function of the bearing horizontal displacement [Ba 91].

The definition of hinges by Barthel (see above), that is, hinges are located where the eccentricity of the trust-line is the highest, explained why he was unable to obtain the maximal displacement that can support the given vault. Moreover, he wrote that the trust-line position as well as the horizontal reaction value does not change up to the maximal lateral displacement of 4 mm.

In respect to the model with fill in the vaulting pocket, the numerical calculations (FEM) gave the following results:

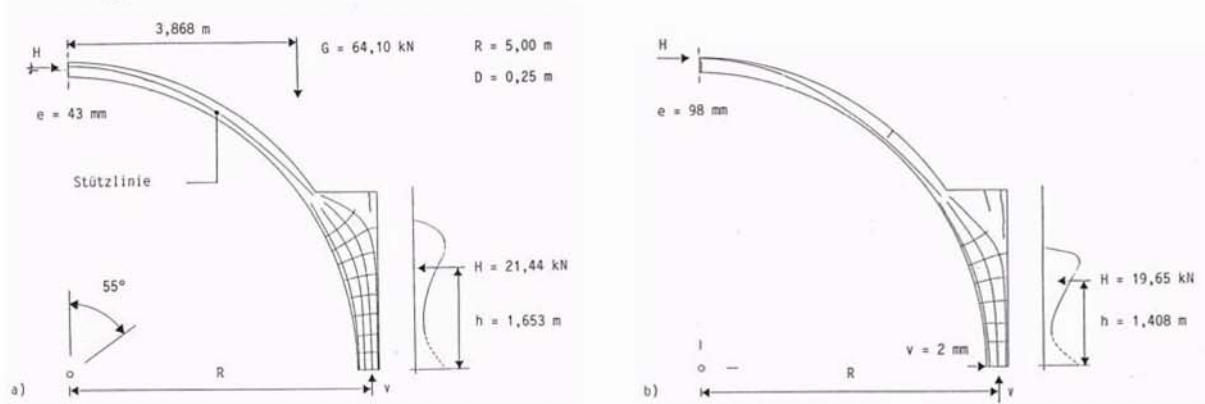


Figure 8.30 : Flow of forces within an arch with a fill under the self-weight and the bearing displacement [Ba 91].

In the field of the abutment, the force from the arch strictly speaking spread in the whole fill; the stress state is no longer unidirectional as within the arch. It can be seen that there is one more vertical crack in the fill compared with the crack pattern under dead-load.

The most interesting result here lay in the position of the thrust-line at the abutment (just above the fill limit); it is along the same side than the above hinge (at 47°). In consequence, and contrary to the thrust-line pattern under H_{min} , which reached the arch extrado at the abutment (and creating then a sort of hinge according to Heyman's assumptions), the thrust-line approaches the intrado of the arch. Though it does not reach it (that would have formed a hinge), it is very close and results in high deformations.

To conclude, collapse of the vault results from the fall of both parts that are at each side of the crown due to the opposite movement of both vault bearings.

8.4.1.2. Groin- and cross-vault

Groin-vaults simply result from the intersection of two equal semi cylindrical barrel vaults; the resulting bay is consequently a square in plan¹; groins correspond then to the square diagonals. The main problem, which is indeed a stereotomy problem, to erect such a vault is the joint between webs, i.e. the groins. Due to the difficulty for cutting the web stones that join at groins, Romans builders started the construction of groin-vaults by carrying out first masonry arches along the diagonally of the squared bay. The vault webs were then erected on these arches, which were partially or entirely embedded within the masonry webs [He 95]. On the light of this account, it is quite easy to understand the evolving that led to the creation of the gothic rib-vault that was built after the same process. The main differences lay in the fact that it is easier and swifter to erect groins with stones dressed without care that will not be visible because hidden by ribs and the ribs also had the function of formwork that made the construction of vaults easier and quicker.

Different kinds of groined- and cross-vaults can be found depending on the open-space to cover and also depending on the location and the era of construction. The main ones are shown here below:

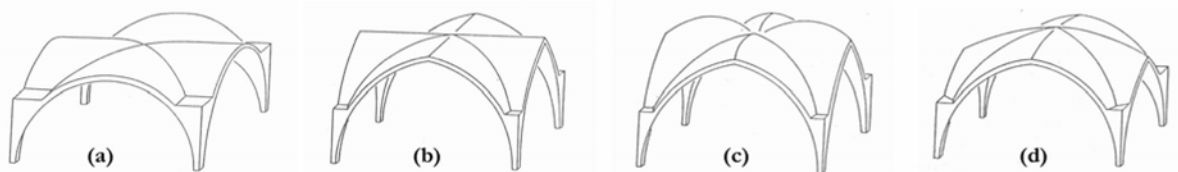


Figure 8.31 : Four selected kinds (the main ones) of quadripartite vaults; the cross-vault or groin-vault(a), the pointed-arch vault (b), vault with dome-webs (c) and dome-like quadripartite vault [Ba 91].

Though every kind can be found in Switzerland, only the groin- and the cross-vault (without and with ribs) will be dealt with since this is the most frequent kind erected in Pre- and Romanesque sacred edifices.

1. Depending on the space to cover, asymmetrical groin-vaults can be found. For instance, the bay plan of vaults in ambulatory is a parallelogram.

STRUCTURAL BEHAVIOUR

In the case of cross-vaults with a level soffit, forces transfer from the webs directly to the groins and/or the ribs as indicated on the Figure 8.32. In such a case, lateral walls do not support the webs; as a matter of interest, this no longer the case for quadripartite vaults with dome webs.



Figure 8.32 : Transfer of forces within cross- and groin-vaults.

Actually, cross-vaults with a level soffit can be treated, under dead load, as a juxtaposition of arches where each arch supports its own weight and carries it down to the groins and/or ribs, as shown on Figure 8.32. Then, these parts leads the vault weight to lateral walls; the trust-line resulting from the vault weight is counteract by the buttresses and the lateral walls.

Regarding the stresses, it must be said that, as in general in masonry, their level is low compared with the stone compressive strength¹; the ratio is about a hundredth. The strength of stone is consequently of no real importance and it is why material used for erecting vault webs is often a light stone, like tufa, with thick mortar joints. Nevertheless, this no longer the case along the groins where stresses are concentrated; it is obvious that this sort of creases (considering the assembly of webs as a whole vault) constitute lines of weakness in the vault. The ribs serve then as a reinforcement; however, it must be said that though they are generally necessary, they are sometimes not essential².

In case of groined-vaults or cross-vaults with a level soffit, transverse arches as well as the formerets (wall ribs) are only subjected to their own weight.

CRACK PATTERNS OF GROIN- AND CROSS-VAULTS

As already seen with arches, masonry vaults will cracked according to the supports movements; in a way, vaults will develop cracks in order to accommodate an increased span (orthogonal to the nave direction, that is north-south). It is worth noting that arches or vaults crack and become then statically determinate.

1. Level of stresses is just high enough to ensure locking stones together by friction.
 2. There are examples of fallen ribs though the vault webs were still standing. It is worth noting that in such a case, instead of being outside the webs, ribs were formed within them along the creases.

Since arch and vault patterns do not differ much from each other, cracks will appear almost always (after the type of vaults) at the same place. P. Abraham [Ab 34] has listed most of them:

- there are cracks along the crown of the west-east webs.
- there often are the so-called «*fissures de Sabouret*» [Ab 34], that are located close to the lateral walls and formerets and also parallel to them. These cracks are due to the deformation of the vault bearings. They involve the separation of the webs from the lateral walls. It is worth noting that these Sabouret's cracks are complemented by other small west-east cracks.

It is important to keep in mind that the cracks at the crown are kind of hinge lines (which let pass forces), whereas the Sabouret's cracks correspond to an actual separation of masonry (the nave ground can be seen by someone who is standing on the vault extrado).

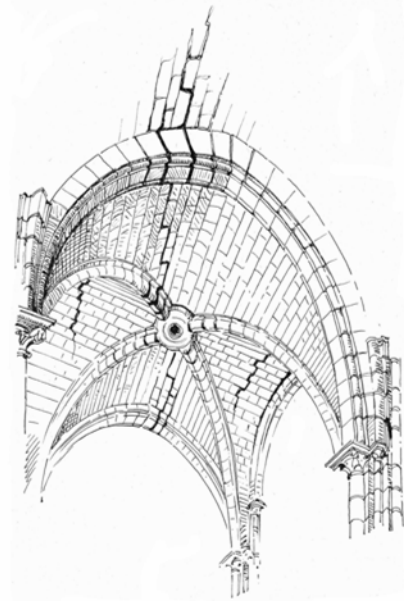


Figure 8.33 : Characteristic cracks in Gothic vaults [Ab 34].

These characteristic cracks, which are essentially due to the movements of the vault bearings, highlights the fact that masonry buildings, such as churches, deform and every part of the edifice accommodates to the changing shape and finds new equilibrium. At this stage, the question is to define the moment when the equilibrium of vaults cannot be achieved.

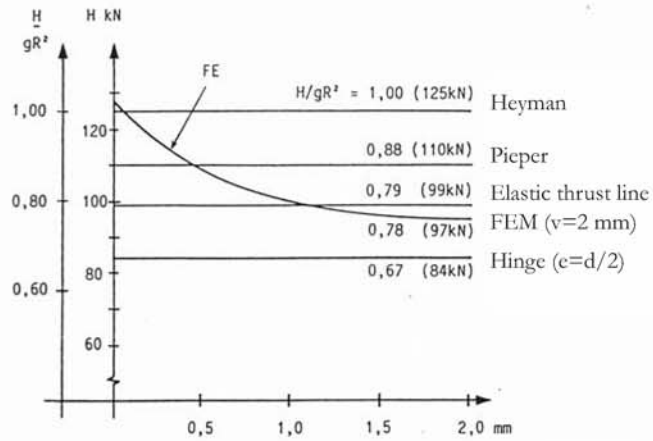
STABILITY

Groined- and cross-vaults generate horizontal thrust at their four bearings; this thrust must be then either brought down to the ground by the lateral walls weight (usually also with vertical abutments) or counteracted by flying buttresses. The first situation is more often found in Pre- and Romanesque sacred edifices whereas the main nave vaults of every Gothic edifice are supported by flying buttresses and also the lateral walls. Under unchanging loading case, a groin- or cross-vault can lose

its stability because of the deformation or movement of its bearings, which are the walls with either simple abutments or flying buttresses.

Maximal lateral displacement per each bearing: 2 mm.

Figure 8.34 : Regular cross-vaults: comparison of the horizontal component of thrust according to different calculations methods and as a function of the transversal displacement of the bearings [Ba 91].



8.4.2. STRUCTURAL BEHAVIOUR UNDER SEISMIC ACTIONS

Concerning the vaults, the main problems come from the out-of-plane deformation of their springings, that is to say, the opposite walls that support the vaults.

Regarding the transversal behaviour of the nave, it is assumed that the out-of-plane movements of the lateral walls are not restrained by vaults (barrel-, groined- and cross-vaults) (Figure 8.35). In other words, the seismic response of vaults have no impact on their bearings. Consequently, their stability under seismic actions only depends on the movements of the opposite lateral walls that constitute their bearings.

The vaults span can increase or decrease according to the boundary conditions of the lateral walls that support the vaults.

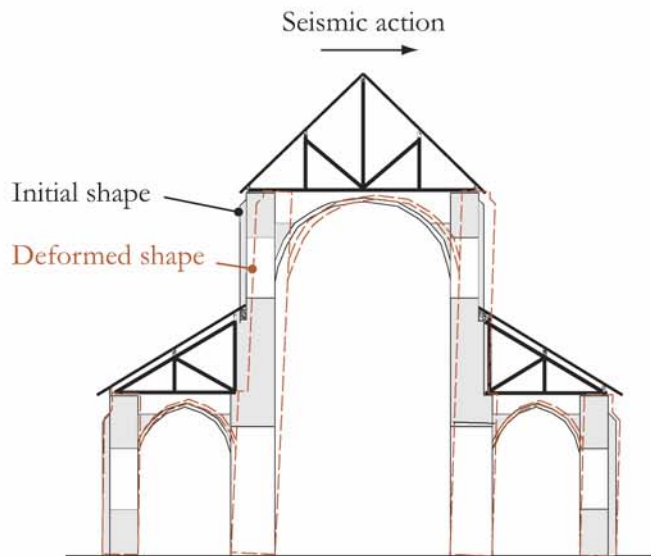


Figure 8.35 : Transversal seismic response of the nave of a basilica church.

When looking at the vaults of a basilica, the situation will be different for each vault (covering the low-aisles or the main nave). Consequently, every situations (i.e. as a function of the direction of the seismic action) for each vault must be addressed.

8.4.2.1. Barrel vault

According to the results obtained by Barthel [Ba 91], barrel vaults whose cross-section is a semicircle lose their stability when one of its bearings moves away of 2 mm (see the Appendix A. 6). In consequence, the drift of lateral walls when subjected to out-of-plane actions must be calculated. The transversal drift corresponds to the difference of the movement of both lateral walls, since they move away more or less similarly under out-of-plane seismic actions.

8.4.2.2. Groined- and cross-vault

The seismic vulnerability of groined- and cross-vaults is treated as the barrel-vaults one.

8.5. BELL-TOWER: SEISMIC BEHAVIOUR

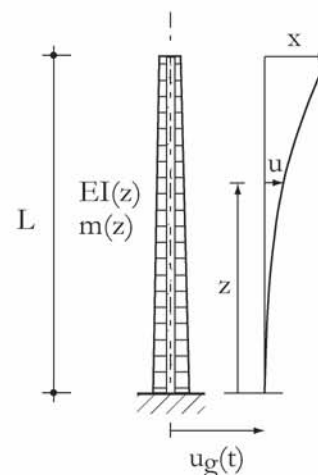
Compared with other structural parts, as the front walls, bell-towers show a few specificities; they are slender, quite compact (in respect to their closed cross-section¹), tall and walls thickness varies along the height.

The aforementioned characteristics make the assumption of a uniform lateral acceleration as the seismic action, which was applied for the other structural parts, no longer valid; such an assumption cannot be accepted for tall and deformable structures, as a bell tower.

Furthermore, especially because of the size, bell-towers must be strong structures in order to resist their self-weight and the lateral actions, such as wind or seismic waves. It is why, they usually were, at least in Switzerland, erected independently from the rest of the edifice; in such a case, they are just put side-by-side with other structural parts.

A bell-tower is a system with a distributed mass (big walls) and stiffness (cross-section changing with height).

Figure 8.36 : Tower made up of masonry and virtual displacements (inspired from Chopra [Ch 00]).



The bell tower in the Figure 8.36 has a distributed mass $m(z)$ per unit of height, and flexural rigidity $EI(z)$; the ground excitation (earthquake) is represented by $u_g(t)$.

1. Moreover, the cross-section is often reinforced through tie-rods that enhance its compactness.

The equation of motion for such a structure is:

$$f(z, t) = -m(z)[\ddot{u}(x, t) + \ddot{u}_g(t)] \quad (\text{EQ 8.42})$$

Where: $m(z)$: distributed mass along the height

$\ddot{u}(x, t)$: spectral acceleration

$\ddot{u}_g(t)$: ground acceleration

The resolution of the equation of motion for the generalized SDF system (Figure 8.36) is done through the application of the principle of virtual displacements [Ch 00]. Moreover, to solve it, the deformed shape of such a structure must be given; the proposal made by Chopra seems to fit the deformed pattern of bell towers under seismic actions.

Then the equation of motion becomes:

$$-\tilde{L}\ddot{\tilde{u}}_g(t) = \tilde{m}\ddot{\tilde{x}} + \tilde{k}\tilde{x} \quad (\text{EQ 8.43})$$

Where:

\tilde{m} : generalized mass

$\ddot{u}(x, t)$: spectral acceleration

\ddot{u}_g : ground acceleration

\tilde{x} : lateral displacement

\tilde{k} : generalized stiffness

$\ddot{u}_g(t)$: ground acceleration

L : factor for the generalized excitation.

Based on EQ 8.43, the natural frequency and the equivalent static forces of the given structure can be defined:

$$\text{Natural vibration frequency} \quad \omega_n^2 = \frac{\tilde{k}}{\tilde{m}} = \frac{0}{H} \frac{\int_0^H ([\psi''(z)]^2 \cdot EI(z)) dz}{\int_0^H ([\psi''(z)]^2 \cdot m(z)) dz} \quad (\text{EQ 8.44})$$

And

$$\text{Equivalent static forces} \quad f_S(z, t) = \omega_n^2 \cdot m(z) \cdot \psi(z) \cdot x(t) \quad (\text{EQ 8.45})$$

Where: ω_n : Natural period

$\Psi(z)$: Shape function

Then, the peak value of lateral displacement can be calculated:

$$x_0 = \frac{\Gamma}{\omega_n} \cdot A \quad (\text{EQ 8.46})$$

Where: A : Pseudo-acceleration (to be drawn from the design spectrum of the Swisscode SIA 261, for a period defined thanks to the natural vibration frequency and for a damping ζ ratio defined in the code too.

And finally, the internal forces, such as the bending moments and the shear force can be determined:

Bending moment
$$M(z) = \tilde{\Gamma} \cdot A \cdot \int_0^z m(z)\psi(z)dz \quad (\text{EQ 8.47})$$

And

Shear force
$$V(z) = \tilde{\Gamma} \cdot A \cdot \int_0^z (m(z)\psi(z))dz \quad (\text{EQ 8.48})$$

Where: A : Pseudo-acceleration (to be drawn from the elastic spectrum).

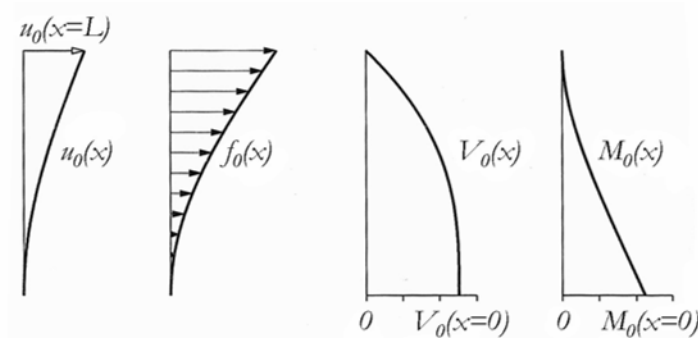


Figure 8.37 : Lateral displacements, equivalent static forces and internal forces of a system with a distributed mass (tower) [Ch 00].

8.6. CHURCHES: GLOBAL BEHAVIOUR

In respect to what is called the global behaviour of a sacred edifice, this is a problem of juxtaposition of structural parts that are characterized by different natural frequencies. In case of sacred buildings, this problem mainly occur at the connections between towers, which usually are taller than the rest of the edifice, and the other parts of the given church that are connected to the towers. It can also appear between vaults and the front wall and the chancel arch if they are tightly connected to each other or between the front wall and the lateral walls if the former is assumed to be supported by them.

Towers dimensions (cross-section and height) make them compact enough to be considered as MDOF in which the mass of the masonry walls are fictitiously concentrated at different levels. These characteristics give towers a lower natural frequency than the church wall to which they might be connected. In consequence, these connecting place will be damaged under seismic actions.

The concept here is to calculate the equivalent forces resulting from the seismic action and to apply them on the connected structural parts if it is required. For instance, this is necessary to calculate them if it is assumed when making the local behaviour calculations that such or such structural part is supported by another one.

8.7. CHURCHES: LOCAL BEHAVIOUR

The out-of-plane and in-plane seismic response of every structural part of a church are dealt with in the following chapters. The structural parts correspond to the standard units presented under the chapter 3.5. They are indeed macro-elements.

8.7.1. FRONT WALLS

According to the chapter 3.5.1.6, seven kinds of front walls were recorded among the Pre- and Romanesque churches in Switzerland. In fact, the structural behaviour (i.e the out-of-plane and the in-plane behaviour) of five types are dealt with here after; these types are: FW2, FW3, FW4, FW6 and FW7. The other ones are not considered because of:

- FW1 actually is a special case of the FW6 type
- FW5 is more often found as a transept unit standard and it is why it is dealt with under the chapter about transept units.

With the transept facades and the rectangular apses sides, front walls are the most vulnerable parts of churches under seismic actions out of their plane.

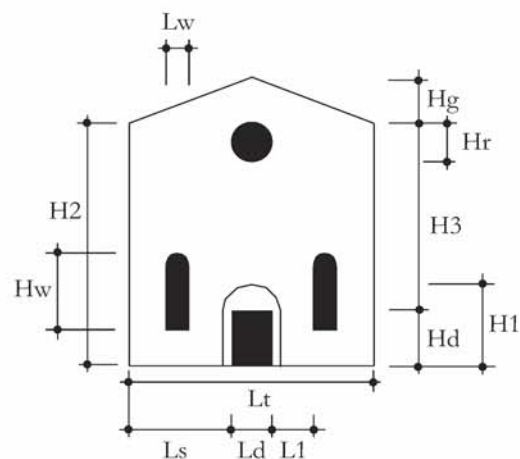
8.7.1.1. FW2

FW2 corresponds to a type of front wall that can be often found in Switzerland, especially in small churches. Consequently, it is generally neither very tall nor very wide.

The proposed configuration for openings is not the most frequent one; FW2 front walls often have only one window above the door.

Proportions are the following^a:

- $(H_2+H_g)/L_t = 1 - 1.5$
- $H_d = 2-3$ m
- $H_r = 1-2$ m
- $H_g = 0.3 L_t/2 - 0.5 L_t$



a. As reminder, these proportions were drawn from a survey on Pre- and Romanesque churches.

Figure 8.38 : FW2 general pattern.

OUT-OF-PLANE BEHAVIOUR

Front walls, which are massive elements, may overturn under seismic actions out of their plane. This phenomenon can struck the gable as well as the whole wall. In consequence, the out-of-plane of both the gable and the facade must be checked.

1. The gable:

It is the most simple system to be dealt with compared with the whole facade. The gable generally corresponds to a triangular structure whose base is assumed to be restrained. Along the other edges, the gable can be either tightly or loosely connected to the timber framework.

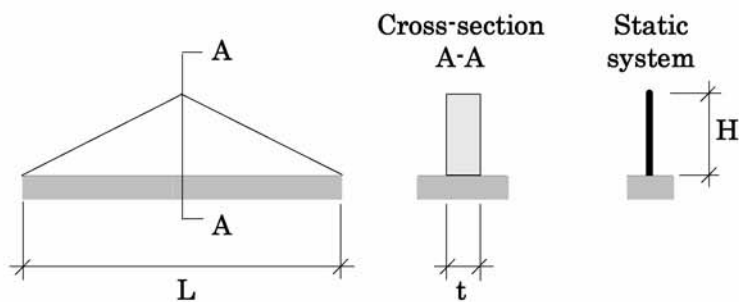


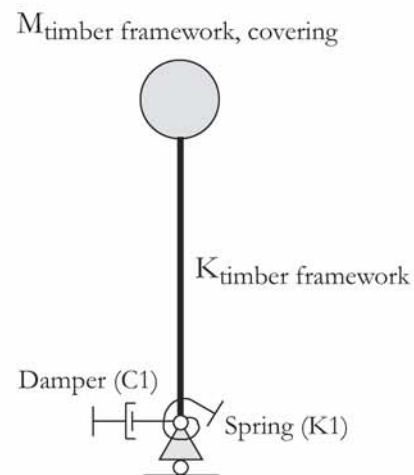
Figure 8.39 : Static system of a gable.

The timber framework can be either stiff or flexible, depending on its structure; its impact on the gable will differ accordingly.

To model the timber framework, it is assumed that the system composed of the timber framework and the covering can be modelled as a SDOF system (see Figure 8.40). In consequence, the mass of the structure itself and the covering is concentrated into the centre of gravity.

First, the boundary conditions (i.e. if the timber trusses are restrained in the lateral walls or simply put on them) have to be determined. Then, the mass of the moving structure (roof and timber structure) and the framework stiffness must be calculated. To calculate the impact force from the timber structure on the gable masonry, it is assumed that the covering and the timber structure are tightly connected together (they form one monolithic structure).^a

Figure 8.40 : SDOF model of the timber structure.



a. It is assumed that the timber structure is not cramped to the gable.

With respect to Figure 8.40, the damper 1 corresponds to the horizontal bearing that is assumed as infinite if the timber trusses are restrained or horizontally fixed in notches dug along the upper

edge of the lateral walls. The damper strength ($C1$) corresponds to the friction force whose value depends on the timber framework weight as well as the coefficient of friction between wood and masonry.

The stiffness of the spring ($K1$) is assumed to be infinite if the timber trusses are restrained in notches; it is equal to zero if the timber structure is simply put on the upper edge of the lateral walls.

The stiffness of the timber framework depends on its structure and assemblies and is to be calculated accordingly. For further information on the seismic response of timber framework, the reader can refer to [CFL 07].

Once the boundary conditions of the timber structure on the lateral walls are defined, it is the turn of the connections between the timber framework and the gable to be considered.

There are two possibilities:

1. the timber structure is simply put on the gable; in this case, there is no difference depending on the wall structure (situation 1).
2. the timber structure is put in a notches (of the gable masonry). The wall structure must be allowed for in this case (situation 2).

Note: if the timber beam does not touch the gable wall, the situation is like the situation 2 on Figure 8.41.

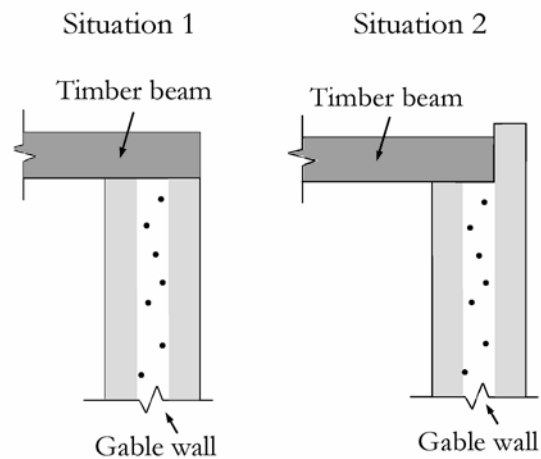


Figure 8.41 : Two boundary conditions (diagrams of cross-sections) for the beams belonging to the timber framework.

Case 1: In this case, timber beams have no impact on the gable masonry under seismic actions. The beams simply slide on the wall; there might be small detachment of masonry due to friction but no real damage.

Case 2: The second case configuration can seriously damage the gable out of its plan. The wall must resist the inertia force from the timber framework (simple-leaf wall) (Figure 8.42):

- this force must be lower than the friction strength of the small part of masonry against which the impact takes place,
- this inertia force from the framework (with the inertia force of the gable) does not make the gable lose its stability
- in respect to the overturning collapse, the increasing of gable speed due to the movement of the timber framework does not exceed the speed leading to the gable collapse.

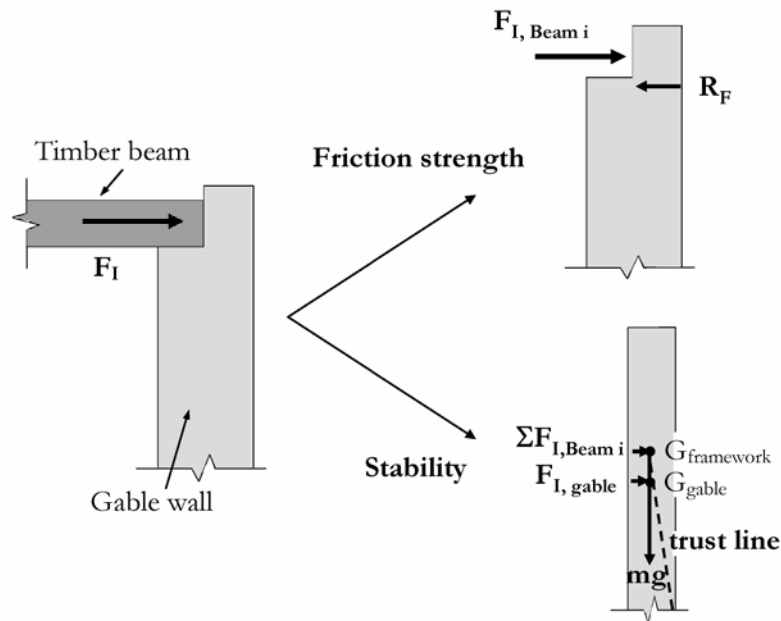


Figure 8.42 : Impact of the seismic response of the timber framework on the gable wall (one-leaf walls).

Note: The centre of gravity of the timber structure differs from the gable one.

Where:

Friction strength:

$$F_{I, \text{beam } i} \leq R_F = \tau_{\text{masonry}} \cdot \Sigma A \quad (\text{EQ 8.49})$$

Where: $F_{I, \text{beam } i}$: inertia force due to the beams of the timber framework

R_F : friction strength

τ : shear strength of masonry

ΣA : friction area¹

Stability of the gable:

$$\Sigma F_{I, \text{beam } i} \cdot h_{G, \text{tfw}} + F_{I, g} \cdot h_{G, g} - mg \cdot \frac{t}{2} \leq 0 \quad (\text{EQ 8.50})$$

Where: $F_{I, \text{beam } i}$: inertia force due to the beams of the timber framework

$h_{G, \text{tfw}}$: height of the gravity centre of the timber framework

$F_{I, g}$: inertia force of the gable wall

1. When masonry is in a good state of maintenance, the friction area corresponds to the area of the notches sides; however, if there are cracks around the notches, the part that is delimited by cracks might move out of its plane due to the inertia force. This case must be allowed for.

$h_{G,g}$: height of the gable gravity centre

m : mass of the gable wall masonry

Then:
$$F_{I,g} \leq \frac{mg \cdot \frac{t}{2} - \sum F_{I, beam i} \cdot h_{G, fw}}{h_{G, g}} \quad (\text{EQ 8.51})$$

In case of a multiple-leaf wall, the procedure is quite similar; however, it slightly differs since it takes into account the strength of the interface between leaves..

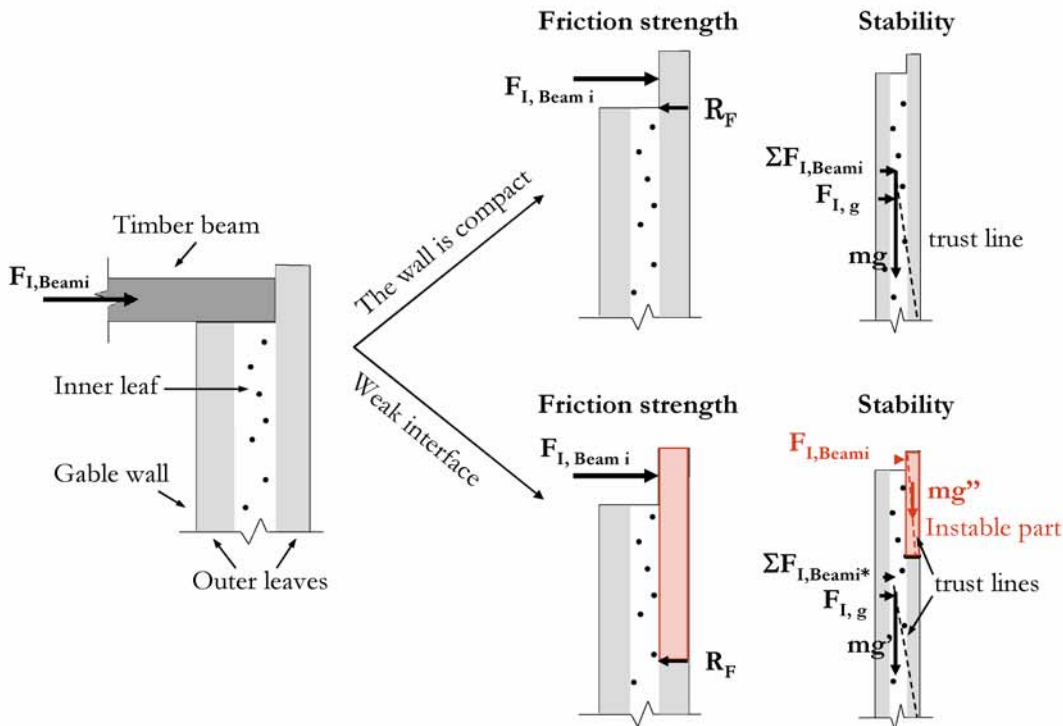


Figure 8.43 : Impact of the seismic response of the timber framework on the gable wall (multiple-leaf walls).

As for the one-leaf walls, the state of masonry (cracks and state of maintenance) must be checked first. In case, a part of masonry might detach from the rest of the gable wall, its out-of-plane stability under the impact of the inertia force of one (or more) beam must be addressed.

The whole facade:

In what concerns the seismic behaviour of front walls in their out-of-plane direction, it is essentially dictated by their boundary conditions, their dimensions, the windows configuration as well as the type and quality of masonry.

The out-of-plane behaviour of facades is treated, as shown under chapter 8.3.2, with the strip method. The idea is to define first a possible transfer of the lateral forces generated by the ground

movements to the facade bearings. Then, based on the chosen flow of forces¹, the seismic demand is compared with the structural element strength.

Usually, the front wall is restrained along its bottom edge and along the vertical edges (connections with the lateral walls); there can be other bearings, as abutments or tie-rods. Timber framework is generally supported by a series of trusses bore by the lateral walls.

As an example, the method is applied to a front wall that is shown on Figure 8.44 and whose dimensions proportion (H_{Total}/L_{Total}) is about 1:1.

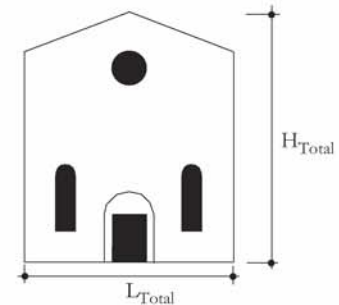


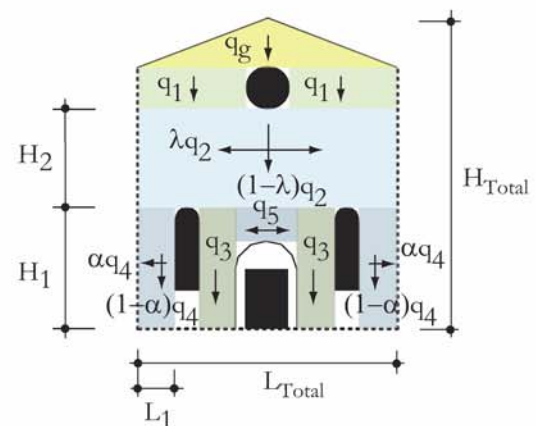
Figure 8.44 : Diagram of a FW2 front wall.

One of the possible flows of forces is shown on the right (Figure 8.45); it fits well the elastic transfer of forces and makes quite easy the calculations of the intern forces.

Such transfer of loads the corners through the creation of an arch is possible only if the masonry is strong enough to support it. In consequence, this will be the first point to be verified.

The redistribution of the horizontal inertia forces (due to the ground acceleration) is: λ is proportional to H_2/L_{Total} and α to H_1/L_1

The strength of parts 1 and 2 is to be calculated according to the way proposed under chapter 8.3.



Note: the dotted lines correspond to restrained bearings.

Figure 8.45 : Possible transfer of forces within FW2 front wall².

Each equivalent lateral load, which is the mass of the given part of masonry multiplied by the peak ground acceleration³, generates by the seismic acceleration must be transferred either to the lateral edges (as for q_2 and q_4) or down to the ground (as for q_g , $q_{i=1,3}$). It is important to keep in mind that this flow of forces is only valid in the linear field; when cracks occur at bearings (or somewhere else), the configuration of the forces transfer must be adapted.

This flow of forces is valid for one-leaf and multiple-leaf masonry walls.

Note: this proposal for a transfer of forces is one possibility; it is obvious that other flows of forces can be chosen.

1. It does not mean that the chosen transfer of forces must be the real and exact one. However, the more it fits the exact elastic transfer, the more accurate it is.
2. The dotted lines correspond to partially restrained bearings
3. It is assumed that front walls are so stiff that they behave as rigid bodies; the spectral acceleration then becomes the peak ground acceleration.

IN-PLANE BEHAVIOUR

The in-plane behaviour of the FW2 type of front wall is treated like the FW7 type (see below).

Note: the treatment of the types FW3, 4, 5 and 6 is presented in Appendix A 7.1

8.7.1.2. FW7

FW7 actually is a special case of the FW6 type of front wall; it corresponds to the main facade of a basilica whose bell-tower is on the church west part.

Proportions are the as for FW6.

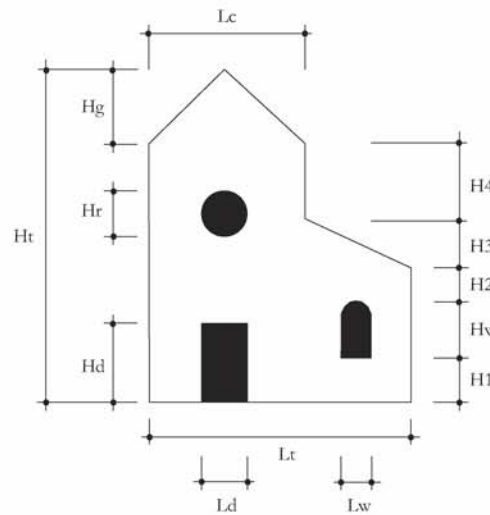
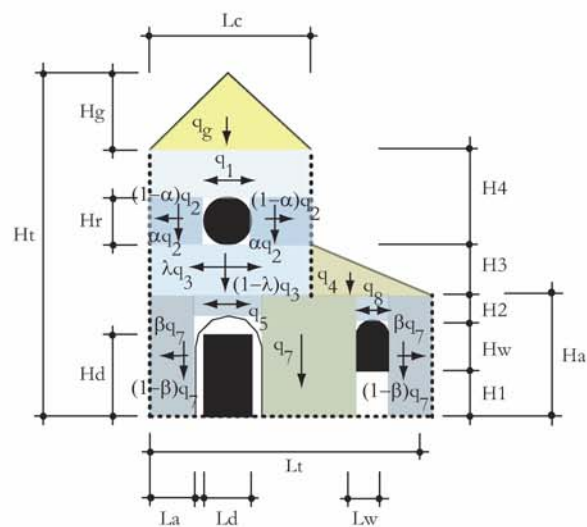


Figure 8.46 : FW7 general pattern.

OUT-OF-PLANE BEHAVIOUR

The fact that the left edge on Figure 8.47 is partially restrained makes a difference with the transfer of forces that could be found within the FW6 facade. Otherwise, there is no difference. This left edge might be not partially restrained (this would be the case for masonry put side-by-side with the bell-tower fabric); in such a case, the transfer would be almost totally different. Regarding the distribution factors, α is proportional to H_r/L_a , λ to H_3/L_c and β to H_a/L_a . The strength of these parts is to be calculated according to the way proposed under chapter 8.3.



Note: the dotted lines correspond to partially restrained.

Figure 8.47 : Possible transfer of forces within FW6 front wall.

IN-PLANE BEHAVIOUR

When the front wall FW7 is laterally loaded in its plane, the main problems occur at its basis. The lateral forces are transferred down to the ground through shear within squat parts (as components 1, 2, 3, 5 and 6 on the next figure) and through bending within slender elements (numbers 4 and 7 on Figure 8.48).

The flow of forces within the FW7 front wall has been determined numerically by linear elastic modelling. A calculation of the flows of forces for a series of peak ground acceleration has been made.

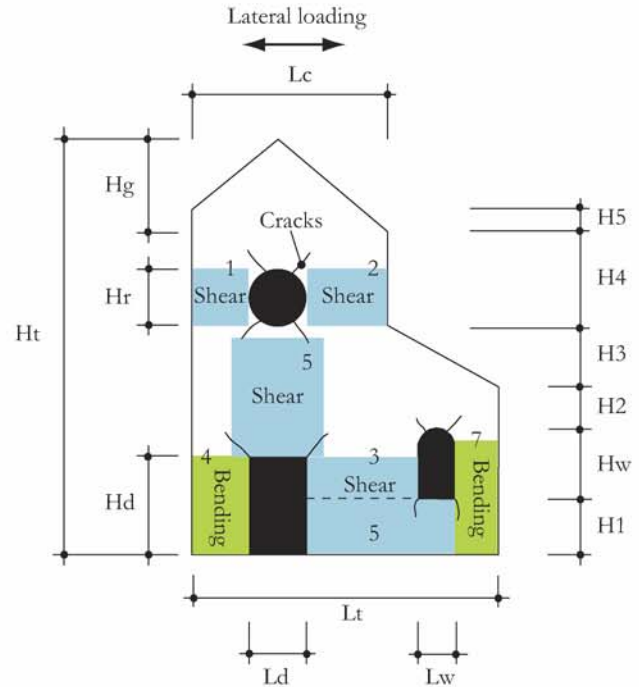
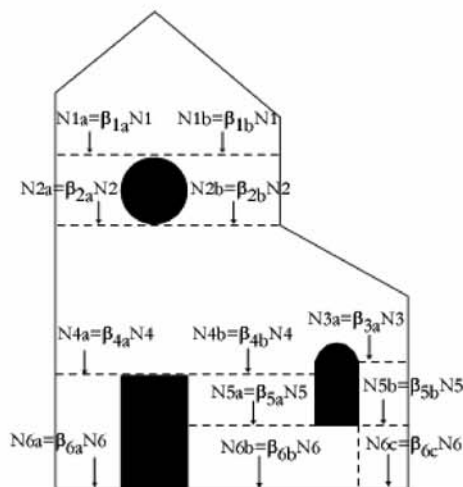


Figure 8.48 : Effects (cracks) and forces within masonry under lateral loading.

In consequence, the shear strength of shear parts must be calculated (by applying Ganz's method, for instance) and compared with the seismic demand; similarly, the state of masonry under bending force must be defined. Furthermore, it must be checked that there is no flexural failure (application of the FEMA or EC 8 method).

Distribution of axial forces (weight)



Distribution of shear forces

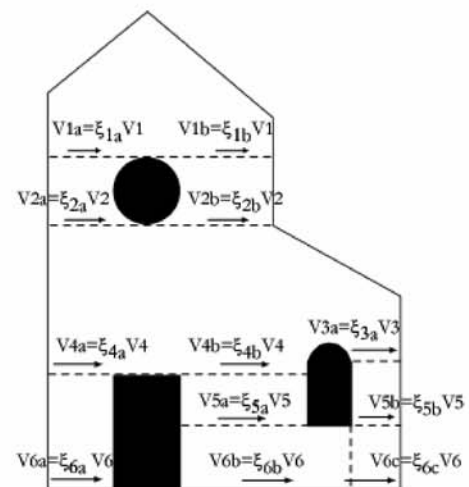


Figure 8.49 : Distribution of forces within a FW7 front wall under seismic loading.

The percentages (β and ξ) of forces (N or V) are determined thanks to linear numerical calculations (determination of stress fields), as explained under 8.3.3.2; they can be found on the following graphs:

Shear forces percentages:

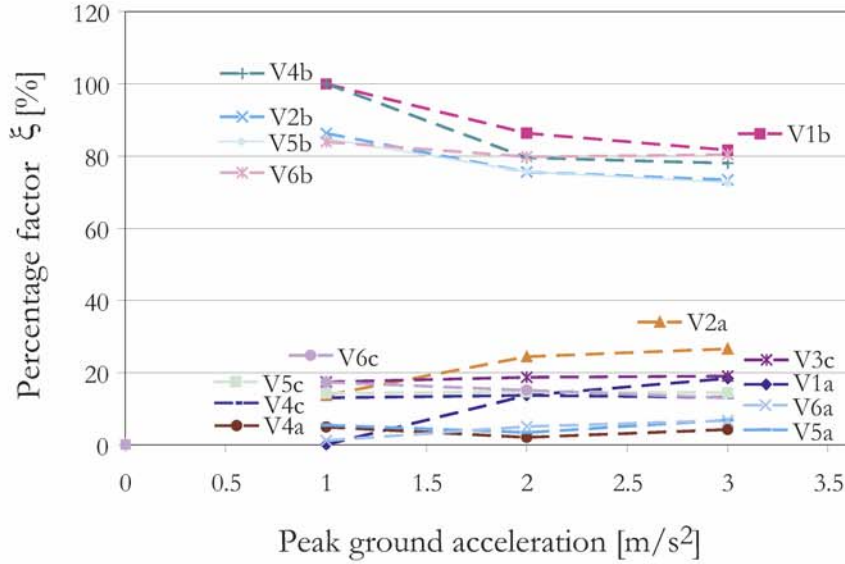


Figure 8.50 : Percentage of V force that transfer through the different parts of FW7 front wall.

Normal forces percentages:

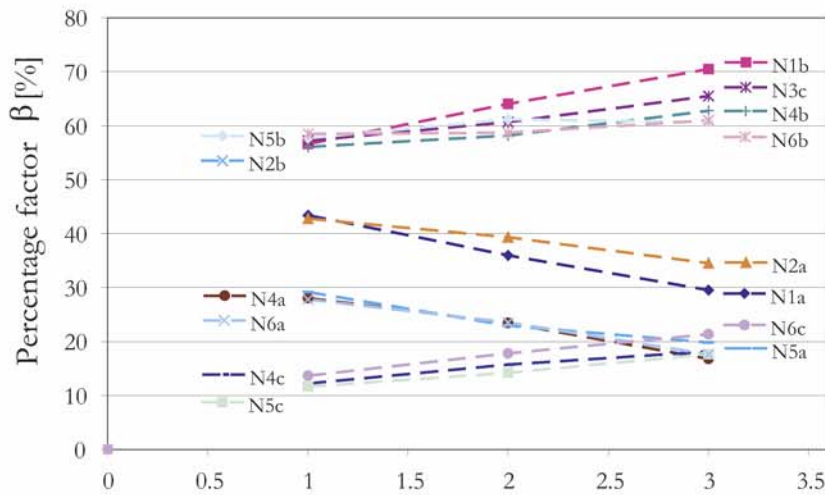


Figure 8.51 : Percentage of N force that transfer through the different parts of FW7 front wall.

While the previous calculations are based on the upper bound theorem of plasticity, the peak ground acceleration that would make the front wall FW7 collapse can also be calculated by the lower bound theorem of plasticity on the basis of the proposed collapse mechanism (Figure 8.52).

In fact, it gives the upper limit for the peak ground acceleration that would lead to the collapse defined thanks to the application of the lower bound theorem (stress fields) of the plasticity theorem.

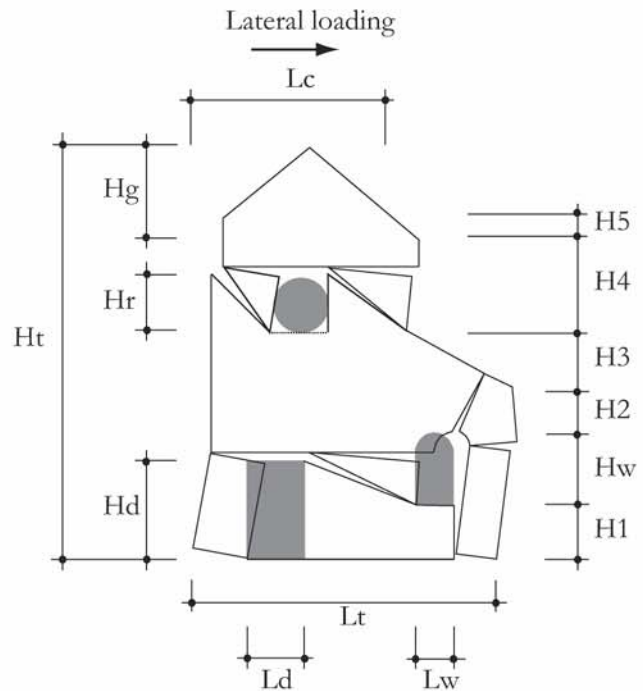


Figure 8.52 : Proposal for a collapse mechanism under a lateral action (left-right directed).

8.7.2. APSES

As seen in chapter 3.5.1.1, there are many kinds of apses. Regarding their structural behaviour under seismic loading, it can be said that they are usually not the most vulnerable part (neither in their plane, nor out of their plane), especially for small churches. Nevertheless, the apses, whose cross-section is rectangular (A4, A5, A6 and A7 types in chapter 3.5.1.1), that have a slender wall might present a higher seismic vulnerability (out-of-plane and in-plane) than smaller apses. Such cases can be found in middle to big size churches. The structural behaviour of the apses (out-of-plane and in-plane behaviour) is analysed the same way as the front walls.

8.7.3. CHOIR

The structural behaviour of the structural components of the choir (out-of-plane and in-plane behaviour) is analysed the same way as the front walls.

8.7.4. TRANSEPT

The structural behaviour of the structural components of the transept (out-of-plane and in-plane behaviour) is analysed the same way as the front walls. Moreover, the «facade» of the transept has indeed the shape of a front wall.

8.7.5. CHANCEL ARCH

The four standard shapes of chancel arches (for their determination, see chapter 3.5.1.2) have been numerically modelled in order to assess their seismic vulnerability.

8.7.5.1. TAH3

The initial meshing for this standard shape of chancel arch was characterized by:

- main height corresponds to the base length (proportion: 1:1)
- all curvatures are a half circle
- Young's modulus is: 4412 MPa
- Poisson's coefficient is: 0.15
- Boundary conditions: every nod along the basis is not restrained, only fixed
- two loading cases: self weight ($\gamma=23 \text{ KN/m}^3$) and lateral acceleration as a function of the self weight

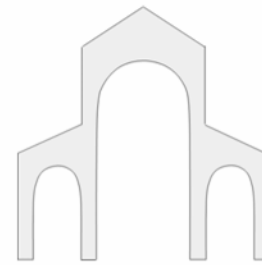


Figure 8.53 : TAH 3 standard shape of chancel arch.

IN-PLANE BEHAVIOUR

The dimensions of the original model are shown in the figure on the right.

Thanks to this numerical model, it has been possible to calculate the peak ground acceleration that leads to different grades of damage for this structural part.

The damage scale is based on the creation of hinges; after the creation of ten hinges (ten damage grades), this structure becomes unstable (for lateral loads) and can collapse later under a certain level.

Note: it is assumed that the masonry behaves like a rigid body; in this case the spectral acceleration corresponds to the peak ground acceleration.

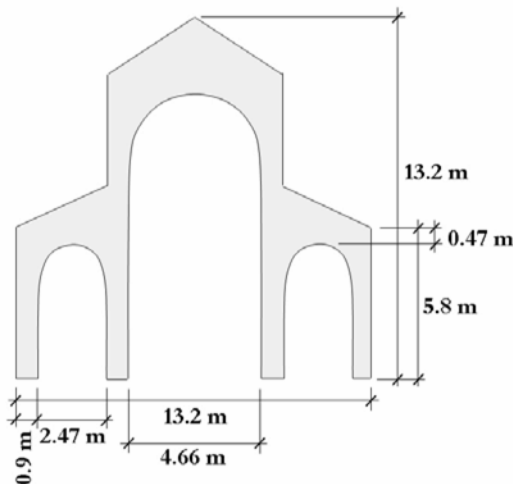


Figure 8.54 : Sketch with dimensions of the original chancel arch TAH 3.

In what concerns the failure modes, the following cases can occur:

- shear failure in one or more pillars
- loss of stability in the arches that support the above masonry
- partial collapse mechanism (8 hinges occurring at the foot and head of each pillar)
- whole collapse mechanism (10 hinges)

Failure modes were drawn from results obtained by the numerical modelling here below.

Seismic actions are modelled by a load in the same way than the self-weight but in x-direction.

Boundary condition are modelled by fix bearings (Fx, Fy are restrained; Rz is free) uniformly distributed along the basis.

Four loading cases were created: self-weight, seismic actions (lateral load), framework load and the lateral component of the framework load under lateral actions. Moreover, combinations of the aforementioned loading cases were also created.

Seismic action is defined as being the weight times a constant peak ground acceleration.

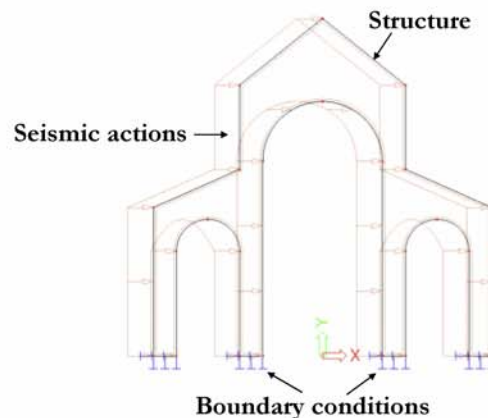


Figure 8.55 : Initial numerical model of TAH 3 structural part.

Masonry is assumed to be elasto-plastic.

Numerical calculations were carried out on the above initial TAH 3 model.

In order to find out failure modes, the numerical model was subjected to an increasing (by step) ground acceleration. After the creation of hinges at the foot of one pillar, the initial boundary conditions were changed in order to model the hinge. Precisely, a rigid bar was added at the foot of the given pillar and this bar was bore by only one fix bearing that was characterized by a certain stiffness in rotation to ensure the correct withstanding.

Here below are presented the results:

The first hinge (on the opposite figure, the hinge is situated on the rotation axis) to be created is located at the foot of the pillar on the right, under a peak ground acceleration of 0.12 g. Then, the pillar on the left is concerned (0.13 g); more or less directly after the creation of this hinge (0.135 g), another one is formed at the head of the same pillar. At this stage, there is no collapse mechanisms, even partial, that is created. This will happen only when 8 hinges (it will be partial in this case) are formed.

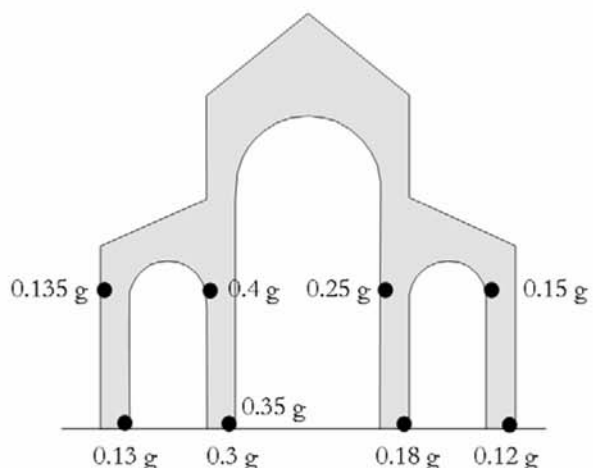


Figure 8.56 : Hinges that occurred on the TAH 3 structural part.

Nevertheless, the shear failure in the left pillar is the most critical moment since it constitutes the first important (i.e. that results in some damage to the fabric) problem to the structure. At this point, there is a separation between the chancel arch and the orthogonal lateral wall.

With respect to the fact that the considered lateral action is cyclic (seismic action), there is also a certain probability that a same level of acceleration that led to the shear failure in the left pillar also results in the right one when the direction of the actions is opposite (i.e. right-left).

Furthermore, the stability of the arches must also be checked. The process of construction must not be forgotten: arches were built on pillars and then, masonry was put on them. In consequence, a part of masonry (even not the whole part of masonry that is above a given arch) is only bore by arches; a loss of their stability would result then in the falling of the supported masonry.

OUT-OF-PLANE BEHAVIOUR

Chancel arches do not present a high seismic vulnerability out of their plane. This statement differs when a chancel arch is linked to lateral walls only on one side. In other words, the structure being on the other side of the lateral walls, usually the apses, is not as tall as the chancel arch. In such a case, the upper part of the chancel arch (kind of gable) can overturn. Consequently, the main point to be checked when calculating the out-of-plane response of a chancel arch under seismic loading is the risk of overturning of the upper part.

8.7.6. LATERAL WALLS

As seen in chapter 3.5.1.4, there are mainly two kinds of standard units for lateral walls (LW1, LW2): first, the lateral walls of the main nave and secondly, the outward walls of the low-aisles.

8.7.6.1. LW1

The LW1 unit corresponds to the main nave lateral walls of a basilica. It is composed of a series of arcades surmounted by a series of windows. In case of Romanesque churches, those windows are quite small.

As reinforcement, there can be pillars on the whole height of both sides of the lateral wall LW1 in order to reinforce the wall against the vault thrust (if there are groined- or cross-vaults)

Abutments are more frequent when the main nave is barrel-vaulted or covered with a wooden ceiling. However, there can be no abutments if the church is rather squat.

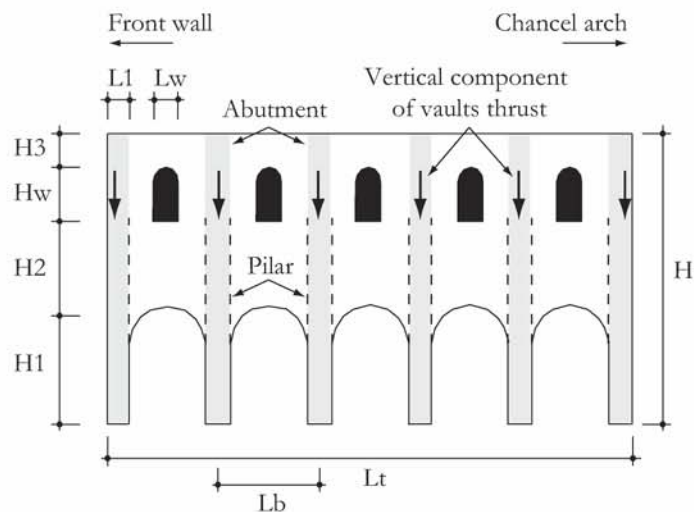
LW1 proportions are related to ones of the front wall; they are (Figure b):

$$H1_{LW} + Hw_{LW} = H1_{FW} + Hw_{FW} + H2_{FW}^a$$

$$H1_{LW} < Ha_{FW}$$

$$H1_{LW} = 0.3-0.6 Ht_{FW}$$

$$Lb_{LW} = 0.25-1.25 Lc_{FW}^b$$



a. LW means Lateral wall and FW: Front Wall. In this case, the front wall corresponding to LW1 lateral walls is the basilica (FW1, FW6 and FW7).

b. This ratio is smaller for churches with a wooden ceiling than for those covered with cross-vaults.

Pattern of the LW1 lateral wall and the ratio of usual dimensions in Romanesque edifices.

At one extremity of the LW1 lateral wall is the front wall of the church and the chancel arch can be found at the other extremity. Regarding the above sketch, the front wall and the chancel arch are perpendicular to the lateral wall.

BOUNDARY CONDITIONS

The boundary conditions of LW1 lateral walls are on one hand the front wall and on the other hand the chancel arch. In fact, the impact of the boundary conditions on the structural behaviour of the LW1 lateral wall differs according to the way it is connected to the front wall and the chancel arch.

Note: according to what was stated in previous chapters, vaults and timber framework do not have an impact on the structural behaviour of the LW1 lateral behaviour (assumption), except with their self-weight or the presence of pillars and abutments.

OUT-OF-PLANE BEHAVIOUR

The out-of-plane response of the LW1 lateral wall is determined by the application of the lower bound theorem of plasticity. As stated under chapter 8.3.2, the strip method is adopted.

The main mass is situated just above the arcades; if the main nave is barrel-vaulted, there is also the mass that comes from the vault and that is transferred into the wall above the windows.

The transfer of forces depends on the boundary conditions and the loading: it differs if the naves are covered either with cross-vaults (or groined-vaults), a barrel-vault or a wooden ceiling. In fact, the cross-section is larger on the height above the pillars of the arcades when the main nave is cross-vaulted.

1. Wooden ceiling or barrel-vault covering

The loading configuration of the LW1 lateral wall when the main nave is barrel-vaulted or covered with a wooden ceiling is given below:

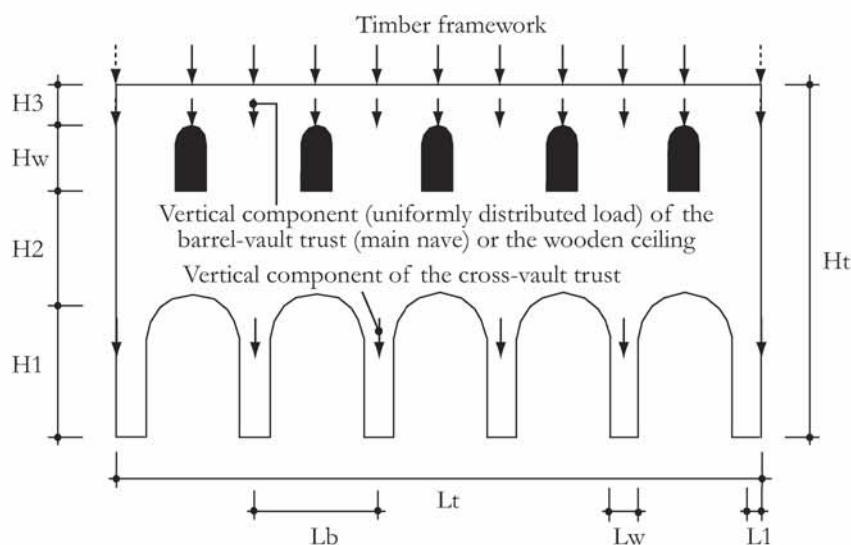


Figure 8.57 : Loading configuration of a lateral wall LW1 when the main nave is covered either by a barrel-vault or by a wooden ceiling.

If the LW1 lateral wall is restrained within the masonry of the chancel arch and that of the front wall, inertia forces resulting from the ground acceleration can transfer to the bearings according to the following sketch.

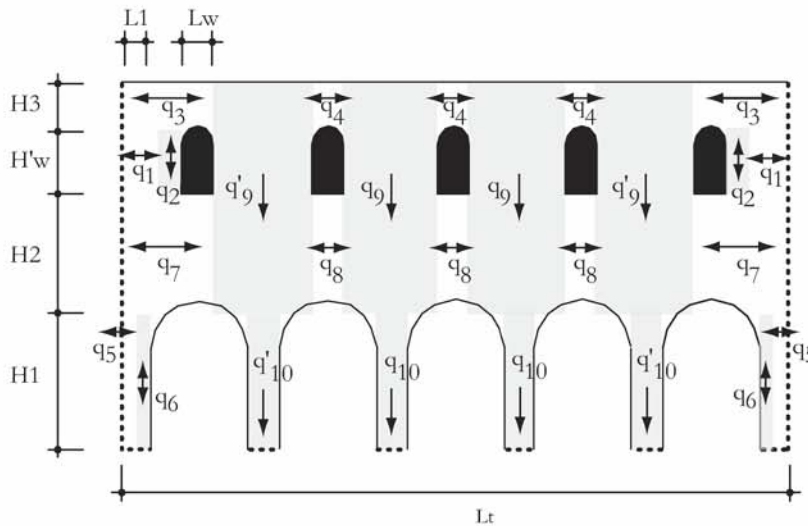


Figure 8.58 : Possible transfer of the inertia forces resulting from a seismic acceleration.

Note: - the above transfer is a possibility and not necessarily the reality (lower bound theorem of plasticity theory),
 - the load coming from the timber beams (ceiling) or from the barrel vault (main nave and low-aisles) as well as of the timber framework must be taken into account,
 - pillars are assumed to be restrained at their basis,
 - numbers correspond to the chronological way for correctly determining every load q_i .

The distribution of inertia forces is defined according to experience. Close to the extremities, the inertia forces get to directly to them; in the centre part, the out-of-plane forces transfer to the ground.

2. Groined- and cross-vault covering

The loading configuration of the LW1 lateral wall when the main nave is groined- or cross-vaulted is given below:

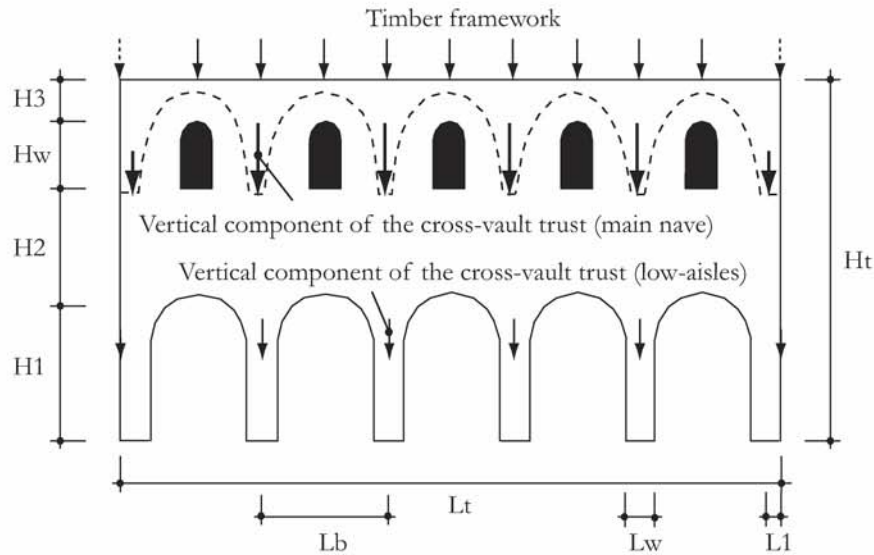


Figure 8.59 : Loading configuration of a lateral wall LW1 when the main nave is covered either by groined-vaults or by cross-vaults.

As previously, in case the LW1 lateral wall is restrained within the masonry of the chancel arch and that of the front wall, inertia forces resulting from the ground acceleration can transfer then to the bearings according to the following sketch:

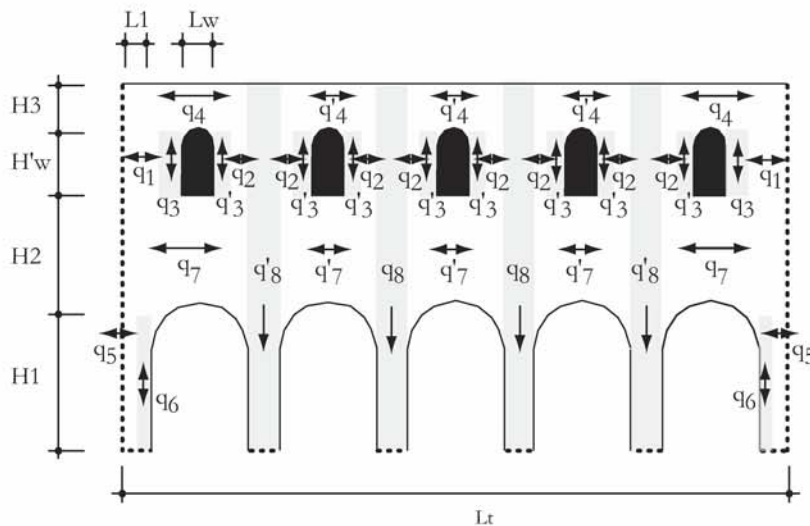


Figure 8.60 : Possible transfer of the inertia forces resulting from a seismic acceleration.

Note: the above transfer is a possibility and not necessarily the reality (lower bound theorem of plasticity theory),

- the load coming from the timber beams (ceiling) or from the cross- or groined vaults (main nave and low-aisles) as well as of the timber framework must be taken into account,
- pillars are assumed to be restrained at their basis,
- numbers correspond to the chronological way for correctly determining every load q_i

What differs from Figure 8.58 is that the presence of pillars on the whole height of the wall and also of bigger abutments than with barrel vault covering of a wooden ceiling. Consequently, forces resulting from an out-of-plane acceleration first transfer to the pillars and then to the ground. Only the distribution at vertical edges is different. Moreover, it might happen that there are buttresses that help transferring the thrust of the vaults down to the ground; in such a case, the out-of-plane response will not be same in both directions.

IN-PLANE BEHAVIOUR

The in-plane behaviour of the LW1 type of lateral walls depends on the bearings conditions, the dimensions of the wall, the configuration of the openings and the forces coming from the timber framework, the vaults (main nave and low-aisles).

In what concerns the Pre-Romanesque and Romanesque sacred edifices, the pillars of the arcades and the windows generally have a small height. Consequently, the piers (part of masonry between two windows) are shear loaded while the pillars, even if not tall, must resist a flexural effort (Figure 8.61).

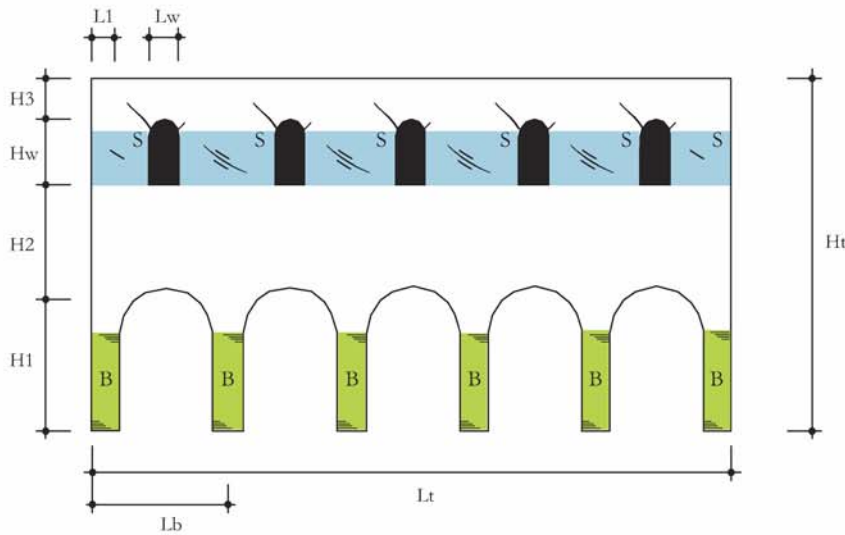


Figure 8.61 : Impact of the transfer of the inertia forces to the ground on the LW1 unit.

The distribution of the shear force amongst the piers is given by a numerical modelling. Furthermore, it also gives the distribution of the axial force amongst pillars.

1. Distribution of shear forces:

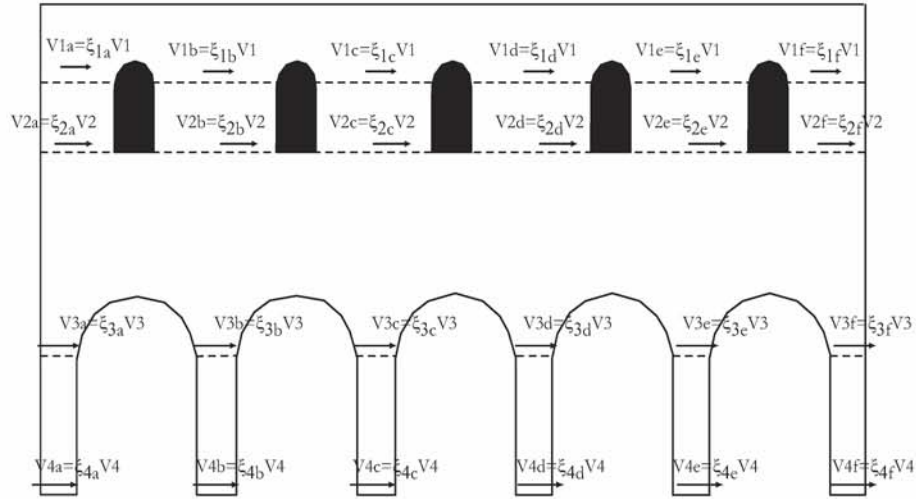


Figure 8.62 : Distribution of shear forces within a LW1 lateral wall under seismic loading.

The percentages ξ of the shear force V are given on the following graphs:

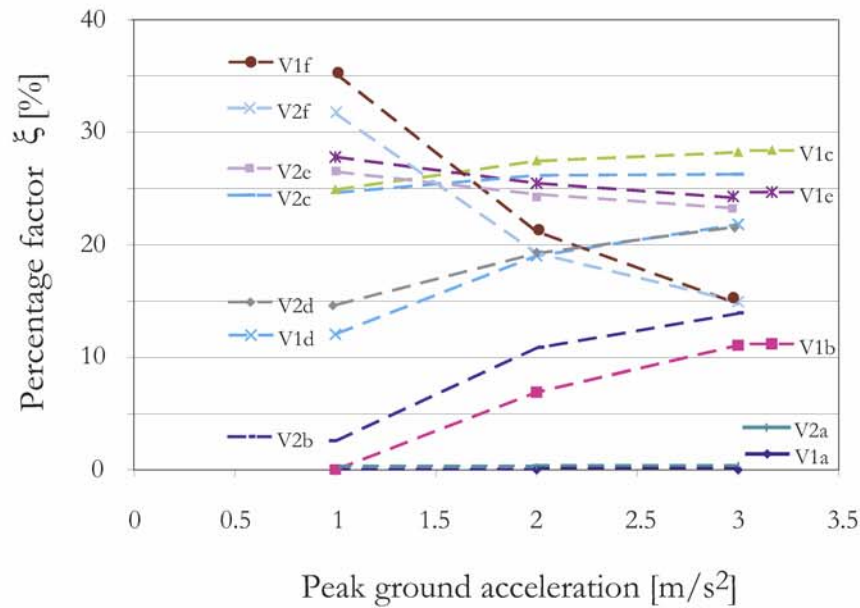


Figure 8.63 : Percentages of distribution of the total shear force amongst the piers situated between the windows.

Under low in-plane acceleration, the component f is the most loaded pier (about 35 % of the total shear at the level 1), followed by the piers e, c, d, b and a. With a higher acceleration, the most

loaded pier becomes the c, followed by the e, d, f, b and a (for the definition of the characters, see Figure 8.62).

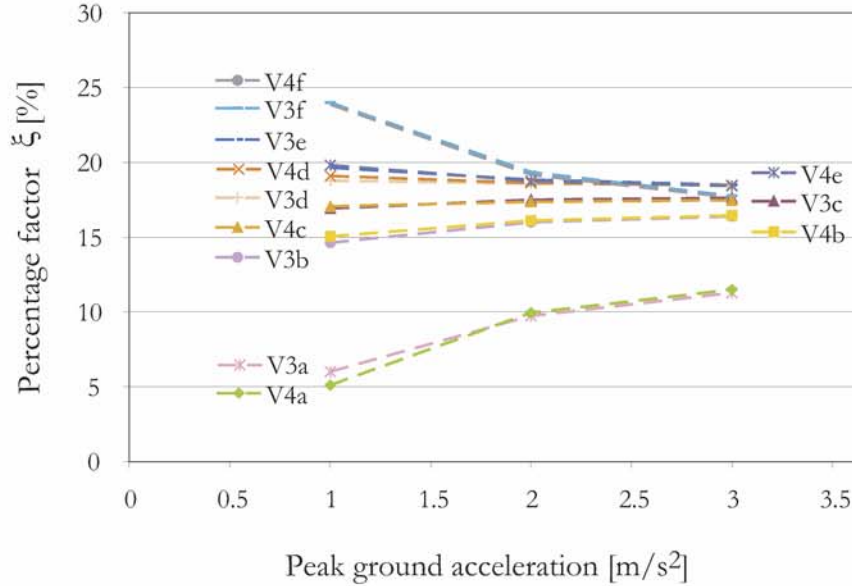


Figure 8.64 : Percentage of distribution of the total shear force amongst pillars.

Though the difference of distribution between the pillars a and f is significant under a low in-plane acceleration, it notably decreases for higher acceleration. Furthermore, it tends to a uniform distribution amongst pillars.

2. Distribution of axial forces (weight):

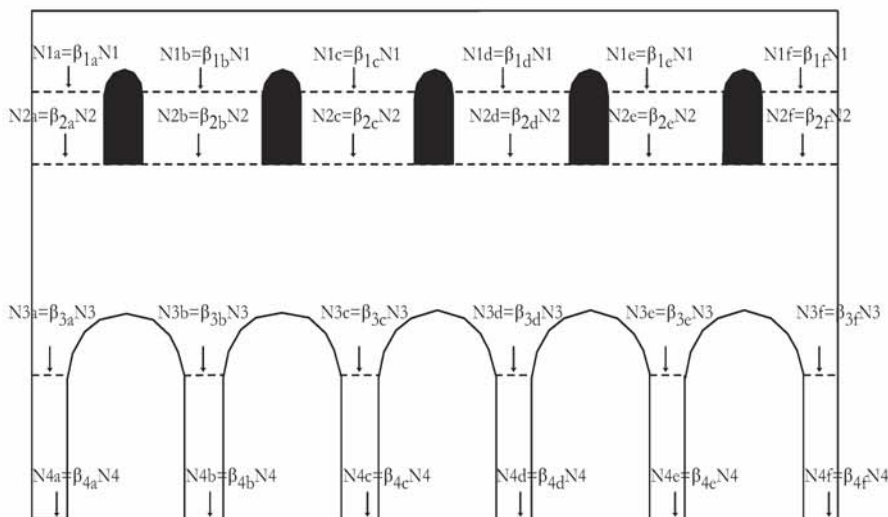


Figure 8.65 : Distribution of axial forces N within a LW1 lateral wall under seismic loading.

The percentages β of the axial force N are given on the following graphs¹:

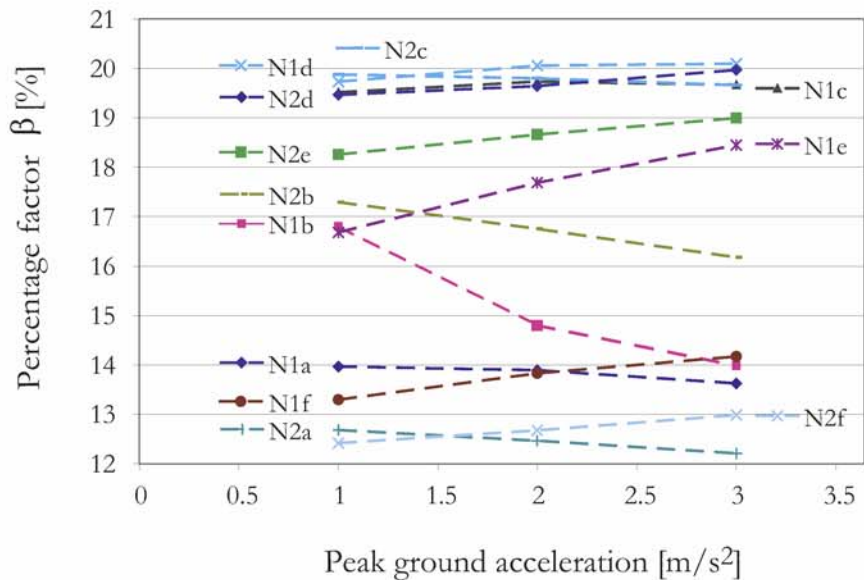


Figure 8.66 : Percentage of distribution of the total axial force N amongst the piers situated between the windows.

The highest percentage of the axial force at the level 1 and under a ground acceleration of 1 m/s² passes through the pier «d»; then come the pier «c», «b», «e», «a» and «f». However, this distribution changes for a higher acceleration; though the piers «d» and «c» are still the most loaded components, the «e» element becomes almost as loaded as the piers «d» and «c». Moreover, the axial load in the pier «f» increases for a higher acceleration while it decreases for the piers «a» and «b».

1. For better readability, the percentages of the four levels are dispatched into two graphs.

The higher percentage of the axial force is about 20 %.

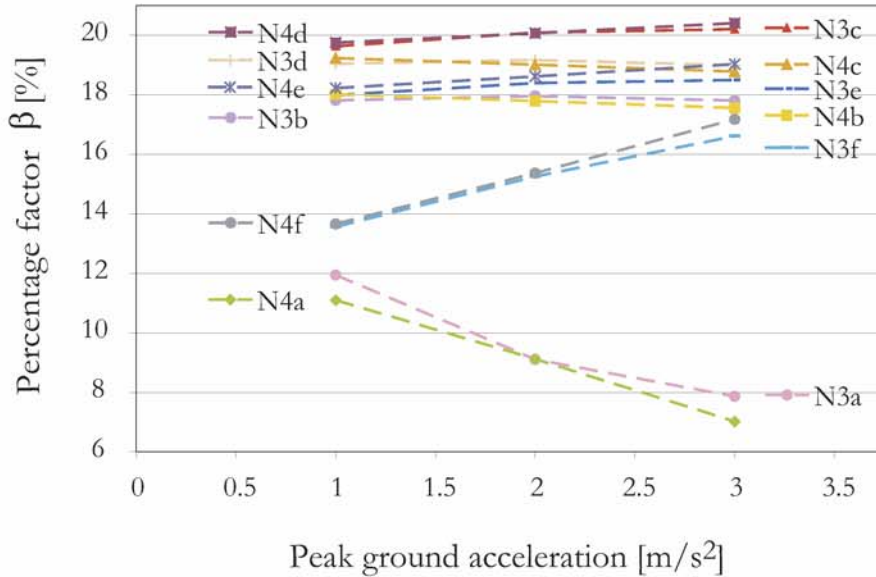


Figure 8.67 : Percentages of distribution of the total axial force N amongst pillars.

The most loaded pillar is the number «c» at its top; this does not change with acceleration. In fact, only the percentage of axial load changes for the piers «b» and «a»; in the former, it significantly increases with acceleration while it diminishes for the pillar «a». Regarding the base of pillars, the number «d» is the one that must resist a higher axial force

If every part fails, i.e. the pillars of the arcades fail because of bending and the piers fail due to the shear force, the following collapse mechanism can be activated.

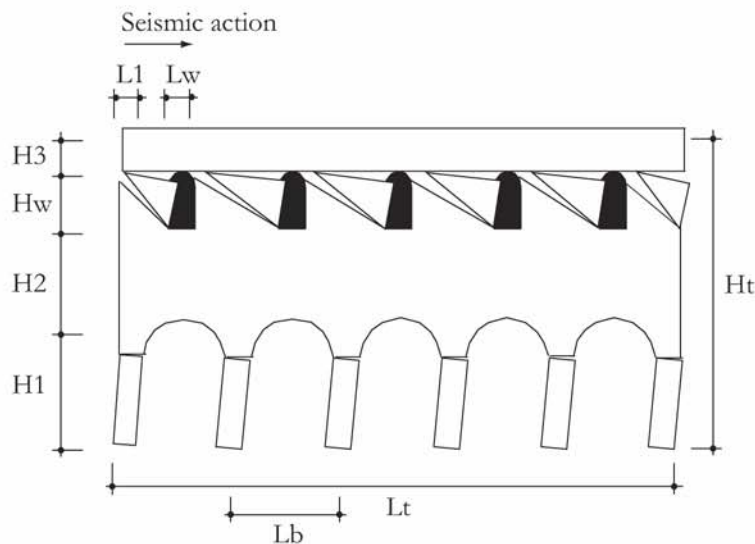


Figure 8.68 : In-plane possible collapse mechanism for LW1 lateral wall.

8.7.6.2. LW2

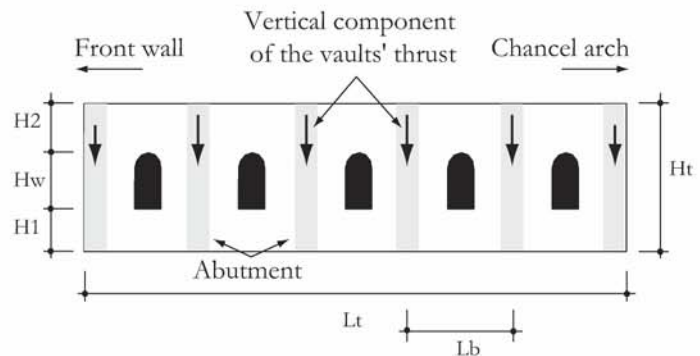
The LW2 lateral walls corresponds either to the lateral walls of a one-nave church or those of the low-aisles of a basilica. As for the LW1 lateral walls, windows are usually small for Romanesque edifices; however, they might have been enlarged after the construction.

To transmit the thrust coming from the vaults (groined-, cross- or even barrel-vaults) down to the ground, there usually are abutments along the wall.

There can be some exceptions if the low-aisle has a wooden ceiling. The usual dimensions and dimensional ratios are:

$$H_{tLW} = H_{aFW}$$

$$L_{bLW} = 0.25 - 1.25 L_{cFW}^a$$



a. This ratio is smaller for churches with a wooden ceiling than for those covered with cross-vaults.

Figure 8.69 : Pattern of the LW2 lateral wall and the usual dimensions and dimensional ratios in Romanesque edifices.

BOUNDARY CONDITIONS

The boundary conditions of the LW2 lateral wall are the same as the ones of the LW1 type.

OUT-OF-PLANE BEHAVIOUR

As for the LW1 type of lateral walls, the strip method is applied.

Compared with the LW1 type, the mass is more uniformly distributed and is not situated high above the ground. Moreover, the inertia forces resulting from an out-of-plane acceleration transfer to the ground according to the boundary conditions. For instance, the transfer is different whether there are abutments or not. In other words, it differs if the ceiling of the low-aisles is vaulted or not.

1. Without abutments (e.g. wooden ceiling):

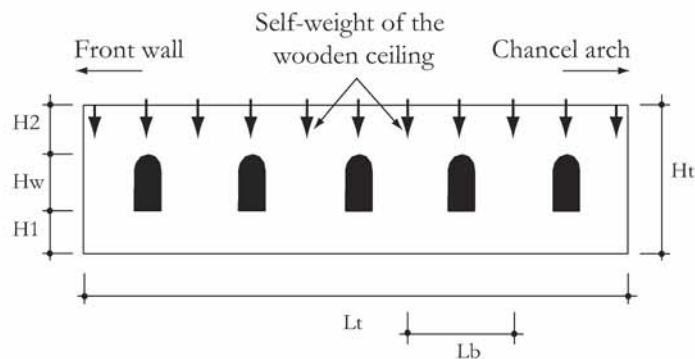


Figure 8.70 : Loading configuration of lateral wall LW2 without abutments.

In such a case, the out-of-plane forces are directly transferred to the ground, except close to the vertical restrained edges.

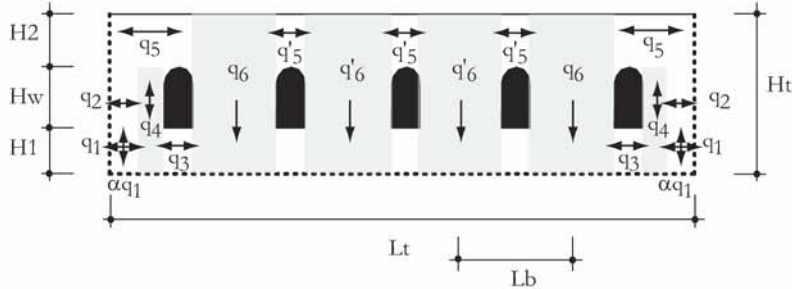


Figure 8.71 : Possible transfer of the forces caused by an out-of-plane acceleration.

- Note:*
- the above transfer is a possibility and not necessarily the reality (lower bound theorem of plasticity theory),
 - the load coming from the timber beams (ceiling) as well as of the timber framework must be taken into account,
 - the wall is assumed to be restrained at its basis and along the vertical edges,
 - numbers correspond to the chronological way for correctly determining every load q_i .

2. With abutments (e.g. cross-vaults)

The loading configuration of the outer lateral wall of a low-aisle is given here below:

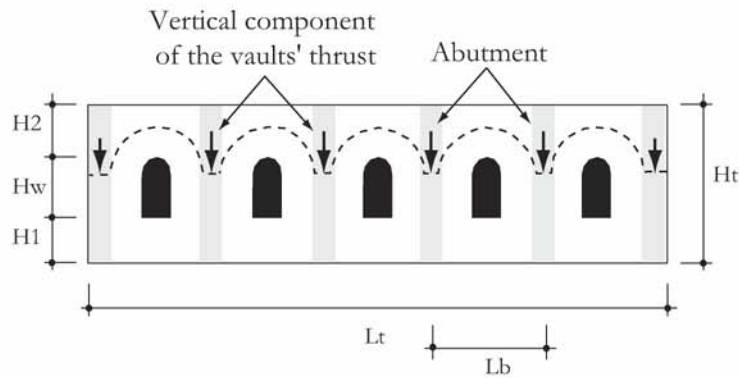


Figure 8.72 : Loading configuration of a LW2 lateral wall when the low-aisle is covered by cross-vaults.

When such a system is shaken out of its plane, the resulting forces transferred to the ground through the abutments, as shown on the next figure:

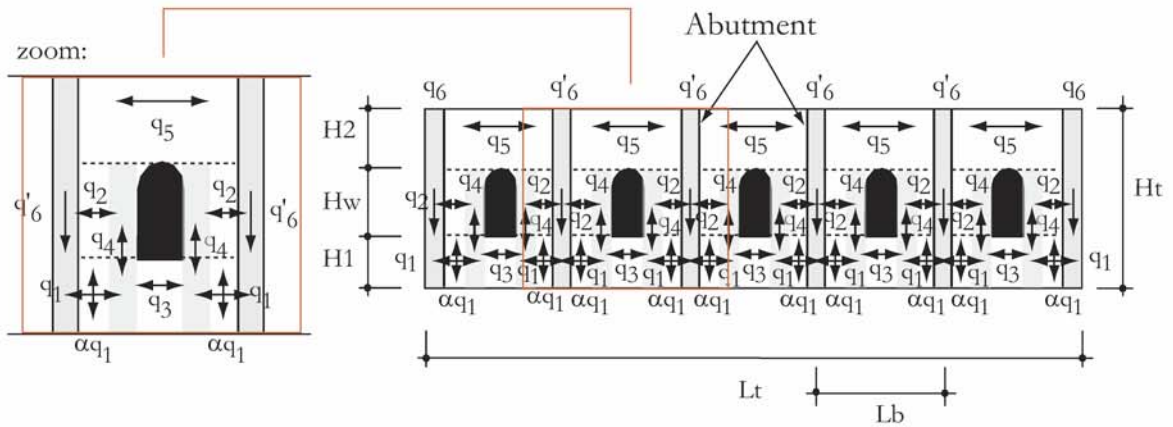


Figure 8.73 : Possible transfer of the out-of-plane forces to the ground.

- Note:*
- the above transfer is a possibility and not necessarily the reality (lower bound theorem of plasticity theory),
 - the load coming from the timber beams (ceiling) as well as of the timber framework must be taken into account,
 - the wall is assumed to be restrained at its basis and along the vertical edges,
 - numbers correspond to the chronological way for correctly determining every load q_i .

Once the first cracks appear, the flow of forces changes and the above proposed transfer must be changed accordingly.

IN-PLANE BEHAVIOUR

In case of Pre-Romanesque and Romanesque sacred edifices, the LW2 lateral walls are usually squat and the windows are of small size. Consequently, there is a large part of wall between windows, as shown on the next figure.

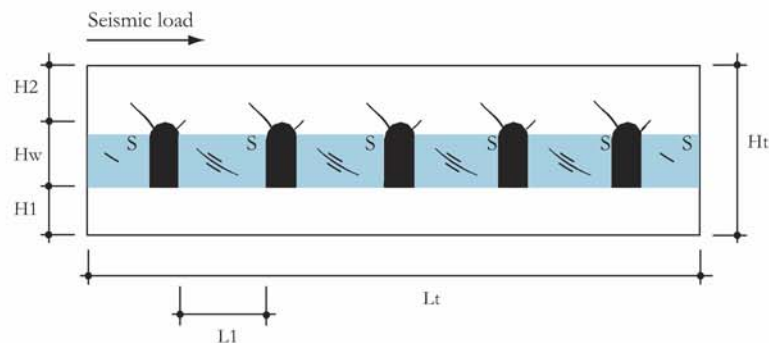


Figure 8.74 : Impact of the transfer of the inertia forces to the ground on the LW2 unit.

Such a configuration of openings causes that, under seismic loading in the plane of the LW2 wall, shear appears in these in-between parts. Thus, the failure of the LW2 lateral wall depends on the shear strength of those elements.

In order to assess the value of the shear force that transfers through each pier (i.e. an part of masonry between two windows), a numerical modelling is carried out. This allows us to determine the amount of the total shear force at one level that goes through each segment as a function of the in-plane acceleration. Moreover, the distribution of the axial force is also done.

1. Distribution of shear forces:

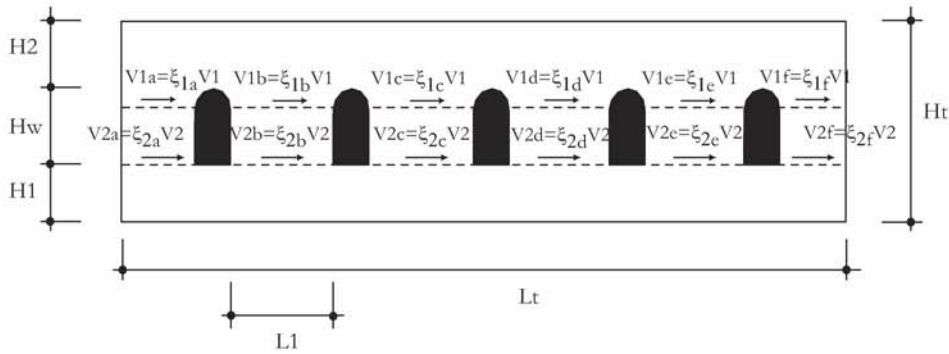


Figure 8.75 : Distribution of shear forces within a LW2 lateral wall under seismic loading.

The values of the percentages that correspond to the ξ of the above figure are given on the following graph.

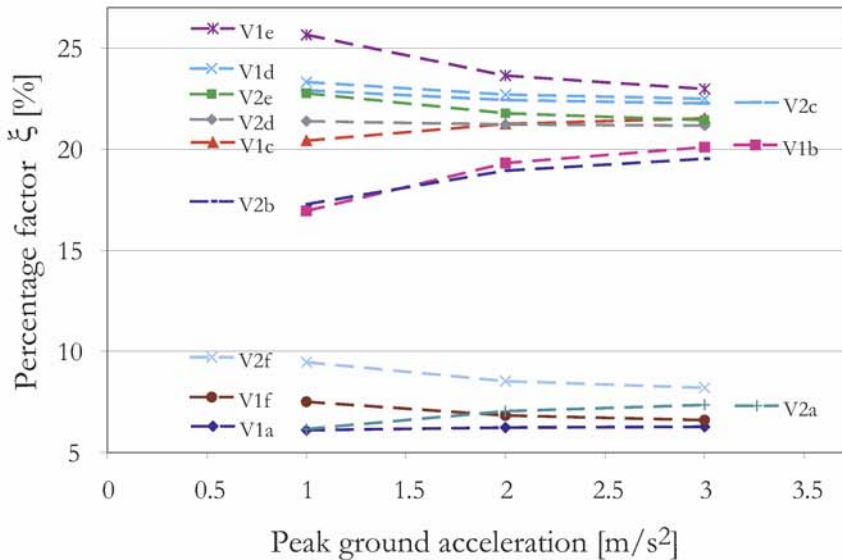


Figure 8.76 : Percentage of the total shear force at the level i ($i=1,2$) that transfer through each pier (given by a, b, c, d, e and f).

The highest percentage of the shear force that passes through one pier is about 26 % (V1e); then, the shear force is distributed with a percentage of 23 % (V1d), 21 % (V1c), 17 % (V1b), 7.5 % (V1f) and 6 % for V1a. It shows that the pier that must resist the higher shear force is the «e» one. Both piers of extremities are less loaded; however, since their cross-section is smaller than the other ones, the resistance is also lower.

The above graph highlights that the distribution of the shear force tends to be homogeneous with higher acceleration. For instance, the ξ_{1e} percentage decreases while the acceleration increases; on

the contrary, the ξ_{1b} increases. In fact, under an acceleration of 3m/s^2 , the shear force is almost uniformly distributed amongst piers; the value of percentage tends to 22 % for piers b, c, e and d. The process is the same for the piers a and f, although the percentage of the total shear force is lower than for the other piers.

2. Distribution of axial forces (weight):

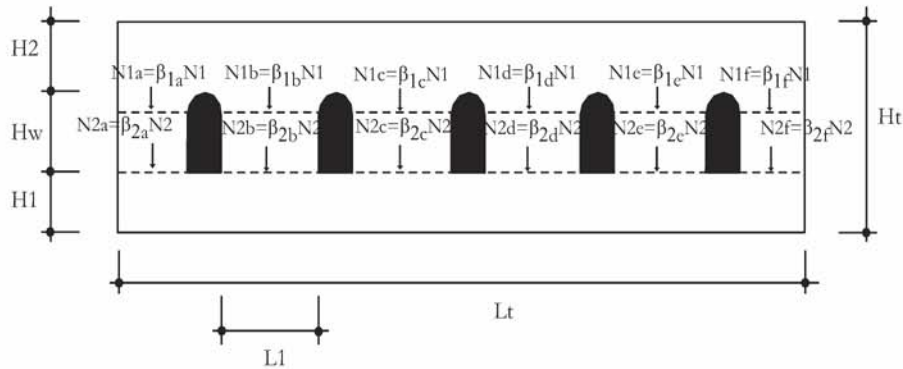


Figure 8.77 : Distribution of axial forces within a LW2 lateral wall under seismic loading.

The values of the percentages that correspond to the β of the above figure are given on the following graph.

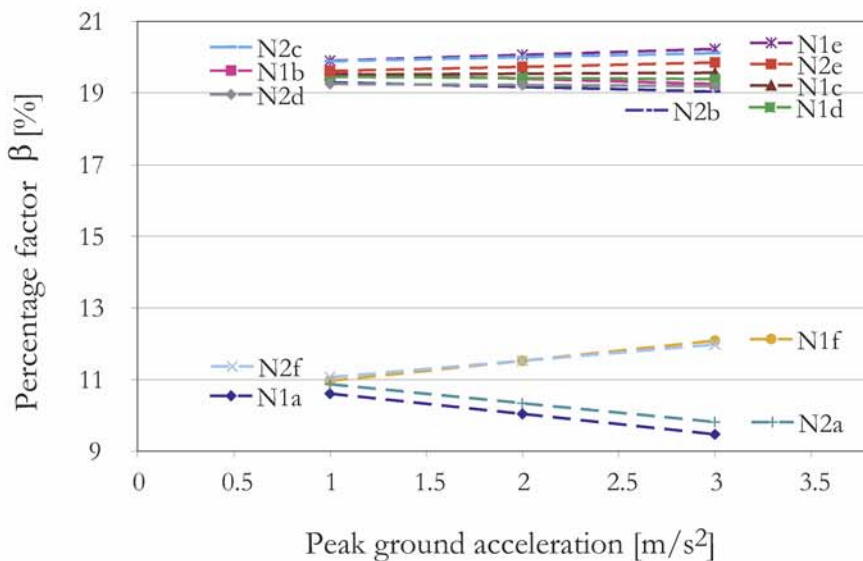


Figure 8.78 : Percentage of the total axial force at the level i ($i=1,2$) that transfer through each pier (given by a, b, c, d, e and f).

The trend is the same than for the distribution of the shear force: the piers at extremities are not too much loaded (though the axial force notably increases on the pier f with acceleration) and the in-between piers are the most loaded ones. Moreover, the percentage do not significantly change with acceleration.

Once every pier has failed, the following collapse mechanism is activated:

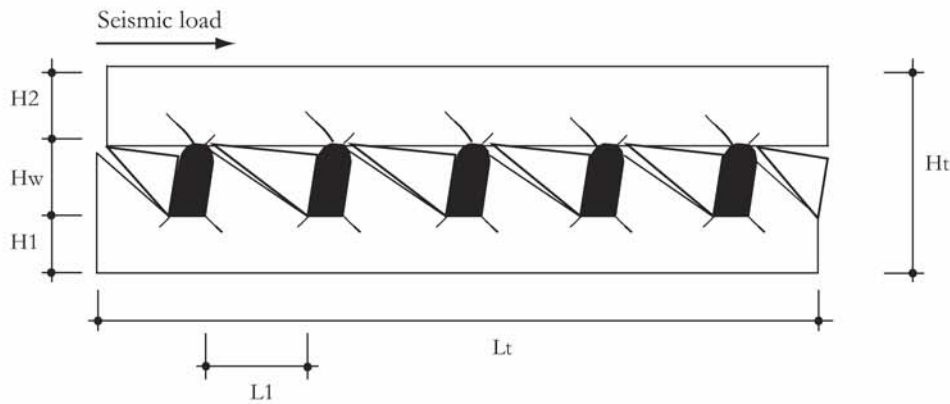


Figure 8.79 : In-plane collapse mechanism for LW2 lateral wall.

8.7.6.3. Discussions

In fact, LW2 is not as seismically vulnerable as LW1; while LW2 type is rather small (or squat), the lateral walls of the main nave (LW2) is tall and its mass is concentrated in the upper part. Furthermore, this mass (a plain wall) is supported by a succession of pillars. Since it is the mass that moves forth and back under seismic actions, this kind of structure is particularly vulnerable.

8.8. DISCUSSIONS AND CONCLUSIONS

As explained in the chapter 8.1, cultural heritage buildings have very different structural features than common buildings. Consequently, their seismic response is different and cannot be treated alike. The main objective of this chapter has been to give an understanding of the structural behaviour of sacred edifices under seismic actions.

Based on in-situ observations, it was stated that the structural parts of small and medium-size churches tend to behave independently from each other [Do 94]. This statement probably constitutes the most important assumption that was put down to address the seismic response of religious edifices. Then, comes the assumption that it is possible to separately treat the out-of-plane and the in-plane responses. However, this assumption is also made for the treatment of common buildings.

The application of the theory of plasticity to macro-elements has proven to be efficient and to give valuable results either for the in-plane or out-of-plane seismic response. This statement shows that the seismic behaviour of sacred edifices, though complex, can be addressed in such a way.

The strip method allows us to obtain the maximal lateral load that can be resisted by the given structural component and also to determine where a damage can happen and under which ground acceleration. However, the obtained value is conservative since the lower bound of the plasticity theory gives under-estimated values.

Because of the presence of openings and of a distributed mass within walls, the in-plane seismic response of walls has to be dealt with by numerical simulations. Since it was possible to list standard units for every Pre-Romanesque and Romanesque edifices, the numerical (linear) treatment of each of them provides a kind of «library» that contains a description (percentage of forces) of the flow of forces under increasing in-plane acceleration.

The assessment of damage resulting from the interaction between macro-elements can be addressed when studying the global behaviour of a given edifice.

In what concerns the seismic behaviour of the vaults, the assumption that their movements under seismic loads have no impact on their bearings must be more thoroughly studied. Moreover, the maximal lateral displacement of 2 mm per each bearing that can be supported by the vaults seems too small and should also be analysed in the future.

9.1. INTRODUCTION

The main purpose of this PhD dissertation is to develop a methodology that help engineers and architects to reach a reasonable decision regarding the seismic vulnerability of sacred edifices.

This chapter is devoted to the methodology; it is shown how the method is structured and how to proceed to apply it in order to assess the seismic vulnerability of a given Pre-Romanesque or Romanesque sacred edifice.

9.2. METHODOLOGY: CONCEPT

This methodology has been developed for small- and medium-size Pre-Romanesque and Romanesque edifices; or at least regular structures. Cathedrals are consequently not considered.

According to the conclusions of chapter 5, the proposed method is composed of four steps that are: three levels of study and one for the diagnosis. This mutli-step approach also looks like to the method proposed by the Federal Office for the Environment [OFEV 1 05], [OFEV 2 05], [OFEV 3 05] for assessing the seismic vulnerability of common buildings.

Before beginning the methodology, a general survey of the sared edifice is carried out in order to identify its main structural features such as the dimensions, the date of construction, structural transformations, type of masonry and its state of maintenance. In fact, all the data that are required to carry out the analysis of the structural behaviour under static and seismic loads must be gathered in this phase.

The main goal of the first step, i.e. the study, is to determine the seismic vulnerability of a given edifice. It is constituted of three levels with an increasing accuracy and complexity. The first level per-

mits to sort out the edifices that are not seismically vulnerable. For this step, the method that has been developed by Lourenço et al. [LR 06] is adopted since it has proven to give good results (see chapter 5.4). The second level of the step 2 is applied only to the edifices that have been previously described as seismically vulnerable at the level 1. More detailed calculations are carried out; because of their efficiency, both theorems of the limit analysis are applied; such an application allows us to obtain two limits that comprehend the real collapse value. The second step results in obtaining the vulnerability curves for each structural element for both their in-plane and out-of-plane directions. Here below is a fictitious graph that could be obtained in the end of this step.

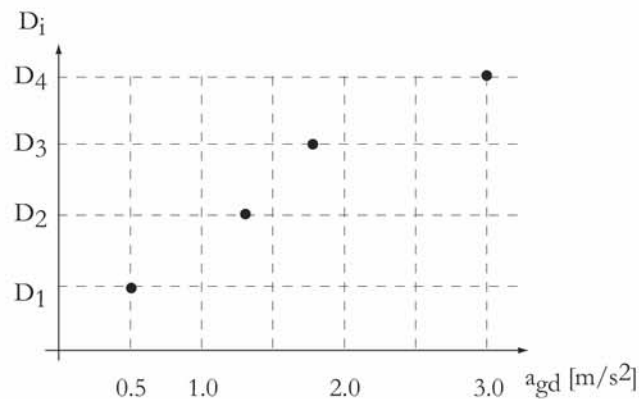


Figure 9.1 : Damage grade as a function of the peak ground acceleration.

Note: the damage grades do not correspond to the EMS-98 list (see under Appendix A. 2.1). They are set by the engineer or architect who makes the assessment.

Once the seismic vulnerability of each macro-elements is determined, that of the whole church must be assessed.

In case of edifices that are too much irregular in plan and in elevation, most sophisticated methods such as the FEM should be applied to refine the accuracy of the level 2 results; this corresponds to the level 3 of the method.

After the three steps are done, the rate of risk for a given building must be addressed; this is the diagnosis phase. Calculations permit to obtain vulnerability curves for every part of a given church and for the whole edifice too. Comparing these results with the maximal peak ground acceleration, which can be expected in the considered region, it becomes possible to assess the resulting damage and also to set down a list of retrofitting that can prevent the expected damage.

The whole procedure is summarized on the following diagram:

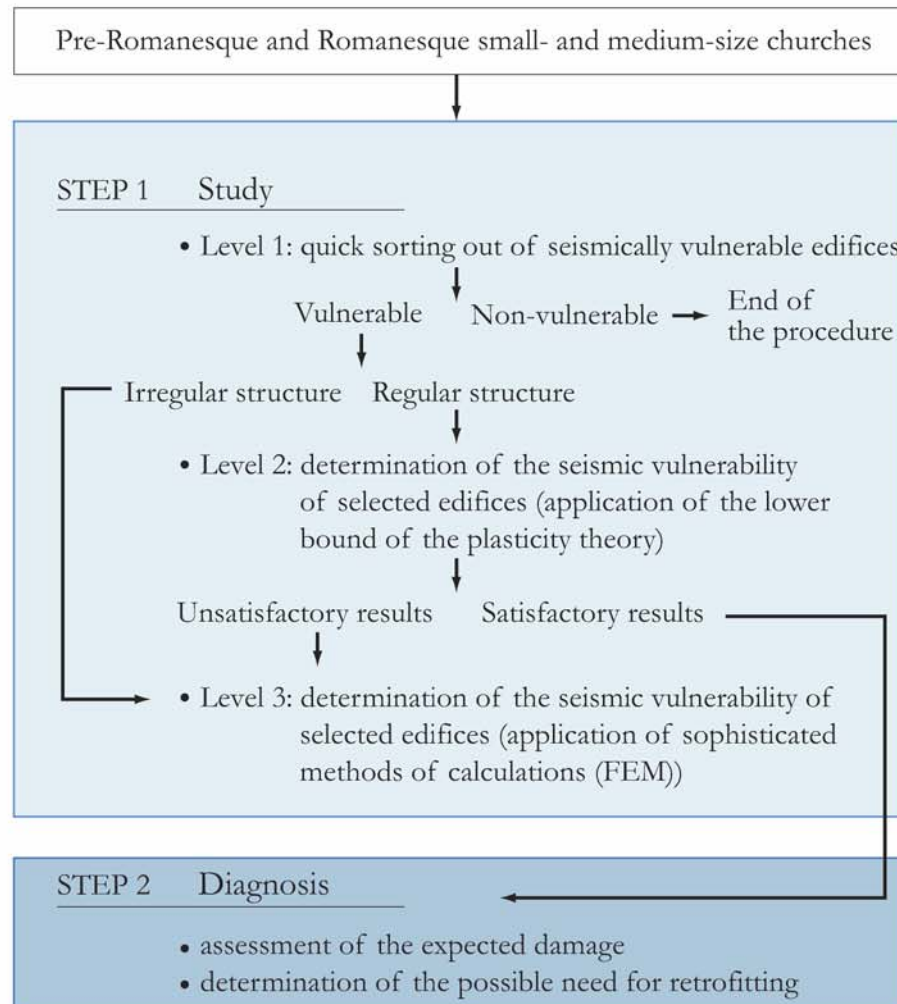


Figure 9.2 : Diagram of the method.

9.3. GENERAL SURVEY

The survey corresponds to the first phase to be done; it somewhat constitutes the basis of the following calculations for defining the structural behaviour of a given edifice dynamic loading. However, it does not constitute a step of the methodology; it is indeed a precondition for the application of the method.

During this phase, the dimensions of the structural elements of a given edifice, the state of maintenance of masonry, the exact static diagram and the mechanical properties of materials such as masonry must be known.

All these data are gathered according to the following procedure:

1. PLANS, DIMENSIONS

Gathering of every plan concerning the edifice (ground plan, transversal and longitudinal elevation, cross-section of structural elements, etc.).

2. IN SITU SURVEY

In order to have a more or less detailed description of the state of maintenance of masonry, an in-situ survey has to be carried out. The idea is to detect any kind of loss of strength such as the crumbling of mortar, the out-of-plumbness of walls, cracks, vegetal organisms (that usually lead to the crumbling of mortar) and dislocations. Furthermore, the change of masonry (due to upraising for instance) should also be recorded (see chapter 6.3.5).

The second step of this in-situ survey is the definition of the causes that result in the afore recorded damage to masonry of the structural elements, like e.g. settlements, masonry creep, bad weather, age and structural transformations. This step must be carried out carefully since every kind of damage highlights not only the way the structure behaves but also problems resulting from external actions such as settlements [MG 90].

3. STATIC DIAGRAM

It matters that the flow of forces within a given edifice is well known before addressing the step 2 of the method. It might be useful to set a static diagram of the edifice.

4. MECHANICAL PROPERTIES

The correct structural behaviour of cultural heritage buildings can be determined only if the mechanical properties of the materials that constitute the given edifice are well known. At first, the structure of walls must be determined, that is, the number of leaves. Moreover, the type of the bonding of masonry must be known (phase 2, in-situ survey) and if masonry is homogeneous or not (transformations, different types of bonding, etc.). In case of multiple-leaf walls, the quality of the interface between leaves must also be assessed.

The mechanical properties of masonry such as the compressive and shear strength as well as the density of rocks must be defined. If there are no experimental results available or that no tests can be done, the compressive strength ($f_{m,x}$ and $f_{m,y}$) of masonry can be defined according to the SIA V 178 [SIA V178 80] (chapter 6.5.1.1), with precaution. The shear strength can be determined with Coulomb's equation (chapter 7.5) and the Young's modulus according to the Swisscode SIA V266/2 (chapter 6.5.1.1).

If walls are composed of three leaves, their mechanical properties can be defined according to the model of Pina-Enriques et al. [PLBA 05] (chapter 6.6.2.3) and the Young's modulus according to Ebner's [Eb 96] (chapter 6.6.2.2) or Egermann's.

Note: the thermal characteristics of masonry are not taken into account in this report.

9.4. STUDY: LEVEL 1

The main goal of the first level is to sort edifices, i.e. to distinguish the ones that are not seismically vulnerable from the ones that are. The method used at this level has actually been developed

by Lourenço et al.; it is based on parameters that are quite easy to obtain as dimensions. Three indexes are obtained; they correspond to ratios of values that characterized edifices such as walls area, ground surface of the whole edifice, the weight and the peak ground acceleration that might subjects it. The indexes are

$$\text{Index 1} \quad \gamma_{1,i} = \frac{A_{wi}}{S} \quad [-] \quad (\text{EQ 9.1})$$

Where: $\gamma_{1,i}$ is the first index in regards to the direction i
 A_{wi} is the plan area of earthquake resistant walls in the direction i
 S is the ground surface of the building

In cases of high seismicity, a minimum value of 10% seems to be recommended for historical buildings [LR 06].

Note: Index 1 ignores walls slenderness and also mass of the construction. Moreover, after Eurocode 8, walls are considered as earthquake resistant if the thickness is wider than 0.35 m and if the height-thickness ratio is smaller than 9.

$$\text{Index 2:} \quad \gamma_{2,i} = \frac{A_{wi}}{G} \quad [\text{m}^2/\text{MN}] \quad (\text{EQ 9.2})$$

Where: $\gamma_{2,i}$ is the second index in regards to the direction i
 A_{wi} is the plan area of earthquake resistant walls in the direction i
 G is the total weight of the construction

This index is somehow the horizontal cross-section of the building per unit of weight.

In case of high seismicity, a minimum value of 1.2 m²/MN seems to be recommended for historical masonry buildings [Me 98] in [LR 06].

$$\text{Index 3:} \quad \gamma_{3,i} = \frac{A_{wi}}{A_w} \cdot \frac{\tan\varphi}{\beta} \quad [-] \quad (\text{EQ 9.3})$$

Where: $\gamma_{3,i}$ is the third index in regards to the direction i
 A_{wi} is the plan area of earthquake resistant walls in the direction i
 A_w is the total area of the earthquake resistant walls
 φ internal angle of friction
 β is an equivalent seismic static coefficient related to the design ground acceleration

Eq. 9.3 is valid if the cohesion is zero. To ensure the safety of the given buildings, $\gamma_{3,i}$ must be greater than 1.

If at least one of the indexes does not satisfy the safety criterion, that is, for instance $\gamma_{1,i} < 1.0$, the seismic vulnerability of the analysed edifice must be assessed with the more sophisticated methods of the level 2.

9.5. STUDY: LEVEL 2

Level 2 is to be applied only to edifices that have been considered seismically vulnerable in level 1. It brings more accuracy to the assessment of the seismic vulnerability but the calculations are more time-consuming than at level 1. They are based on the theory of plasticity; both lower and upper bound theorems are applied for defining the in-plane strength as well as the out-of-plane resistance to seismic actions.

As already explained in chapter 8, each edifice should be locally and globally approached. With the local approach, the seismic vulnerability of each structural parts is assessed. The global approach of a sacred edifice (seen as a group of macro-elements connected to each other) allows the identification of the incompatibilities of deformation at connections between two different structural system (bell-tower and nave, for instance).

9.5.1. DESCRIPTION OF THE STRUCTURE

First, in order to give a basis for the analysis of the local behaviour, the given structure must be described through standard units (see chapter 3) that correspond to macro-elements.

9.5.2. SEISMIC DEMAND

Swisscode SIA 261 is applied for defining the seismic demand. The procedure is the same as for common buildings though the spectral acceleration of macro-elements actually corresponds to the peak ground acceleration. However, no correcting factors (γ_f or behaviour coefficient) are applied. The impact of the ground quality is also taken into account as the Swisscode SIA 261 proposes. If seismic micro-zonation maps exist for the place where a given edifice is placed, they have to be used.

9.5.2.1. Choice of a suitable peak ground acceleration

For determining the seismic demand, it is proposed to used the design spectrum in the construction codes. However, at least in Switzerland, the peak ground acceleration in the Swisscodes as well as the seismic hazard (distribution of areas characterizing the seismic hazard) has been defined for common buildings. The earthquake of reference is indeed characterized by a return period of $T=475$ years. Since the life span of cultural heritage buildings is generally longer than 475 years, the peak ground acceleration given in usual construction codes is not really suitable for old edifices.

As the seismic demand is an important for determining the seismic vulnerability of buildings, the chosen value must fit the real situation. Consequently, the determination of a suitable value for the peak ground acceleration as well as for the seismic hazard in general must be undertaken in the future.

9.5.3. LOCAL BEHAVIOUR

The method for calculation is based on the application of the plasticity theory. The lower bound theorem is applied to each macro-element of a church; if required, the upper bound theorem can be applied in order to have the upper limit of the peak ground acceleration that results in a given damage of the studied case.

The out-of-plane behaviour of macro-elements (or standard units) is calculated by the application of the strip methods. Differently, the in-plane response of the studied macro-elements is defined thanks to the «library» of linear numerical simulations carried out for finding the flow of forces within each standard units recorded in Pre-Romanesque and Romanesque edifices.

Procedures for treating the local behaviour of each macro-element presented in chapter 3.5 are given in the next chapter. In order to be able to account for the impact of macro-elements on each other, the following order must be respected. In fact, the seismic response of bell-towers might have an impact on the neighbour macro-elements such as the front wall or the chancel arch (depending to which elements the bell-tower is connected to). Then, the front wall can influenced the seismic response of the lateral walls.

9.5.3.1. Bell-towers

Because of their slenderness and the impact they might have on the seismic response of other structural parts, the seismic response of bell-towers must be first analysed. The procedure for determining the seismic vulnerability of bell-towers is:

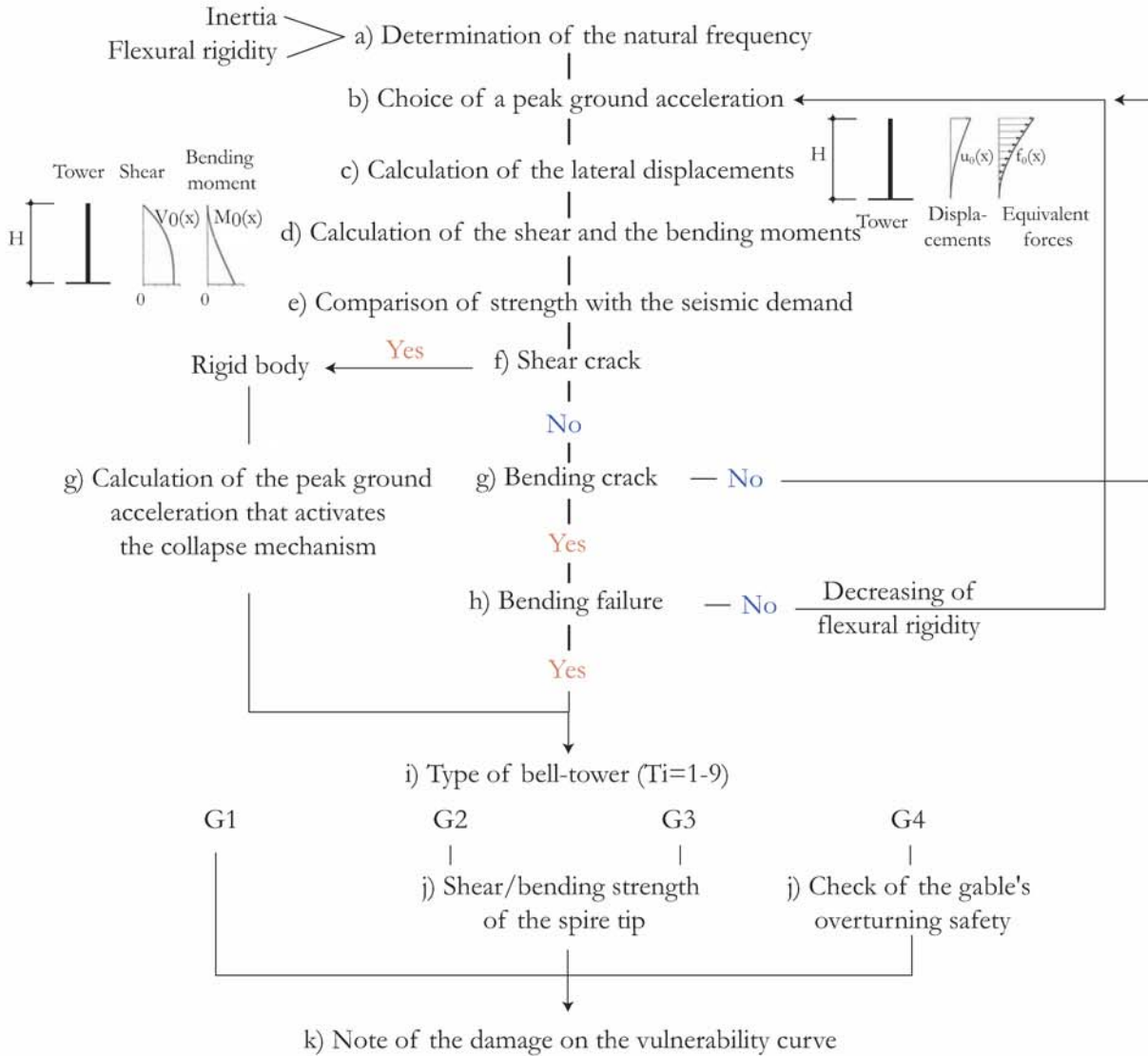


Figure 9.3 : Procedure for defining the seismic vulnerability of bell-towers.

Note: the G1 group comprehends the T5, T6 and the T9 types; G2: T1, G3: T4 and T8, G4: T3 and T7.

First, the moment of inertia (I), the flexural rigidity (EI) and the natural period and frequency (ω, f) must be defined for both axis (x, y) of the cross-sections. These values are calculated on the basis of the following assumptions: the mass is uniformly distributed on the height, the deformed structure has a ($\psi(z)=1-\cos(\pi z/2L)$) shape (chapter 8.5); it is assumed that the heavy self-weight makes the material stay in the elastic domain and the stiffness is constant along the height.

Based on the obtained values, lateral displacements and equivalent forces are calculated; from equivalent forces, it is quite an easy task to find the shear and bending moments. The comparison between the seismic demand and the strength of the cross-sections allows us to determine the peak ground acceleration that leads the most loaded cross-section to enter the plastic domain. The crack can be either due to the bending moment or shear; the aftermath are obviously not the same. In case of shear crack, the upper part of the structure (that was cut from the below one by the shear crack) will move like a rigid body.

In case of a bending crack, which is the most likely to happen (according to the observed damage (chapter 3)), the lateral load and the peak ground acceleration that lead to a loss of 20% of the flexural inertia are reported on a graph (lateral load vs peak ground acceleration). The flexural strength and natural period are then recalculated with the new inertia (that is 20% less than the initial one).¹ The seismic demand is once again compared with the structure bending and shear strength; if shear cracks appear, the aforementioned way must be followed. Otherwise, the lateral load and the peak ground acceleration that lead to a loss of 50% of flexural inertia are reported.

This process must be followed until a shear or a bending failure happens. The bending failure happens when, for a loss of 90% of flexural rigidity, the peak ground acceleration leads the rocking part of the tower, which is considered as being a rigid body, to its loss of stability. According to Betbeder, the loss of stability does actually not correspond to the collapse of the tower moving part; the peak ground acceleration must actually be higher to make this instable part collapse. Nevertheless, as the assumptions made for the overturning of plain massive walls cannot be apply for a tower (whose cross-section is composed of four walls), the maximal damage that a tower can sustain in this method is related to the peak ground acceleration that make the tower collapse without allowing for the cyclic movement generates by an earthquake. In consequence, such a value is not exact and in the safety side.

The seismic vulnerability of the upper part, that is, the tower tip or the gable, must also be checked.

Note: though the walls of bell-towers look like being connected to the masonry of neighbour parts, they often are not. Moreover, if masonries of two parts are interconnected, the cross-section of the bell-tower is massive compared with the thickness of other walls; the difference is too large for causing torsion in the bell tower. However, this no longer the case if there are tie-rods that connect tightly the bell-tower to the neighbour macro-element; then, the strength of the bell-tower to torsion must be verified. The determination of the location of the embedment can be found by applying the method of ambient vibrations, as shown in a study carried out on the Cathedral of Strasbourg.

1. From that time on, the flexural inertia is no longer constant along the height; to be exact, the variation of this value should be integrated as a function of the height.

9.5.3.2. Front walls

First, the structural behaviour of front walls under seismic loading must be assessed in one direction, that is, for instance, in their plane and then, out of their plane.

IN-PLANE STRUCTURAL BEHAVIOUR

The in-plane structural behaviour of front walls under lateral loading is assessed thanks to the graphs given under chapter 8.7.1. The proposed procedure is the following:

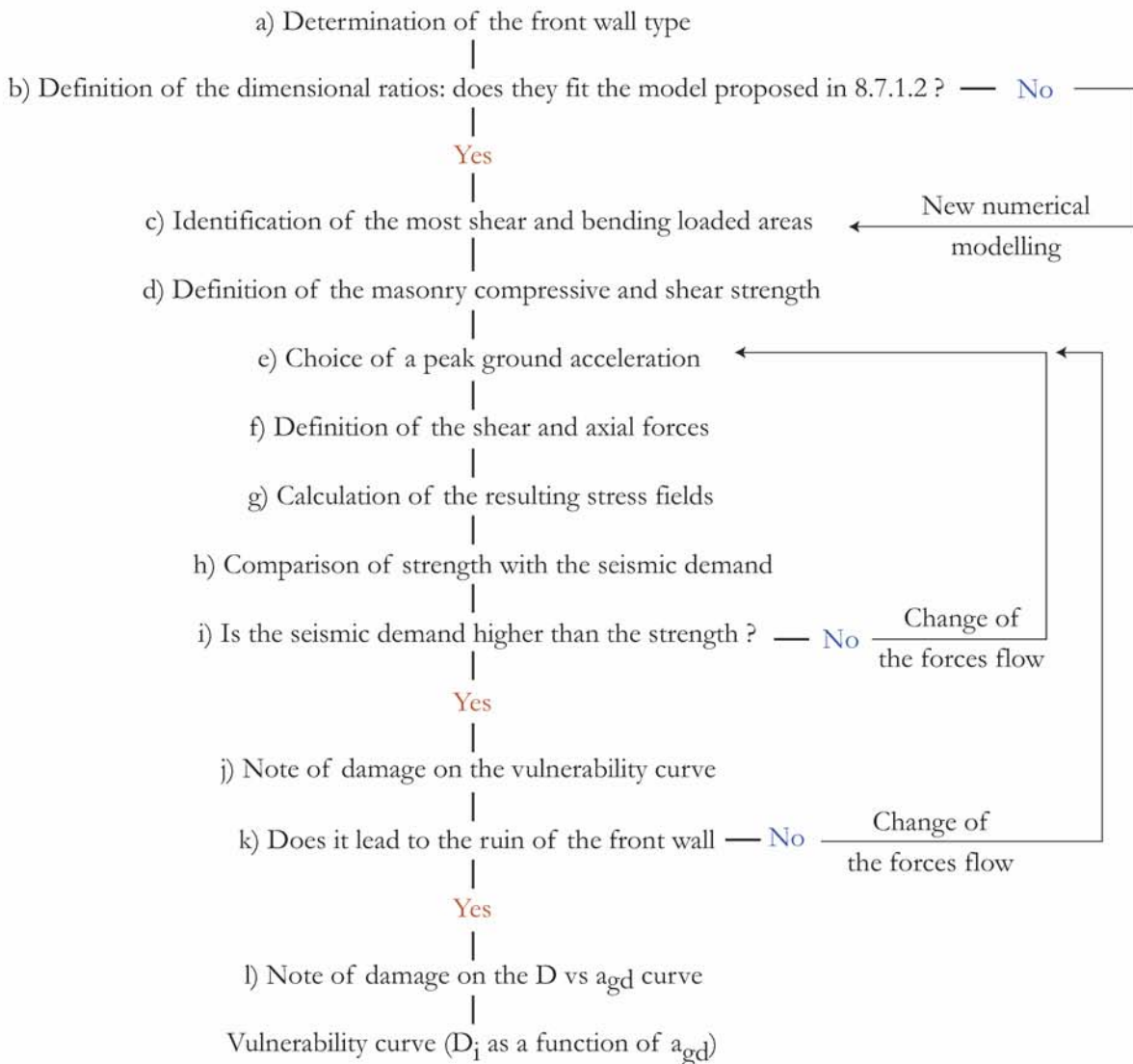


Figure 9.4 : Procedure for assessing the in-plane seismic vulnerability of front walls.

If the given type of front wall does not exist in the list given in chapter 4 or that there is no percentages available, a simple numerical modelling should be done.

Explanations

- a) The boundary conditions, i.e. the bearing conditions and the loading configuration must be determined.
- b) To apply the results (the flow of forces) of the model that is presented under 8.7.1.2, the dimensional ratios of the given FW front wall must be similar to that of the model in the «library». In case they are not too much different from the model's, the percentages given in 8.7.6.1 can be used. Otherwise, another numerical modelling must be done.
- c) Based on the chosen model and its results, the critical points must be highlighted.
- d) The mechanical properties of masonry must be calculated and/or measured.
- e) First, a low peak ground acceleration should be chosen; for instance, $a_{gd}=1\text{m/s}^2$.
- f) The flow of forces is defined according to the chosen model; in particular, the shear and axial force that load the critical elements of masonry must be defined according to the actual masses of the given lateral wall.
- g, h) Based on the values that are defined in the previous step, the resistance of the critical masonry parts must be calculated. In chapter 7, it is stated that Ganz's model (stress fields) is well adapted to find out the shear strength of a squat wall (or part of wall). Consequently, it is proposed to apply this model. However, if the bending moment is high in the studied part, Ganz's model gives an approximately strength value¹. In such a case, Coulomb's model can be used, also giving approximate values but easier to be calculated than that with Ganz's model. On the other hand, in the same chapter, it is seen that the FEMA model suits well for determining the flexural resistance of walls or parts of wall. Pillars with a circular cross-section must be adapted through the use of an equivalent rectangular area.
- i, j) If the masonry strength (shear or flexural strength) is higher than the forces resulting from the chosen peak ground acceleration, a new acceleration is to be chosen. On the contrary, if the forces are higher than the strength of masonry, the corresponding damage must be recorded on a D_i - a_{gd} graph (vulnerability curve). At the next step, with a higher peak ground acceleration, the positive difference² of percentage of shear force that would have flown within the damaged part must be dispatched into the neighbour parts.
- k) This procedure goes on the same way until the ruin of the front wall is reached.

1. Because of the difficulty to accurately define the eccentricity of the axial force.

2. i.e. the difference compared with the percentage of shear force that led to the failure of the damaged part (at the previous step, with a lower acceleration).

OUT-OF-PLANE BEHAVIOUR

The out-of-plane seismic response of the gable must be assessed first according to the procedure presented here below:

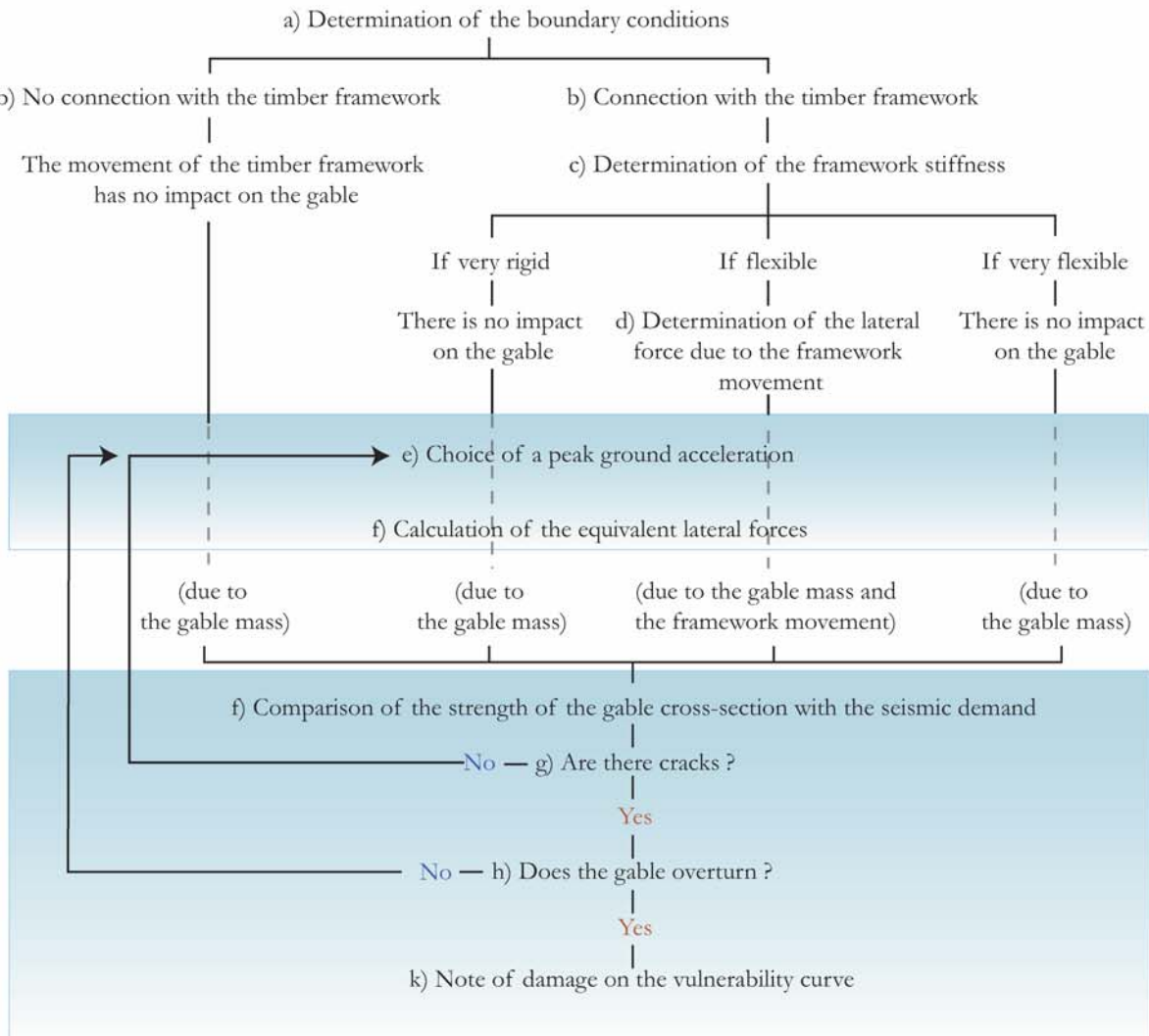


Figure 9.5 : Assessment of the out-of-plane seismic vulnerability of gables.

Note: by no connection, it is meant that the timber framework is simply put on masonry and when the timber beams are put in notches, it is called in the above diagram a connection. It does not mean that the beams are cramped to masonry.

- multiple-leaf masonry:

The procedure is similar to the previous one, which was adapted for one-leaf tympanums. Nevertheless, since one, two or the three layers of a multiple-leaf walls can overturn, the quality of the interfaces must be first determined in order to calculate the maximal acceleration that leads to the loss of stability. Then, the speed that makes the tympanum collapse has also to be determined.

2. The out-of-plane of the whole front wall is assessed with the following method:

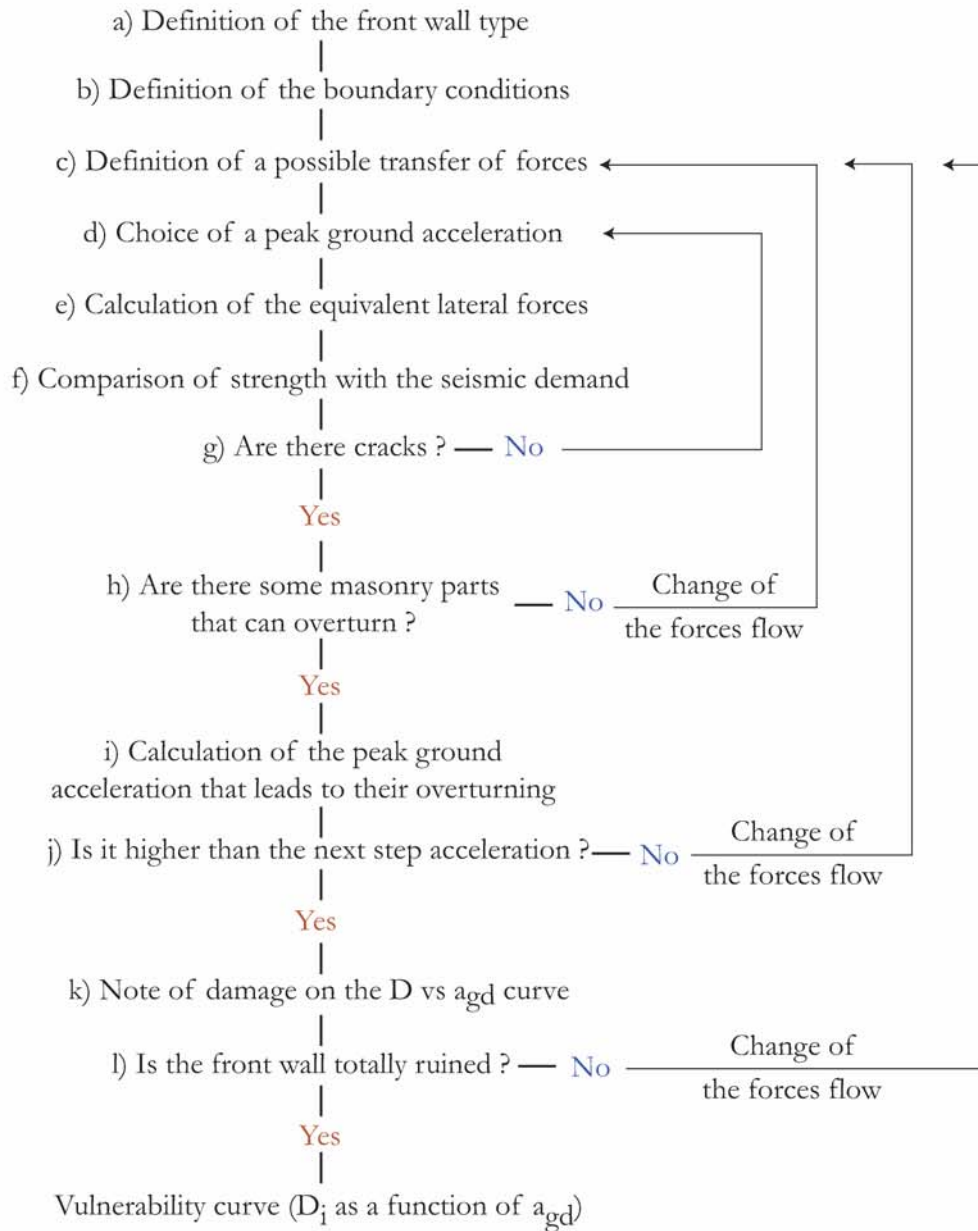


Figure 9.6 : Assessment of the out-of-plane seismic vulnerability of front walls.

Explanations

- a) First, the type of front wall is defined ($FW_{i=1-7}$)
- b) Boundary conditions must be defined first in order to set a possible transfer of forces within the structure. How bearings (front wall edges) are connected to the lateral walls and how strong are

the connections must be defined. Moreover, the presence of tie-rods must be taken into account.

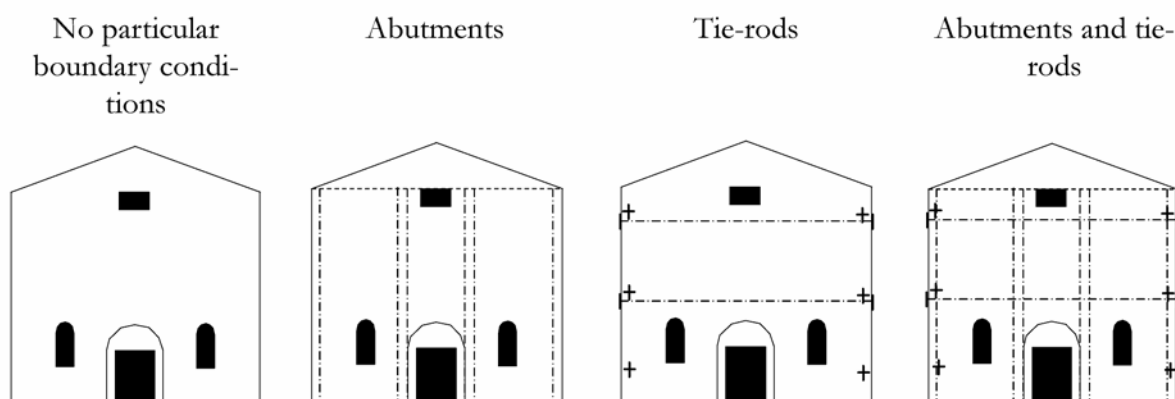


Figure 9.7 : Examples of boundary conditions.

- c) Possible transfer of forces is defined according to the type of front wall as well as the boundary conditions. Proposals for the most cases are made under chapter 8.7.1.
- d) Before the following calculations, a series of peak ground accelerations must be chosen. This choice will be based on the Swiss code SIA 261 [SIA 261 03], in relation with the seismic hazard of the area where the given edifice is located. Nevertheless, as aforementioned, the maximal peak ground acceleration that can be expected in the given area is higher than the value proposed in the Swisscode since a return period of 475 years was chosen for defining the seismic hazard.
- e) The equivalent forces (perpendicular to the wall) are calculated on the basis of what have been defined earlier; the forces generated by the equivalent forces are calculated too.
- f) Shear forces and bending moments are compared with the strength of cross-sections that are most likely to be overloaded.
- g) The above comparison leads to this point: are there cracks? If not, a new cycle with another peak ground acceleration can be undertaken. On the contrary, that is, if there are cracks, the stability of the separated part (there are actually at least two parts that are separated; what follows is only about the one that might move) must be checked (h). If the given part does not overturn under the chosen peak ground acceleration (i, j), a new cycle can begin (with a new value for the peak ground acceleration and the transfer of forces must be consequently adapted). If the part can overturn, the corresponding point, that is, a peak ground acceleration and the associated damage must be noted on the damage vs a_{gd} curve (k).
- l) Procedure goes on this way until the front wall is ruined.

9.5.3.3. Lateral walls

As for front walls, the structural behaviour of lateral walls under seismic loading must be assessed in both directions separately.

IN-PLANE STRUCTURAL BEHAVIOUR

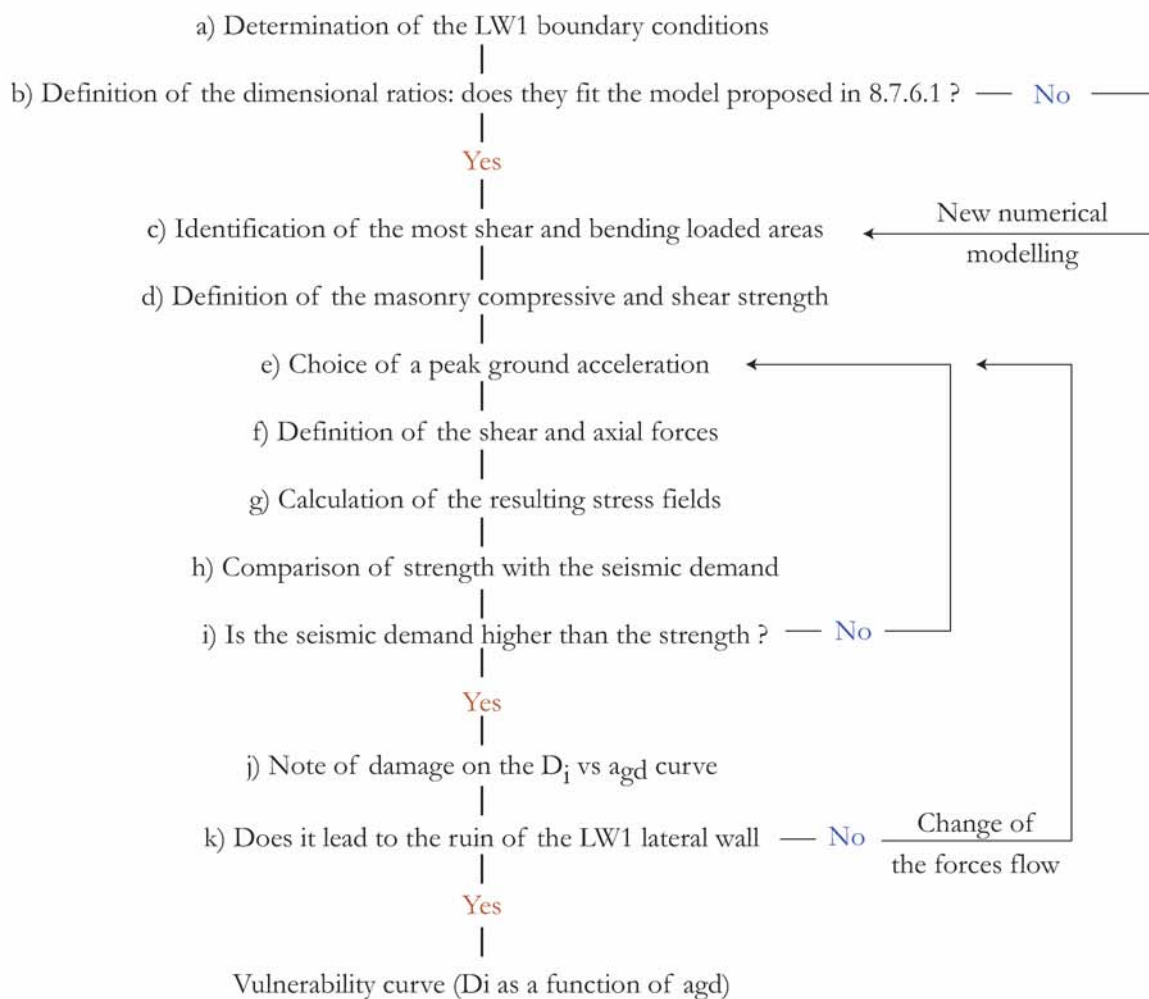


Figure 9.8 : Procedure for assessing the in-plane seismic vulnerability of the LW1 lateral walls.

Explanations

- The boundary conditions, i.e. the bearing conditions and the loading configuration must be determined.
- To apply the results (the flow of forces) of the model that is presented under 8.7.6.1, the dimensional ratios of the given LW1 lateral wall must be similar to that of the model. In case they are not too much different from the model's, the percentages given in 8.7.6.1 can be used. Otherwise, another numerical modelling must be done.
- Based on the chosen model and its results, the critical points must be highlighted.

- d) The mechanical properties of masonry must be calculated. If the whole procedure is followed and that the inner structure of walls as well as the bonding type are the same as that of the front wall, the mechanical properties found for the front wall can be reused.
- e) First, a low peak ground acceleration should be chosen; for instance, $a_{gd}=1\text{m/s}^2$.
- f) The flow of forces is defined according to the chosen model; in particular, the shear and axial force that load the critical elements of masonry must be defined according to the actual masses of the given lateral wall. Furthermore, forces corresponding to the bearing reactions of the front wall must be taken into account (see global behaviour).
- g, h) Based on the values that are defined in the previous step, the resistance of the critical masonry parts must be calculated. In chapter 7, it is stated that Ganz's model (stress fields) is well adapted to find out the shear strength of a squat wall (or part of wall). Consequently, it is proposed to apply this model. However, if the bending moment is high in the studied part, Ganz's model gives an approximately strength value¹. In such a case, Coulomb's model can be used, also giving approximately values but better than that from Ganz's model. On the other hand, in the same chapter, it is seen that the FEMA model suits well for determining the flexural resistance of walls or parts of wall. Pillars with a circular cross-section must be adapted through the use of an equivalent rectangular area.
- i, j) If the masonry strength (shear or flexural strength) is higher than the forces resulting from the chosen peak ground acceleration, a new acceleration is to be chosen. On the contrary, if the forces are higher than the strength of masonry, the corresponding damage must be recorded on a D_i - a_{gd} graph. At the next step, with a higher peak ground acceleration, the positive difference² of percentage of shear force that would have flown within the damaged part must be dispatched into the neighbour parts.
- k) This procedure goes on the same way until the ruin of the lateral wall is reached.

1. Because of the difficulty to accurately define the eccentricity of the axial force.

2. i.e. the difference compared with the percentage of shear force that led to the failure of the damaged part (at the previous step, with a lower acceleration).

B. OUT-OF-PLANE BEHAVIOUR

The out-of-plane seismic response must be assessed first according to the procedure presented here below:

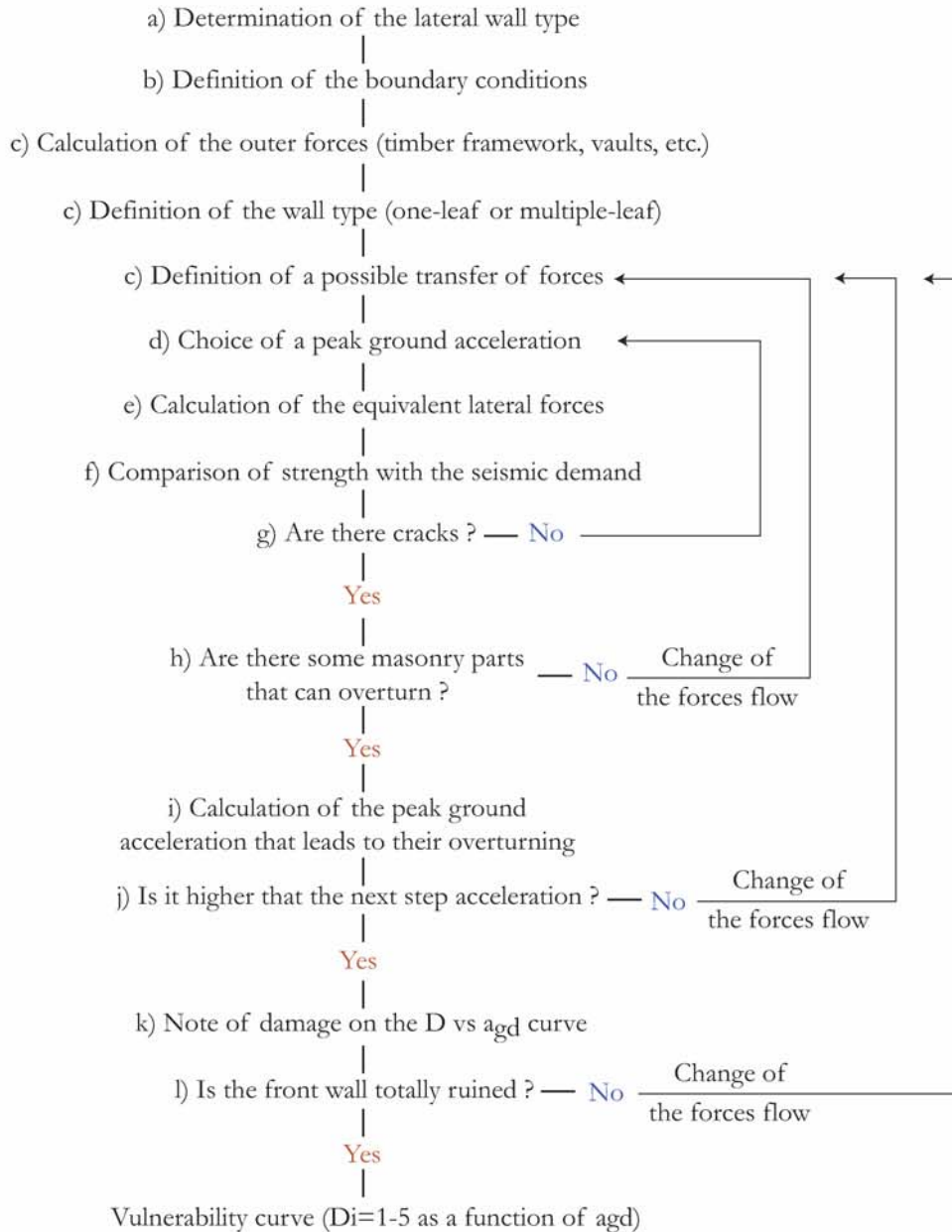


Figure 9.9 : Procedure for assessing the out-of-plane seismic vulnerability of the lateral walls.

As this procedure is the same as that for the front walls, the reader can find the explanations under the chapter 9.5.3.2.

9.5.3.4. Chancel arches

As all macro-elements, the seismic response of chancel arch must be addressed in both directions: in-plane and out of their plane. In fact, the procedures for the in-plane and out-of-plane check are similar to the ones presented for other macro-elements.

9.5.3.5. Ceilings

The seismic vulnerability of ceilings is treated differently according to their type. However, the main parameter for every kind of covering is the difference of displacement between the bearings. When considering the ceiling of the main nave, the vulnerability of the ceilings depends on movements of the LW1 lateral walls while the response of the LW2 walls influences the vulnerability of the low-aisles ceiling.

WOODEN CEILING

Usually, wooden ceilings are supported by transversal beams. Consequently, their seismic vulnerability depends on the stability of the bearings of those beams. The in-plane seismic response of lateral walls is generally the same since the nave of churches is symmetric. Consequently, only the out-of-plane movement of lateral walls, which can be different due the boundary conditions, can cause the loss of stability of the ceiling bearings.

To calculate the seismic vulnerability of the wooden ceilings, the difference of movement between two lateral walls must not be larger than the bearings length.

BARREL-VAULT

Barrel vaults are particularly vulnerable to different movements of their bearings. According to Barthel, only a displacement of 4 mm can result in the collapse of the barrel-vault. As for the wooden ceiling, the difference in the movement of both opposite walls that support the barrel vault must be assessed.

CROSS- AND GROINED VAULTS

According to Barthel, the case of the cross- and groined vaults are similar to that of the barrel vault.

9.5.4. GLOBAL BEHAVIOUR

The church as a whole is studied.

At that point, the impact of the macro-elements that can load another elements is taken into account. For instance, bell-towers can have an impact on the front wall, the lateral walls or even the chancel arch. Also, the front wall can have an impact on the lateral walls.

9.6. STUDY: LEVEL 3

Calculations at this level are the most accurate of the proposed methodology. Seismic response of a given edifice is defined through the use of numerical simulations (FEM). To be correct and close to reality, the calculations must be non-linear and must allow for the specificities of the composite material that masonry is.

Level 3 is devoted to sacred edifices whose results, that is, the seismic vulnerability, obtained with the level 2 calculations are not accurate enough compared with the required objectives. It also can be applied for some parts of the building that are too much complex to only be addressed with the level 2 models.

When the sacred building is characterized by a complex static system, such as the Cathedral of Basel, its seismic response, should be analysed through this level 3.

9.7. DIAGNOSIS

This step, which is actually the last one, can be considered as a summary of the three previous levels. Based on the results that are obtained at the level 2 or 3, the following path must be followed:

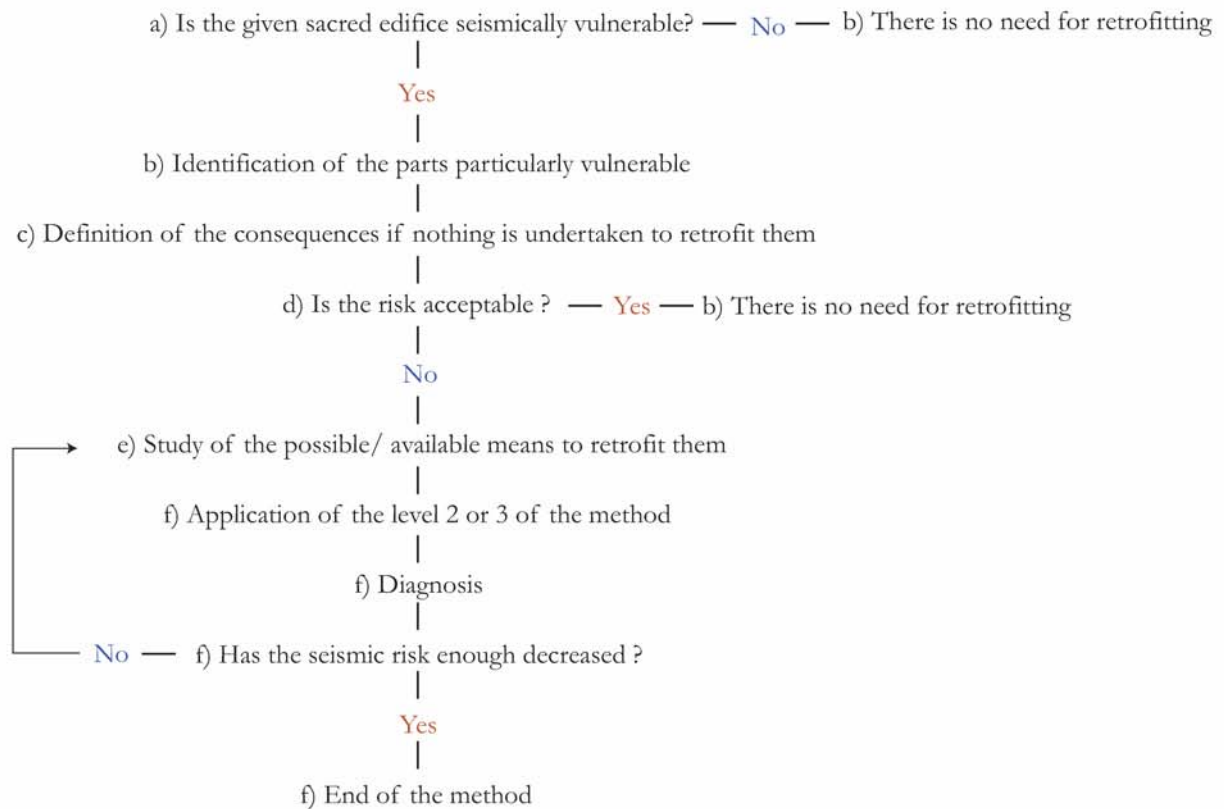


Figure 9.10 : Procedure for the diagnosis phase.

9.8. DISCUSSIONS AND CONCLUSIONS

The fact that this methodology is based on four steps is very useful; the first level permits to sort out the churches that are not seismically vulnerable. Since calculations at this step are quickly made, it permits a gain of time.

Calculations of the second step are also easy to make because they use simplified models (theorems of the plasticity theory). However, even if the applied models simplified reality, they proved to give valuable results. Moreover, the procedures for the assessment of the out-of-plane and in-plane seismic vulnerability are similar for every macro-element. This contributes to the rapidity of execution

of this method. Nevertheless, if the «library» with the in-plane flow of forces does not contain the studied standard units or if the proportions are too much different from the existing one (in the «library»), a new numerical simulation must be carried out. However, since the required numerical simulation is a linear one, it can be rapidly made with a common FEM software.

If the edifice is too complicated, the level 3 can be applied. Furthermore, it can be applied for more accurate results when the sacred edifice is of prime importance for the building heritage.

When the seismic vulnerability of every macro-element is assessed, their vulnerability curve is compared with the seismic demand. Every graph put side-by-side gives a good overview of the seismic vulnerability of the edifice.

10.1. INTRODUCTION

This section is devoted to a case study; the objective is to show how to proceed with the methodology by applying it to an example that is fictitious. The edifice is a representative medium-size Romanesque basilica.

10.2. GENERAL SURVEY

1. PLANS, DIMENSIONS

The given edifice is composed of a five-bay main nave and two low-aisles, each being ended by a semicircular apse. The front wall was built side-by-side with a bell-tower whose foundations coincide with the first bay of one lateral aisle. The nave is covered by cross-vaults, while the semicircular apses ceiling is half a dome.

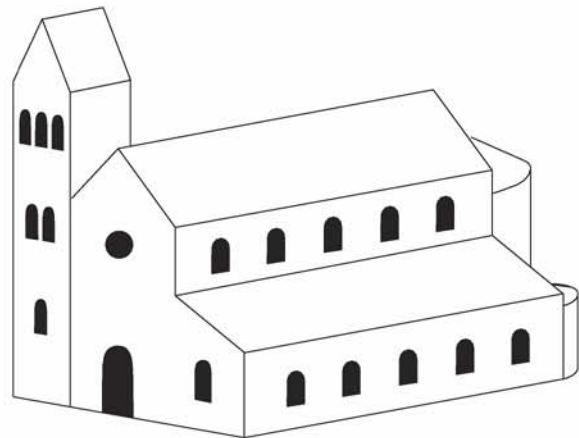


Figure 10.1 : View of the church.

Here below are a ground plan.

PLAN

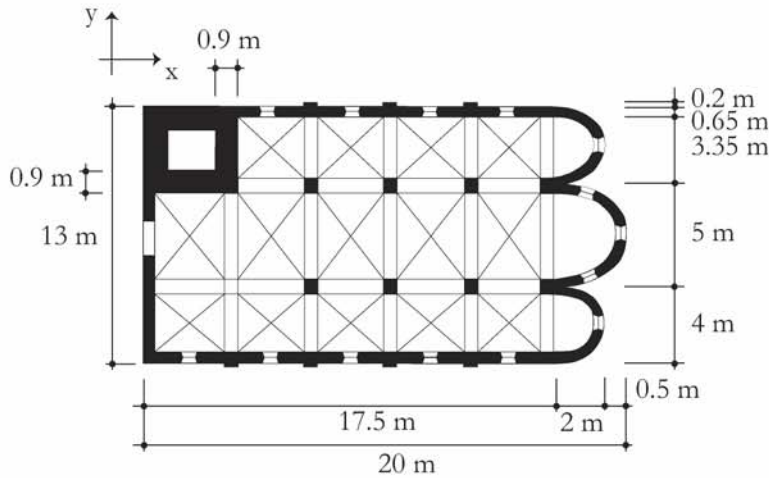


Figure 10.2 : Plan of the church.

The church was built on a rocky ground (soil class A in the Swisscode SIA 261); there is no site effects.

2. IN SITU SURVEY

The edifice is undamaged; there are no cracks, no damage, no degradation of materials and no transformations that took place after the building completion.

3. STATIC DIAGRAM

The vertical bearing structure is composed of the lateral walls (LW1 and LW2, x direction) as well as the front wall and the chancel arch (y direction).

4. MECHANICAL PROPERTIES

The masonry is made up of square dressed stone of molasse; experimental investigations allowed us to obtain the molasse compressive strength, the masonry shear strength and its displacement ductility. The masonry compressive strength (f_x , f_y) of the outer leaves is then defined according to the Swisscode SIA V178 as the Young's modulus. These values are:

Table 10.1: Mechanical properties of the given masonry (one-leaf walls)

$f_{x, \text{mol}}$ [MPa]	$f_{x, \text{ma}}$ [MPa]	$f_{y, \text{ma}}$ [MPa]	$\tan\phi$ [-]	E [MPa]
31.5	15	7.5	0.75	4412

Walls are constituted of three leaves; the compressive and shear strength of the multiple-leaf walls are:

Table 10.2: Mechanical properties of the multiple-leaf walls:

$f_{x, \text{filling}}$ [MPa]	$f_{x, \text{ma}}$ [MPa]	$f_{y, \text{ma}}$ [MPa]	$\tan\phi$ [-]	E [MPa]
31.5	15	7.5	0.75	4412

Assumption: masonry is similar and of constant quality every where in the edifice.

10.3. STUDY: LEVEL 1

As a first look at the seismic vulnerability of the given edifice, the index method that has been developed by Lourenço et al., is applied.

10.3.1. INDEX 1

IN X-DIRECTION

$$\gamma_{1,x} = A_{wx}/S = 35.6^1 / 249.9 = 0.14 > 0.1$$

Where:

- A_{wx} is the ground area of the resisting walls in x-direction
- S is the ground surface of the edifice.

IN Y-DIRECTION

$$\gamma_{1,y} = A_{wy}/S = 21.5^2 / 249.9 = 0.086 < 0.1$$

10.3.2. INDEX 2

IN X-DIRECTION

$$\gamma_{2,x} = A_{wx}/G = 35.6 / 11.72 [\text{MN}] = 3.04 > 1.2^3$$

Where:

- A_{wx} is the ground area of the resisting walls in x-direction
- G is the structure self-weight.

IN Y-DIRECTION

$$\gamma_{2,y} = A_{wy}/G = 21.5 / 11.72 [\text{MN}] = 1.8 > 1.2$$

10.3.3. INDEX 3

IN X-DIRECTION

$$\gamma_{3,x} = A_{wx}/A_w * \tan(\varphi) / \beta = 35.6 / 57.1 * 0.4 / 0.16 = 1.56 > 1.0$$

Where:

- A_{wx} is the ground area of the resisting walls in x-direction
- A_w is the ground area of every bearing walls
- $\tan(\varphi)$ is the tangent of the internal angle of friction; a value of 0.4 is proposed by [LR 06] and corresponds to the EC8.
- β is a factor for allowing for the ground acceleration; in this case, it is $\beta = 0.16$ ($a_{gd} = 1.6 \text{ m/s}^2$; Zone 3b, SIA 261, ground category: A).

1. As simplification for the calculation, the apses shape is assumed to be rectangular.
2. As simplification for the calculation, the apses shape is assumed to be rectangular.
3. The maximal value of 1.2 is proposed for places characterized by a high seismicity.

IN Y-DIRECTION

$$\gamma_{3,y} = A_{wy} / A_w * \tan(\varphi) / \beta = 21.5 / 57.1 * 0.4 / 0.16 = 0.94 < 1.0$$

10.3.4. DISCUSSIONS

Table 10.3: Summary of the index values:

$\gamma_{1,x}$ [-]	$\gamma_{1,y}$ [-]	$\gamma_{2,x}$ [m ² /MN]	$\gamma_{2,y}$ [m ² /MN]	$\gamma_{3,x}$ [-]	$\gamma_{3,y}$ [-]
0.14	0.086	3.04	1.8	1.56	0.94

According to the obtained values ($\gamma_{1,y}, \gamma_{3,y}$), the given edifice is seismically vulnerable in its y-direction, that is, perpendicular to the vessel axis. Although this conclusion is not confirmed by the second index, this church is considered as seismically vulnerable since there are two indexes that do not satisfy the required value.

Based on these conclusions, the church seismic vulnerability is checked through the application of more sophisticated methods.

10.4. STUDY: LEVEL 2

10.4.1. DESCRIPTION OF THE STRUCTURE

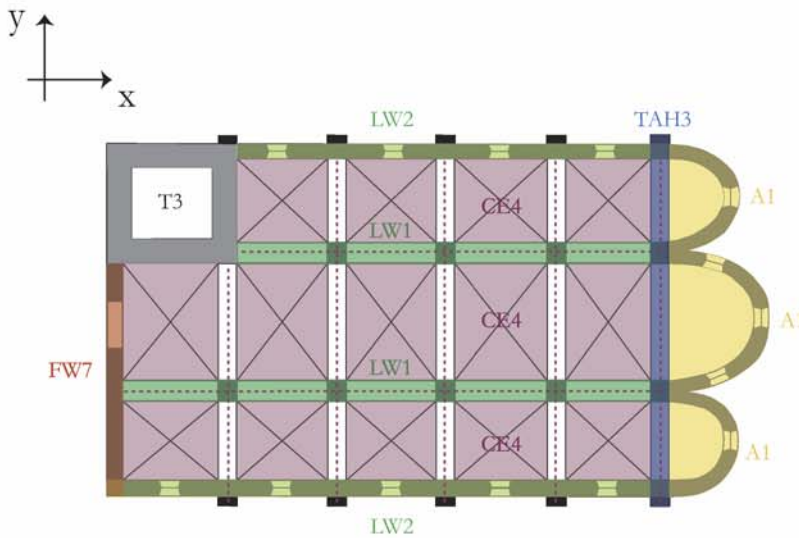


Figure 10.3 : Application of the characterization method on the given church.

Church part	Units	Comments
East side	A1 (3x)	The east side is composed of three half-dome-shaped apses.
Chancel arch	TAH3 (1x)	There is one unit that shares the east side of the church.
Nave	LW2 (2x), LW1 (2x), CE4 (14x)	The whole nave is covered by cross-vaults.

Front wall	FW7 (1x)	The bell-tower had existed before the construction of the rest of the church.
Tower	T3	

10.4.2. LOCAL BEHAVIOUR

Following the description of the edifice, a first global understanding of the seismic response must be done. In particular, the structural parts that might influence the seismic behaviour of other parts must be identified. In respect to the given example, the bell-tower can damage other structural parts because of its natural frequency is different.

10.4.2.1. Bell-tower

The bell-tower was built independently from the rest of the church. Masonry of the front wall, the north lateral wall and the transversal structure of the nave is only put against the masonry of the bell tower; there is no tight connection between the tower and the rest of the church.

3D VIEW, PLAN AND ELEVATION

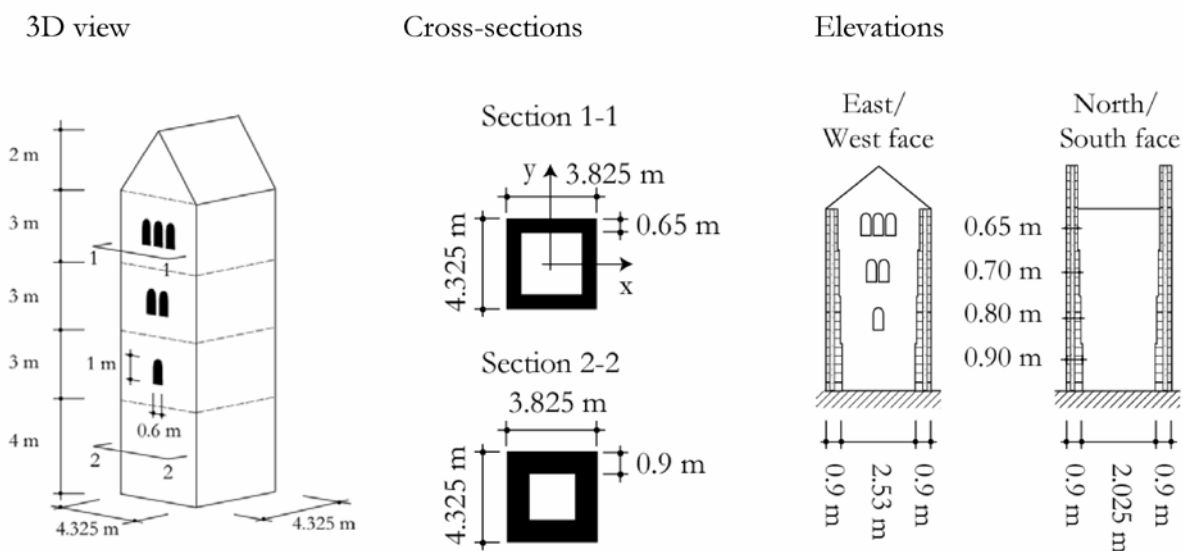


Figure 10.4 : 3D view, cross-sections and elevation of the tower.

DEFINITION OF THE NATURAL FREQUENCY

The tower properties:

Height: 13 m^a

Cross-sectional area: $A=9.55 \text{ m}^2$ ^b

Mass per unit of height: $m=21954 \text{ Kg}^c$

Second moment of area (moment of inertia):

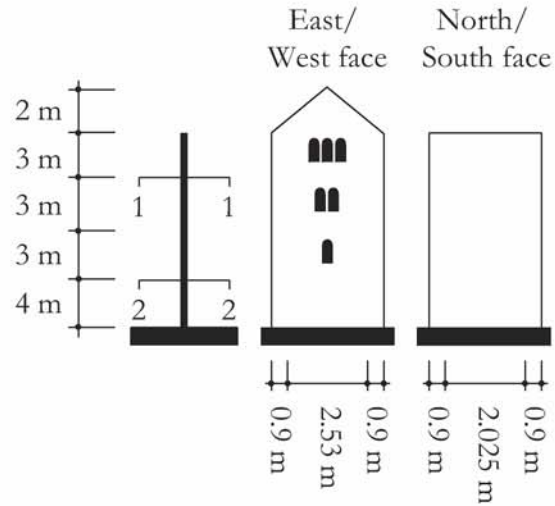
In x-axis: 15.88 m^4 .

In y-axis: 13.21 m^4 .

Flexural rigidity:

In x-axis: 7.07 Nm^2 .^d

In y-axis: 5.88 Nm^2 .



- a. The gable does not take in the global movement.
- b. The cross-sectional area is calculated with a mean thickness.
- c. The weight per unit of volume is: $\gamma=23\text{KN}/\text{m}^3$.
- d. The flexural rigidity is assumed to be constant on the height of the tower, though it is not right.

Figure 10.5 : Model (cantilever) of the tower.

The natural period is:

In x-axis: $\omega_n=38.85 \text{ rad/sec}$.

In y-axis: $\omega_n=35.43 \text{ rad/sec}$.

Then, the period and the natural frequency are:

In x-axis: $T_n=0.16 \text{ sec}; f_n= 6.18 \text{ sec}^{-1}$

In y-axis: $T_n=0.18 \text{ sec}; f_n= 5.64 \text{ sec}^{-1}$

Contrary to design calculations where a new building must resist a peak ground acceleration defined by building codes, the idea here is to find the peak ground acceleration that leads to the edge of the elastic domain. The lateral acceleration is then defined thanks to the elastic spectrum given in the SIA 261 [SIA 261 03]; the foundation ground (rock) belongs to the category A, the viscous damping level is fixed to 3% for unreinforced masonry (see [PP 92]). The elastic lateral acceleration becomes:

$$S_e = 2.5 \cdot a_{gd} \cdot S \cdot \eta \quad \text{for} \quad T_B \leq T \leq T_C$$

Where :

- a_{gd} is the peak ground acceleration
- S a factor for taking into account the ground quality (for category A, $S=1$)

- η is a correcting coefficient depending on the viscous damping ratio.

$$\eta = \sqrt{\frac{1}{0.5 + 10\xi}} = 1.12 > 0.55$$

RESULTS:

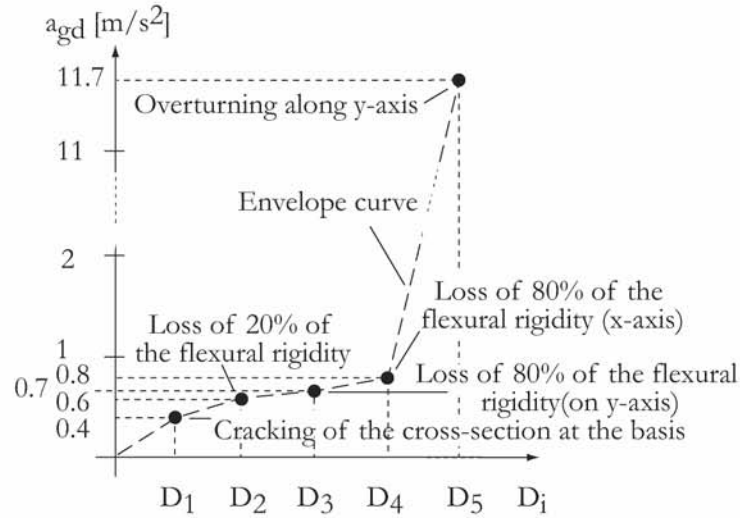


Figure 10.6 : Vulnerability curve of the bell-tower.

The out-of-plane behaviour of the gable is given on the following graph:

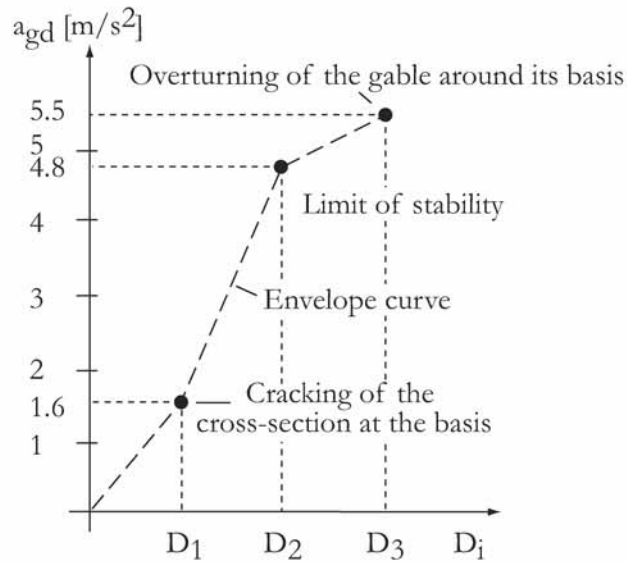


Figure 10.7 : Vulnerability curve of the gable.

Note: the limit of stability corresponds to the moment the resultant goes out of the cross-section.

10.4.2.2. Front wall

The front wall plan:

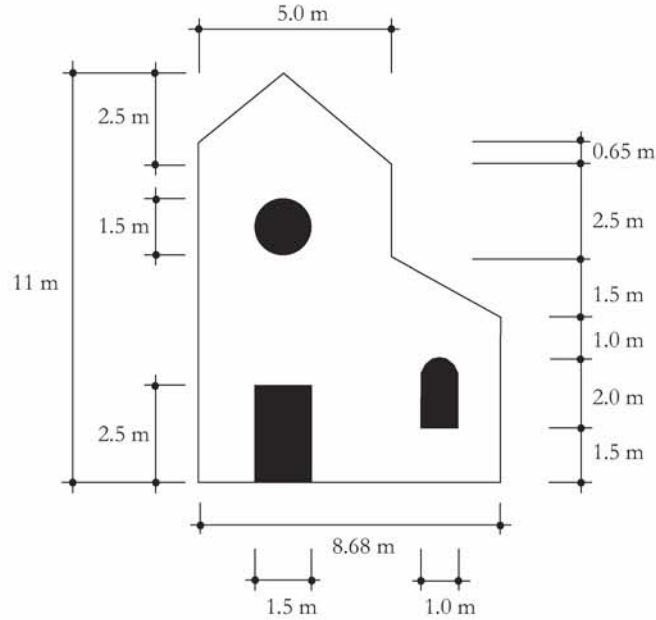


Figure 10.8 : Plan of the front wall.

OUT-OF-PLANE BEHAVIOUR

1. Out-of-plane response of the gable

It is assumed that the masonry (multiple-leaf) is compact; furthermore, the rosace is far enough from the basis cross-section of the gable and the cracks it can generate (in-plane response) have no influence on the gable out-of-plane response.

- a) Boundary conditions: restrained along the basis
- b) There is no connection with the timber framework of the nave (beams are put above masonry).
- c) Calculation of the equivalent forces and the resultant eccentricity:

According to the calculation, the peak ground acceleration that make the resultant go out of the cross-section is: $a_{gd}=3.8 \text{ m/s}^2$; after Betbeder, the peak ground acceleration that would lead to the overturning is: $a_{gd}= 5.5 \text{ m/s}^2$. It is worth noting that the gable cross-section is cracked under an a_{gd} of 1.2 m/s^2 .

2. Out-of-plane response of the whole facade

The front wall is of FW7 type.

With respect to boundary conditions, there are neither tie-rods, nor abutments.

Only the outward-directed seismic forces are considered (most defavourable case).

The distribution of forces (α , β , etc.) is defined according to the dimensions of the given areas.

The chosen transfer of forces is the following:

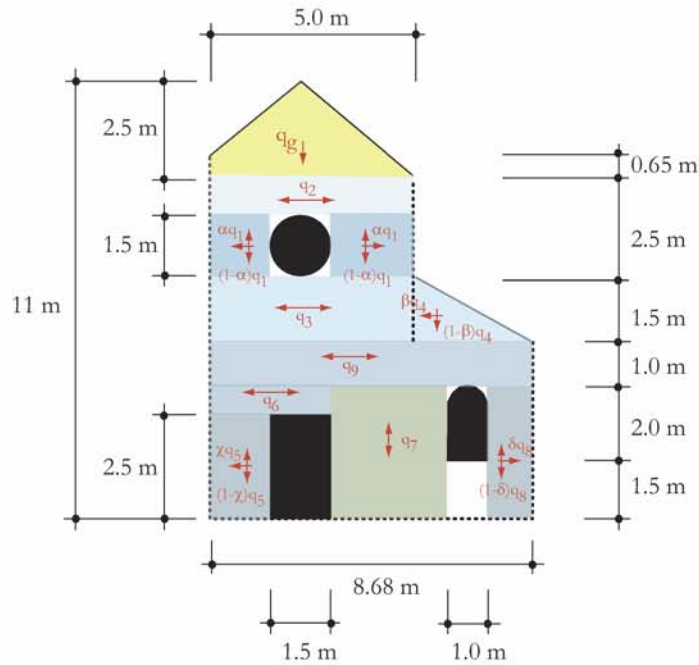


Figure 10.9 : Chosen transfer of forces within the FW7 front wall of the case study.

According to the above transfer of forces, the creation of hinges is observed along the edges of the parts 1, 2, 3, 4, 6 (the left edge) and 9 under a small out-of-plane acceleration ($a_{gd} < 0.05 \text{ m/s}^2$). These hinges change the transfer of forces.

Then, a few parts get separated (detachment) from the perpendicular walls; this is the case for the part 2 ($a_{gd} = 0.082 \text{ m/s}^2$), 9 ($a_{gd} = 0.085 \text{ m/s}^2$), 4 ($a_{gd} = 0.1 \text{ m/s}^2$) and 6 (along the left edge; $a_{gd} = 1.15 \text{ m/s}^2$). At that time, another transfer of forces must be allowed for.

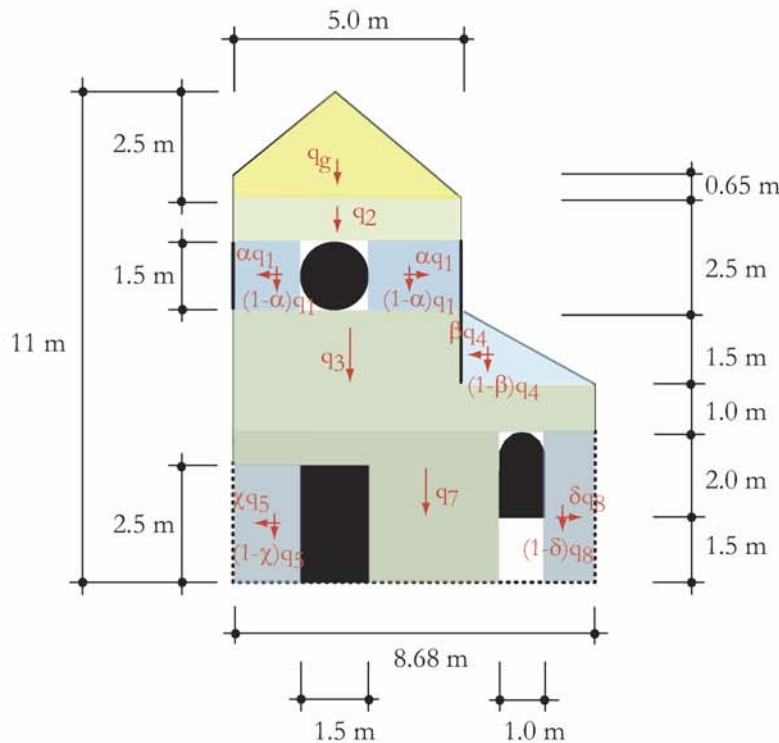


Figure 10.10 : Transfer of forces within the FW7 front wall of the case study after a out-of-plane acceleration of 1.15 m/s^2 .

Note: the bold continued lines mean a hinged edge; the thin continued lines mean a detachment (crossing crack) and the dotted lines still mean a restrained edge.

Since the boundary conditions of the gable changed, its stability must be checked once again: if the vertical edges of part 1 and 4 can resist the lateral bearing reactions, cracking would occur under an out-of-plane acceleration of 0.8 m/s^2 , while the lost of stability happens for an acceleration of 2.57 m/s^2 . This upper part would collapse under an acceleration of 4.54 m/s^2 .

Quick further calculations show that the vertical edges of parts 1 and 3-4 can no longer resist the action coming from the out-of-plane response of the upper part (gable and part 2): they get completely cracked (detachment of the parts 1, 3 and 4). The transfer of forces changes then.

On the contrary, parts 5 and 8 vertical edges still resist the lateral forces coming from the parts above them. First, the cross-section gets cracked ($a_{gd}=0.3 \text{ m/s}^2$) and the edges of parts 5 and 8 finally detached from the lateral walls ($a_{gd}= 0.8 \text{ m/s}^2$).

From then, the whole facade is free to move out of its plane and, from an engineering point of view, behaves like a cantilever (restrained along its basis). The basis cross-section gets cracked

under $a_{gd}=0.2 \text{ m/s}^2$, the resultant goes out of its for a $a_{gd}=0.6 \text{ m/s}^2$ (loss of the facade stability); it collapse under a peak ground acceleration of $a_{gd}=2.2 \text{ m/s}^2$ (according to Betbeder).

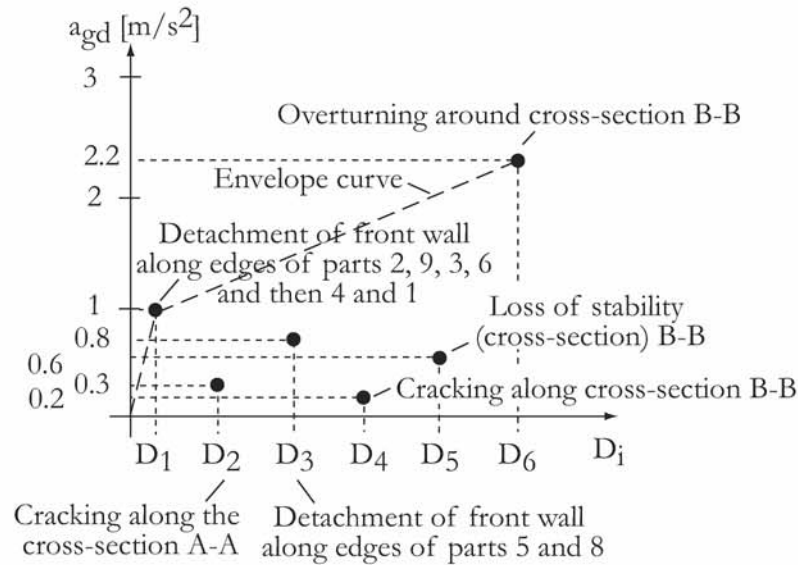


Figure 10.11 : Out-of-plane vulnerability curve of the front wall.

Note: the cross-section A-A is situated at the gable's base whereas the cross-section B-B is at the base of the whole façade.

What is shown on the above figure is that a peak ground acceleration of 1 m/s^2 is first required to cause the first damage D1 that is the detachment of a few edges. Then, if the peak ground acceleration is greater than 1 m/s^2 , all the following damage, except D6, will happen. However, if this is not the case, that means that at the next cycle, the peak ground acceleration must be greater than 0.3 m/s^2 to cause damage D2. This information is valuable in the context of a cyclic loading like earthquakes. Moreover, this also indicates which parts could be reinforced first in order to enhance the level of the first damage to a given edifice.

IN-PLANE BEHAVIOUR

1. Shear strength

The proportions correspond to the model. According to the percentages given under chapter 8.7.6.1, the following safety factor are obtained:

Table 10.4: Safety factors for the strength to shear of the parts 1, 2 and 3 (Figure 8.48).

Parts	$a_{gd}=1 \text{ m/s}^2$	$a_{gd}=2 \text{ m/s}^2$	$a_{gd}=3 \text{ m/s}^2$	$a_{gd}=4 \text{ m/s}^2$
1	3.9	2.5	1.9	1.4
2	5.1	3.0	2.1	1.6
3	5.1	3.0	2.0	1.5

In consequence, part 1 will fail before both parts 2 and 3. However, this will probably not happen in Switzerland since the required peak ground acceleration is great.

2. Strength to bending moments

The parts that might be damaged because of a high bending moments are parts 4 (to the left of the door) and 7 (to the right of the window). Once again, graphs of Figure 8.50 and Figure 8.51 of chapter 8 are used; applying the FEMA equation for rocking failure, the safety factor for these three sections is (for an a_{gd} of 3m/s^2):

- Part 4: 3.8
- Part 7: 2.3

Once again, if we assume that the distribution of forces will be still the same under higher ground accelerations, then a rocking might appear in part 7 for an a_{gd} of 7m/s^2 .

10.4.2.3. Lateral walls

The main nave walls are of LW1 type; there is the front wall at one extremity and the apses at the other. Moreover, in respect to the boundary conditions, since the naves are covered with cross-vaults, the arcades pillars go forth up to the vaults springings.

The LW1 units:

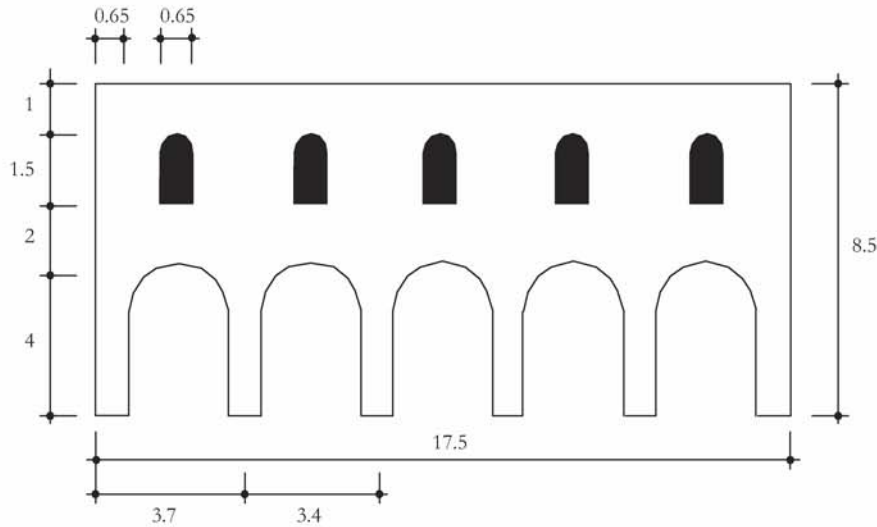


Figure 10.12 : Plan of the main nave lateral walls.

Low-aisles lateral walls are of LW2 type:

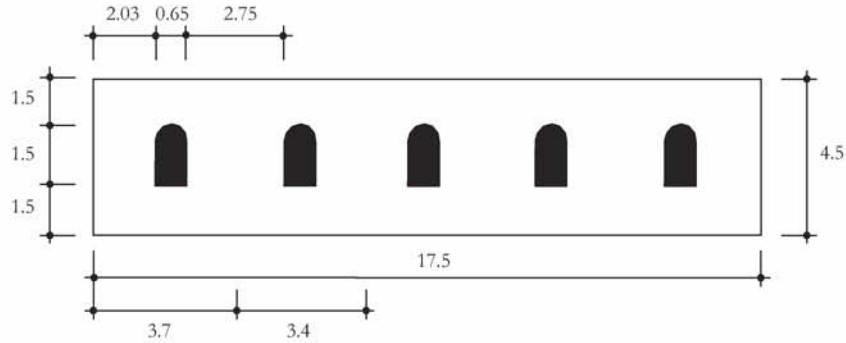


Figure 10.13 : Plan of the low-aisles lateral walls.

OUT-OF-PLANE BEHAVIOUR

The lateral walls of the main nave are dealt with at first; the treatment of the low-aisles walls follows.

1. Lateral walls of the low-aisles

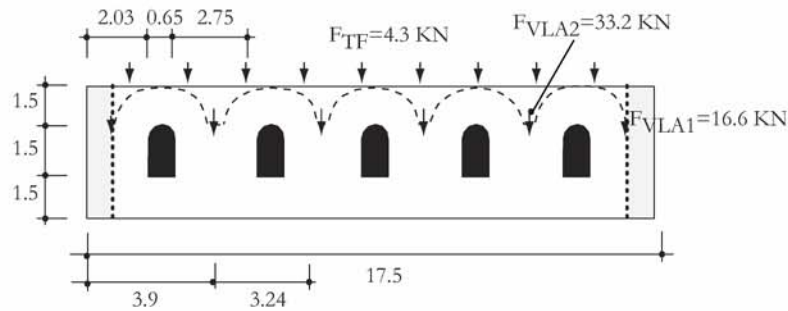


Figure 10.14 : Actions loading the low-aisles lateral walls.

OUT-OF-PLANE

The transfer of forces is:

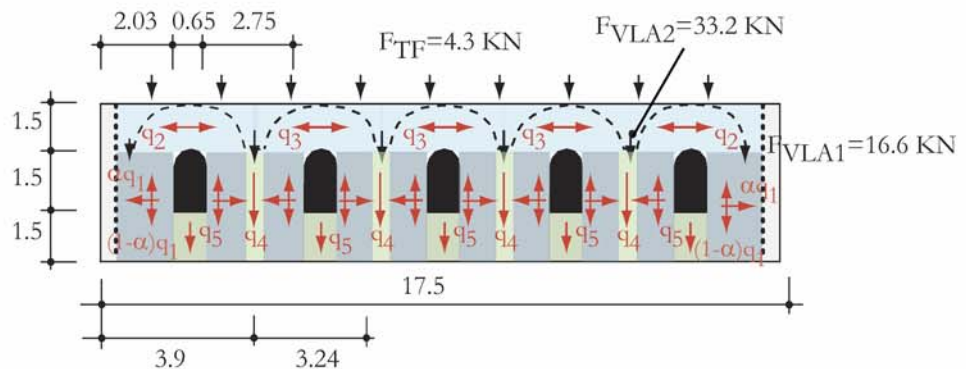


Figure 10.15 : First chosen transfer of forces for the low-aisles lateral wall.

1. First, the q_1 load is calculated; in every case, as masonry does not resist any bending moments, the edges are directly cracked for a small out-of-plane acceleration ($a_{gd} < 0.01 \text{ m/s}^2$). In consequence, the resulting transfer of forces is different.

At that point, a quick calculation shows that parts at the wall extremities cannot resist more than the horizontal thrust resulting from an arch (in part 2) created under an a_{gd} of 0.02 m/s^2 . At that moment, the only way to keep a constant thrust is to increase the arch rise; doing so results in the cracking of the vertical edge at the extremity under a slightly higher acceleration.

The resulting transfer of forces is:

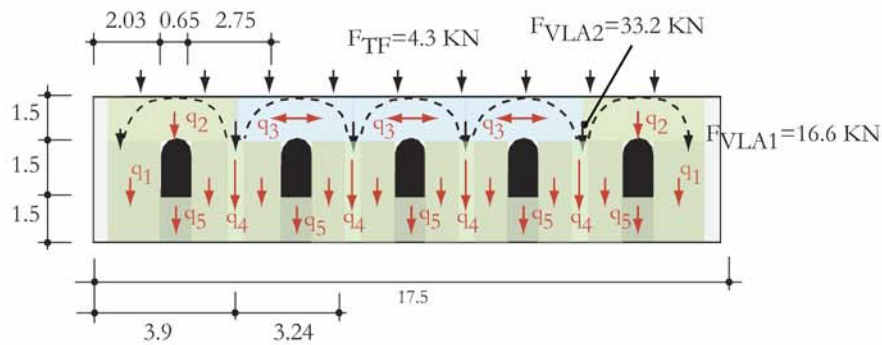


Figure 10.16 : Resulting transfer of forces after a peak ground acceleration of 0.02 m/s^2 .

Based on the assumption that the bay walls at the extremities can no longer counteract the q_3 arch horizontal thrust since they are cracked, parts 3 get detached from the part 4 under an acceleration of 0.4 m/s^2 . The transfer of forces changes and becomes:

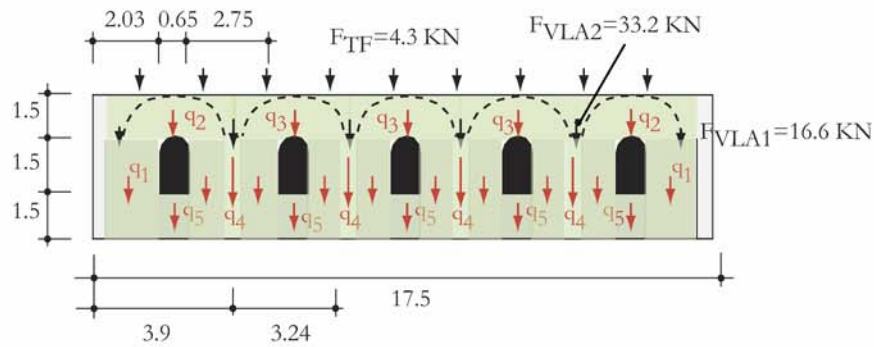


Figure 10.17 : Resulting transfer of forces after a peak ground acceleration of 0.4 m/s^2 .

The loss of stability of parts 1 and 2¹ happens for an acceleration of 1.36 m/s², while it would overturn under an a_{gd} of 3.3 m/s².

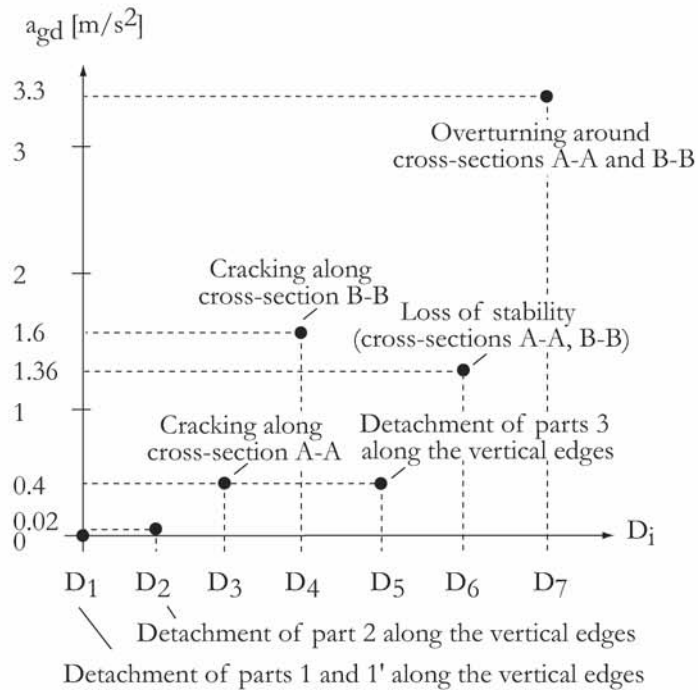


Figure 10.18 : Vulnerability curve (out-of-plane) of the LW2 lateral walls.

Note: the cross-sections A-A and B-B are situated at the base of the facade (they correspond to the abutments cross-section and the cross-section of the normal wall).

IN-PLANE BEHAVIOUR

1. Shear strength

A simplified approach of the method that is proposed under chapter 9.5.3.2 is used: the maximal chosen peak ground acceleration is directly applied. Proportions of the model in the «library» correspond to the given structural component. As flexion forces are lower than shear, only the resistance to shear must be checked. According to the percentages given under chapter 8.7.6.2, the following safety factor are obtained:

Table 10.5: Safety factors for the resistance to shear of the piers between windows.

Parts	a _{gd} =1 m/s ²	a _{gd} =2 m/s ²	a _{gd} =3 m/s ²	a _{gd} =4 m/s ²
a	18.1	8.4	5.2	3.9
b	12.0	5.2	3.3	2.5
c	10.0	4.8	3.2	2.4
d	8.7	4.5	3	2.2

1. The loss of stability of parts 1 and 3 (in the middle)

e	8.1	4.4	3.1	2.3
f	15.2	8.8	6.4	4.8

2. Lateral walls of the main nave

According to the methodology (see chapter 8), the next step is the calculation of the outer forces, such as the timber framework dead load¹, the wooden ceiling load and the vaults self-weight.

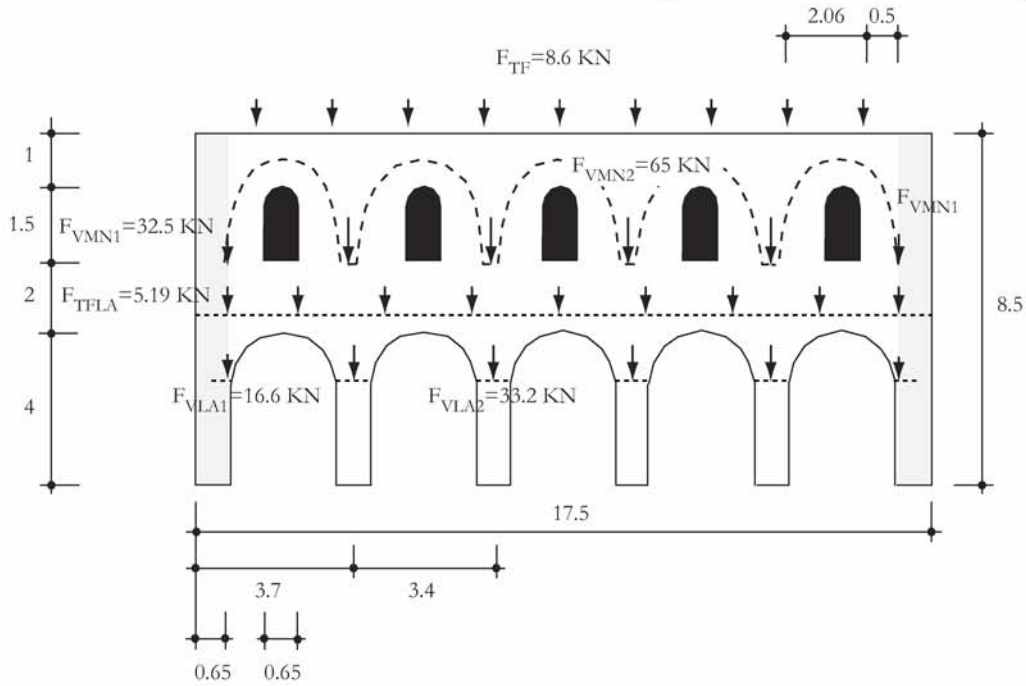


Figure 10.19 : Vertical forces on the main nave lateral walls².

1. No other actions, such as snow for instance, are taken into account.
 2. The longer lateral wall is considered here; however, though there one bay less in the opposite lateral wall, the transfer of forces does not change.

The initial transfer of forces is (choice):

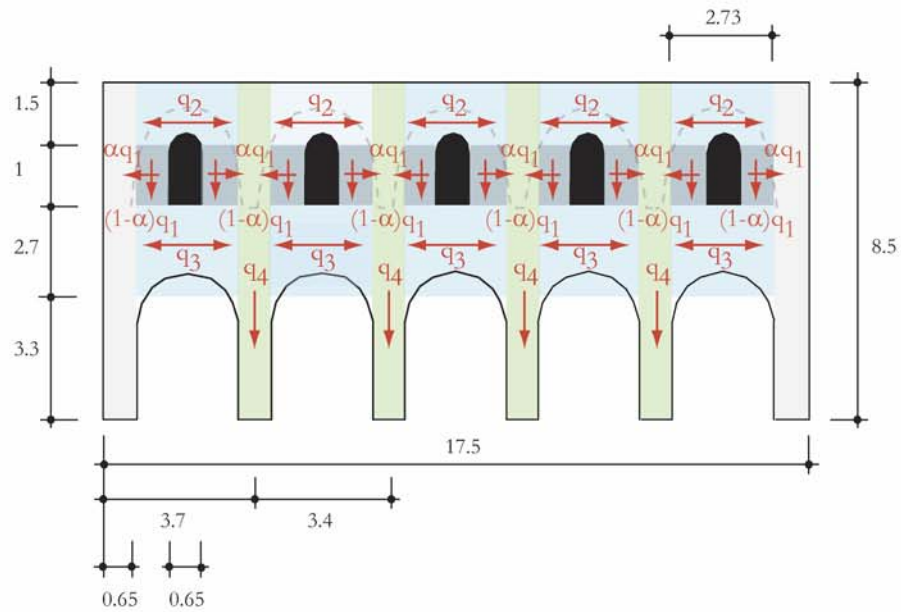


Figure 10.20 : Chosen initial transfer of forces.

1. Calculation of α and q_1

Note: since the resisting bending moment is very low, the edge is quite quickly cracked and the transfer of forces is changed.

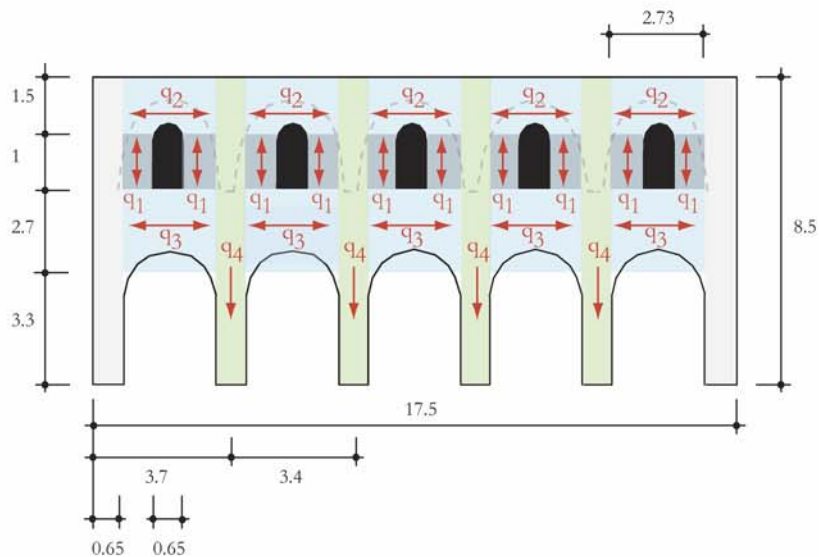


Figure 10.21 : Resulting transfer of forces after a very small out-of-plane acceleration ($a_{gd} < 0.01 \text{m/s}^2$).

2. Calculation of q_2 : $q_2 = m_2 \cdot a_i + q_1'$

Where $q_1' = (1-\alpha) q_1 \cdot (2 \cdot 1.04) / 2.7^1$

3. Calculation of q_3 : $q_3 = m_2 \cdot a_i + q_1'$

4. Calculation of q_4 : $q_4 = m_4 \cdot a_i + q_2 \cdot 2.07 + \alpha q_1 \cdot 1 + q_3 \cdot 2.07$

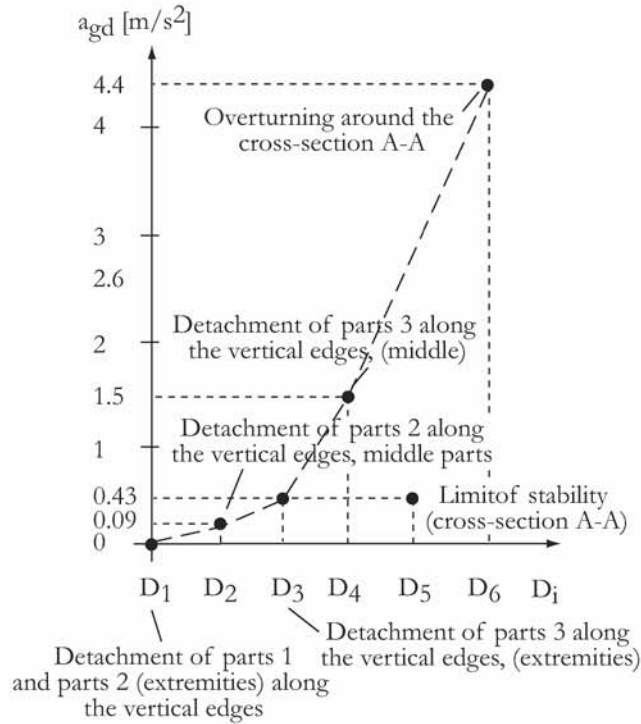


Figure 10.22 : Vulnerability curve (out-of-plane) of the LW1 lateral walls.

Note: the cross-section A-A is situated at the base of the LW1 wall.

IN-PLANE BEHAVIOUR

1. Shear strength

The proportions correspond to the model. According to the percentages given under chapter 8.7.6.1, the following safety factor are obtained:

Table 10.6: Safety factors for the resistance to shear of the piers between windows.

Parts	$a_{gd}=1 \text{ m/s}^2$	$a_{gd}=2 \text{ m/s}^2$	$a_{gd}=3 \text{ m/s}^2$	$a_{gd}=4 \text{ m/s}^2$
a	-	-	-	-
b	46.9	4.9	6.8	5.1
c	5.7	2.7	2.2	1.6
d	9.6	3.7	3.3	2.5
e	4.5	2.6	2.1	1.6
f	3.0	2.6	1.6	1.2

1. Simplification with a distribution of the q_1 load on the field 2; this simplification is correct when the window is not too wide.

2. Flexural strength

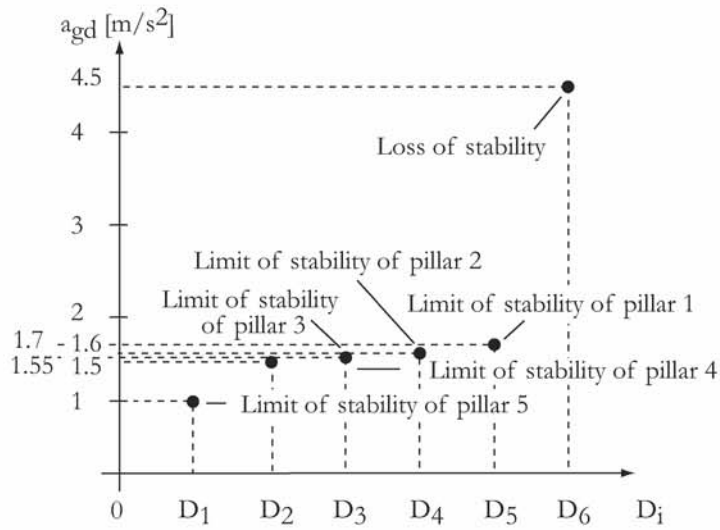


Figure 10.23 : Vulnerability curve (in-plane) of the LW1 lateral walls.

10.4.2.4. Chancel arch

OUT-OF-PLANE BEHAVIOUR

The main problem regarding the out-of-plane seismic response of the chancel arch is the gable; this is the only part to be checked.

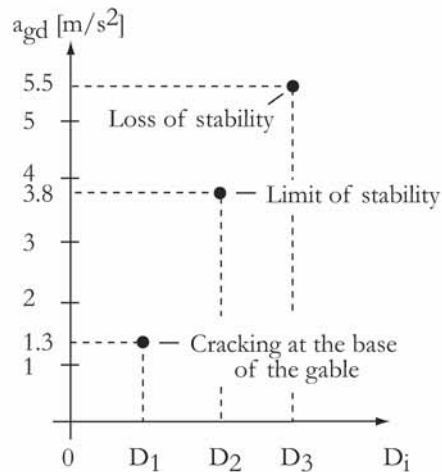


Figure 10.24 : Vulnerability curve (out-of-plane) of the TAH 3 chancel arch.

IN-PLANE BEHAVIOUR

According to the Figure 8.56, the following damage curve as a function of the peak ground acceleration can be set down:

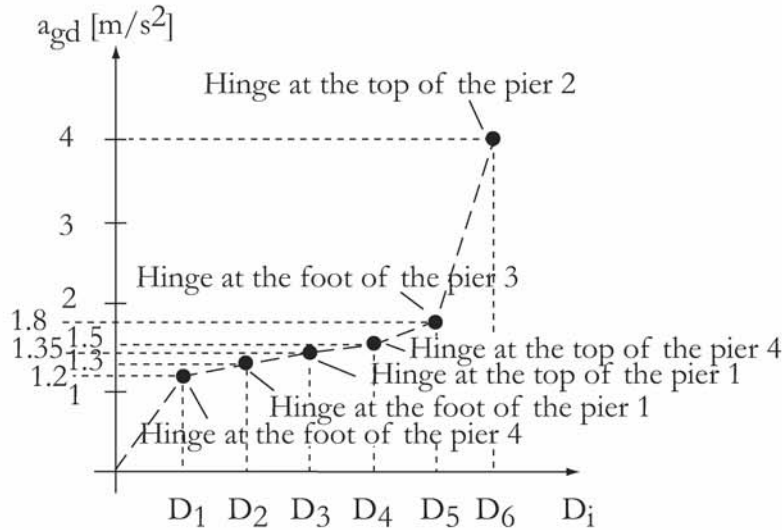


Figure 10.25 : Vulnerability curve for the in-plane seismic response of the TAH 3 chancel arch.

10.4.2.5. Apses

A check of the timber framework showed that every component is well tight to each other; apparently, there will be no problem of hammering due to rafters incorrectly connected to the rest of the framework. In consequence, the given semicircular apses are not seismically vulnerable.

10.4.2.6. Vaults

MAIN NAVE

According to the chapter 8.4.2.2, the seismic vulnerability of cross-vaults depends on the movement of opposite walls. The movement of these walls is influenced by the flow of forces, i.e. the position of the resultant. In fact, the deformation grows larger since the resultant of inertia forces gets out the central third until reaching the cross-section edge. When the resultant gets out of the cross-section, the wall loses its stability. However, for the seismic loads are cyclic it does not mean that the wall is going to fall. However, at this moment, the drift of the wall can be very large.

According to [Ba 91], cross-vaults fall down when their opposite bearings get away of 4 mm. In the case of the LW1 lateral wall, it means that the angle of deformation at the basis of the wall must be of 0.01 degree which is almost nothing. However, both opposite walls, if the shape and the boundary conditions are the same moves in the same way since they are parallel. Consequently, if they move together, there will not be a difference of drift. This situation can change when the resultant of inertia forces is out of the cross-section because the movement is not necessarily the same between the opposite walls. Therefore, a difference of 4 mm in the drift between the bearings can appear since this moment on.

When referring to the graph with the damage curve as a function of the peak ground acceleration that loads the wall out of its plane (Figure 10.22), the resultant gets out of the cross-section for an

acceleration of 1.5 m/s^2 . Consequently, according to the aforementioned assumptions, vaults of the main nave are at risk since this moment on.

LOW-AISLES

In the case of the low-aisles, both opposite walls (one being a LW1 lateral wall and the other a LW2 wall) have not the same shape. Consequently, their out-of-plane drift is not the same too. According to this statement, the vaults of low-aisles are more vulnerable than that of the main nave. In the present case, they become clearly vulnerable when the resultant in the LW1 lateral wall is out of the cross-section while it is still not the case in the LW2 walls. As for the cross-vaults of the main nave, they become vulnerable from an out-of-plane acceleration of 1.5 m/s^2 .

It is assumed that cross-vaults are not seismically vulnerable when the lateral walls are loaded in their plane by a moderate ground acceleration.

10.4.3. GLOBAL BEHAVIOUR

Problems at the connections between the tower and:

- the front wall
- the nave transversal structure

can appear. However, these incompatibilities of deformation are difficult to be assessed. In fact, it constitutes a topic to address in the future. However, it can be assumed that for moderate peak ground accelerations, such as in Switzerland, these incompatibilities have not much influence on the damage of the whole church.

When the front wall is loaded out of its plane, it results in loading the lateral walls (LW1 and LW2) in their plane. This overloading must be added to the in-plane loading determined under chapter 10.4.2.3.

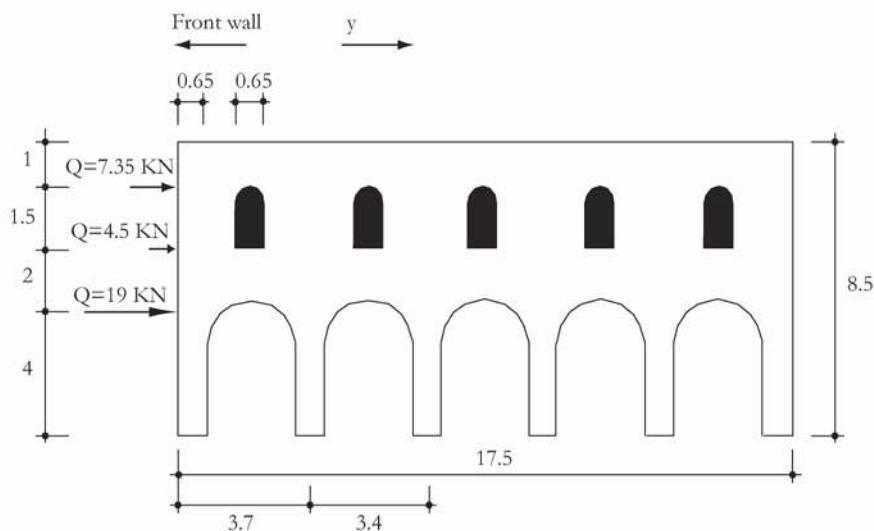


Figure 10.26 : The lateral wall LW1 supports the reaction forces of the front wall when it is loaded by seismic load in the y direction.

These forces make diminish the safety factors of the shear resistance of the piers (Table 10.6) of 0.1; even for an acceleration of 4 m/s^2 , that has no impact. Because of the above result and also

because the safety factors for the LW2 lateral wall (Table 10.5) are high, the effect of the reaction forces of the front wall (when moving in the y direction) is not addressed.

The impact on the flexural resistance is no greater. The limit of stability is reached under an acceleration 0.05 m/s^2 lower than it was without taking into account the impact of the front wall. In fact, the loss of not of safety is not important.

10.4.3.1. The whole church

THE BELL-TOWER:

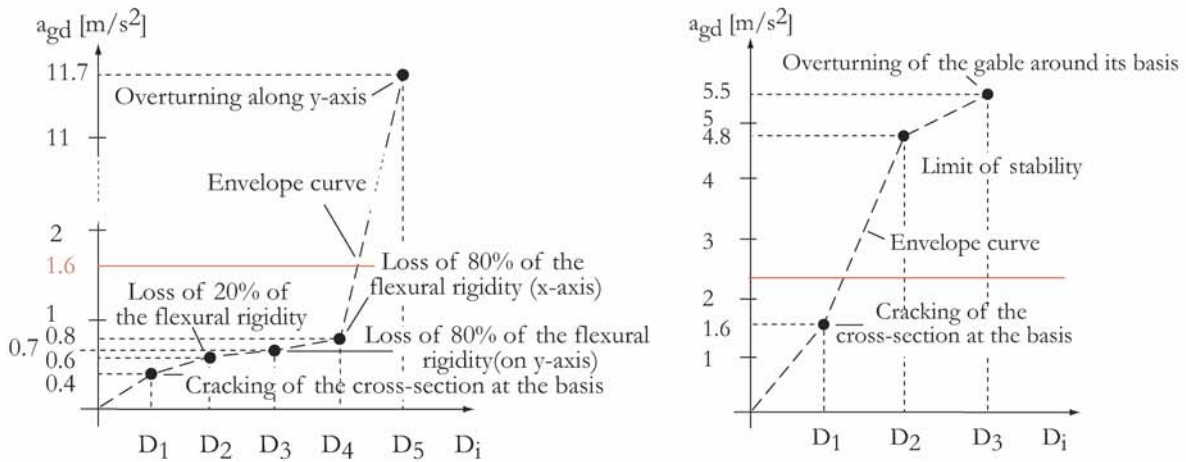


Figure 10.27 : Comparison of the vulnerability curve of the bell-tower and the gable's with the seismic demand.

First, it can be seen that the gable is not seismically vulnerable. Under a peak ground acceleration of 2.2 m/s^2 , that leads to the overturning of the whole front wall, the gable is only cracked at its basis. The resultant of inertia forces is out of the central third of the cross-section. However, in what concerns the bell-tower, the cross-section at the basis is highly cracked; the cross-section would loose 80% of the initial stiffness. Nevertheless, though the amplitude of the movement under the seismic loads is great, this will not result in the collapse (overturning) of the tower.

THE FRONT WALL:

The seismic demand ($a_{gd}=1.6 \text{ m/s}^2$) will not cause the collapse of the front wall (overturning of the whole facade). However, it can be seriously damaged: the facade will be detached from the lateral walls and the bell-tower.

According to the results obtained for the in-plane direction, no important damage will happen.

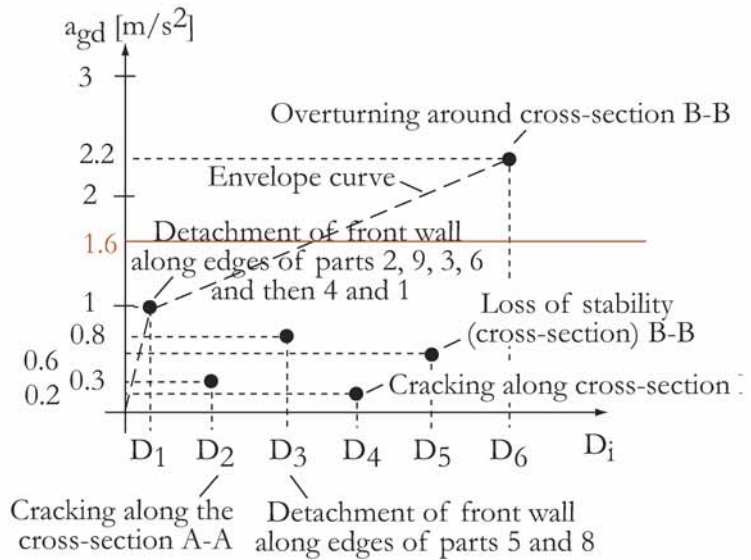


Figure 10.28 : Comparison of the vulnerability curve (out-of-plane) of the front wall with the seismic demand.

THE LW2 LATERAL WALL:

The LW2 lateral wall shows a small seismic vulnerability. Only the parts close to the vertical edges would be cracked under the seismic demand (an out-of-plane acceleration of $a_{gd}=1.6 \text{ m/s}^2$). However the other parts would not be hurt.

According to the values obtained for the in-plane resistance of the LW2 lateral wall, the safety factors would be for each piers (between windows) under an out-of-plane $a_{gd}=1.6 \text{ m/s}^2$:

$FS_a=13.3$; $FS_b=8.6$; $FS_c=7.4$; $FS_d=6.6$; $FS_e=6.3$ and $FS_e=12$. They are all higher than 1.

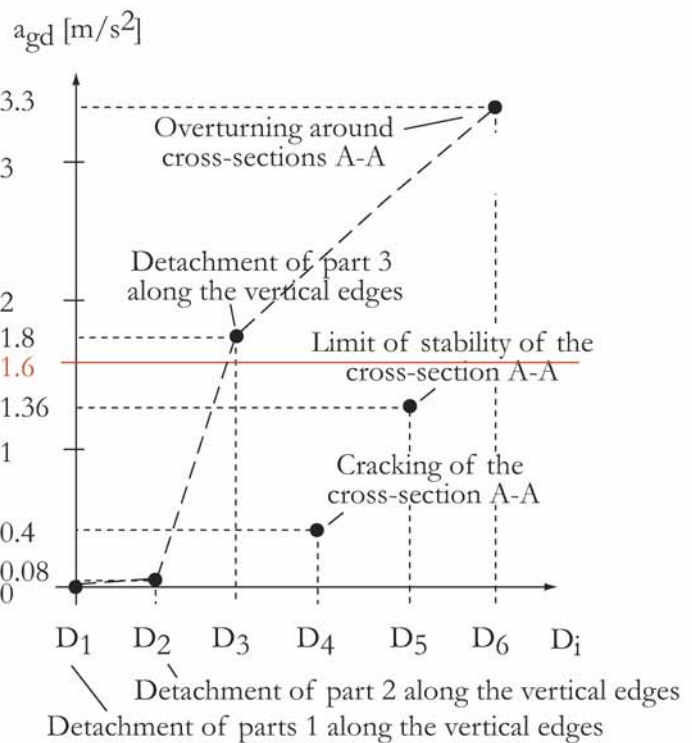


Figure 10.29 : Comparison of the vulnerability curve (out-of-plane) of the LW2 lateral wall with the seismic demand.

THE LW1 LATERAL WALL:

Under the acceleration of the seismic demand ($a_{gd}=1.6 \text{ m/s}^2$), the lateral walls do not resist very well. They are damaged along their vertical edges (that connect them to the chancel arch or the front wall/ bell-tower) and also at the axis of the part 4 (rectangular area above the pillars of the arcade).

However, even if they are damaged, they will not overturn though the amplitude of the movement will be important.

The in-plane shear resistance is guaranteed. However, this not the case of the flexural strength of pillars. Under an acceleration of $a_{gd}=1.6 \text{ m/s}^2$, every pillar would be at the limit of its stability, except the pillar a.

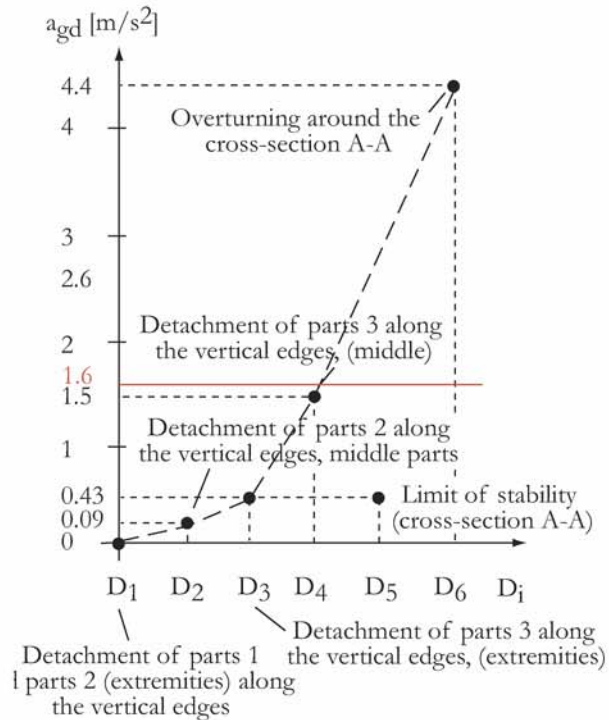


Figure 10.30 : Comparison of the vulnerability curve (out-of-plane) of the LW1 lateral wall with the seismic demand.

THE CHANCEL ARCH:

According to the obtained results, the chancel arch is not vulnerable out of its plane.

However, there would be at least four hinges at the top and the foot of both extremity piers under the acceleration of the seismic demand ($a_{gd}=1.6 \text{ m/s}^2$). Nevertheless, this does not mean the collapse of the chancel arch since the other two piers must also be damaged (with hinges) to activate the collapse mechanism.

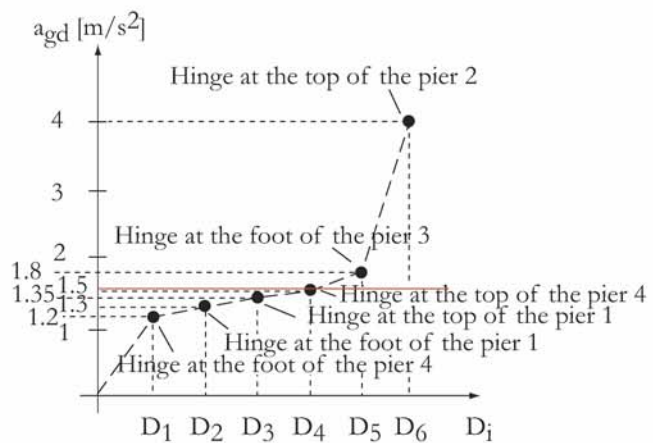


Figure 10.31 : Comparison of the vulnerability curve (in-plane) of the chancel arch with the seismic demand.

As aforementioned, the cross-vaults of the main nave and the low-aisles could be highly damaged and even collapse under the peak ground acceleration of 1.5 m/s^2 .

10.5. STUDY: LEVEL 3

It is not necessary; results are satisfactory.

10.6. DIAGNOSIS

In the previous chapter, it is stated that almost every macro-element would be moderately damaged (cracking of the cross-section at the base of the element). However, the most damaged parts are the front wall (out-of-plane) and the LW2 lateral wall out of its plane too. However, LW2 is less vulnerable than the front wall.

Since the front wall would collapse under a higher ground acceleration than the one given in the Swisscode SIA 261, it is *a priori* not necessary to retrofit it as an emergency case. However, the collapse acceleration is not so far from what you could expect for earthquakes whose return period is higher than 475 years. Therefore, it would be recommended to reinforce the front wall against the out-of-plane collapse. *A priori*, the easiest way to proceed would be the use of tie-rods.

The cross-vaults might also be damaged for the design peak ground acceleration; a retrofitting could be envisaged.

For the other macro-elements, it must be kept in mind that they can be moderately damaged even if they do not collapse. The question for them is: do we agree that this church would be moderately damaged or not? If yes, there is no need for reinforcement. On the contrary, if no damage is acceptable, a solution of retrofitting must be given.

10.7. DISCUSSIONS AND CONCLUSIONS

The proposed method allows us to obtain not only the seismic vulnerability of a whole church, but it also permits to define which parts of such and such macro-element are vulnerable and the reasons. This is a very valuable tool for deciding which kind of retrofitting must be used and in which extent.

As mentioned and shown in the chapters 1 and 4, sacred buildings in Switzerland are at risk for earthquakes. However, no studies have been carried out on their seismic vulnerability. On the contrary, after the Friuli earthquake (1976), European countries, especially Italy, took notice of the fact that their cultural heritage buildings were at risk. Therefore, research has been made on the development of methodologies that allow engineers and architects to assess their seismic vulnerability. The most important of the existing methodologies were dealt with in chapter 5. While efficient and applicable in certain cases, in general, they are based on damage observed on different cultural heritage buildings than the Swiss ones. For structure (configuration of structural parts) and masonry can differ a lot between countries, a new procedure that is more adapted to the Swiss building heritage has been developed. However, this methodology could also be applied to cultural heritage buildings elsewhere than in Switzerland. Only the standard units should be changed according to the structural patterns found in the respective countries.

Some results from previous research on this topic, such as the macro-elements approach, are used as input for the developed methodology presented in this thesis. The multi-level structure of a few existing methodologies is also adopted for the present method. Also, one method that presents many advantages such as speedy evaluation and valuable results was adopted for the first level. This enables a rapid selection of the seismically vulnerable buildings.

Because of the numerous kinds of different cultural heritage buildings, an homogenous group had to be chosen first. Since religious edifices, such as churches, constitute the most important category of cultural heritage buildings in Switzerland, it was chosen, though containing different types of structure. In this category, the Pre-Romanesque and the Romanesque edifices form an homogeneous

group from a structural point of view. Consequently, the present methodology is particularly adapted for such kind of edifices though it can also be applied for sacred buildings from other eras. However, since they might have other structural characteristics, this method should be extended in order to be applicable for other types of churches such as Gothic and Baroque edifices. This task is indeed part of the future work list.

To study every Pre-Romanesque and Romanesque sacred edifice in Switzerland, a list of standard units is drawn up. These units actually correspond to macro-elements and are essential for the study of the seismic response of given edifices. As aforementioned, this list should be completed in the future in order to adapt the present method to other architectural types, such as Gothic or Baroque. Moreover, a data base with good quality plans and profiles of Swiss sacred buildings should be created.

The approach by macro-elements has proven to be efficient and correct for small- and medium-size churches [La4 04]. Its application to such types of edifices is correct because the structural components are not too highly interconnected to each other. This is indeed not the case of many cathedrals. However, based on the aforementioned explanation, this approach could also be applied for large-size sacred edifices whose structural components are not linked through many connections. Consequently, the present method could also be applied to large-size religious buildings only if the above condition (the presence of a few connections between structural components) is satisfied.

While the first level consists in separating the buildings that are seismically not vulnerable from those that are vulnerable, the second level gives quantitative results on the seismic vulnerability of previously selected buildings. Contrary to other methods, the ground acceleration that makes the edifice (or a part of it) collapse is not the only sought-after parameter. The evolution of damage is indeed of prime importance, especially in Switzerland since the seismic hazard is qualified as moderate (chapter 1). Therefore, the damage that can happen under low ground acceleration such as 1 or 1.6 m/s^2 is also important. Moreover, the determination of the evolution of damage gives clear indications on the part(s) that might be damaged and where retrofitting should be inserted in order to diminish the seismic vulnerability of the studied edifice.

The approach by macro-elements is linked to the corollary that macro-elements behave independently from each other. Since religious edifices have no rigid diaphragm to ensure a compact behaviour under seismic loading, this assumption is *a priori* valid. Moreover, masonry can resist only a low level of tensile stresses and that highest stresses usually (depending on the global shape of the edifice) appear at corners. Nevertheless, the stiffness of the horizontal diaphragm that vaults may generate should be addressed in the future for it might modify the application of the approach by macro-elements.

Furthermore, the seismic response of vaults must be one of the future work since they certainly constitute one of the most vulnerable parts of the structure of sacred buildings under seismic actions. Also, their impact on the seismic response of the supporting walls (usually the lateral walls and abutments) is to be more deeply studied than it is in the context of this PhD thesis. In fact, a lateral displacement of 4 mm to cause the collapse of barrel-, groin- and cross-vaults should be verified. Such future work would fulfil a clear void of knowledge in this field; there are indeed no published research that deals with the seismic response of vaults.

The impact of the timber framework should also be more deeply addressed within the framework of future work.

The methodology is based on the assumption that there is no interaction between movements along the two perpendicular directions; however, it is not always true. The methodology should be completed in that direction. Also, the interaction between the ground and the building is not taken into account, as it is in Swisscodes; however, this aspect must be addressed.

The application of the theory of plasticity to macro-elements has proven to be efficient and to give valuable results either for the in-plane or out-of-plane seismic response. This statement shows that the seismic behaviour of sacred edifices, though complex, can be addressed in such a way.

Regarding the out-of-plane seismic response, the strip method allows us to obtain the maximal lateral load that can be resisted by the given structural component. Also, it permits to determine where a damage can happen and under which ground acceleration. However, the obtained value is conservative since the lower bound of the plasticity theory gives under-estimated values. Because of the presence of openings and of a distributed mass within walls, the in-plane seismic response of walls has to be dealt with by numerical modelling in order to obtain the flow of forces (stress fields) within a wall. Since it was possible to list standard units for every Pre-Romanesque and Romanesque edifices, the numerical (linear) treatment of each of them provides a kind of «library» that contains a description (percentage of forces) of the flow of forces under increasing in-plane acceleration. It becomes then possible to treat every Romanesque sacred edifices by consulting this library. However, if proportions of the studied parts do not correspond to the proportions of the related structural parts in the «library», a new modelling must be carried out.

Contrary to walls, the seismic response of bell-towers was studied by applying an elastic method. This approach suits more such slender structures because they cannot be considered as rigid bodies as it is for walls. Bell-towers are characterized by a natural frequency and the study of their structural behaviour must consider this feature. However, the loss of stiffness under seismic actions should be addressed in the future in order to increase the accuracy of the method. In this context, it would be interesting to carry out a wide testing program for applying the ambient vibrations method in order to build a data base with natural frequency of bell-towers. This would permit to better understand the structural behaviour of such structures under seismic actions.

Another important subject that must be dealt with in the future is the choice of the peak ground acceleration for the calculations. As aforementioned in the previous chapters, the peak ground acceleration that is given for common buildings (which is found in most building codes) is not suitable for cultural heritage buildings whose life span is really different from this of common buildings. The determination of the seismic vulnerability of religious edifices highly depends on this value and on the seismic hazard (distribution of areas) indeed.

Though based on all the aforementioned assumptions and simplified models, the level 2 gives reasonable and valuable results. They are valuable since they permits to obtain the type of damage expected for different levels of ground accelerations and also the location. This information is particularly useful for defining required reinforcements, if needed. Furthermore, once the adapted reinforcements are chosen, the level 2 procedure is to be once again applied.

In case the results from level 2 are not satisfactory or if its application is not possible because of irregularities, it is proposed to numerically study the given edifice (FEM). However, the application of such a method must be made very carefully because the structural behaviour of masonry is diffi-

cult to simulate numerically. An elastic model, which models a whole edifice (3D model), can give valuable results only under very low ground acceleration. In fact, once some parts of masonry enter the non-linear domain, such kind of elastic models are no longer valid. Furthermore, since masonry takes only negligible tensile stress, the boundary conditions of the structure of a sacred edifice can change quickly and invalidate the previously used model. However, such kinds of models can give valuable results if the modelling is accurate and the results are carefully interpreted.

The proposed method to assess the seismic vulnerability of Pre-Romanesque and Romanesque sacred buildings gives interesting results. Nevertheless, it should be applied to other edifices, and particularly, to existing ones that were damaged by seismic events. This would help refining the methodology, in particular in what regards the vaults seismic response and its impact on the out-of-plane behaviour of the lateral walls (that bear them). Furthermore, the structural behaviour and the arches collapse mechanisms of the arcades (lateral walls) and of the chancel arches have to be dealt with through the use of a sophisticated software with which the interaction of voussoirs with the above masonry can be treated.

With respect to stone masonry, it exists a few models that have been developed to define its mechanical properties. The model proposed in the Swisscode V178, proved to be accurate when applied for the analytical determination of the shear strength of the tested specimen, which is presented in chapter 7 through the Ganz's method. Nevertheless, if that model would be still exact for other kind of masonry (especially in what regard the shear strength), remains a question that has to be answered by carrying out many experimental investigations (of the kind that was made in chapter 7) on other kinds of stone masonry.

Methods for assessing the seismic vulnerability of common buildings are not suitable for sacred buildings because of many reasons. On one hand, the structure of common buildings are really different from this of religious edifices and on the other hand, the fabrics also differ. Masses are indeed differently distributed (concentrated masses in common buildings vs more uniformly distributed masses in sacred edifices) and the structural components, which resist the seismic forces, are also differently distributed. Consequently, a methodology for religious buildings must be created.

In this report, a methodology for assessing the seismic vulnerability of cultural heritage buildings has been developed. This method is specifically adapted for Pre-Romanesque and Romanesque religious edifices in Switzerland. However, it could be applied to other types of edifices, such as Gothic or Baroque sacred buildings, and also to cultural heritage in other countries with a few modifications.

The methodology takes into account structural characteristics that can be found in every Pre-Romanesque and Romanesque edifices, especially in Switzerland. Moreover, the three-level configuration of the method makes it possible to first sort out the sacred buildings that are seismically vulnerable. This can significantly speed up the assessment process. Then, only the edifices that are assessed as being vulnerable are studied more deeply with the models proposed in the levels 2. When parts of the given building are structurally very complex or if the structure of the whole edifice is complicated, a numerical model can be created; this corresponds to the last level.

This new methodology is based on the strength of the structural component rather than on deformations that tend to be more used in the field of earthquake engineering nowadays. However, the structural behaviour under seismic loading of old masonries is still not well understood, in particular the displacement curve as a function of the shear load. Consequently, it was given up setting up a

methodology based on deformations. Future work is indeed needed in this research field.

With respect to the structural behaviour of masonry, an experimental investigation was carried out at EPFL in order to obtain information on the seismic response of an old masonry. This is indeed one of the first times that such experimental investigation on an old masonry is performed in the world. The high displacement ductility and shear strength of the tested masonry (ashlar masonry with regular courses made up of large sandstone blocks) are promising results in regard to the seismic response of such kind of masonry. In order to be able to assess other types of fabrics, the panel of tested masonries should be extended.

The creation of this methodology raised the problem related to the choice of the peak ground acceleration. In fact, it is proposed in the present method to apply the maximal peak ground acceleration defined by design spectrum for common buildings. Nevertheless, as is the case in Switzerland, this peak ground acceleration was defined for an earthquake with a return period of $T=475$ years. Since this period of time is shorter than the life span of many cultural heritage buildings, it is no longer correct. Consequently, more accurate values for the peak ground accelerations to be chosen for the assessment of the seismic vulnerability of cultural heritage buildings must be defined.

It is worth reminding that this methodology allows architects and engineers to address the structure of cultural heritage buildings and not the movable goods inside the edifices.

To sum up, the method that is presented in this report permits to assess the seismic vulnerability of Pre-Romanesque and Romanesque sacred buildings within a reasonable amount of time. Moreover, it makes it possible to determine the evolution of damage due to earthquake, that is, which damage to expect at which place and for which ground acceleration. This valuable information can be then used to define accurately which reinforcement should be used and where. Results obtained with this method efficiently help diminishing the risk of sacred buildings for earthquakes. Though this methodology permits to locate the damage and the ground acceleration for which the given damage can happen, this PhD work does not include a description of the available reinforcement today. This topic should be addressed in the future.

- [Ab 34] Abraham P., Viollet-le-Duc et le rationalisme médiéval, Edition Vincent, Fréal & Cie, Paris, 1934.
- [AS 04] Aoudia A., Suhadolc P., Il terremoto del 6 maggio 1976 e la tettonica attiva in Friuli, Università di Trieste, 2004.
- [Ar 95] Arbellay R., Grône, un passé à découvrir, Sierre, 1995, p. 428
- [AR 05] Arbellay R., Roch C., Le Valais : chroniques illustrées de la préhistoire au XXI^e siècle, Impr. centrale Sierre, 2005.
- [ANA 85] Atkinson R. H., Noland J.L., Abrams D.P., A deformation failure theory for stack-bond brick masonry prisms in compression, proceedings of the 7th International Brick/Block masonry Conference, Melbourne, 1985.
- [ACG 00] Augusti G., Ciampoli M., Giovenale P., A procedure for the seismic reliability assessment of monumental buildings, 8th ASCE Specialty Conference on Probabilistic Mechanics and Structural Reliability, 2000.
- [AC 00] Augusti G., Ciampoli M., Heritage buildings and seismic reliability, Prog. Struct. Engng Mat., 2000.
- [Au 01] Augusti G. et al., Seismic vulnerability of monumental buildings, Structural safety, 2001.
- [ACZ 02] Augusti G., Ciampoli M., Zanobi S., Bounds to the probability of collapse of monumental buildings, structural safety, 2002.
- [Ba 91] Barthel R., Tragverhalten gemauerter Kreuzgewölbe, PhD Thesis, Universität Karlsruhe, 1991.
- [Be 89] Berger F., Assessment of old masonry by means of partially destructive methods, Structural Repair and Maintenance of Historical Buildings (STREMA), Computational Mechanics Publications, Southampton, Boston, 1989.

References

- [BS 91] Berndt E., Schöne I., Tragfähigkeitsuntersuchungen an Natursteinmauerwerk aus sächsischem Sandstein zur Beurteilung historischer Konstruktionen, 9th International Brick/Block masonry conference, Berlin 1991.
- [BS 94] Berndt E., Schöne I., Eine Bemessungsvorschlag für Mauerwerk aus Eldsandsstein auf der Grundlage experimentell ermittelter Tragfähigkeiten, Erhalten historisch bedeutsamer Bauwerke, Jahrbuch des SFB 15, Berlin 1994.
- [Be 96] Berndt E., Zur Druck- und Schubfestigkeit von Mauerwerk - experimentell nachgewiesen an Strukturen aus Elbsandstein, Bautechnik 73, Volume 4, 1996.
- [BBJPSS 99] Bessac J.-C., Journot F., Prigent D., Sapin C., Seigne J., La construction en pierre, Collection «Archéologiques», Ferdière A., Editions Errance, 1999.
- [Be 56] Bertrand Elie, Mémoires sur les tremblements de terre, Ed. P. A. Chenebié, Vevey, 1756.
- [Be 03] Betbeder-Matibet J., Prévention parasismique, Génie parasismique, volume 3, Lavoisier, Paris, 2003.
- [Be2 03] Betbeder-Matibet J., Phénomènes sismiques, Hermès Science Publications, Paris 2003.
- [BKQ 97] Beuchat A., Krüttli C., Quadroni D., La collégiale de Saint-Imier, Paroisse réformée de Saint-Imier, 1997.
- [BFA 91] Binda L., Fontana A., Anti L., Load transfer in multiple leaf masonry walls, proceedings of the 9th International Brick/Block masonry conference, Berlin, 1991.
- [Bl 46] Blondel L., Report on the collegial of Valère, Commission for the protection of cultural heritage buildings in Switzerland, 1946.
- [Bo 01] Boothby T. E., Analysis of masonry arches and vaults, Prog. Struct. Engng Mater., 2001.
- [BSI 96] Borer A., Schuppisser S., Ineichen S., Leben zwischen den Steinen ; Sanierung historischer Mauern, Documentation SIA, Zürich, 1996.
- [BP 06] Boscotrecase L., Piccarreta F., Edifici in muratura in zona sismica, Dario Flaccovio Editore, Palermo, 2006.
- [Br 79] Braunschweiler E. et al., Sankt Peter Mistail, Schweizerischen Kunstführer, Gesellschaft für Schweizerische Kunstgeschichte, Basel, 1979.
- [Cant ArC] Archives of the canton Valais
- [CFL 07] Ceccotti A., Follesa M., Lauriola M. P., Le strutture di legno in zona sismica, Edizioni C. L. U. T., Torino, 2007.
- [Cha ArP] Archives of the parish in Chalais.
- [Chippis BP] Bulletin paroissial de Chippis, 1981 (1982).
- [Ch 01] Chopra A. K., Dynamics of structures, theory and applications to earthquake engineering, second edition, Prentice Hall, 2001.
- [CVLR 82] Christe Y., Velmans T., Losowska H., Recht H., Grammaire des formes et des styles, Office du livre, Fribourg, 1982.

-
- [CG 83] Como M., Grimaldi A., A unilateral model for the limit analysis of masonry walls, proceedings of the Conference on Unilateral Problems in Structural Analysis, Ravello, 1983.
- [Cl 50] Clotert. P., Notre-dame-des-neiges à Crételles, 1950.
- [Co 70] Corboz A., Architecture universelle : Haut Moyen-Age, Office du livre, Fribourg, 1970.
- [Co 99] Cosse J., Initiation à l'art des cathédrales, 1999.
- [Cr 03] Crettol A., Crételles, terre de prière, Commune de Randogne, 2003.
- [Cr 98] Croci G., The conservation and structural restoration of architectural heritage, Computational Mechanics Publications, Southampton, 1998.
- [Da 85] Dahmann W., Untersuchungen zum Verbessern von mehrschaligem Mauerwerk durch Vernadeln und Injizieren, Karlsruhe Universität, Dissertation, 1985.
- [DS 96] D'alfonso E., Samsa D., L'architecture : Les formes et les styles de l'Antiquité à nos jours, Ed. Solar, Paris, 1996.
- [De 70] Delapraz A., Eglises de Suisse, Editions Avanti, 1970.
- [DeR 87] De Raemy D., Grandson, le bourg et le château, Guides de monuments suisses, Société d'Art et d'Histoire de l'Art en Suisse, Bern, 1987.
- [Do 94] Doglioni F., Le chiese e i terremoti, Ed. Trieste, 1994.
- [Dr 87] Drusin N., Il Duomo di Gemona del Friuli, Italy, 1987.
- [Du 69] Dunca N., Engineering geology and Rock mechanics, Vol. 2, Leonard Hill, London, 1969.
- [DSC 96] Dolce M., Sabetta F., Colozza R., Seismic risk assessment in the historical centre of Rome, 11th World Conference on Earthquake Engineering, Acapulco, Mexico, 1996.
- [EA 03] Techniques et pratique de la chaux, Ecole d'Avignon, Ed. Eyrolles, 2003.
- [Eb 96] Ebner B., Das Tragverhalten von mehrschaligem Bruchsteinmauerwerk im regelmässigen Schichtenverband, Dissertation, Technische Universität Berlin, 1996.
- [ECOS 02] Earthquake Catalogue of Switzerland (ECOS), Swiss Seismological Service, 2002.
- [EC 6 01] Norme, Calcul des ouvrages en maçonnerie, partie 3: méthodes de calcul simplifiées et règles de base pour les ouvrages en maçonnerie. PR XP ENV 1996-3. Projet définitif, Comité Européen de Normalisation (CEN), Bruxelles, Novembre 2001.
- [EC 8 04] Norme, Calcul des structures pour leur résistance aux séismes, partie 3: Evaluation et modernisation des bâtiments. prEN 1998-3. Projet définitif, Comité Européen de Normalisation (CEN), Bruxelles, Novembre 2004.
- [Eg 93] Egermann R., Tragverhalten mehrschaliger Mauerwerkskonstruktionen, Dissertation, Universität Karlsruhe, 1993.

References

- [EMS 98] European macroseismic scale 1998 : EMS-98, Centre Européen de Géodynamique et de Séismologie, Ed. Grünthal G. et al., Luxembourg, 1998.
- [En 02] Enlart C., Architecture religieuse, Manuel de l'architecture française, Vol. 1, A. Picard et Fils éditeurs, 1902.
- [Fä 03] Fäh D. et al., Earthquake Catalogue of Switzerland (ECOS) and the related macroseismic data base, *Eclogae geol. Helv.* 96, 2003, Basel.
- [Fa 99] Falter H., Untersuchungen historischer Wölbkonstruktionen-Herstellverfahren und Werkstoffe, PhD Thesis, Institut für Konstruktion und Entwurf II, Universität Stuttgart, 1999.
- [Fa 07] Favez P., Détermination de la résistance sismique de maçonneries anciennes par essais expérimentaux, Master thesis, ENAC-IS-IMAC, EPFL, 2007.
- [Fa 05] De Fátima Moreira de Vasconcelos G., Experimental investigations on the mechanics of stone masonry: characterization of granites and behavior of ancient masonry shear walls, PhD thesis, University of Minho, Portugal, 2005.
- [FEMA 310 98] Handbook for the Seismic Evaluation of Buildings - A prestandard, Federal Emergency Management Agency, Washington D.C., January 1998.
- [FEMA 356 00] Prestandard and Comentary for the seismic Rehabilitation of buildings, Federal Emergency Management Agency, Washington D.C., November 2000.
- [FFG 05] Fritsche, S., Fäh, D., Giardini, D., Damage Fields and Site-Effects. Investigations on the 1855 Earthquake in Switzerland. Proceedings of the 250th Anniversary of the 1755 Lisbon earthquake, 2005.
- [FFGG 06] Fritsche S., Fäh D., Gisler M., Giardini D., Reconstructing the damage field of the 1855 earthquake in Switzerland: historical investigations on a well-documented event, *Geophysical Journal International*, 2006.
- [Fi 81] Fitchen J., Structure of Gothic Cathedrals: Study of Mediaeval Vault Erection, Chicago Univrsity Press, 1981.
- [FJBC 90] Favre R., Jaccoud J.-P., Burdet O., Charif H., Dimensionnement des structures en béton, Presses Polytechniques et Universitaires Romandes, Lausanne, 1990.
- [Fr 94] Frey, F., Analyse des structures et milieux continus, Volume 2, Traité de génie civil, PPUR, Lausanne, 1994.
- [Fr 93] Froidevaux Y.-M., Techniques de l'architecture ancienne, construction et restauration, Mardaga, Liège, 1993.
- [Ga 96] Gaillard A., L'église Saint-Jean Ardon-Magnot, Conseil de gestion de la paroisse d'Ardon-Magnot, 1996.
- [GL 96] Gambarotta L., Lagomarsino S., On dynamic response of masonry panels, Proc. National Conference on Masonry mechanics between theory and practice, Messina, 1996.
- [GL 97] Gambarotta L., Lagomarsino S., Damage models for the seismic response of brick masonry shear walls, Part II: the continuum model and its applications, *Earthquake engineering and Structural Dynamics*, 26, 1997.

-
- [GT 84] Ganz H.-R., Thürlimann B., Versuche an Mauerwerksscheiben unter Normalkraft und Querkraft, Institut für Baustatik und Konstruktion, ETH Zürich, Versuchsbericht Nr. 7502-4, Birkhäuser Verlag, Basel, 1984.
- [Ga 85] Ganz H.-R., Mauerwerksscheiben unter Normalkraft und Schub, Institut für Baustatik und Konstruktion, ETH Zürich, Bericht Nr. 148, Birkhäuser Verlag Basel, 1985.
- [Gi 04] Gisler M. et.al., The Valais earthquake of December 9, 1755, *Eclogae geol. Helv.* 97, 2004.
- [GWF 05] Gisler M., Weidmann M., Fäh D., Erdbeben in Graubünden: Vergangenheit, Gegenwart, Zukunft, Verlag Desertina, Chur, 2005.
- [Gi 91] Giuffré A., *Lecture sulla meccanica delle murature storiche*, Ed. Kappa, 1991.
- [Gi 93] Giuffré A., *Sicurezza e conservazione dei centri storici: Il caso Ortigia*, Editrice Laterza, Bari, 1993.
- [GS 01] Graubner C.-A., Simon E., Zur Tragfähigkeit von Mauerwerk aus grossformatigen Steinen, *Mauerwerk* 26, Berlin, 2001.
- [Gr 03] Grünenfelder J., *Die Burg Zug: Archäologie, Baugeschichte, Restaurierung*, Kantonsarchäologie/Schweizerischer Burgenverein, Zug/Basel, 2003.
- [GA 02] Guerreiro L., Azevedo J., Seismic analysis and reinforcement of the «Torre do relógio» in Horta, Faial, 12th ECEE, 2002.
- [HGK 90] Häring S., Günther K., Klausen D., *Technologie der Baustoffe: Handbuch für Studium und Praxis*, Verlag C.F. Müller, Karlsruhe, 1990.
- [Ha 42] Haller P., *Natursteine, künstliche Steine, Leichtbaustoffe*, Polygraphischer Verlag A.G., Zürich, 1942.
- [Ha 74] Haller H., *Die romanische Kirche in Spiez*, Gesellschaft für schweizerische Kunstgeschichte, Basel, 1984.
- [Ha 77] Harris C. M., *History architecture sourcebook*, McGraw-Hill, Inc., USA, 1977.
- [Ha 05] Hatot T., *Bâtisseurs au Moyen-Age*, Ed. L'instant durable, 2005.
- [He 90] Hendry A. W., *Structural masonry*, MacMillan Education LTD, 1990.
- [He 56] Heusser J.C., *Das Erdbeben im Visper-Thal im Jahr 1855. An die zürcherische Jugend auf das Jahr 1856*. Neujahrsblätter der Naturforschenden Gesellschaft, Vol. 58, 1856.
- [He 82] Heyman J., *The masonry arch*, Ellis Horwood limited, John Wiley & Sons, 1982.
- [He 95] Heyman J., *The stone skeleton*, Cambridge University Press, 1995.
- [He 96] Heyman J., *Arches, Vaults and Buttresses-masonry structures and their Engineering*, Variorum, Hampshire, 1996.
- [Hi 75] Hillerborg A., *Strip method of design*, Viewpoint Publication, William Clowes & Sons Ltd, London 1975.
- [Ho 88] Horat H., *L'Architecture religieuse*, *ARS Helvetica III*, Arts et culture visuels en Suisse, Ed. Desertina, Disentis, 1988.

References

- [Hu 00] Huster U., Tragverhalten von einschaligem Natursteinmauerwerk unter zentrischer Druckbeanspruchung, PhD Thesis, 2000.
- [Me 96] Meier H.-R., Suisse Romane, 3ème édition, Ed. Zodiaque.
- [Is 82] Ishiyama Y., Motions of rigid bodies and criteria for overturning by earthquake excitation, International Journal for Earthquake Engineering and Structural Dynamics, 1982.
- [Je 76] Jenny H., Kunstführer durch die Schweiz, Société d'Art et d'Histoire Suisse, Böhler-Verlag, Zürich, 1976.
- [Jo 00] Jossen E., Naters, das grosse Dorf im Wallis, Rotten Verlag, Visp, 2000.
- [JWK 97] Junge Wirtschaftskammer, Brig, 1997.
- [KH 73] Khoo C.L., Hendry A.W., Strength tests on brick and Mortar under complex stresses for the development of a failure criterion for brickwork in copression, proceedings British Ceramic Society, Stoke-on-trent 1973.
- [Ki 96] Kirchner-Zufferey P., Séisme, Ed. Monographic SA, Sierre, 1996.
- [Ko 02] Koch I. A., Zum Tragverhalten von schubbeanspruchten gemauerten Wandscheiben mit Öffnungen, Dissertation, Technische Universität München, 2002.
- [LPR 02] Lagomarsino S, Podesta S, Resemini S., Seismic response of historical churches, 12th ECEE, 2002.
- [La 98] Lagomarsino S., A new methodology for post-earthquake investigation of ancient churches, 11th ECEE, 1998.
- [La1 04] Lagomarsino et al., Observational and mechanical models for the vulnerability assessment of monumental buildings, 13th WCEE, Vancouver, 2004.
- [La2 04] Lagomarsino S. et al., Seismic vulnerability of ancient churches: I. Damage assessment and emergency planning, Earthquake spectra, volume 20, 2004.
- [La3 04] Lagomarsino S. et al., Seismic vulnerability of ancient churches: II. Statistical analysis of surveyed data and methods for risk analysis, Earthquake spectra, volume 20, 2004.
- [La4 04] Lagomarsino S. et al., Vulnerability assessment of historical and monumental buildings, Handbook, WP5, Risk-UE, 2004.
- [La 05] Lagomarsino et al., Mechanical models for the seismic vulnerability assessment of churches, Structural analysis of Historical Constructions- Modena, Lourenço and Roca, 2005.
- [La 06] Lagomarsino S. et al., Sicurezza e protezione delle chiese in zona sismica, working document, 2006.
- [La 02] Lang K., Seismic vulnerability of existing buildings, PhD Thesis, ETHZ, 2002.
- [Lau 04] Laupper H. et al., Expert report: earthquakes and cultural property, Federal Office for Civil Protection, 2004, Bern.
- [Le 49] Lenoir D., Récit du tremblement de terre du Valais (25 juillet 1855), Bulletin de la Muritienne, Fasc. 66 (1949), 1949.
- [Lens ArPr] Lens, archives of the priory.

-
- [Le 05] Lestuzzi P., Dimensionnement parasismique, Polycoié EPFL, 2005.
- [Le 08] Lestuzzi P., Séismes et construction, Presses Polytechniques et Universitaires Romandes, Lausanne, 2008.
- [LM 06] Lestuzzi P., Mittaz X., Maçonnerie sollicitée parallèlement à son plan: cisaillement combiné avec un effort normal centré, Détermination de la résistance latérale, exemples numériques, Publication de l'EPFL en collaboration avec le CREALP et l'Office Fédéral de l'Environnement, 2006.
- [Lo 94] Lourenço P. B., Analysis of masonry structures with interface elements, Report, Delft University of Technology, 1994
- [Lo 01] Lourenço P. B., Analysis of historical constructions: from thrust-lines to advanced simulations, Historical Constructions, P.B Lourenço, P. Roca (Eds.), 2001.
- [Lo 05] Lourenço P. B., Overview of seismic risk for large span buildings heritage, Improving the seismic resistance of cultural heritage buildings, EU-India Economic Cross Cultural Programme, 2005.
- [LO 05] Lourenço P. B., Oliveira D. V., Seismic vulnerability of churches, Improving the seismic resistance of cultural heritage buildings, EU-India Economic Cross Cultural Programme, 2005.
- [LR 06] Lourenço P.B., Roque J.A., Simplified indexes for the seismic vulnerability of ancient masonry buildings, Construction and building materials, 2006.
- [Ma 02] Maier J., Handbuch Historisches Mauerwerk, Birkhäuser, 2002.
- [Ma 83] Mann W., Zum Tragverhalten von Mauerwerk aus Natursteinen, Mauerwerkskalender, Ernst und Sohn, Berlin, 1983.
- [MM 82] Mann W. and Müller H., Failure of shear stressed masonry- an enlarged theory, tests and application to shear walls, Proc. Br. Ceram. Soc., 1982.
- [MMS 97] Maret M., Meyer C.-A., Sarbach J., Eglises de pierre, églises de lumière/ Kirchen aus Stein, Kirchen sein, Evêché de Sion, Editions Saint-Augustin, Saint-Maurice, 1997.
- [MC 79] Mayer-Rosa D., Cadiot B., A review of the 1356 Basel earthquake, basic data, Tectonophysics, 1979.
- [Me 98] Meli R., Ingeniería Estructural de los Edificios Históricos, Fundación ICA ; 1998.
- [Me 05] Meyer W., Da verfiel Basel überall. Das Basler Erdbeben von 1356, Schwabe Verlag, Basel, 2005.
- [Me 06] Meyer W., Das Basler Erdbeben von 1356- Verlauf und Bewältigung einer Katastrophe, Mittelalter, Zeitschrift des Schweizerischen Burgenvereins, 2006.
- [Mi 07] Michel C., Vulnérabilité Sismique, de l'échelle du bâtiment à celle de la ville - Apport des techniques expérimentales in situ - Application à Grenoble, Thèse de Doctorat, Université Joseph Fourier, Grenoble, 2007.

References

- [MDF 05] Mirabella Roberti G., Donati L., Fontana A., Out-of-plane behaviour of multiple-leaf stone masonry, *Structural analysis of Historical Constructions*, Modena, Lourenço and Roca, 2005.
- [Mon ArP] Archives of Montana's parish.
- [Mo 72] Morgan S., *Eglises romanes et châteaux forts en Suisse romande*, Ed. Bon-vents S.A., Genève, 1972.
- [MP 04] Mühlhaus-Ebersole S., Patitz G., *Zerstörungsfreie Voruntersuchungen an Kirchenbauten mittels Seismik, Mauerwerksdiagnostik in der Denkmalpflege* (Hrsg. Dr.-Ing. Gabriele Patitz), *Monudocthma 01*, Fraunhofer IRB Verlag, Stuttgart, 2004.
- [MG 90] Müller N., Gücker R., *Gründungsschäden an historischen Bauwerken*, Landesinstitut für Bauwesen und angewandte Bauschadensforschung Aachen, 1990.
- [MST 97] Muttoni A., Schwartz J., Thürlimann B., *Design of Concrete Structures with Stress Fields*, Birkhäuser, Basel, 1997.
- [Mu 04] Muttoni A., *L'art des structures - une introduction au fonctionnement des structures en architecture*, Presses Polytechniques et Universitaires Romandes, Lausanne, 2004.
- [Nö 55] Nöggerath J., *Die Erdbeben im Visperthale*, Besonderer Abdruck für Freunde des Verfassers aus Nr. 282 bis 286 der Kölnischen Zeitung von 1855, Köln, Selbstverlag, 1855.
- [OFEV 1 05] *Vérification de la sécurité parasismique des bâtiments existants et directives pour l'étape 1*, Directives de l'OFEG, Office Fédéral de l'Environnement, Berne, 2005.
- [OFEV 2 05] *Vérification de la sécurité parasismique des bâtiments existants et directives pour l'étape 2*, Directives de l'OFEG, Office Fédéral de l'Environnement, Berne, 2005.
- [OFEV 3 05] *Vérification de la sécurité parasismique des bâtiments existants et directives pour l'étape 3*, Directives de l'OFEG, Office Fédéral de l'Environnement, Berne, 2005.
- [OI 03] Oliveira C.S., *Seismic vulnerability of historical constructions: a contribution*, *Bulletin of Earthquake engineering*, Kluwer Academic publishers, 2003.
- [ÖL 06] Ötes A., Löring S., *Zum Tragverhalten von Mauerwerksbauten unter Erdbebenbelastung*, *Mauerwerk*, Ernst & Sohn Verlag, Berlin, 2006.
- [Pa 82] Page A. W., *An experimental investigation of the bi-axial strength of brick masonry*, 6th International Brick Masonry Conference, Rom, 1982.
- [PP 92] Pauley T., Priestley M. J. N., *Seismic design of reinforced concrete and masonry buildings*, John Wiley & Sons, Inc., 1992.
- [Pf 81] Pfister F., *Pfarrkirche Sankt Peter und Paul*, Schlussbericht, Ingenieurbüro W.Galli, Zürich, 1981.

-
- [PLBA 05] Pina-Henriques J., Lourenço P. B., Binda L., Anzani A., Testing and modelling of multiple-leaf masonry walls und shear and compression, Structural analysis of Historical Constructions, Modena, Lourenço and Roca, 2005.
- [PSWOS 92] Pohl R., Schneider K.-J., Wormuth R., Ohler A., Schubert P., Mauerwerksbau: Baustoffe-Konstruktion-Berechnung-Ausführung, 4. Auflage Werner Verlag, Düsseldorf 1992.
- [PS 96] Pöschel G, Sabha A., Ein theoretisches Modell zum Tragverhalten von Elbesandstein, Erhalten historisch bedeutsamer Bauten: Jahrbuch 1993, SFB 315, Ernst und Sohn, Berlin, 1983.
- [Qu 34] De Quervain F., Die nutzbare Gesteine der Schweiz, ??, 1934.
- [RCom 60] Rapport du Comité central de bienfaisance chargé de la répartition des secours recueillis pour les victimes du tremblement de terre qui a dévasté, en 1855, les districts de Rarogne, de Brigue et de Viège, Sion, 1860.
- [Re 91] Reinsch D., Natursteinkunde, Enke Verlag, Stuttgart, 1991
- [Ri 98] Rizzoni G., Cattedrali e basiliche in Italia, Ed. Giorgio Mondadori, Milano, 1998.
- [RGOL 98] Roca P., Gonzáles J.L. , Oñate E., Lourenço P.B., Experimental and numerical issues in the modelling of the mechanical behaviour of masonry, Structural analysis of historical constructions II, Barcelona, 1998.
- [Ro 1852] Rondelet J.-B., Traité technique et pratique de l'art de bâtir, Firmin Didot Frères, Paris, 1852.
- [Ru 94] Ruppen W., Visp: Siedlung und Bauten, Gesellschaft für schweizerische Kunstgeschichte, Bern, 1984.
- [SHF]M 95] Salvadé P., Hauser M., Prongué J.-P., Fischer H., Jardin R., Migy P., Saint-Ursanne, guide de la Collégiale, Comme ecclésiastique de Saint-Ursanne, 1995.
- [SPH 81] Samaringhe W., Page A., Hendry A. W., Behaviour of brick masonry shear walls. The structural Engineer, Volume 59B, 1981.
- [Sc 89] Schaad W., Scénarios de tremblements de terre en Suisse. Résumé de rapport de recherche. Pool suisse pour l'assurance contre les tremblements de terre, Berne, 1989.
- [Sc 04] Schermer D. C., Verhalten von unbewehrtem Mauerwerk unter Erdbebenanspruchung, Dissertation, Berichte aus dem Konstruktiven Ingenieurbau, Technische Universität München, 2004.
- [Sc 00] Schibler R., Makroseismische Untersuchung der Erdbeben von 1946 im Mittelwallis, Diplomarbeit, Institut für Geophysik, ETHZ, 2000.
- [SA 91] Schiessl P., Alfes C., Festigkeit und Verformbarkeit von Sandstein-Bedeutung für die Verwitterungsresistenz und Messmethoden, Bautenschutz und Bausanierung 14, 1991.
- [Sc 71] Schmid A. A., Dictionnaire des églises suisses, Ed. Robert Lafont, 1971.
- [Sc 01] Schmid V., Brig-Glis, Naters und Ried-Brig, Kulturführer zur Geographie, Geschichte, Wirtschaft, Sprache und Kultur, Wir Walser Verlag, Brig, 2001.

References

- [Se 92] Sennhauser H.-R., L'abbatiale de Payerne, Guides de monuments suisses, Société d'Art et d'Histoire de l'Art en Suisse, Bern, 1992.
- [ST 99] Shao Y., Tung C. C., Seismic response of unanchored bodies, earthquake spectra, vol 15, august 1999.
- [Si 67] Sinha B. P., Model studies related to load bearing brickwork, PhD thesis, University of Edinburgh, 1967.
- [Sion ArB] Archives of the Sion bishopric
- [SS 79] Speich K., Schläpfer H. R., Eglises et monastères suisses, Ed. Ex-Libris, Zürich, 1979.
- [St 72] Stuart M., Eglises romanes et châteaux forts, Suisse romande (Vol 1.), Les Ed. de Bonvent SA, Genève, 1972.
- [St 74] Stuart M., Eglises romanes et châteaux forts, Suisse alémanique (Vol 2.), Les Ed. de Bonvent SA, Genève, 1974.
- [St 77] Stuart M., Eglises romanes et châteaux forts, Suisse rhétique et italienne (Vol 3.), Les Ed. de Bonvent SA, Genève, 1977.
- [St 94] Studer-Freuler G., Vispertemenen, Versuch einer Beschreibung von Geschichte und Kultur eines Walliser Bergbauernvolkes, Rotten Verlag, Brig, 1994.
- [SIA V178 80] Swisscode, Maçonnerie de pierre, Société suisse des ingénieurs et des architectes, Zürich, 1980.
- [SIA 266 03] Swisscode, Construction en maçonnerie, Société suisse des ingénieurs et des architectes, Zürich, 2003.
- [SIA 261 03] Swisscode, Actions on structures, Société suisse des ingénieurs et des architectes, Zürich, 2003.
- [SIA 2018 04] Swisscode, Verification of the seismic vulnerability of existing common buildings, technical handbook, Société suisse des ingénieurs et des architectes, Zürich, 2004.
- [SIA D 0211 05] Swisscode, Vérification de la sécurité parasismique des bâtiments existants. Introduction au cahier technique SIA 2018. Société Suisse des Ingénieurs et des Architectes, Zürich, 2005.
- [SIA 266 07] SIA 266 (Swisscode), Construction en maçonnerie, Société suisse des ingénieurs et des architectes, Zürich, 2003, on-going project.
- [TSUM 02] Theodossopoulos D., Sinha B. P., Usmani A. S., Macdonald A. J., Assessment of the structural response of masonry cross vaults, Blacwell Science Ltd, 2002.
- [To 99] Tomazevic M., Earthquake-resistant design of masonry buildings, Imperial college press, 1999.
- [Tr 98] Trautz M., Zur Entwicklung von Form und Struktur historischer Gewölbe aus der Sicht der Statik, PhD Thesis, Institut für Baustatik, Universität Stuttgart, 1998.
- [Un 01] Ungewitter G., Lehrbuch der Gotischen Konstruktionen, 4th version, Chr. Herm. Tauchnitz, Leipzig, 1901.

-
- [VL 06] Vasconcelos G., Lourenço P. B., Assessment of the in-plane shear strength of stone masonry walls by simplified models, Structural analysis of historical constructions, New Delhi, 2006.
- [VR 93] Vermeltfoort A. Th., Raijmakers T. M. J., Deformation controlled tests in masonry shear walls, Part 2, Report TUE/BKO/93. 08, University of Eindhoven, 1993; (reference find in [Ko 02]).
- [VD 74] Viollet-le-Duc E.-E., Damish H., L'architecture raisonnée, Paris, 1978.
- [Vi 04] Viollet-le-Duc E.-E., Encyclopédie médiévale, Bibliothèque de l'image, 2004.
- [Visp ArP] Archives of the city of Visp.
- [Vi 05] Vitruvius P. M., De Architectura, translated by C. Perrault, reviewed by M. Nisard, Ed. Errance, Paris, 2005.
- [Wa 95] Warnecke P., Tragverhalten und Konsolidierung von historischem Natursteinmauerwerk, Dissertation, Institut für Baustoffe, Massivbau und Brandschutz, TU Braunschweig, Heft 114, 1995.
- [WRB 95] Warnecke P., Rostásy F.S., Budelmann H., Tragverhalten und Konsolidierung von Wänden und Stützen aus historischem Natursteinmauerwerk, Mauerwerk-Kalender 1995, Verlag Ernst und Sohn, Berlin 1995.
- [Wa 03] Warth O., Die Konstruktionen in Stein, J. M. Gebhardt's Verlag, Leipzig 1903; 7th version, Ed. «Libri rari» Th. Schäfer GmbH Hannover, 1981.
- [We 02] Weidmann M., Earthquakes in Switzerland, Desertina, 2002, Chur.
- [We 03] Weidmann M., Tremblements de terre en Suisse, Verlag Desertina, Chur, 2003.
- [Wi 06] Wild W., Auf der Suche nach archäologischen Spuren von Erdbebenkatastrophen, Mittelalter, Zeitschrift des Schweizerischen Burgenvereins, 2006.
- [www 1] www.library.thinkquest.org
- [www 2] www.flholocaustmuseum.org
- [www 3] www.arch.montana.edu
- [www 4] www.academic.udayton.edu
- [ZA 98] Zalewski W., Allen E., Shaping structures: statics, John Wiley & Sons, Inc., New York, 1998.
- [Zi 05] Zimmerman T., Dynamique des structures, méthodes numériques, notes de cours, EPFL, 2005.

Roman upper case

A	area
$A_{wx,y}$	plan area of earthquake resistant walls in the direction x and y.
A_w	plan area of all earthquake resistant walls.
D	damage
E	Young's Modulus
E_m	Young's Modulus for masonry
$E_{m,x}$	masonry Young's Modulus (vertical (x) axis)
E_s	stone Young's Modulus
E_{mo}	mortar Young's Modulus
$E_{o,i}$	Young's modulus of the outer leaf, inner leaf respectively (multiple-leaf wall)
F	force in general
G	weight of the whole structure
H_u	maximal shear-loading capacity (idealised curve)
I	second moment of Inertia
I	seismic intensity according to the EMS
I_o	epicentral intensity
K	correcting factors in general
K_e	secant stiffness
K_o	initial stiffness
M	bending moment
N	normal force

Symbols

N_n, N_v	normal force transmitted through vertical or inclined stress strut
P_{cr}	critical buckling load
Q	resultant of the seismic action
S	ground surface of the whole building
S_a	spectral acceleration
S_d	spectral displacement
T	period
V	shear force
V_i^*	average of the vulnerability index (Lagomarsino's method)
V_i^+	average value and maximal standard deviation (Lagomarsino's method)
V_i^-	average value diminished by the maximal standard deviation (Lagomarsino's method)
V_I	vulnerability index
$V_{R,S}$	maximal lateral load (in case of a shear failure)
$V_{R,R}$	maximal lateral load (in case of a flexural failure)

Roman lower case

a	acceleration
a_{gd}	peak ground acceleration
c	cohesion
f	natural frequency
$f_{c,w}$	compressive strength of the wall
$f_{c,e}$	compressive strength of the external leaves
$f_{c,i}$	compressive strength of the inner leaf
f_a	failure strength of the outer leaf (multiple-leaf wall)
$f_{s,c}$	stone compressive strength
$f_{s,t}$	stone tensile strength
f_{ml}	failure strength of a multiple-leaf wall (with two outer leaves)
f_{sd}	design shear strength (EC 8)
$f_{m,c}$	masonry compressive strength
$f_{m,c,am}$	failure stress of an ashlar masonry
$f_{m,c,ssm}$	failure stress of a squared-stone masonry
$f_{m,t}$	masonry tensile strength

$f_{m,x}$ or f_{mx}	compressive strength of masonry perpendicular to the bed joint
$f_{m,y}$ or f_{my}	compressive strength of masonry parallel to the bed joint
$f_{m,c,k}$	specific compressive strength of masonry (5% fractile)
$f_{m,o,c}$	mortar compressive strength
$f_{m,o,c,p}$	mortar compressive strength on prism
$f_{w,FK}$	strength of a stone-mortar-stone sandwich according to Berger's method
g	gravity acceleration
l_{2n}, l_{2v}	length of the vertical and inclined stress strut
q	seismic action

Greek lower case

α	angle of inclination
α_λ	factor for slenderness [Eg 93]
α_φ	factor for the influence of the loading direction [Eg 93]
β	equivalent seismic static coefficient related to the design ground acceleration
δ	drift
γ	specific weight
φ	internal angle of friction
κ	parameter that controls the slope of the curve; given in [La4 04].
λ	collapse multiplier
$\mu\Delta$	displacement ductility
μ_D	mean damage grade
ν_m	Poisson's coefficient of mortar
ν_d	design shear strength of masonry
σ_1, σ_2	principal stresses
σ_x, σ_y	stress in x- and y-direction
σ_N	normal stress
τ_{xy}	shear stress
τ_S	shear strength
θ_i	correction factor for the inner leaf [PLBA 05]
θ_e	correction factor for the outer leaves [PLBA 05]
ω	circular frequency

Abbreviations

DPM	Damage Probability Matrix
EMPA	Institute for the Testing of Buildings Materials
EMS	European Macroseismic Scale
EPFL	Federal Institute of Technology Lausanne
FEMA	Federal Emergency Management Agency
MDG	Mean Damage Grade
MDOF	Multi Degree Of Freedom
SDOF	Simple Degree Of Freedom
SIA	Swiss Society of Engineers and Architects

Word	Explanation
Abutment	A masonry mass which receives the thrust of an arch, vault, or strut.
Ambulatory	1. Passageway around the apse of a church, or for circumambulating a shrine. 2. Covered walk of a cloister.
Apse	Usually semicircular or polygonal, often vaulted recess, especially the termination of the sanctuary end of a church.
Arcades	A series of arches supported by columns, piers, or pillars, either freestanding or attached to a wall to form a gallery.
Arcatures	An ornamental, miniature arcade
Arris or groins	Arris is an architectural term that describes the sharp edge formed by the intersection of two surfaces.
Ashlar masonry	A squared block of building stone.
Baptistery	A building or part of one wherein the sacrament of baptism is administered.
Barrel-vault	A masonry vault of plain, semicircular cross-section supported by parallel walls or arcades.
Basilica	Form of the early Christian church: a central nave with clerestory, lower-aisles along the sides, with a semicircular apse at the end.
Bay	Within a structure, a regularly repeated spatial element defined by beams or ribs and their supports.
Bell tower	A tower in which a bell or a set of bells is hung.

Bond header, bondstone, throughstone	A bond header extends the full thickness of a wall.
Buttress	An exterior mass of masonry set at an angle to or bonded into a wall which it strengthens or supports.
Campanile	A bell tower, especially one near but not attached to a church or other public building.
Capacity curve	Or push-over curve. Curve representing the total shear force acting on a structure as a function of the lateral deflection at the top of the structure or element.
Cell	A small enclosed cavity or space.
Chancel	The sanctuary of a church, including the choir; reserved for the clergy. Is often enclosed by a lattice or railing.
Chancel arch	Arch which, in many churches, marks the separation of the chancel from the nave or body of the church.
Chapel	A place of worship that is smaller than and subordinate to a church.
Chevet	An apse having a surrounding ambulatory; usually opens into three or more chapels which radiate from the apse [Ha 77].
Crossing	In a church, the place where the nave and chancel cross the transept.
Cupola	A small dome set on a circular or polygonal base or resting on pillars.
Diaphragm	Horizontal structural element that ensure the distribution of the inertial forces to the vertical structural elements (walls) that can resist lateral forces.
Displacement capacity	Maximal displacement that can be reached by a structure under given forces.
Ductility	Ability of a structure to maintain its strength without significant degradation once its yield point is undergone.
Extrado	The exterior curve or boundary of the visible face of the arch.
Fabric	A structural material, such as masonry or timber.
Flying buttress	A characteristic feature of Gothic construction, in which the lateral thrusts of a vault are taken up by an arch and transferred then to a pier.
Formeret	Or wall rib. One of the ribs against the walls in a ceiling vaulted with ribs.
Fragility curves	Functions describing the probability of a building to reach or exceed a particular damage grade under a particular spectral acceleration.
Gable	A triangular, usually ornamental architectural section, as one above an arched door or window.
Groin-vault or groined-vault	A compound vault in which barrel-vaults intersect, forming arises called groins.
Haunches (vaults)	The middle part between the crown and the springing of an arch.

Headstone	The central wedge-shaped stone of an arch that locks its parts together (Keystone).
In- and out-bond	In masonry, a bond formed by headers and stretchers alternating vertically, especially at corners, as by quoins.
Intrado	The inner curve or face of an arch or vault forming the concave underside.
Intensity	Evaluations of the perceived local effects of an earthquake on the environment.
Keystone	In masonry, the central voussoir of an arch.
Lesenes	Or pilaster strip. Same as pilaster mass but usually applied to slender piers of slight projection; in medieval architecture and derivatives, often joining an arched corbel table.
Low-aisles or aisles	The space flanking and parallel to the main nave.
Narthex	The narthex of a church is the entrance or lobby area, located at the end of the nave, at the far end from the church's main altar.
Nave	The central part of a church, extending from the narthex to the chancel and flanked by aisles.
Pendentive	One of a set of curved wall surfaces which form a transition between a dome (or its drum) and the supporting masonry.
Presbytery, presbyterium	The actual sanctuary of a church beyond the choir and occupied only by the officiating clergy [Ha 77].
Purlin	One of several horizontal timbers supporting the rafters of a roof
Rib	A curved structural member supporting any curved shape of panel.
Rib-vault	A vault in which the ribs support (partially or fully) the web of the vaults.
Roof rafters	One of the sloping beams that supports a pitched roof.
Sacristy	A room in a church housing the sacred vessels and vestments; a vestry.
Shrine	Receptacle to contain sacred relics; by extension, a building for that purpose.
Spire	A top part or point that tapers upward; a pinnacle. Any slender pointed construction surmounting a building; generally a narrow octagonal pyramid set above a square tower [Ha 77]
Steeple	A tall ornamental structure; a tower, composed of a series of stories diminishing in size, and topped by a small pyramid, spire or cupola.
Stereotomy	The art of cutting stones.
Stonework	Masonry construction in stone. Preparation or setting of stone for building or paving.
Tambour	A circular or polygonal wall supporting a dome or cupola.
Transept	The transverse portion of a church crossing the main axis at a right angle and producing a cruciform plan.

Glossary

Truss	A rigid framework, as of wooden beams or metal bars, designed to support a structure, such as a roof.
Tuf or tufa	A rock composed of compacted volcanic ash varying in size from fine sand to coarse gravel.
Tympanum	A similar space between an arch and the lintel of a portal or window.
Vulnerability curve	Curve defining the expected damage as a function of an lateral motion input (e.g. the ground acceleration).
Web	Portion of a ribbed vault between the ribs.

A. 1. SWISS PRE-ROMANESQUE AND ROMANESQUE EDIFICES

A. 1.1. A BRIEF DESCRIPTION

A. 1.1.1. WESTERN SWITZERLAND

Romanesque Switzerland, its western part

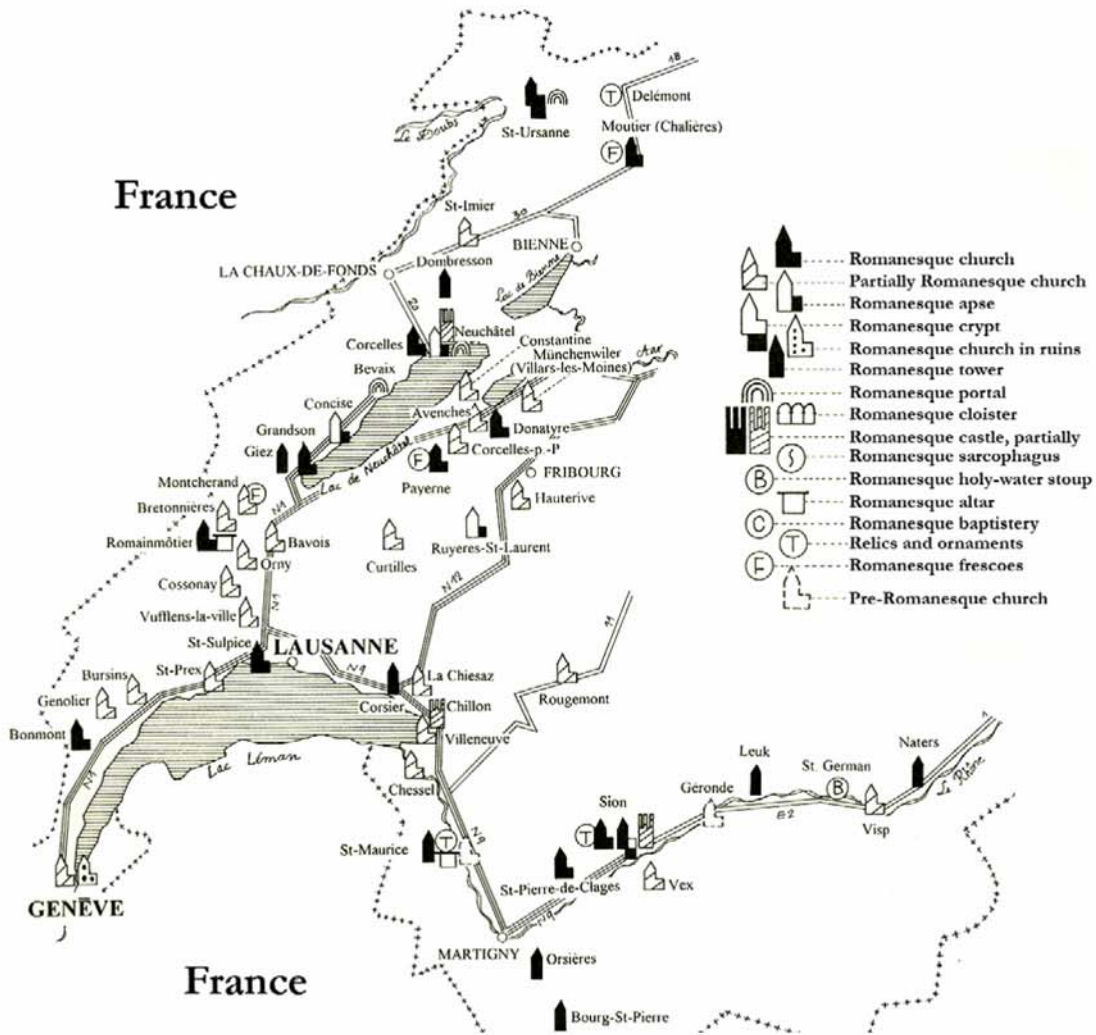


Figure 16.1 : Pre-romanesque and Romanesque edifices in Western Switzerland [Me 96]

A. 1. 1. 2. EASTERN SWITZERLAND

Romanesque Switzerland, its eastern part

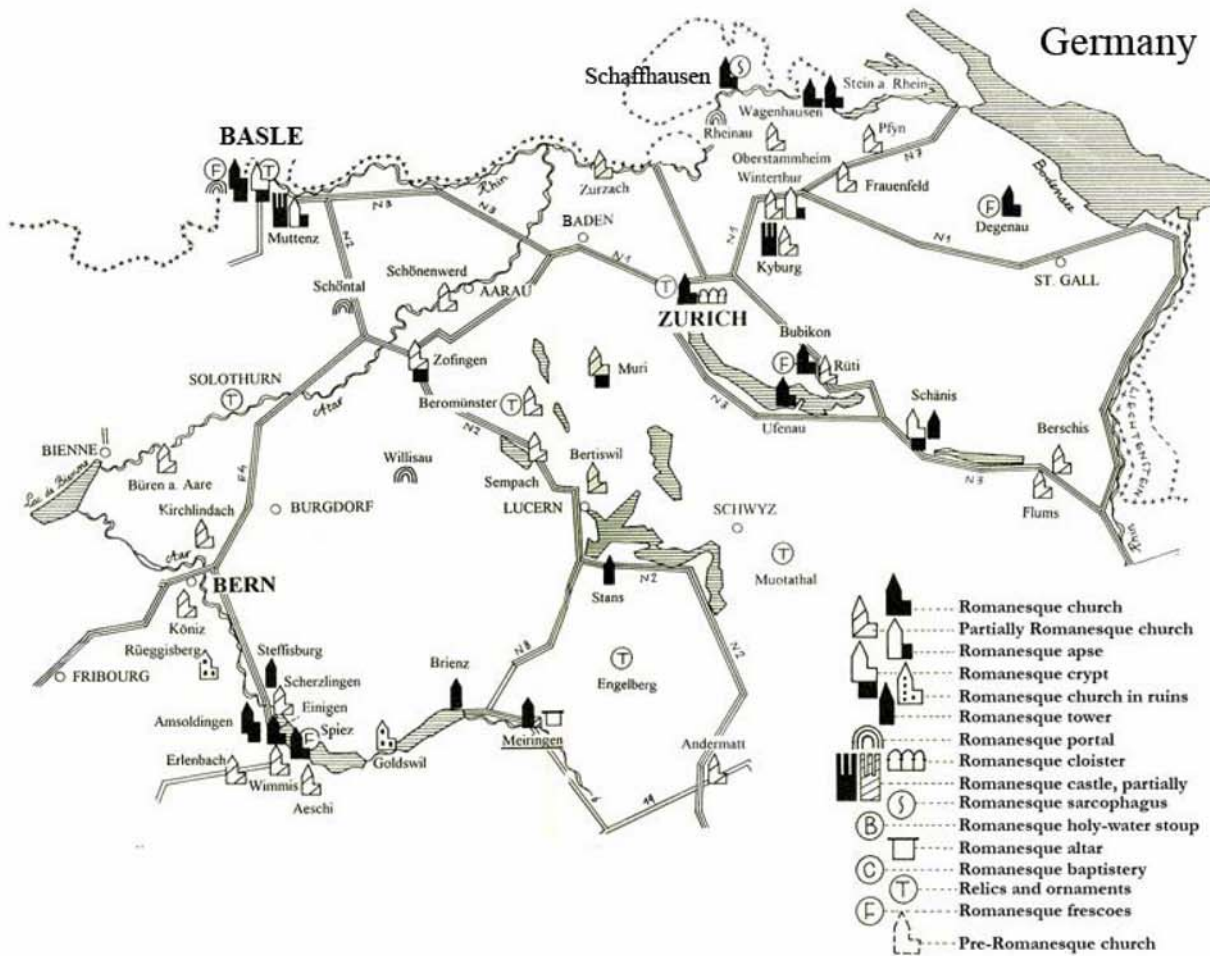


Figure 16.2 : Pre-romanesque and Romanesque edifices in Eastern Switzerland [Me 96].

A. 1. 1. 3. SOUTHERN SWITZERLAND

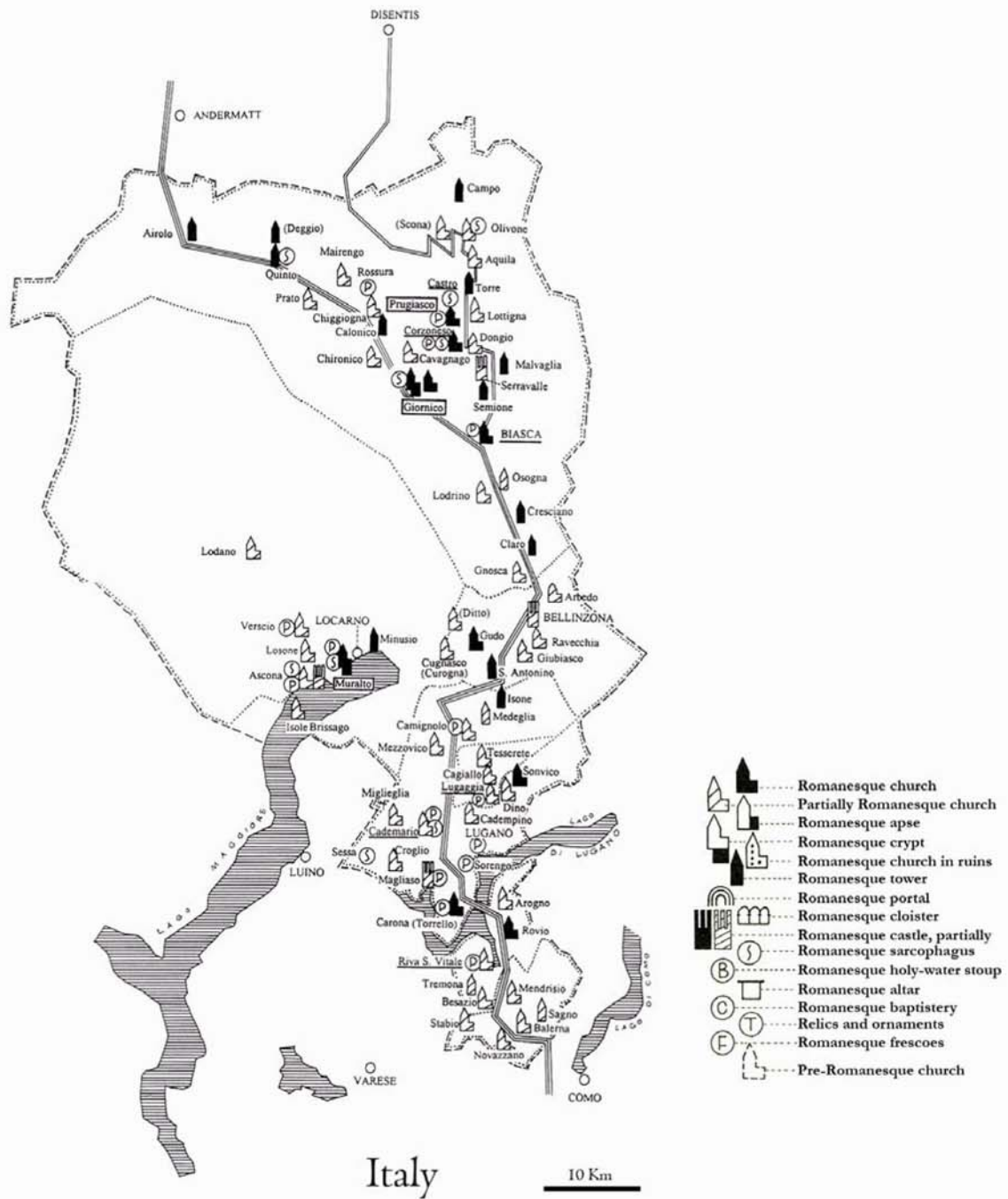


Figure 16.3 : Pre-romanesque and Romanesque edifices in Southern Switzerland [Me 96].

A. 1. 1. 4. SOUTH-EASTERN PART OF SWITZERLAND

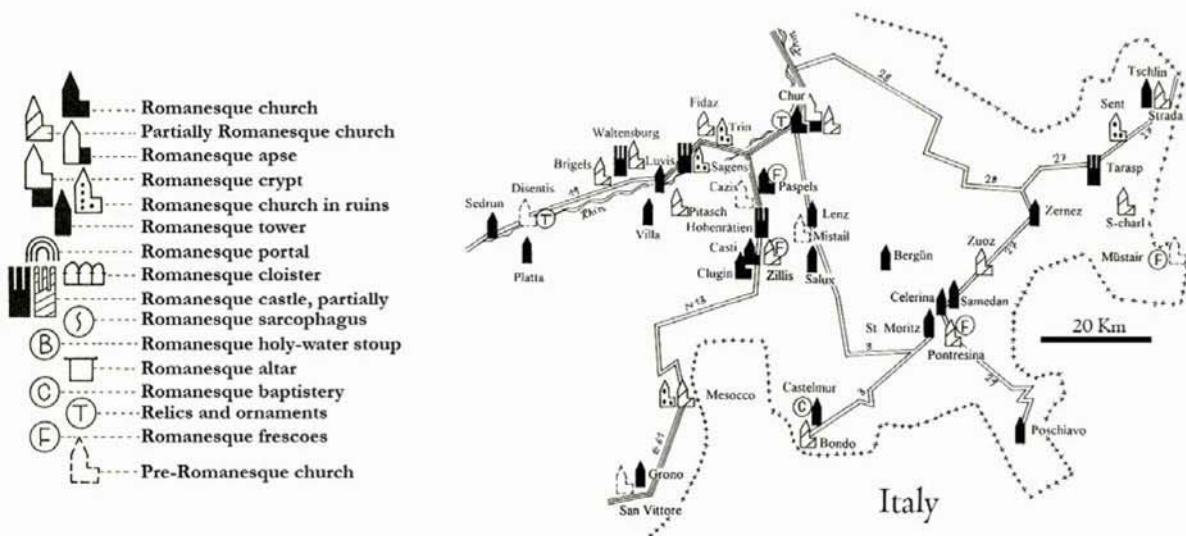


Figure 16.4 : Pre-romanese and Romanesque edifices in South-eastern Switzerland [Me 96].

A. 1.2. ARCHITECTURAL ACCOUNT

The purpose of this chapter is to give an overview of the architecture development throughout time. The present thesis deals with Pre-Romanesque and Romanesque sacred edifices, knowing that this period of time extends from the beginning of Christianity up to the second half of the 12th century. In order to set it in historical context, it is also complemented by a historical (mainly related to Christian history) account.

The following section is divided into homogeneous periods of time from an artistic standpoint.

A. 1. 2. 1. BEGINNING OF CHRISTIANITY

In the 2nd century, even if prohibited by Roman authorities, the Christian faith propagated from Rome through the main roads of the Roman Empire which linked the principal handcraft and business centres. The business centres in the Swiss geographical area were: Aventicum (Avenches, the capital of Helvetia), Augusta Raurica (Augst, close to the current city of Basel) and Geneva (Geneva). Christians were persecuted until the Edict of Milan, which was signed by the Emperor Constantine in 313 and which ensured freedom of worship to Christians. Christianity settled in Switzerland in the end of the Roman Empire; it is attested that bishoprics already existed in the 4th and 5th centuries. The first Episcopal cities were: Chur, Vindonissa, Augusta Raurica, Basle, Avenches, Yverdon, Martigny, Nyon and Geneva [Sc 71].

In the end of the 4th century, the migration of nations in Europe began. The Goths attacked the Roman Empire on the ground of the future Italy; to riposte, the Roman generals gathered all the available troops along the attack front. Consequently, the defence line along the Rhine was abandoned and never again provided. The relationship with Rome stopped with the north-eastern region of Helvetica whereas it went on with the future Western and Southern Switzerland as well as the Rhetia. It lasted until 476 when the Western Roman Empire collapsed under the attack of Ostrogoths. After Romans, Theodoric the Great, King of the Ostrogoths, beat Odoacer, King of the Hunnic, in Ravenna in 493. This city became the capital of the Ostrogothic kingdom of Italy as well as the cultural metropolis of Italy during the first Middle Age centuries. In 540, the Emperor Justinian I invaded Italy and conquered Ravenna, which became the seat of the Byzantine government in Italy. The construction of the San Vitale Basilica was finished in 547.

The year 568 witnessed another Germanic invasion of Italy, by the Lombards this time, a West Germanic people originally settled along the Danube. Lombards were less interested in Roman administration than Theodoric had been, and Italy became administered by the Germanic law (the Lombards). However, they never came to rule the whole Italy as Theodoric had done before them. They only established authority over discontinuous patches of Italy while the Byzantine Empire exerted control over the other parts, including Rome and Ravenna. In the end of the 6th century, the Lombards went north to the valley of the Ticino.

To the north of Italy, other Germanic tribes also settled, after a few devastating raids, in the future Swiss territories in the 5th century. Burgundians, who came from the west, was stopped on their way by Roman armies and settled then in the western part of the present Switzerland in 443. They were keen to adopt the Gallo-Roman culture they found, learned Latin, forgot their German language and became Christians. They converted to Roman Catholicism in 515. After the rapid break-up of Roman power, they set their capital in Lyon. At the same time, another Germanic people, the Alamannen, was infiltrating Switzerland in little groups, settling far from the Roman towns in small villages. There was no mixture with the indigenes culture and they stuck to their German language and mentality while Celtic and Roman indigenes gathered themselves inside Roman fortresses.

Frankish tribes invaded the north of the present France. Unlike Theodoric of the Ostrogoths, and the Visigothic kings, the Frankish leader Clovis (and thus many of his subjects) converted to Orthodox Christianity early on. This facilitated the fusion of the very separate entities of German and Roman societies into a single new civilisation, unseen in the Ostrogothic or Visigothic kingdoms. Moreover, this conversion highly contributed to make the Christianization of Europe progress. Clovis, who founded the Merovingian Dynasty in the beginning of the 6th century, rapidly extended its Empire borders. For instance, Sigismond, the King of Burgundians was defeated in 534 by Franks while the Alamannen were already under their domination.

A 1.2.1.1. Sacred edifices

The first Christian sacred edifices were not influenced by Roman temples; they adopted the basilica (built for the Roman public manifestations) pattern because their buildings had to be a place where people could gather for worshipping, as Roman basilicas had been before. The basilica was divided into naves separated by two ranges of arcades; there was also often a small room (barrel-vaulted) where the judges sat. This room was called an apse. This architectural configuration became the

prototype for the first Christian churches. When the terrain at disposal was large enough, the basilica was aligned along the west-east direction.

From this time onwards, the basilica shape became one of the two fundamental patterns of churches for many centuries (until the end of the 19th c.). The other essential Christian architectural type, was the square, octagonal or circular construction. This was predominant mainly in the Byzantine areas. This shape was probably inspired by small Roman graves or public baths.

The most famous Christian building, which dates from the beginning of Christianity and still standing, is probably the basilica of San Vitale in Ravenna (547), whose construction had begun under the reign of Theodoric the Great in 532.

The octagonal pattern of baptisteries came from this architecture; the baptistery of Riva San Vitale in the canton of Ticino, which dates to the 5th century, is the only example of this architecture still existing in Switzerland.



Figure 16.5 : Outer view of the basilica San Vitale in Ravenna (532-547).

The period of Germanic invasions was synonymous with fear and precariousness in the bordering regions of the Roman Empire such as Switzerland. It became difficult to find good workers, money and the motivation to build sacred edifices. Consequently, wide edifices were very rarely built as has been proven by ground excavations; the basilicas, like those found in Geneva (bishopric), with more than one nave were exceptions (Figure 16.7). In the end of Antiquity, the one-nave small edifice with poor-quality masonry, one simple two-slope roof and an apse at one end was the most widespread sacred building. This kind of building was long the archetype of the first Christians' oratory in countryside [SS 79].

It is assumed that sacred edifices were erected at the same place than previous pagan buildings. For instance, in Geneva, the Saint Madeleine's church was built on the foundations of a temple dedicated to Maïa. Moreover, it was also frequent to find a church erected on the foundations of a Roman villa.

Construction of most sacred edifices were financed by bishops or kings, in order to worship one or more Saints, whose relics were kept in the sanctuary of the edifice. These sacred buildings attracted pilgrimages from pious people throughout Europe for worshipping many Saints. In Switzerland, a notable example is the church in Saint Maurice (Sion bishopric) where relics of the Theban legion were venerated.

Swiss territory was divided into a few bishoprics, which corresponded to the previous configuration of the Roman states [SS 79]. The early Christian landscape seems to have been composed of cathedrals (Episcopal seats) and parish churches. The abbey churches came later; during the 4th and the 5th centuries, monks were still nomads or sometimes already organised in small communities, living in groups.

EPISCOPAL CHURCHES

In 340, an Episcopal church was erected in Augst (foundations of an Episcopal church were found in the present Kaiseraugst church ground) that was composed of a long nave and an apse with lateral appendixes; there also was a baptistery (Figure 16.6).

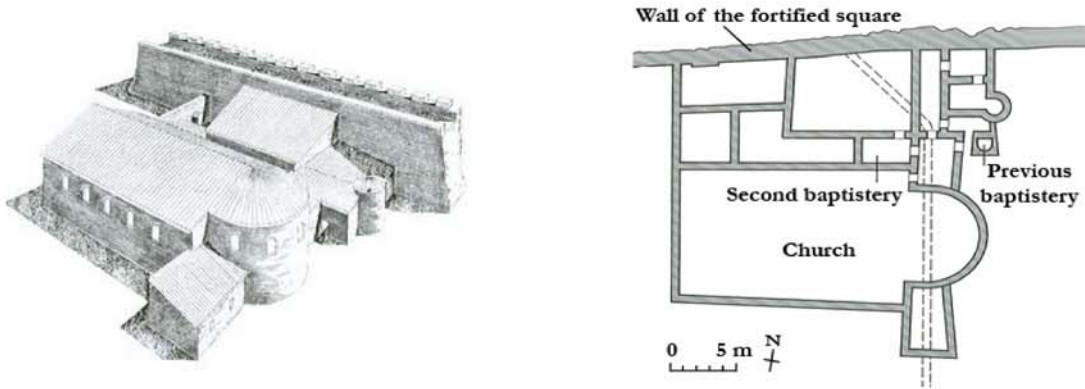


Figure 16.6 : Episcopal seat in Augst around 340 AD [Ho 88].

At the same time, the Episcopal seat in Geneva had two cathedrals (one for the bishop and where the sacraments were performed and the other for the faithfuls), basilica shaped, 30 m long, with a baptistery in-between (Figure 16.7). Chur also had an important ecclesiastic complex [Ho 88]. A similar building complex was found in the Tenedo castle in Zurzach; both churches were probably built around 400 [Sc 71]

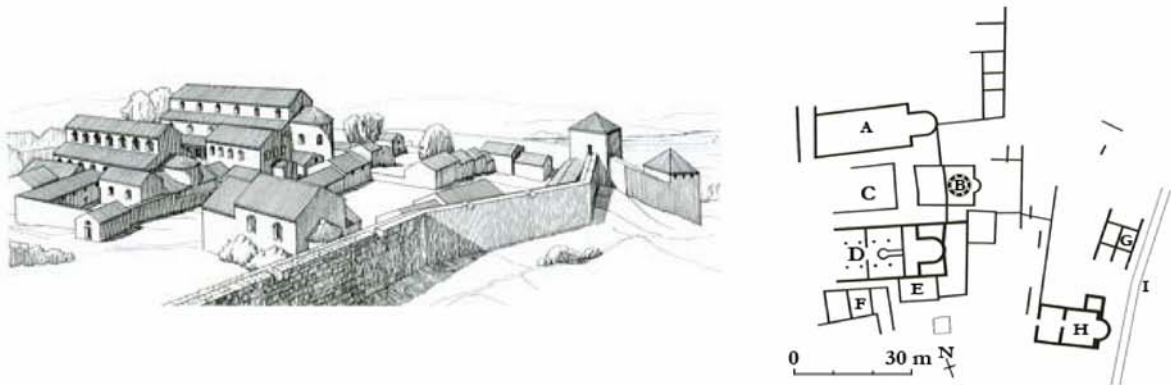


Figure 16.7 : Episcopal seat of Geneva around 400 AC [Ho 88]

Legend:	A Cathedral	F Appendices
	B Baptistery	G Episcopal castle
	C Atrium between both edifices	H Episcopal chapel
	D Recently built cathedral	I Roman villa fence
	E Reception hall	

The episcopal edifices, which were made of masonry, were of small dimensions. The nave, which was a sort of large room whose ceiling was made up of visible beams (wooden ceiling), was finished at one end by a semi-circular apse; a chancel arch separated the nave from the apse. The entrance was usually situated at the west whereas the apse was built toward the east. This shape was actually the archetype of many future churches.

Though many sacred buildings were erected during this period in Switzerland, the only edifice built at this time which is still standing, is the baptistery of San Vitale in the Ticino (500).

PARISH CHURCHES

Beside Episcopal edifices, which were built in most important cities of that time, many smaller churches were built throughout the countryside, like in Commugny, Corsier, etc. To build them, parts of masonry taken from previous Roman villas or fortresses were generally used. They usually had a simple rectangular nave finished by a narrower semi-circular apse, like in Schiers, Zillis and in Schaan (Liechtenstein) [Sc 71].

After the collapse of the Roman Empire, Germans invaded the centre of Europe and in 537 [Sc 71], the Swiss region was under the Merovingian Kingdom.

A. 1. 2. 2. MEROVIGIAN PERIOD

The Merovingian Dynasty, which started with Clovis, lasted until the middle of the 8th century. Although Clovis' conquered lands were distributed among his four sons upon his death, the Franks wielded authority over a large portion of Europe long after Clovis. Nevertheless, with respect to the future Swiss territory, the canton Ticino was outside the Merovingian kingdoms.

Since the decline of the Roman Empire, the Merovingian Dynasty was the first to reorganize the Christian Church throughout its kingdoms.



Figure 16.8 : Merovingian kingdoms and its tributary regions [www 1].

A 1.2.2.1. Sacred edifices

At this time, sacred edifices were still built (and also belonged to) by sovereigns or bishops. Moreover, they were endowed with goods by their founder. Founding lords frequently required a tithe for the use of goods they put at disposal of the clergy.

Merovingian period was also characterized by the coming of missionary monks. In this framework, two Irish monks played an important role in the Christianization of Switzerland: Saint Columban and Saint Gall. The former (543-615) founded monasteries in the Frankish kingdoms as Luxeuil (Vosges), from where his monastic rules rapidly spread throughout France. Because of political conflicts with bishops and Merovingian kings, including disagreements over the date for the celebration of Easter, Saint Columban moved south into Italy around 612, passing by Switzerland. Saint Gall (550-645), who was Saint Columban's disciple, joined him on his way to Frankish Empire (from Ireland). After founding Luxeuil in France, they set off to Alemania, went to Zurich, Tuggen and Arbon, where they built a monastery in an old Roman castle. While his master went on to Italy, Saint Gall stopped in the Steinachtal where he founded the future foyer of the Christian culture in Alemania, i.e. Saint Gall's abbey.

Beside the bishoprics of Basel, Chur, Geneva, Lausanne and Sion, a new diocese was created in the end of the 6th century: the diocese of Constance. This newly created diocese was under the archbishopric of Mainz protection. Under the archbishopric of Besançon, Lausanne was influenced by the Burgundian culture, as also was Basel, although to a less extent. The archbishop of Milan wielded a certain power on the southern area of the present Switzerland (since Ticino was invaded by Lombards in 568) as well as on the bishopric of Chur. The dioceses of Sion and Geneva were influenced by the Savoy and the Provence (Vienne) archbishopric, respectively.

However, due to its geographical situation, Rhetia was more or less separated from the Lombards' influence and also from the Frankish culture (though it was linked to the Franks Empire in 539) and kept their Roman traditions. Moreover, a noble family (Victorids) appropriated both spiritual and political powers in Rhetia and ruled over it from 550 to 775. The diocese of Chur broke up from the archbishopric of Milan and joined the one of Mainz in 843.

Except the baptistery of Riva San Vitale, no sacred buildings from this age survived because of abandon, destruction by humans, deterioration over time, etc. Furthermore, according to literature and vestiges [SS 79], it seems that the Merovingians' art of building was fair and the constructions were not durable.

A. 1. 2. 3. CAROLINGIAN PERIOD

During the period from 400 to 800, Western Europe was dominated by small kings, dukes and noblemen. In fact, Frankish and Burgundian kings had limited influence. In the beginning of the 8th c., Charles Martel (688-741) was the leading member of one of the most important aristocratic families within the Frankish kingdom. In the Merovingian world, the aristocracy got a certain immunity from royal authority, creating a system where power was not wielded by kings, but rather by regional aristocratic families led by dukes. Charles Martel had come into power as a Mayor of the Palace, who acted as an advisor to the king on behalf of the aristocracy. By the 8th c., he had amassed such a large support base that he was the recognised acting leader of the Franks though he did not have the title of a king. Moreover, he maintained a strong army of heavily armoured cavalrymen through a system of vassalage. A vassal's absolute allegiance to Martel would be reciprocated with an estate and wealth (often taken from subdued rivals or enemies). This relationship of mutual

responsibilities between vassals and lords formed the fabric of social interaction among the higher class of European society in the Middle Ages. Regarding religion, Charles Martel also supported the spread of the hierarchical, Roman form of Christianity in the Frankish kingdom, which had been strengthened by Anglo-Saxon missionaries from Ireland, as aforementioned. The highly centralized nature of the Roman form of Christianity was in Martel's favour, especially as he could extend his ruling influence by designating his supporters as bishops within the Church.

Eventually, Martel's son, Pippin III, used this blossoming relationship with the papacy to formally obtain the title of king (in addition to the practical power of king that he inherited from his father) and finally supplanted the last of the Merovingian Dynasty in 751. This seeking of papal approval set a precedent in Europe for the Church's involvement in the recognition of royal power, which had been until that time a secular mixture of noble birth and military prowess.

Charlemagne (747-814), the 3rd of the Carolingian line, not only inherited the Frankish kingdom (768), but also influenced the whole of Europe through his strong (and long) leadership of the Carolingian Empire.

He organized an administration based on counties all over Western Europe. Charlemagne subdued and absorbed the Aquitainians, Bavarians, Lombards, Avars, Saxons, and the Spanish in Catalonia. When Lombardy was linked to the Holy Empire in 774, the Swiss region was geographically in the heart of the great Empire; among others, this increased the importance of the Alpine passes. From then on, the Swiss territory became a sort of gravity centre of the Carolingian culture, which is proven by the primordial rights received by Swiss monasteries (Saint Gall for instance).



Figure 16.9 : Map of Charlemagne's Empire after 800 AD [www 2].

In terms of governance, the vassalage system Martel had employed still continued. At the regional level, counts with close personal bonds of allegiance to Charlemagne presided over estates and the courts of the county. The relative autonomy granted to the counts was balanced by visiting royal delegations composed of other counts and bishops, called *missi dominici*. This network of ruling aristocrats and *missi* who were personally tied to the king set a model of governance for the latest leaders of the Middle Ages.

Charlemagne's rule was also closely tied to the Church. Rather than unifying the vast kingdom through the imposition of Frankish traditions and laws, Charlemagne tried to hold the kingdom together through religion. To do so, he set up a strategic network of palaces (which were the prototype of castles) and especially of abbeys throughout his Empire as well as along its borders such as along the Alps. It is worth noting that abbeys (derived from the Roman *castrum* and *villa*; it was as much a fortified town as a kind of colony), which were built along pilgrimage roads, were actually the foundation of the Romanesque civilization [Mo 72]. The Roman form of Christianity that the Frankish kingdom had adopted was hierarchical and therefore extremely well suited to be aligned with a centralized system of government.

Moreover, Charlemagne was allied with the papacy in such a way that on Christmas in the year 800, he was crowned Emperor by the pope in St. Peter's Basilica in Rome. Considering the significant role Christianity played in Charlemagne's kingdom, it is not surprising that Charlemagne reformed his clergy. In the few centuries before Charlemagne's rule, Frankish monasteries had degraded, such that the clergy had little education and the monasteries were no longer recognised as institutions of learning. Also, other centres of learning, which were separated from the Church, had also disappeared, resulting in a deplorable state of education.

In an effort to reform the Frankish clergy, Charlemagne supported a variety of educational programs within the royal court under the charge of a man called Alcuin of York. The best minds from all over Europe, including those from England, Ireland and Italy, were brought to the Frankish court to set a new and strong educational program. In the monasteries of Saint Gall and Fulda, Charlemagne supported the establishment of schools. Hence, with these educational reforms, the Carolingian Renaissance was ushered into the 9th century.

The reform of education was in some ways part of the clergy reform: education was being reformed in order to reorganize the clergy. In parishes, the clergy was trained to perform the Christian rituals in a standard and unified form. At monasteries, the Benedictine version of monasticism was encouraged as the established form (it became the Empire monastic rule in 817), and the knowledgeable clerics were cultivated in order to effectively serve both the Church and the Frankish government. Besides spiritual education and teaching, monks helped to clear the forests, to plant vines and they also introduced new processes in agriculture. In 747, the monastery of Saint Gall abandoned the monastic rule of Columban and instead adopted the Benedictine rule.

Whereas the Frankish scribes had salvaged old Roman texts and on their basis, developed their own culture of education of their own, Carolingian art was characterised by a fresh synthesis that combined traditions from both Roman and Barbarian worlds. In the late 8th century, Charlemagne commissioned a palace complex to be built in Aachen, and the Chapel at the Waters became the centrepiece of this architectural complex. This chapel is probably the most famous example to illustrate the combination of Roman and Barbarian worlds.

A 1.2.3.1. Sacred edifices

Under the Carolingian Reign, Europe came through a relatively peaceful period which was good for an architectural renewal. Although Roman techniques were still applied, the original Roman model of a basilica for the church was abandoned for new architectural shapes.

In fact, the Empire's emblem became the cathedral which was designed to show the union between temporary and spiritual powers. The shape of Cathedrals was based on the famous plan of Saint

Gall (presented at synods in 817 or 818), given by the bishop of Basel (Haitto) to Gozbert, who wanted to erect a cathedral at Saint Gall's hermitage place: it was characterized by a westwerk (with the Emperor tribune), a Carolingian feature that symbolized the Imperial power. The basilica had then a nave whose extremities were composed of apses, a choir area and a transept with a lantern-tower. The nave became then the link between the Episcopal seat and the Emperor's. Moreover, this edifice had to be the church for monks, pilgrims and laymen. To sum up, it represented a sort of universal edifice that pre-dated the Middle Ages cathedrals. The crypt was also a typical Carolingian feature, where the Saints relics are conserved and worshipped. Pilgrimages in the beginning of the Middle Ages were almost always undertaken for worshipping tombs and relics. In Switzerland, Saint Maurice, where the Theban legion's relics were conserved, was a spiritual point of convergence in the Empire.

In comparison, Lombard cathedrals (or Duomo) were simply composed of a nave leading to a transept surmounted by a lantern-tower and then a chancel. This kind of edifice was erected within the city precincts and a square was always built in front of them [DS 96].

Amongst the main Carolingian buildings, the Palatine chapel in Aachen (790-805, designed by Eudes from Metz) must be quoted. This edifice, which was a part of Charlemagne's palace, was covered by a cupola with two levels of galleries surmounted by an octagonal lantern-tower, like the church in Ravenna (532-547) [DS 96].

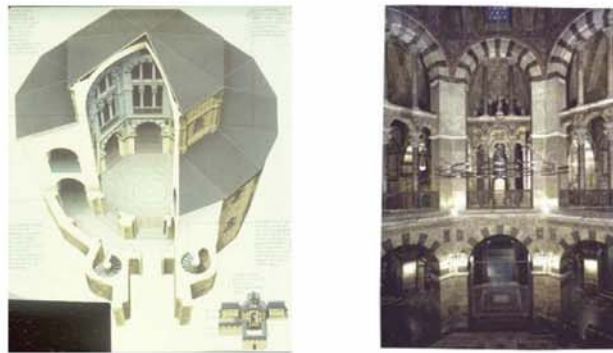


Figure 16.10 : 3D and inner view of the Palatine chapel [www 3].

This building, which had been built upon the remains of Rome and the glory of the Frankish king, housed the three strands that composed the fabric of medieval Europe - the Christian religion, Roman traditions, and Germanic leadership.

The Carolingian churches in Switzerland were usually composed of a nave with three apses. Famous example still standing are the convents of Mistail and of Mustair in Rhetia (8th c.). It is worth noting that foundations of many great Swiss sacred buildings date from the Carolingian period like the Fraumünster of Zürich, the cathedral of Saint Gall or the abbey of Saint Maurice. The church of Spiez and both first pre-medieval churches of Romainmôtier were also beautiful examples of buildings from this time. An interesting fact is that all the aforementioned edifices show diverse architectural influences. Switzerland, at that time, was at the centre of Charlemagne's Empire, which was in the midst of Artistic currents and was also a place of cultural exchanges and trends. Nevertheless, it must be also said that its Alpine geography prevented a complete mixture of styles.

A. 1. 2. 4. HIGH MIDDLE AGES

Upon Charlemagne's death in 814, his only surviving son, Louis, became the king of Franks and the Emperor. When the Emperor Louis himself died, a civil war erupted amongst his sons Lothar, Charles the bald and Louis II for the throne. This conflict was finally solved in 843 by the treaty of Verdun that split the Holy Empire into three parts: western (France), central (Lorraine-Burgundy-Italy) and eastern (Germany). So Switzerland was then split between Burgundy and Germany for a while. But soon the central Empire decayed and around 900 the German king had seized control over Burgundy and Italy. From an economical and social point of view, this was a difficult and dangerous period in Switzerland.

The legacy of Charlemagne's purpose, that is, the extension of the Empire borders as far as the Roman borders were at the Western Roman Empire apex, was resumed by the Saxon kings after the victory of Henry I on the Hungarians in the end of the first millennium. His son, Otto I, was crowned in 962 as the Emperor of the Holy Roman Empire in Aachen by the dukes of Frankish, Lorraine, Swabia (Alamannic southern Germany) and Bayern. Otto I settled the feudal system that helped to organise the political structure. Since then, civil wars stopped and peace made its way in Europe.



Figure 16.11 : Map of the Holy Roman Empire in the 12th century [www 4].

While other German dukes quarrelled with each other about power within the German Empire, the traditional disinterest or even aversion of the Alamannen to national organisation deprived the Swabia dukes of support (Alemania was a part of the Swabia dukedom). Consequently, they played a minor role in Southern Germany as well as in Switzerland. The power in Alemania was actually exercised by counts rather than by dukes; several counts, namely those of Habsburg (North-eastern Switzerland), Kyburg (midland), Toggenburg (Turgau) and Zähringen (midland), gained remarkable influence in Switzerland during the Middle Ages. Nevertheless, most of the dynasties were extinct by the end of the Middle Ages. Western Switzerland was under the influence of the Burgundian Kingdom and, as in Alemania, counts tried to extend their territories: for instance, the counts of Savoy had interests in the cantons of Vaud and Geneva, whereas the counts of Gruyere were interested in Freiburg.

Amongst them, the counts of Habsburg were probably the most ambitious. Starting from a castle in Northern Switzerland they had acquired territories in Austria and also tried to acquire the heritage of the counts of Kyburg, Zähringen and Toggenburg.

Regarding Arts and architecture, this political and economical situation was stable enough to lead towards an Artistic renewal after the long interruption due to political troubles after Charlemagne's reign. People were once again able to make long journeys and pilgrimages throughout Europe without problems; this situation was also favourable to cultural and economic exchanges as well as new artistic currents.

A 1.2.4.1. Sacred edifices

In parallel to the political development of the Holy Roman Empire, the monastic societies also initiated a reform. After a period of inactivity, the abbey of Cluny wanted to break free from the protection of the Emperor and noblemen; the abbey obtained it and the abbey was only under the pope protection in 910. The main abbot was elected without any bishops or laymen opinion. Moreover, the prior of the congregation monasteries only had to obey the main abbot of Cluny. They built many monastic communities throughout Europe and also many existing communities asked for joining them; at its apogee, Cluny's monastery had 1500 convents under its control. The first monastery that belonged to Cluny in Switzerland was Romainmôtier.

Eastern Switzerland was influenced by the abbey of Hirsau, which was the most prestigious monastery united with Cluny. The abbey of Schaffhausen (The all Saints' church, 1150) is probably the most famous example of the architecture from Hirsau. The monastery of Cluny had a great influence on society of that time; at its peak, the community began the construction of the biggest edifice of Christianity (5 naves, 8 towers, 2 transepts and one narthex). However, it has never been finished.

The power and wealth of Cluny softened the initial principles of the Benedictine monastic rule. In 1115, to counteract what he thought to be a decline of the Benedictine rule, Bernard de Clairvaux and other monks founded a new monastic order: the Cistercians. At Bernard's death, 343 abbeys were under the Cistercian protection. In 1153, the abbey of Bonmont was founded in Switzerland, then came Lucelle in Eastern Switzerland and finally Canobbio in the Ticino. About 30 abbeys and Cistercian convents were founded in Switzerland between the 12th and the 13th centuries.

The creation of new monastic orders and their growth in the 11th century resulted in building a lot of sacred edifices [Fr 93]. Romanesque period actually corresponds to an era of revival of Art and

growth in Europe. Nevertheless, building techniques as well as the configuration of sacred buildings did not differ a lot from the ones applied during the Carolingian era, which were inspired from Roman techniques [CVLR 82]. Romanesque architecture derived from the Antiquity and the ten books of *De Architectura* [Vi 05] were the architectural and technical basis out of which the new style arose.

At this time, scholars belonged to the ecclesiastic society. The supervision of building sites and the construction were the prerogative of the regular clergy only; the abbots and monks were becoming great builders. Moreover, they were the first to be able to directly adapt the shape of sacred buildings to the liturgy, space and light requirements.

Benedictine rule made monks adapt the configuration of sacred buildings especially for liturgy. On the contrary, Cistercian order implemented specific rules for their buildings: masonry was not whitewashed, the floor was just covered by paving stones and the naves had to be barrel-vaulted. It is worth noting that since the construction of the first edifice, pointed-arches were applied to arcades, windows and vaults. It must be said that Cistercian builders were particularly skilled in construction in comparison with other orders.

In the 11th century, political stability made possible an economical and social growth. The multiplicity and diversity of the first Romanesque edifices followed two main artistic currents: the first one, which is the direct legacy of the Carolingian past, can be found in the Holy Roman Empire (Central and Northern Europe), and the second is a more rustic and widespread current in Northern Italy, Catalonia, Provence and in the Rhone and Saone valleys. While in the north they used wood for the ceiling of their edifices, the southern countries covered the edifices naves with stone vaults (direct legacy of the Christian churches in Ravenna). It is worth noting that the Kingdom of Burgundy, which was situated between the north and the south, was influenced by both the Carolingian and the southern architectural style.

The plans, though different all over Europe, had similar features due to liturgy. Most churches adopted the basilica configuration. The Carolingian basilica was enlarged and the new architectural style added an area between the chancel and the area for the lays: the transept. The basilica was broadly composed of one or three naves, transept, lantern-tower, towers, crypt, and chancel with choir and sometimes an ambulatory; there was sometimes also a narthex. The chancel ground was often slightly raised above the nave floor, which was also sometimes the crypt ceiling. Whereas the chevet had a semicircular cross-section at the beginning of the Romanesque era, it became flat towards the end (premises of Gothic style [CVLR 82]). It is worth noting that only a few parts of the church were vaulted at first; later, the whole edifice was vaulted and then the cupola placed on the transept crossing appeared too. The west entrance was sometimes conceived, as in the areas of the Holy Roman Empire, as a space independent (the westwerk) from the rest of the church and was flanked by towers (Carolingian legacy). Windows were quite small, except in buildings whose covering was a timber framework; the outer side of walls was ornamented by lesenes and arcatures.

The first Romanesque edifices in Switzerland were erected in the beginning of the 11th century. Western Switzerland was one of the first regions influenced by the Benedictine (Cluny) and the Cistercian orders and their monastic reforms. Romainmôtier and Payerne abbeys, which were under Clunisian influence as soon as the 10th century, set up a large network of smaller congregations in this part of the country. This contributed to the introduction of new building techniques such as the stone vaults and the Clunisian stone sculpture.

The first signs from the Cistercian reform in this area appeared in the 12th century; the abbey churches of Bonmont and Hauterive are good examples.

It is worth noting that the edifices that were completely erected during the Romanesque period were few and those which are still intact today are even fewer. In fact, many great buildings, such as the cathedrals of Geneva, Lausanne, Basel, Chur or the Grossmünster in Zürich were built in many stages and only the first one was Romanesque. Other Romanesque (or Pre-Romanesque) edifices have been transformed since their completion.

A. 2. OBSERVED DAMAGE

A. 2.1. EMS-98

A. 2.1.1. DAMAGE SCALE

Intensity	EMS-98	Description
Not felt	I	a) Not felt, even under the most favourable circumstances. b) No effect. c) No damage.
Scarcely felt	II	a) The tremor is felt only at isolated instances (<1%) of individuals at rest and in a specially receptive position indoors. b) No effect. c) No damage.
Weak	III	a) The earthquake is felt indoors by a few. People at rest feel a swaying or light trembling. b) Hanging objects swing slightly. c) No damage.
Largely observed	IV	a) The earthquake is felt indoors by many and felt outdoors only by very few. A few people are awakened. The level of vibration is not frightening. The vibration is moderate. Observers feel a slight trembling or swaying of the building, room or bed, chair etc. b) China, glasses, windows and doors rattle. Hanging objects swing. Light furniture shakes visibly in a few cases. Woodwork creaks in a few cases. c) No damage.

Strong	V	<p>a) The earthquake is felt indoors by most, outdoors by few. A few people are frightened and run outdoors. Many sleeping people awake. Observers feel a strong shaking or rocking of the whole building, room or furniture.</p> <p>b) Hanging objects swing considerably. China and glasses clatter together. Small, top-heavy and/or precariously supported objects may be shifted or fall down. Doors and windows swing open or shut. In a few cases window panes break. Liquids oscillate and may spill from well-filled containers. Animals indoors may become uneasy.</p> <p>c) Damage of grade 1 to a few buildings of vulnerability class A and B.</p>
Slightly damaging	VI	<p>a) Felt by most indoors and by many outdoors. A few persons lose their balance. Many people are frightened and run outdoors.</p> <p>b) Small objects of ordinary stability may fall and furniture may be shifted. In few instances dishes and glassware may break. Farm animals (even outdoors) may be frightened.</p> <p>c) Damage of grade 1 is sustained by many buildings of vulnerability class A and B; a few of class A and B suffer damage of grade 2; a few of class C suffer damage of grade 1.</p>
Damaging	VII	<p>a) Most people are frightened and try to run outdoors. Many find it difficult to stand, especially on upper floors.</p> <p>b) Furniture is shifted and top-heavy furniture may be overturned. Objects fall from shelves in large numbers. Water splashes from containers, tanks and pools.</p> <p>c) Many buildings of vulnerability class A suffer damage of grade 3; a few of grade 4. Many buildings of vulnerability class B suffer damage of grade 2; a few of grade 3. A few buildings of vulnerability class C sustain damage of grade 2. A few buildings of vulnerability class D sustain damage of grade 1.</p>
Heavily damaging	VIII	<p>a) Many people find it difficult to stand, even outdoors.</p> <p>b) Furniture may be overturned. Objects like TV sets, typewriters etc. fall to the ground. Tombstones may occasionally be displaced, twisted or overturned. Waves may be seen on very soft ground.</p> <p>c) Many buildings of vulnerability class A suffer damage of grade 4; a few of grade 5. Many buildings of vulnerability class B suffer damage of grade 3; a few of grade 4. Many buildings of vulnerability class C suffer damage of grade 2; a few of grade 3. A few buildings of vulnerability class D sustain damage of grade 2.</p>

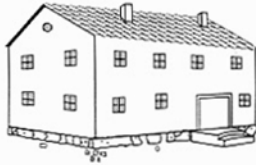
Destructive	IX	<p>a) General panic. People may be forcibly thrown to the ground.</p> <p>b) Many monuments and columns fall or are twisted. Waves are seen on soft ground.</p> <p>c) Many buildings of vulnerability class A sustain damage of grade 5. Many buildings of vulnerability class B suffer damage of grade 4; a few of grade 5. Many buildings of vulnerability class C suffer damage of grade 3; a few of grade 4. Many buildings of vulnerability class D suffer damage of grade 2; a few of grade 3. A few buildings of vulnerability class E sustain damage of grade 2.</p>
Very destructive	X	<p>c) Most buildings of vulnerability class A sustain damage of grade 5. Many buildings of vulnerability class B sustain damage of grade 5. Many buildings of vulnerability class C suffer damage of grade 4; a few of grade 5. Many buildings of vulnerability class D suffer damage of grade 3; a few of grade 4. Many buildings of vulnerability class E suffer damage of grade 2; a few of grade 3. A few buildings of vulnerability class F sustain damage of grade 2.</p>
Devastating	XI	<p>c) Most buildings of vulnerability class B sustain damage of grade 5. Most buildings of vulnerability class C suffer damage of grade 4; many of grade 5. Many buildings of vulnerability class D suffer damage of grade 4; a few of grade 5. Many buildings of vulnerability class E suffer damage of grade 3; a few of grade 4. Many buildings of vulnerability class F suffer damage of grade 2; a few of grade 3.</p>
Completely devastating	XII	<p>c) All buildings of vulnerability class A, B and practically all of vulnerability class C are destroyed. Most buildings of vulnerability class D, E and F are destroyed. The earthquake effects have reached the maximum conceivable effects.</p>

Table 16.1 : EMS-98 damage scale [EMS 98].

Note: the single intensity degrees can include the effects of shaking of the respective lower intensity degree(s) also, when these effects are not mentioned explicitly.

A. 2. 1. 2. DAMAGE CLASSIFICATION FOR MASONRY BUILDINGS

Classification of damage for masonry buildings



Grade 1: Negligible to slight damage (no structural damage, slight non-structural damage).

Hair-line cracks in very few walls.

Fall of small pieces of plaster only.

Fall of loose stones from upper parts of buildings in very few cases.



Grade 2: Moderate damage (slight structural damage, moderate non-structural damage)

Cracks in many walls.

Fall of fairly large pieces of plaster.

Partial collapse of chimneys.



Grade 3: Substantial to heavy damage (moderate structural damage, heavy non-structural damage)

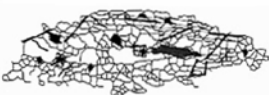
Large and extensive cracks in most walls.

Roof tiles detach. Chimneys fracture at the roof line; failure of individual non-structural elements (partitions, gable walls).



Grade 4: Very heavy damage (heavy structural damage, very heavy non-structural damage)

Serious failure of walls; partial structural failure of roofs and floors.



Grade 5: Destruction (very heavy structural damage)

Total or near total collapse.

Table 16.2 : EMS-98 classification of damage on masonry buildings

A. 2.2. QUOTATION FROM THE RED BOOK OF BASEL CITY

„Man soll wissen, dass diese Stadt durch das Erdbeben zerstört und zerbrochen wurde; keine Kirche, kein Turm und kein Haus aus Stein blieb heil, weder in der Vorstadt noch in den Vorstädten, sondern wurden größtenteils zerstört. Auch fiel der Burggraben an vielen Stellen ein. [...]...brach Feuer aus in der Nacht und dauerte die folgenden acht Tage an, sodass niemand dem Erdbeben zu widerstehen getraute noch mochte. Die Stadt innerhalb der Ringmauer brannte beinahe vollständig ab...“

A. 2.3. DAMAGE RECORDED AFTER THE 1946 EARTHQUAKE (EPICENTRE: SIERRE, SWITZERLAND)

AIGLE

The seismic event seriously damaged the church and the bell tower; both need to be restored quickly [Sion ArB].

ALBINEN

The church was seriously damaged by the severe earthquake of Friday, January 25, 1946. Whereas the chancel was specially hit, the rest of the church was not too much damaged. according to the priest Andermatten, if the sacristy would not have been built, the chancel south side would have overturned and made the vaults collapse along. The old stone vault was still in the chancel, whereas the ceiling nave was replaced by a lighter vault in 1911.

Letter written by the parish priest, Mr Andermatten, to the bishop of Sion, January 28, 1946 [Sion ArB].

ARDON

In 1524, an earthquake caused the tower collapse. A new tower was erected according to the plan designed by Ulrich Ruffiner (1480-1544).

The church and its bell tower were especially hit after the seismic event of 1946 [Ga 96]. The tower spire was cut four meters below the cross; the upper part was moved that resulted in hollowing the masonry spire on two sides. Thanks to the timber framework, it did not break down.

CHALAIS

The spire of the bell tower was damaged; the seismic event seriously damaged the church and the bell tower; both need to be restored quickly. It would seem that the earthquake caused the fall of the spire tip [Cha ArP].

CHAMOSON

The bell tower was damaged (L.Pflug).

CHIPPIS

After the shock (January 25, 1946), the tower spire was damaged and its tip was horizontally cracked 6 m below the top and slid 30 cm aside [Chippis BP]. The tip was broken during the first motion and however did not fell down. The plaster vaults were cracked and plaster covered the nave pews. Repair began in April 1946. Nevertheless, in May 30, two strong shakes of 3 secondes struck again the region (Magnitude on the Richter's scale: 6; Ayent [ECOS 02]). This time, the whole spire was highly cracked and was about to fall down. Inside the church, the vault next to the organ was sagged and its south half part was highly cracked.

June 1, 1946, some parts of plaster detached from the vault and after a noisy cracking from the tribune place (and a strong upwards shake (?)), the vault fell down slowly. Suddenly, the whole vault collapsed with a terrible noise; every pew was broken as well as the lustre and the candelars.

CONTHEY

The church was highly damaged in 1946: according to human memories, the tower got too cracked to ring the bells and the vaults were so highly cracked that they collapsed two weeks later.

The whole church was destroyed in 1947 and a new building was erected somewhere else in the town. Nothing is remaining; it is presently the churchyard.

GRÔNE

The earthquake of 1946 resulted in the falling down of the spire tip of the Grône bell tower. The church was restored in 1947 [Ar 95].

LENS

The bell tower of the parish church of Lens is repaired in 1948, after the earthquake of 1946 [**Arch prio Lens**].

MASSONGEX

The church in Massongex was also damaged by the 1946 seismic event. According to the priest, the walls seemed to wobble along their basis; he also had the impression that the edifice was collapsing. The church had already sustained bad weather and soil settlements and there were cracks on the walls and the vault (the vault was no longer well connected to the walls). The earthquake enlarged them; the covering with roughcast was no longer enough and rapid reinforcement was required [**Arch Bish Sion**].

MIÈGE

On October 22, 1946, it was decided to reinforce the east wall which had been cracked by the earthquake. In 1958, a survey of the vault was carried out in order to assess its stability since it was highly cracked by the 1946 seismic events [Sion ArC].

MONTANA

The 1946 earthquake (January 25) resulted in a few small cracks along the vault and the walls. One stained-glass was partially damaged and three were split. Two big stones from the spire tip of the tower fell down [Mon ArP].

RANDOGNE

The chapel main edifice was 9.85 m. long and 5 m. wide; the vault was 6.2 m high. The saint sepulchre edifice was 6.55 m. long and 3.85 m. wide; the vault was 5.65 m high. It was written that the edifice walls were damp [Cr 03]. When the bishop visited the chapel in 1861, he wrote that it was in a bad state of conservation. In 1908, the edifice was restored. In 1946 [Cl 50], the chapel was still in a bad state and it was recorded that the vault of the sacristy was in such a state that the pilgrims were frightened to enter in.

In 1946, the chapel was highly damaged by the earthquake. The front wall was split into two parts by a wide vertical crack, whereas both twin vaults were highly cracked and the rock itself (floor) was damaged [Cl 50]. Damage even reached the building basis. In 1947, the damaged building was destroyed and in 1953, the new one consecrated.

SEMBRANCHER

After the 1946 earthquake, the spire of the bell tower had to be repaired and a pillar had to be added to each gothic window of the bell tower.

SIERRE

The tower roof of the church Our-Lady of the Moor was hollowed and the rest of the church was highly cracked. It is worth noting here that the ground soil is of bad quality (alluvium).

SION

Cathedral of Sion:

The spire of the bell tower was like cut and the upper part moved of about 20 cm aside.

Collegiate of Valère:

According to [Bl 46], the collegiate sustained serious damage resulting from the earthquake occurred in 1946. They are serious enough to threaten the structural safety of the edifice. They cracks probably existed before the shake and this might merely have enlarged them. Except the apse, every part of the church is in a bad state. The nave aisles were, compared with the whole structure, highly damaged; there were longitudinal (lateral?) cracks along vaults. The arch tympanum on the outer sides, like the arch bands, presents a sort of detachment from the pillars and walls. This deformation was so important that a voussoir (close to the keystone, the 3rd one actually) detached from the arch, fell down and broke a corner of the Jube. A large and vertical crack was observed beneath the first timber beam crossing the nave (1st bay, southward) (where exactly?). Besides, the vaults of this first bay are also cracked. Alike, the cage of the stairs up to the organ tribune is also cracked. The first part of the north aisle presents a large fracture on its outer wall and the arch band is broken. The arch wall which contains the Rose (at the intersection of the nave with the transept) is completely detached and the rose partially fell down. On the contrary, the north transept, which had a barrel vault, better faced the seismic displacement than the aisles; a transversal crack was yet observed. Although the crossing resisted in its centre, there was a detachment along the arch which divided it from the south transept. The south transept (which is actually the sacristy) is seriously damaged. The thin wall between the south aisle and the transept was fractured, the remplace of one window was broken and finally, the vault detached towards (where?) the crossing.

The chapels that flanked the nave also suffered from the earthquake. The arch and the vault of the south one (above the sacristy) were fractured. The wall against the choir of the north chapel had a large fracture.

To sum up: the cracks direction in the aisles vaults and the fall of the rose highlighted that the aisles were no longer well tight up to the nave structure and this one is no more laterally supported. The church was merely getting opened like a fan; if it had gone on, the vaults would have collapsed.

A. 2.4. DAMAGE RECORDED AFTER THE 1976 EARTHQUAKE IN FRIULI (ITALY)

A. 2.4.1. SANTO STEFANO A CESCLANS

The church of Santo Stefano a Cesclans was situated to the north of the region of Gemona del Friuli and Venzone, at about 15 km from the epicentre of the Tolmezzo earthquake. It was built on a rock peak that was made of compact conglomerate (conglomerato del Tagliamento) and surrounded by layers composed with fragments detached from the conglomerate.

Archaeological survey showed tracks of a church anterior to the church, which was damaged by the earthquakes in 1976, and that was erected during the 9th century. The last edifice, which collapsed because of an earthquake, was built in the 16th century.

STRUCTURAL CHARACTERISTICS

The church was made up of a central nave with two aisles, an apse, an appendix leaning against the right lateral wall and a campanile connected to the front wall. There were also lateral arches (between the central nave and its aisles) as well as a chancel arch between the nave and the apse.

The edifice is about 12 m wide and 8 m high; the campanile is 6 m taller than the rest of church. There were no vaults in stones.

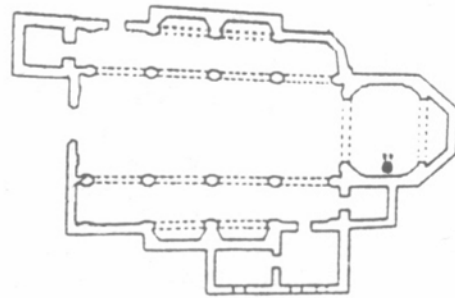


Figure 16.12 : Plan of the church Santo Stefano a Cesclans.

OBSERVED DAMAGE

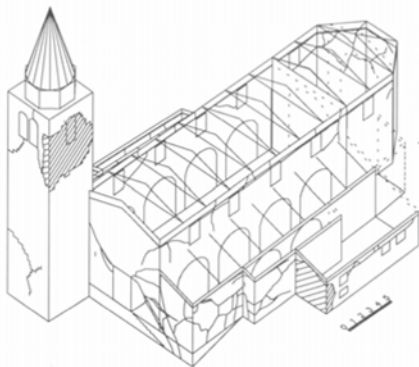


Figure 16.13 : Observed damage to the fabric of the church after the main (left) and second (right) seismic event.

1. The front wall

The main seismic shock was at the root of the first cracking of the front wall; after the second tremor, the facade totally collapsed like a major part of the church (likely due to the fall of the campanile upper part on the church).

After the main shock:

- There was a vertical fracture right at the connection between the front wall and the campanile, along half of the height. This split went across the façade down to the upper left corner of the door and after passing through the door lintel, crossed again the facade and finally reached the ground.
- The right part of the wall was seriously damaged by diffuse cracking (right-hand figure).



Figure 16.14 : Front wall damaged by the main seismic shock occurred in May 1976.

2. Nave walls

Like the front wall, the nave walls were still standing after the main seismic shock but did not resist the second earthquake.

Note: as no information was available about the damage following the second seismic event, only the damage resulted from the main shock is presented.

There was a fracture right at the connection of the wall with the concrete cord (along the upper edge of the lateral wall) that started from the front wall and ended at the chancel arch. Moreover, splits, which were close to the edge bound with the front facade as well as with the chancel arch, were observed.

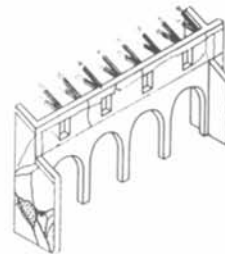


Figure 16.15 : Outline of the damage observed on the lateral wall (right one) of the nave.

3. Lateral walls

Every part of the lateral walls was still standing after the first seismic event, save a wall belonging to the sacristy. Following the second event, only the left lateral wall still remained while the oppo-

site one was completely destroyed (the sacristy included). As there was information only about a part of the right wall, this is the only one dealt with.

Cracks concentrated within the middle part of the lateral and chapel walls were observed. There also was a split along the joint of the lateral wall with the chapel structure. A part of the outer leaf of the lateral wall, just beneath the cord at the corner with the front wall, fell down too.

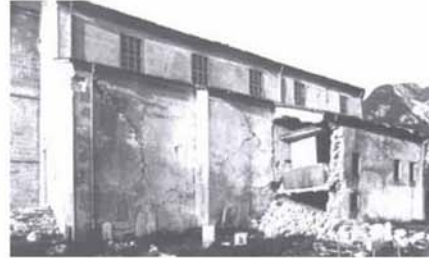


Figure 16.16 : Observed damage to the right lateral wall after the seism of May 1976.

A complete wall of the sacristy broke down; it did not bring along the cord, which was on the wall upper edge, but the corner with the lateral wall of the sacristy. The connection of the chapel masonry with the sacristy fabric was actually rather mediocre.

4. Chancel arch

The chancel arch belonged to the structural components that were still standing after both seismic events.

The masonry of the arch was separated from the cord. The fabric being on the sides of the arch were fractured by oblique cracks going from the intrados to the upper angles of the wall. Only a small part of masonry, close to the arch keystone, fell down. On the contrary, the headstone remained in place, being well attached to the cord. Some of the dressed stones alongside the arch intrados also fell down too (figure to the right).



Figure 16.17 : Chancel arch after the main seismic shock in May 1976.

5. Apse

The state of damage changed a lot before and after the second seismic shake: the walls of the apses cracked during the main seism shock and the second event caused the fall of the wall parts that were previously separated from the rest of the fabric.

Following the main seismic shock, the parts of the apse wall making an angle with the lateral walls were split by clean cracks, which were mainly situated along the upper edge of the walls (separation between the cord and masonry); such cracks were also observed along the polygonal part of the apse. There were also cracks parallel to the ground at about 1 m high.

The second seismic event resulted in the collapse of the structural parts that were already separated by cracks from the rest of the masonry after the main seismic shock. Both opposite walls were then hollowed by the tumble of a big part of their own fabric.

It is worthy noting that the cord did not break down, even after the second earthquake. The left lateral wall presented two distinct fractures: the first one was vertical and went from the annexe wall up to the cord, while the second split had its root at one of the lower corners of the window and ended at half the height of the same appendix (see next Figures).

After the main shock of May:



After the seismic event in September:



Figure 16.18 : Damage observed on the apse after both seismic tremors.

6. Campanile

After the main seismic shock:

A part of the cell collapsed and then only a small section remained to support the structure above the cell. On the opposite side, an independent behaviour between the upper part and the lower one of the cell was observed: the upper part displaced out of its plan while the lower part did not move.

There was also an oblique crack that crossed both first vertical segments of the tower (from the ground); according to [Do 94], it might be due to a twisting action and influenced by a discontinuity created during the construction.

Following the second seismic event, only the first three segments were still standing (see Figure 16.13).



Figure 16.19 : Campanile after the main seismic event.

DAMAGE MECHANISMS

1. Front wall

After the main seismic shock:

The vertical split between the front wall and the campanile, which was actually a detachment, was likely due to the different oscillations of both structural bodies (front wall and campanile). These latter disconnected, they certainly hammered against each other. As the lower part of the front wall was embedded in the foundations, the hammering phenomenon caused the formation of a

diagonal crack starting from the lowest point of the vertical crack at the connection between the front wall and the campanile.

The other cracks were also due to the same phenomenon of hammering between the front wall and the campanile. The diffuse cracking was probably influenced by the poor masonry quality.

After the second seismic event:

As the second shake totally destroyed the front wall, it is only possible to make assumptions about the mechanism of failure. Then, although the fracture across the wall was large and went through the wall on its width, it seems likelier that the front wall collapse resulted from the fall of the upper part of the campanile onto the church.

Note: the connections between the elements of foundations had certainly played an important role within the mechanisms of damage, it is actually neither known how the foundations were nor how were the connections between them and the front wall.

2. Nave walls

The horizontal fracture at the cord foot was certainly promoted by the timber trusses movements (hammering phenomenon) during the earthquake, if it was not the origin of the damage. The cracking within the corners region was probably due to the connection with the orthogonal walls (the front wall and the chancel arch).

3. Lateral walls

The configuration of the cracks and deformations, i.e especially concentrated within the central part of the wall with oblique fractures going up to the wall corners and with out-of-plane displacements, was typical of a wall connected at both horizontal edges (upper and lower edges) with rigid bodies (membrane-like structural behaviour). In this case, these latter clearly corresponded to the foundations along the lower edge and the cord along the upper extremity.

The collapse of the sacristy wall had its root likely in the weak connection with the chapel and the miss of cohesion of the masonry (the sacristy was built after the chapel construction).

4. Chancel arch

The observed cracking mainly resulted from the seismic in-plane movement. It also seems that the fabric of the triumphal arch was actually quite well bound to the cord since the cracked parts of the masonry were still attached to it after the seism event (like the keystone). This is also confirmed by the cracking configuration that encompassed oblique cracks (see on Figure 16.17).

5. Apse

The damage observed on the walls of the polygonal part of the apse was probably influenced by discontinuities inside the fabric, caused by previous transformations. The fractures in the lateral walls of the apse certainly resulted from lateral movements partially restrained by the appendix.

CONCLUSIONS

This church damage allows highlighting the following points:

- A restrained wall, even partially, along the upper and lower edges might suffer an out-of-plane movement (membrane-like structural behaviour) and then cracked especially on its middle part. The cord put along the upper edge of walls contributed to partially restrain them.

- The discontinuities or changes of stiffness inside the masonry, which might be caused by structural transformations, often resulting in fracturing the fabric. This was the case, in respects with the Santo Stefano a Cesclans church, between the sacristy building and the chapel wall.
- The hammering action from the roof rafters laid on a concrete cord seems to lead to the detachment of the cord from the underneath masonry (lateral walls of the central nave).
- When two building parts are side-by-side, but not linked (like the campanile and the front wall), this generally causes the cracking of both bodies part.

A. 2. 4. 2. SANTO STEFANO DI VALERIANO

The church of Santo Stefano di Valeriano was situated in the south of Tolmezzo at about 17- 18 km from the epicentre. The ground, above which was located the church, was composed of two layers: the upper one being made up of old alluvium (about 17 m thick) and the lower one was old alluvium compacted.

STRUCTURAL CHARACTERISTICS

The edifice encompassed a rectangular nave prolonged by an apse ending with a polygonal wall, two annexes (one along each lateral wall), a sacristy and a campanile. The apse was separated from the nave by a chancel arch. The nave and the apse ceilings were actually made up of cross vaults (slightly drawn on the next Figure) in brickwork.

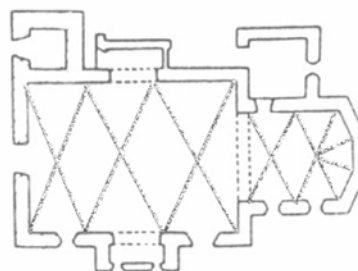


Figure 16.20 : Plan of the church Santo Stefano di Valeriano.

The roof was supported by the lateral walls of the nave through timber trusses and towards the apse through trusses composed of timber rafters and metallic tie. The roof structure of the apse took in three trusses and three rafters. The church size was about 17 m x 26 m per a height of 11 m (campanile excluded).

OBSERVED DAMAGE

There is information only about the damage caused by the seismic event occurred in May 1976; what happened after the second tremor is not presented in [Do 94] and there was even no picture

Globally, half of the roof collapsed as well as half of the upper part of the Campanile, the cross vaults and a big part of the wall belonging to the apse perimeter.

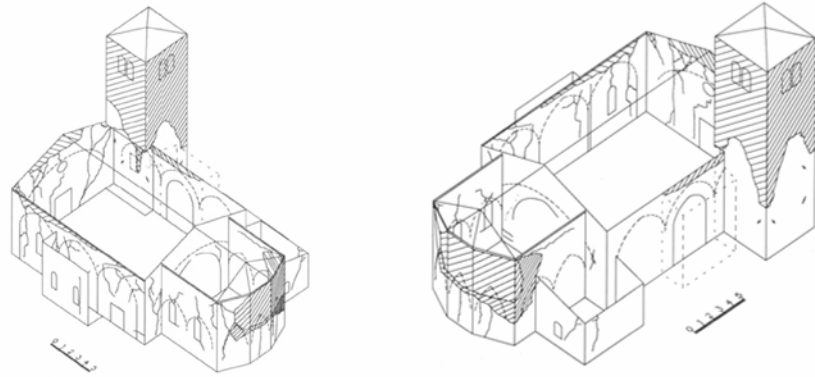


Figure 16.21 : Observed damage on the church Santo Stefano di Valeriano.

1. The front wall.

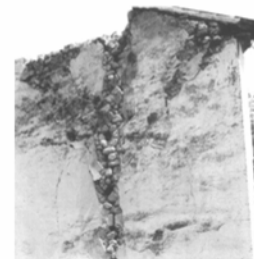
The main damage was situated at the gable level: a quite big part of brickwork tumbled down. The bottom edge of the fallen part seems also to be the start of many vertical cracks (there was also a vertical crack close and parallel to the right corner edge). The left part of the wall was crossed by crack that started from the gable upper edge, close to the connection with the campanile, down to the ground.

Figure 16.22 : Front wall damaged by the main seismic shock occurred in May 1976.



The pre-existing and already repaired crack, which followed the right corner of the facade, reappeared and was enlarged (moreover it cut the wall on its whole thickness). A large crack (on the whole thickness) appeared along the right corner of the front wall but on the lateral wall face.

Figure 16.23 : Pre-existing crack enlarged during the second seismic event of Sept. 1976.



2. Lateral walls.

A long part of the cord in concrete fell down (the phenomenon also appeared on the opposite side) and also resulted in damaging the masonry underneath. One third of the cord was still standing after the earthquake. The other types of damage were more of cracking kind.

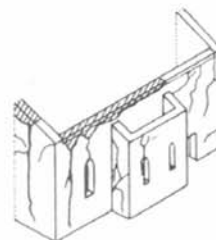


Figure 16.24 : Outline of the damage on a lateral wall.

3. Apse

The most serious damage concerned a large fraction of the upper part of the polygonal wall (about the half). Moreover, the fall of these elements promoted the dislocation of the outer wall part. The cord and the roof structure yet remained in place.

There were many splits around the windows that begun at the angles, corners on the lateral parts of the apse and their surroundings



Figure 16.25 : Damage observed on the apse after the earthquake.

4. Campanile

The most severe damage was the collapse of a big fraction of the superior part of the bell tower. There was a vertical crack that crossed a face of the campanile, which was parallel to the principal face of the church, and the front wall of the church (down to the ground). This crack followed the discontinuity between the quoins and the rest of the masonry in the campanile face.



Figure 16.26 : Failure of the upper part of the campanile.

DAMAGE MECHANISMS

1. Front wall

As the gable fabric was not connected to the roof structure, its upper edges were free to move and behaved like a cantilever. It was then fractured at its foot and the gable fell down. The crack that started right at the connection place with the campanile would seem to be due to the hammering of the campanile on the upper left corner of the front wall and also likely to a discontinuity within the foundations. The other diagonal cracks were merely due to the flow of shear forces within the front wall.

The enlargement of the pre-existing crack highlighted the behaviour of a split structure (the detached parts behaved almost independently from each other). The large crack appeared along the right corner might be due to independent movements of the corner part of the fabric, as well as of the lateral wall itself.

2. Lateral walls

The fall of the cord was certainly due to the fall of the upper part of the campanile on the roof of the church.

The part of the wall towards the apse (presenting a diffuse kind of cracking) and the large crack close to the corner with the front wall were probably due to the independent oscillations of the lateral wall and the other structural parts (front wall for the crack along the corner on the front wall).

3. Apse

The failure of a major part of brickwork would seem to start at the connection with the sacristy and to occur by an out-of-plane mechanism where the maximal displacements appeared in the middle of the wall.

4. Campanile

The fracture pattern of the upper part was such that it seems highly probable the tower experienced a twisting action under the earthquake (May 1976) [Do 94]. This phenomenon was also confirmed by the detachment of few quoins along the four angles.

The fracture, which passed at the upper corner of the front wall, actually began right at this point since it resulted from the hammering of both buildings (bell tower and church) on each other.

CONCLUSIONS

- The campanile experienced a torsion action; it means that it was enough connected to the nave body to displace the shear centre of its section.
- Although the campanile was quite well bound to the nave body, its oscillations were not similar to the structural response of the front wall and they consequently hammered each other
- The metallic ties linking both opposite sides in the campanile structure at 5 m high appeared to be actually quite efficient
- The cross vaults failed mainly because their supports moved from their initial position
- Before the earthquake, it would seem that the front wall was already injured along its corner with the right lateral wall; it existed there a vertical crack indeed.
- The gable of the front wall behaved like a cantilever structure, as it was confirmed by its failure (which was also helped by the miss of connection with the roof structure); the lateral walls also behaved in similar way as confirmed by the fractures along their corners with orthogonal walls
- According to the vertical cracks on the lateral walls along the corners between the lateral walls and the front wall, the front wall response to the earthquake appeared to differ from the lateral walls one
- A big part of the apse broke down because of the detachment of the masonry from the cord and certainly also because of the presence of the sacristy building.

A. 2. 4. 3. DUOMO DI VENZONE

Venzone is small town situated to the northeast of Udine at about 7-8 km of the epicentre.

STRUCTURAL CHARACTERISTICS

The dome (also called San Andrea's church), whose construction was finished in 1338, was composed of a central nave crossed by a transept, a chancel with an apse and two chancel aisles with an apse in each, sacristy, appendices along the lateral walls and two towers.

The edifice was about 27 m width, 48 m long and around 19 m high.

As only information about the front wall was available, the facade of the north transept with its campanile, the facade of the south transept with its tower, the chancel apse, the lateral walls, annexe buildings and the chancel arch are not presented.

OBSERVED DAMAGE

There is information only about the damage caused by the earthquake occurred in May 1976; what happened after the second tremor is not presented in [Do 94] and there was even no picture

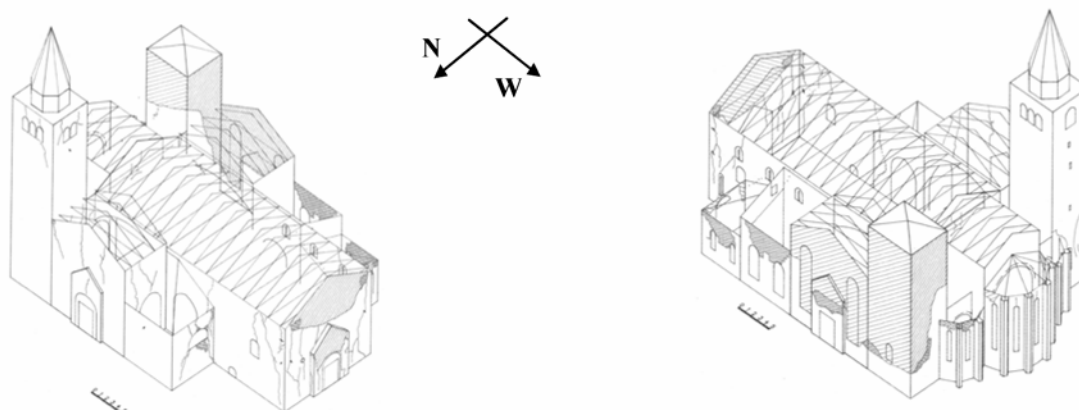


Figure 16.27 : Observed damage on the duomo di Venzone after the 1976 seismic event.

1. The front wall.

The following paragraph describes the damage observed after the main seismic shock. Although there is no information about what happened to this facade after may 1976, it might have totally collapsed after the second seismic event occurred in September.

The pebbledash entirely fell down and let the masonry totally exposed.



Figure 16.28 : Front wall damaged by the main seismic shock occurred in May 1976.

The fabric being above the door tympanum also collapsed and the main fractures followed the cracks that existed before the seism. Vertical cracks could also be observed on the perpendicular walls, close to the front wall, within 1 m.

2. Facade of the north transept and north tower.

There was no information about this part of the structure after the earthquake of September 1976, but only after the earthquake occurred in May 1976. Nevertheless, I saw on a picture of the apse ruins in late September that there was no serious aggravation of the damage on the bell tower as well as the side-by-side facade. The assessment of the damage caused by the main seismic shock of May 1976 is based on only two pictures and cannot be hence very exact, nor exhaustive.

The pre-existing failure between the upper right corner of the facade and the portal corner was enlarged.



Figure 16.29 : North side after the earthquake.

The perpendicular walls were crossed by a vertical large crack, which seemed to go through the front wall roof (both slopes).

From outside



From inside



Figure 16.30 : Separation of the front wall belonging to the north transept.

According to [Do 94], the bell tower presented vertical cracks along its east face (toward the apse).

3. South transept facade and south tower.

The south facade of the transept totally collapsed during the main seism shock of May, although the roof structure was yet still standing afterwards. According to [Do 94], the front wall broke all

along the windows perimeter and the door lintel. This fracture went on at the same height in the tower walls and after crossing the south face. The tower collapsed quite entirely..

After the main shock of May:



After the second shock of September:



Figure 16.31 : East side of the dome after each seismic tremor.

4. Chancel apses

All the apses survived (though seriously damaged) the seismic event occurred in May 1976. The damage was situated especially in the upper parts of the apses where small parts of the outer part of the wall fell down on the south apse, for instance. The piers were also slightly cracked in their height. Nevertheless, the piers must have been more damaged or even slight (in appearance) cracks may promote collapse of this kind of piers, since it remained quite nothing after the second seismic event. Following the second seismic event, it was noted that the piers (belonging to the apse of the central chancel), which were still standing, were dismembered in their lower part.

DAMAGE MECHANISMS

1. Front wall

The connections with the roof structure being not strong enough to resist the earthquake (the gable was then free to behave like a vertical cantilever), the upper part of the facade broke down in a way according to the anterior damage (old displacements or deformations, miss of connections, etc.).

The way the portal broke down, which was a clear separation of two independent masonry parts, indicates that it was built after the front wall.

The Vertical cracks, which could be observed on the perpendicular walls, close to the front wall, might have been promoted by the roof structure, but not necessary, and then enlarged as well as prolonged towards the ground by the transversal (west-east) movements of the front wall.

2. Facade of the north transept and north tower

The enlargement of the pre-existing failure between the upper right corner of the north facade and the portal corner was probably due to the difference of oscillations between both parts of the structure, which led to a kind of hammering of both parts on each other.

3. South transept facade and south tower.

The collapse of the south facade of the transept was probably due to an overturning mechanism (out-of-plane); the wall then took along parts of the brickwork belonging to the transept lateral

walls. The apse piers became certainly independent of each other and behaved like vertical cantilevers (not well restrained in the ground) during the second seismic event.

4. Chancel apses

The collapse of the apses might be promoted by the collapse of other structural elements like roof parts, walls, etc. For example, the roof of the south aisle chancel apse collapsed because of the overloading due to the south tower material that fell down on the apse roof.

Following the main seismic shock, the piers of the central chancel apse, which were still standing, were dismembered in their lower part that likely shows a problem with the basement.

CONCLUSIONS

- The gable of the front wall behaved like a cantilever and took along a part of the wall that was beneath itself, certainly because this latter was likely not well connected to the rest of the face (difficult to assess).
- Few parts of the portal that belonged to the front wall collapsed according to pre-existing cracks [Do 94].
- The parts of the lateral walls being close to the front wall were damaged by vertical cracks that were supposed to result from the lateral movement of the front wall.
- On the south walls, quite every upper part of the appendices collapsed; this seemed to be probably due to the combination of the roof rafters hammering against upright structure and the being (and in respects to the position of each one) of gothic windows.
- The south face of the transept quite totally collapsed; the limit of the failure began at the west side at the level of the upper edge of the side-by-side appendix, went on according to the windows shape and then continued on the tower south facade.
- The north face of the transept was cracked by hammering with the side-by-side campanile and separated from the transept body by a fracture that came across the building in parallel to the face. The main differences between both transept facades were: presence or not of windows and shape of the side-by-side tower.

A. 2. 4. 4. DUOMO DI GEMONA

The Duomo di Gemona is located in the same town as the church of Santa Maria del Fossale, that is to say, at the foot of the Alps, on an alluvium ground.

This famous roman-gothic edifice was consecrated in 1337 (its construction had began about fifty years before). At this date, the dome was composed of three naves separated by two lines of columns and of one rectangular presbyter. Since the consecration date until nowadays, the dome has encountered many structural transformations, including repairs, adjunctions, modifications and experienced disastrous events like earthquakes.

STRUCTURAL CHARACTERISTICS

Just before the Tolmezzo earthquake, the Duomo di Gemona was composed of one central nave with two aisles, a presbyter with apse, a sacristy and numerous chapels situated along the lateral walls of the aisles. The present dome was actually built up on the foundations of a previous roman church, the Santa Maria della Pieve.

From the front wall to the apse, the cathedral was about 50 m long and it was about 30 m wide (from the Cappella di SS. Sacramento (5) to the Cappella della beata vergine (11)).

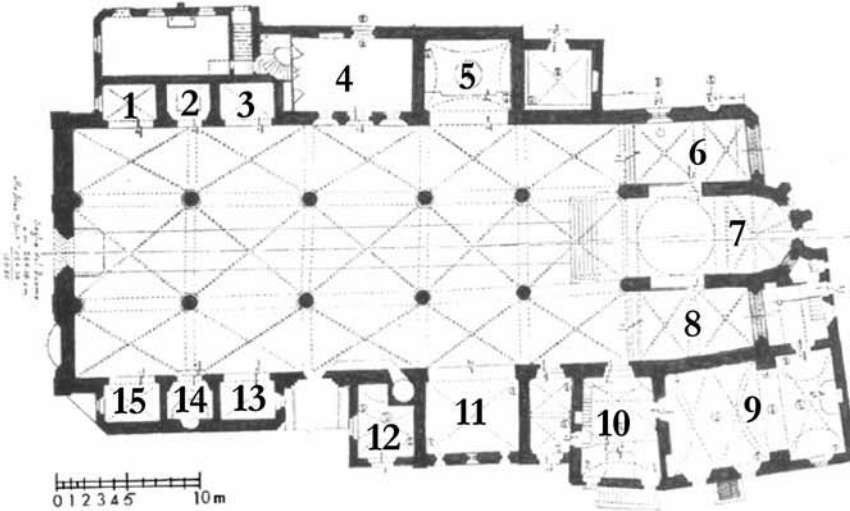


Figure 16.32 : Plan of the Duomo di Gemona.

Note: numbers 1, 2, 3, 4, 5, 6, 11, 12, 13, 14, 15 are chapels; number 9 is the sacristy. The axis of the nave is West-East.

This dome, like the Duomo di Venzone, has not been as well described by Doglioni et. al. [Do 94] as the three other churches were. Consequently, the description of structural characteristics is not very exhaustive.

It seems worthy highlighting the miss of regularity in the dome geometry, as you can see on the next Figure.

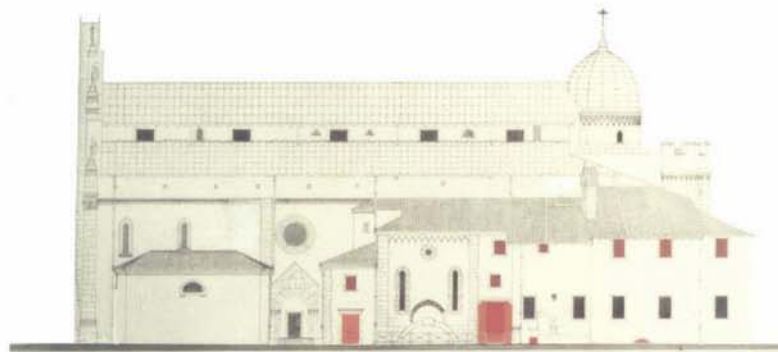


Figure 16.33 : Vertical plan of the dome of Gemona.

OBSERVED DAMAGE

There is information only about the damage caused by the seism event occurred in May 1976; what happened after the second tremor is not presented in [Do 94] and there was even no picture

The Duomo di Gemona was actually highly damaged by the Tolmezzo earthquake: all its right part was indeed quite demolished (enclosing three chapels and the sacristy), as well as the apse roof and the campanile. The tip of the main facade also tumbled down. Moreover, almost every wall was cracked and the columns of the main nave remained deformed, even after the restoration



Figure 16.34 : The Duomo di Gemona after the second seismic event in September 1976.

1. The front wall.

Few cracks were observed around the roses, but these latter were not seriously damaged. On the contrary, the tip of the facade turned around a horizontal axis, which was located just above the main rose and was formed during the main seismic shock, and then fell down after the second seismic event. There was no other serious damage recorded on the front wall.

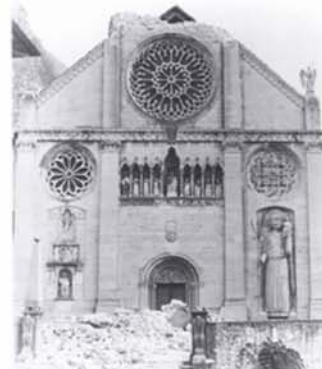


Figure 16.35 : Front wall damaged by the main seismic shock occurred in May 1976.

Though the masonry of the lateral walls, including those of the aisles and those of the central nave, was not similar to the front wall fabric, the observation of the damage seems to indicate that the connection between these structural components was quite efficient (efficient enough to resist the Tolmezzo earthquake; according to [Do 94], there were many metallic ties between the front wall and the lateral walls). Concerning the bound between the roof structure and the front wall, it was almost inexistent.

2. Lateral walls

As already mentioned, the lateral walls on the left side of the dome were more slightly damaged than those belonging to the right part, and far from. The lateral walls on the right side, as well as the chapels bound to, were actually almost totally destroyed, save the walls above the line of pillars and the presbyter right wall.

According to the pictures taken after the earthquake, the columns of the central nave were no longer verticals after the earthquake. It is actually unknown whether they were originally vertical or not.

3. Lateral chapels and sacristy

The sacristy and the chapels, which were situated along the right side of the dome, partially or completely collapsed.

As there is little information about the damage experienced by the appendices on the left side of the dome, save a picture of the Cappella dell'Annunziata, the chapels being on the right side are mainly dealt with.

Chapels 13-15 (cappella del Cristo, della pieta and del Battistero):

These three chapels totally broke down: nothing remained even after the main seismic shock save small parts of the walls close to the ground.

The timber vaults also broke down.



Figure 16.36 : Collapse of the aisle buildings.

South door:

The wall encompassing the south door was partially destroyed: it let only the doorframe with the surrounding arcades and a part of the window structure. The breaking, which was oblique, began close to the eleventh chapel, circumvented the arcades, cut the circular window and stopped at the intersection with the perpendicular wall of the appendix 12.

The appendix 10 a:

The roof totally disappeared, as well as the part of the right aisle wall related to the appendix. The fracture edge was horizontal along the transversal wall and cut the window.

The cappella della beata vergine degli angeli (11):



In this case, only the roof and the part of wall of the right aisle broke down; the lateral wall of the chapel was yet highly cracked, especially around the bull's-eye window and above the high window.

Figure 16.37 : Rest of the cappella della beata vergine degli angeli.

The appendix 10:

The roof, the shared wall with the right aisle and the part of wall related to the sacristy collapsed. Moreover, there were cracks that started from the windows corners (belonging to the lateral wall).

Sacristy (9):

From the sacristy building, only the masonry parts of the first floor outlived the earthquake. The fracture edges followed the windows lintel in the lateral wall and the sacristy ceiling everywhere else. The part of fabric connected to the appendix 10b yet remained not demolished.

The pinnacle obviously fell down and very likely on the sacristy roof.

4. Apse

The roof was completely destroyed, like the embattled part of the wall and the fabric around the windows was cracked, especially at their top.

Before the main seismic shock the apse wall was in a quite bad state of decay and was also passably cracked.

Figure 16.38 : Interior of the duomo di Gemona after the seismic event occurred in September 1976.



5. Cupola

The cupola was still standing after the second seismic shake and there is no picture at disposal to assess any state of damage.

6. Campanile



After both seismic events, the campanile broke almost completely and only 10 m of structure remained after the earthquake

Figure 16.39 : Campanile after the seismic event of September 1976.

MECHANISMS OF DAMAGE

1. Front wall

The fall of the facade tip was certainly due to the miss of connection with the roof structure that hammered against the facade and accentuated the out-of-plane displacements due to the cantilever structural behaviour of the gable. It is very interesting to note that the rose, which was just below the axis of failure (and below the level of trusses tie), was not damaged.

2. Lateral walls

Seeing the miss of information, relevant mechanisms of damage that might have occurred cannot be established. Nevertheless, it may be possible that the hammering caused by the rafters of the roof structure contributed to the destruction of the dome external lateral walls.

3. Lateral chapels and sacristy

Chapels 13-15 (cappella del Cristo, della pieta and del Battistero):

The collapse of these chapels was likely due to the hammering of the roof structure against the lateral walls (of the aisle as well as of the chapels).

The appendix 10 a:

Once again, the collapse seemed to be partially due to the hammering of the roof structure on the walls.

The cappella della beata vergine degli angeli (11):

The inner face of the lateral wall (configuration of the pebbledash plates) showed cracks resulting from a shear mechanism.

The appendix 10:

The damage configuration does not look like being issued from any hammering between the chapel and the appendix, nor with the sacristy.

4. Apse

The state of decay and cracking before the earthquake highly contributed to the failure, since the limits of some fractures corresponded to the pre-existing cracks.

5. Campanile

According to [Do 94], the collapse of the bell tower began at its top at the windows level (in the cell). The fabric around the windows, which looked like piers, would have been fractured at their top and foot and would have then moved towards outside in pair with the fabric beneath them (which was also cracked).

CONCLUSIONS

"The front wall tip behaved like a cantilever, since it had no connection with any lateral structure (like the roof structure for instance). However the front wall survived the earthquake quite without severe injuries; it was due to many metallic ties that were put between the front and lateral walls during the last transformation that took place before 1976.

- Quite every appendix was damaged; this phenomenon was certainly due to the discontinuities created following their construction (that necessarily corresponded to the destruction of parts belonging to the previous fabric).
- The roof of the aisle totally broke down; it is difficult to establish if the roof structure was at the root of the failure of the aisle walls (that supported it) or if it broke down following the collapse of the supporting walls.
- In the case of the appendices, the roof rafters probably hammered the vertical structure and promoted their collapse.
- The failure limits of the apse roof followed actually the pre-existing cracks.

- The columns of the nave (supporting the arcades) would seem to have moved during the earthquake and it would seem that they remained slightly inclined after the tremor. However it is not known whether they already had an angle with the ground before the earthquake or not.

A. 3. EXISTING METHODOLOGIES

A. 3.1. RISK-UE: CORRECTING FACTORS

1. The first part helps collecting general data, such as the name and the place as well as data related to general points of seismic emergency, such as frequency of use and accessibility to emergency exits.

Name of the building	
Address	
Period of construction	
Prevalent period	When transformations led to the present structure
Ownership	Public, private, church-owned, etc
Type of use	Residential, offices, library, etc
Frequency of use	Daily, weekly, occasionally, etc
Crowding of immediate surroundings	Yes/ No
Accessibility to emergency exits	Difficult, good, excellent, etc

Table 16.3 :General information about a given edifice; taken from [La4 04].

2. The second part contains the main factors that may influence the seismic vulnerability of the given typology of edifices such as the plan regularity and the height of walls.

General parameters		V_i
Plan regularity: nave typology	Central	-0.02
	One	0
	Three	0.02
Section regularity: sailing facade/ raised elements	Yes	0.04
	No	0
Position	Included	-0.02
	Additions	0.02
	Isolated	0
Domes, vaults	Yes	0.04
	No	0
Height of lateral walls	Low (H<6m)	-0.02
	Medium (6m<H<12m)	0
	High (H>12m)	0.04

Table 16.4 :Specific vulnerability parameters for churches; taken from [La4 04].

3. The obtained values are then changed according to modifier scores that account for the state of preservation, the damage level, etc.

General parameters		V_i
State of preservation/ maintenance	Bad (worst)	0.04
	Medium	0
	Good	-0.04
Damage level	Severe	0.04
	Light	0.02
	Null	0
Architectural transformations	Yes	0.02
	No	0
Recent interventions	Yes	-0.02
	No	0.02
Masonry quality	Yes	0.05
	No	0
Site morphology	Ridge	0.04
	Sloping	0.02
	Flat ground	0
Plan regularity	depending on the typology	
Section regularity	depending on the typology	
Position	depending on the typology	

Table 16.5 :General vulnerability parameters; taken from [La4 04].

A. 3.2. LOURENÇO'S METHOD: APPLICATION

P.B. Lourenço et al. have developed a methodology to assess the seismic vulnerability of churches in Portugal; it is based on three different simplified safety indexes: in-plane area ratio (I_1), area to weight ratio (I_2) and base shear ratio (I_3). The methodology was applied to a sample of 58 Portuguese churches and the results showed that quite valuable information can be obtained from this simplified method. By extension, they also concluded that simplified methods in general give helpful information about the seismic vulnerability of churches.

A. 3.2. 1. APPLICATION TO THE OLD CHAPEL IN VISPETERMINEN

INDEX 1: A_{w1}/S

Where A_{wi} is the area of the walls in the considered direction and S is the whole ground area of the church.

For this church, based on the schema on Figure 5.15, $S= 156.3 \text{ m}^2$.

Note: the real plan is unknown; the above schema has been reconstituted according to archive texts [St 94].

On x and supposing a thickness of 0.85 m , $A_{wx}= 35.7 \text{ m}^2$; on the y axis, A_{wy} is 13.43 m^2 .

The index 1 is then: $\gamma_{1,x}=0.23$ and $\gamma_{1,y}=0.09$. It is worth noting that, according to the method, the values must be higher than 0.1 (according to [LR 06]) to indicate that the building is safe regarding the seismic vulnerability. It means that the surfaces of resisting walls must be higher or equal to 10% of the whole ground surface of the edifice. Furthermore, this way of calculation is essentially about the in-plane seismic response.

Discussion

Results indicate that the chapel is seismically relatively unsafe on the y axis (the ground surface is wider in comparison with the transversal resisting walls). This fact proves more or less to be correct since the main facade does not exist any more and the transversal wall of the apse is crossed with a large crack. Nevertheless, it must be kept in mind that the aforementioned damage was not necessarily caused because of a weak in-plane resistance.

It seems worth noting that regarding the resistance on the y axis, index 1 reaches a value equal to or higher than 0.1 with a thickness of 0.9 m ; as it might be possible to find such a thickness, the church might be also safe on y axis. This result shows that, in this case, an index of 0.9 does not necessarily indicate that the building is really seismically unsafe since a very slight change in dimensions can give a different result.

INDEX 2: A_w/G

As a reminder: G is the weight of the whole structure (walls, vaults/ceiling and covering).

Assumptions:

- masonry (limestone masonry) weight per unit of volume: 25 KN/m^3 (SIA 260)
- vault masonry (limestone tuff masonry) weight per unit of volume: 20 KN/m^3 (SIA 260)
- roof weight per unit of surface: 1.25 KN/m^2 (0.75 KN/m^2 for the tiles and 0.5 KN/m^2 for the framework; values based on [SIA 261 03])
- the inner structure looked like the reconstituted one.

The index 2 is then: $\gamma_{2,x}=3.88$ and $\gamma_{2,y}=1.54$

In both directions, the indexes are higher to 1.2 , which is indicated as the bottom limit in [Me 98] for old masonry buildings. According to index 2, the building is seismically safe in both directions. However, as $\gamma_{2,y}$ is rather close to 1.2 , it tends to the result obtained with the first index. Nevertheless, a value of 1.2 could be reached by adding a mass of 300 tons, which is quite high and is almost impossible to be covered by the incertitude in dimensions.

On the other hand, the inner structure (vaults) was certainly different from the reconstituted one; in this way, the indications given by this index have to be carefully handled.

Discussions

Although the ground surface was wider in comparison with the transversal resisting walls (index 1), it is not the case of the weight. It can be said that the chapel might have been too wide but not too heavy in regards to the resisting walls ground surface.

INDEX 3: $AWI/AW^* \tan(\theta)/B$

Assumptions:

- $\tan(\beta)$: 0.4 ($\varphi=22^\circ$); proposed value in [LO 05]
- zero cohesion

Index 3	Z1 ($a_{gd}=0.06$ g)	Z3b ($a_{gd}=0.16$ g)	$a_{gd}=0.2$ g
$\gamma_{3,x}$	4.77	1.79	1.43
$\gamma_{3,y}$	1.9	0.71	0.57

Under a peak ground acceleration of $a_{gd}=0.16$ g (Area Z3b, in [SIA 261 03]; return period of 475 years), index 3 on y-axis is already lower than 1. This result means that the chapel is on its transversal axis quite highly vulnerable to dynamic loadings.

A calculation has been carried out for a peak ground acceleration of 0.2 g (according to specialists, this might have been the peak ground acceleration that hit the chapel in Visperterminen during the 1855 earthquake).

If a same calculation is carried out with a value of $\tan(\beta)$: 0.72 [SIA V178 80], the index value along y-axis is equal to 1. Even if it is not under the value level of 1.0, it more or less confirms the fact that the chapel might be highly damaged on its transversal axis.

RESULTS SUMMARY

Index 1: $\gamma_{1,x}=0.23$ and $\gamma_{1,y}=0.09$.

Index 2: $\gamma_{2,x}=3.88$ and $\gamma_{2,y}=1.54$

Index 3:

Index 3	Z1 ($a_{gd}=0.06$ g)	Z3b ($a_{gd}=0.16$ g)	$a_{gd}=0.2$ g
$\gamma_{3,x}$	4.77	1.79	1.43
$\gamma_{3,y}$	1.9	0.71	0.57

Both indexes 1 and 3 show that the chapel is seismically vulnerable on its y-axis. As aforementioned, index 2 is exact only for the reconstituted plan and elevation that do not exactly represent the chapel real structure.

DISCUSSION

Compared with the damage observed on the chapel, it must be said that the aforementioned results seem to more or less match the reality. The transversal parts are indeed either highly dam-

aged (transversal wall in the apse) or simply does not exist any more (main facade). However, it is difficult to say whether these transversal walls were damaged or destroyed because of their weak in-plane resistance or not. Furthermore, it must be added that the vertical crack in the transversal wall in the apse does not look like an in-plane failure. It seems rather due to horizontal-vertical shocks caused by the timber framework. This cause, which can be allowed for as a local one, was indeed put down after the 1855 earthquake. According to the same source, the «loose» framework was at the basis of the damage.

Otherwise, the fact that the indexes do not take into account the irregularity (in plan and in elevation) of the building is also a disadvantage. In the church, the impact of the chancel arch on the transversal seismic response is not considered. The presence and position of windows is also forgotten though it might influence the seismic resistance of a building (indexes only allowed for walls surface at the ground). Moreover, the shape of the existing north-west wall, which is like cut along the bottom level of the windows, makes think that the out-of-plane response was of importance. This is also not taken into account in Lourenço's method since it allows for only the building in-plane seismic response.



Figure 16.40 : View of the still existing north-west wall.

Furthermore, it must be said that the close other chapel, whose shape is more or less like the studied chapel, was damaged after the seismic event of 1855 but not destroyed. In consequence, there no particular reason that both structures were so different to behave so differently under seismic actions. In this case, the different quality of soil might be an explanation. However, this impact is not taken into account in this method.

To sum up, this method gives tools to assess the global seismic behaviour of the structure; according to what has been mentioned, it can give quite a good assessment of the general structural response under seismic actions. Nevertheless, it did not give a realistic appraisal of the seismic vulnerability of the given building.

A. 3. 2. 2. APPLICATION TO THE COLLEGIATE CHURCH OF VALÈRE

INDEX 1: A_{w1}/S

The ground surface of the collegiate church of Valère is $S= 915.42 \text{ m}^2$.

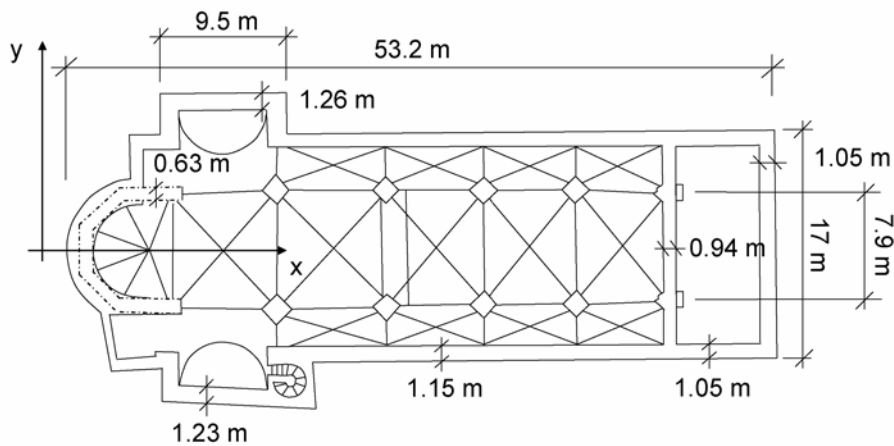


Figure 16.41 : Plan of the colegiate church of Valère, Sion.

Assumptions:

- Tower wall that includes the staircase is assumed to be as thick as the tower opposite wall
- Apse length for the A_{wy} corresponds to the y length component

Two calculations have been made; in the first one, the gain of resistance that might be provided by the pillars ground surface is not taken into account whereas it is accounted for in the second calculation.

	$A_{wx} \text{ [m}^2\text{]}$	$A_{wy} \text{ [m}^2\text{]}$	$\gamma_{1,x}$	$\gamma_{1,y}$
Without the gain provided by the pillars	124.5	76.9	0.14	0.08
With the gain provided by the pillars	154.4	106.8	0.17	0.12

Discussion

As a first result, the indexes show that, as for the chapel in Visperterminen, the transversal direction is more vulnerable than the lateral one. This is not really surprising since it is well known that the cross-shaped churches are transversally more flexible.

It is also interesting to see that in case the pillars contribute to its seismic response, the building is no longer seismically vulnerable in its transversal direction. The matter-of-fact there is: could the pillars provide a certain strength under seismic actions and to which extent?

Nevertheless, if it is accounted that the collegiate is transversally vulnerable, it is worth wondering which part of the church is the most vulnerable (the main facade, the transept, the tower, the apse).

INDEX 2: A_{Wl}/G

Assumptions:

- Masonry (limestone masonry) weight per unit of volume: 25 KN/m³ (SIA 260)
- Vault masonry (limestone tuff masonry) weight per unit of volume: 20 KN/m³ (SIA 260)
- Roof weight per unit of surface: 1.25 KN/m² (0.75KN/m² for the tiles and 0.5 KN/m² for the framework; values based on [SIA 261 03].)
- Organ weight: 1 ton
- 4 bells in the tower; weight for one bell: 500 Kg
- Weight per unit of surface of each floor of the tower: 3.5 KN/m² (estimation based on the SIA260)
- The pillars ground surface has been taken into account.

The index 2 is then: $\gamma_{2,x}=1.4$ and $\gamma_{2,y}=0.97$

Discussion

Index 2 shows that there might be a problem in the transversal direction. Nevertheless, a parametric study has shown that the value of index 2 is highly (and almost only) depending on the masonry weight per unit of volume; for instance, in case the masonry weight per unit of volume is lower than the initial value of $\gamma=25$ KN/m³, the index goes up to $\gamma_{2,y}=1.2$ (for $\gamma=20$ KN/m³). It is worth noting here that the value of masonry weight per unit of volume has been chosen according to the Swiss code 178 and on the basis of assumed homogeneous walls. It is obvious that reality is different and the above value of index 2 cannot be in consequence the exact value; it is only an approximate value. On the other hand, the chosen value for the masonry γ is certainly close to its real average value.

It must be written that the calculation of the weight of a complex church is not only highly time-consuming but also not completely reliable since it is difficult to deduce the weight of every part by only basing the calculation on plans and elevations.

INDEX 3: $AWI/AW* \text{TAN}(9)/B$

Assumptions:

- $\text{tg}(\beta)$: 0.4 ($\varphi=22^\circ$); proposed value in [66]
- zero cohesion

Index 3	Z1 ($a_{gd}=0.06$ g)	Z3b ($a_{gd}=0.16$ g)	$a_{gd}=0.2$ g
$\gamma_{3,x}$	3.94	1.48	1.18
$\gamma_{3,y}$	2.73	1.02	0.82

According to this index, the collegiate, which is situated in the zone 3b (Swiss code 260), tends to be seismically vulnerable in its transversal direction. Under a peak ground acceleration of $a_{gd}=0.2g$,

the collegiate is clearly vulnerable along the y-axis; on the other hand, it also tends to be vulnerable on the longitudinal axis.

Discussion

The values of index 3 have been defined while the gain of resistance provided by the pillars was taken into account. In case this gain is not allowed for, the index 3 shows a certain seismic vulnerability on x-axis under a peak ground acceleration of $a_{gd}=0.2g$ whereas along the y-axis, the value goes down to $\gamma_{3,y}=0.82$.

RESULTS SUMMARY

	A_{wx} [m ²]	A_{wy} [m ²]	$\gamma_{1,x}$	$\gamma_{1,y}$
Without the gain provided by the pillars	124.5	76.9	0.14	0.08
With the gain provided by the pillars	154.4	106.8	0.17	0.12

Index 2: $\gamma_{2,x}=1.4$ and $\gamma_{2,y}=0.97$

Index 3:

Index 3	Z1 ($a_{gd}=0.06$ g)	Z3b ($a_{gd}=0.16$ g)	$a_{gd}=0.2$ g
$\gamma_{3,x}$	3.94	1.48	1.18
$\gamma_{3,y}$	2.73	1.02	0.82

The three indexes show that the collegiate is seismically vulnerable on its y-axis and might suffer quite high damage under the seismic actions defined for the hazard zone 3b. As the values of indexes 1 and 3 are close or equal to the level value, it cannot be said that the collegiate is clearly vulnerable; nevertheless, in this kind of limit cases, it might be reasonable to undertake a few interventions (like reinforcing masonry; enhancement of $\tan(\varphi)$ for index 3) in order to keep the collegiate safe in case of a seismic event.

Note: in regard to the index 1, the exact value is probably situated between both values (0.12 and 0.08).

DISCUSSION

Like the chapel in Visperterminen, the collegiate of Valère seems to be seismically vulnerable mainly along its transversal axis. Nevertheless, it does not really match the damage observed after the 1946 earthquake.

Otherwise, same notices as for the chapel in Visperterminen have to be made. Moreover, regarding the collegiate structure (three naves, transept, tower), which is different from the chapel in Visperterminen, it must be added that the method do not take into account the impact of the transversal and lateral arches and walls (that divide the three naves). In regard to the structure, the miss of regularity (in the three directions) is of great disadvantage.

Moreover, as the collegiate was built about 8 centuries ago, the state of maintenance of the masonry is an important point to consider, as the reconstructions (structural and/or material additions or changes) and the impact of reinforcements (tie-rods, etc.).

A 3.2.2.1. Plan of the Italian churches

SANTA MARIA DELL FOSSALE: PLAN

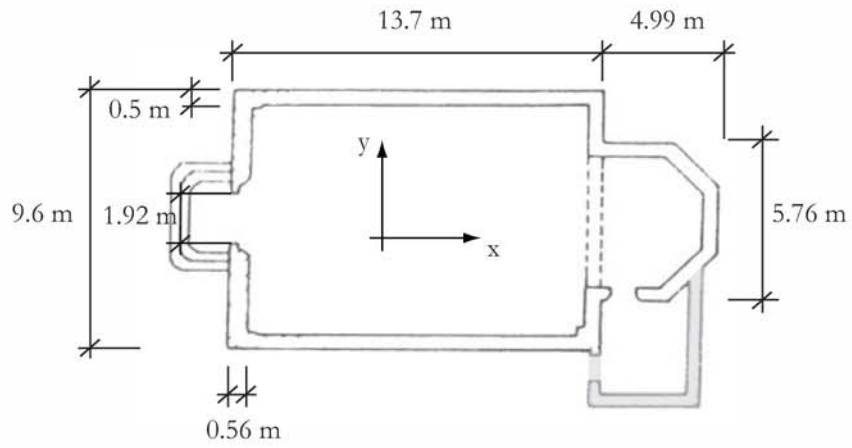


Figure 16.42 : Plan of Santa Maria del Fossale, with dimensions (the plan is taken from [Do 94]).

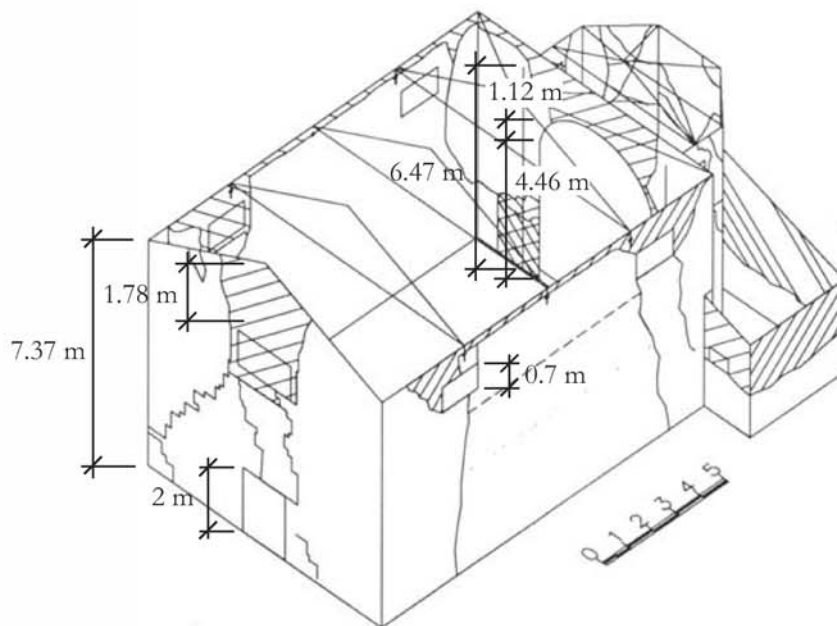


Figure 16.43 : 3D view of Santa Maria del Fossale, with dimensions (the plan is taken from [Do 94]).

SANTO STEFANO A CESCLANS

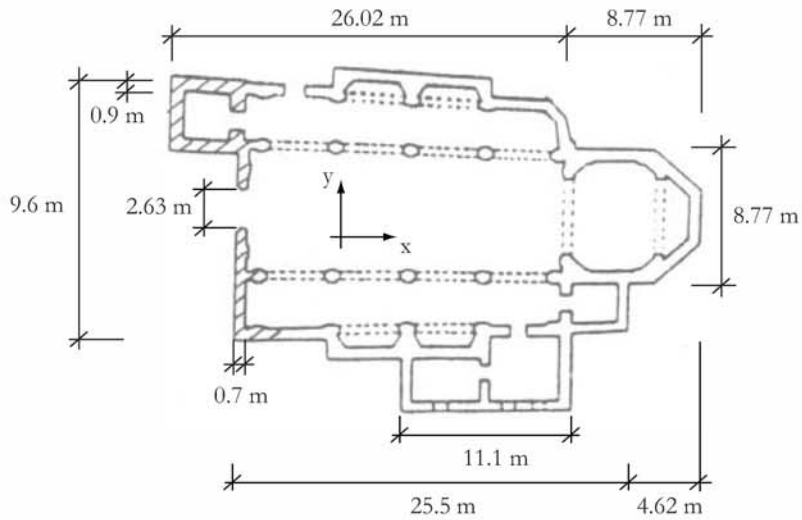


Figure 16.44 : Plan of Santo Stefano a Cesclans, with dimensions (the plan is taken from [Do 94]).

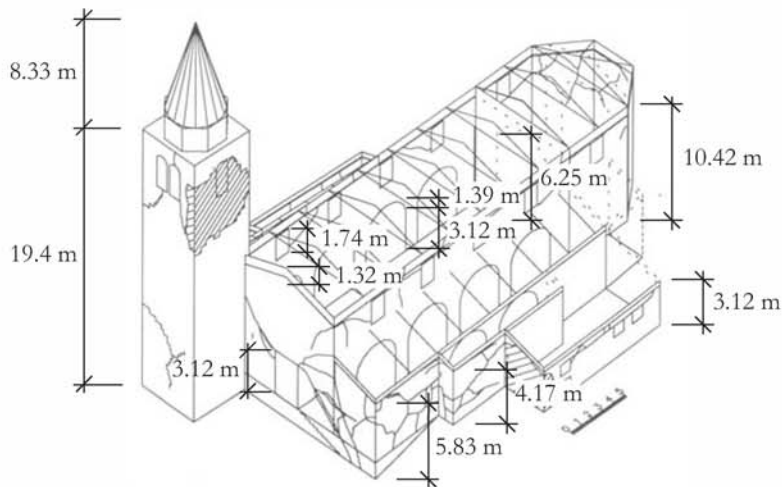


Figure 16.45 : 3D view of Santo Stefano a Cesclans, with dimensions (the plan is taken from [Do 94]).

SANTO STEFANO DI VALERIANO

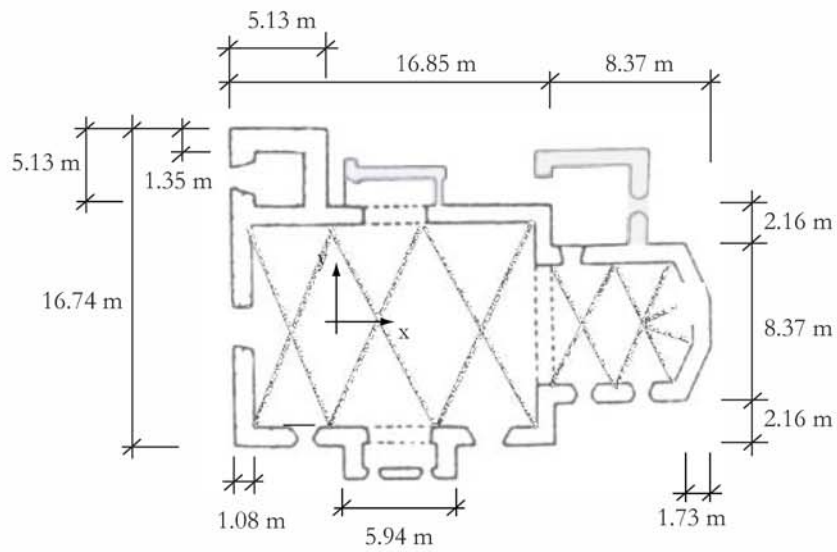


Figure 16.46 : Plan of Santo Stefano di Valeriano, with dimensions (the plan is taken from [Do 94]).

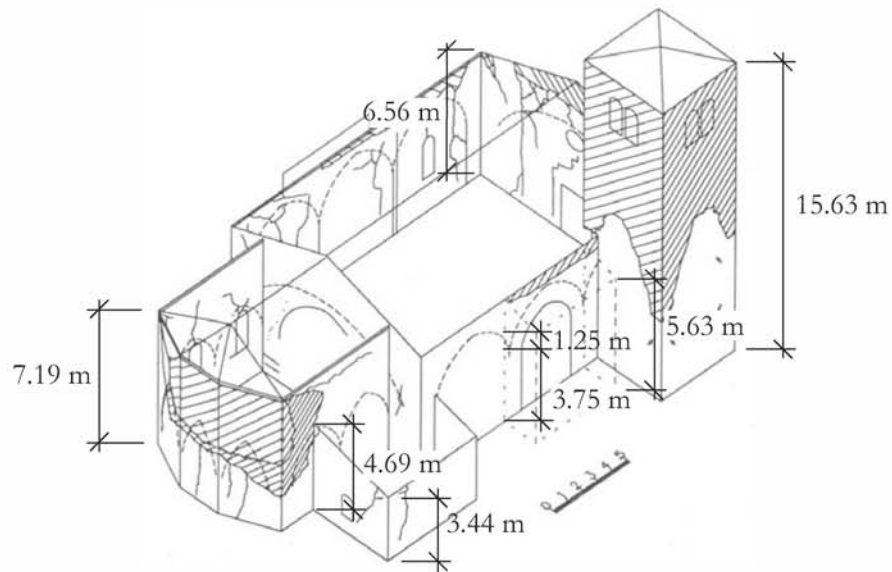


Figure 16.47 : 3D view of Santo Stefano di Valeriano, with dimensions (the plan is taken from [Do 94]).

DUOMO DI GEMONA

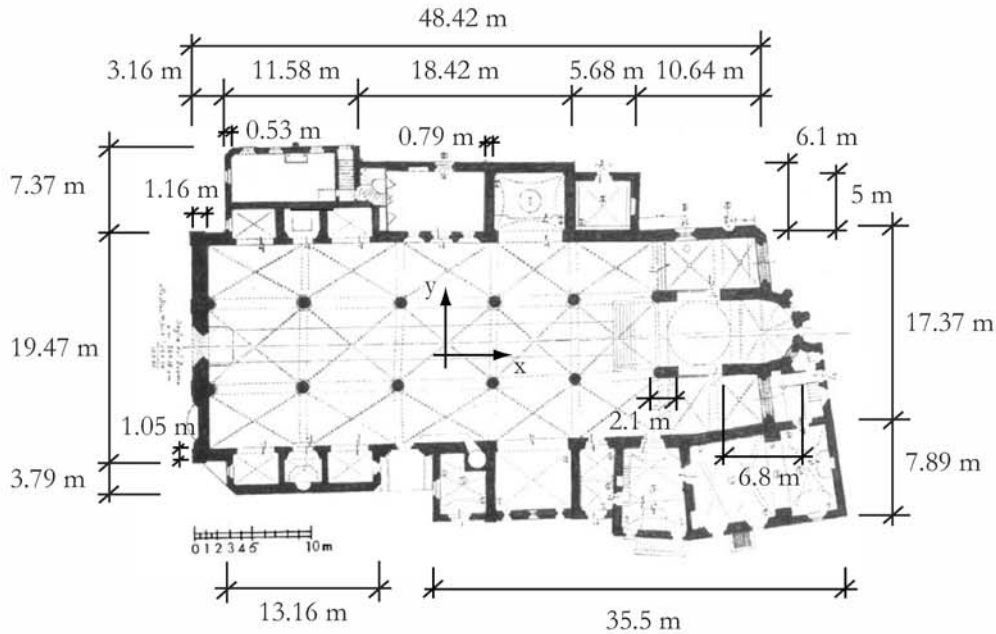


Figure 16.48 : Plan of the Duomo di Gemona, with dimensions (the plan is taken from [Dr 87]).

A. 3.3. RISK-UE METHOD: APPLICATION

A. 3.3.1. APPLICATION TO THE CHAPLE OF VISPETERMINEN

A 3.3.1.1. Level 1

Since the chapel was highly damaged after two successive earthquakes: 1755 and 1855. It is interesting to see the difference of assessment in both cases.

BEFORE THE SEISMIC EVENT OF 1755

Note: the following information is linked to the chapel when it was in use and more precisely before the seismic event of 1755.

Name of the building	Waldkapelle (Chapel in the forest)
Address	-
Period of construction	1730-1740
Prevalent period	1730-1740
Ownership	? (probably to the parish of Visperterminen)
Type of use	Mass, pilgrimage
Frequency of use	Weekly essentially

Crowding of immediate surroundings	No
Accessibility to emergency exits	Good (there were at least three exits; they were however quite small) ^a

a. Since the given building has not been used for years (about 150 years), the above description is of no prevalent interest.

Table 16.6 :General information about the chapel in Visperterminen.

		Vi
Plan regularity: nave typology	Central	-0.02
	One	0
	Three	0.02
Section regularity: sailing façade/ raised elements	Yes (?)	0.04
	No	0
	Included	-0.02
Position	Additions	0.02
	Isolated	0
	Yes	0.04
Domes, vaults	No	0
	Low (H<6m)	-0.02
	Medium (6m<H<12m)	0
Lateral alls height	High (H>12m)	0.04

Table 16.7 :Specific vulnerability parameters for the given chapel.

		Vi
State of preservation/ maintenance	Bad (worst)	0.04
	Medium	0
	Good	-0.04
Damage level	Severe	0.04
	Light	0.02
	Null	0
Architectural transformations	Yes	0.02
	No	0
	Yes	-0.02
Recent interventions	No	0.02
	Yes	0.05
	No (?)	0

Site morphology	Ridge	0.04
	Sloping	0.02
Plan regularity	Flat ground	0
	depending on the typology	?
Section regularity	depending on the typology	?
Position	depending on the typology	?

Table 16.8 :General vulnerability parameters for the given edifice.

The total of the modifier scores is: $V_{i,total}=0.06$

The vulnerability index results then from the sum of all the values: $V_i = V_i^* + V_{i,total}=0.89 + 0.06=0.95$.

The expected damage grades for different seismic intensities (EMS-98):

I	VI	VII	VIII	IX
μ_D (EMS-98)	1.58	2.36	3.18	3.86

The value of β for the church typology is $\beta = 3$ (given value).

Note: no hints are given to assess the corrector factor for the irregularities in plan, in elevation and in position (Table 16.8). In consequence, no value has been defined for them.

BEFORE THE SEISMIC EVENT OF 1855

The above tables give:

Note: the chapel had been damaged after the earthquake of 1755; since then it was almost no longer used.

Plan regularity: nave typology	Central	-0.02
	One	0
Section regularity: sailing facade/ raised elements	Three	0.02
	Yes (?)	0.04
Position	No	0
	Included	-0.02
Domes, vaults	Additions	0.02
	Isolated	0
Lateral walls height	Yes	0.04
	No	0
Lateral walls height	Low (H<6m)	-0.02
	Medium (6m<H<12m)	0
	High (H>12m)	0.04

Table 16.9 :Specific vulnerability parameters for the damaged chapel.

	Bad (worst)^a	Vi
		0.04
State of preservation/ maintenance	Medium	0
	Good	-0.04
	Severe	0.04
Damage level	Light	0.02
	Null	0
Architectural transformations	Yes	0.02
	No	0
Recent interventions	Yes	-0.02
	No	0.02
Masonry quality	Yes	0.05
	No (?)	0
Site morphology	Ridge	0.04
	Sloping	0.02
	Flat ground	0
Plan regularity	depending on the typology	?
Section regularity	depending on the typology	?
Position	depending on the typology	?

a. Walls were, according to written sources, highly cracked.

Table 16.10 : General vulnerability parameters for the damaged edifice.

The total of the modifier scores is: $V_{i,\text{total}}=0.14$

The vulnerability index results then from the sum of all the values: $V_i= V_i^* + V_{i,\text{total}}=0.89 + 0.18=1.07$.

The expected damage grades for different seismic intensities (EMS-98):

I	VI	VII	VIII	IX
μ_D (EMS-98)	2.16	2.98	3.71	4.24

The value of β for the church typology is $\beta = 3$ (given value).

A 3.3.1.2. Level 2

This level corresponds to the level 2 of Lagomarsino's method; please, see A 3. 4. 1.

A. 3. 3. 2. APPLICATION TO THE COLLEGIATE CHURCH OF VALÈRE

A 3.3.2.1. Level 1

Note: the following information is linked to the chapel when it was in use and more precisely before the seismic event of 1755.

Name of the building	Collegiate church of Valère
Address	-
Period of construction	Around 1300.
Prevalent period	?
Ownership	? (probably to the parish of Visperterminen)
Type of use	Museum, organ concerts
Frequency of use	Daily
Crowding of immediate surroundings	No
Accessibility to emergency exits	Medium (the room is separated into two parts by a jube)

Table 16.11 :General information about the collegiate of Valère.

		Vi
Plan regularity: nave typology	Central	-0.02
	One	0
	Three	0.02
Section regularity: sailing facade/ raised elements	Yes	0.04
	No	0
	Included	-0.02
Position	Additions	0.02
	Isolated	0
	Yes	0.04
Domes, vaults	No	0
	Low (H<6m)	-0.02
	Medium (6m<H<12m)	0
Lateral walls height	High (H>12m)	0.04

Table 16.12 :Specific vulnerability parameters for the collegiate of Valère.

		Vi
State of preservation/ maintenance	Bad (state in 1946)	0.04
	Medium	0
	Good	-0.04

Damage level	Severe	0.04
	Light	0.02
	Null	0
Architectural transformations	Yes	0.02
	No	0
	Yes	-0.02
Recent interventions	No (?)	0.02
	Yes	0.05
	No (?)	0
Masonry quality	Ridge	0.04
	Sloping	0.02
	Flat ground	0
Plan regularity	depending on the typology	?
Section regularity	depending on the typology	?
Position	depending on the typology	?

Table 16.13 :General vulnerability parameters for the given edifice.

The total of the modifier scores is: $V_{i,total}=0.24$

The vulnerability index results then from the sum of all the values: $V_i= V_i^* + V_{i,total}=0.89 + 0.24=1.13$.

The expected damage grades for different seismic intensities (EMS-98):

I	VI	VII	VIII	IX
μ_D (EMS-98)	2.47	3.28	3.93	4.39

The value of β for the church typology is $\beta = 3$ (given value).

Note: once again, no hints are given to assess the corrector factor for the irregularities in plan, in elevation and in position (Table 16.13). In consequence, no value has been defined for them.

A 3.3.2.2. Level 2

This level corresponds to the level 2 of Lagomarsino's method; A 3.4.1.2.

A. 3.4. LAGOMARSINO'S METHOD: APPLICATION

Only the results of the method second level are recorded hereafter. The first level index has been dealt with in the previous chapter (Risk-UE). As reminder, both methods have been developed by Lagomarsino et al. and both first levels are similar.

A. 3. 4. 1. APPLICATION TO THE OLD CHAPEL IN VISPERTERMINEN

The shape of the chapel in Visperterminen has been drawn thanks to the information found in [LR 06]. The below presented scheme is the fruit of a few assumptions. Among them, the following ones can be listed:

- It is written that the chapel was built according to the plan of the «three kings» church in Visp; in consequence, they must have been similar though the chapel must be smaller,
- It also probably looked like the nearby chapel that survived both shaking events.

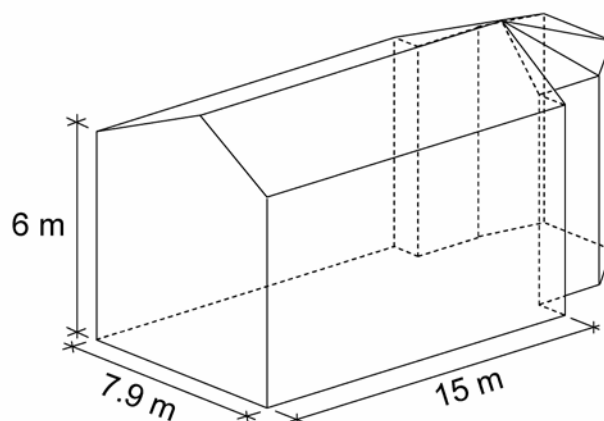


Figure 16.49 : 3D view of the chapel in Visperterminen.

MATERIALS PROPERTIES

The values of materials have been defined according to the SIA 260; walls are made up of quite heavy ashlar limestone masonry whereas the vaults are in lighter material, maybe in tuff.

The weights per unit of volume of both materials are:

Walls	25 KN/m ³
Vaults	20 KN/m ³

MACRO-ELEMENTS

According to the method that has been developed by Lagomarsino et al., the chapel has been divided into macro-elements, which are:

- the main façade,
- the nave (lateral walls),
- the chancel arch,

- the apse.

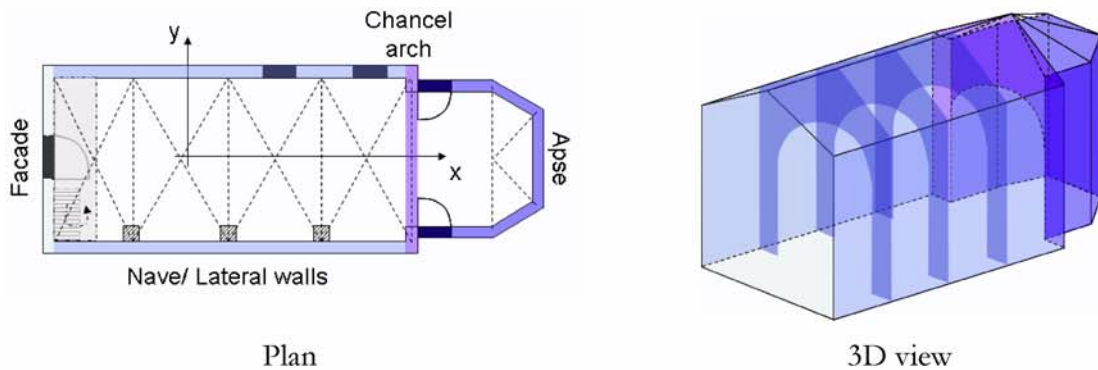


Figure 16.50 : Plan and overview of the old chapel in Visperterminen.

ASSUMPTIONS

- It was allowed for that there is no portal,
- The framework is made up of trusses that are supported by the lateral walls (for the apse: every wall supports the framework),

The results from the Level 1 calculations are the same as the ones calculated under the first level of the Risk-UE method. In regard to Level 3, no FEM analyses have been made for the moment. This step is a very sophisticated one and it was not the main interest of this report to carry out numerical modelling. This will be made in a next future.

A 3.4.1.1. The main façade

The real façade of the chapel in Visperterminen is actually unknown since it collapsed long ago; no pictures or engravings could have been found. As for the whole chapel, the below presented scheme is based on the few aforementioned assumptions.

Moreover, we assume that there were no horizontal tie-rods that helped tightening the lateral walls to the façade.

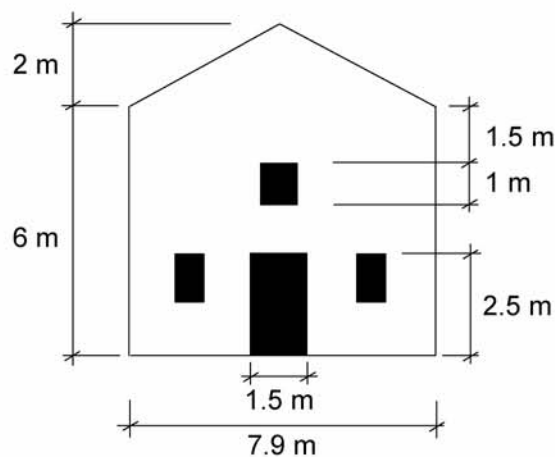
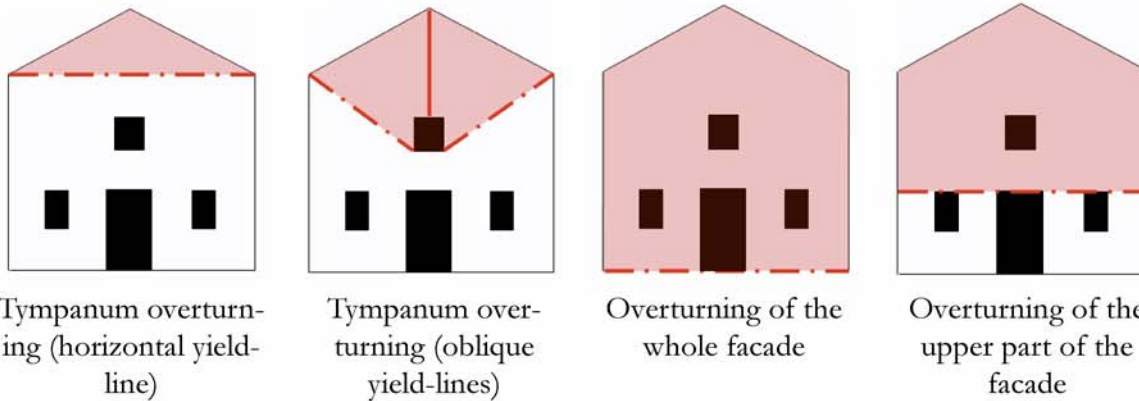


Figure 16.51 : The main façade of the old chapel in Visperterminen; thickness: 0.85 m.

According to the damage Lagomarsino et al.[La 06] observed on churches after seismic events in Italy, the following collapse mechanisms were taken into account:

1. CAPACITY CURVE OF THE OUT-OF-PLANE BEHAVIOUR OF THE FACADE

According to the possible out-of-plane collapse mechanisms presented under 5.2.3, the following ones have been analysed:



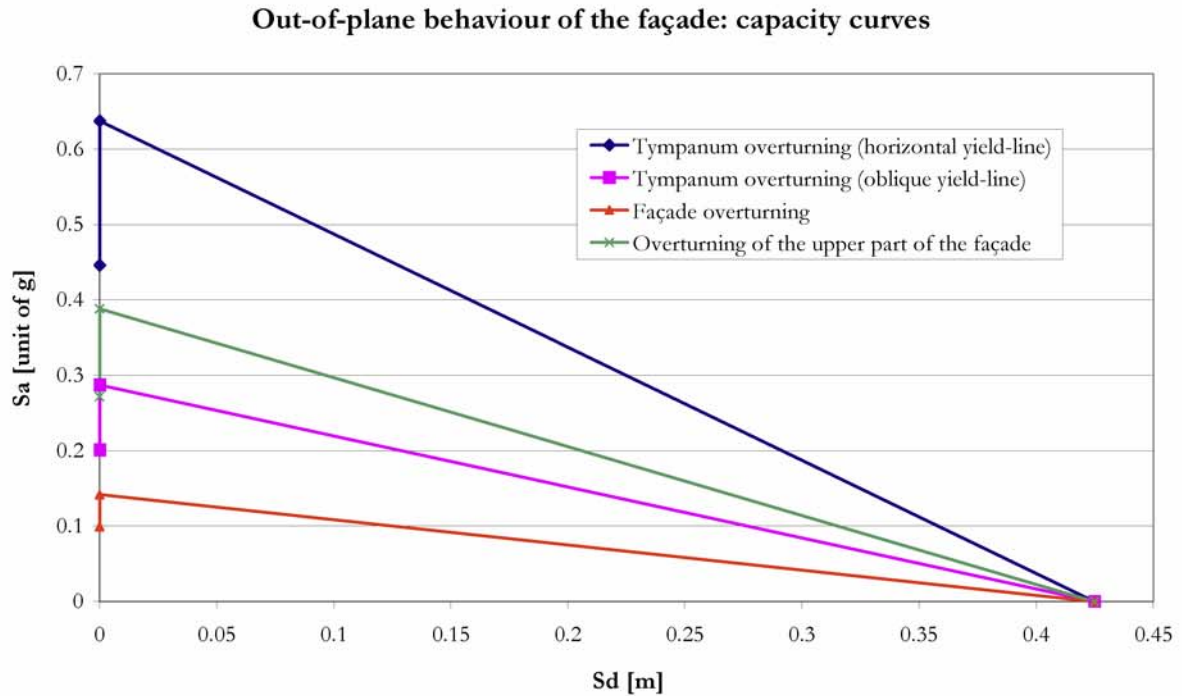
Note: the overturning part is hatched and the yield lines are indicated by dotted outlines; the plain lines correspond to cracks.

ASSUMPTIONS

- the tympanum (top of the main facade) does not support the framework,
- the tympanum is as thick as the facade,
- there was probably one opening above the main door and two on each side; the positioning of each window has been assumed,
- there is no particular link between the facade and the lateral walls (tie-rods for instance)
- in calculations (especially for the gravity centre), the openings areas have not been taken into account,
- calculations have been carried out according to the theorem of the virtual works; moreover it is assumed that the rigid block turns around one point.

RESULTS

According to the dimensions showed in Figure 16.51, the capacity curves of the three possible out-of-plane collapse mechanisms of the façade are:



Graph 1 : Capacity curves of out-of-plane behaviour of the façade.

Where:

- S_u | ultimate horizontal displacement; recorded on Sd axis; it is equal to half the thickness, i.e., in this case, 0.425 m.
- S_a | corresponds to the spectral acceleration; in this method (based on the assumption of rigid blocks), the spectral acceleration is equal to the peak ground acceleration.

Regarding to graph 1, the tympanum overturning through the creation of two oblique yield-lines is the less probable because of the high value of the spectral acceleration (about 6.3 m/s^2) requested to initiate the mechanism. The whole façade overturning seems to be less favourable since the needed spectral acceleration ($S_a=1.4 \text{ m/s}^2$) to activate the overturning the façade is very small. It is worth reminding here that the ground acceleration due to an earthquake in the canton Valais has been defined as being 1.6 m/s^2 . (Swiss Seismological Service).

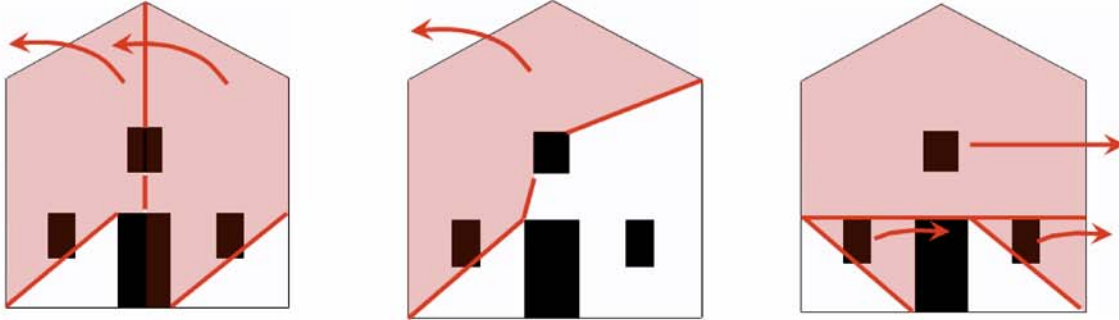
In regard with the tympanum overturning, the spectral acceleration that is required to activate the collapse mechanism is quite high (around $S_a=6.5 \text{ m/s}^2$); this result is probably not realistic since it is known that this part is one of the most vulnerable under seismic actions. This is generally due to the impact of the framework lateral beams that hammer the tympanum. In this case, the method might give an unrealistic value.

Note: the first point of every curve corresponds to a kind of «cracking» point of masonry (so-defined by Lagomarsino

et al.); it is the starting point for the rigid block behaviour of the wall (or part of wall).

2. CAPACITY CURVE OF THE FAÇADE IN-PLANE BEHAVIOUR

The collapse mechanisms that are taken into account:



1. Shear collapse and overturning of both halves of the facade.

2. Shear collapse and overturning of a facade part (oblique crack).

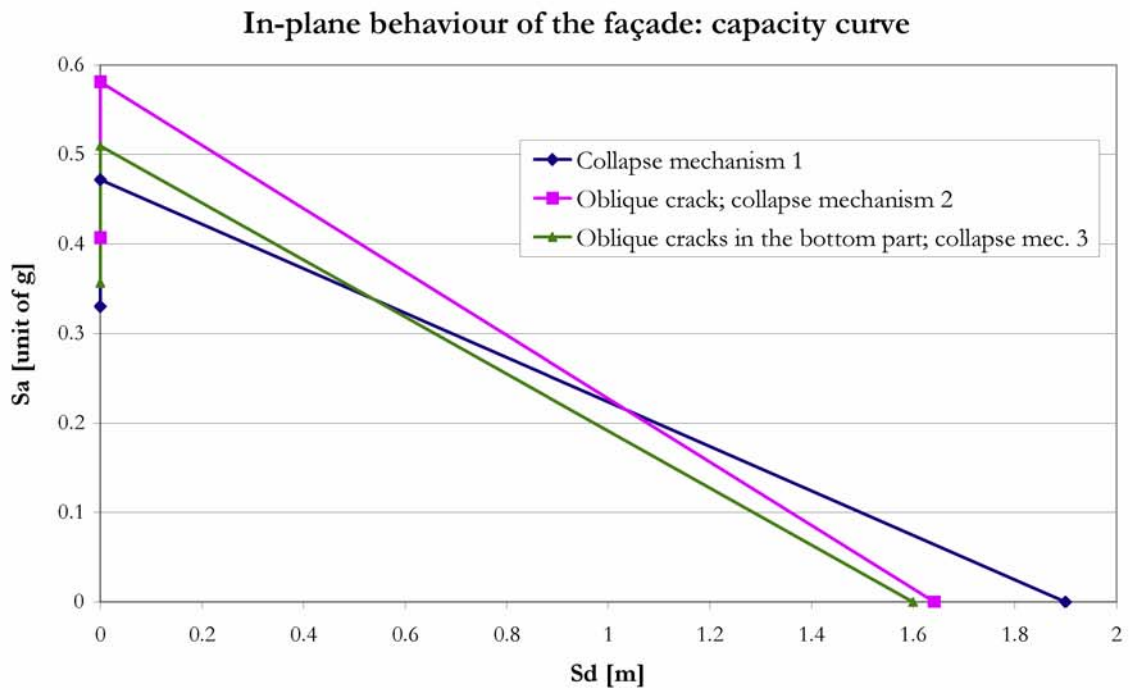
3. Shear collapse in the bottom part of the facade and overturning of every rigid block.

ASSUMPTIONS

- There is no particular link between the facade and the lateral walls (tie-rods for instance)
- In calculations (especially for the gravity centre), the openings areas have not been taken into account,
- Calculations have been carried out according to the theorem of the virtual works; moreover it is assumed that the rigid block turns around one point.
- The multiplier (that corresponds to the spectral acceleration in these cases) has been calculated according to [Gi 93].

RESULTS

According to the above schemes, the capacity curves of the three possible (in respect with the list of collapse mechanisms given by Lagomarsino et al.) in-plane collapse mechanisms (shear mechanisms) of the facade are:



Graph 2 : In-plane seismic response of the façade of the chapel in Visperterminen.

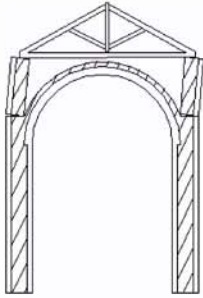
In the three situations, the spectral acceleration that is required to activate the in-plane mechanisms is quite high regarding the peak ground acceleration that could be measured in Switzerland.

The results show that the in-plane collapse of the façade due to seismic actions is not very realistic; nevertheless it might be a cause of indirect out-of-plane collapse. The cracking configuration of the façade, which would result from the in-plane seismic response, should be dealt with the same tools previously used to assess the seismic out-of-plane response of the façade. However, this iterative calculation would considerably increase the number of collapse mechanisms.

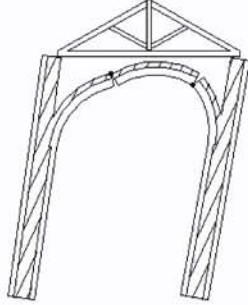
A 3.4.1.2. Lateral part of the church: the nave

The collapse mechanisms that are taken into account:

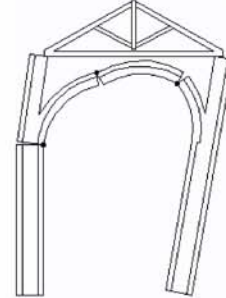
Nave covered by vaults:



Overturning of the upper parts.



Global overturning.



Overturning of one lateral wall.

Note: the above schemes are taken from [La 06].

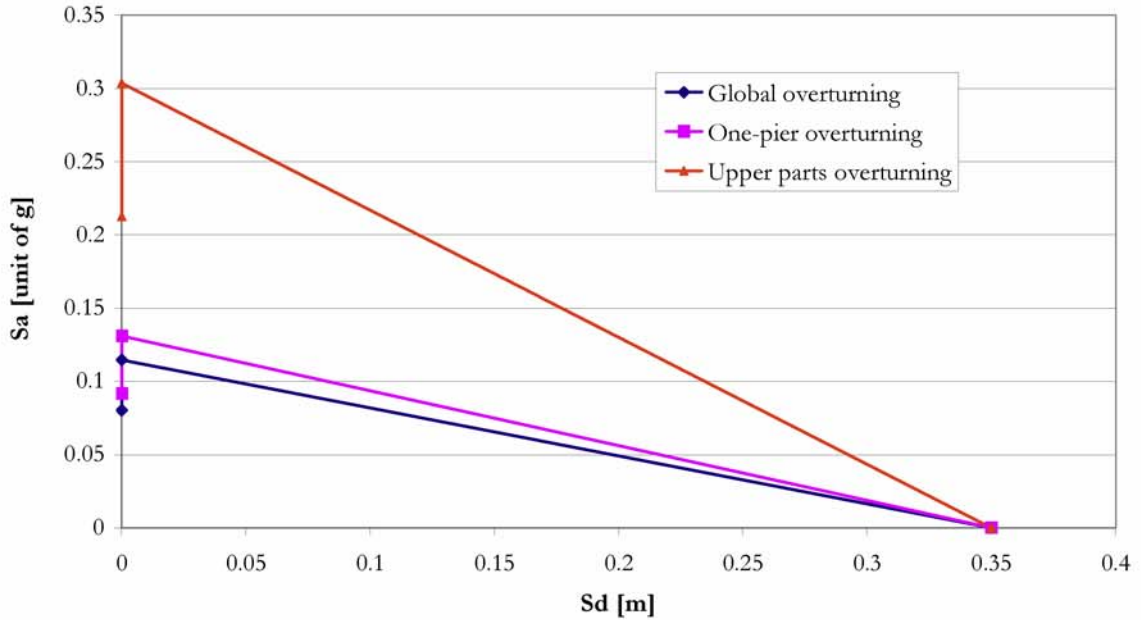
The seismic vulnerability of vaults has been taken into account through the treatment of the transversal seismic response of the nave. Since the method does not proposed any way to deal with the seismic vulnerability of groined or rib-vaults, as there probably were in the chapel, the vaults are modelled as being barrel-shaped.

ASSUMPTIONS

- it has been assumed that there were two ranges of prominent pillars (one along each lateral wall) and that the vaults came up from them (like in the «Three Kings» church in Visp),
- the weight due to framework and covering (slates) has been taken into account (loading case: own weight); the load has been defined according to SIA 261,
- possible vaults fillings have not been allowed for,
- the vaults shape has been assumed as a barrel vault with a radius of 2.95 m,
- the position of hinges has been assumed ($1/4 L$, $1/2 L$, $3/4 L$; L is the vault span),
- the vault is 0.25 m thick,
- every part of the model turns with the same angle,
- it has been assumed that the whole model collapsed when one part got unstable.

RESULTS

Overturning of lateral walls: capacity curves



Graph 3 : Capacity curves of the overturning of lateral walls, chapel in Visperterminen.

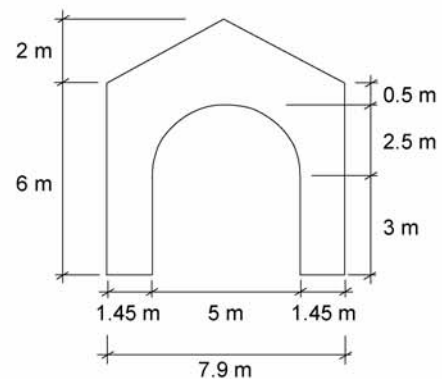
According to the graph 3, the most probable collapse mechanisms are the global overturning at first and then the one-pier overturning. Both require a spectral acceleration ($S_a=1.15 \text{ m/s}^2$ for the global overturning and $S_a=1.31 \text{ m/s}^2$ for the one-pier overturning mechanism) that might be clearly achieved in case of an earthquake in Switzerland.

It has to be said that the collapsed mechanism has been forced, that is to say, the position of hinges has been defined in advance. It is almost certain that the collapse multiplier that has been calculated above is not the lowest ones. Nevertheless, the calculated one could not be too far from the real solution. Moreover, regarding the assumptions of the method, the obtained value would be more or less close to the real value.

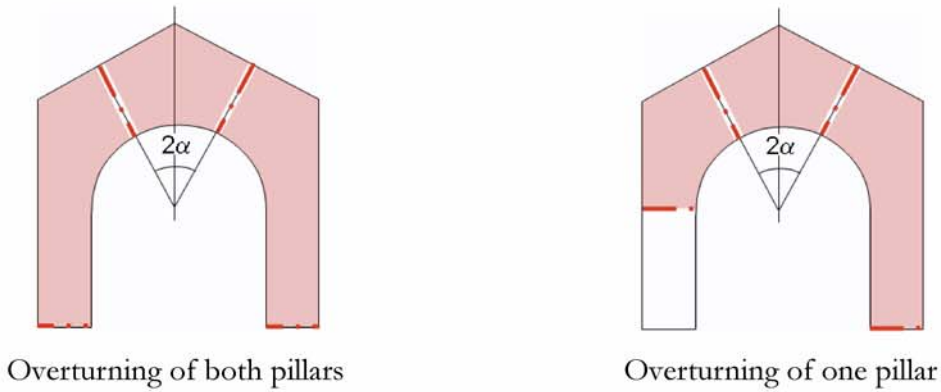
A 3.4.1.3. Chancel arch

The assumed dimensions of the chancel arch:

Note: to simplify the calculations, the upper part of the chancel arch opening has been assumed as being a round arch radius with a radius of 2.5 m.



The collapse mechanisms that have been taken into account are:

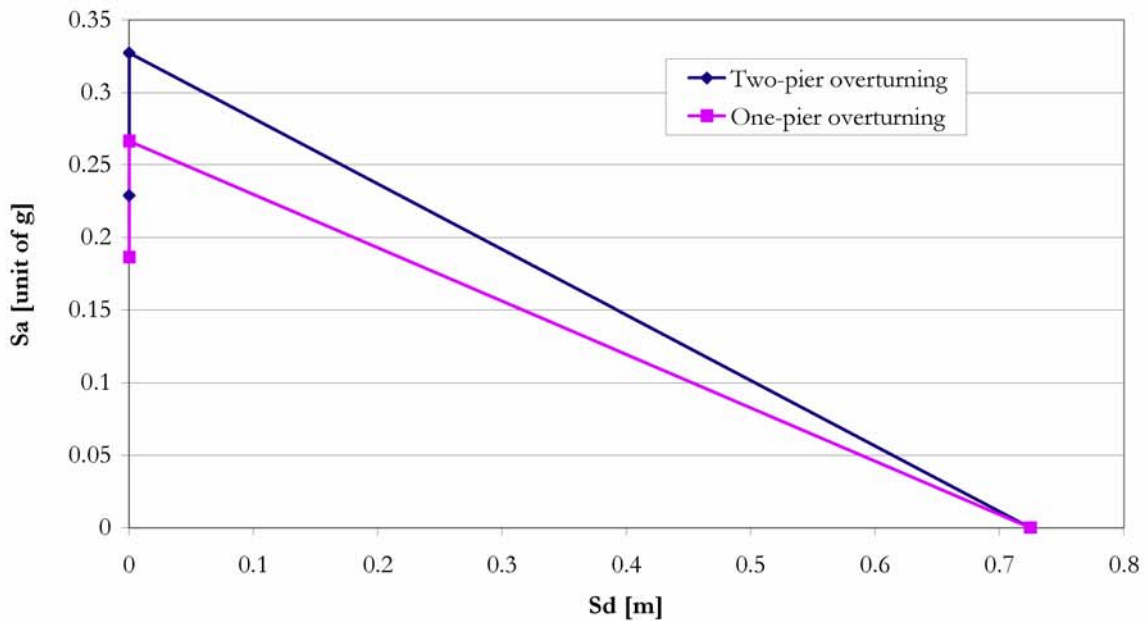


ASSUMPTIONS

- the arch shape has been assumed as a barrel arch with a radius of 2.5 m,
- the chancel arch is no support for any framework and covering,
- the position of hinges has been assumed (the middle part is cut symmetrically with 30° from the vertical),
- every part of the model turns with the same angle,
- it has been assumed that the whole model collapsed when one part got unstable.

RESULTS

Overturning of the chancel arch: capacity curves



Graph 4 : Capacity curves of the chancel arch; chapel in Visperterminen.

According to the graph 4, the activation of the one-pier collapse mechanism is the most probable. Nevertheless, the required spectral acceleration is higher than the peak ground acceleration due to the possible earthquakes in the canton Valais.

A 3.4.1.4. Apse

The assumed dimensions of the apse are:

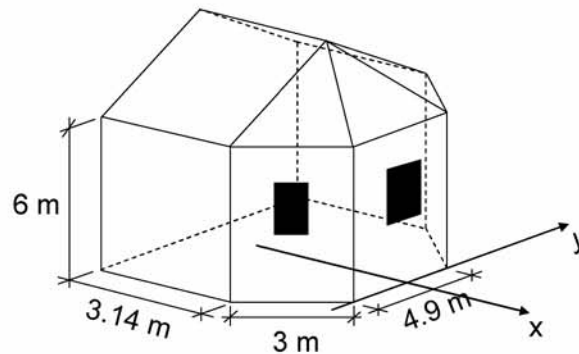


Figure 16.52 : Sketch of the chapel in Visperterminen apse.

The collapse mechanisms that have been taken into account are:

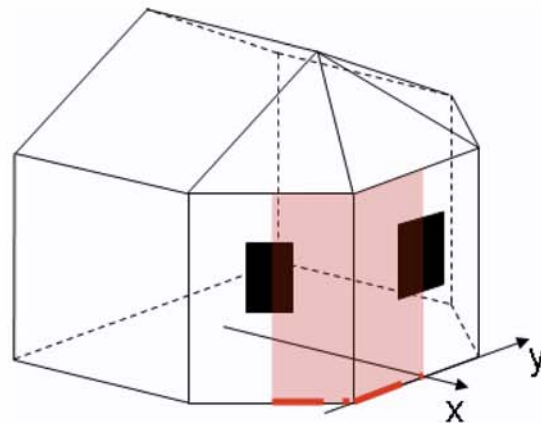


Figure 16.53 : Collapse mechanism that has been dealt with.

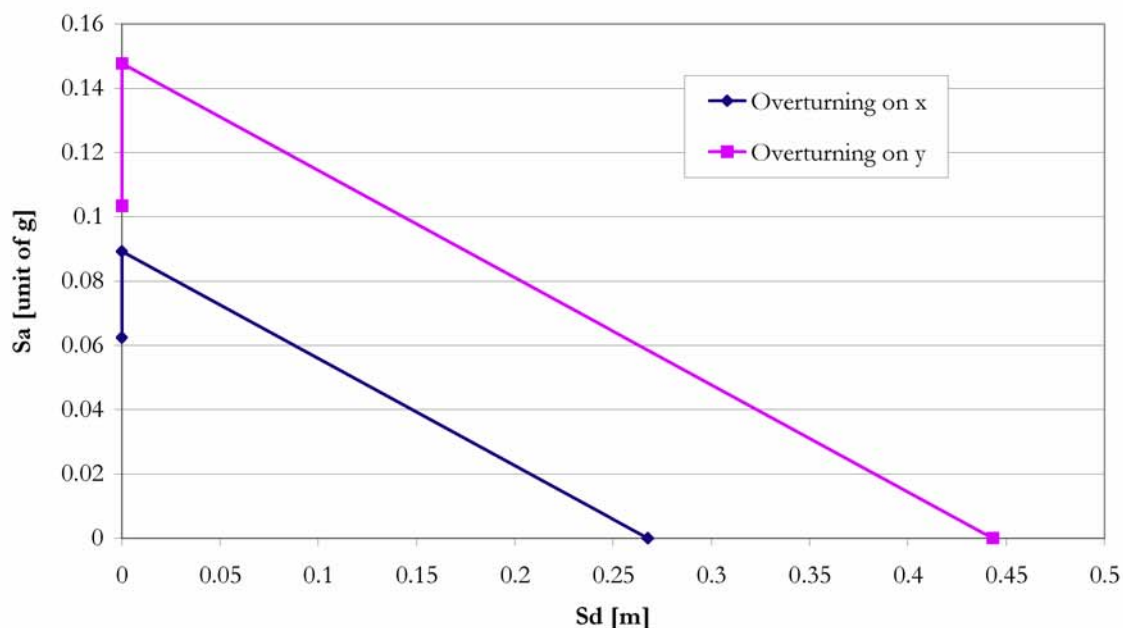
The first mechanism is in fact the collapse part (hatched part in Figure 16.53) that overturns along x direction; in the other mechanism, the same part overturns in y direction. This collapse mechanism was dealt with since this pattern was observed in situ (with the structure in ruins).

ASSUMPTIONS

- the collapse lines are vertical and situated in the middle of each apse part,
- the horizontal component of the action due to rafters does not load the walls.

RESULTS

Apse overturning: capacity curves



Graph 5 : Capacity curves of the apse overturning; chapel in Visperterminen.

The required spectral acceleration to turn around y-axis (i.e. on x-axis) is smaller than the one needed for the turn around the x-axis. This result might seem logical when looking at the apse geometry; nevertheless, it does not exactly match reality since the apse turned more around x axis than around y axis as the calculations indicate.



Figure 16.54 : View of the apse of the chapel in Visperterminen.

Otherwise, both values of acceleration are rather small and indicate then that this part was seismically particularly vulnerable. This result is indeed completely right.

A. 3. 4. 2. APPLICATION TO THE COLLEGIATE OF VALÈRE

Plan of the collegiate of Valère (schema):

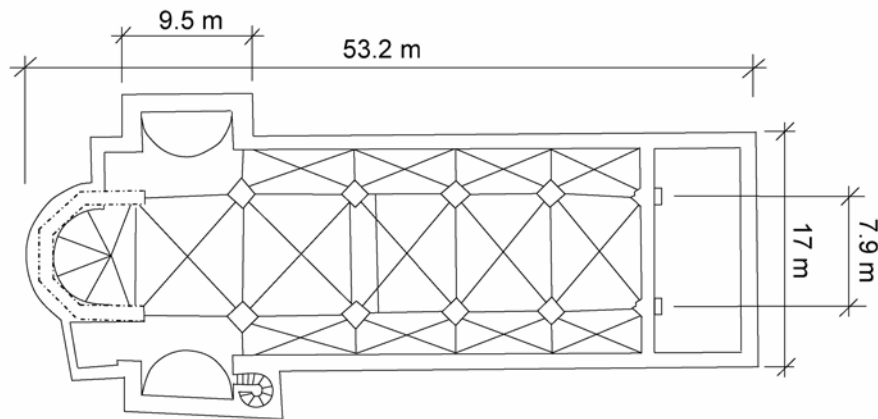


Figure 16.55 : Plan of the collegiate of Valère, Sion.

MATERIALS PROPERTIES

The values of materials have been defined according to the experience; walls are made up of ashlar limestone masonry whereas the vaults are in lighter material, maybe in tuff. The walls are made up of two leaves whose middle part is filled in with rubbles and mortar.

The weights per unit of volume of both materials are:

Walls	25 KN/m ³
Vaults	20 KN/m ³

In absence of further information, it has been assumed so.

MACRO-ELEMENTS

According to the method that has been developed by Lagomarsino et al., the chapel has been divided into macro-elements, which are:

- three facades (the main one, the nave facade and the transept facade),
- the nave/ lateral walls
- the chancel arch,
- the apse,
- the tower

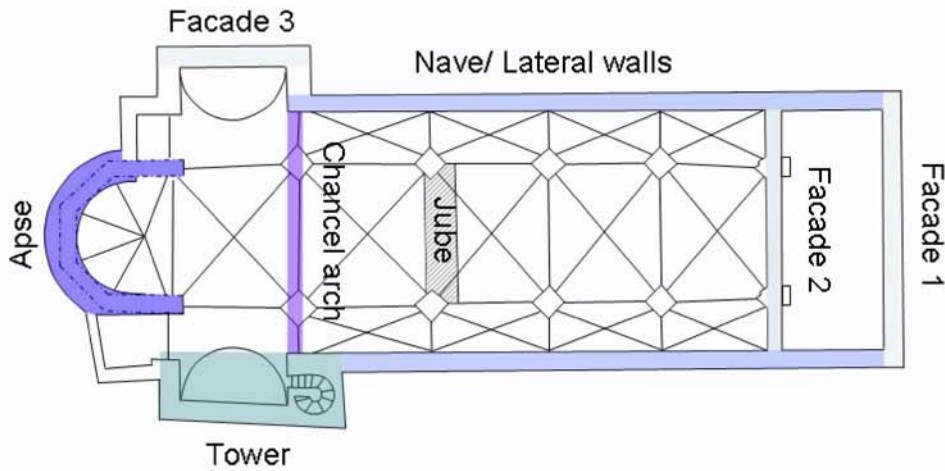
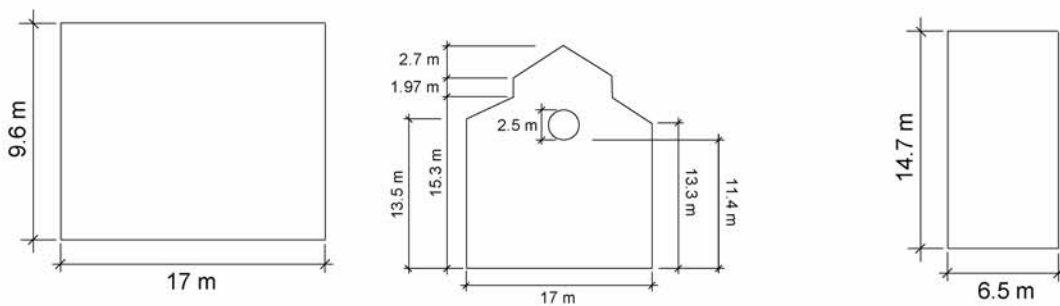


Figure 16.56 : Plan of the collegiate of Valère.

The results from the Level 1 calculations are the same as the ones calculated under the first level of the Risk-UE method. In regard to Level 3, no FEM analyses have been carried out for the moment. This step is a very sophisticated one and it was not the main interest of this report to think of numerical modelling. This may be carried out in a next future.

A 3.4.2.1. Macro-element: façade

The collegiate of Valère has three walls than can be described as being a macro-element: façade. The first one is the gable wall; it seems to have been built later than the main body of the church. The second wall is actually the main façade of the building even though it was concealed later with the gable wall. The last part of the collegiate to be dealt with as a façade macro-element is the southern wall of the southern transept.



Gable wall

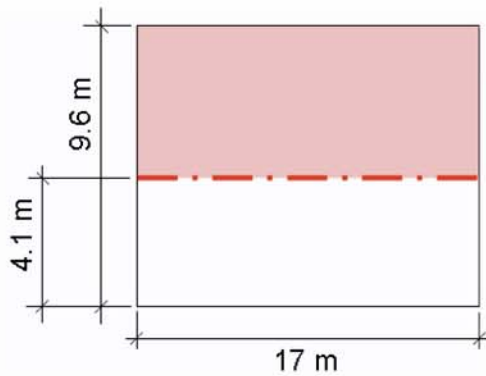
Main facade

Transept «façade»

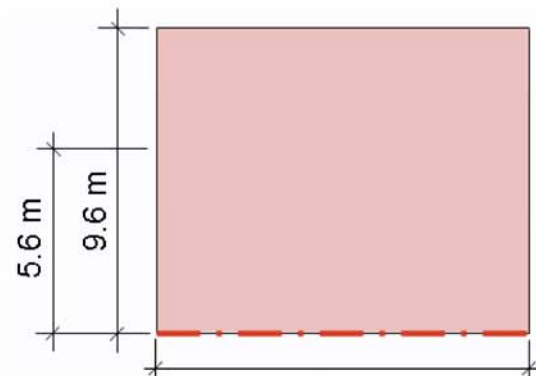
1. CAPACITY CURVE OF THE OUT-OF-PLANE BEHAVIOUR OF THE THREE FACADES

1. Gable wall

The out-of-plane collapse mechanisms of the gable wall are: the tympanum and the whole façade overturning.



1. Overturning of the upper part (tympanum)



2. Facade overturning

Though there is actually no real tympanum, this case has been taken into account because of the side-by-side building that might more or less restrained the wall at the position that is 4.13 m high from the ground. This limit (4.13 m high) also corresponds to a change of the wall thickness; the real out-of-plane behaviour of the gable wall is certainly between both cases.

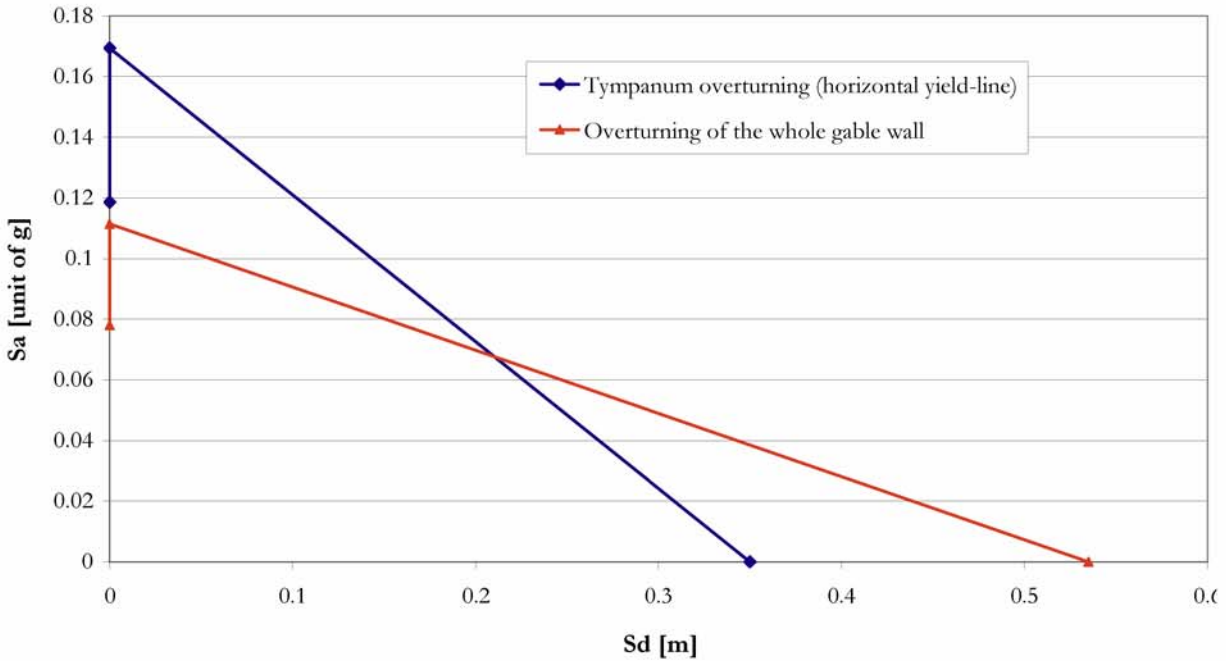
Note: the gable wall is 1.07 m thick up to 4.13 m high; it is 0.7 m thick in the upper part.

ASSUMPTIONS

- there are no tie-rods between the gable wall and its lateral walls,
- the covering and framework weight has not been taken into account,
- the impact of the openings has not been taken into account.

RESULTS

Out-of-plane behaviour of the gable wall: capacity curves



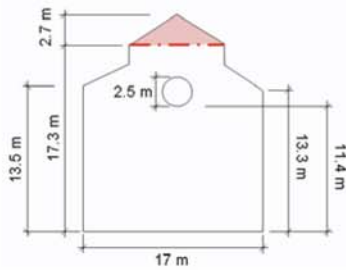
Graph 6 : Capacity curves of the out-of-plane behaviour of the gable wall; collegiate of Valère.

Though the tympanum is less thick than the bottom part of the entire gable wall, the whole facade is more vulnerable under dynamic actions and the collapse mechanism is activated with a low value of spectral acceleration. Moreover, the required multiplier is even under the pea ground acceleration defined in the Swiss code ($Z3b = 1.6 \text{ m/s}^2$).

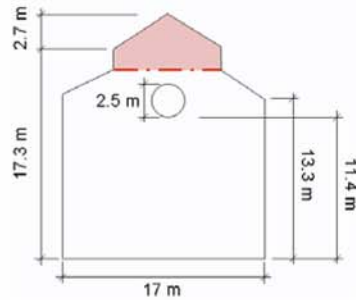
Note: there are almost certainly tie-rods that connect this gable wall to the lateral ones.

2. Main facade

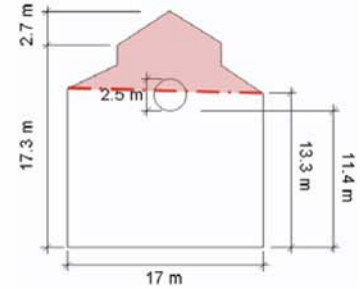
The out-of-plane collapse mechanisms of the main facade are: the tympanum and the whole facade overturning.



1. Tympanum overturning



2. Tympanum overturning
(yield-line at a lower level)



3. Tympanum overturning
(oblique yield-lines)

The fourth out-of-plane collapse mechanism is the overturning of the whole facade.

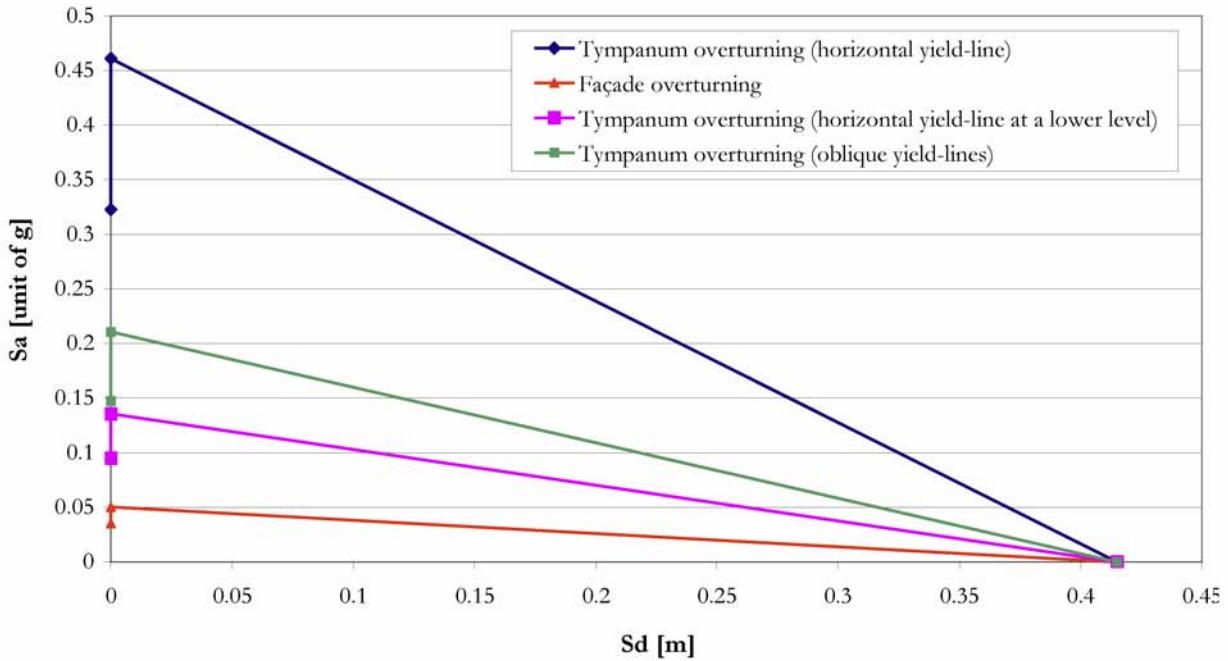
Note: the facade is asymmetric in regards to its middle vertical axis.

ASSUMPTIONS

- the main facade does not support any weight due to the nave framework,
- there are no tie-rods that link the main facade to the nave lateral walls,
- the weight due the organ is not allowed for.

RESULTS

Out-of-plane behaviour of the main façade: capacity curves



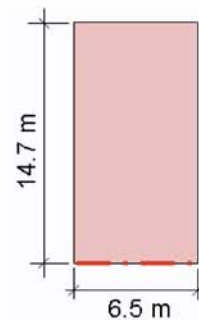
Graph 7 : Capacity curves of the out-of-plane behaviour of the main façade; collegiate of Valère.

The most seismically vulnerable part (in its out-of-plane behaviour) is the whole facade; this quite an astonishing result since the tympanum is the highest part and then is likely to be damaged at first. However the multiplier value to activate the tympanum out-of-plane collapse mechanism (collapse mechanism 2) is not much higher than the facade one. Furthermore, the tympanum is reinforced at its basis with vertical and horizontal iron strips that indicate it had already to be reinforced in the past. In this case, the impact of a possible hammering of the framework lateral beams should be investigated.

Note: as for the gable wall, the main facade is almost certainly connected to the lateral wall through tie-rods.

3. Transept wall

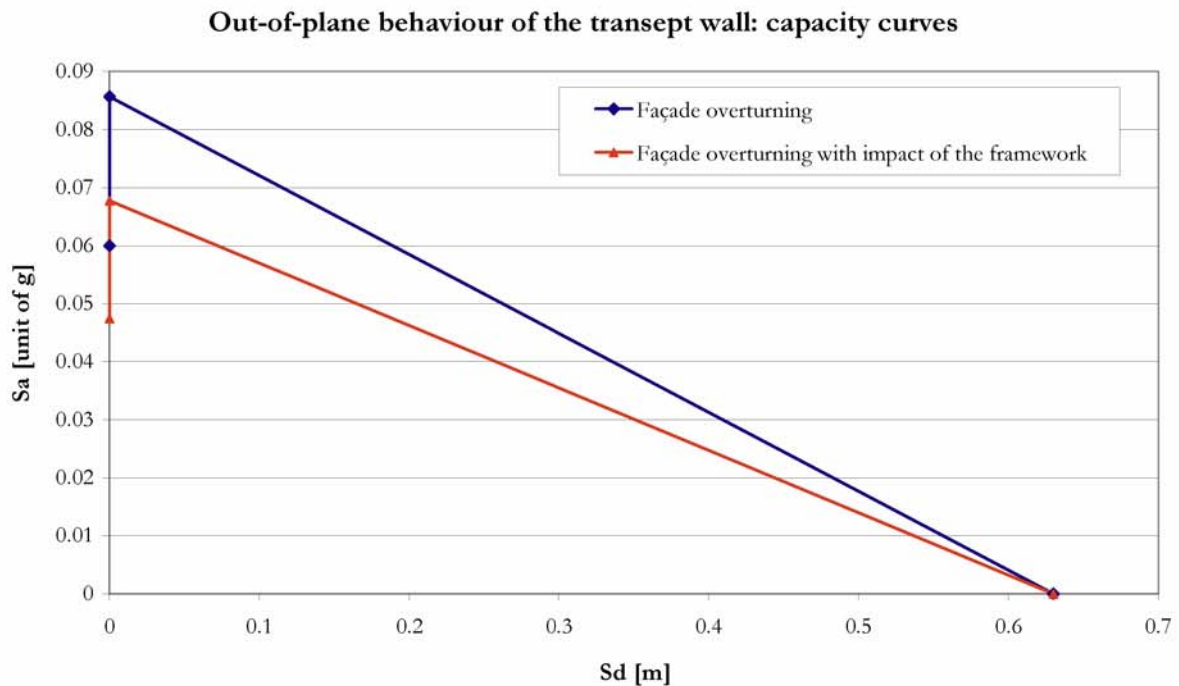
According to the assumption that the window has no impact on the out-of-plane collapse mechanisms, the only one collapse mechanism that is taken into account is: the whole facade overturning.



ASSUMPTIONS

- the transept facade supports the weight due to the nave framework,
- there are no tie-rods that link the main facade to the nave lateral walls,
- the impact of the openings has not been taken into account.

RESULTS



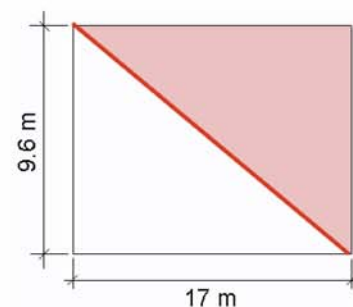
Graph 8 : Capacity curve of the transept wall; collegiate of Valère.

On the above graph, it can be seen that the transept facade is seismically highly vulnerable. Moreover, the graph shows that the framework has a negative impact on the value of the spectral acceleration that activates the out-of-plane mechanism. Once again, since this wall has already experienced seismic event that were characterized by higher peak ground acceleration, it must be well connected to its perpendicular walls.

2. CAPACITY CURVE OF THE IN-PLANE BEHAVIOUR OF THE THREE FAÇADES

1. Gable wall

According to Lagomarsino et al., a possible in-plane collapse mechanism is the creation of an oblique crack followed by the in-plane overturning of the upper half part of the wall.

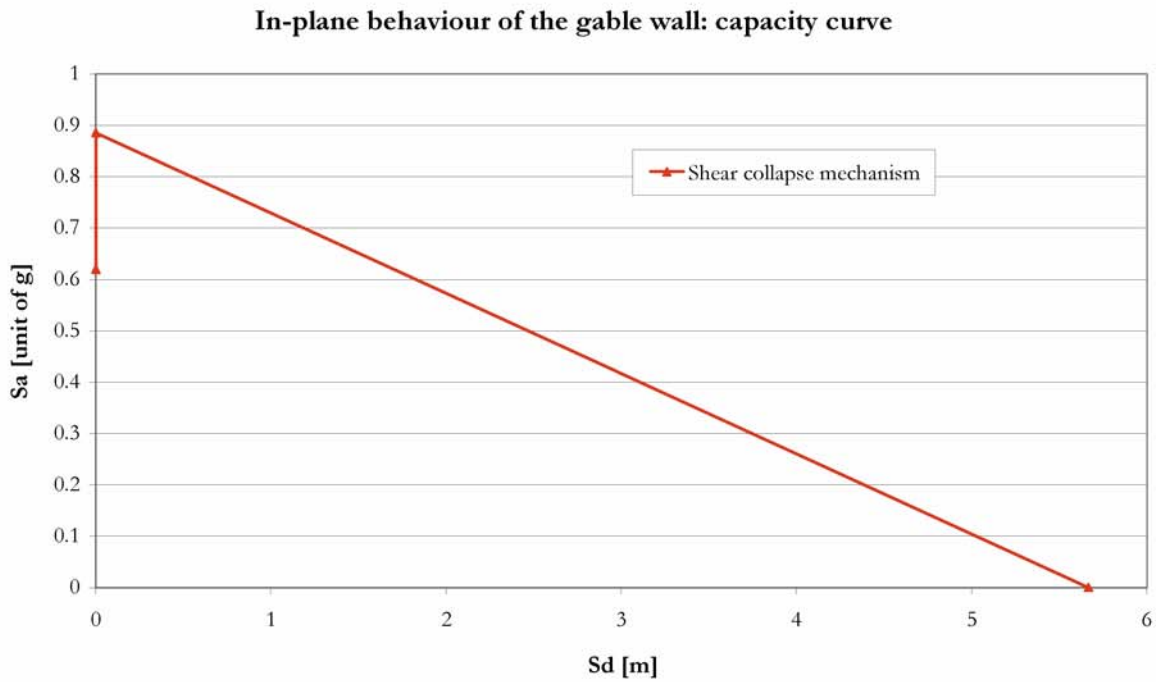


Note: it is worth reminding here that the presented scheme only approximately represents a collapse mechanism that can really happen.

ASSUMPTIONS

- the impact of the openings has not been taken into account,
- there is no particular links between the gable wall and the lateral walls.

RESULTS



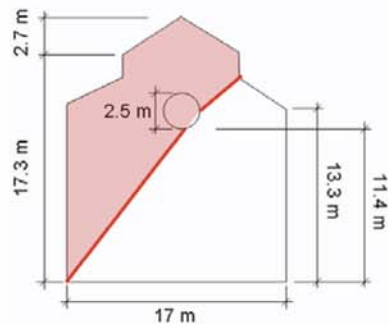
Graph 9 : Capacity curve of the shear mechanism of the gable wall; collegiate of Valère.

As it can be seen on the previous graph, the required spectral acceleration to activate the mechanism is quite high. Moreover it can be said that just only because of dimensions this collapse mechanism is almost impossible to be activated.

2. Main facade

The in-plane collapse mechanisms of the main facade are: the tympanum and the whole facade overturning.

There is only one visible opening that can have an impact on the mechanisms; it is why no other in-plane collapse mechanisms are taken into account.

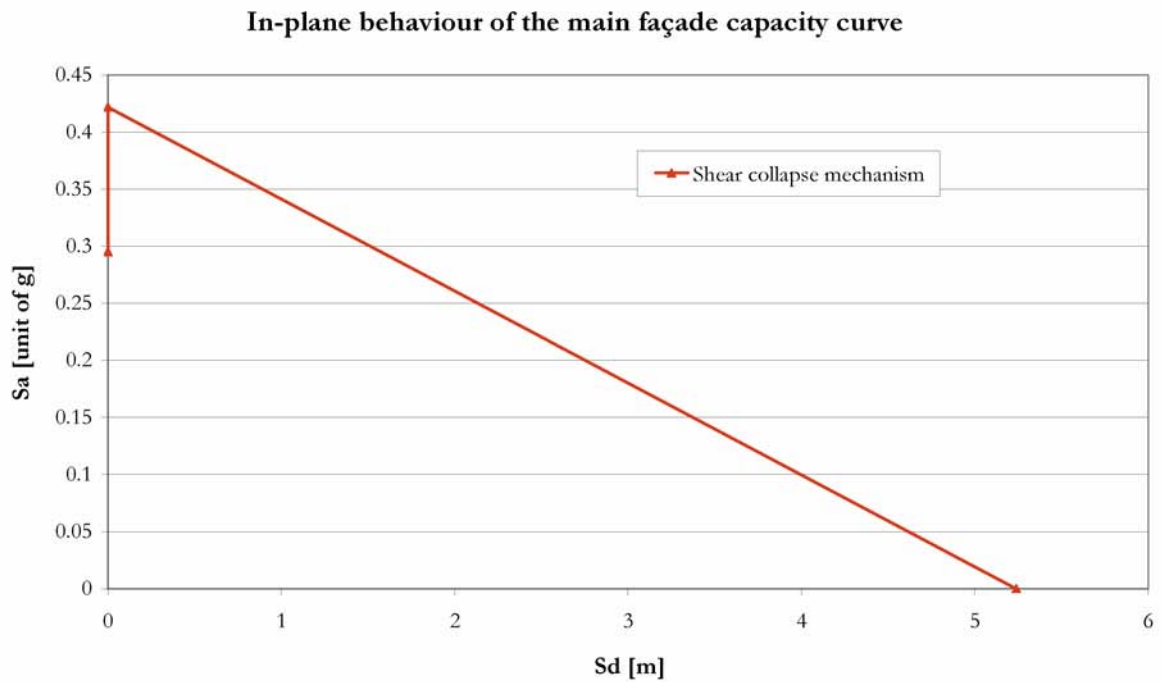


Note: the facade is asymmetric in regards to its middle vertical axis.

ASSUMPTIONS

- The impact of the openings has not been taken into account,
- There is no particular links between the gable wall and the lateral walls.

RESULTS

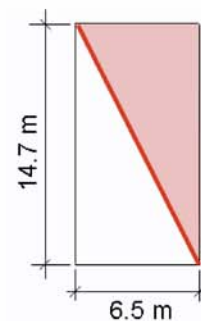


Graph 10 : Capacity curve of the shear mechanism of the main façade; collegiate of Valère.

Once again, as for the gable wall, the required spectral acceleration to activate the mechanism is quite high.

3. Transept facade

Like the gable wall, there is mainly one in-plane collapse mechanism that can be allowed for and it is the following one. It corresponds to the creation of an oblique crack followed by the in-plane overturning of the upper half part of the wall.

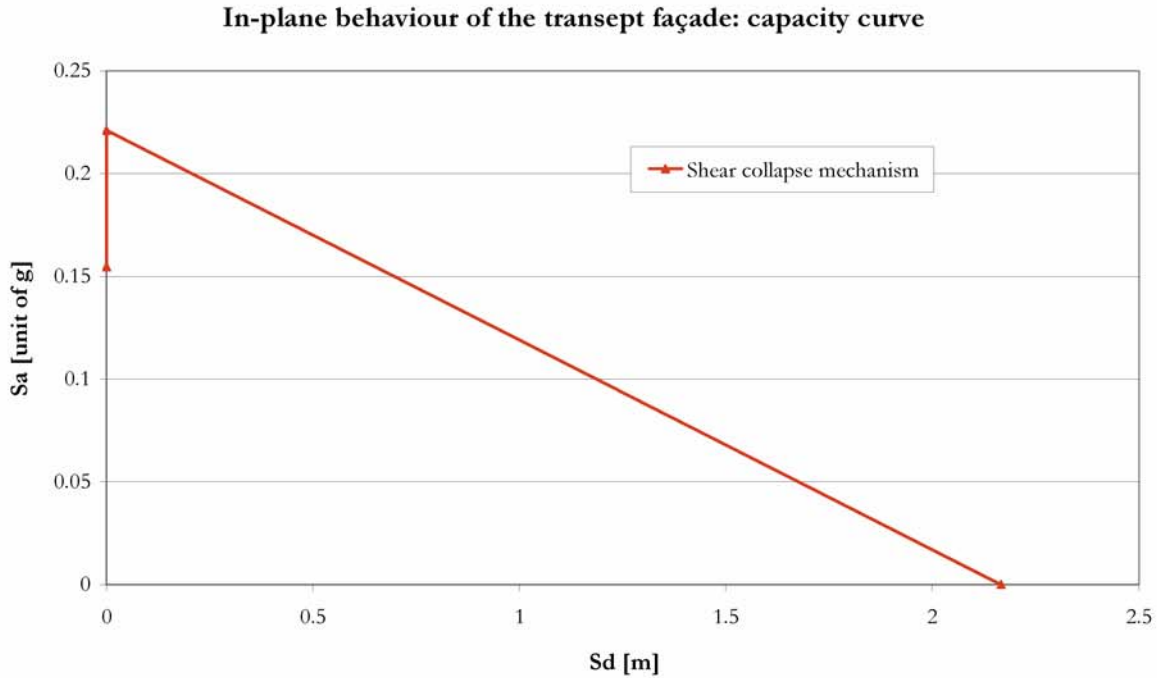


Note: the facade is asymmetric in regards to its middle vertical axis.

ASSUMPTIONS

- the impact of the openings has not been taken into account,
- there is no particular links between the gable wall and the lateral walls.

RESULTS



Graph 11 : Capacity curve of the shear mechanism of the transept façade; collegiate of Valère.

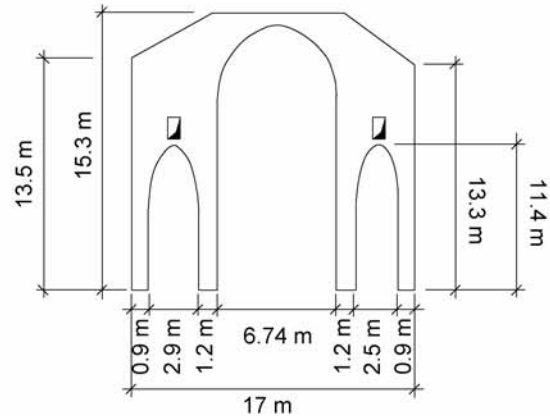
The shear collapse mechanism of the transept wall might be activated under a spectral acceleration of 2.3 m/s^2 .

DISCUSSION

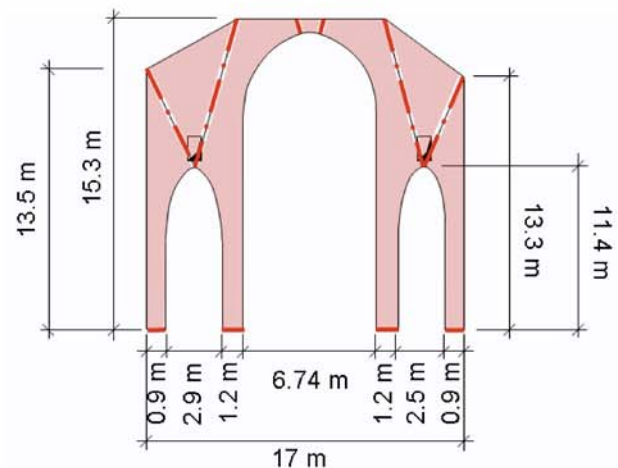
The in-plane collapse mechanisms proposed in the given method do not exactly correspond to shear collapse mechanisms. The failure is indeed a shear failure but the mechanism of collapse is an overturning around one edge. Moreover, the seismic motion that is required to result in such a collapse must be larger, at least for the given front walls and transept façade, than the peak ground acceleration that can be expected in Switzerland.

A 3.4.2.2. Lateral part of the church: the nave

The cross-section of the nave is composed of three naves; both side aisles are surmounted by a massive buttress that rather looks like a wall. There is a small opening (door to go from one bay after the other) under the ceiling of each side aisle. The wall above each arch of the main nave does not go up to the roof ridge.



One collapse mechanism had to be chosen in order to calculate the collapse multiplier that is required to activate the mechanism. According to the surveys carried out by Lagomarsino et al., the following mechanism has been individuated:



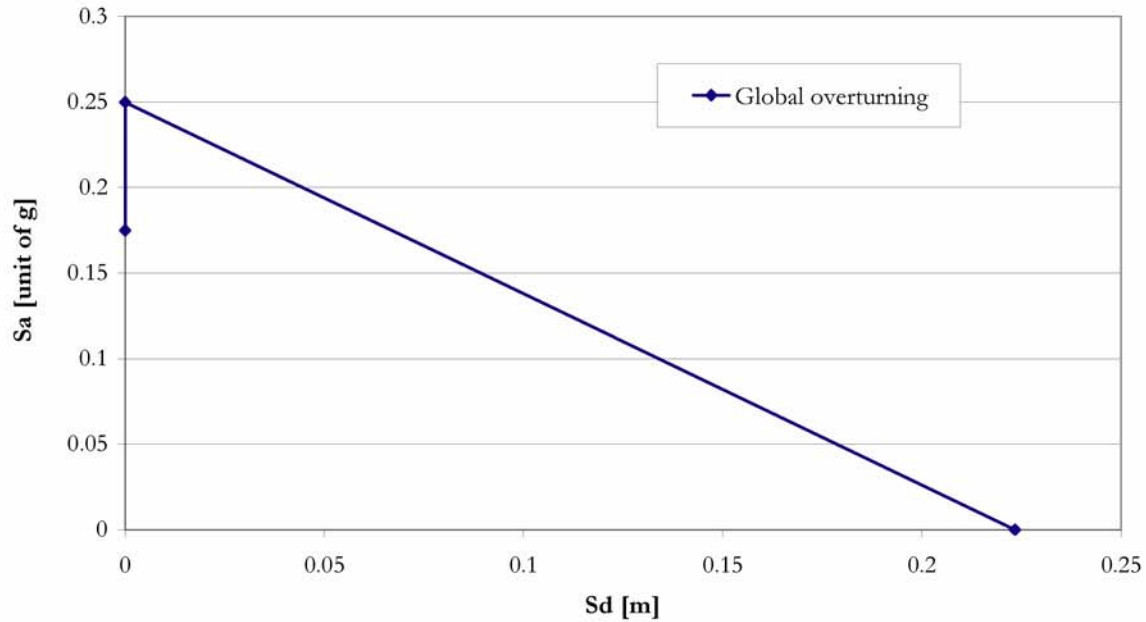
The seismic vulnerability of vaults has been taken into account through the treatment of the transversal seismic response of the nave.

ASSUMPTIONS

- the weight due to framework and covering (slates) is not supported by the transversal part of the nave; the nave walls support this weight,
- the position of hinges has been assumed,
- the rib-vaults have been modelled as barrel vaults,
- the vault is 0.25 m thick,
- every part of the model turns with the same angle,
- the buttresses have been included within what it is called the transversal structure of the nave,
- it has been assumed that the whole model collapsed when one part got unstable.

RESULTS

Overturning of lateral walls: capacity curve



Graph 12 : Capacity curve of the in-plane overturning of the transversal structure of the collegiate of Valère.

The spectral acceleration that would lead to the activation of the above mentioned collapse mechanism is about 2.5 m/s^2 . Regarding the seismic hazard in Switzerland, it seems rather impossible to be activated without site effects. Nevertheless, the first damage might occur under a peak ground acceleration of 1.7 m/s^2 , which could happen.

A 3.4.2.3. Chancel arch

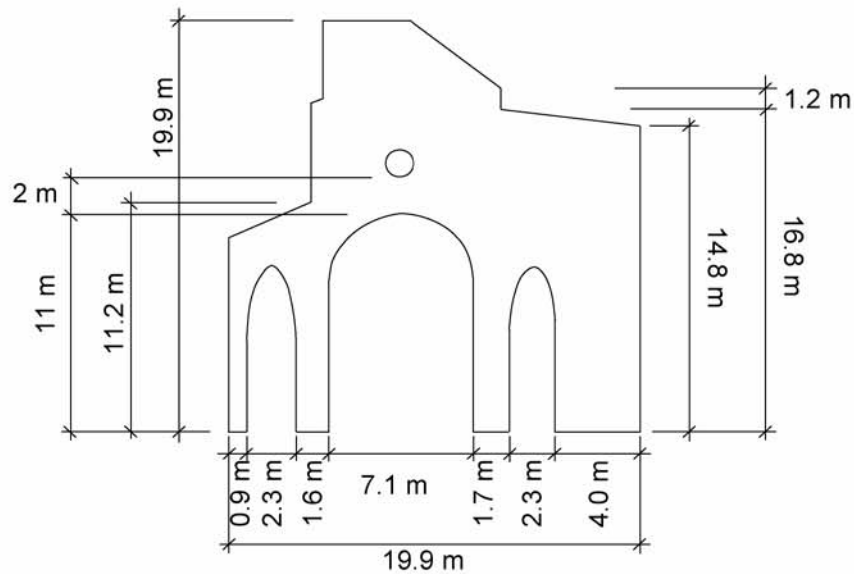


Figure 16.57 : Plan of the chancel arch

To the left of this structural part is the tower. It has not been included in the chancel arch part because the masonry of both parts is actually separated; both parts were just built side-by-side. Nevertheless, the shape of this part looks rather weird; it is difficult to exactly know if it could be partially included or not. On the contrary, the transept west wall has been included in the so-called chancel arch part.

Lagomarsino's method proposes no collapse mechanisms for such sacred edifices because it is limited to one-nave churches. However, in [La4 04], an example with a three-nave chancel arch is given and the following mechanisms was chosen on the basis of this example.

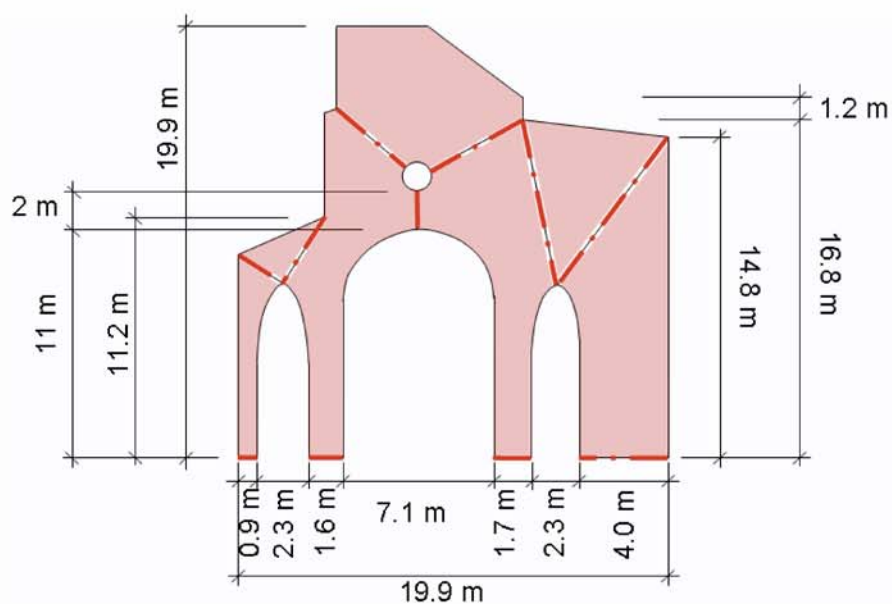


Figure 16.58 : Collapse mechanism of the chancel arch.

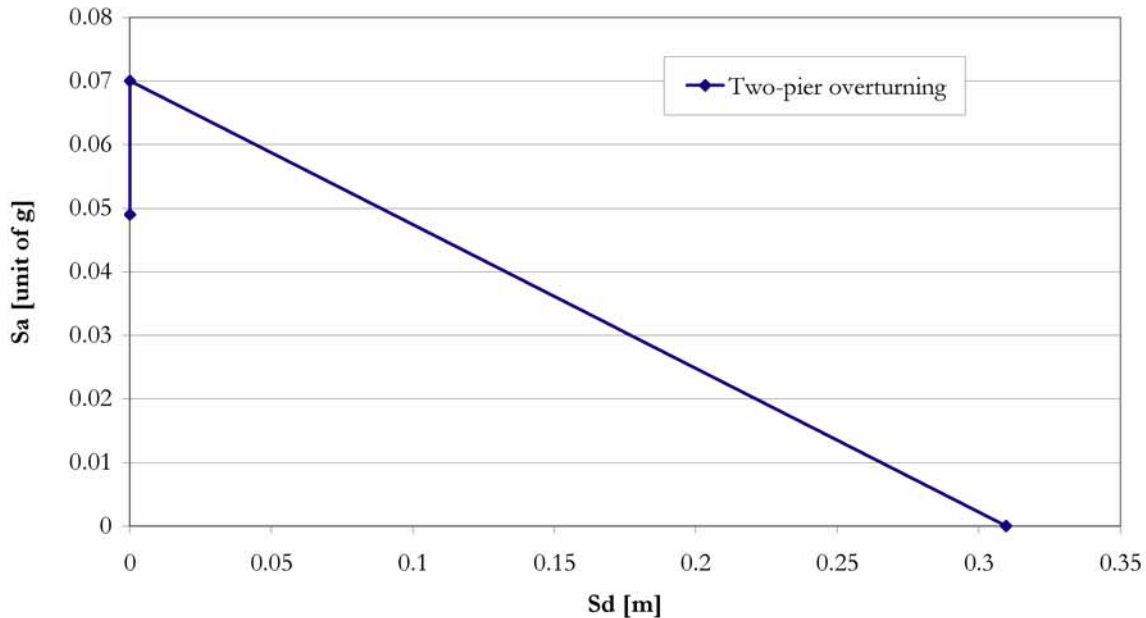
Note: this structural part can be found twice in the collegiate: between the nave and the crossing and between the crossing and the nave.

ASSUMPTIONS

- the weight due to framework and covering (slates) is not supported by the chancel arch; the nave lateral walls support this weight,
- the position of hinges has been assumed (this is the most important assumption),
- the vault is 0.25 m thick,
- every part of the model turns with the same angle,
- it has been assumed that the whole model collapsed when one part got unstable.

RESULTS

Overturing of the chancel arch: capacity curves



Graph 13 : Capacity curve of the chancel arch overturning; collegiate of Valère.

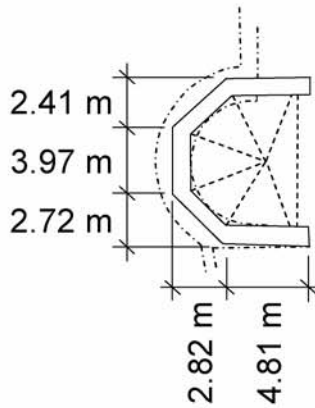
The results show that this part of the structure might be seismically highly vulnerable.

It must be kept in mind that the chosen collapse mechanism is of great importance because the collapse multiplier depends on it. If the collapse mechanism is not correct (and this probably the case for the chancel arch), i.e. too unfavourable, the collapse multiplier is lower than the value for the real mechanism. The upper bound theorem gives either the right value for the collapse mechanism of a structural part (which also correspond to the lowest value of collapse multiplier given by the Static theorem) or a higher one. This is actually the Achille's heel of the method; nevertheless, the upper bound theorem is easier and less time-consuming than its counterpart, the Static theorem. The problem is that its application to «easy» structures is rather safe, even if we obtain a higher collapse multiplier (i.e. not exactly the real collapse mechanism) for a structural part than

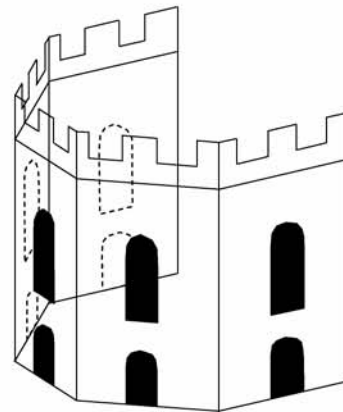
the real one because they normally could not be too much different. This is no longer the case with quite complex structures like this chancel arch part.

To sum up, this structural part might be vulnerable though not necessarily to such an extent.

A 3.4.2.4. Apse

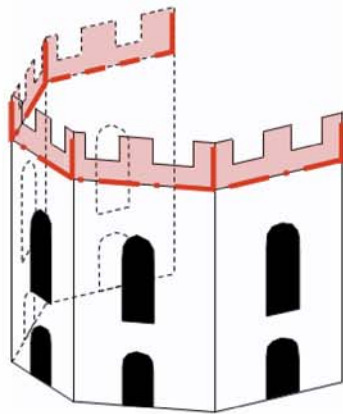


Plan and dimensions

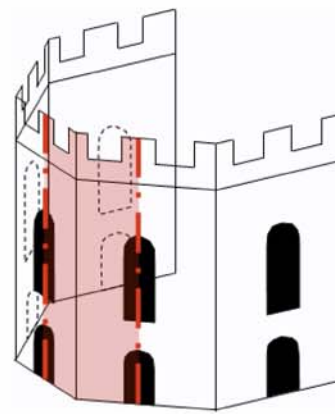


View in elevation

The collapse mechanisms that have been studied (they were chosen on the basis of Lagomarsino's method, but they are not given in it):



1. Crenels overturning



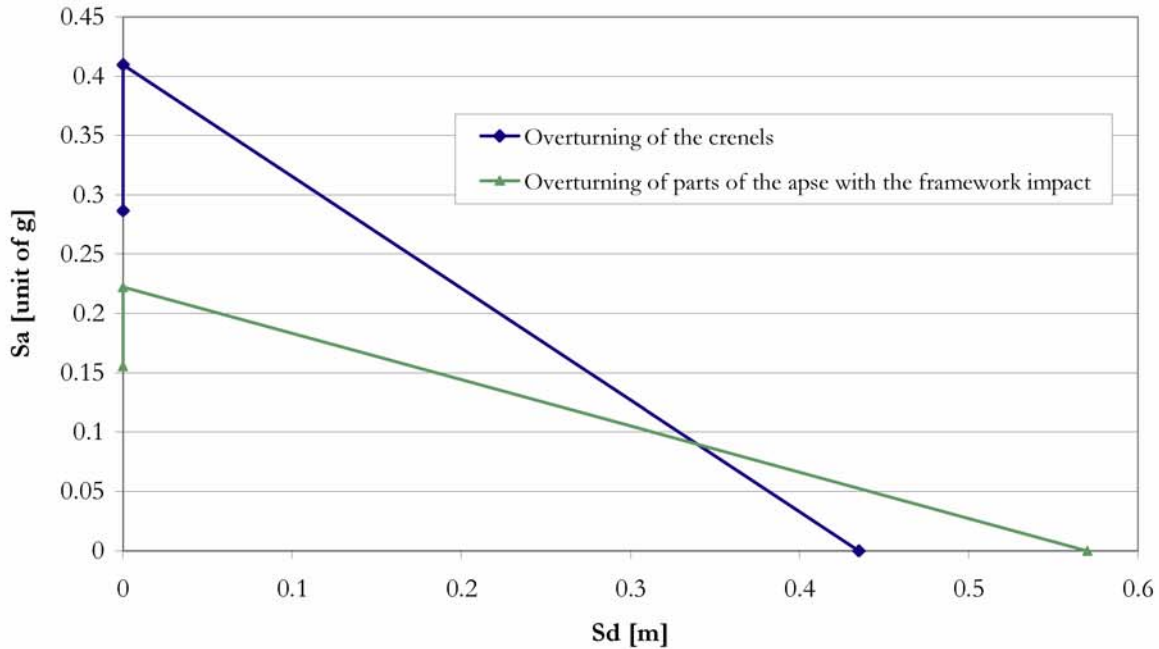
2. Part of the apse walls overturning

ASSUMPTIONS

- the collapse lines are vertical and situated in the middle of each apse part,
- the horizontal component of the action due to the rafters is taken back by the framework.

RESULTS

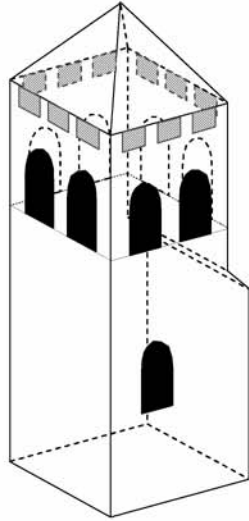
Overturning of the apse: capacity curves



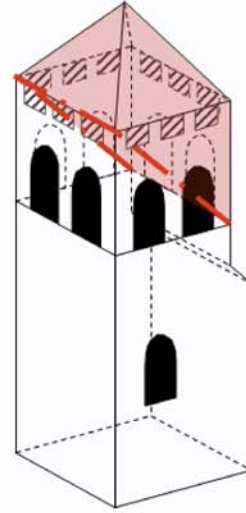
Graph 14 : Capacity curves of the overturning of the crenels and of horizontal strips belonging to the apse; collegiate of Valère.

The apse seems not to be too much vulnerable. This fact is confirmed by the damage survey carried out by L. Bondel in July 1947.

A. 3. 4. 3. BELL TOWER



View (schema) of the tower in elevation



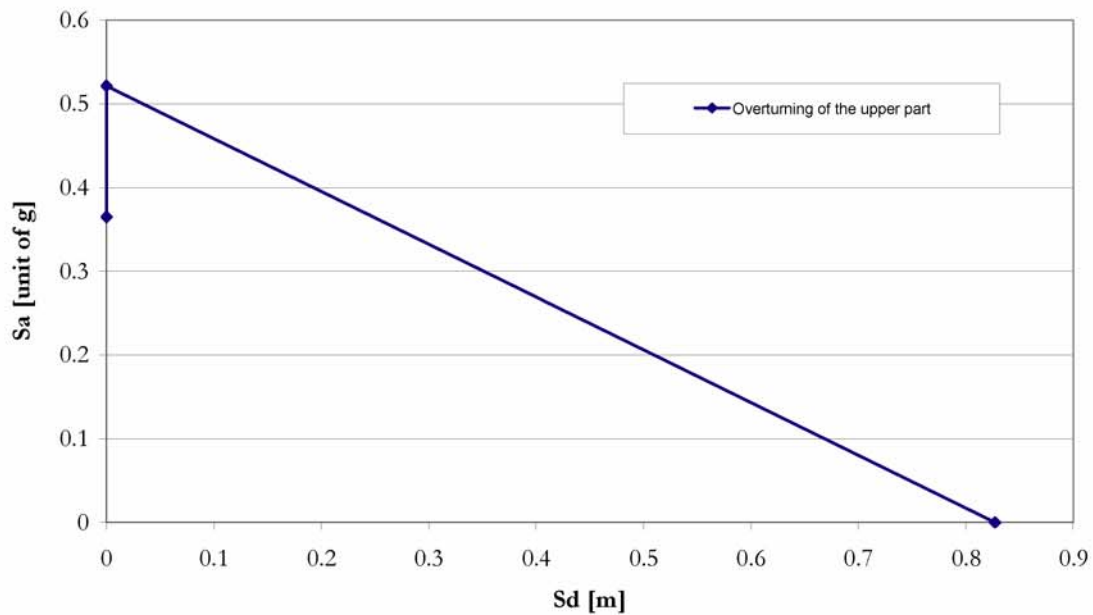
Collapse mechanism that has been studied.

ASSUMPTIONS

- the framework is constructed in the way to induce no horizontal components on the masonry,
- the covering with the framework moves with the below masonry in one block.

RESULTS

Overturning of the bell tower: capacity curve



Graph 15 : Capacity curve of the overturning of the upper part of the tower.

As more or less expected, the tower is rather safe regarding this collapse mechanism. Nevertheless, it might be worth studying the required spectral acceleration to activate a shear mechanism just below the covering.

A. 3.5. AUGUSTI'S METHOD: APPLICATION

A. 3.5.1. APPLICATION TO THE OLD CHAPEL IN VISPERTERMINEN

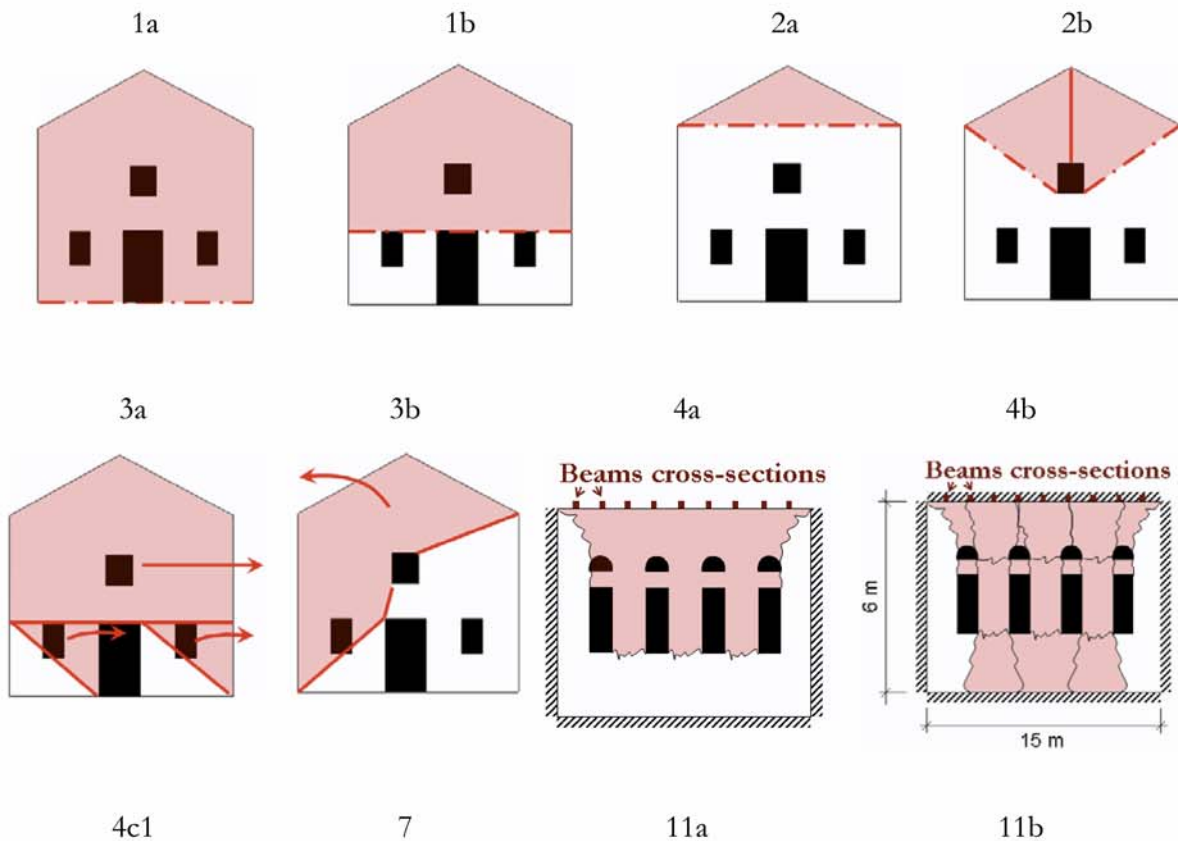
The estimation of the collapse probability of each macro-element is dealt with at first; the obtained results are then used to calculate the collapse probability of the whole church.

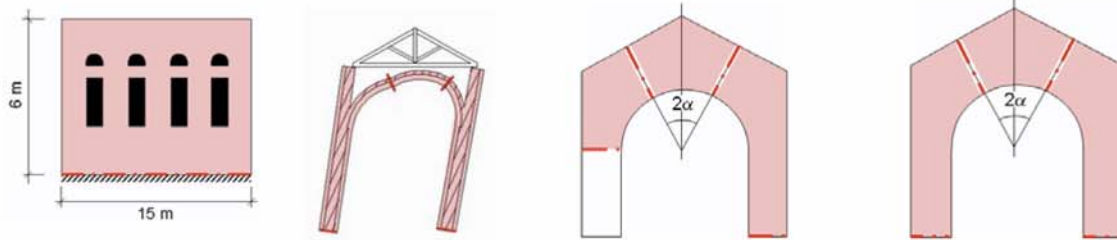
Note: both kind of evaluation have been carried out according to the way proposed in [Au 01] and [Au 02].

ASSESSMENT OF THE COLLAPSE PROBABILITY OF EACH MACRO-ELEMENT

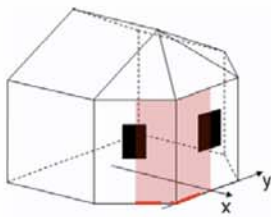
1. With respect to the present ruins still standing in Visperterminen, the most significant collapse mechanisms are for each macro-element:

the tympanum (top of the main facade) does not support the fram





12a



Note: the hatched surface correspond the part that collapses due to the mechanism.

2. By means of the limit analysis (upper bound theorem and application of the theorem of virtual works), nominal values of the seismic coefficients C_{ij} are obtained.

All the assumptions made for the application of the method of Lagomarsino et al. are also made for this method application. A few more have been made because of the method particularities.

ASSUMPTIONS

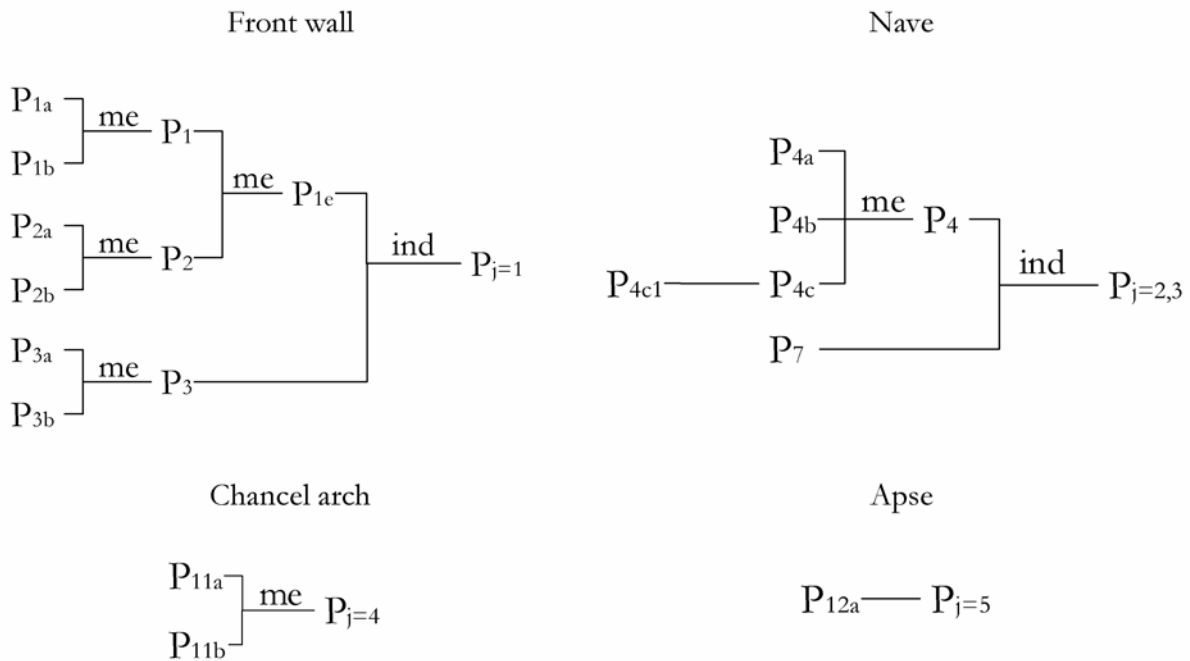
- the overturning of the facades and tympanums has been calculated by taking into account a part of the wall that was in high compression (triangular distribution of stresses) instead of one theoretic point (as in the Lagomarsino's method). In this case, the compression strength of masonry was assumed to be 20 MPa,
 - for other collapse mechanisms, this compression part has not been taken into account and the rotation point has been idealized in one point.
3. The probability density functions f_{cij} of the seismic coefficients C_{ij} are defined (C_{ij} have been assumed to be normally distributed [Au 01] and the coefficient of variation (c.o.v) is estimated on the basis of the number and significance of the geometrical and mechanical parameters considered under step 2. and also of their uncertainties

Table 16.14 : Seismic coefficients and their combined probabilities for three different level of ground acceleration.

<i>Mechanism</i>	<i>Macroelement</i>	$E[C_{ij}]$	<i>c.o.v</i>	P_{ij} ($a_g=0.06\text{ g}$)	P_{ij} ($a_g=0.1\text{ g}$)	P_{ij} ($a_g=0.16\text{ g}$)
1a	1	0.244	0.375	0.018	0.054	0.175
1b	1	0.39	0.375	0.0084	0.0201	0.0566
2a	1	1.27	0.390	0.0021	0.0039	0.0102
2b	1	0.632	0.465	0.0098	0.0193	0.0379
3a	1	0.51	0.325	0.0024	0.0058	0.0164
3b	1	0.504	0.390	0.0067	0.0145	0.035
4a	2, 3	0.33	0.450	0.0204	0.05	0.11
4b	2, 3	0.626	0.315	0.0013	0.003	0.0083
4c1	2, 3	0.23	0.345	0.015	0.052	0.2
7	2, 3	0.115	0.375	0.12	0.37	0.86
11a	4	0.27	0.375	0.0154	0.04	0.14
11b	4	0.33	0.375	0.011	0.028	0.083
12 a	5	0.09	0.390	0.195	0.62	0.97

Note: bold numbers indicate the most probable collapse mechanism.

4. For given earthquake intensities, the collapse probability P_j of the j th macroelement is calculated; in the case of the chapel in Visperterminen, P_j ($j=1-5$) is calculated according to the following schemes:



RESULTS

Macroelement	Collapse probability (P_c), $a_{gd}=0.06 \text{ m/s}^2$	(P_c), $a_{gd}=0.1 \text{ m/s}^2$	(P_c), $a_{gd}=0.16 \text{ m/s}^2$	$a_{gd}=0.16$
Façade (1)	0.017	0.044	0.11	
Nave (2, 3)	0.13	0.39	0.87	
Chancel arch (4)	0.015	0.038	0.129	
Apse (5)	0.195	0.62	0.97	

ASSESSMENT OF THE COLLAPSE PROBABILITY OF THE WHOLE EDIFICE

1. The critical and non-critical macro-elements have to be individuated at first. In the case of the old chapel in Vipsperterminen, it is assumed that every element is critical since the collapse of each of them involve the failure of the structure. The logical diagram of the old chapel in Visperterminen is:

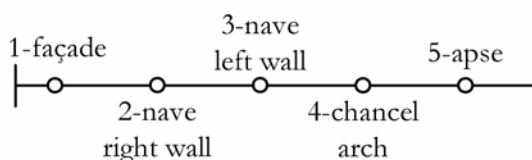


Figure 16.59 : Logical diagram of the old chapel in Visperterminen.

2. The collapse probability of the whole building is given in 5.21.

DISCUSSION

According to the graph 16, the whole chapel would have a probability of 1 to collapse under a peak ground acceleration of 1.6 m/s^2 that characterized the zone 3B where is situated Visperterminen [SIA 261 03]. Since the chapel collapse has been defined through the logical diagram (that meant: the chapel collapses if the nave or the facade or the chancel arch or the apse collapses), this result is correct. Though it is also quite right in respect of the present ruins of the chapel, it seems to be overstated because the chapel was not so damaged after the 1755 earthquake; it got so damaged only after the 1855 earthquake. It is worth noting that the method gives no possibility to take into account the initial state of maintenance of the edifice; the above graph must correspond to both states: before 1755 seismic event and before 1855 earthquake. In this sense the method, as well as the second level of the method of Lagomarsino et al., presents a great disadvantage.

The apse is the most seismically vulnerable part of the chapel; it is followed by the nave (lateral seismic response), the facade and then the chancel arch. With respect to the ruins and in regarding the already cracked chapel before 1855, it is quite right except for the facade. Since there is nothing that is still standing at the place of the facade it can be deduced that it was moderately or highly damaged after the 1855 earthquake. Since the collapse multiplier has been calculated according to the assumption that the facade did not idealistic turn around one point but a surface, this value is maybe too much conservative or on the other hand, the other ones (collapse multiplier of the nave, apse, etc.) are too much unfavourable. This assumption is indeed more realistic than the idealistic movement around one point; however the definition of the compressive strength as well as the surface of compression is quite delicate and makes the result more uncertain.

The low seismic vulnerability of the chancel arch seems to be quite right with respect to the ruins. To sum up, though the valuable results obtained, it must be kept in mind that the chapel was already damaged in 1855, when it was struck by an earthquake. This must have had an impact on the seismic response of the chapel but no ones of the applied methods give the possibility to consider it.

A. 3. 5. 2. APPLICATION TO THE COLLEGIATE OF VALÈRE

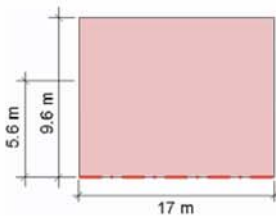
The evaluation of the collapse probability of each macro-element is dealt with at first; the obtained results are then used to calculate the collapse probability of the whole church.

Note: both evaluations have been carried out according to the way proposed in [Au 01] and [Au 02].

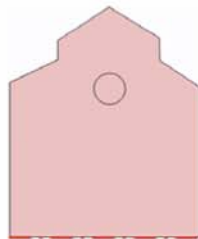
A 3.5.2.1. Assessment of the collapse probability of each macroelement

1. With respect to the present ruins still standing in Visperterminen, the most significant collapse mechanisms for each macro-element are:

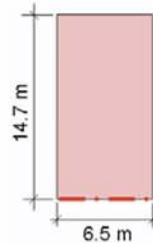
1a; Gable wall (A)



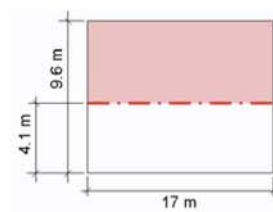
1a; Main facade (B)



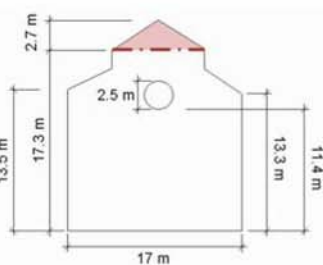
1a; Transept wall



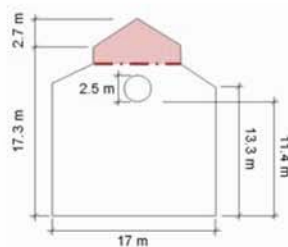
2a; Gable wall (A)



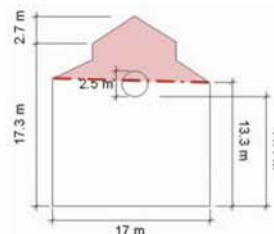
2a; Main facade (B),
Tympanum 1



2a; Main facade (B),
Tympanum 2

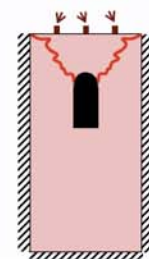


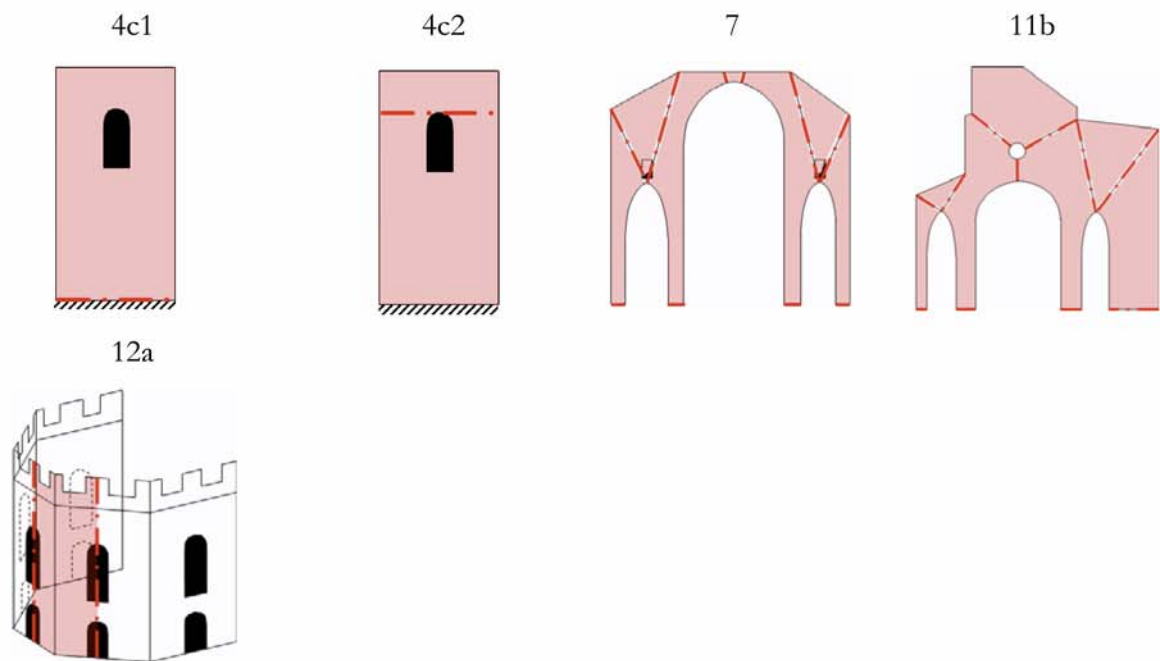
2b; Main facade (B),
Tympanum 2



4a

Beams cross-sections





Note: the hatched surface correspond the part that collapses due to the mechanism.

2. By means of the limit analysis (upper bound theorem), nominal values of the seismic coefficients C_{ij} are obtained.

As for the application to the chapel in Visperterminen, all the assumptions made for the application of the method of Lagomarsino et al. are also made for this method application. A few more have been made because of the method particularities.

ASSUMPTIONS

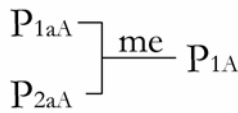
- the overturning of the facades and tympanums has been calculated by taking into account a part of the wall that was in high compression (triangular distribution of stresses) instead of one theoretic point (as in the Lagomarsino's method). This assumption seems more reasonable. In this case, the compression strength of masonry was assumed to be 20 MPa (based on the figure 6.16, [SIA V178]),
 - for other collapse mechanisms, this compression part has not been taken into account and the rotation point has been idealized in one point.
3. The probability density functions f_{cij} of the seismic coefficients C_{ij} are defined (C_{ij} have been assumed to be normally distributed [Au 01] and the coefficient of variation (c.o.v) is estimated on the basis of the number and significance of the geometrical and mechanical parameters considered under step 2. and also of their uncertainties

Table 16.15 : Fragility functions (collapse probability vs. horizontal load coefficient) of the macro-elements and the whole collegiate.

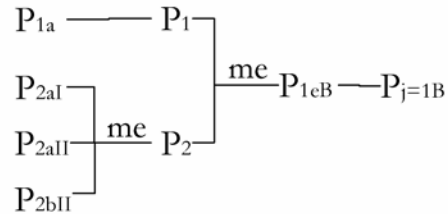
<i>Mechanism</i>	<i>Macroelement</i>	$E[C_{i,j}]$	<i>c.o.v</i>	P_j ($a_g=0.06 g$)	P_j ($a_g=0.1 g$)	P_j ($a_g=0.16 g$)
1a	1A	0.25	0.375	0.018	0.053	0.17
2a	1A	0.34	0.390	0.012	0.03	0.08
1a	1B	0.097	0.375	0.15	0.528	0.954
2a	1B, Tymp.1	0.92	0.390	0.004	0.007	0.013
2a	1B, Tymp.2	0.47	0.390	0.003	0.017	0.039
2b	1B	0.21	0.465	0.046	0.113	0.29
4a	2, 3	0.47	0.450	0.012	0.027	0.06
4c1	2, 3	0.15	0.345	0.039	0.16	0.42
4c2	2, 3	0.7	0.345	0.002	0.005	0.006
7	2, 3	0.25	0.375	0.017	0.05	0.16
11b	4	0.07	0.375	0.35	0.87	0.996
12 a	5	0.22	0.390	0.026	0.074	0.23
1a	8	0.17	0.375	0.04	0.14	0.45

4. For given earthquake intensities, the collapse probability P_j of the j th macro-element is calculated; in the case of the collegiate of Valère, P_j ($j=1-8$) is calculated according to the following schemes:

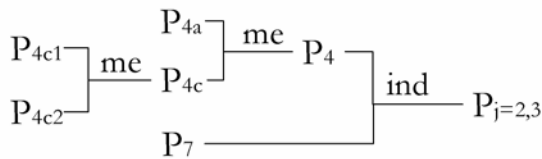
Gable wall



Main Facade



Nave



Chancel arch



Apse



Transept



RESULTS

Macroelement	Collapse prob. $(P_i), a_{gd}/g=0.06 \text{ m/s}^2$	$(P_i), a_{gd}/g=1.0 \text{ m/s}^2$	$(P_i), a_{gd}/g=1.6 \text{ m/s}^2$
Gable wall (1 A)	0.017	0.044	0.11
Façade (1 B)	0.14	0.48	0.86
Nave (2, 3)	0.027	0.08	0.22
Chancel arch (4)	0.35	0.87	0.996
Apse (5)	0.026	0.074	0.23
Transept (8)	0.04	0.14	0.45

ASSESSMENT OF THE COLLAPSE PROBABILITY OF THE WHOLE EDIFICE

1. The critical and non-critical macro-elements have to be individuated at first. In the case of the old chapel in Vipserterminen, it is assumed that every element is critical since the collapse of each of them involve the failure of the structure. The logical diagram of the collegiate of Valère is:

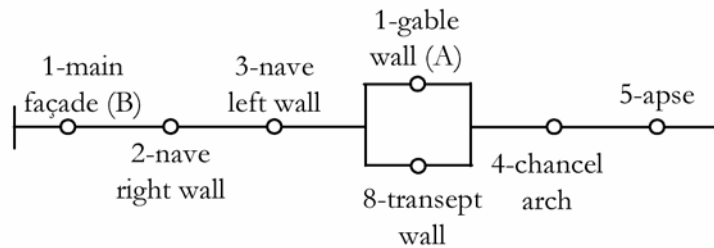


Figure 16.60 : Logical diagram of the collegiate of Valère, Sion.

2. The collapse probability of each subsystem composed of macro-elements working in parallel is evaluated through Eq 5.10, where P_k corresponds to the collapse probability of each branch k of the subsystem,
3. The collapse probability of the whole building is to be found in the Figure 5.22.

DISCUSSION

According to the graph 17, the whole collegiate would collapse under a peak ground acceleration of about 1.2 m/s^2 . The most seismically vulnerable part of the collegiate is the chancel arch; it is not surprising since the chosen collapse mechanism is the same than the one chosen for the application of the Lagomarsino's method. Obviously, the same notes have to be made regarding this result; though the chancel arch is probably seismically vulnerable, this result is certainly overstated.

The main façade is also highly vulnerable under seismic actions. Come after the transept wall (out-of-plane mechanism), the apse, the nave (transversal collapse mechanism) and the gable wall.

Except the chancel arch, it can be seen that the other parts are particularly vulnerable in their out-of-plane direction; this concerns especially the main façade and the transept wall (the south one since the north one is side-by-side with the tower).

The apse and the nave (transversally) seem to be the less vulnerable in case of a seismic event; at least in case of an undamaged structure, which is not really the case.

A. 4. MASONRY

A. 4.1. GEOLOGY OF SWITZERLAND: A BRIEF DESCRIPTION

Switzerland can be geologically divided into 13 areas (Figure 16.61). Though geographically quite homogeneous, rocks of the Jura Mountains are to be divided into 2 unities from a geologically-tectonically point of view. The former, which is called the «Folded Jura» (number 3 in Figure 16.61), is characterized by formations with folded layers dating from Tertiary time. The second unity is named «Tabular Jura» (number 4 in Figure 16.61) and is made up of flat slabs as its name tells us. Though we can find gneiss in the second unity, rocks that can be exploited there are essentially limestone-marl alternations from the Jurassic formation. The eastern section enclosed the oldest banks (Triassic up to Malm) whereas the youngest (Dogger up to Cretaceous) are situated to the west.

Between Jura Mountains and the Alps, there is the Molasse basin which is composed of the flat (number 1 in Figure 16.61) and the sub alpine Molasse (number 2 in Figure 16.61). Molasse basin components, which results from the erosion of the Alps, are gravels, sands and clay more or less consolidated to form conglomerates, sandstones and marls. The basin is divided into four formations (each characterized by typical types of rocks) that were created at four different eras under two different conditions of sedimentation. However, though presenting a few differences regarding their components and compaction degree, Molasse enclosed more or less strong sandstones and also shell limestones. The main differences between sub alpine and flat Molasse layers regard the porosity and the strength. Furthermore, unlike the sub alpine Molasse, the flat one is not crossed by splits [Ha 42].

North Alpine foreland basin, whose rocks are constituted of limestones, marls, marl schists, dolomites, sandstones, breccias, conglomerates and clay schists, was divided into two main zones because of the different way of the creation of their rocks. The Helvetic area (number 5 in Figure 16.61), which spreads over a large part of the north alpine foreland basin, is composed of many nappes. Amongst them, there are the nappes of Glaris, Blüemisalpe, Diablerets and the Dent de Morcles'. It is worth noting that the nappes follow the west to east axis of the Helvetic zone. As this, Romanic zone also encloses limestones and marls essentially; however, their creation was different than the one of the Helvetic nappes rocks. Furthermore, after F. de Quervain [Qu 34], this zone is difficult to describe with accuracy because formations (different rocks and creation eras) are intertwined.

Central massif corresponds to a part of the Alps whose rocks have not sustained big thrusts but only accumulations (aufstauen), ground rising (Hebung) or splitting here and there; moreover, crystalline rocks show almost vertical schistosity. Those rocks are actually part of an old formation, older than surrounding areas. In detail, central massif is composed of four parts: the Aar's, Gotthard's, Mont Blanc's and red sharp peaks' massif. The former is mostly made up of a granite zone in sandwich between (northward and southward) schists and gneiss areas; all crystalline stones are older than the Triassic era and have been from slightly to strongly modified through the Alps creation. The Gotthard' massif, to the south of the Aar's massif, is made up of mica-gneisses and feldspath-gneisses often with intrusions of Amphibolites and Serpentine. At a few places, granite blocs can also be found. Due to Alpine tectonic, Gotthard's massif rocks are at many places metamorphic. The central part of the Mont Blanc's massif is made up of granites; along

both sides, we find schists and gneisses with, like in the Gotthard's massif, Amphibolites and Quartzite (Quarzporphyren) intrusions. In the whole massif, metamorphism is clearly visible. Massif of the red sharp peaks is essentially made up of diverse types of little-metamorphic granites, gneisses, hornblende rocks (Hornfelsen) and mica-schists.

All the Southern Alps are gathered under what is called the penninic area; for the most part, it encompasses wide gneiss banks that can be horizontal, little-sloping or sometimes sloping. This area is to be divided into an upper and a bottom formation. The second encloses a large range of thick gneiss banks (resulting from granites metamorphism) with mica-gneiss and Amphibolites intrusions. Amongst the most well-known, there are the gneisses of the Levantine valley, the Verzasca valley and of the Maggia valley. The upper formation can be essentially found in the Valais, between the Saint Bernard's pass to the Mont Rose's massif. It essentially consists of diverse kinds of gneisses, mica-schists and green schists; it also presents a wide area with sandstones and clay-schists dating from the Carboniferous era. The highest penninic bank, which is called the Dent Blanche's bank and composed of granite-gneisses as well as diorite-gneisses (close to mica-gneisses), can be found at the top of many 4000 peaks of the Alps. Eastward, canton of Graubünden is mainly covered by the Adula and Mishabel banks; both are made up of gneisses. In front of those banks and also at a few places between them, there are sedimentary rocks from the Triassic, the Jurassic, the Cretaceous as well as the Tertiary eras; banks can be either a few meters thick or more than 1000 m tall. Except Triassic sediments, which resulted in Quartzite, dolomite and marble (from limestones) often come with Rauhacken and Gypsum rocks, rocks are similar as the ones belonging to the northern alpine foreland basin. It seems worth noting the important schists of Graubünden that resulted from the metamorphism of rocks during the Jurassic up to the Cretaceous era.

The ground of the Eastern Alpine region (number 11 in Figure 16.61) nappes (the Errgroups, Albula groups and Bernina groups) has a crystalline core of old eruptive rocks as Granites, Diorites, Quartzite-Diorites, Monzonites, Syenites and Gabbros-Diorites that is surrounded by gneisses, Mica-schists and Mesozoic sediments. At the upper level, we find the Campo banks as well as the Silvretta banks that are composed of complex gneisses and of diverse sediment formations.

The underground of the area called "Southern Alps" (number 12 in Figure 16.61) is made up of Gneisses, Mica-schists and of basic rocks as Amphibolites, Gabbros and Peridotites that, in the region of Ivrea, raised up close to the surface. Above those basis formations, we can find banks made up of carbonated rocks created from the Perm to the Cretaceous eras, going through Triassic and Jurassic periods. In consequence, Limestones, Marl-schists, Dolomites and Conglomerates can be found in the Southern Alps region.

The 13th region in Figure 16.61, the Bergel's massif, is essentially composed of Mesozoic sediments. However, what characterize him are the numerous intrusions of Granites and Tonalites at

the Alps creation. Finally, it is worth noting the latest geological formation: the Quaternary, which has resulted from Alps erosion; it can be mainly found in valleys bottom, along rivers shores.

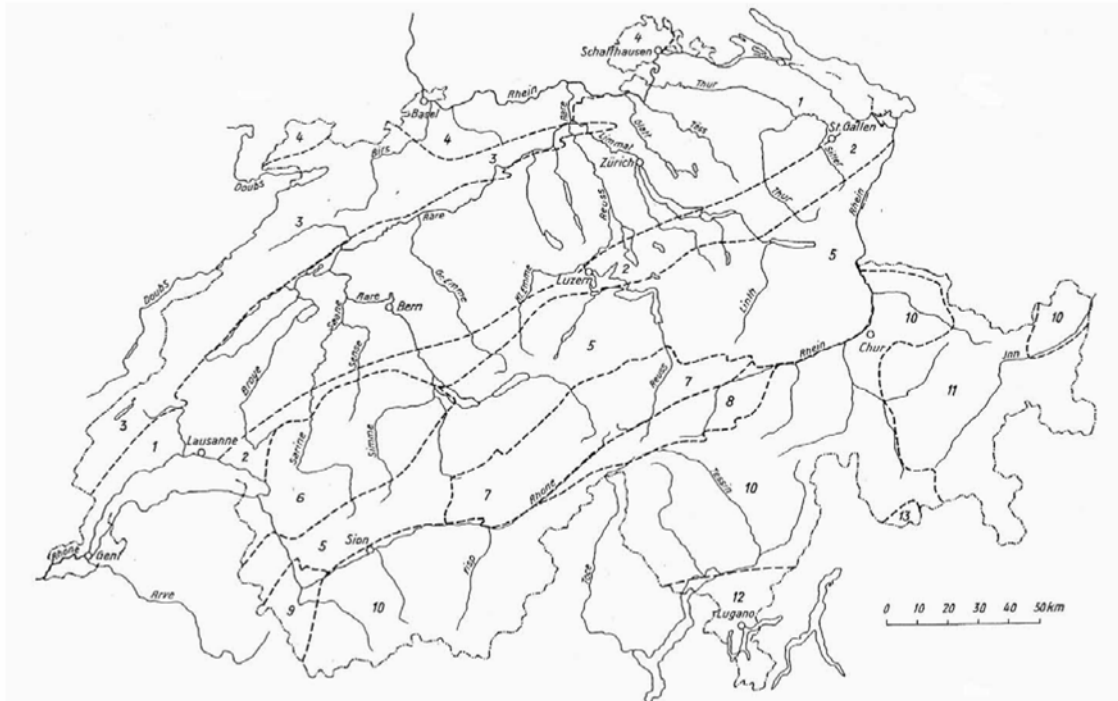


Figure 16.61 : overview of the geologist areas in Switzerland [Ha 42].

Legend:

1	Flat Molasse	2	Sub Alpine Molasse	3	Folded Jura
4	Tabular jura	5	North alpine foreland basin (helvetic nappes)	6	North Alpine foreland basin (Romanic nappes)
7	Aar massif	8	Gotthard massif	9	Mont Blanc and red sharp peaks massifs
10	Penninic unit	11	Eastern alpine region	12	Southern Alps
13	Bergel massif				



Figure 16.62 : main quarries in 1942 [Ha 42]

Legend:

	<i>Nr in the previous figure</i>	<i>Rock type</i>	<i>Canton</i>	Quarry/ Place
A	1	Aar Granite	Bern	Hasli valley
	1		Uri	Reuss valley
B	2	Mont-Blanc Granite	Valais	Monthey, Martigny
C	3	Granite-Gneiss	Tessin	Leventine valley (upper)
	4		Tessin	Leventine valley (middle)
	5		Tessin	Leventine valley (under)
	6		Tessin	Verzasca valley
	7		Tessin	Maggia valley
	8		Tessin	Centovalli
	9		Graubünden	Hinterrhein
	10		Graubünden	Val Poschiavo
	10		Graubünden	Engadin valley
D	11	Gneiss-Quartzite		Averser valley
E	12	Serpentine	Graubünden	Poschiavo
	12		Uri	Hospen valley
F	13	Verrucano	Saint Gall	Murg, Mels
	13		Graubünden	Ilanz
G	14	Gravel Marble-schists	Wallis	Sembrancher

Appendices

<i>H</i>	<i>15</i>	<i>Gravel limestone (Under Cretaceous)</i>	<i>Central Switzerland</i>	Matt, Kehrsiten, Rozloch, Hergiswil, Brunnen
	16		Central Switzerland	Seewen
	16		Glarus	Mollis, Näfels
	16		Saint Gall	Quinten, Weesen, Ober-Toggenburg
	16		Bern	Balmholz (Lake of Thun)
I	17	Valangin Limestone	Bern	Ringgenberg (Lake of Brienz)
K	18	Echinoderm Limestone	Wallis	Collombey
	18		Vaud	Villeneuve (Arvel)
L	19	Green sandstone	Saint Gall	Buchserberg, Sevelen
	19		Nidwald	Beckenried
M	20	Schilfsnstein (reed sandstone)	Aargau	Gansingen
	20		Schaffhausen	Schleitheim
N	21	Triassic Limestone	Vaud	Saint-Triphon
O	22	Calc silicate rock	Tessin	Castione
P	23	Flysch sandstone	Glarus	Matt-Sernf valley
	23		Fribourg	Plasselb, Zollhaus
	23		Bern	Mitholz-Kander valley, Schwarzenburg-Gurnigel
	23		Obwald	Alpnach
	23		Uri	Attinghausen, Bolzbach
	23		Wallis	Massongex, Illiez valley, Saint Gingolph

<i>Q</i>	24	<i>Compact Limestone</i>	<i>Vaud</i>	Yverdon, Sainte-Croix
	24		Neuchâtel	Valangin, la Chaux-de-Fonds
	24		Bern	Pruntrut, Bienne-Biel, Reuchenette, Neuveville
	24		Basle (countryside)	Läufelfingen
	24		Solothurn	Solothurn
	24		Aargau	Baden, Rümikon
	24		Schaffhausen	Schaffhausen, Hemmenthal
	24		Zurich	Dielsdorf
R	25	Oolithic Lime Sandstone	Jura	Laufen
	25		Solothurn	Balsthal
	25		Basle (countryside)	Muttenz
S	26	Porous Limestone	Neuchâtel	Saint Blaise, Hauterive
T	27	Granite Sandstone	Saint Gall	Uznarberg, Saint Magrethen
	27		Schwyz	Buchberg
	27		Zug	Lothenbach-Zugersee
U	28	Lime Sandstone (Appenzell stone)	Saint Gall	Ebnat, Krummenau, Schänis
	28		Schwyz	Buchberg
	28		Fribourg	Echarlens, Corbières, Attalens
	28		Vaud	Chexbres

<i>V</i>	29	<i>Platy Sandstone</i>	<i>Saint Gall</i>	Rorschach
	29		Schwyz	Bäch
	29		Lucerne	Rooterberg, Lucerne
W	30	Muschelkalksteine (shell Limestone)	Aargau	Würenlos, Mägenwil, Othmarsingen-Dottikon
	30		Neuchâtel	Seiry (Estavayer-le-lac)
	30		Saint Gall	Staad
X	31	Bern Sandstone	Bern	Krauchthal, Bolligen, Ostermundigen
Y	32	Fine- grained Conglomerate	Saint Gall	Herisau, Degersheim
	32		Zurich	Rüti
Z	33	Lime Tuff	Saint Gall	Bütschwil, Mosnang, Libingen
	33		Graubünden	Surava, Lenzerheide
	33		Nidwald	Oberdorf
	33		Fribourg	Corpataux
	33		Wallis	Saxon, Sembrancher

A. 4.2. TYPES OF STONES

Stones are usually classified in regards to the way they have been created; one generally distinguishes amongst three groups: volcanic, metamorphic and sedimentary rocks.

Types of stones used for construction in Switzerland ranges from limestone, sandstone and granite to gneiss and even marble, which has been mainly used as stone facing.

In respect to the mechanical properties of stones, it can be roughly written that: they usually have a very low resistance under tensile load; it is actually so a small value that it is generally considered null. The mechanical behaviour is from far better under compression than under traction; nevertheless, considering a plane stress within the compression-tensile stress domain, the resistance is higher than only under traction or in the tensile-tensile stress domain. Nevertheless, either under traction or compression, rocks have a brittle mechanical behaviour, which means that collapse occurs suddenly without any kind of yielding before rupture.

Under loading, rocks behave elastically at first up to a certain load, where micro-cracks parallel to the action direction appear at the stone-mortar interface. Micro-cracks get bigger as the force gets stronger until reaching the strength of masonry and finally the collapse. Once micro-cracks begin to form, the mechanical behaviour enters in its non-linear phase. The collapse occurs more or less quickly after entering into the plastic phase, depending on the rock ductility.

LIMESTONE

Limestone was probably one of the first rock types to be used in Switzerland either by Celtic (Helvetians) people, Roman or even before them. There are quarries, which were already exploited in Roman times, that still exist nowadays. Nevertheless, for 2000 years, many quarries have been opened and many of them have also been closed; in the beginning of the 20th century, only about ten quarries were still exploiting limestone.

Limestone used in the stone masonries belonging to the Swiss building heritage came from three geological formations: Triassic, Jurassic and Cretaceous. Limestone of Castione: called black granite, this limestone is made up of many diverse coloured minerals that make him looks like granite.

The mechanical properties of the aforementioned rocks will be found under A 4.3.

SANDSTONE

The geological Tertiary formations in the middle country and also in the Jura Mountains, which were essentially composed of Molassic sandstone, were exploited a lot for building. Most of churches, cathedrals and public buildings were erected with sandstones coming from this Tertiary formation.

The mechanical properties of the aforementioned rocks will be found under A 4.3

GRANITE AND GNEISS

Granite and gneiss are found in the Alps area; to the north, Aar granite is exploited in Gurtellen, Wassen and Göschenen. In Eastern Switzerland, there are many places where granite is exploited; it is worth noting that other eruptive rock, the serpentine, is quarried in Pontresina. To the south, each valley of the Tessin has its own granite type: the granite-gneiss of the Leventina valley (Lavorgo, Giornico, etc.), the Riviera granite-gneiss (Biasca, Osogna, etc.), the Verzasca granite

(Lavertezzo, Brione, etc.). Finally, in Western Switzerland, the Mont-Blanc granite is quarried in Monthey-Collombey.

A. 4.3. MECHANICAL PROPERTIES OF THE MAIN STONES USED FOR THE CONSTRUCTION IN SWITZERLAND

Values can be found in the Appendix 3 of the Swisscode [SIA V178 80].

A. 4.4. DEFINITION OF THE THICKNESS

The wall thickness can be calculated through the equation:

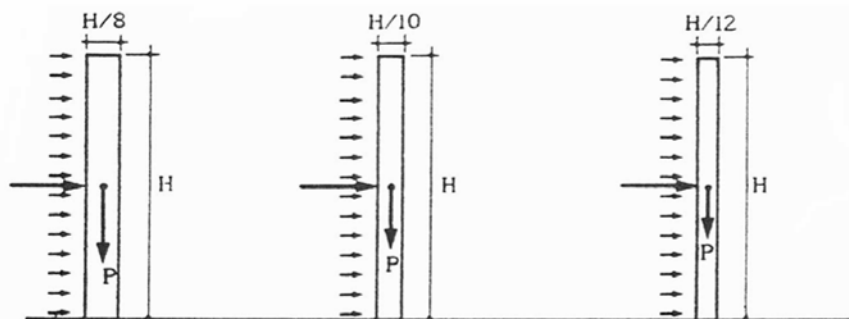


Figure 16.63 : method to define thickness of isolated walls.

After the isolated walls, Rondelet also dealt with the ones connected to lateral walls. In this respect, he pointed out that if a wall is laterally supported by two other walls, it can be thinner than an isolated wall though as stable as the latter. Mathematically he proposed the following equation:

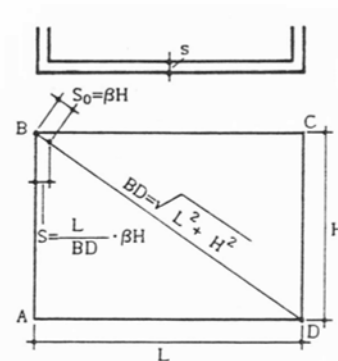


Figure 16.64 : method to calculate the thickness of connected walls.

Where:

L	Wall length
H	Wall height
$BD = \sqrt{H^2 + L^2}$	Diagonal length
β	Coefficient linked to H in order to obtain the wall thickness in respect to the each lateral connection.

Compared with the equation that give the possibility to calculate the wall thickness ($s=H$), the factor of correction is then: $\beta'=L/BD \cdot \beta$; in consequence, if the wall is not isolated, $\beta' < \beta$.

In his article II, Rondelet dealt with the topic of the walls thickness of tall basilicas. Compared to isolated walls, they required thinner walls since the framework efficiently helps containing them. Nevertheless, such action decrease with the nave width and Rondelet proposed a way to calculate it, based on several surveys he did on churches. According to him, if the lateral walls of a nave have no other connection than the roof timberwork, the wall thickness will be a twelfth of the height, reduced according to the nave width with the same equation developed to allow for the distance between the lateral walls.

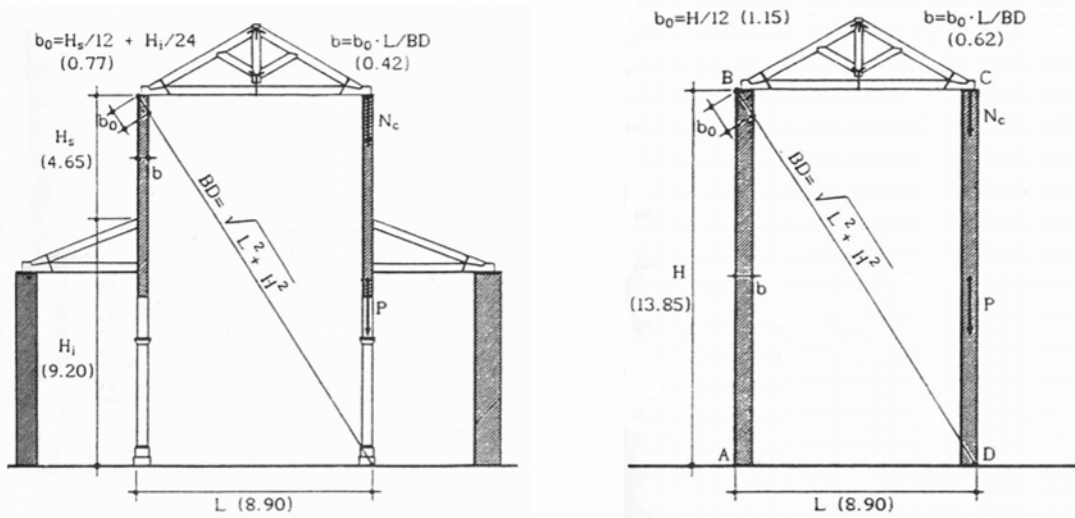


Figure 16.65 : Method to calculate the thickness of basilicas walls.

In case there are low-aisles whose timberworks lean against the main nave walls, these latter thickness corresponds to a twelfth of the vertical dimension from the low-aisles timberwork up to the main nave timberwork with a twenty-fourth of the lower part of the wall and once again reduced according to the nave width.

A. 4.5. DIAGRAM OF FAILURE OF MASONRY UNDER DIFFERENT STRESS LOADING; AFTER PAGE

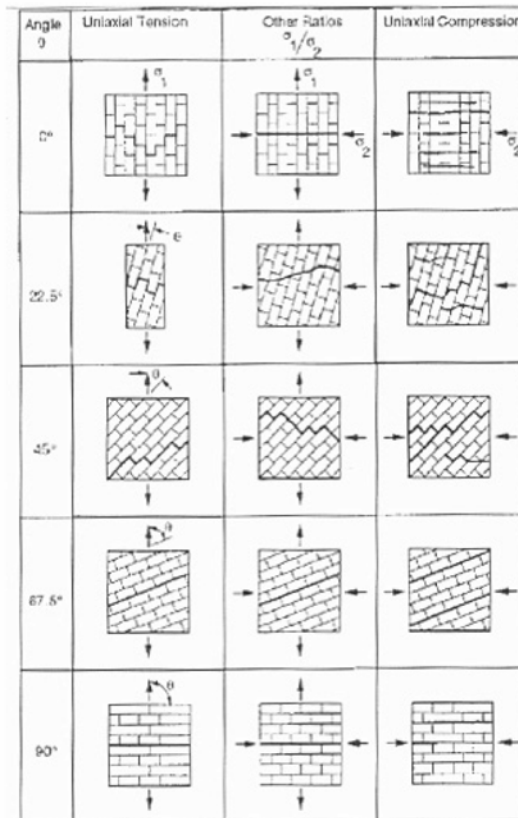


Figure 16.66 : Failure of masonry under different loading conditions; according to Page [Pa 92].

A. 5. SAMPLE: NUMERICAL CALCULATIONS

A. 5.1. DEFINITION OF THE YOUNG'S MODULUS OF THE MASONRY WITH MOLASSE BLOCKS, ACCORDING TO THE SIA V178:

$$E_x^1 = E_s (\text{volume of the stone part in \%}) + E_m (\text{volume of the mortar part in \%})$$

$$E_s: 4497 \text{ MPa}^2$$

$$E_m: 1933 \text{ MPa}^3$$

$$\text{The volume of the stone part is: } V_s = (1.345^4 - 0.035) * 0.53 * 2.1 - 7 * 0.01 * 0.34 * 0.53 = 1.45 \text{ m}^3$$

1. x corresponds to the x-axis (vertical).
2. Value defined by wave velocity [MP 04]
3. Value experimentally defined [Fa 07]

The volume of the mortar part is: $V_m = 3.5 \cdot 0.01 \cdot 0.53 \cdot 2.1 + 7 \cdot 0.01 \cdot 0.34 \cdot 0.53 = 0.052 \text{ m}^3$

The volume of the whole part: $V_T = 1.345 \cdot 2.1 \cdot 0.53 = 1.5 \text{ m}^3$

Then, the volume in %: for the stone part: 96.7 % and the mortar part: 3.3%

$E_x = 4497 \cdot 0.967 + 1933 \cdot 0.033 = 4412.4 \text{ MPa}$

-
4. Bed and head joints are 1 cm thick; the bed joints between the molasse part and the limestone layer is consider for a half.
-

A. 5.2. RESULTS FROM THE DEFOMETER TARGETS

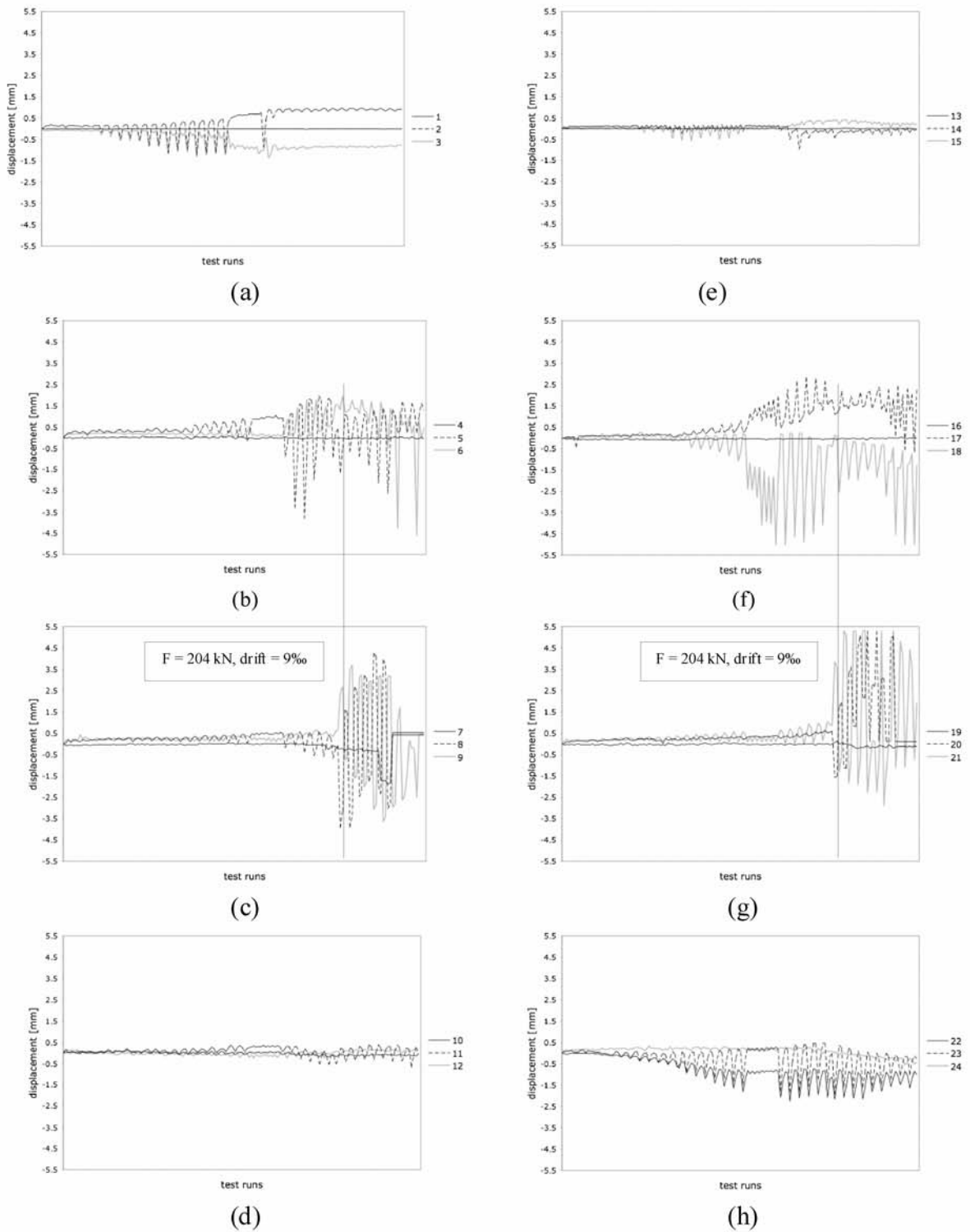


Figure 16.67 : Results obtained with the defometer targets [Fa 07].

A. 6. FLOW OF FORCES WITHIN A BARREL-VAULT

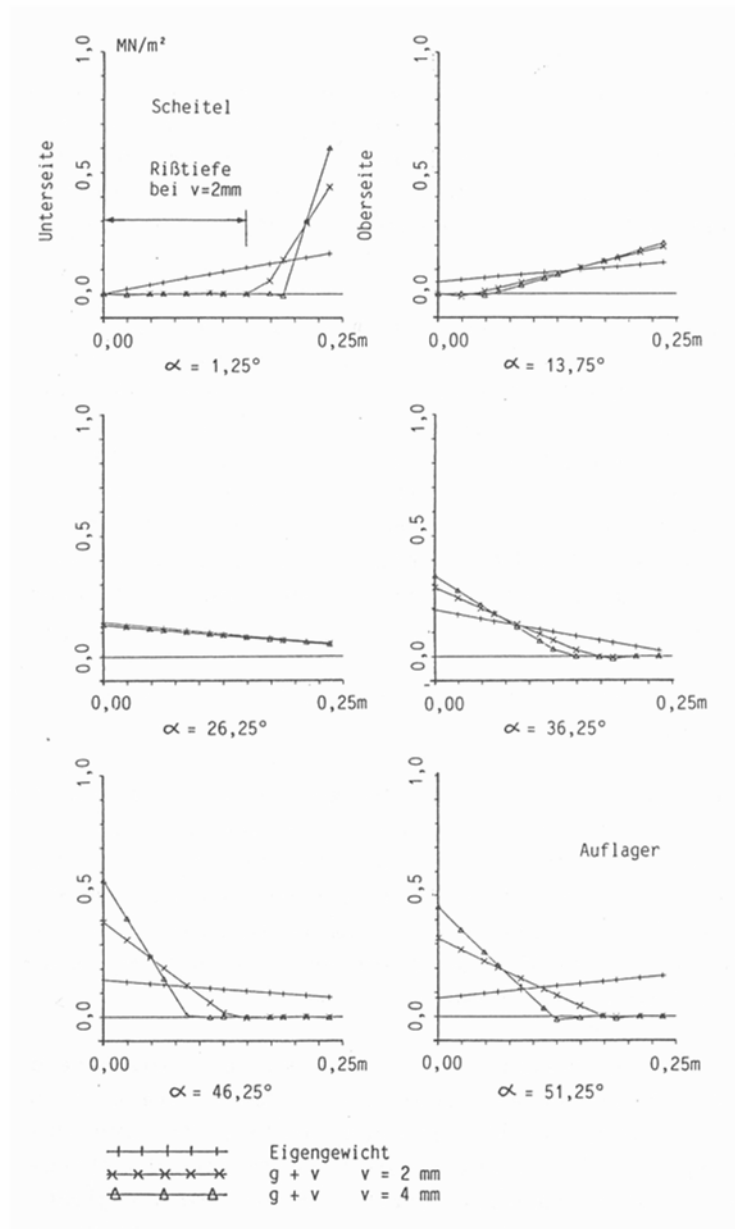


Figure 16.68 : Flow of forces within a barrel vault [Ba 91].

A. 7. SEISMIC RESPONSE OF STANDARD UNITS

A. 7.1. FRONT WALLS

A. 7.1.1. FW3

Contrary to FW2, FW3 is not frequently found in Switzerland; it actually constitutes a part of narthexes that can be found in Romanesque Burgundian edifices.

The proposed configuration with six openings is one possibility; in fact, it is the same pattern than the narthex of the abbey church in Payerne.

Proportions are the following:

- $H_t/L_t = 0.75 - 1$
- $H_d = 2-3$ m
- $H_w = 1-2$ m

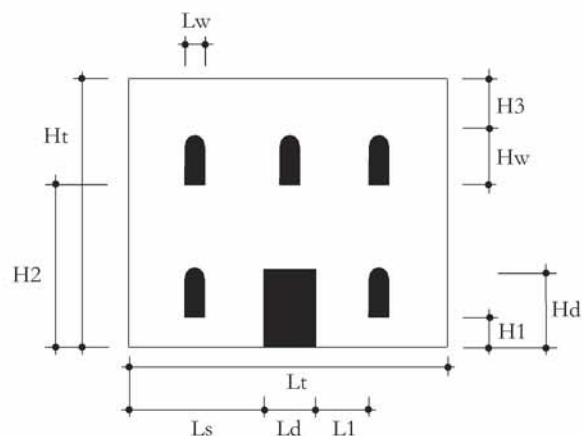


Figure 16.69 : FW3 general pattern.

OUT-OF-PLANE BEHAVIOUR

As aforementioned, front walls may overturn under seismic actions out of their plane. Nevertheless, there is no gable on this type of front wall; only the overturning of the whole façade must be consequently checked.

Whole façade

One of the possible flows of forces is shown on the Figure 16.70: there are three columns where equivalent lateral forces are directly transferred down to the ground thanks to the masonry self-weight and six sections where they are horizontally transferred by arch effect.

It must be said that another flow of forces where there is no horizontal transfer could also be possible and may make the calculations less time-consuming; however, this easier transfer of forces does not give the possibility to determine under which ground acceleration the front wall will get separated from the lateral walls along the vertical edges.

Note: the dotted lines correspond to partially restrained bearings.

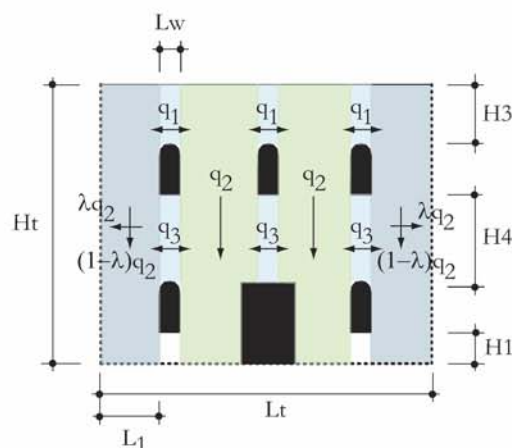


Figure 16.70 : Possible transfer of forces within FW3 front wall.

The in-plane behaviour is treated as for the FW7 standard unit.

A. 7. 1. 2. FW4

The FW4 type of front wall is essentially found as a part of Westwerk façade, like on the Basel cathedral or the «Fraumünster» in Zürich.

The component itself can be characterized by a certain seismic vulnerability (due to its own structural behaviour under seismic loading); nevertheless it is more vulnerable because of the movement of the adjacent structural components.

The proposed configuration for openings is quite frequent one, though it might have no window but a door instead.

Proportions are the following:

- $H_2/L_t = 2-3$; $H_2/H_1 = 1.25-1.6$; $H_1/L_t = 1.5-2.5$
- $H_3 = 1-2$ m

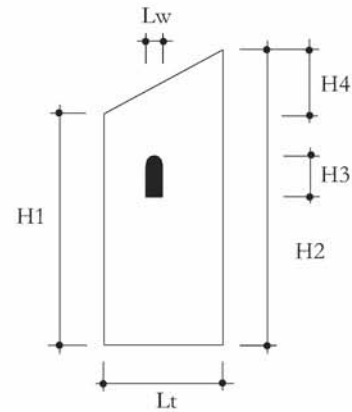


Figure 16.71 : FW4 general pattern.

OUT-OF-PLANE BEHAVIOUR

This kind of front wall is quite slender and might overturn when no longer connected to lateral components. As the previous case, there is no gable and consequently, only the overturning of the whole façade must be consequently checked.

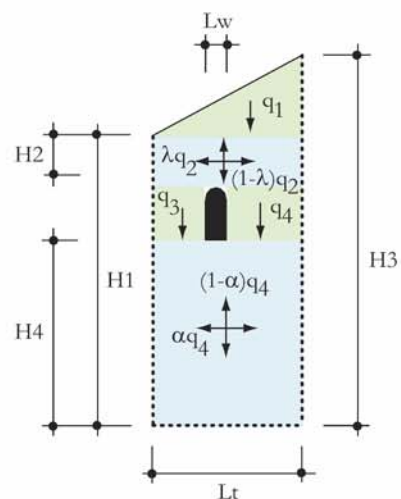
Whole façade

One of the possible flows of forces is shown on the Figure 16.70: there are four columns where equivalent lateral forces are directly transferred down to the ground thanks to the masonry self-weight and two sections where they are horizontally transferred by arch effect.

It must be said that another flow of forces where there is no horizontal transfer could also be possible and may make the calculations less time-consuming.

In this case, λ is proportional to H_2/L_t and α to H_4/L_t

The strength of the part 2 is to be calculated according to the way proposed under chapter 8.3.



Note: the dotted lines correspond to partially restrained bearings.

Figure 16.72 : Possible transfer of forces within FW4 front wall

The in-plane behaviour is treated as for the FW7 standard unit.

A. 7. 1. 3. FW6

FW6 corresponds to the most widespread type of front wall in Switzerland; it is basilicas front wall.

The proposed configuration for openings is not the most frequent one (windows can be taller and wider).

Usual proportions are the following:

- $L_t = 1.5-2 L_a$
- $H_t = 0.75-1.5 L_t$
- $H_a = 0.4-0.6 H_t$
- Rosace radius varies as a function of the main nave width
- The main door height varies as a function of the aisles height.

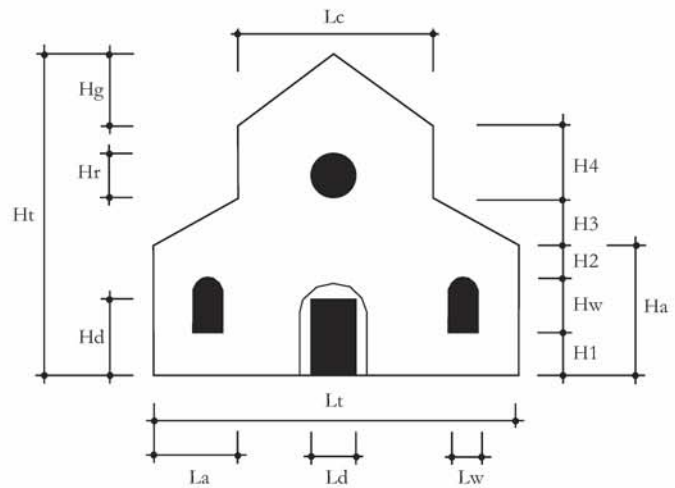


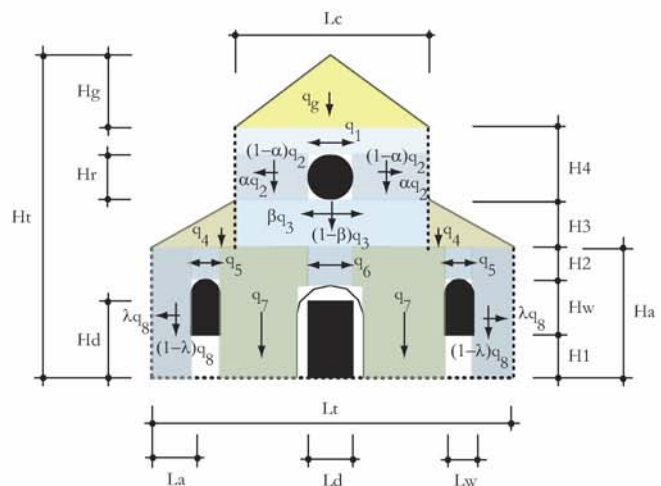
Figure 16.73 : FW6 general pattern.

OUT-OF-PLANE BEHAVIOUR

One of the possible flows of forces is shown on the Figure 16.74. Due to particular boundary conditions^a, the equivalent forces of the upper part transfer first to the lateral edges.

In this case, α is proportional to $H_r / (0.5L_c - 0.5L_d)$ and β to H_3 / L_c and $\lambda = H_a / L_a$. The strength of these parts is can be calculated according to the way proposed under chapter 8.3.

Note: the dotted lines correspond to partially restrained bearings.



a. The walls of the main nave do not stop at the top of the aisles roof; it go down a bit further (arcades level).

Figure 16.74 : Possible transfer of forces within FW6 front wall.

The in-plane behaviour is treated as for the FW7 standard unit.

A. 8. SEISMIC HAZARD IN SWITZERLAND

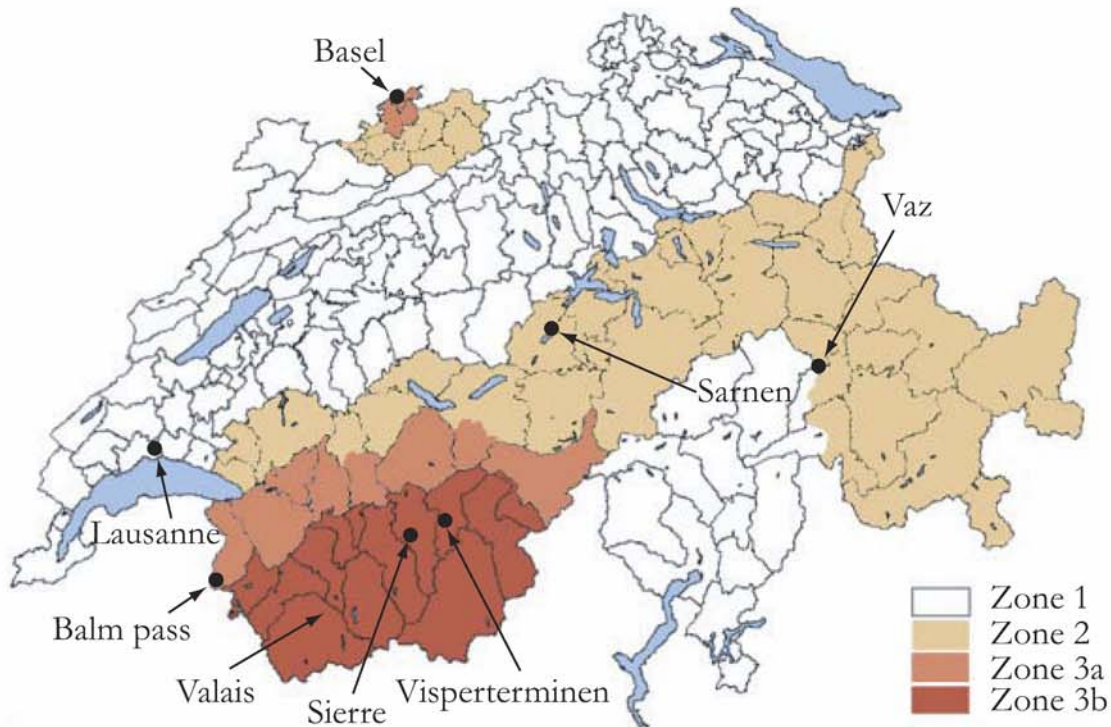


Figure 16.75 : Seismic hazard in Switzerland for an earthquake with a return period of $T=475$ years (Swiss Seismological Service).

Each zone, which describes a different seismic hazard, is characterized by a peak ground acceleration that are:

- zone 1: $a_{gd}=0.6 \text{ m/s}^2$
- zone 2: $a_{gd}=1.0 \text{ m/s}^2$
- zone 3a: $a_{gd}=1.3 \text{ m/s}^2$
- zone 3b: $a_{gd}=1.6 \text{ m/s}^2$

Mylène Devaux

Rte de la Chérard 4
1027 Lonay
Mobile phone : 078/ 857.32.99
E-Mail: mylene.devaux@epfl.ch

25.08.1977
Single
Swiss



EDUCATION

2002 1998-1999 1995	Swiss Federal Institute of Technology Lausanne (EPFL): Master's degree in Civil Engineering Swiss Federal Institute of Technology Zürich (ETHZ) : exchange year Secondary school (option : scientific), Neuchâtel
--	---

PROFESSIONAL EXPERIENCE

2004 - 2008	Research assistant at the Applied Computing and Mechanics Laboratory at EPFL (IMAC).
2002 - 2003	Researcher at the Timber Structures Laboratory at Tokyo University : Study on the structural behaviour (static and dynamic loadings) of the Kintai bridge in Iwakuni.
2002 - 2002	Research assistant at the Structural Concrete Laboratory at EPFL (IS-BETON) : Creation of an e-learning course on structures.
Été 2000 (2 months)	Training at the Timber Structures Laboratory at EPFL (IBOIS) : Creation, construction and numerical modelling of a shell made up of screwed-laminated timber components.

PUBLICATIONS

Devaux M., Lestuzzi P., Seismic vulnerability of Swiss heritage buildings, First European Conference on Earthquake Engineering and Seismology, Geneva, 2006.

Devaux M., Lestuzzi P., Seismic vulnerability of monumental buildings in Switzerland, Structural Studies, Repairs and Maintenance of Heritage Architecture IX, Malta, 2005.

Devaux M., Lestuzzi P., Seismic vulnerability of cultural heritage buildings in Switzerland, D-A-CH Tagung, Köln, 2005.

Devaux M., Sakamoto I., Analysis and improvement of the dynamic performances of the Kintai Bridge, Interaction between Science, Technology and Architecture in Timber Construction, Heritage Series, Ed. Elsevier, 2004.